PERFORMANCE INVESTIGATION of PILE DRIVING HAMMERS and PILES

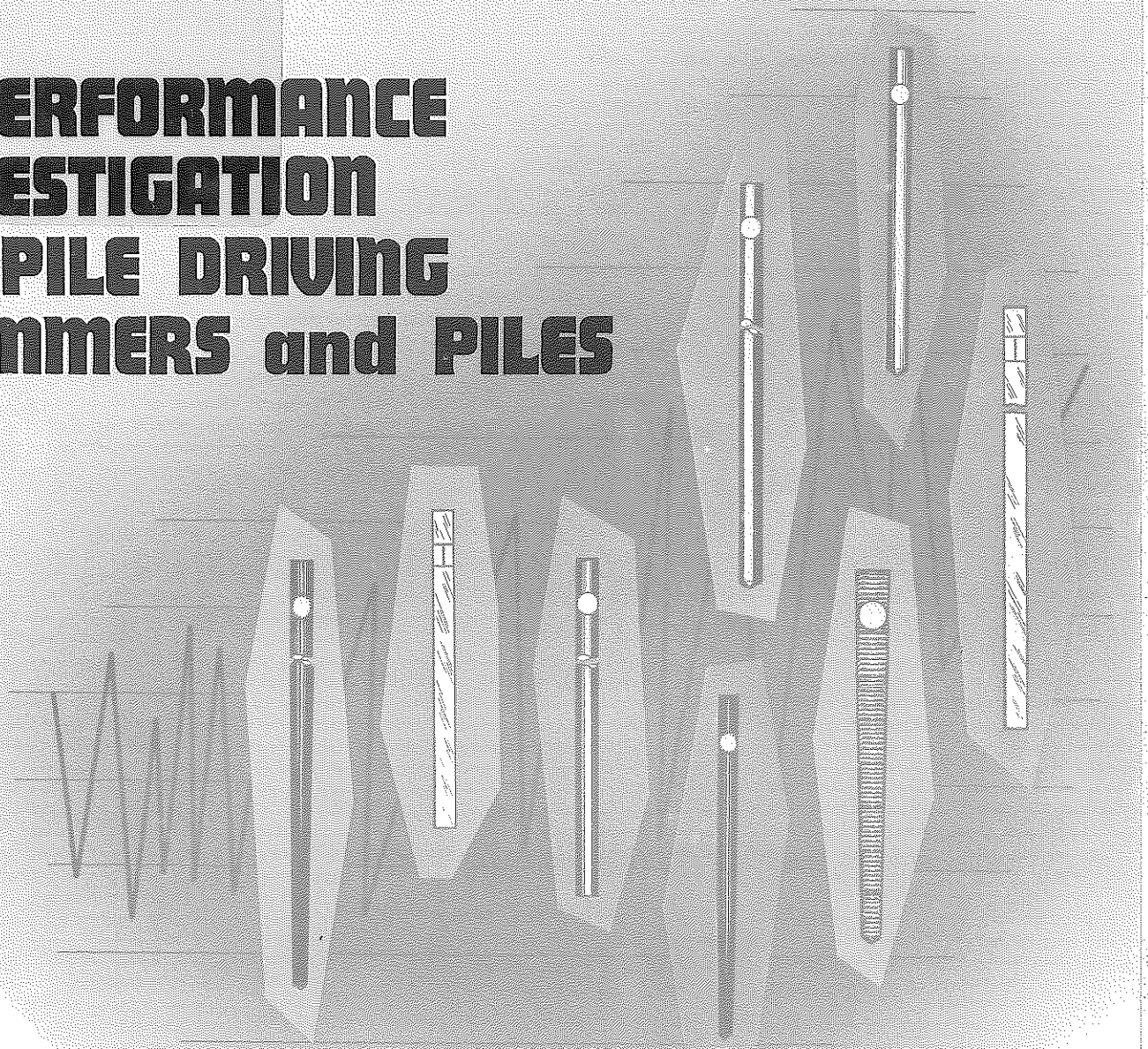

MICHIGAN
STATE HIGHWAY COMMISSION

MARCH 1965

REPORT
TEXT

APPENDICES A AND B TO THIS REPORT ARE BOUND SEPARATELY

INFORMATION

RETRIEVAL

DATA

KEY WORDS: pile drivers; energy transfer ("Enthru"); formulas; statistical analysis; instrumentation, electronic; piles and pile driving; soil mechanics; bearing capacity; elastic limit; yield strength.

ABSTRACT: In one of the largest experimental field pile driving operations in recent years, Michigan has tested air-, steam-, and diesel-powered pile driving hammers on piling of various configurations at sites selected to represent a varied range of soil conditions. Hammer performance was recorded by conventional methods and also through electronic transducers for experimental determination of force, acceleration, and deflection. Resulting data were evaluated and compared in terms of blow count, pile penetration rate, and "Enthru" (net energy delivered to the pile top). Selected piles also underwent extensive static loading tests. From data obtained, measured pile supporting capacity was correlated with that estimated from soil boring data secured prior to pile driving. Eleven common dynamic pile formulas were analyzed in light of this correlation of estimated and measured pile capacity. Guidelines are presented for selection of hammers and for good pile driving practice.

REFERENCE: A Performance Investigation of Pile Driving Hammers and Piles. Lansing: Michigan State Highway Commission, March 1965.

A PERFORMANCE INVESTIGATION OF PILE DRIVING HAMMERS AND PILES

Final Report of a Study in Cooperation with
The Bureau of Public Roads - U. S. Department of Commerce,
The Michigan Road Builders Association, Wayne State University,
and Representative Hammer Manufacturers

Office of Testing and Research
Research Project 61 F-60

Michigan State Highway Commission

Ardale W. Ferguson, Chairman; Charles H. Hewitt, Vice-Chairman;
Wallace D. Nunn; Richard F. Vander Veen; Howard E. Hill, Director

Lansing, March 1965

Fourth Printing, September 1966

IN MEMORIAM

Mr. Leo V. Garrity, Project Manager for this research study, died February 28, 1963, eighteen months after his appointment. He had been hospitalized during the early stages of the field study, but returned to guide the first operations in data reduction and organization of the project report. He continued in active leadership until a few weeks before his death.

A 1923 graduate in civil engineering from the University of Wisconsin, his home state, he came to Detroit in 1927 as one of a group of "exceptional engineers" recruited by the Detroit Water Board. From 1932 to 1940 he accepted positions in public service in Michigan including the directorship of Michigan State Highway Department Testing and Research Laboratory at Ann Arbor. In 1940 he returned to the Detroit Water Board where he held the position of Assistant General Manager and Chief Engineer until retirement in 1955. Subsequently, he engaged in consulting practice and in 1955 re-entered public service with the Wayne County Road Commission, until his second retirement in 1961. At the time of his appointment to this project, he was associated with the Civil Engineering Department of Wayne State University.

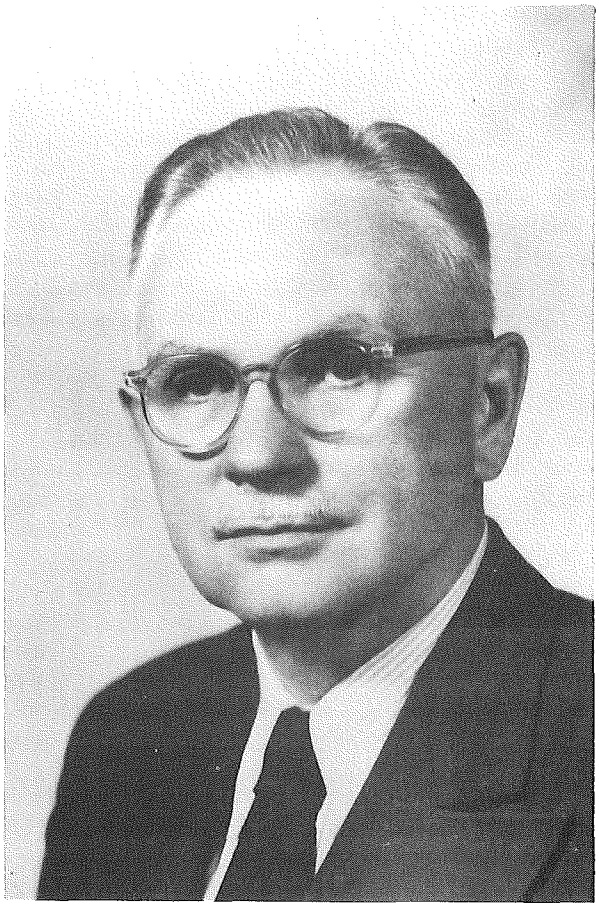

Leo V. Garrity, 1899 - 1963

The Michigan Section of The American Society of Civil Engineers, of which he was a past president, wrote of Mr. Garrity after his death:

"Mr. Garrity's contributions to the improvement of Detroit, and to his profession, were outstanding. A thoroughly practical and skilled construction engineer, he was equally capable as designer, researcher, teacher and administrator."

His talents and knowledge of construction problems were a vital element in the execution of this research investigation. His guidance and counsel have been severely missed by his co-workers.

PREFACE

In recent years, diesel pile driving hammers have come into increasing use in bridge construction. These diesels appear to have certain advantages over air and steam powered hammers, in size and weight and in absence of auxiliary power supply equipment. Nevertheless, questions remain concerning their performance, in terms of results--the driving of piles and development of load bearing capacity of piles.

Manufacturers publish energy ratings for their hammers that have been developed by several methods, most involving modifications of maximum potential energy of the ram. Some engineers have accepted the manufacturers' energy ratings for the diesels while others have felt that the ratio of actual energy output to the manufacturer's rating is much smaller for diesel hammers than for steam or air hammers. As a result certain modifying factors are sometimes used in pile driving formulas when working with diesels, which have the result of reducing the computed load bearing capacity. Thus, in some cases the full potential of the diesel hammers is probably not being realized, and it is also clear that preparation of construction specifications and reliable guides for design and construction practice has been complicated considerably.

Formulation of the Study

As more Michigan contractors began using diesel hammers on State projects, more reliable rating of diesel hammer energy was required and the need for guidelines in design and construction practice became urgent. At a joint meeting of representatives of the Michigan State Highway Department and the Michigan Road Builders Association in September 1960, action was taken by initiating a cooperative research project involving pile driving hammers, their performance, and load bearing capacity of piles under varying field conditions.

A memorandum describing such a project was prepared by P. A. Nordgren, Bridge Construction Engineer, reviewed at the September 1960 joint meeting, and provided the basis for continued planning. L. W. Lamb, Sr. enlisted the support of the MRBA and presented the contractor's

viewpoint. At the MRBA's annual meeting in December 1960, action was taken to support the project through their Specifications-Structure Committee of which Mr. Lamb was chairman.

Beginning in January 1961, a series of meetings were held, including representatives of the Highway Department, the Bureau of Public Roads, the Michigan Road Builders Association, and various hammer manufacturers. As a consequence of these meetings, a research project proposal was prepared, and in July 1961 approved by the Bureau of Public Roads for Federal financial participation.

Objectives and Scope

As the proposal was developed, it became apparent that the scope of the investigation should extend beyond the operating characteristics of the diesel hammers, to include their comparison with steam and air hammers, as well as problems in pile design, soil variation, and driving practice. The following general goals emerged:

a. Development of a procedure, in terms of measurable quantities, to determine hammer energy delivered to the pile and its effectiveness in driving the pile, and comparison of these quantities with the manufacturers' published ratings.

b. Correlation of measured static load bearing capacity with that computed on the basis of blow count or penetration per blow, using a selected group of well-known pile driving formulas.

c. Correlation of measured static load bearing capacity with soil boring information and soil resistance data from field and laboratory tests, and determination of whether these data provide a more reliable basis for predetermination of load capacity for design purposes.

In order to define the scope of the investigation, the following specific objectives were outlined in the proposal:

"1. To develop a method for determining the driving energy output of various types of pile driving hammers.

"2. To determine by load tests the bearing capacity of certain piles driven under test conditions.

"3. To determine what factors, if any, relate the measured pile-driving energy to the bearing capacity of a pile.

"4. To determine the proper wall thickness of pipe piles under certain driving conditions.

"5. To determine the correlation between bearing capacity of the load-tested piles and estimated pile bearing capacity as obtained by (eleven) selected pile-driving formulas.

"6. To determine the best methods or procedures for jetting of piles through intermediate soil layers when driving resistance is large but bearing capacity in these layers is not satisfactory.

"7. To determine the effect of pile cross-section or surface configuration on the energy required for driving.

"8. To determine the effect of pile cross-section or surface configuration on pile load bearing capacity."

In addition to these eight formally stated objectives, two particular phases of the investigation should be emphasized, due to their importance in terms of results achieved. From the project's inception, particular attention was given to the development of experimental technique, equipment, and instrumentation to measure energy input to a pile, and the pile's response in terms of force, deflection, and acceleration. At the conclusion of field testing operations, it was found that so large a volume of experimental data had been accumulated over so wide and varied a range of driving conditions that the data analysis required computer processing and application of statistical techniques.

Project Administration and Acknowledgments

Throughout the investigation, from its inception to completion of this final report, the project has had the active and understanding administration support through Howard E. Hill, formerly managing Director of the Michigan State Highway Department and since January 1965, Acting Director for the Michigan State Highway Commission.

Administrative responsibility for the entire research program was vested in the Office of Testing and Research, Michigan State Highway Department, under direction of W. W. McLaughlin, Testing and Research Engineer and Chairman of the Steering Committee which defined the project's scope and assisted in its supervision. The Chairman was assisted in various phases of the project by P. A. Nordgren, Bridge Construction Engineer, Michigan State Highway Department, and Research Consultant Prof. W. S. Housel, University of Michigan. Other Steering

Committee members included E. A. Finney, G. O. Kerkhoff, L. T. Oehler, O. L. Stokstad, U. W. Stoll, C. H. Voss, and J. H. Williams, for the Michigan State Highway Department; L. W. Lamb, Sr., Chairman of a Michigan Road Builders Association Committee for this study including L. D. Abbey, LeRoy Feldkamp, F. W. Neu, and Walter Toebe; and Harry Krashen and James Gordon for the Bureau of Public Roads. Representatives of the Bureau of Public Roads have maintained contact with the project, met with the Steering Committee, and made comments and suggestions contributing considerably to the group effort. In addition, special operational assignments were executed by A. E. Matthews and E. N. Noble, Michigan State Highway Department.

The Steering Committee placed administration of the project with Wayne State University, which engaged L. V. Garrity as Project Manager, designated Prof. Dudley Newton as Project Director, and assigned R. E. Wilshaw as a research associate. After Mr. Garrity's death, through mutual agreement of the University and the Department, the manager's duties were transferred to Department personnel. Over a period of more than three years the study's active technical operations were carried out by the Department's Testing Laboratory Division (Soils Section) in the Soil Mechanics Laboratory at the University of Michigan, Ann Arbor, and Research Laboratory Division (Physical Research Section) in Lansing.

Field operations were directed initially by Mr. Garrity and later by G. O. Kerkhoff, Acting Project Manager, who was assisted by George Langen, District Soils Engineer, Michigan State Highway Department. Project Engineer throughout field operations was Earl Knott, Bridge Construction Division, Michigan State Highway Department.

Design and fabrication of transducers and the automatic recording system were the responsibility of L. T. Oehler and Paul Milliman, of the Research Laboratory Division in Lansing, and C. J. Arnold assisted in development of the load cell. During field operations, Paul Milliman was in charge of automatic recording equipment and D. A. Davis and R. E. Wilshaw were in charge of all other recording procedures. F. T. Higgins, Jr., conducted the pile loading tests.

Field data were coordinated and compiled by D. A. Davis, J. M. Ritchie, and R. E. Wilshaw at the Testing Laboratory Division. The computer programs were set up and carried to conclusion by J. M. Ritchie and J. R. Darlington and the statistical analyses were planned by L. F. Holbrook. The facilities of the University of Michigan Computer Center and the Michigan State University Computer Laboratory were used in data processing.

Preparation of the report was coordinated by G. O. Kerkhoff, L. T. Oehler and W. S. Housel. Editorial review and processing was the responsibility of A. D. Emerich and R. W. Ormsby designed and executed the graphic presentation and printing format.

Authors and others contributing materially to the completion of this report include the following (listed alphabetically):

D. A. Davis - Chapters 2 and 3
F. T. Higgins, Jr. - Chapter 10
L. F. Holbrook - Chapters 5, 6, and 7
W. S. Housel - Chapters 11 and 13
G. O. Kerkhoff - Chapters 1 and 10
Paul Milliman - Chapter 4
J. M. Ritchie - Chapters 8 and 12, Apps. A and B
U. W. Stoll - Chapters 8, 9, and 12
R. E. Wilshaw - Chapters 8 and 12, Apps. A and B

Manufacturers and distributors of pile driving hammers who cooperated by furnishing hammers for the study, included the McKiernan-Terry Corporation (MKT Corporation), the Vulcan Iron Works, the Link-Belt Speeder Company (Division of the Link-Belt Company), the Foundation Equipment Corporation (Delmag), and the Raymond Concrete Pile Division of Raymond International, Inc. Other pile driving equipment and the labor force were provided by the Reid Construction Company, Battle Creek, under contract with the Michigan State Highway Department. The step-taper shell was donated by Raymond Concrete Pile Division of Raymond International, which also paid the cost of its driving. The Ford Motor Company loaned steel ingots for the pile load tests.

Before reaching its final form, this report went through several revisions and an unusually extensive series of reviews by all participants in the investigation. The Department particularly appreciates the time and effort devoted to this phase of the project by the cooperating manufacturers, whose suggestions and comments have been most valuable. The manufacturers' representatives who took part in these reviews were: G. G. Brode, R. M. Brode, Mogens Rand, W. H. Rabe, F. Kuemmel, M. J. Tschirch for the Foundation Equipment Corporation (Delmag); T. M. Leigh, K. E. Bailey, L. D. Bassett and L. M. Proctor for the Link-Belt Speeder Company; L. L. Frederick, W. H. Guest, and G. M. Anderson for the McKiernan-Terry (MKT) Corporation; F. M. Fuller, H. W. Hunter, E. A. Smith, G. J. Gendron, and J. H. Owens for the Raymond Concrete Pile Division of Raymond International, Inc; and C. V. Adams for the Vulcan Iron Works.

CONTENTS

CONTENTS (Cont.)

CHAPTER ONE

SOILS INVESTIGATION

After preliminary investigation considering typical soil conditions found in Michigan, three representative sites were selected. These included the Belleville site, located 2 miles east of Belleville and within the right-of-way of the Huron River Drive; the Detroit site, in the interchange area of Greenfield Road and I 94 (Detroit Industrial Expressway, Section II); and the Muskegon site, northeast of Muskegon in the Muskegon River drainageway.

The first of these sites provided cohesive subsoils highly resistant to pile penetration, so that hammer performance in hard driving could be measured. At the second site, deep soft cohesive subsoils offered extremely weak resistance, so that hammer performance under easy driving conditions could be measured. The third site, with its deep granular deposits and intrabedded organic materials, presented driving problems typical of buried drainageways emptying into the Great Lakes.

At each site a detailed field subsoil investigation was made by an experienced Michigan State Highway Department hydraulic boring crew. In each of these investigations, a soils engineer was assigned to assist in boring operations. The Michigan method of making hydraulic (wash) borings, obtaining undisturbed samples, and testing penetration resistance,[1] was used for a total of eight borings (Fig. 1). For each boring, a 2-in. ID casing was advanced continuously during drilling. The core sampler for taking undisturbed samples had an 1-3/4-in. OD and contained a series of intersectional liners with an ID of 1-3/8 in. The split spoon sampler had an OD of 1-3/4 in. and an ID of 1-3/8 in. No borings were made after driving or load testing of piles.

Undisturbed samples were tested by the Department's Testing Laboratory Division (at Ann Arbor) for shearing resistance, unconfined

[1] "Field Manual of Soil Engineering" (4th Edition). Lansing: Michigan State Highway Dept. (1960), pp. 36-40.

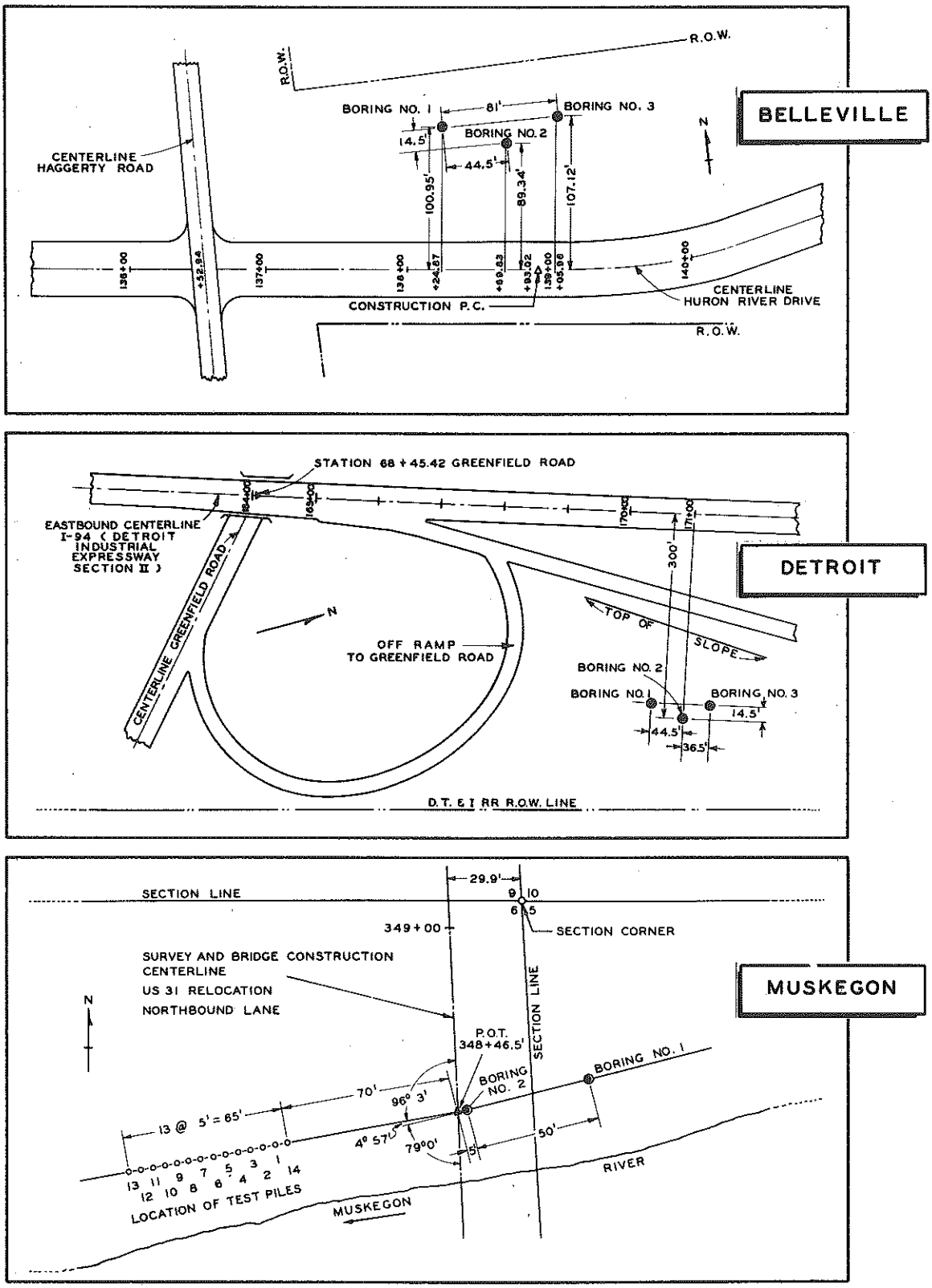

Figure 1. Test boring locations at the three test sites. Relative positions of piles are shown for Belleville and Detroit in Figs. 22 and 23. Those for Muskegon are shown above and in Fig. 24.

compressive strength, moisture content, and unit weight. On selected samples, mechanical analyses and moisture limit tests were also performed.

Laboratory results and field information were compiled on individual profile charts for each individual boring, and in addition a composite subsoil analysis chart was constructed from all borings at each site to provide a comprehensive soil report. [2,3]

Belleville Site (Stiff-to-Firm Cohesive Subsoils)

Undisturbed samples were taken and penetration resistance was measured at 2.5-ft intervals with the core sampler (Figs. 2, 3, 4, 5). The three borings showed that the major feature of the subsoil is the top 45 ft of stiff-to-firm clay. Later examination of subsoil material pre-excavated before pile driving showed that the surface clay was weathered and desiccated to a depth of about 10 ft before it changed to a saturated blue clay. Shearing resistance test results for the upper 45 ft indicated variations in strength among the borings. Fig. 6 shows these variations specifically in terms of "cumulative average shearing resistance," defined here as average shearing resistance for a given interval of depth measured from the surface, or from any selected horizontal plane, to the elevation at which the average shear value applies. These values were used in computing side shear capacity of the test piles (Chapter 11). In particular, these results showed greater strength in the subsoils at the west side of the site than at the east, a difference reflected later in performance evaluation of test hammers and piles.

Underlying the 45 ft of clay is a 14-ft alluvial deposit of mineral silt and very fine sand, with thin laminations of clay. Sampled materials from this deposit were studied in detail. In appearance, they were a clayey silt and clayey fine sand, and laboratory tests on the combined whole sample showed a high amount of mineral silt with a substantial percentage of clay. Transverse shearing resistance test results could not be obtained. Compressive tests were made, but the test values were low and were not considered a complete measure of the strength properties of this soil body. The engineering properties of the alluvial deposit are estimated to be granular in character.

---

2 "Procedure for Testing Soils." Philadelphia: ASTM (April 1958), pp. 317-320, 360-363.

3 "Field Manual of Soil Engineering" (4th Edition). Lansing: Michigan State Highway Dept. (1960), pp. 64-72.

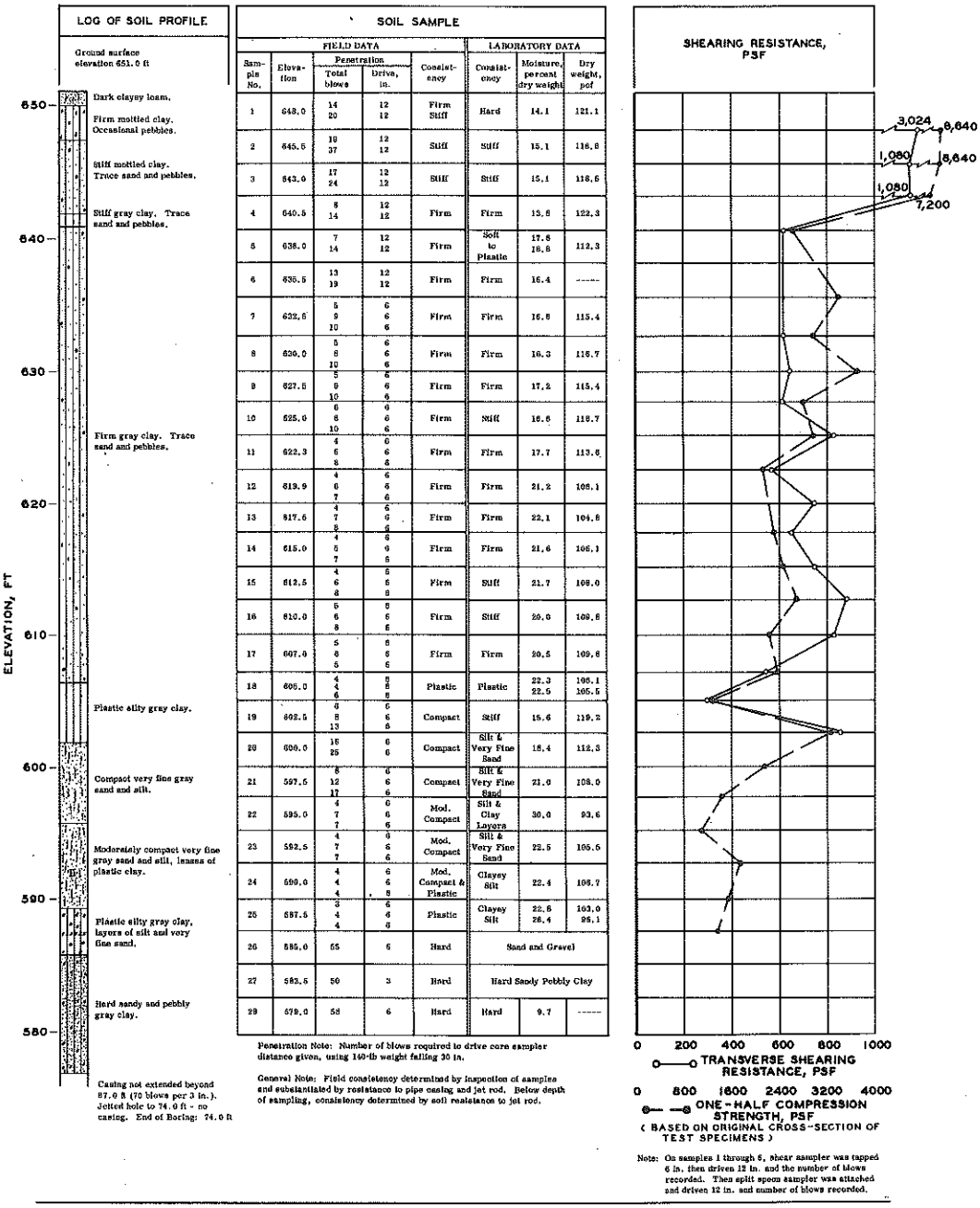

Figure 2. Belleville Boring No. 1 profile.

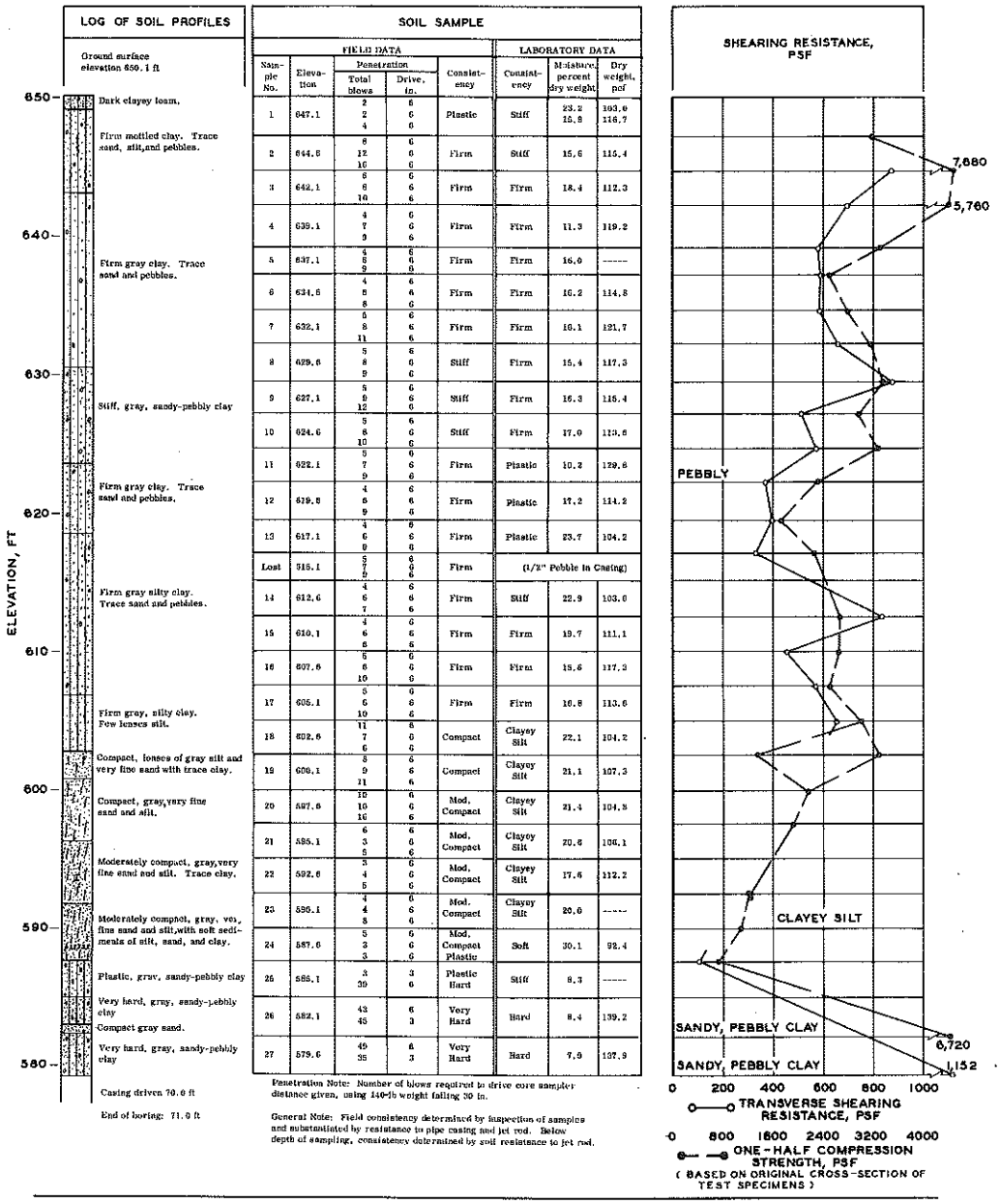

Figure 3. Belleville Boring No. 2 profile.

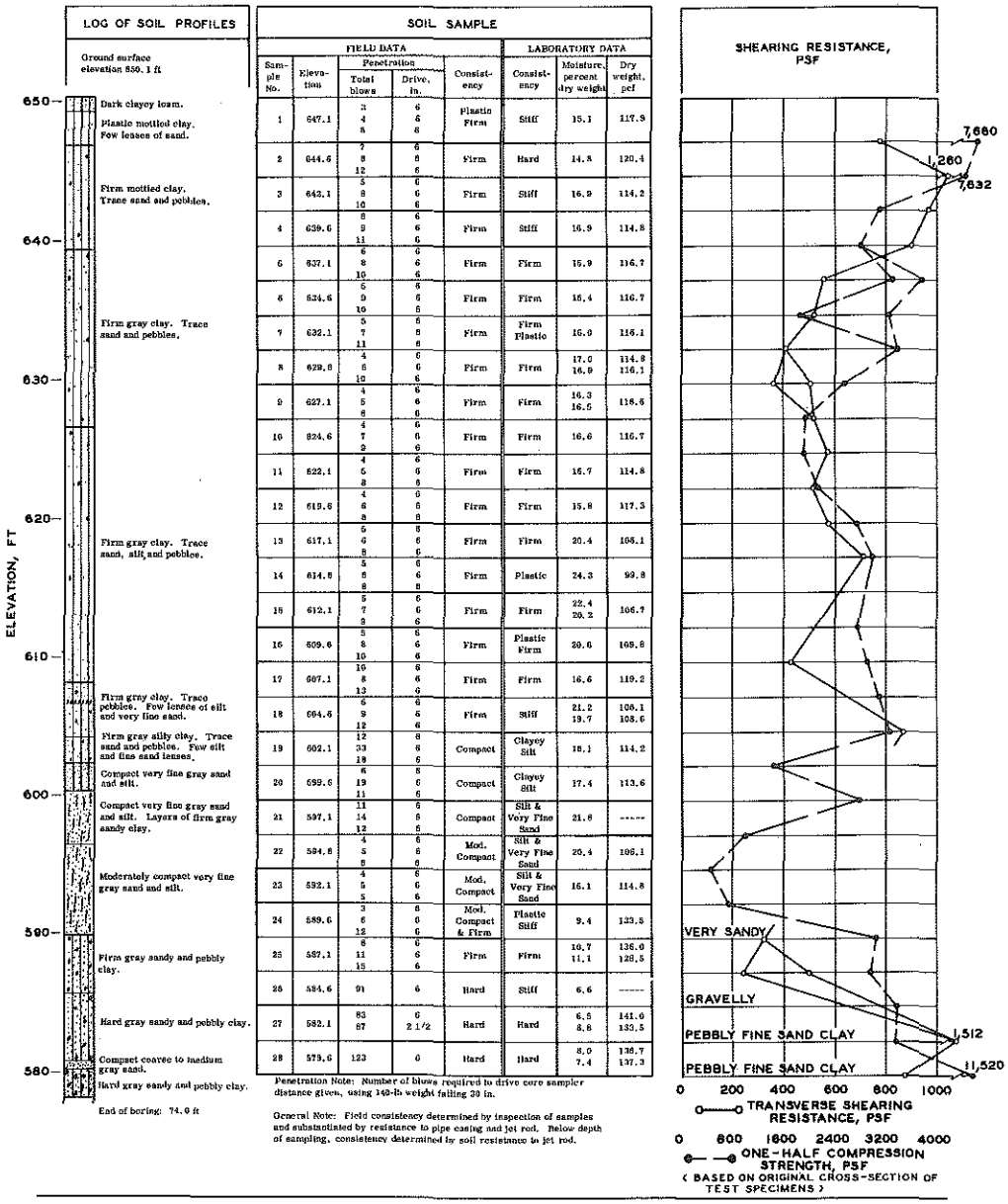

Figure 4. Belleville Boring No. 3 profile.

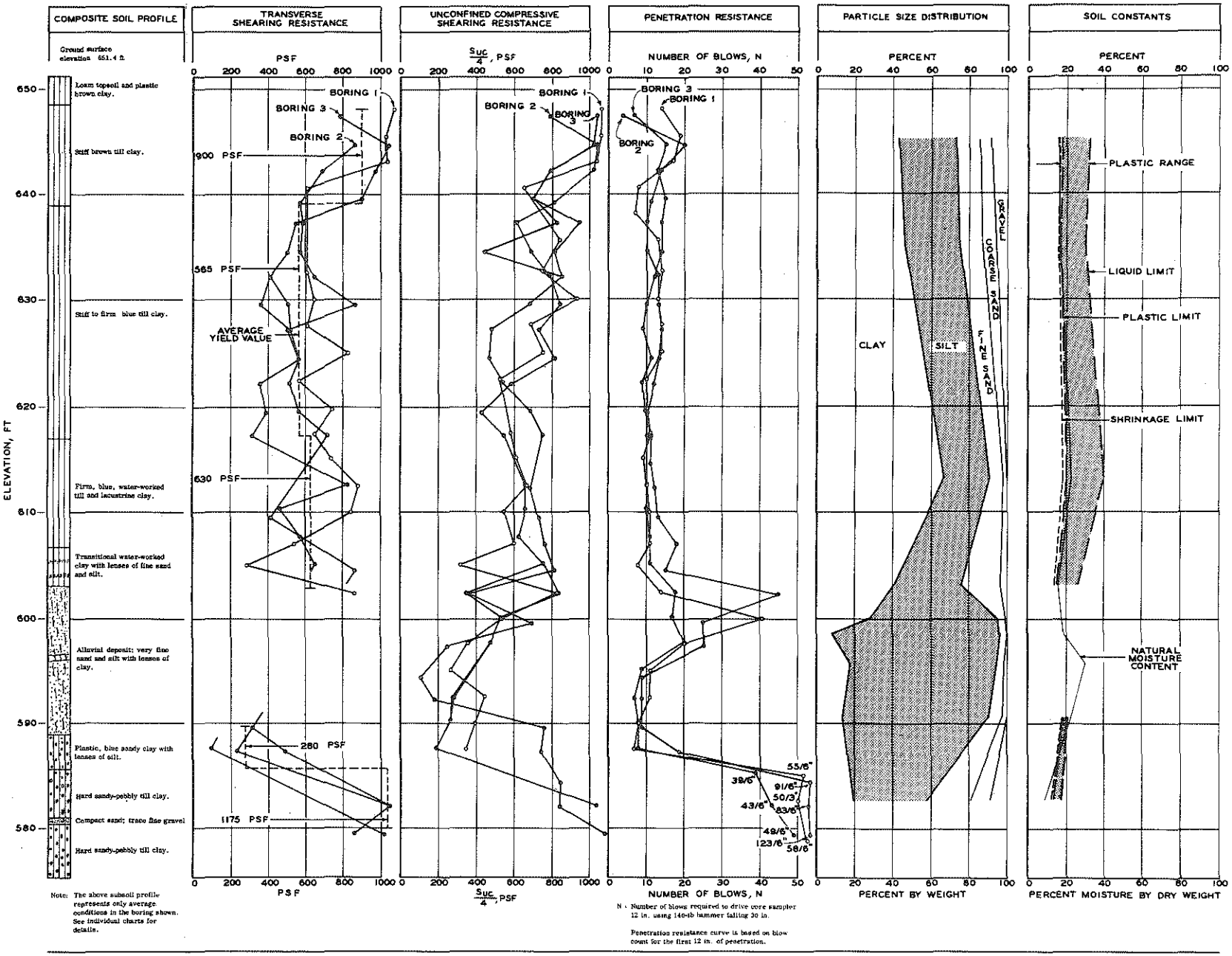

Figure 5. Belleville composite subsoil analysis (Borings No. 1, 2, 3).

Below the alluvial stratum is the basal formation of hard till clay of Pre-Wisconsin origin. This basal formation is almost level, varying approximately 1 ft over the test area. It is a sandy pebbly clay with very high density, high penetration resistance, and high shearing resistance. The appropriate engineering treatment would consider both granular and cohesive resistance properties.

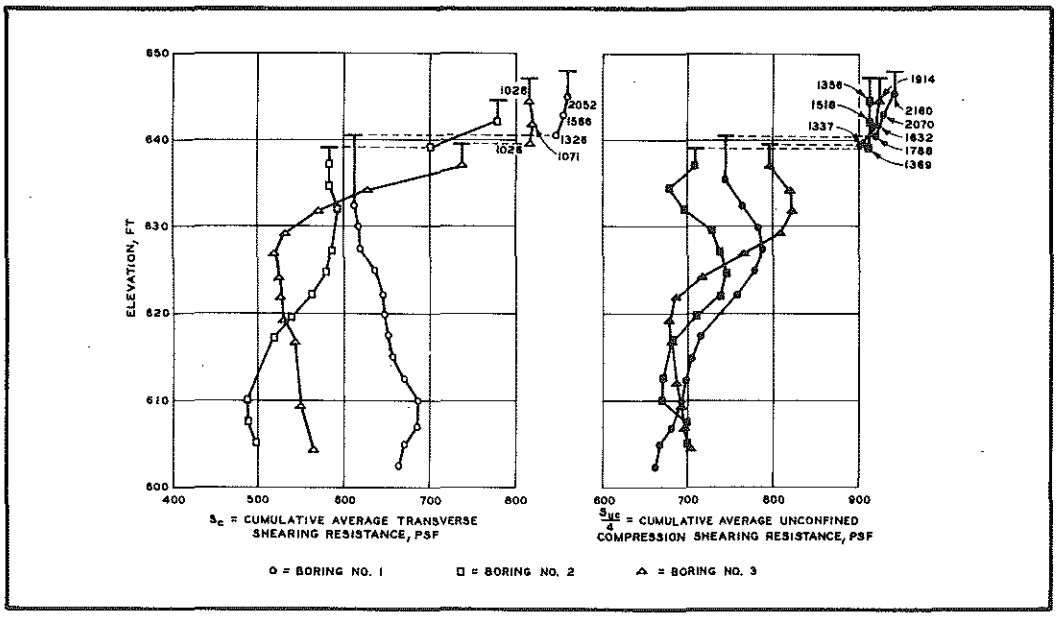

Figure 6. Cumulative average shearing resistance of Belleville Borings 1, 2, and 3.

Detroit Site (Soft Cohesive Subsoils)

Three borings were made at this site (Figs. 7, 8, 9, 10). Undisturbed samples were taken at 2.5-ft intervals, with the core sampling spoon, in the soft and plastic subsoils. Penetration resistance was measured independently with a split spoon sampler directly below the depth of each undisturbed sample. Boring information and laboratory test results compared well with 1942 boring information obtained for nearby structures.

The main subsoil feature is a 66-ft deposit of uniform soft clay of lacustrine origin with some evidence of waterworked till clays resulting from a re-advancing ice sheet. In terms of engineering properties, the soft clay soils are cohesive in character. Cumulative test results were

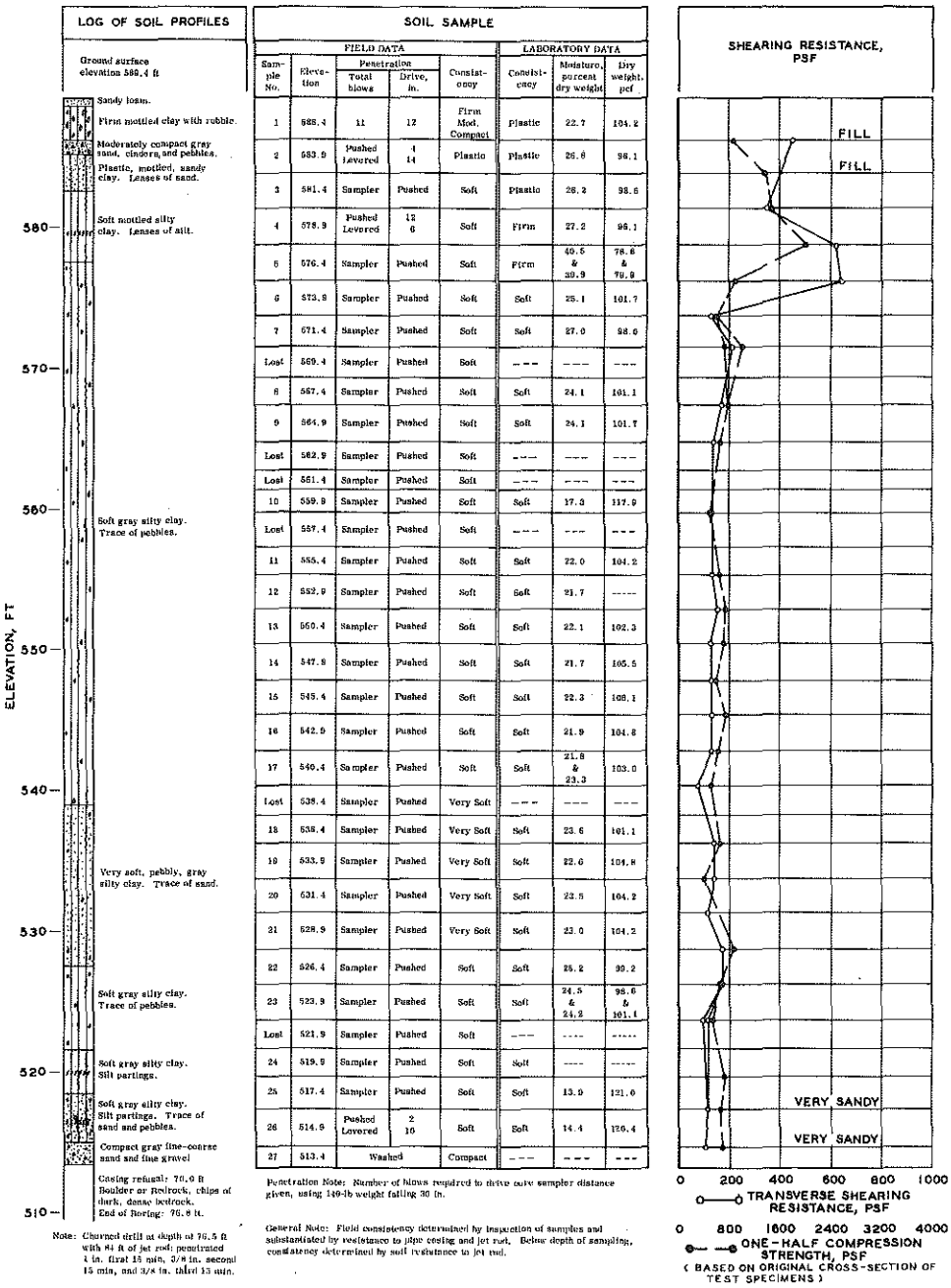

Figure 7. Detroit Boring No. 1 profile.

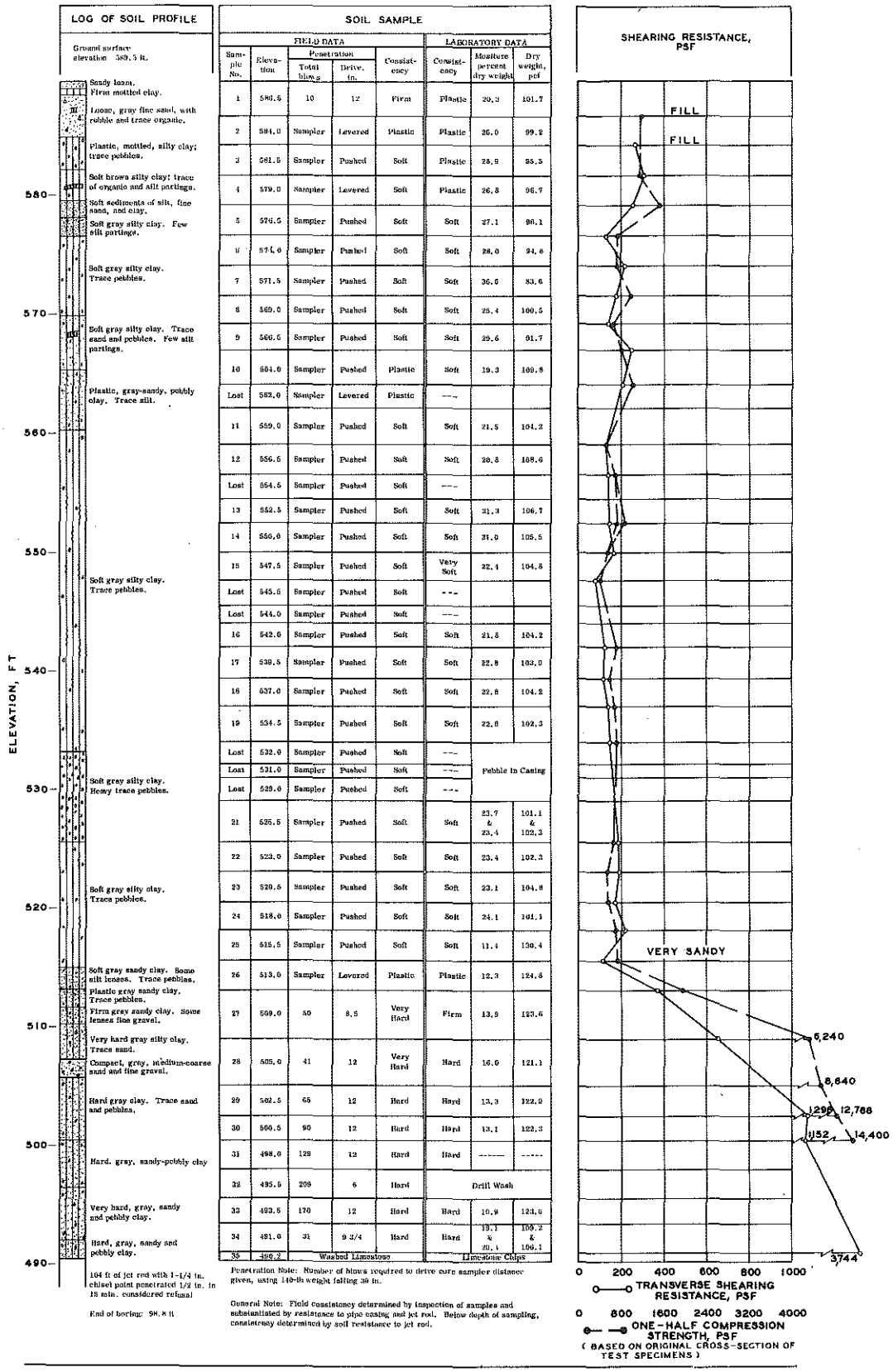

Figure 8. Detroit Boring No. 2 profile.

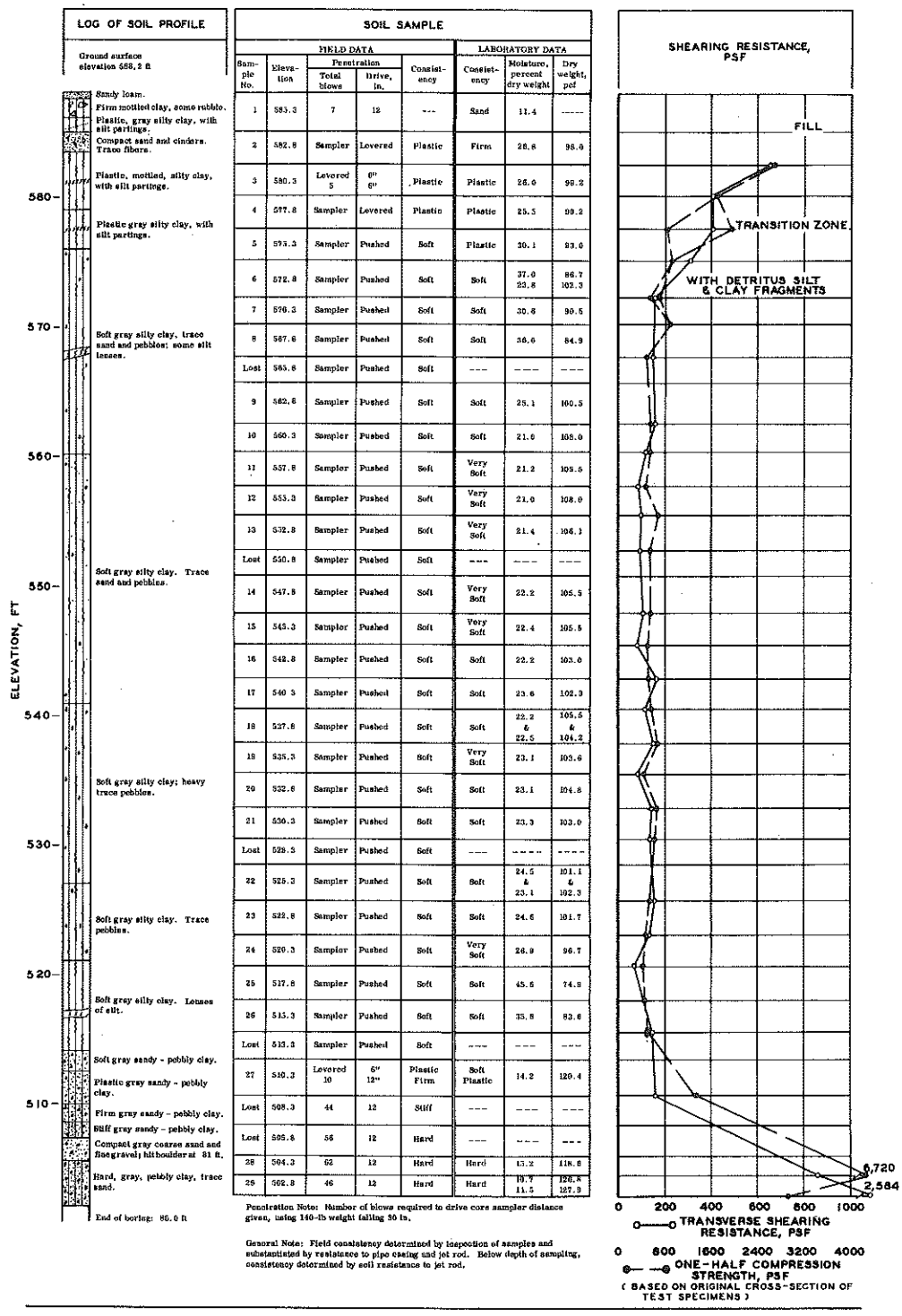

Figure 9. Detroit Boring No. 3 profile.

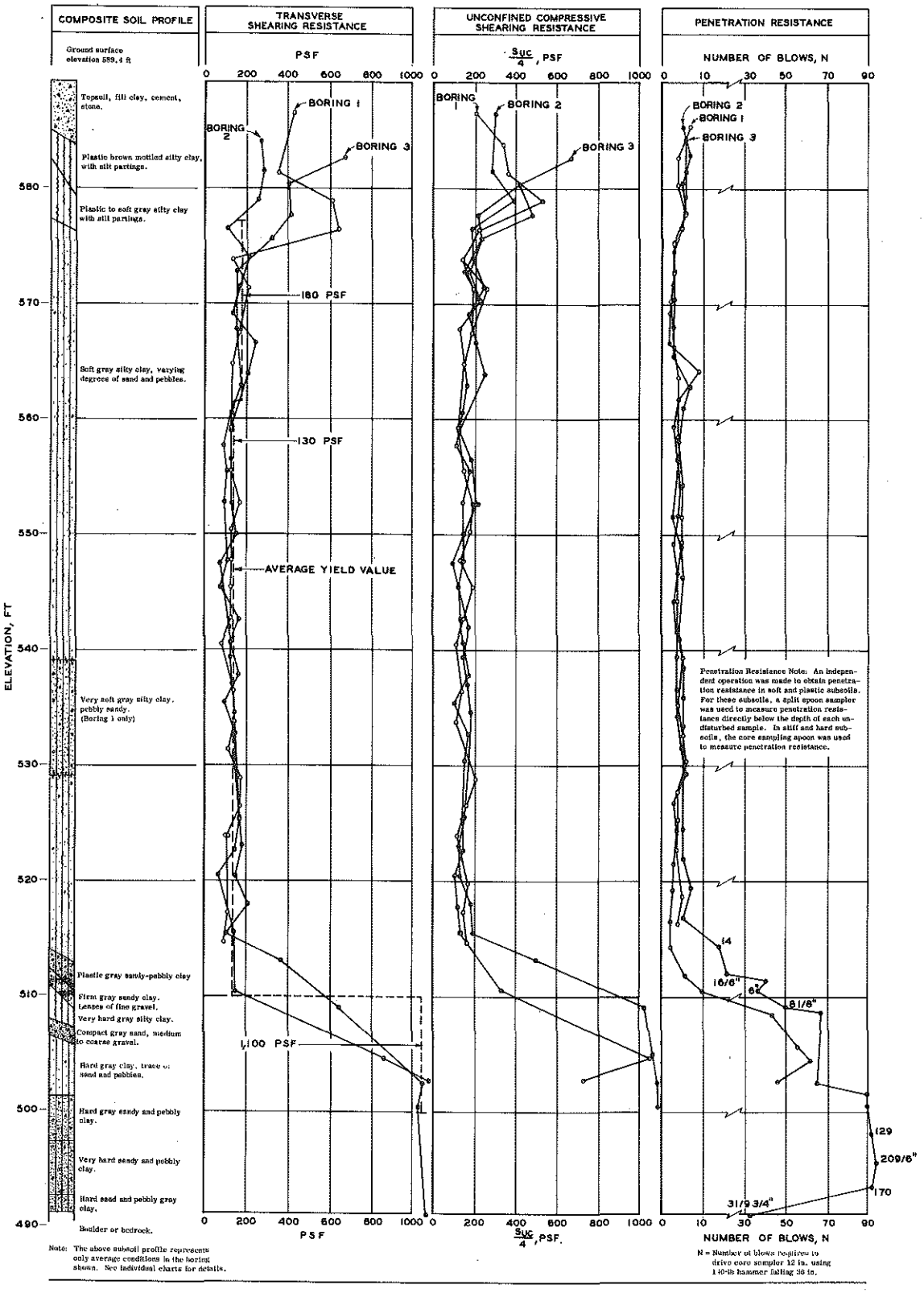

Figure 10. Detroit composite subsoil analysis (Borings No. 1, 2, 3).

plotted for this site (Fig. 11) in the same manner as for Belleville borings, and showed a notable uniformity of strength and of ratios between transverse and unconfined shearing resistance. These values, in turn, were used in computing side shear resistance for Detroit test piles (Chapter 11), and indicated consistent conditions across the site.

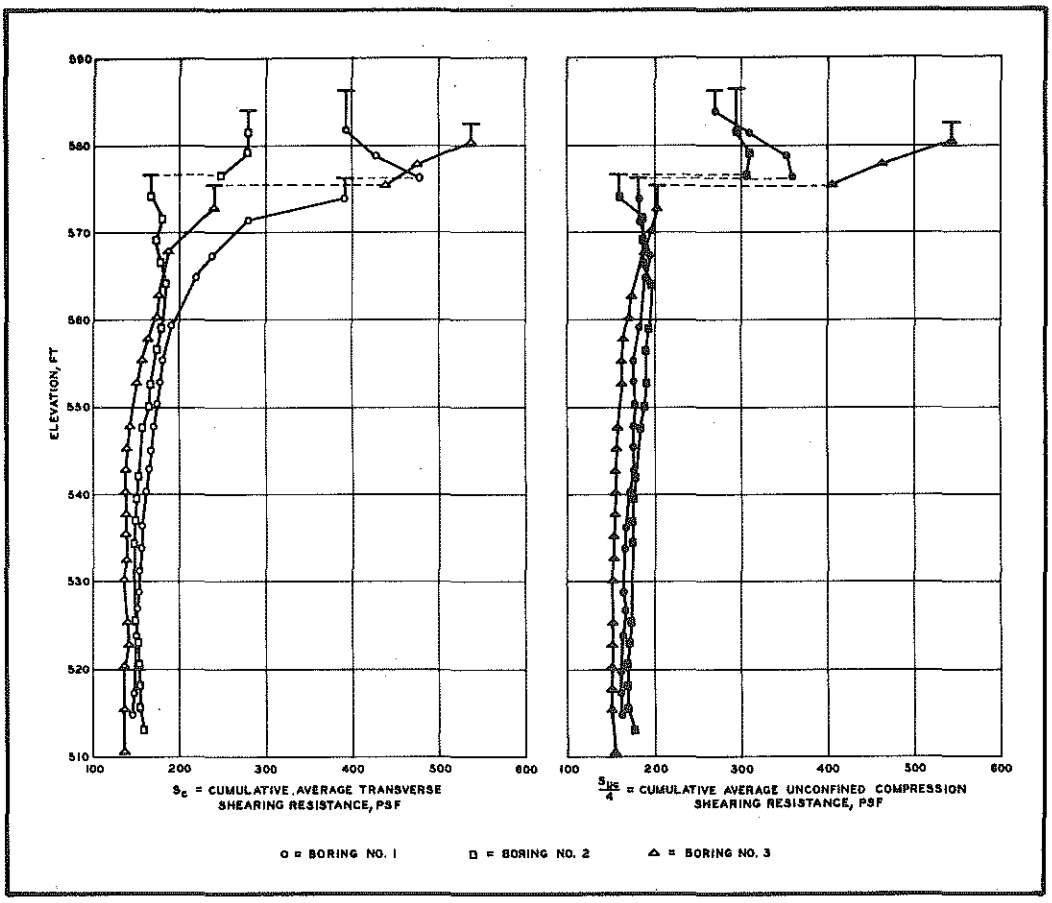

Figure 11. Cumulative average shearing resistance at Detroit Borings 1, 2, and 3.

The soft clay is underlaid by a hard, gray, sandy-pebbly till clay ("Detroit hardpan"). Boring 1 indicated the presence of boulders on the floor of the hard clay. In the bottom hard clays, undisturbed samples and penetration resistance tests were obtained simultaneously with the core sampling spoon.

Muskegon Site (Granular Subsoils)

Two borings were made to depths of 180 ft, with sampling and penetration tests performed at 5-ft intervals. The split spoon sampler was

used in the granular layers, and the core sampling spoon in the organic sediments and the deep plastic clays. Difficulty was encountered in obtaining penetration tests due to inflow of sand up into the casing. This was corrected by using the split spoon as a drilling tool to advance the hole and casing, instead of using the wedge-shaped chopping bit. Details of this operation appear in the boring profile charts in Figs. 12, 13, 14.

The test site was on a broad, filled-in drainageway. The test borings disclosed that the channel or valley was cut down by stream erosion to a depth of 181 ft below the existing surface. At this depth one boring showed a Pre-Wisconsin till clay, highly resistant to penetration.

Initial refilling began with a 7-ft basal deposit of compact coarse sand and fine gravel, which exhibited a very high penetration resistance. The next or second stage of filling is indicated by a 43-ft deposit of thinly laminated lacustrine clay. The third stage of filling is a 24-ft accumulation of an alluvial deposit formed in shallow water. This deposit appears to be formed of numerous thin layers of sand interbedded with wood and bark particles, and some thin layers of peat, marl, and peaty clay. The physical properties of the third-stage material are considered granular in character. Experience during test pile driving indicated that the high-resistance sand layers vary considerably in elevation and thickness within this third stage of filling.

The fourth stage of filling is 45 ft of a semi-organic sedimentary deposit, believed to have been formed during various stages of inundation and ponding. The first accumulation consists of sediments of organic silty clays with thin lenses of sand and a trace of marl. This texture changes, from the center to the top of this deposit, to a higher organic content and includes more frequent layers of fine sand. It is believed that enough organic material is present in the deposit to affect its engineering properties, and that some allowance also must be made for the intrabedded granular material. However, the total deposit is considered compressible and cohesive in behavior.

A special study was made of the material in this fourth-stage semi-organic subsoil formation (-60 to -108 ft). Mechanical analysis of seven representative samples showed average results grouped by the following particle size ranges: 30-percent clay, 55-percent silt, and 15-percent sand. It should be pointed out that these sizes contain both mineral and organic particles. The average liquid limit is 48 percent and the average plasticity index is 4, indicating an organic silty clay material. The loss on ignition of the material is approximately 21 percent by weight, and the

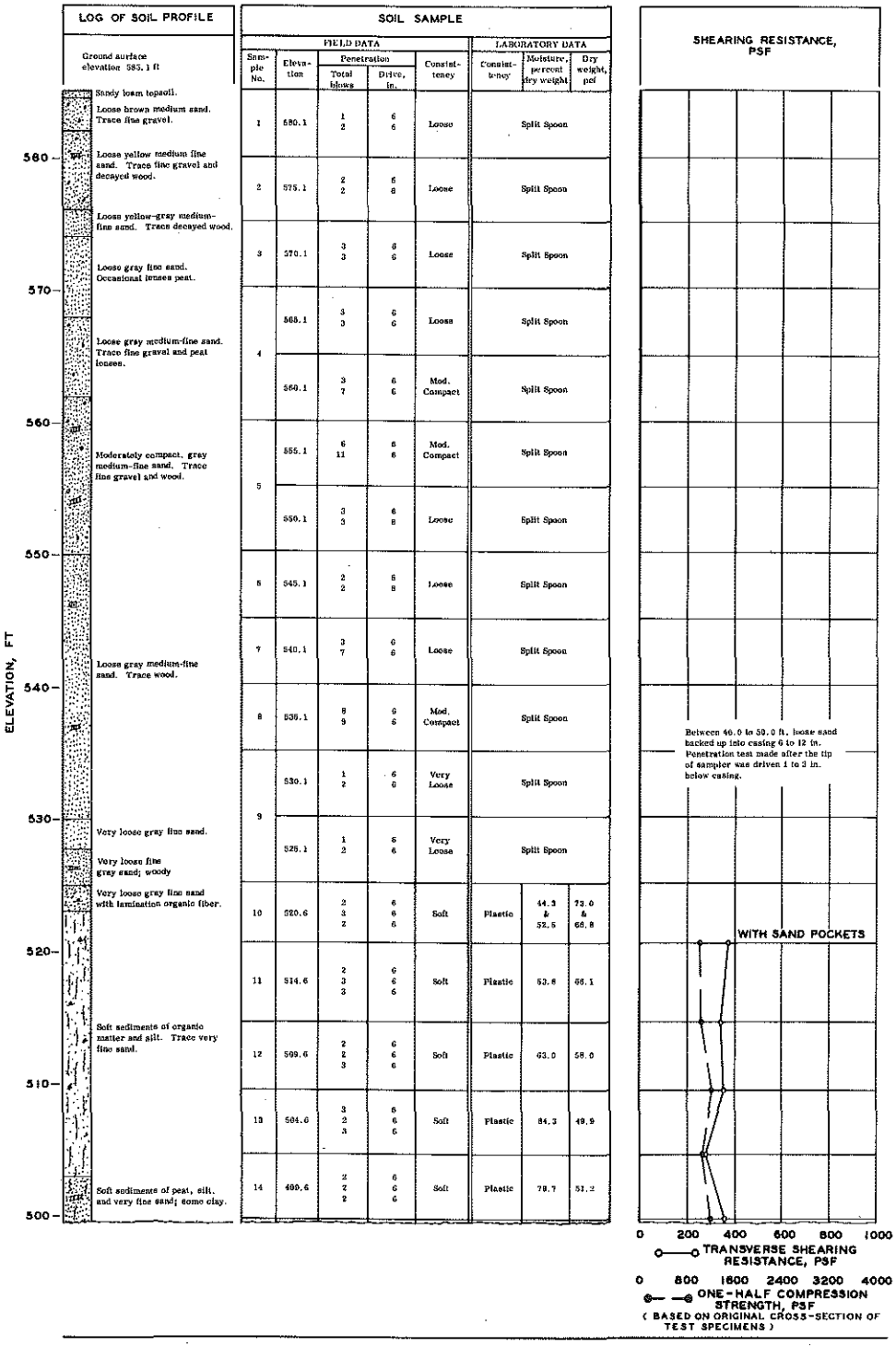

Figure 12. Muskegon Boring No. 1 profile.

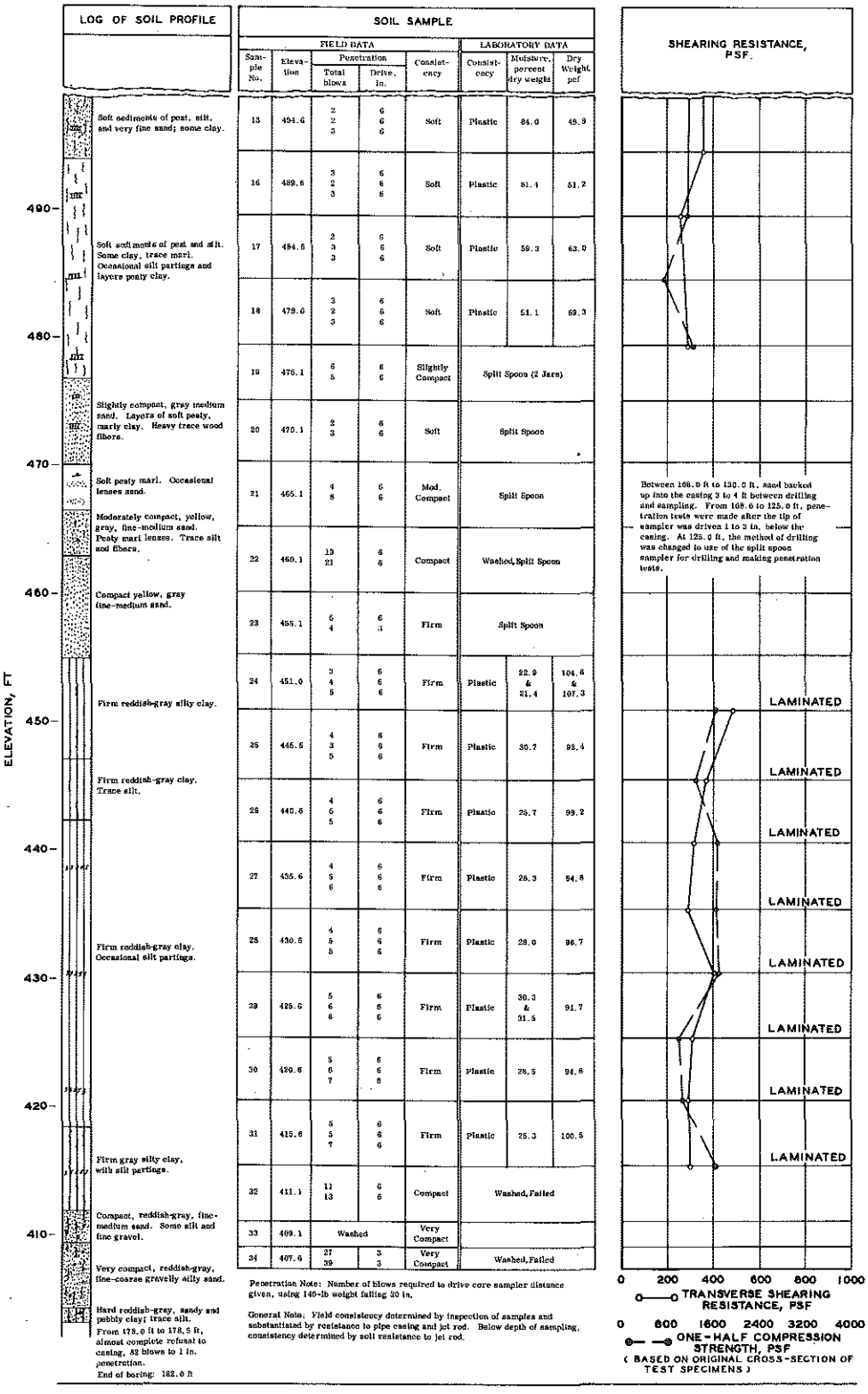

Figure 12 (Cont.). Muskegon Boring No. 1 profile.

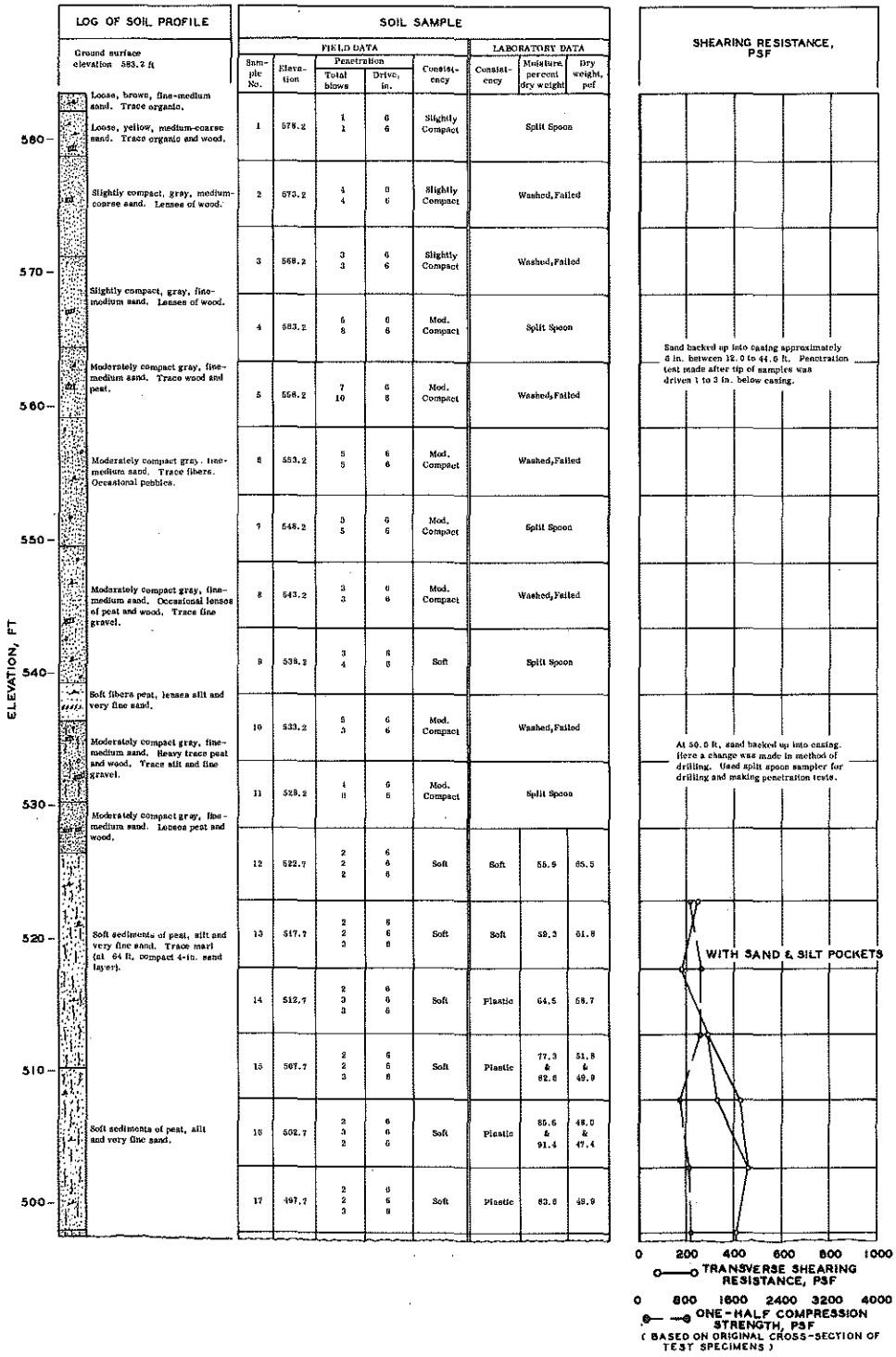

Figure 13. Muskegon Boring No. 2 profile.

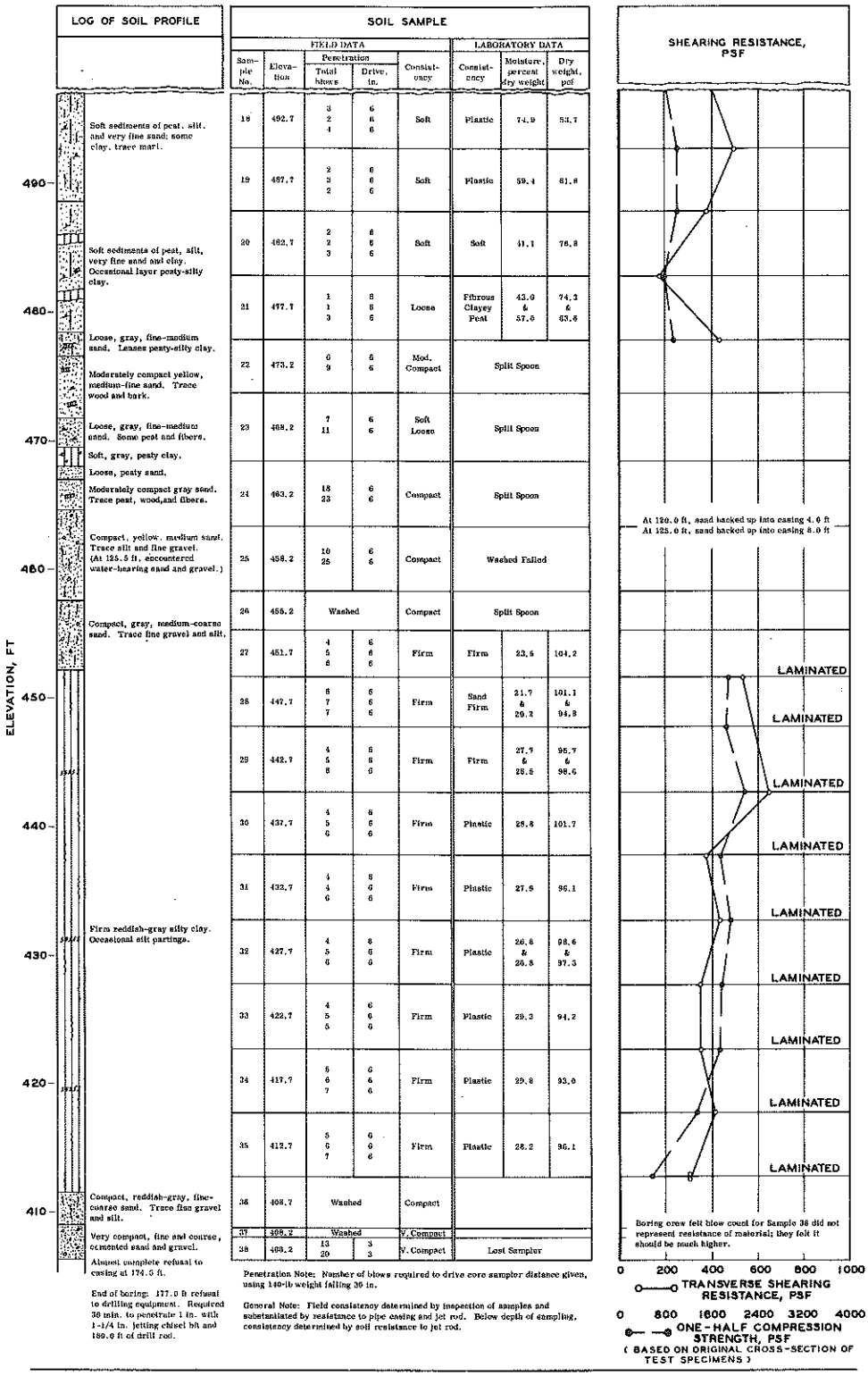

Figure 13 (Cont.). Muskegon Boring No. 2 profile.

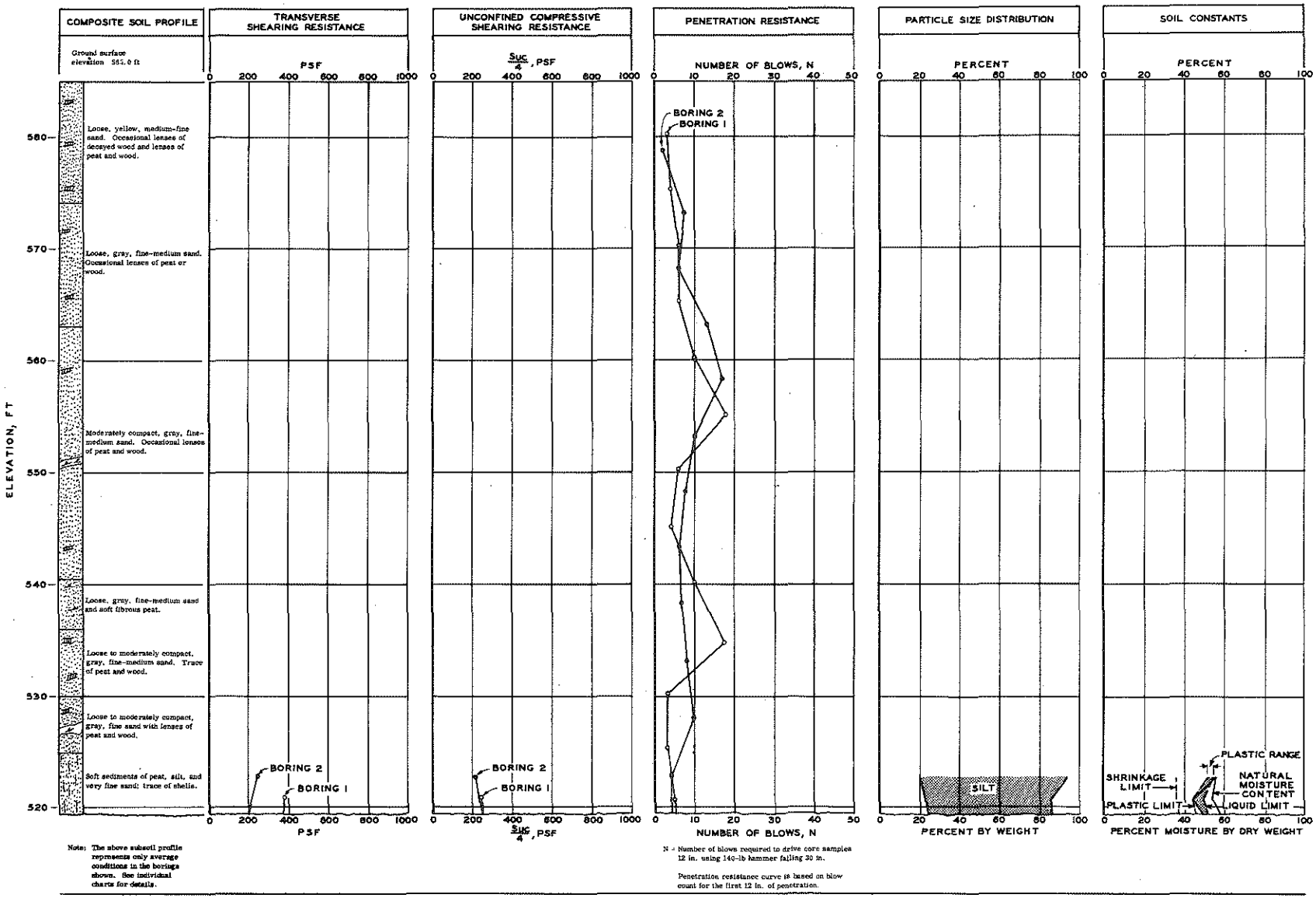

Figure 14. Muskegon composite subsoil analysis (Borings No. 1 and 2).

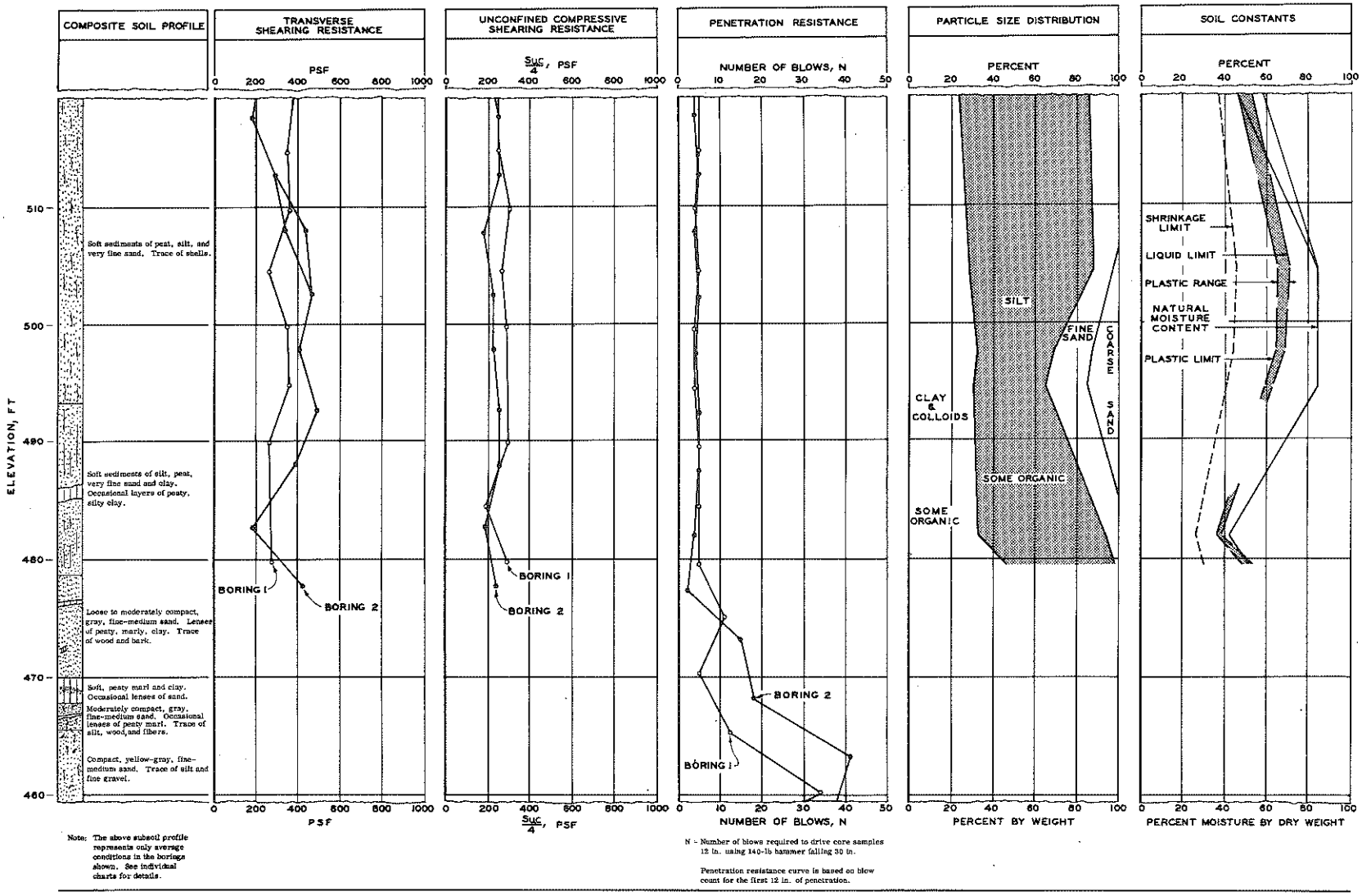

Figure 14 (Cont.). Muskegon composite subsoil analysis (Borings No. 1 and 2).

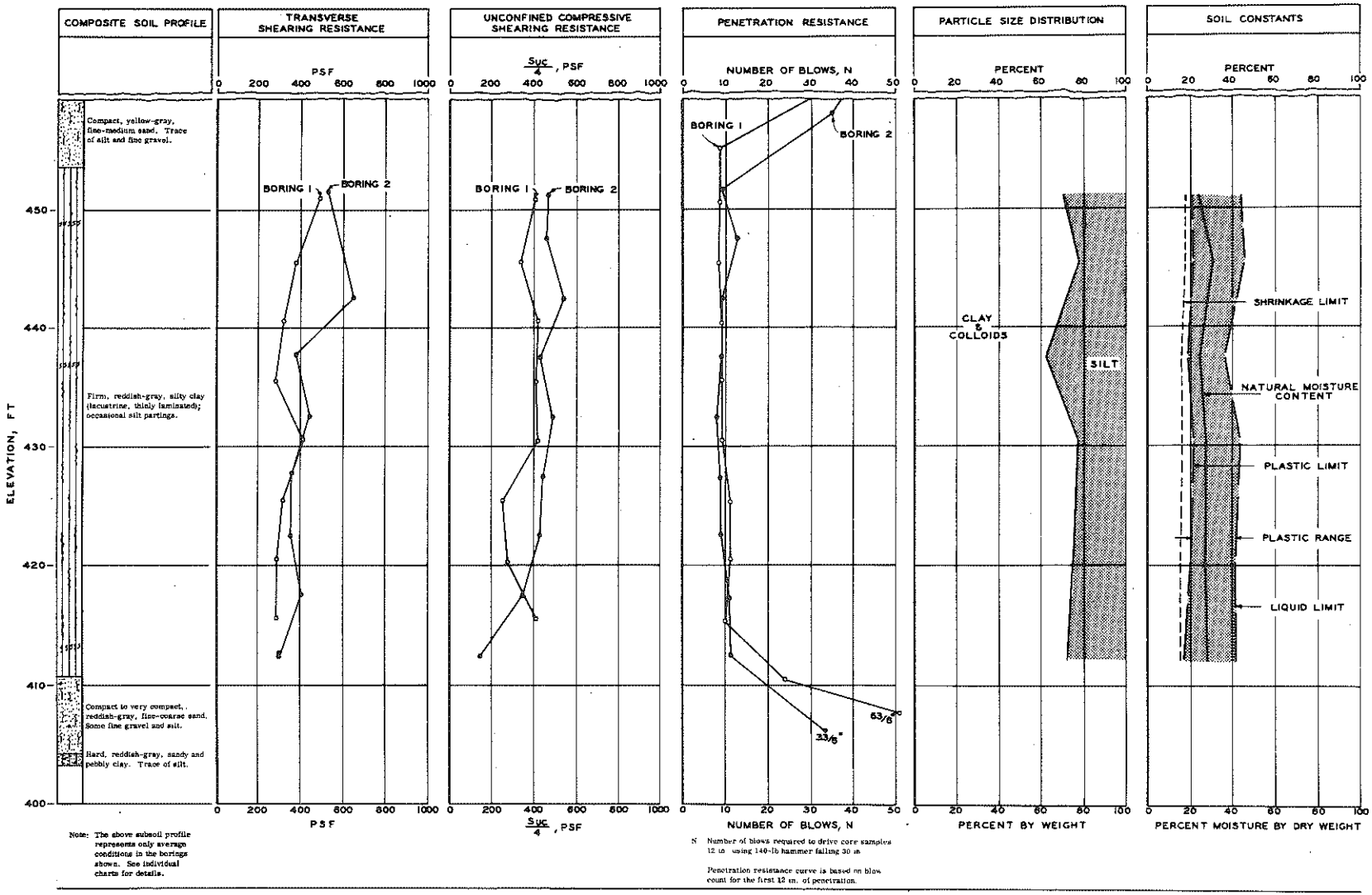

Figure 14 (Cont.). Muskegon composite subsoil analysis (Borings No. 1 and 2).

organic content ranges by weight from 5 to 12 percent. Study of the volumetric proportions of mineral solids, organic content, calcium carbonate content, and water content (Fig. 15) showed that the combined calcium carbonate and organic contents were generally greater than 20 percent. This index definitely indicates that the material is highly organic.

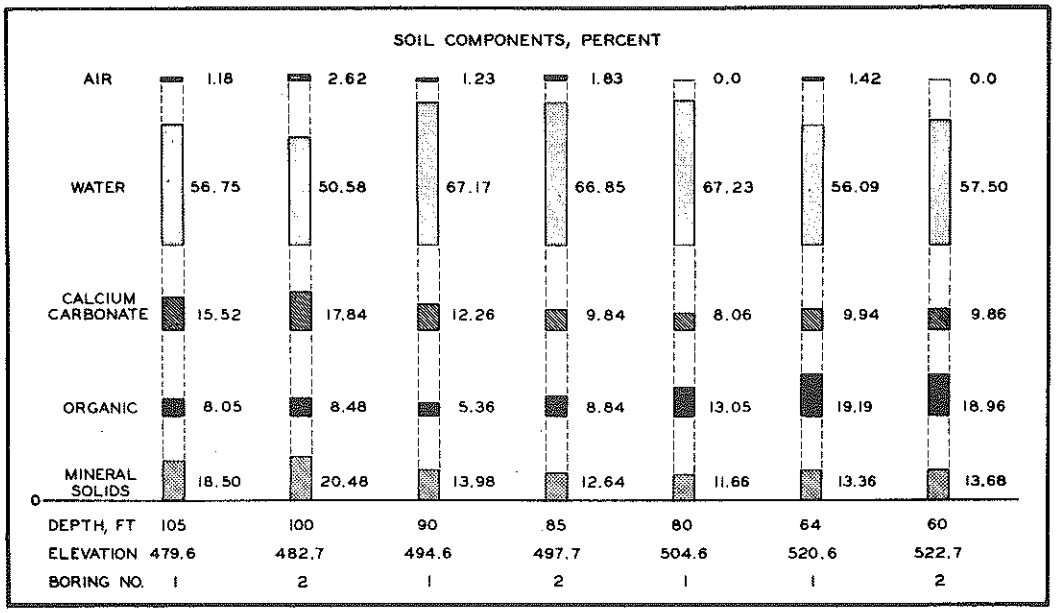

Figure 15. Volumetric analysis of semi-organic sedimentary deposit (Muskegon).

The fifth stage of filling extends to the surface, and is approximately 60 ft of recent alluvial accumulation of loose sand. It contains wood and bark particles, and a continuous irregular pattern of thin lenses of peat. From the standpoint of soil engineering evaluation, the physical properties of this deposit may be considered granular. The existing surface is wet and subject to flooding, and organic materials, such as muck and peat, are forming under this environment.

Boring data for this site were also evaluated in terms of side shear capacity, but due to the greater complexity of the granular and cohesive deposits encountered, several other factors had to be considered. This analysis is discussed in Chapter 11.

The location for actual pile driving was moved 75 ft west of Boring 2 after completion of the boring investigation because of possible interference with construction of the northbound bridge structure crossing the north channel of the Muskegon River on the US 31 relocation. A study of nearby structural foundation borings indicated that Test Borings 1 and 2 are representative of subsoil conditions at the relocated test site.

CHAPTER TWO

TEST HAMMERS AND PILES

The history of pile driving hammers starts with the drop hammer, which essentially involves raising a given mass by mechanical means to a predetermined height and then releasing the mass, allowing it to fall by gravity.

With the advent of air and steam power, more sophisticated mechanisms were developed to speed up pile driving operations. The first was the single-acting hammer in which steam or air pressure raises the ram, which then falls by gravity. This modification allows the hammer manufacturer to increase the striking repetitions considerably, shorten the stroke, and still retain a heavyweight ram if desired.

From the basic single-acting hammer evolved the faster double- and differential-acting hammers. The double-acting hammer is constructed with two separate steam chests, one above and one below a single piston. This construction allows the upper chest to be exhausted while steam pressure in the lower raises the ram; similarly, the lower chest is exhausted while steam pressure in the upper chest drives the ram downward.

The differential-acting hammer is essentially the same as the double-acting in construction, except that a small piston is connected to the piston rod at the bottom of the lower chest. Raising the ram is effected by steam or air maintained at constant pressure in the lower chest, between the large and small piston, during the complete operating cycle of the hammer. During the upstroke the upper chest is exhausted, while on the downstroke the steam or air in the lower chest is also applied to the upper chest above the large piston, assisting the force of gravity in accelerating the ram downward. Net downward force, due to the pressure, is equal to applied pressure times the effective area of the smaller piston.

For the double- and differential-acting hammers, the additional kinetic energy which can be developed by air or steam pressure acting on the hammer is generally limited to the product of the hammer jacket dead

weight and stroke of the ram. Some manufacturers recognize the development of additional energy from upward acceleration of the hammer jacket dead weight before impact. The main difference between these two types of hammer action is that in the double-acting the two steam chests are independent and act on the same piston, while in the differential-acting they are interdependent and act on different piston areas. This energy increment (contributed by air or steam pressure), added to that resulting from the free fall of the ram, makes up the total kinetic energy available. It can be shown that the operating characteristics of a hammer may be varied by varying the ratio of ram weight to hammer jacket dead weight and the height of ram rise. In the differential-acting hammers, the weight ratio can be adjusted, since the lifting area under the piston is independent of the downward thrusting area above the piston. This adaptation allows the manufacturer to design a hammer with a heavy ram and light dead weight components, resulting in a desirable total weight.

Diesel hammers in general use are of two types: open-top and closed-top cylinder. The work cycle of the open-top type starts with raising of the piston (ram) by means of a lifting cable attached to a tripping device. At a predetermined height the piston is released and falls due to gravity, activating a fuel pump cam which deposits a gaged amount of fuel into the cup of the anvil block. The piston continues falling, compressing the air beneath, which pre-loads the anvil block and seats it firmly on the driving cap and subsequently on the pile. Upon impact, the piston drives the anvil block downward and also ignites the fuel. The expanding gases add to the downward movement of the anvil and start the piston moving upward until it is arrested by gravity, and the cycle starts again.

The closed-top cylinder is a modification of the open-top, having a sealed pressure chamber above the piston. This bounce chamber assists in arresting the piston on the upward stroke by compressing the air in the chamber. At the point of maximum upstroke, the piston starts its downstroke and is accelerated by gravity and expansion of the compressed air in the bounce chamber. With this modification, hammer speed is increased by shortening the ram stroke while maintaining energy output equivalent to a longer stroke.

In a normal field driving situation all hammers deliver kinetic energy to a cushion assembly which is normally set in the top of a driving cap. The bottom surface of the driving cap is so constructed as to fit the piles to be driven. The mechanical purpose of the cushion and driving cap assembly is to reduce impact stresses so that they will not damage the pile top or the hammer mechanism.

TEST HAMMERS

The steam and air hammers used in the project were selected on the basis of their long use in field construction; familiarity with their characteristics facilitated their comparison with products of three major producers of diesel hammers. It should be borne in mind that throughout this report the hammers described are those furnished for testing in 1961-62 (Table 1). Some models currently available may have been altered by manufacturers' improvements or modifications since the testing reported here. Cushion block and cap assemblies used in the project were those recommended by the manufacturers.

Air and Steam Hammers

In the current project, one single-acting air hammer and three differential-acting steam hammers were used: the Vulcan No. 1, Vulcan 50C, Vulcan 80C, and Raymond 15-M (Figs. 16, 17, 18). Their specific ram weights, total weights, and rated energies may be compared in Table 1.

The single-acting Vulcan No. 1 (Fig. 16) was activated by two 600-cfm mobile air compressors, raising the ram a total of 36 in. before release, and creating a theoretical gross striking energy at the point of impact of 15,000 ft-lb. The point of impact was the top of an oak block placed on top of two steel plates, held by a plain driving cap. At maximum efficiency, the energy cycle repeats 60 times each minute, with net striking energy averaging about 85 percent of gross striking energy (manufacturer's estimate), due to such losses occurring within the hammer as back pressure, pre-admission, and friction.

The differential-acting, steam-powered Vulcan 50C and 80C hammers (Fig. 17) are similar in design, the latter being a larger version of the former. The same concept of heavy ram design is used for these hammers as for the Vulcan No. 1, and the manufacturer estimates about the same maximum efficiency (84 percent of rated energy) due to internal mechanical losses. In addition, the differential-acting hammers have a higher frequency of blows which is desirable to increase the pile penetration rate. There is an additional advantage to increasing the blows per minute; in some soils the resistance to driving decreases due to momentary releases of the frictional grip of soil around the pile. For this project, the ram of these hammers struck directly on a cushion composed of phenol fiber blocks.

TABLE 1
SUMMARY OF PILE HAMMER CHARACTERISTICS
Based on Manufacturers' Specifications

	Characteristic	Vulcan No. 1	Raymond 15-M*	Vulcan		Link-Belt		McKiernan-Terry		Delmag	
				50C	80C	312	520	DE-30	DE-40	D-12	D-22
OPERATION	Manufacturer's Rated Energy Output per Blow	15,000 ft-lb	15,000 ft-lb	15,100 ft-lb	24,450 ft-lb	15,000 ft-lb[e] 18,000 ft-lb (max)[f]	26,300 ft-lb[e] 30,000 ft-lb (max)[f]	16,800 ft-lb (mean) 22,400 ft-lb (max)	24,000 ft-lb (mean) 32,000 ft-lb (max)	22,500 ft-lb	39,700 ft-lb
	Power Source	Air	Steam[a][b]	Steam[c]	Steam[d]	Diesel		Diesel		Diesel	
	Type of Action	Single	Differential	Differential		Modified Single		Single		Single	
	Manufacturer's Rated Operating Speed (blows per minute)	60[g]	75 to 90	120[g]	111[g]	100 to 105	80 to 84	48 to 52		42 to 60	
	Stroke	36 in. (normal)	18 in. (normal) 36 in. (equiv.)	15.5 in. (normal) 36.1 in. (equiv.)	16.5 in. (normal) 36.6 in. (equiv.)	30.89 in. (max.) 46.41 in. (equiv.)	43.17 in. (max.) 62.19 in. (equiv.)	72 in. (avg.) 96 in. (max.)		72 in. (avg.) 102 in. (max.)	
WEIGHTS AND CUSHIONS	Hammer Weight Including	9,700 lb (net, with standard base)	10,305 lb[h] (less core)	11,782 lb (net, with standard base)	17,885 lb	10,375 lb (net, with standard anvil)	12,245 lb	8,125 lb (net)	9,900 lb (net)	5,512 lb (net)	10,055 (net)
	Ram	5,000 lb	5,000 lb	5,000 lb	8,000 lb	3,855 lb (net, piston)	5,070 lb (net, piston)	2,800 lb (piston)	4,000 lb (piston)	2,750 lb (piston)	4,850 lb (piston)
	Anvil	---	---	---	---	1,188 lb	1,179 lb	774 lb	1,350 lb	754 lb	1,147 lb
	Cushion Type Used for This Study	Oak block 11-1/4-in. diam by 6-1/4-in. thick, on top of two steel plates, each 11-1/4-in. diam by 3/4-in. thick; total thickness: 7-3/4 in.	Alternating layers of eleven micarta fiber plates 11-in. diam by 1-in. thick with eleven plates 11-in. diam by 1-in. thick sandwiched between two steel plates 11-in. diam by 4-5/8-in. thick; total thickness: 31-1/4-in.	50C: Two phenol fiber blocks 11-3/8-in. diam, one 5-in. thick, the other 3-in. thick; total thickness: 8 in. 80C: Two phenol fiber blocks, each 14-in. diam by 5-in. thick; total thickness: 10 in.		Alternating layers of five phenol fiber plates 11-in. diam by 1/2-in. thick with four aluminum plates 11-in. diam by 1/8-in. thick; total thickness: 3 in.		DE-30: Oak block 18-1/2-in. diam by 2-1/4-in. thick. DE-40: Oak block 18-1/2-in. diam by 2-1/4-in. thick, plus an adapter cushion of two plywood plates 23-1/4-in. diam, one 3/4-in. thick, the other 1-1/4-in. thick; total thickness of adapter: 2 in.		Steel block 15 in. by 15 in. by 3 in. thick on top of sectioned block of German oak 15 in. by 15 in. by 5 in. thick; total thickness: 8 in.	
	Weight of Plain Driving Cap and Cushion Assembly[i]	1,000 lb	---	1,000 lb	2,140 lb	1,381 lb		1,400 lb (driving cap only)	2,900 lb (1,400-lb driving cap plus 1,500-lb adapter cap)	1,100 lb	1,463 lb
	Manufacturer's Information Bulletin	68H	---	70G		2852B (Sep. '59)		674		ZRE/SCM-D-26	

* Internal Mandrel Hammer
(a) Belleville: 150-hp horizontal boiler (ASME rating)
(b) Muskegon: 100-hp vertical boiler
(c) 150-hp horizontal boiler (ASME rating)
(d) 100-hp vertical boiler
(e) Maximum equivalent WH (gage)
(f) Manufacturer's performance rating
(g) At zero set, normal stroke, and specified pressure
(h) Plus 10,780 lb for 64-ft mandrel (core)
(i) Weight not included in hammer-and-component weight given above

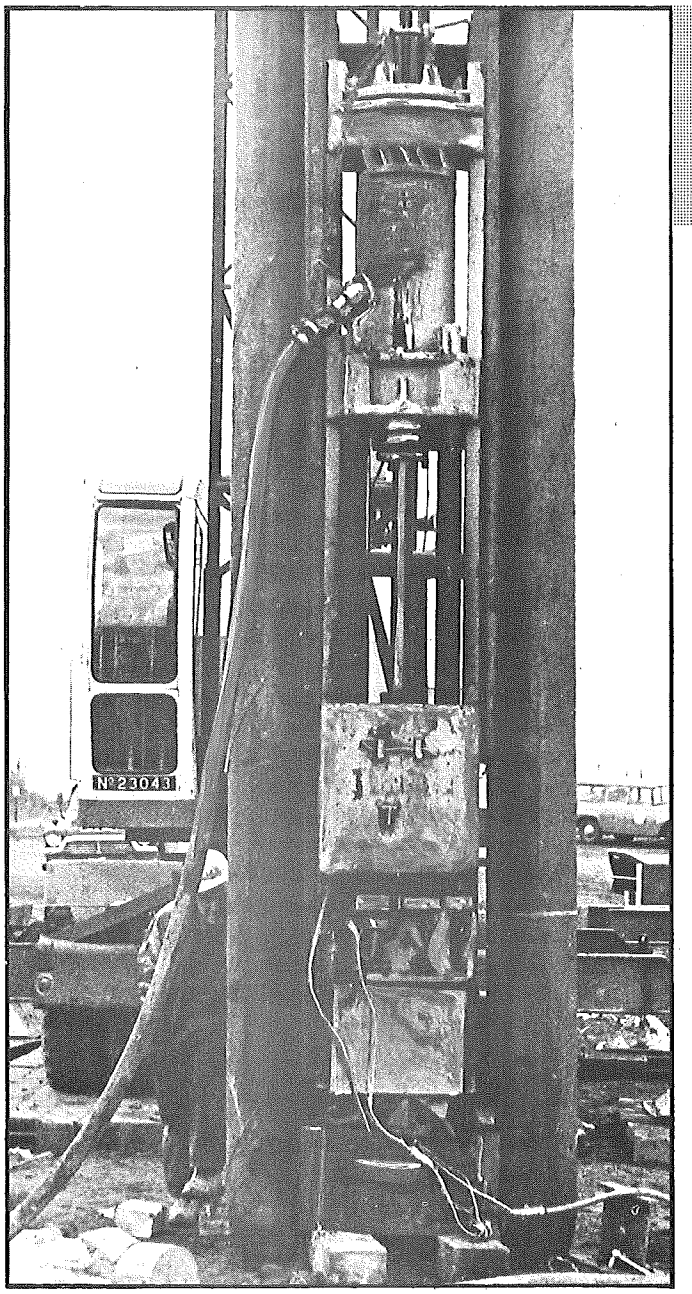

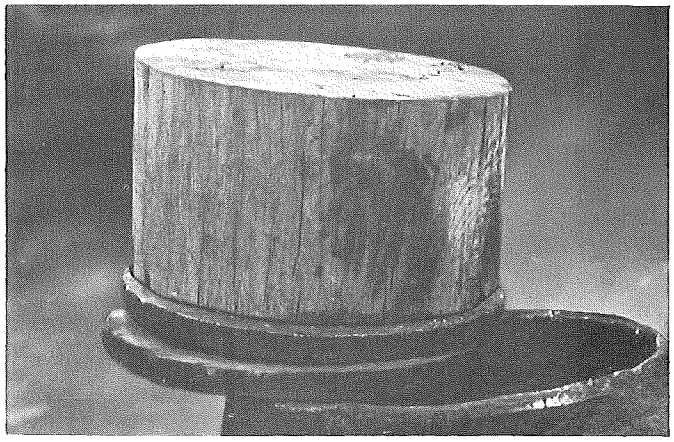

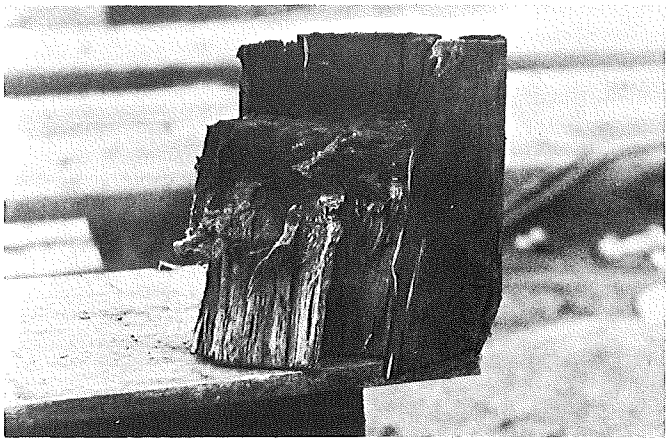

Figure 16. Single-acting, air-activated Vulcan No. 1. Cushion assembly is shown at lower left before driving (oak block resting on steel plates), and a typical block after hard driving at lower right (note area compressed by ram blows at center of block). Block at right was split during extraction from driving cap.

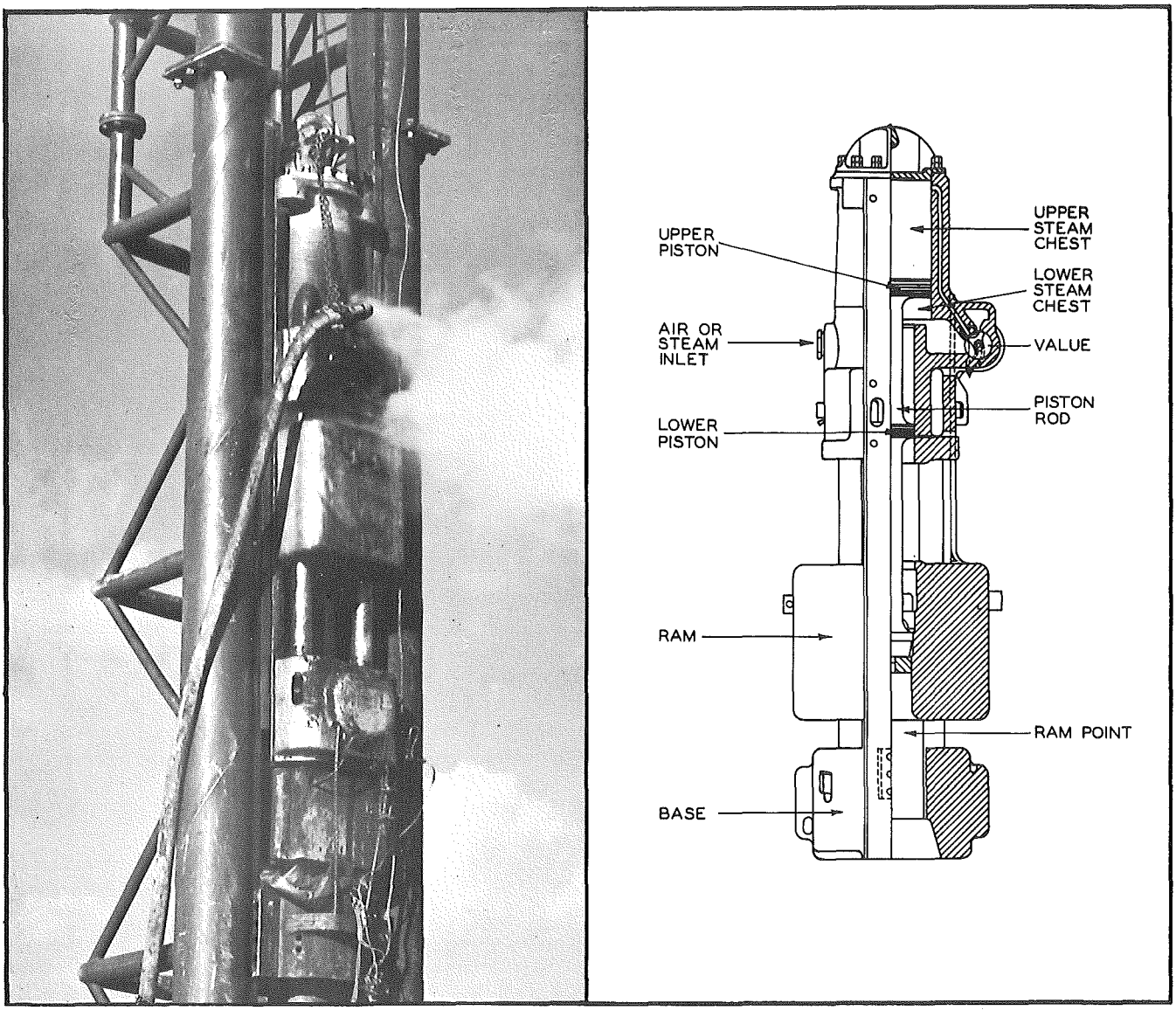

Figure 17. Differential-acting, steam-activated Vulcans 50C and 80C. Phenol fiber upper cushion block is shown at lower left before driving, resting on rim of driving cap. At lower right, after hard driving, the lower block is partially burnt within driving cap, while the bottom of the upper block exhibits crumpling and partial burning.

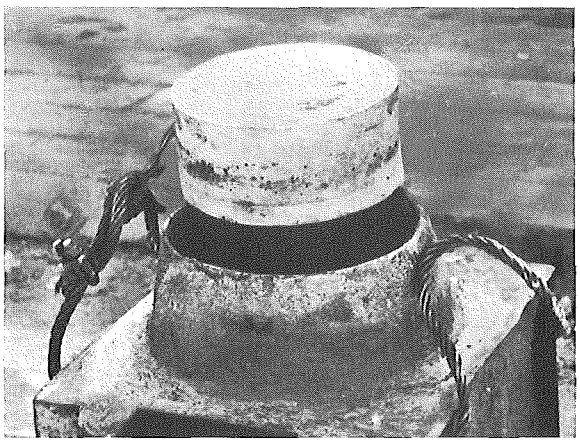

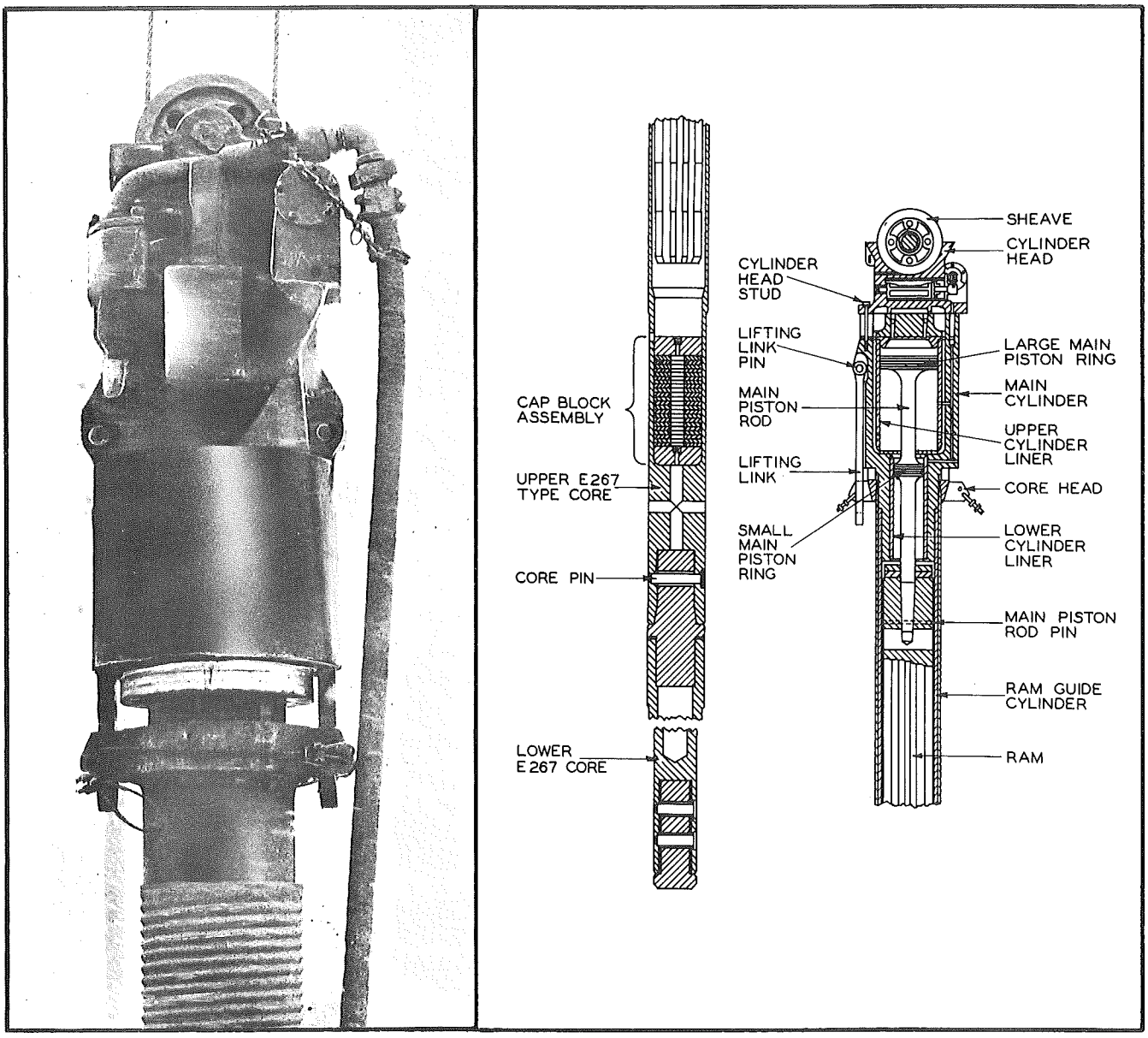

Figure 18. Differential-acting, steam-activated Raymond 15-M (internal hammer). Mandrel is shown at lower left prior to assembly, and cushion component at lower right.

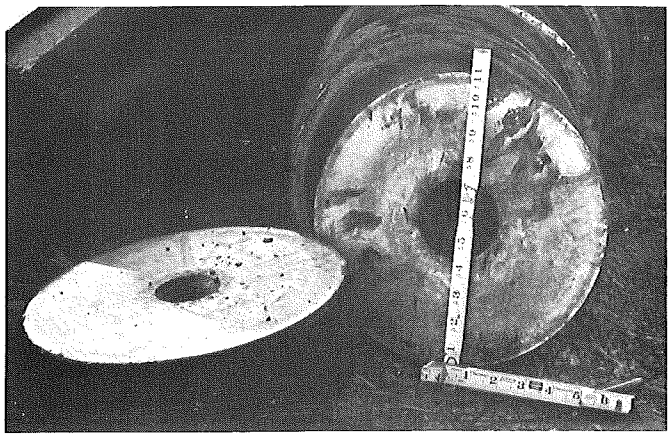

In addition to the Vulcan 50C and 80C, a third steam hammer, the Raymond 15-M, was used in driving two piles, and is essentially a modification of the 50C. The main difference is the long, narrow Raymond ram (Fig. 18) adaptable for use with a mandrel (core). The mandrel hammer provides for direct transfer of energy to the tip of the pile and intermediate "driving rings." Thus, the pile shell is actually pulled into the soil. In this case the cushion consisted of an alternating series of phenol fiber plates and aluminum heat dissipator plates, sandwiched between two steel blocks.

Diesel Hammers

In addition to the air and steam hammers, four single-acting diesels and two modified single-acting diesels were supplied by their manufacturers: the Delmag D-12 and D-22, the McKiernan-Terry DE-30 and DE-40, and the Link-Belt 312 and 520 (Figs. 19, 20, 21). Their specific ram weights, total weights, and rated energies may be compared in Table 1.

Two open-top Delmag hammers (Fig. 19) were supplied, the D-12 and D-22, similar in design except that the D-22 is heavier and has a greater rated energy. The hammers are so designed that the overall weight of the D-12 is less than any of the three Vulcan hammers and the weight of the D-22 is less than the Vulcan 50C or 80C. The manufacturer achieves this relatively light weight by the long stroke of the piston, combined with impact atomization, with the energy being transmitted through compression, impact, and combustion.

The energy values are reported by the manufacturer to be practically constant for each hammer blow, because a measured quantity of fuel is squirted, in its raw, liquid state, into the cup of the anvil block. Thus, theoretically, with constant combustion efficiency, the energy output would be identical for each blow. Energy is transmitted from the anvil block to the cushion assembly, consisting of a steel plate placed atop a very hard oak block.

The McKiernan-Terry DE-30 and DE-40 hammers (Fig. 20) are identical to each other in design, and differ only in size. Although they are constructed on the same operating principle as the Delmags, the two manufacturers differ in energy rating method and cushion assembly design. McKiernan-Terry specifies that the energy of each blow is dependent on the distance of the ram fall times the ram weight, rather than being an essentially constant value as stated by Delmag. Therefore, it is necessary to measure the height of ram rise if rated energy is to be determined.

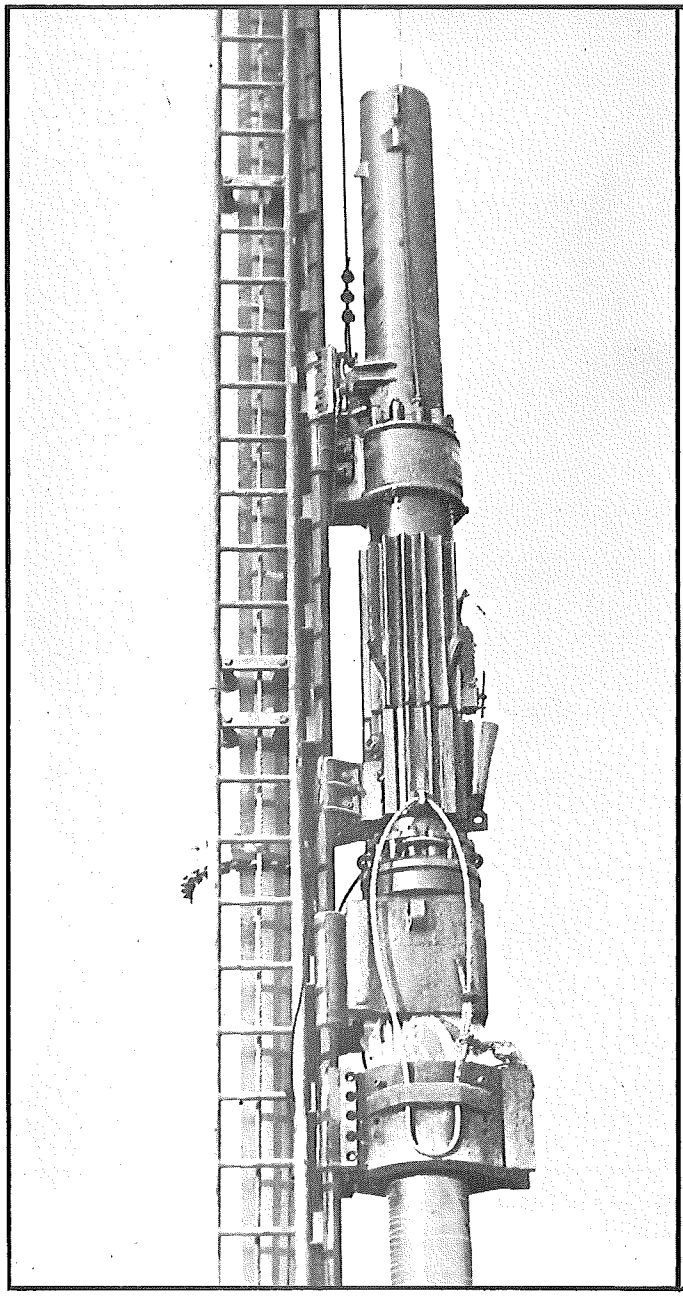

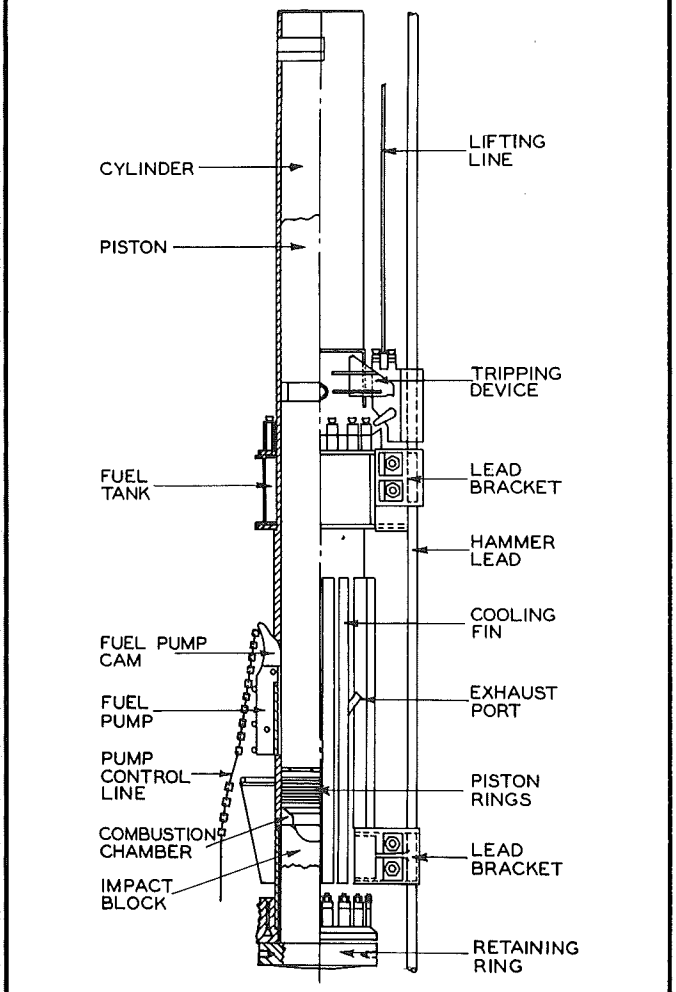

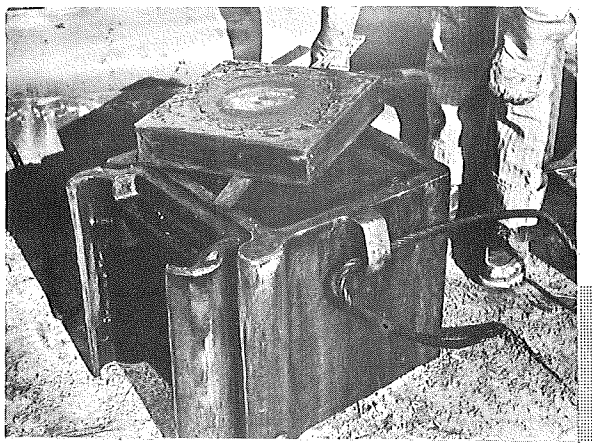

Figure 19. Single-acting diesel Delmags D-12 and D-22. Cushion assembly as driven is shown at left, with steel plate resting on driving cap.

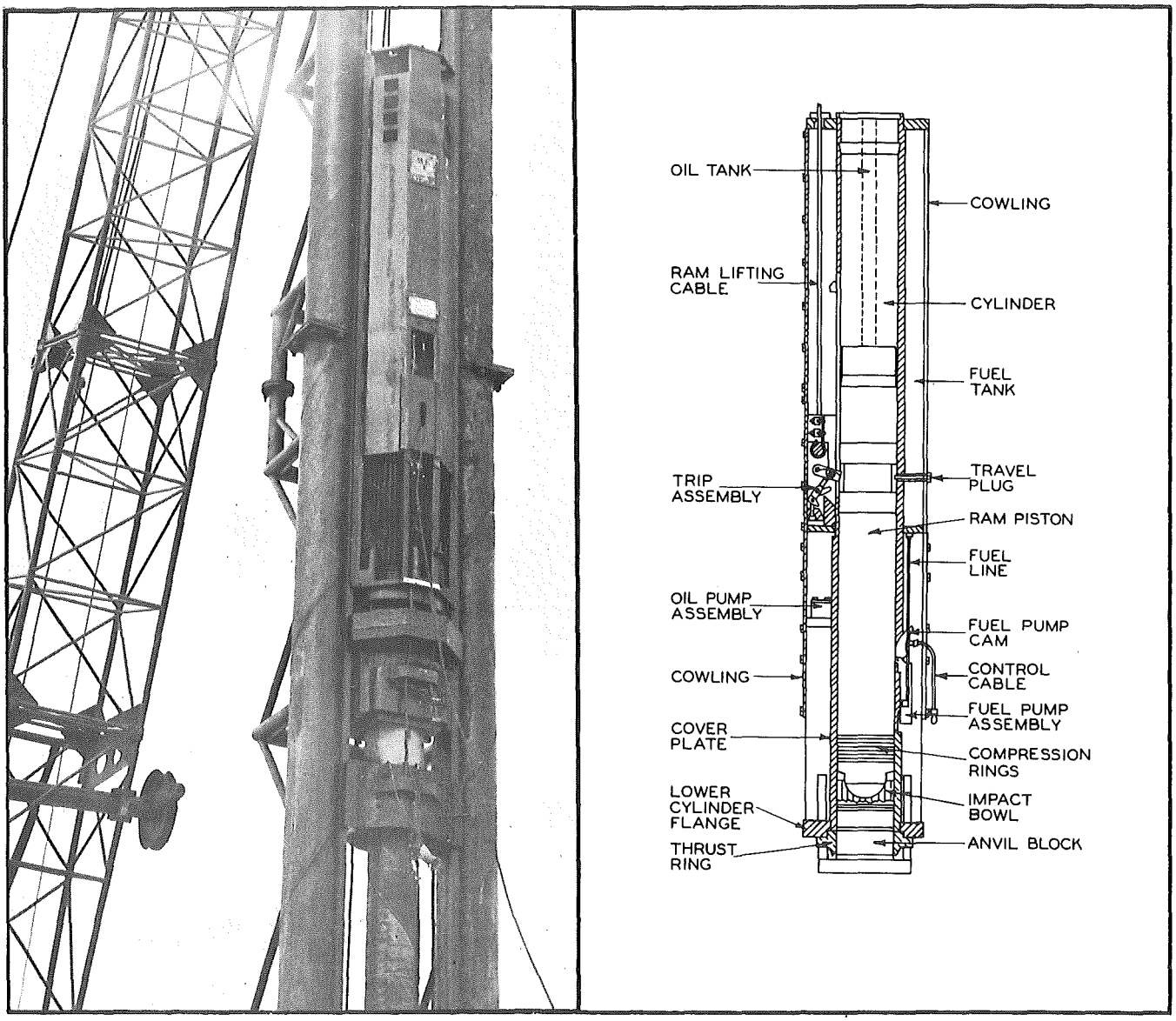

Figure 20. Single-acting diesel McKiernan-Terrys DE-30 and DE-40. Oak cushion block is shown before driving at lower left, resting on driving cap. At lower right, a section of a similar block is shown after hard driving, resting on an unused block.

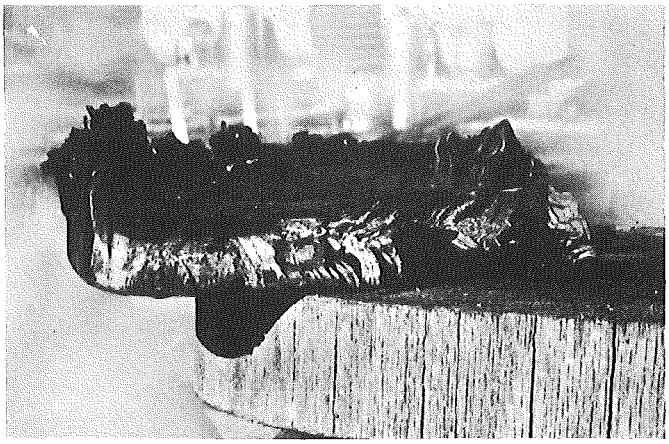

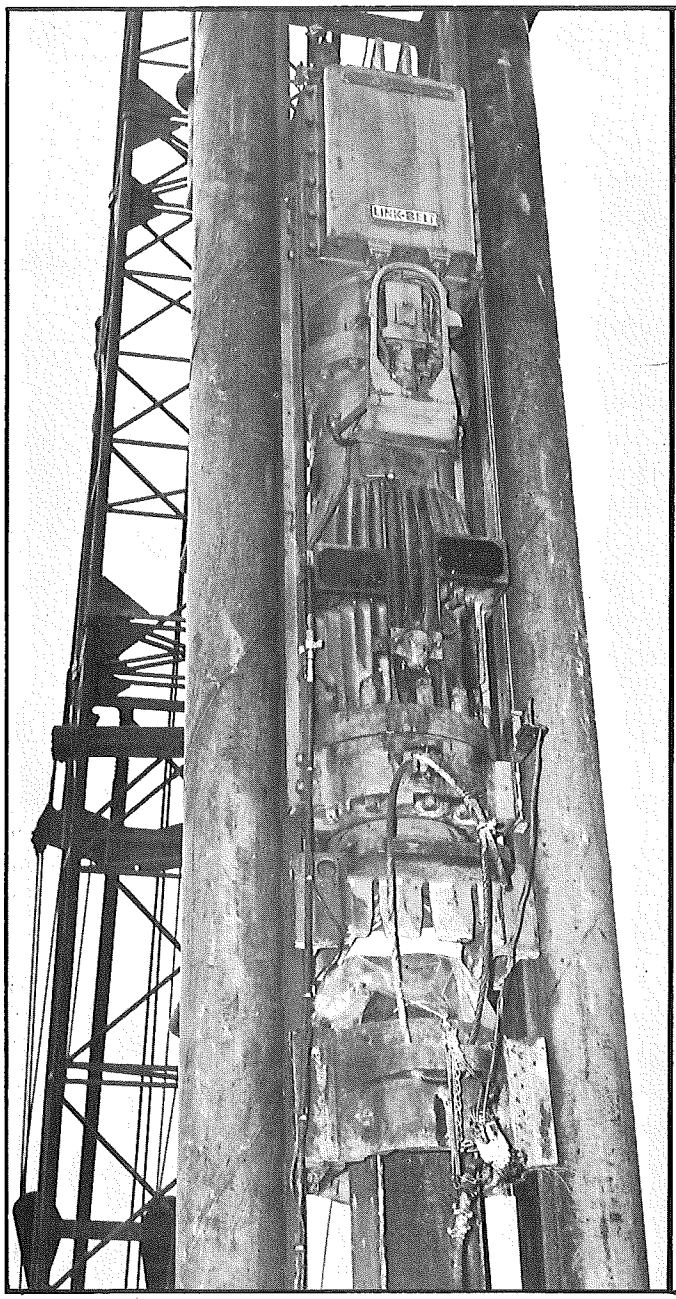

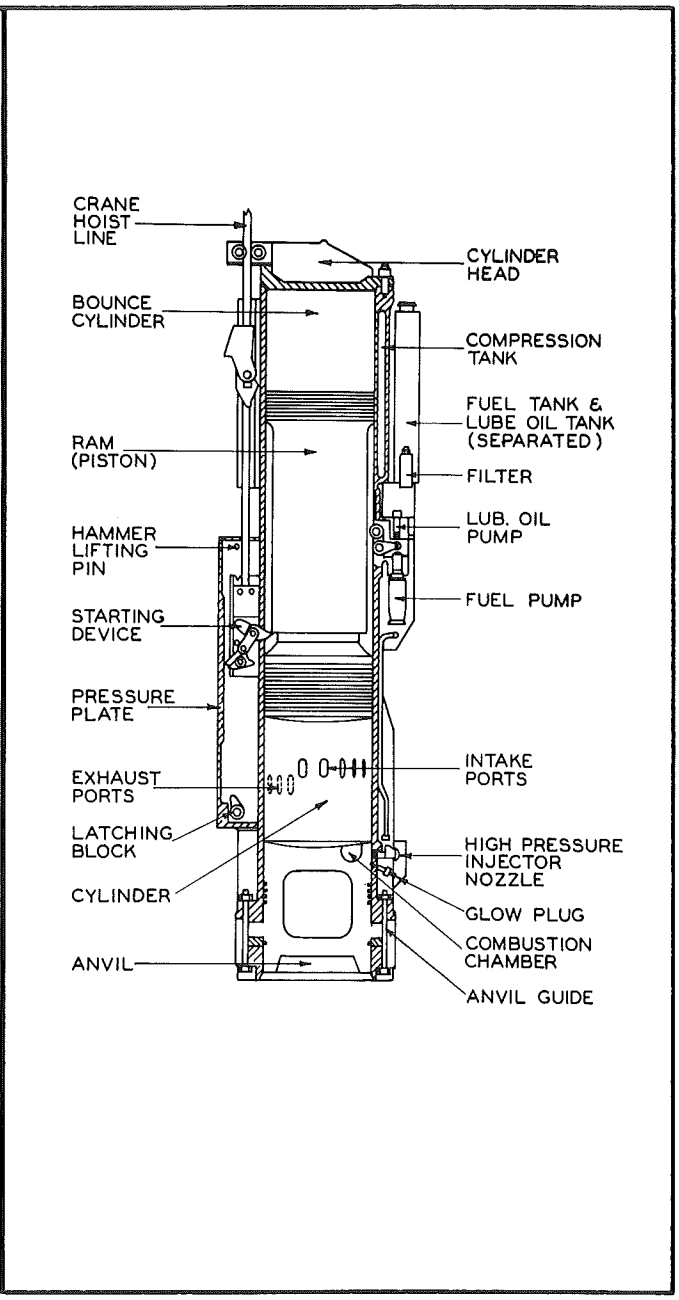

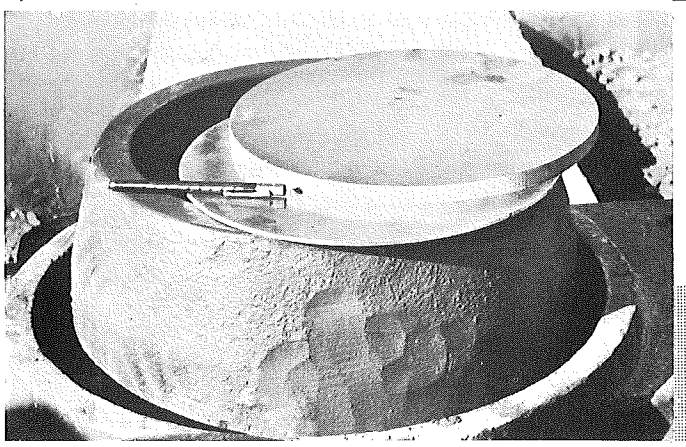

Figure 21. Modified single-acting diesel Link-Belts 312 and 520. Typical phenol fiber and aluminum thin cushion plate elements are shown at lower left, resting on driving cap.

The cushion used for the lighter hammer was a solid oak block, and for the heavier hammer, an oak block plus two plywood plates.

The tests also included two diesel hammers with closed cylinders, the Link-Belt 312 and 520 (Fig. 21). Again, both hammers are identical in design, but differ in size. The Link-Belt bounce chamber at the top of the piston cylinder allows greater hammer speeds than the other diesels. Their design also incorporates a fuel-injection system which provides a fine spray of fuel into the combustion chamber.

Since energy output may be varied by the fuel input and also depends somewhat on pile resistance, the manufacturer offers and recommends a bounce-chamber positive-acting pressure gage, so that the hammer operator or inspector may read the pressure value for any particular blow. The pressure reading is then converted into an energy value by means of a graph of bounce chamber pressure versus rated energy. The graph essentially converts the pressure into equivalent stroke and then multiplies it by the ram weight. Hammer energy is regulated by the amount of diesel fuel injected. Maximum energy is limited by the dead weight of the hammer (excluding anvil and piston), since the maximum downward reaction cannot be greater than this dead weight. The cushion consisted of phenol fiber plates and aluminum heat dissipator plates.

TEST PILES

The testing program initially called for driving of a total of 44 piles offering several cross-sections and types of surface configuration (Table 2). The H-piles and pipe piles are commonly used in Michigan, and the other types were selected for comparative evaluation of their driving characteristics and performance. Of this total, 26 were test piles (TP's) to determine driving characteristics of hammers and piles and the remaining 18 were load test piles (LTP's) specifically designated for static load testing to determine individual load capacity. In reviewing this program, the cooperating hammer manufacturers expressed concern over the possible inadequacy of the number of piles to be driven to demonstrate the driving characteristics of their hammers. They also suggested that if soil conditions varied within the test areas, results for their hammers could be adversely affected. It was agreed that 38 H-piles would be added to the pile driving schedule at Belleville, and six H-piles at Detroit, which would also serve as anchor or reaction piles (RP's) for load testing. Thus, the final total was 88 piles distributed among the three sites.

TABLE 2
SUMMARY OF PILE CHARACTERISTICS

Pile Type	Dimensions	Weight, lb per lin ft	Manufacturer	References (for additional data)
H-section, CBP 124	12-in. (flange width)	53	U. S. Steel	Chellis, R. D. Pile Foundations. N.Y.: McGraw-Hill (1961) p. 531 (Second Edition)
Pipe	12-in. OD (.250-in. wall)	31.37	Armco Foundation Products	Armco Foundation Pile Catalog FP 13559 (1959) and other Armco sources
	12-in. OD (.230-in. wall)	28.98		
	12-in. OD (.179-in. wall, #7 gage)	22.60		
Monotube, fluted-tapered F 12-7 (30-ft taper section), and N 12-7 (extension)	12-in. ND (.179-in. wall, #7 gage)	F: 19.63 N: 24.50	Union Metal Mfg. Co.	Union Catalog No. 91 (May 1959)
Step-Taper Shell (8-ft sections)	9-1/2-in. OD tip, with 1-in. step each 8 ft	Variable* by Section	Raymond International	Chellis, p. 528

*168 lb per ft for Mandrel, 9 to 11 lb per ft for shell

CHAPTER THREE

TESTING PROGRAM AND OPERATIONS

Planning of the field testing program for the three test sites was completed in the Summer of 1961, work began in October 1961, and was continued without interruption through March 1962. The 88 piles were driven at the three sites with ten different makes or models of pile driving hammer, nearly all of which were electronically instrumented for dynamic measurements and automatic data recording during driving. Table 3

TABLE 3
SUMMARY OF HAMMER AND PILE DISTRIBUTION

	Hammer and Model	H-Section	12-in. Pipe			Monotube Fluted-Tapered	Step-Taper Shell	Total Piles per Hammer	Site Totals
			.250-in. Wall	.230-in. Wall	.179-in. Wall (#7 Gage)				
Belleville	Vulcan No. 1	7	3(a)		1	1		12	
	Raymond 15-M						1	1	
	Vulcan 50C	8			1			9	
	Link-Belt 312	8	1		1			10	
	McKiernan-Terry DE-30	8	1		1	1		11	
	Delmag D-12	9	1		1			11	
									54
Detroit	Vulcan No. 1	1			2(a)	1		4	
	Vulcan 50C		1		1			2	
	Link-Belt 312	2		1	1			4	
	McKiernan-Terry DE-30	2	1(b)		1	1		5	
	Delmag D-12	3		1	1			5	
									20
Muskegon	Vulcan No. 1			4(c)		1		5	
	Raymond 15-M						1	1	
	Vulcan 80C		2					2	
	Link-Belt 520		2					2	
	McKiernan-Terry DE-40		2					2	
	Delmag D-22		2					2	
									14
	Total	48	16	6	11	5	2		88

(a) One open end (set-up pile).
(b) Combination of 45 ft of .23-in. wall and 40 ft of .25-in. wall.
(c) One pile driven open-end with 19 ft of .25-in. wall and 45 ft of .23-in. wall; two piles open-end and internally jetted during driving; one pile driven closed-end.

summarizes hammer and pile distribution among the sites. At each site, the pile schedule and hammer assignments were arranged to provide a uniform, dispersed pattern of pile driving (Figs. 22, 23, 24). A technical

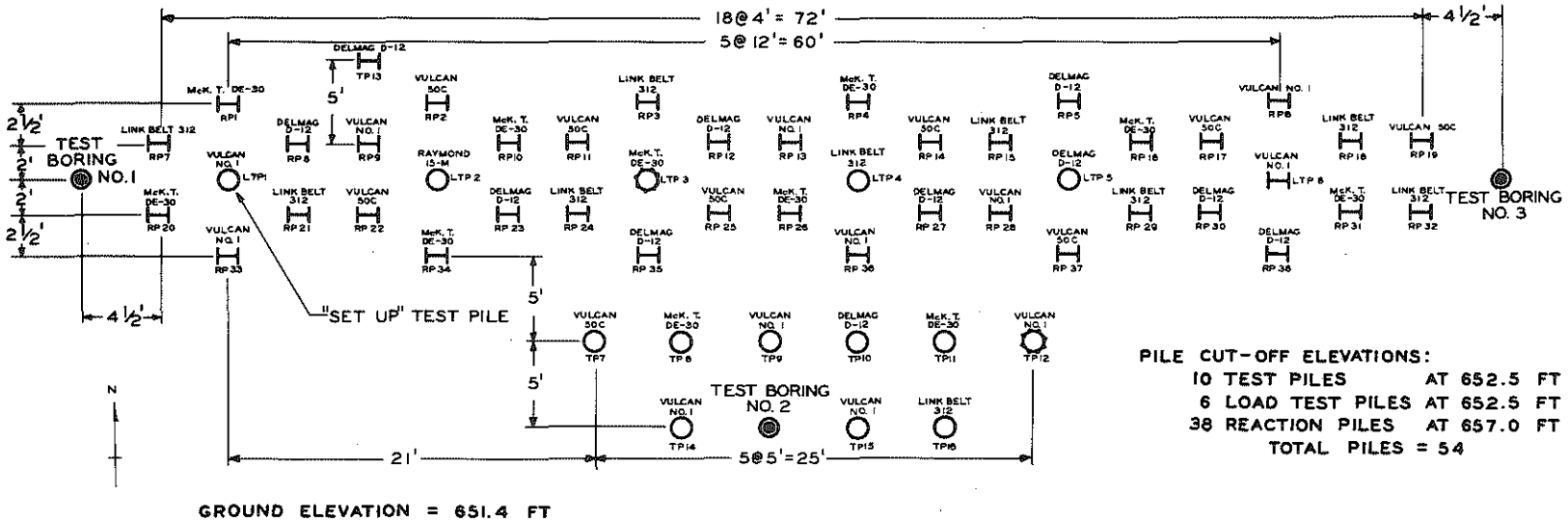

PILE AND HAMMER SCHEDULE

Vulcan No. 1

Pile No.	Pile Type	Depth Driven, ft	Depth Tip Elevation
LTP 1	12-in. pipe, .25-in. wall	44.4	607.0
LTP 6	12- by 12-in. H, 53 lb per ft	58.0	593.4
TP 9	12-in. pipe, #7 gage wall	54.8	596.6
TP 12	12-in. fluted-tapered, #7 gage wall	55.1	596.3
TP 14	12-in. pipe, .25-in. wall	66.3	585.1
TP 15	12-in. pipe, .25-in. wall	55.2	596.2
RP 6	12- by 12-in. H, 53 lb per ft	53.8	597.6
RP 9	12- by 12-in. H, 53 lb per ft	53.2	598.2
RP 13	12- by 12-in. H, 53 lb per ft	44.5	606.9
RP 28	12- by 12-in. H, 53 lb per ft	53.0	598.4
RP 33	12- by 12-in. H, 53 lb per ft	61.4	590.0
RP 36	12- by 12-in. H, 53 lb per ft	52.8	598.6

Raymond 15-M

Pile No.	Pile Type	Depth Driven, ft	Depth Tip Elevation
LTP 2 (a)	step-taper shell, 9-1/2-in. tip with 1-in. step each 8 ft.	67.1	584.3

Vulcan 50C

Pile No.	Pile Type	Depth Driven, ft	Depth Tip Elevation
TP 7	12-in. pipe, #7 gage wall	66.3	585.1
RP 2	12- by 12-in. H, 53 lb per ft	53.0	598.4
RP 11	12- by 12-in. H, 53 lb per ft	53.4	598.0
RP 14	12- by 12-in. H, 53 lb per ft	53.0	598.4
RP 17	12- by 12-in. H, 53 lb per ft	53.0	598.4
RP 19	12- by 12-in. H, 53 lb per ft	53.1	598.3
RP 22	12- by 12-in. H, 53 lb per ft	67.8	583.6
RP 25	12- by 12-in. H, 53 lb per ft	53.2	598.2
RP 37	12- by 12-in. H, 53 lb per ft	53.5	597.9

Link-Belt 312

Pile No.	Pile Type	Depth Driven, ft	Depth Tip Elevation
LTP 4	12-in. pipe, .25-in. wall	66.5	584.9
TP 16	12-in. pipe, #7 gage wall	66.5	584.9
RP 3	12- by 12-in. H, 53 lb per ft	53.3	598.1
RP 7	12- by 12-in. H, 53 lb per ft	68.0	583.4
RP 15	12- by 12-in. H, 53 lb per ft	53.4	598.0
RP 18	12- by 12-in. H, 53 lb per ft	53.1	598.3
RP 21	12- by 12-in. H, 53 lb per ft	53.4	598.0
RP 24	12- by 12-in. H, 53 lb per ft	53.0	598.4
RP 29	12- by 12-in. H, 53 lb per ft	53.2	598.2
RP 32	12- by 12-in. H, 53 lb per ft	53.2	598.2

McKiernan-Terry DE-30

Pile No.	Pile Type	Depth Driven, ft	Depth Tip Elevation
LTP 3	12-in. fluted-tapered, #7 gage wall	60.9	590.5
TP 8	12-in. pipe, #7 gage wall	63.8	587.6
TP 11	12-in. pipe, .25-in. wall	66.7	584.7
RP 1	12- by 12-in. H, 53 lb per ft	53.0	598.4
RP 4	12- by 12-in. H, 53 lb per ft	53.0	598.4
RP 10	12- by 12-in. H, 53 lb per ft	53.0	598.4
RP 16	12- by 12-in. H, 53 lb per ft	53.0	598.4
RP 20	12- by 12-in. H, 53 lb per ft	67.6	583.8
RP 26	12- by 12-in. H, 53 lb per ft	53.0	598.4
RP 31	12- by 12-in. H, 53 lb per ft	53.0	598.4
RP 34	12- by 12-in. H, 53 lb per ft	53.0	598.4

Delmag D-12

Pile No.	Pile Type	Depth Driven, ft	Depth Tip Elevation
LTP 5	12-in. pipe, #7 gage wall	66.7	584.7
TP 10	12-in. pipe, .25-in. wall	66.6	584.8
TP 13 (a)	12- by 12-in. H, 53 lb per ft	67.1	584.3
RP 5	12- by 12-in. H, 53 lb per ft	53.0	598.4
RP 8	12- by 12-in. H, 53 lb per ft	67.6	583.8
RP 12	12- by 12-in. H, 53 lb per ft	53.0	598.4
RP 23	12- by 12-in. H, 53 lb per ft	53.2	598.2
RP 27	12- by 12-in. H, 53 lb per ft	53.0	598.4
RP 30	12- by 12-in. H, 53 lb per ft	53.0	598.4
RP 35	12- by 12-in. H, 53 lb per ft	53.0	598.4
RP 38	12- by 12-in. H, 53 lb per ft	53.0	598.4

(a) Driven without load cell assembly

Figure 22. Pile layout and hammer schedule at Belleville.

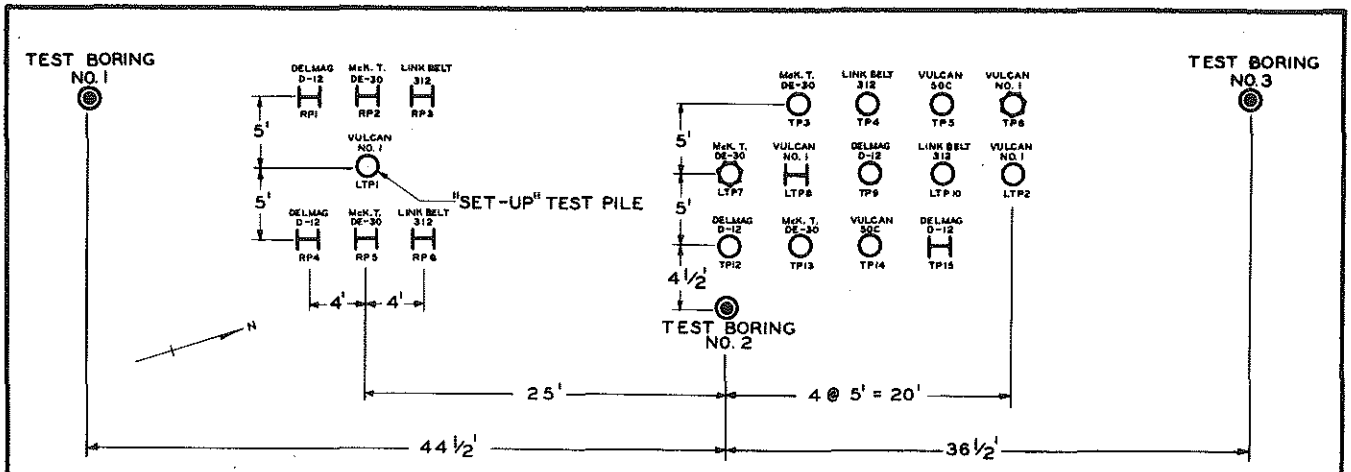

GROUND ELEVATION = 589.4 FT

PILE CUT-OFF ELEVATIONS:

4 LOAD TEST PILES (NOS. 2, 7, 8, 10)	AT 591.5 FT
1 LOAD TEST PILE (NO. 1)	AT 592.7 FT
9 TEST PILES	AT 591.5 FT
6 REACTION PILES	AT 595.9 FT
TOTAL PILES = 20	

PILE AND HAMMER SCHEDULE

Vulcan No. 1

Pile No.	Pile Type	Depth Driven, ft	Depth Tip Elevation
LTP 1	12-in. pipe, #7 gage wall	69.5	519.9
LTP 2	12-in. pipe, #7 gage wall	78.6	510.8
LTP 8	12- by 12-in. H, 53 lb per ft	81.1	508.3
TP 6	12-in. fluted-tapered, #7 gage wall	79.6	509.8

Vulcan 50C

Pile No.	Pile Type	Depth Driven, ft	Depth Tip Elevation
TP 5	12-in. pipe, #7 gage wall	82.8	506.6
TP 14	12-in. pipe, .25-in. wall	81.8	507.6

Link-Belt 312

Pile No.	Pile Type	Depth Driven, ft	Depth Tip Elevation
LTP 10	12-in. pipe, .23-in. wall	81.0	508.4
TP 4	12-in. pipe, #7 gage wall	80.6	508.8
RP 3	12- by 12-in. H, 53 lb per ft	73.6	515.9
RP 6	12- by 12-in. H, 53 lb per ft	73.5	515.9

McKiernan-Terry DE-30

Pile No.	Pile Type	Depth Driven, ft	Depth Tip Elevation
LTP 7	12-in. fluted-tapered, #7 gage wall	81.1	508.3
TP 3	12-in. pipe, 45 ft of .23-in. wall and 40 ft of .25-in. wall	80.7	508.7
TP 13	12-in. wall, #7 gage wall	81.2	508.2
RP 2	12- by 12-in. H, 53 lb per ft	73.5	515.9
RP 5	12- by 12-in. H, 53 lb per ft	73.5	515.9

Delmag D-12

Pile No.	Pile Type	Depth Driven, ft	Depth Tip Elevation
TP 9	12-in. pipe, #7 gage wall	81.3	508.1
TP 12	12-in. pipe, .23-in. wall	84.2	505.2
TP 15	12- by 12-in. H, 53 lb per ft	88.1	501.3
RP 1	12- by 12-in. H, 53 lb per ft	63.5	525.9
RP 4	12- by 12-in. H, 53 lb per ft	73.5	515.9

Figure 23. Pile layout and hammer schedule at Detroit.

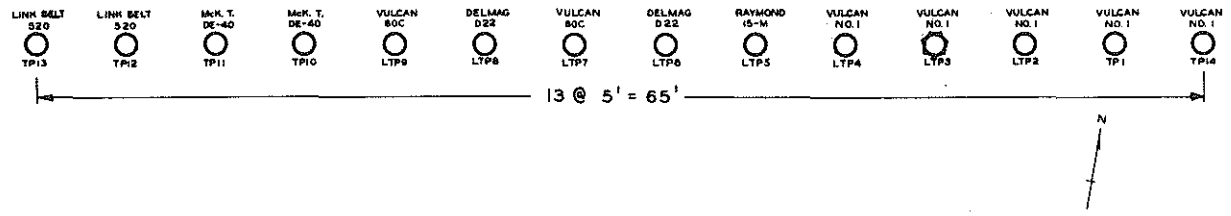

PILE CUT-OFF ELEVATIONS:
6 TEST PILES AT 590.0 FT
8 LOAD TEST PILES AT 590.0 FT
TOTAL PILES = 14

GROUND ELEVATION (FILL) = 588.0 FT

PILE AND HAMMER SCHEDULE

Vulcan No. 1

Pile No.	Pile Type	Depth, Driven, ft	Depth, Tip Elevation
TP 1 (a)	12-in. pipe, .23-in. wall	56.4	531.6
LTP 2	12-in. pipe, .23-in. wall	58.0	530.0
LTP 3	12-in. fluted-tapered, #7 gage wall	57.9	530.1
LTP 4 (b)	12-in. pipe, .23-in. wall	58.0	530.0
TP 14 (d)	12-in. pipe, 18 ft of .25-in. wall and 45 ft of .23-in. wall	61.0	527.0

Raymond 15-M

Pile No.	Pile Type	Depth, Driven, ft	Depth, Tip Elevation
LTP5 (c)	step-taper shell, 9-1/2-in. tip with 1-in. step each 8 ft.	58.0	530.0

Vulcan 80C

Pile No.	Pile Type	Depth, Driven, ft	Depth, Tip Elevation
LTP 7	12-in. pipe, .25-in. wall	178.4	409.6
LTP9	12-in. pipe, .25-in. wall	128.2	459.8

Link-Belt 520

Pile No.	Pile Type	Depth, Driven, ft	Depth, Tip Elevation
TP 12	12-in. pipe, .25-in. wall	128.0	460.0
TP 13	12-in. pipe, .25-in. wall	174.4	413.6

McKiernan-Terry DE-40

Pile No.	Pile Type	Depth, Driven, ft	Depth, Tip Elevation
TP 10	12-in. pipe, .25-in. wall	128.1	459.9
TP 11	12-in. pipe, .25-in. wall	175.3	412.7

Delmag D-22

Pile No.	Pile Type	Depth, Driven, ft	Depth, Tip Elevation
LTP 6	12-in. pipe, .25-in. wall	128.0	460.0
LTP 8	12-in. pipe, .25-in. wall	178.2	409.8

(a) Internal jetting attempted during driving; first 43 ft unsuccessful
(b) Internally jetted during driving
(c) Driven without load cell assembly
(d) Driven open-end

Figure 24. Pile layouts and hammer schedule at Muskegon. Relative positions of test borings are shown in Fig. 1.

field staff of 11 engineers and technicians directed the field operations, operated the electronic data recording equipment, and also recorded events by conventional manual-verbal techniques. Compiled records for the driving of each pile are given in Appendix A.

Driving Procedure and Pile Splicing

Pile driving was performed by a standard spread of contractor's equipment, with some modifications for the test situation. The pile driving leads were held by a P&H truck-mounted 40-ton crane. Two

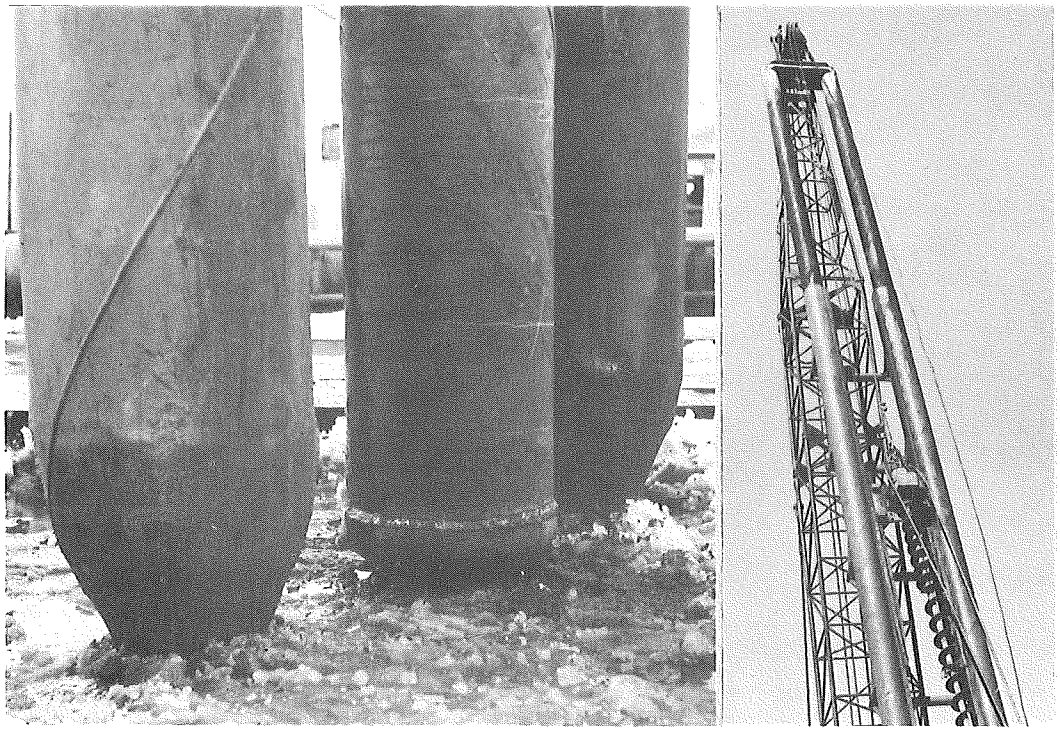

Figure 25. Tubular leads used for all hammers except Delmags, showing pointed ends (left), and telescoping section pinned to crane boom (right).

makes of telescoping leads were used: a tubular frame type and a modified Delmag 18-in. single-tube shaft type. The telescoping sections allowed the crane operator to move and align the leads easily; the bottom of the leads was spudded into the ground and the top telescoping section was pinned to the crane boom (Figs. 25, 26).

At the commencement of driving for the individual pile, the driving assembly was rigged in the leads, and the crane then spotted the leads in position and placed the driving assembly and pile hammer on top of a

prepared pile section. Each pile was marked at 6-in. intervals to facilitate observations during penetration. In the case of pipe piles a pressed steel cone point was welded to the pile tip (Fig. 27). After the pile was positioned, the first or bottom pile section was driven until about 4 ft remained above ground level, and driving was stopped, the hammer was removed,

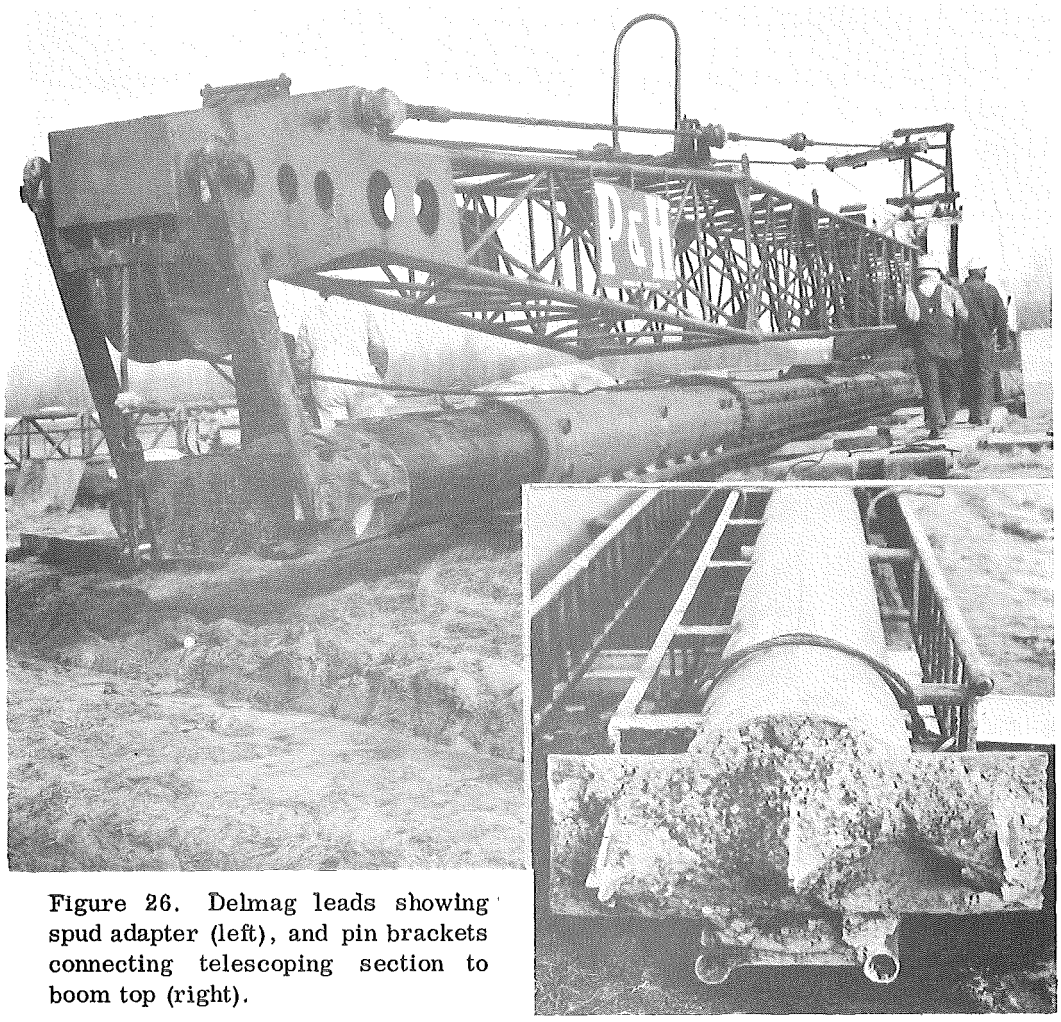

Figure 26. Delmag leads showing spud adapter (left), and pin brackets connecting telescoping section to boom top (right).

and an extension section was welded into position (Fig. 28). At the completion of welding, driving resumed until additional extensions were required or final penetration was reached.

It was decided during initial field operations (at Belleville) that driving of H-piles was being delayed excessively due to the time required to splice-weld extension sections. To expedite this procedure, an H-extension section was tack-welded into position on top of a driven bottom section. The crane and hammer then moved to another pile position,

drove a second bottom section to splice depth, and an extension section was immediately tack-welded into position. During driving of this second pile, the first pile's extension section was being welded into place. Next, the crane and hammer could either return to the first pile and continue driving, or could drive additional bottom sections at other pile locations. Then, in turn, the pile driving equipment could return and drive each extended pile to its final penetration.

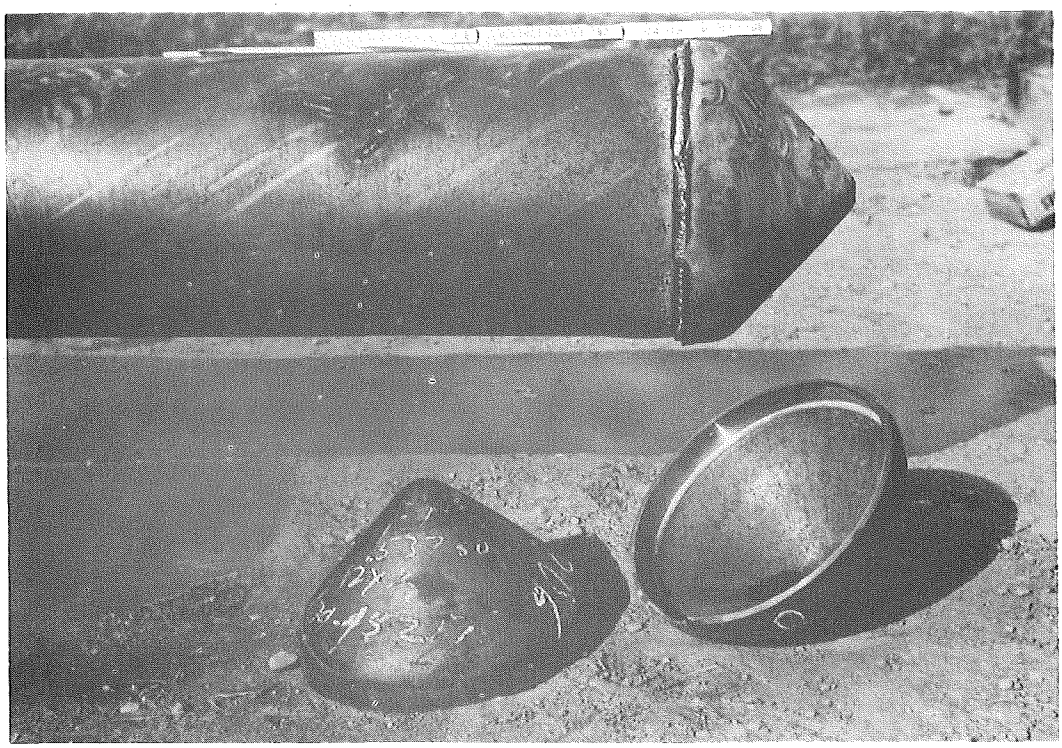

Figure 27. Closed-end pipe pile with pressed-steel cone points.

Belleville Site Operations (Stiff-to-Firm Cohesive Subsoils)

Belleville was selected for the initial field testing because of the character of the site's subsoil, the excellent conditions for reaction piles, and the large number of piles scheduled to be driven there, as well as the convenience of its location.

All reaction piles and test piles were driven before the load test piles. All H-piles were driven without pre-excavation, and all closed-end tubular piles were pre-excavated to a depth of 10 ft (elevation $\pm$ 640) with a 10-in. continuous flight, expandable bit, spiral auger (Fig. 29). Drilling diameter was held to slightly less than the outside diameter of the piling.

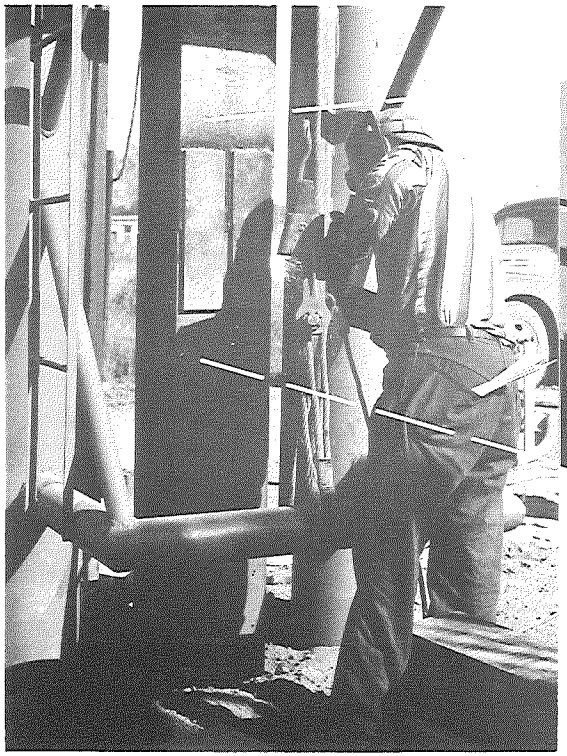

H - SECTION

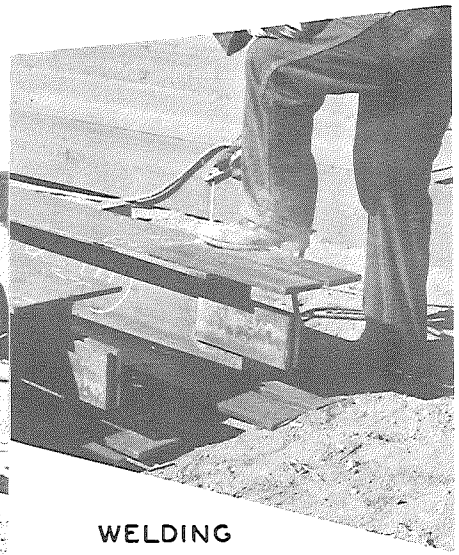

WELDING
SPLICE PLATE

FLUTED - TAPERED PILE

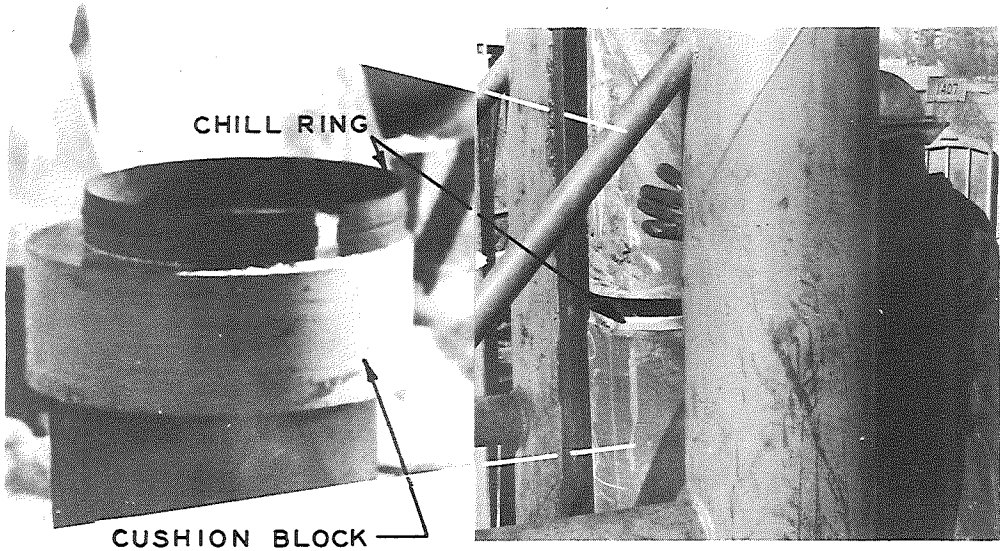

PIPE PILE WITH CHILL
RING IN PLACE

Figure 28. Splice welding of extension sections to bottom sections.

This pre-excavation was intended to eliminate possible failure of the closed-end tubular piles in the hard upper 10-ft layer of desiccated clay.

Before test driving began, 33 blows per inch was selected as the refusal criterion. LTP's 2 through 6 and TP's 7 through 16 (Fig. 22) were driven to this refusal condition. In the case of reaction piles, each hammer drove one pile to this refusal condition, and all others to a depth of 53 ft (tip elevation 598.4). This penetration provided sufficient side shear to develop the estimated pull-out capacity required in performing the subsequent load tests.

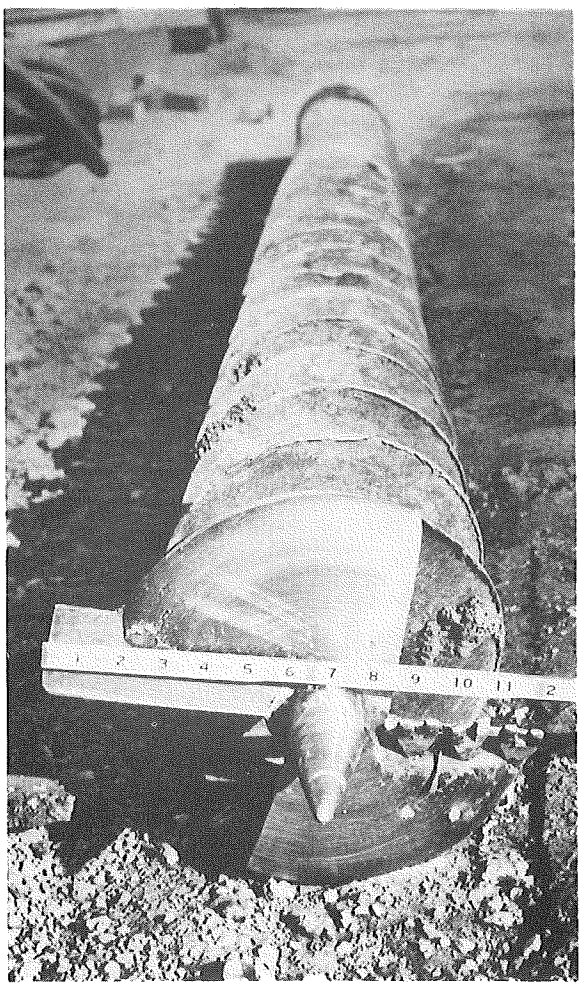

Figure 29. Air-operated, 10-in. diam, spiral auger with expandable bit extended.

The last pile driven in the test area was the friction pile, LTP 1. Before driving, all load test equipment and personnel were in readiness to being the load test as quickly as the reaction frame could be assembled after completion of driving. When the necessary preparations were completed, the open-end pile was driven without pre-excavation to a penetration of 43.4 ft (elevation 608). The soil plug measured 10.5 ft, and was removed by a power auger to a depth of 41.4 ft (elevation 610), leaving a 2-ft plug. Then the pile was driven another 1 ft (tip elevation 607), leaving a final 3-ft soil plug. The elasped time between the completion of driving and the first load cycle was held to 3 hr 40 min.

Detroit Site Operations (Soft Cohesive Subsoils)

The same hammers used at Belleville, except the Raymond 15-M, were assigned to drive piling at Detroit. All piles, except LTP 1 (open-end friction pile) and the adjacent six reaction piles, were driven through

the soft clay to refusal in the hard clay. All reaction piles were driven to a tip elevation of 523.9 (73.5 ft) which provided sufficient side shear to develop the estimated anchor capacity necessary in performing the load tests. Soil was not pre-excavated for Detroit piles.

The procedure for driving the open-end pile at Detroit was the same as at Belleville. LTP 1 was driven to 41 ft 1 in., a soil plug of 19 ft 6.5 in. was measured, the pile was spliced, and then driven to a final penetration of 69 ft 6 in. The soil plug then measured 33 ft 8 in. and was not removed from the pile interior before load testing, since point bearing was considered insignificant. The interval between completion of driving and beginning of the pile load test was 2 hr 35 min.

Muskegon Site Operations (Granular Subsoils)

For determination of the effects of pile cross-section and surface configuration on energy required for driving and on pile load bearing capacity in granular materials, five piles were driven with the Vulcan No. 1. These piles were driven into the upper 58-ft deposit of loose-to-moderately compact sands.

In addition to these five piles, one corrugated thin shell was driven with the Raymond 15-M internal hammer to the same penetration. The Vulcan 80C, Link-Belt 520, McKiernan-Terry DE-40, and Delmag D-22 hammers each drove one pile to a penetration of 125 ft (in order to test carrying capacity on a compact sand layer), and one pile to refusal at approximately 175 ft. In all, eight piles were load tested at Muskegon.

Special Studies and Observations

Certain studies were scheduled at each site in conformance with project objectives, and in the course of work, certain developments suggested other pertinent measurements and experiments. These observations, described separately and in varying detail later in this report, included the following:

1. Cushion Block Study (Chapter 8). Two attempts were made at Muskegon to measure hammer force and pile displacement with the cushion block and cap removed from the pile driving assembly.

2. Pile Failures (Chapter 9). In the process of checking all piles for failure and alignment after driving, a total of 7 of the 88 piles were found to have failed. These failures were considered in subsequent analysis.

3. Internal Jetting of Piles (Chapter 9). In fulfillment of the sixth project objective, internal jetting was used at Muskegon to reduce driving resistance of piles when penetrating granular soils.

4. Blow Count Increase Due to Soil Set-Up (Chapter 9). After interruptions in driving operations, increases in blow count were noticed, attributable to soil set-up along and around the pile, and special recording procedures were established to measure this increase.

5. Soil Drag-Down in H-Pile Flanges (Chapter 9). At Belleville, it was found that soil adhering within the flanges of nearly every H-pile was being dragged down during driving. Measurements were made to determine possible effects.

6. Increase in Load Capacity Due to Soil Set-Up (Chapter 11). Two special piles (Belleville LTP 1 and Detroit LTP 1) were load-tested immediately after driving, and after varying time intervals, to evaluate the increase in capacity due to soil set-up.

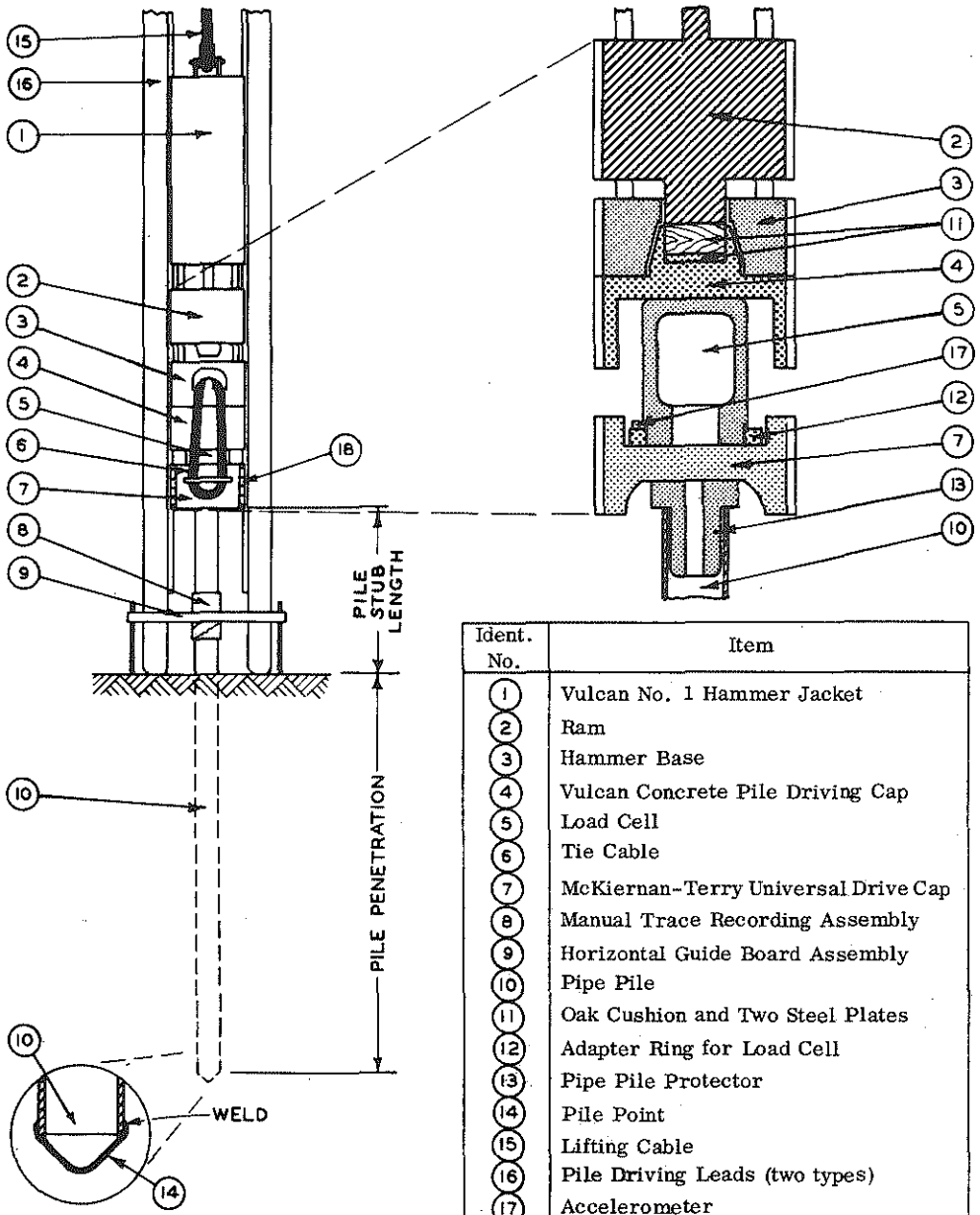

Ident. No.	Item
1	Vulcan No. 1 Hammer Jacket
2	Ram
3	Hammer Base
4	Vulcan Concrete Pile Driving Cap
5	Load Cell
6	Tie Cable
7	McKiernan-Terry Universal Drive Cap
8	Manual Trace Recording Assembly
9	Horizontal Guide Board Assembly
10	Pipe Pile
11	Oak Cushion and Two Steel Plates
12	Adapter Ring for Load Cell
13	Pipe Pile Protector
14	Pile Point
15	Lifting Cable
16	Pile Driving Leads (two types)
17	Accelerometer
18	Lead Adapters (two types)

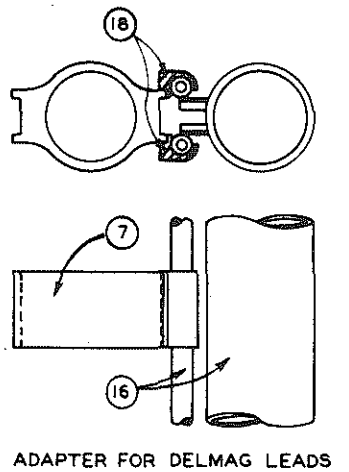

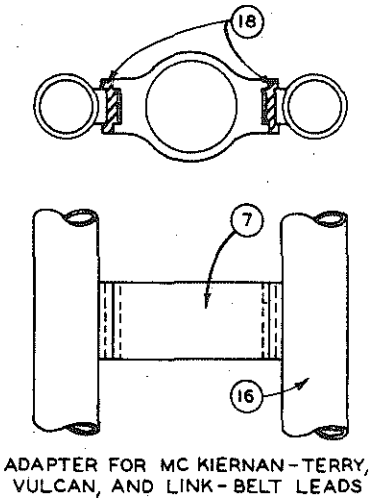

Figure 30. Typical pile driving assembly and cap-to-lead adapters; components (5) (8) (9) (12) (17) used in measuring and recording data.

CHAPTER FOUR

MEASURING AND RECORDING PROCEDURES

Measuring and recording of data during driving operations involved a number of procedures conventional in pile and hammer testing, and in fulfillment of project objectives, also included developmental experiments in electronic measurement through the use of transducers (sensing devices converting such physical phenomena as force, acceleration, or deflection into measurable electrical output signals).

The instrumentation problem presented in this study was somewhat unusual, in that a fully instrumented driving assembly was required, applicable to nine hammers of four different manufacturers (excluding the Raymond hammer and pile), and compatible with two different types of leads and three pile types. Before attempting design and construction of the required assembly, a number of conferences were held between representatives of the hammer manufacturers and members of the study group. The resulting driving assembly, shown schematically in Fig. 30, consisted of a pile driving hammer, the hammer manufacturer's recommended cushion, a plain drive cap normally used for driving 14-in. concrete piles, a load cell, a McKiernan-Terry U-2308 universal drive cap, and in the case of pipe piles a special pipe protector. Also shown in Fig. 30 are cap-to-lead adapters bolted to the universal drive cap, allowing use of the driving assembly with either conventional or Delmag leads.

MEASURING SYSTEMS (Transducers)

The instrumentation system, shown schematically in Fig. 31, consisted of three primary transducers: 1) a load cell for measuring force output of the pile hammer, 2) an accelerometer for measuring acceleration of the pile and pile driving assembly, and 3) a pile deflectometer or "penetrometer" for measuring gross and net pile deflections. The output of these transducers was fed to a high-writing-speed oscillographic

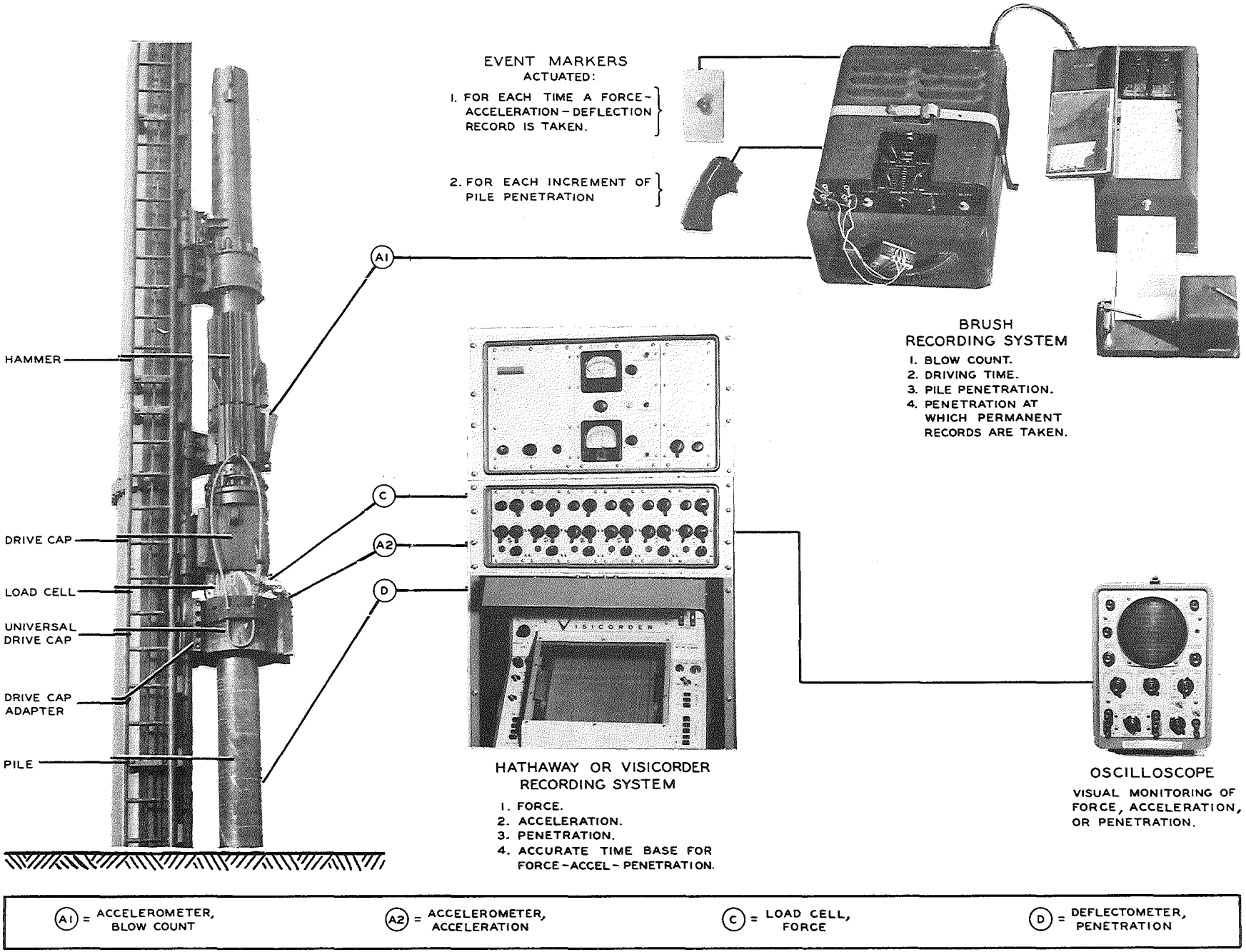

Figure 31. Pile driving instrumentation system.

recorder, permitting permanent, simultaneous, dynamic trace records of force, acceleration, and deflection. A sample of one of these records including three consecutive blows is shown in Fig. 32. An oscilloscope monitor was also used throughout automatic and non-automatic recording operations.

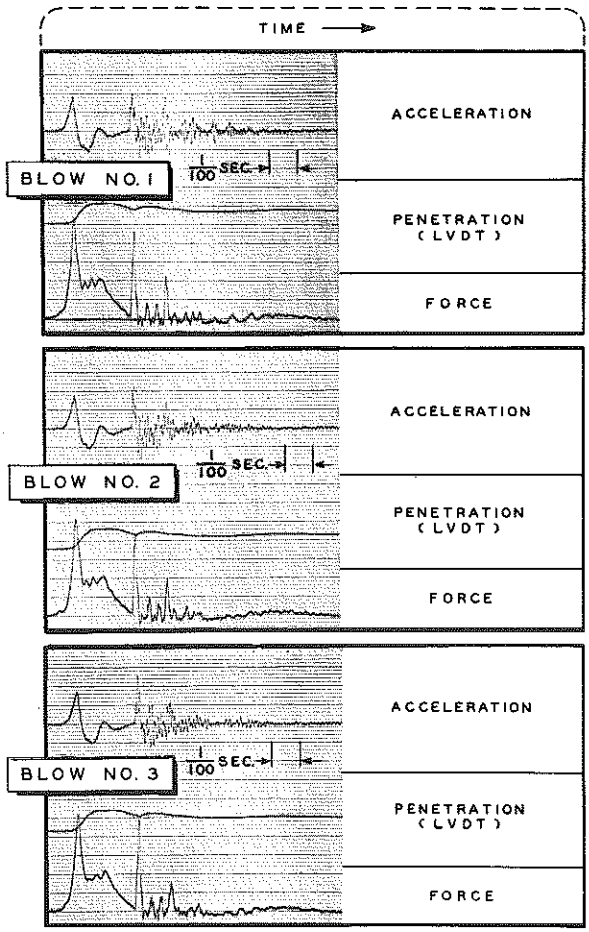

Figure 32. Record of three consecutive hammer blows at a given penetration.

Load Cells

The minimum height and and outer diameter of the cell were dictated by the dimensions of the plain and universal driving caps. It was machined from a solid blank of Heppenstall "hard tem, B-hardness" steel[1], and instrumented with 24 Type AB3 SR-4 strain gages--12 active and 12 temperature compensating (Fig. 33). The gages were mounted at 30° intervals around the internal surface at a point midway between the top and bottom of the bored-out area, a distance minimizing any corner effects on the measured strains. As may be seen, the gage installation at each 30° increment consisted of an active gage with its strain-sensitive axis parallel to the principal axis of the load cell, and a temperature compensating gage with its strain-sensitive axis perpendicular to the cell axis.

[1] Steel properties and alloy contents were as follows:

Steel Properties
Ultimate strength--150,000 to 171,000 psi
Yield strength--130,000 to 145,000 psi
Elongation at break--13 to 16 percent
Reduction of area at break--37 to 43 percent
Rockwell--36 to 40 "C"

Alloy Content, percent	
Carbon	0.50-0.60
Manganese	0.60-0.95
Molybdenum	0.38-0.48
Silicon	0.20-0.35
Chromium	0.85-1.15
Vanadium	0.03

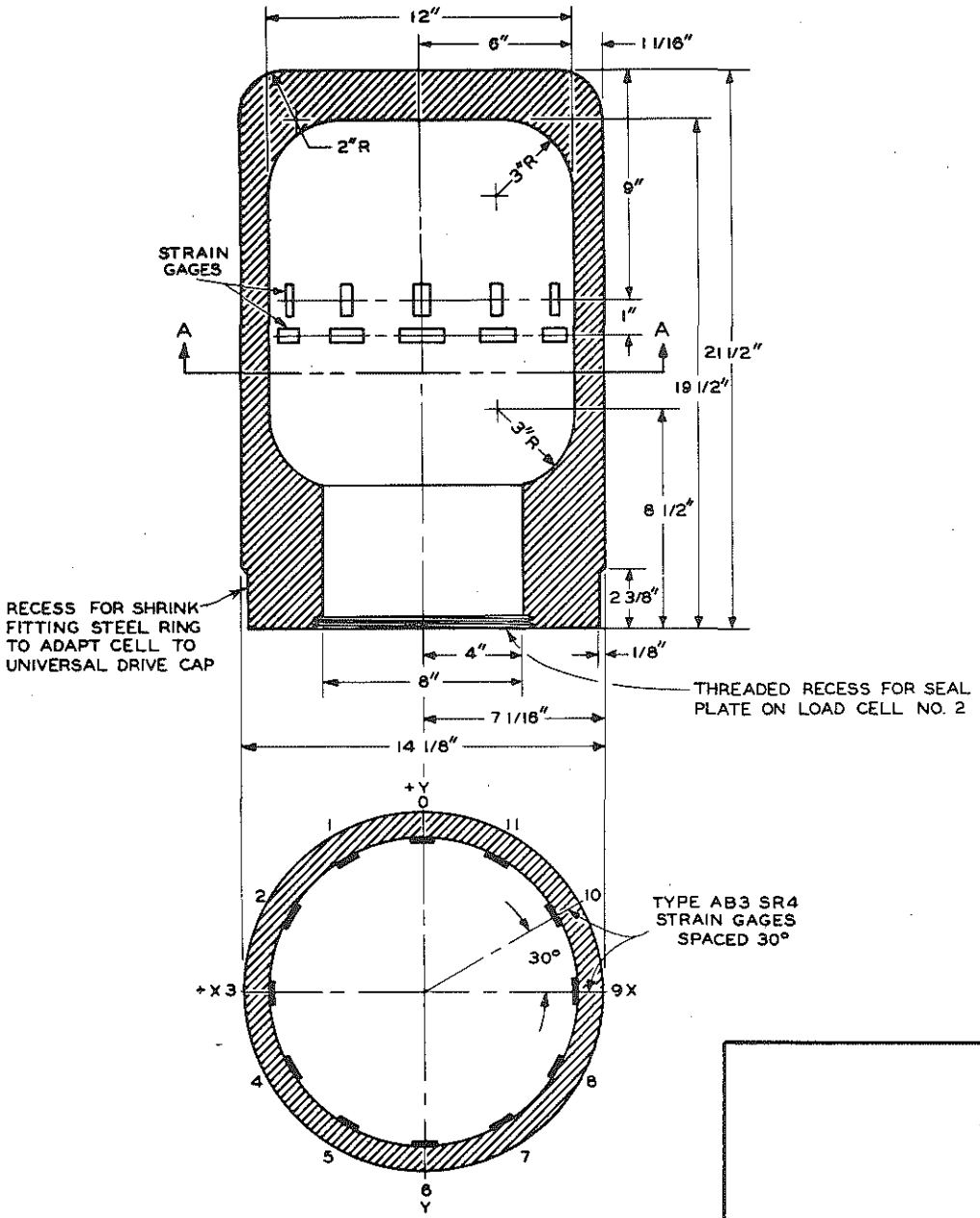

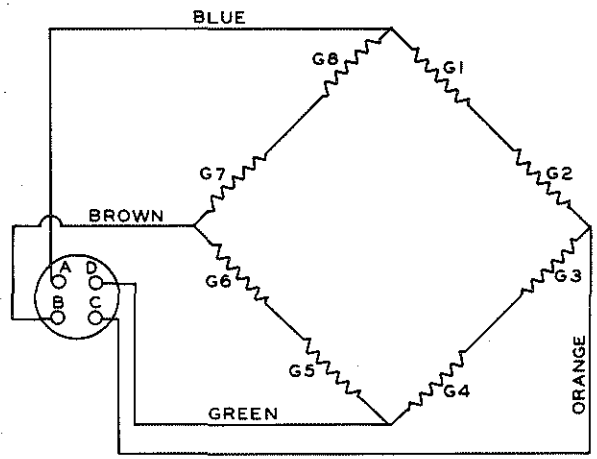

GAGES	BRIDGES		
	0-3-6-9	1-4-7-10	2-5-8-11
G1	3 COMP.	4 COMP.	5 COMP.
G2	9 COMP.	10 COMP.	11 COMP.
G3	9 ACT.	10 ACT.	11 ACT.
G4	3 ACT.	4 ACT.	5 ACT.
G5	6 COMP.	7 COMP.	8 COMP.
G6	0 COMP.	1 COMP.	2 COMP.
G7	0 ACT.	1 ACT.	2 ACT.
G8	6 ACT.	7 ACT.	8 ACT.

GAGE AND WIRING DETAILS:
GAGE AND WIRING BONDED WITH ARMSTRONG A1 EPOXY RESIN WITH ACTIVATOR A.
WIRE #24 AWG ENAMELED SINGLE COTTON COVERED MAGNET WIRE FROM GAGE TO GAGE AND #24 AWG SOLID VINYL INSULATED FROM GAGES TO CONNECTOR.
STRAIN GAGES 1 5/8" LONG AND 5/16" WIDE.

Figure 33. Pile hammer load cell.

Each of the three separate eight-gage bridges contained in the cell was made up of four active and four compensating gages. The purpose of this arrangement was to allow each bridge to contain active gages spaced at 90° intervals around the cell interior, thereby providing a strain-averaging effect in the event of any eccentric impacts. Three bridges were installed in the cell as a precaution against down time in the event of a gage failure, as only one bridge was used at any given time.

Gages and leads were bonded to the internal cell surface with Armstrong A1 epoxy resin with Activator A. The surface of this first cell was prepared for gage application by roughing with emery paper and thorough cleaning with acetone. In the subsequent gage applications to this cell, and also to the second cell, the surface was prepared by sandblasting and then again using acetone as the cleaning and degreasing agent. The resin was cured after gage application by placing a heater blower in the open end of the cell and heating the entire unit to approximately 200 F. The internal cell wiring was with No. 24 AWG enameled, single-cotton-covered magnet wire from gage to gage, and No. 24 AWG solid vinyl insulated wire from gages to cell connectors. The extension lead running from the cell connector to the recording equipment was Belden 8404, four-conductor shielded. This lead and the two accelerometer leads were enclosed in a 1-in. diam steel-reinforced plastic sheath from driving assembly to instrument van.

The first load cell was taken to the University of Illinois for calibration on the University's 3,000,000-lb Southwark-Emery universal testing machine (Fig. 34). Strains were read from a Hathaway Instrument Co. RS-20C, 12-channel strain indicator and recorded manually. The calibration procedure consisted of first cycling the setup from 0 to 2,000,000 lb twice, and then applying loads in 100,000-lb increments to 3,000,000 lb. Strain on each of the three bridges was recorded at each increment of load. At the completion of these concentric loadings, a check was performed to determine the response to eccentric loads. This was accomplished by inserting a 2- by 2- by 20-in. square steel bar between the loading head and the top of the cell, and positioning the bar so that its longitudinal centerline was located in relation to the cell centerline as shown in Fig. 35. Six such positions were checked and in each case the load was applied only to 500,000 lb, with the results shown.

After bond failure of the gages in the first cell (described later) and subsequent regaging, the cell was check-calibrated on Michigan State University's Tinius-Olsen 300,000-lb capacity testing machine. This check calibration consisted of applying loads in 20,000-lb increments to

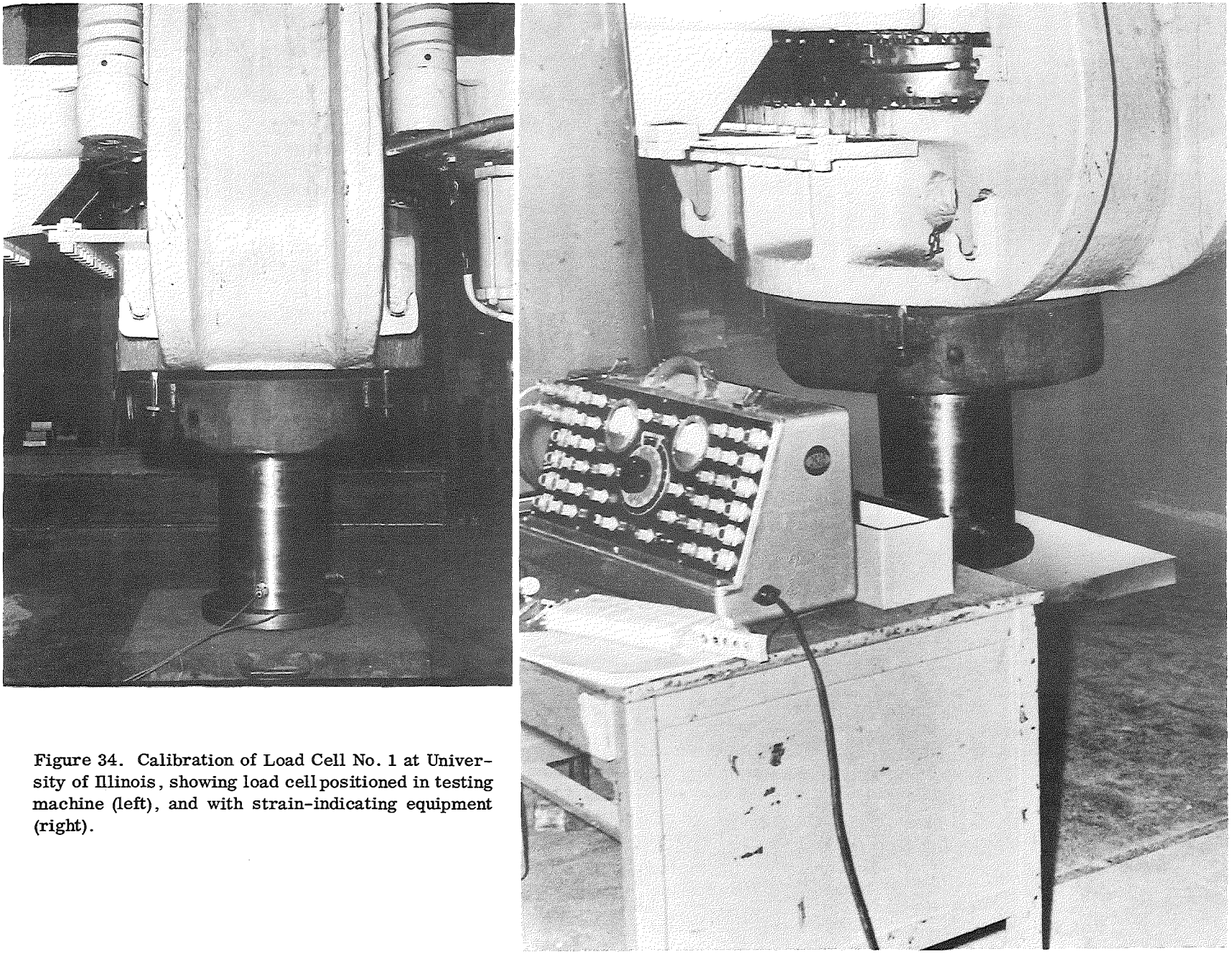

Figure 34. Calibration of Load Cell No. 1 at University of Illinois, showing load cell positioned in testing machine (left), and with strain-indicating equipment (right).

a total load of 300,000--the testing machine's maximum capacity. The load-strain relationship thus determined was then checked and found to be linear and slightly more sensitive than in the first gaging. On the basis of the demonstrated linearity, it was assumed that some extrapolation would be reasonable and consequently the unit was placed back into operation. However, after completing fabrication of the second or standby cell, it was taken to Illinois and calibrated in the same manner as in the first calibration of the first cell. Fig. 35 shows the results of all calibrations including the check on eccentric loadings.

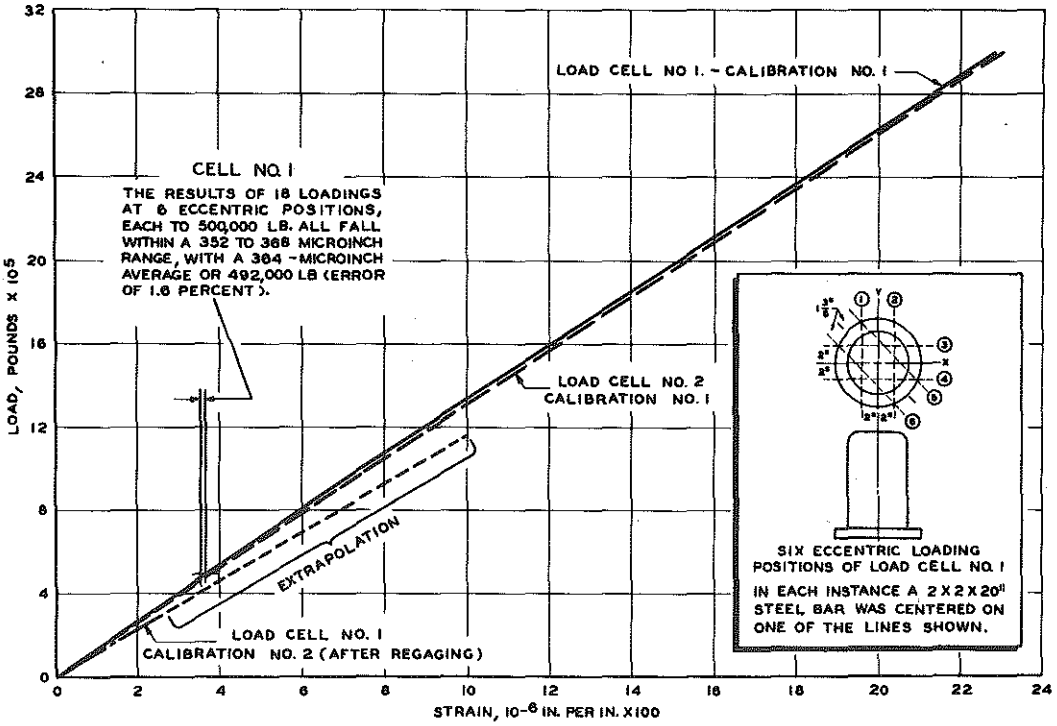

Figure 35. Load cell calibration curves.

Some readers may ask whether a static calibration for a load transducer is valid when that transducer is to be used in measuring dynamic loads. The answer is yes, providing: 1) that the transducer is properly designed, and 2) that properties of the material of which it is fabricated are not altered by dynamic loading.

Proper transducer design requires selection of material and configuration ensuring that the elastic limit is not exceeded. The load cells were made using a very tough steel, machined into a configuration (Fig. 33) minimizing stress concentrations, and requiring a force of 6,000,000 lb to reach its elastic limit. The greatest force applied during the field

work, however, was only 1,500,000 lb (about 25 percent of the elastic limit). This application itself was not part of regular test driving, but occurred during a special study of force transmitted to the load cell by the hammer with the driving cap and cushion removed (Chapter 8). Further, proper transducer design requires placement of measuring strain gages, properly temperature compensated, in series with the applied force (as described earlier and also shown in Fig. 33). Finally, the design must by characterized by a high natural frequency and low mechanical hysteresis. The cell's natural frequency under this study's support conditions (fixed at both ends) was about 5000 cps, and low mechanical hysteresis is characteristic of the steel used in its fabrication.

Regarding the second of these considerations, possible modifications of the cell materials' static properties under dynamic loading include the following:

a) increase in ultimate strength
b) increase in yield strength
c) apparent lack of ductility at very high strain rates
d) delay of initiation of yielding
e) rise in the entire stress level of the stress-strain curve, in the region above the elastic limit, at very high strain rates.

Of these possible property changes, the last is the only one that might affect load cell accuracy. However, this characteristic, like the other four, becomes significant only when approaching or exceeding the elastic limit of the material being loaded. Since the elastic limit was never approached during this study, none of these possible modifications appear to apply.

One final point may be noted regarding dynamic loading as performed in this study. In this report, dynamic force being measured by the load cell is often referred to as "impact." This word may raise some question regarding use of static calibration. However, by the usual technical definition, an impact occurs when load is applied to a structure (load cell) in a time less than half the period of the fundamental frequency of vibration of the structure. For the load cell, any applied load properly to be termed an impact must occur in less than 0.0001 sec. None of the dynamic forces recorded during this study occurred that rapidly.

A number of problems were encountered in field use of the first cell, because the severity of the environment had been underestimated. The load cell, accelerometers, deflectometers, and lead wires had to function

in an atmosphere of oily steam, fuel oil, low temperature, and considerable rain, snow, ice, and mud, in addition to being subjected to large accelerations and forces.

To overcome these environmental conditions and thereby prevent field failures, it was necessary to make some equipment modifications and to provide as much protection as possible during driving. This included encasing the extension leads in a weatherproof sheath, placing a polyethylene sheet skirt on the load cell, wrapping all connectors, and sealing the opening in the bottom of the load cell. In addition, at the end of each day's driving the load cell was placed under a specially built plastic-covered frame with a heater in its open end to dispel any moisture accumulated during the day's operations.

The failure of the first cell resulted from bond fatigue between the epoxy resin and the cell wall. In removing and examining the gages and wiring after the failure, it was concluded that acceleration-induced forces on the combined mass of gage wiring and resin had been the cause. The wiring required for the 24 gages and 3 bridges, along with the resin necessary to bond all of this wiring to the cell wall, probably amounted to 1/2-lb or more. After submitting this mass to 200- to 400-g accelerations 300,000 to 400,000 times, the failure is understandable.

After determining the type of failure that had occurred it was decided that no advantage would be gained from multiple bridges in the cell, since with this type of failure, if one bridge is destroyed the others are destroyed as well. Consequently, when the cell was re-instrumented only one bridge was installed.

Since a load cell is not normally included in a driving assembly, question arose regarding its possible effect on blow count. In an attempt to answer this question, TP 13, a Belleville H-beam pile, was driven to refusal by the Delmag D-12 hammer with the load cell and universal driving cap removed. This pile's blow count record was then compared with those of eight other H-beam piles driven at the same site with the same hammer, but with load cell and driving cap in place.

Fig. 36 indicates that the load cell had no consistent or significant effect on blow count at any elevation. However, in spite of this obvious qualitative indication, statistical tests were performed for further verification. These tests indicated that the degree to which the load cell absorbed energy was well within the limits of experimental error encountered on the project. Indeed, the similarity of blow counts for piles

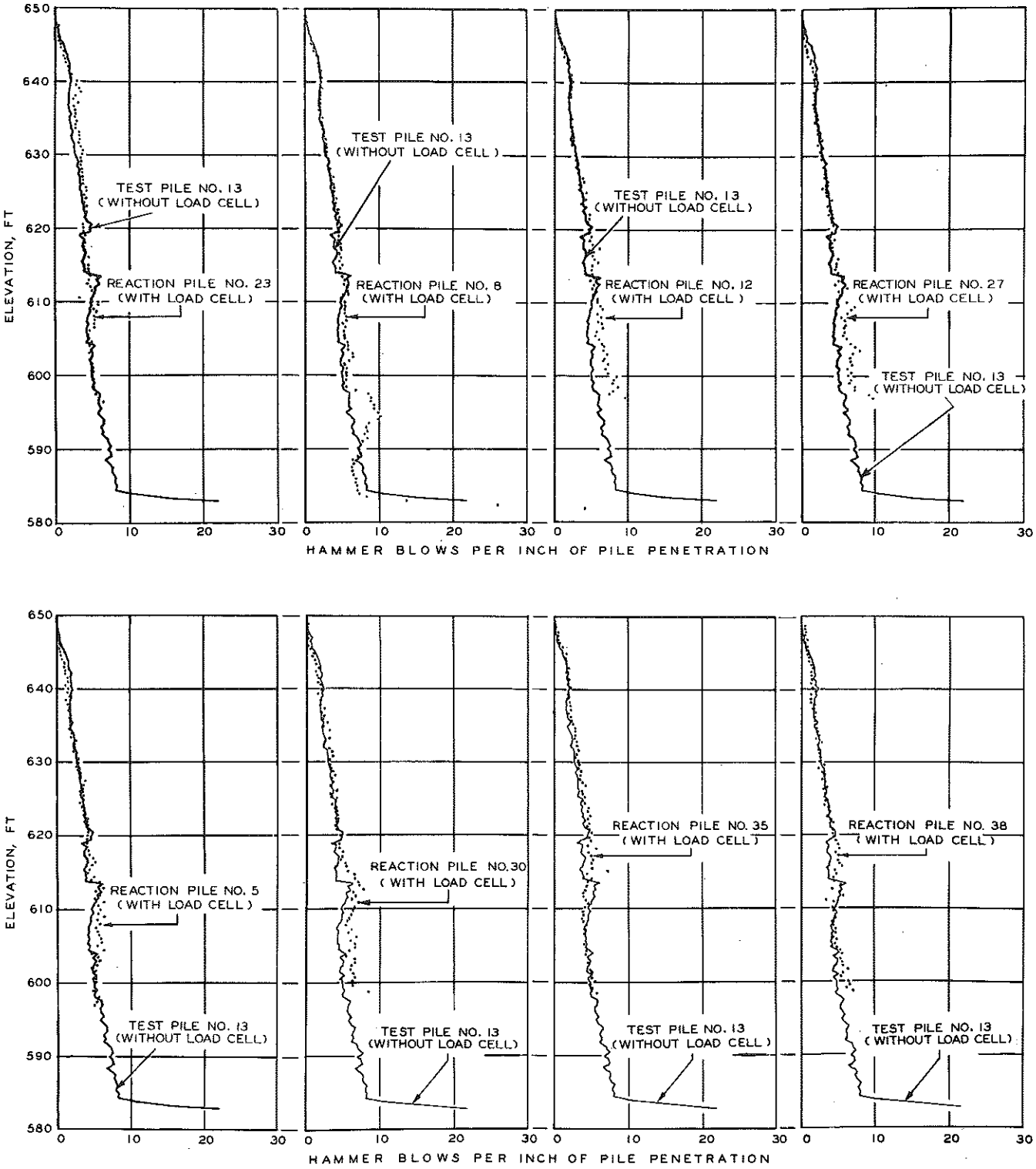

Figure 36. Influence of presence or absence of load cell on pile penetration resistance (Delmag D-12 driving Belleville H-piles).

driven with and without load cells seems noteworthy (either in terms of statistical tests or the appearance of the Fig. 36 profiles), particularly considering the variations in soil resistance and hammer operation that would be expected for a selection of nine piles.

Accelerometers

Three different accelerometer models were used, one 250-g (No. A69TC-250-350) and two 500-g (A69TC-500-350 and A5-500-350), all manufactured by the Statham Instrument Co. Initially, it was planned to

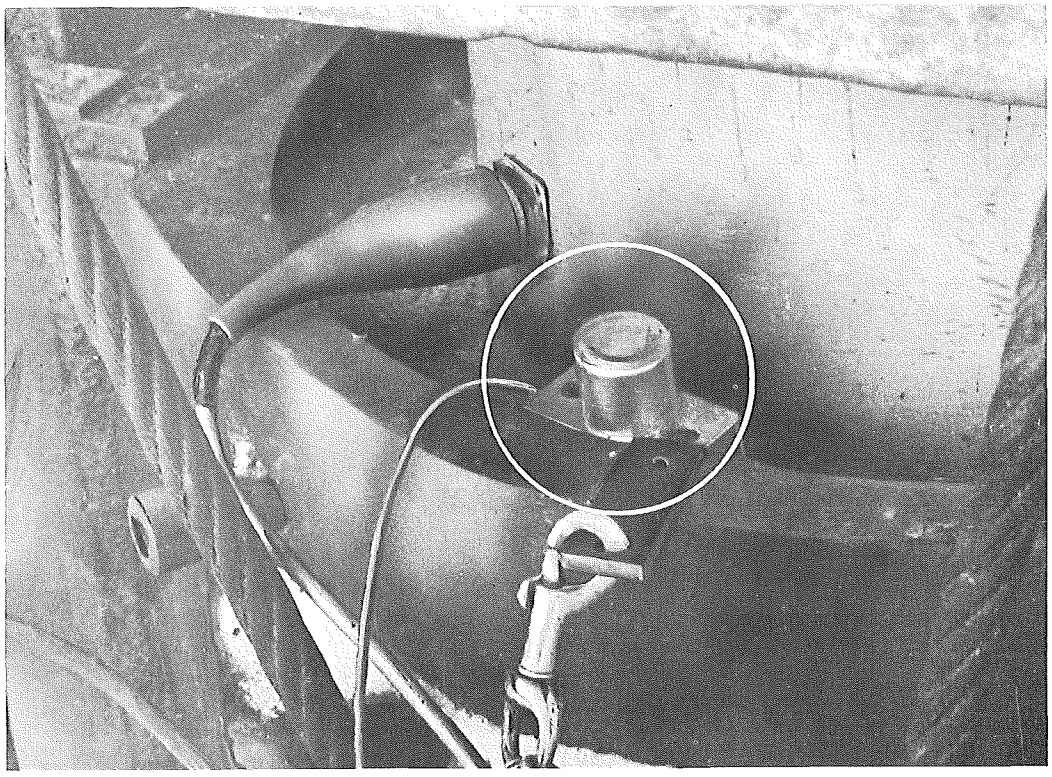

Figure 37. A 500-g accelerometer (enclosed in aluminum housing) mounted in position on a load cell ring.

mount accelerometers on the hammer body, on the hammer ram where possible, and at the top of the pile, but due to internal failures of the A69 models and procurement difficulties it was never possible to have more than one accelerometer, which was located at the top of the pile, in operation at any given time (Fig. 37). Of the models used, the A5-500-350 was found to be the most durable and satisfactory. Also, a field problem was encountered in keeping the units firmly mounted, since the anchoring bolts tended to loosen under the high acceleration impacts.

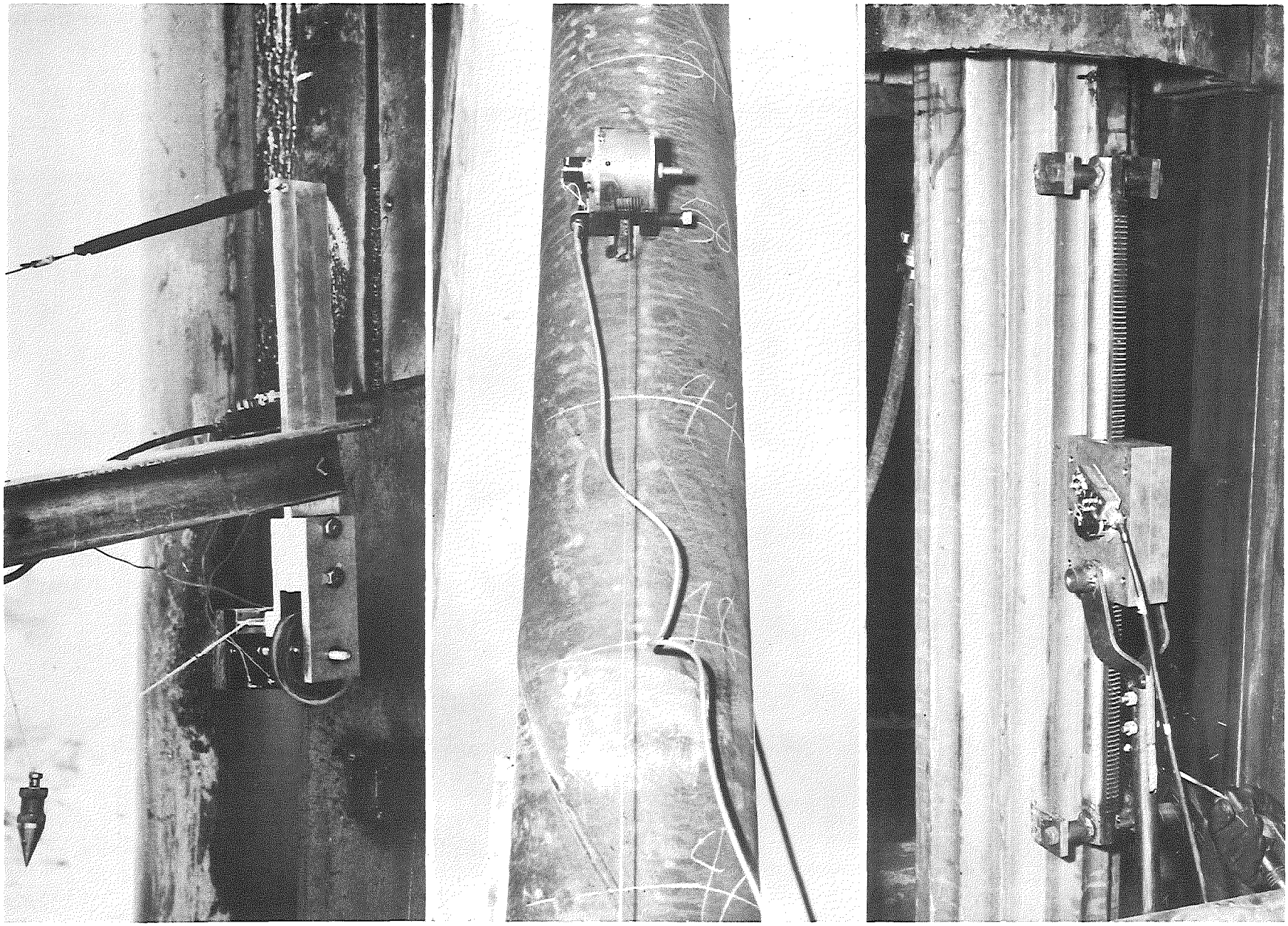

Figure 38. Deflectomer types used included No. 1 (left), No. 2 (not shown), No. 3 (center), and No. 4 (right).

Whenever a transducer such as an accelerometer is used, question arises as to the fidelity of the output amplitudes and waveforms, as compared with the amplitudes and waveforms of the input. To answer this question for this study, it was necessary to obtain solutions to the appropriate differential equation of motion. Response solutions were obtained for the two 500-g accelerometers, for single, half-wave triangular and sine pulses of 100- to 1000-cps frequencies in 100-cps increments (Table 4). No corrections for time lag were applied in the computation of energies. The time offset corrections for the trace readings would be approximately 0.005 and 0.010 in. for the triangular and sine wave pulses, respectively.

Deflectometers

The initial goal was to obtain a device that would give a continuous signal of pile movement during driving, from which to deduce temporary elastic compression of pile and soil and permanent set, for each hammer blow. This would allow a permanent record to be taken at any elevation without stopping the hammer. This goal was not fully achieved.

TABLE 4
TIME LAG AND
AMPLITUDE ATTENUATION
OF ACCELEROMETER RESPONSE

Input Frequency, cps	Response Amplitudes, percent of input			
	Accelerometer A5-500-350*		Accelerometer A69TC-500-350*	
	Triangular Pulse	Half-Sine Wave Pulse	Triangular Pulse	Half-Sine Wave Pulse
100	98.6		99.2	
200	97.7		99.0	
300	96.4		98.5	
400	95.3	No Significant Attenuation	98.0	No Significant Attenuation
500	94.1		97.6	
600	93.0		97.2	
700	91.9		96.8	
800	90.7		96.3	
900	89.5		95.8	
1000	88.2		95.4	

* Time lag found to be constant without regard to frequency or shape of input pulse: 0.0002 sec for the A5-500-350 and 0.0001 for the A69TC-500-350.

The first unit built (Fig. 38) was a rubber-tired wheel which was spring-loaded against the edge of the pile, and which would rotate as the pile moved downward. The axle of this wheel was connected to the shaft of a rotary variable resistor whose electrical resistance changed with shaft position. The unit was checked for linearity in the laboratory and then check-calibrated in the field. It proved unsatisfactory for the following reasons: a) lateral movement of pile sections during driving was sufficient to knock the wheel out of contact with the pile; b) unless the surface of the pile was clean and dry the wheel would not follow its movement, but would slip; c) after increasing the spring tension to overcome the slipping, the pile movement crushed the pressed steel wheel or destroyed the rubber contact surface of the solid steel wheel; and d) the accelerations of the contact arm on the

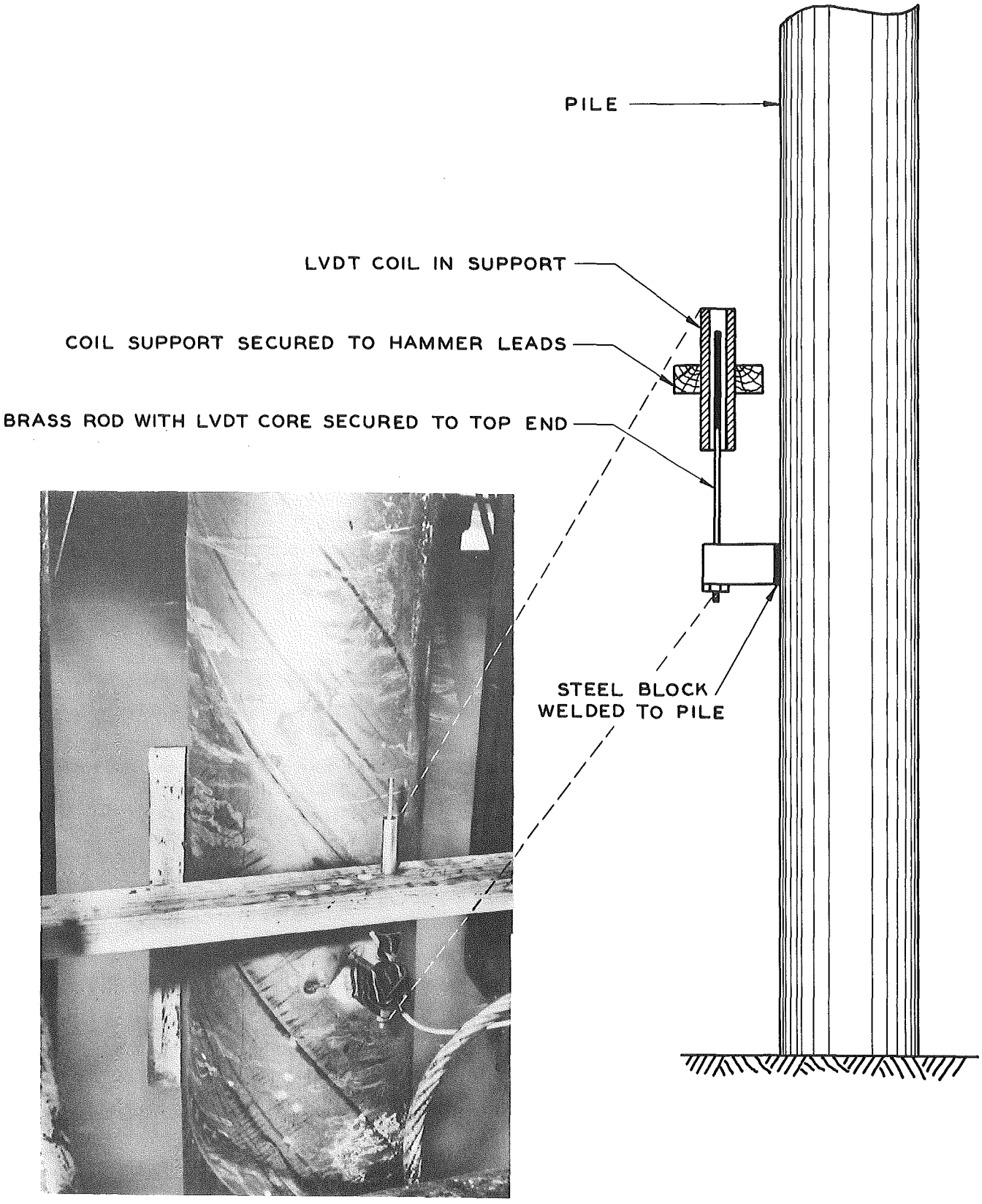

Figure 39. Deflectometer No. 5 (LVDT).

laboratory-built variable resistor were high enough to cause the arm momentarily to lose contact with the resitance wire.

The second deflectometer was a modification of the first. It consisted of a cable, secured to the pile and then wrapped around a rotating drum, with the other end connected to a spring load. When the cable end was secured so that downward pile movement caused the drum to unwind, the drum's momentum would cause it to overshoot. When the cable was secured so as to take-up during downward pile movement, the drum inertia would allow the cable to slacken, and thus again distort the record. This device would therefore give an accurate record of net deflection only, and consequently it was also abandoned.

The third deflectometer (Fig. 38), represented an improvement over the second. This unit consisted of a cylindrical steel case housing a spring-loaded cable take-up drum. The drum was fabricated from aluminum to reduce the inertial effects, and a commercially available, high-quality rotary variable resistor was procured. This device also proved a complete failure. When the drum was secured to the ground and the cable was fastened to the pile, the inertia of the drum was such that it would give only net pile deflection (or "set"). When the drum was secured to the pile and the cable secured to ground, the instrument was destroyed, breaking the steel case and the mounting clamps.

For the fourth device (Fig. 38), the measurement goals were modified in that the unit was designed to give continuous deflections over only a 2-ft length of pile. This device was a rack and gear assembly, with the two ends of the rack welded to the pile and the gear box secured to the ground. Therefore, as the rack moved down with the pile it caused a rotation of the gear and this in turn rotated the rotary variable resistor. This instrument proved unsatisfactory. It was nearly impossible to keep the base, which supported the gear, from moving and thereby distorting the deflection data recorded.

The fifth and partially successful unit was based on a commercially available linear variable differential transformer (LVDT). The particular model used was a Sanborn Co. Model 585 DT 1000 "Linearsyn." This type of transducer (Fig. 39) consists of a cylindrical tube-type transformer with the primary and secondary wound concentrically and a separate coaxially mounted movable core. As its core position changes it varies the coupling between the primary and secondary, with the magnitude of the secondary electrical output being a linear function of the core position.

This device's advantage was in presenting no inertial or acceleration-induced force problems. There was no physical connection between coil and core, and the core, which was mounted on the pile, was extremely light.

This unit gave an excellent signal of dynamic deflection, but was limited to a total pile movement range of only 2 in. Because of the device's extremely short linear range, it was necessary to stop the driving operations each time a force-acceleration-deflection record was to be taken. After stopping the hammer, the core mounting block was welded to the side of the pile approximately 3 ft above the ground, and the transformer, which was secured to a support fastened to the hammer leads, was placed over it so that the full throw of the device would be usable. The hammer was started and a permanent record was taken during the next 2 in. of driving. Then the hammer was stopped and the core and mounting block removed before driving resumed.

The unit was calibrated at the start of each day's operation and then check calibrated at various times throughout the day. This was accomplished by a small laboratory-built calibrator to which the LVDT core was securely mounted, and which incorporated a 0.001-in. dial gage to indicate coil displacements. After positioning the core in the coil and fastening it to the dial gage stem, it was then displaced through measured distances and the recording oscillograph galvanometer displacement was adjusted to give the desired ratio of core-to-galvanometer movement.

Oscilloscope Monitor

Dynamic driving information was monitored at all times, to allow detection and permanent recording of any unusual occurrences or conditions at points other than the predetermined sampling elevations, and to detect transducer malfunctions. This was accomplished by paralleling the separate outputs of the load cell, accelerometer, and deflectometer to a Model 122A Hewlett-Packard oscilloscope (Fig. 31). This made it possible to display any one of these three signals on the face of the scope tube.

RECORDING SYSTEMS

Automatic Trace Recording

Two different recording systems were used for dynamic force-acceleration-deflection data. At Detroit and Belleville, a Hathaway

Instrument Co. system was used (Fig. 40), consisting of an S8-B recording oscillograph with Type OA-2, Group 27 galvanometers (frequency response flat ± 2 percent to approximately 750 cps and flat ± 5 percent to approximately 1000 cps), and a Type MRC-17 control unit with Type MRC-15C carrier amplifiers. This system had certain limitations and was subject to periodic malfunctions. Its maximum chart speed of 40 in. per sec

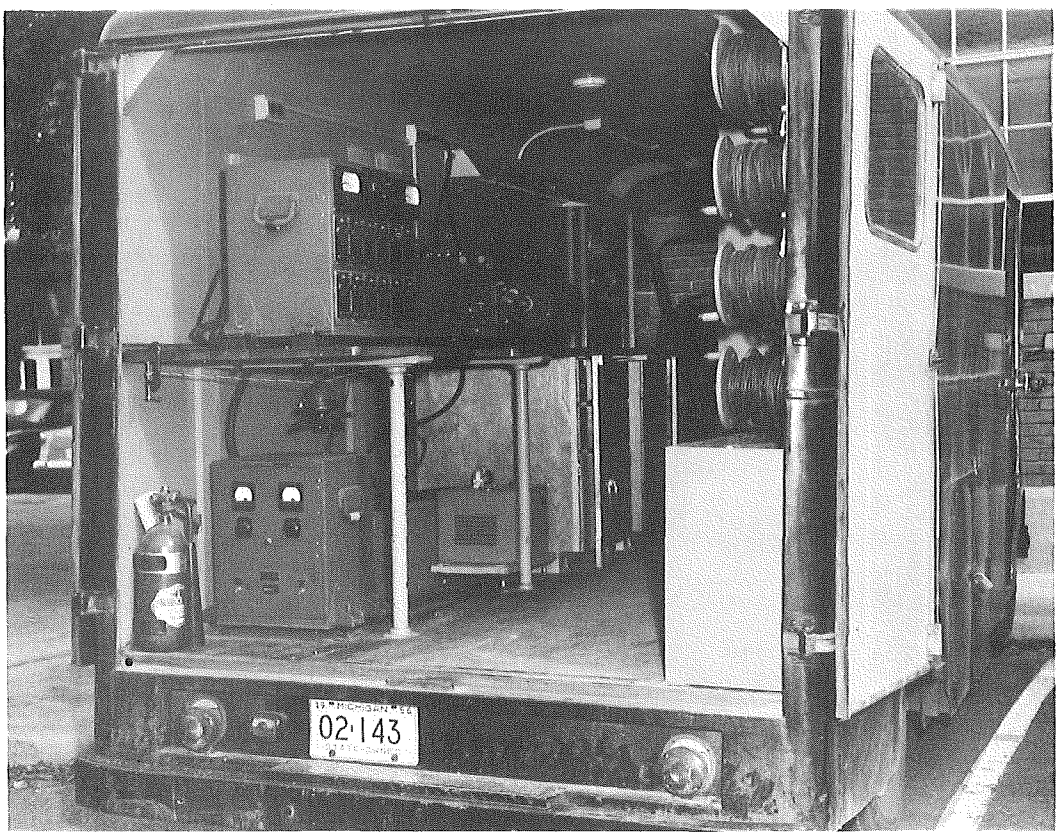

Figure 40. Hathaway recording system as used at Belleville and Detroit.

was not fast enough to spread the data adequately from a hammer blow lasting only a few hundredths of a second. In addition, the system was not direct writing, and photographic development of traces was required before they could be examined to determine whether the data were being recorded properly and to detect malfunctions.

The first system was replaced at Muskegon by a Minneapolis-Honeywell Co. Model 1108 Visicorder oscillographic recorder with M1650 galvanometers (frequency response flat ± 5 percent to 1000 cps), using 119B carrier amplifiers (Fig. 31). In this case, the maximum chart speed was 80 in. per sec and was direct writing at the discretion of the

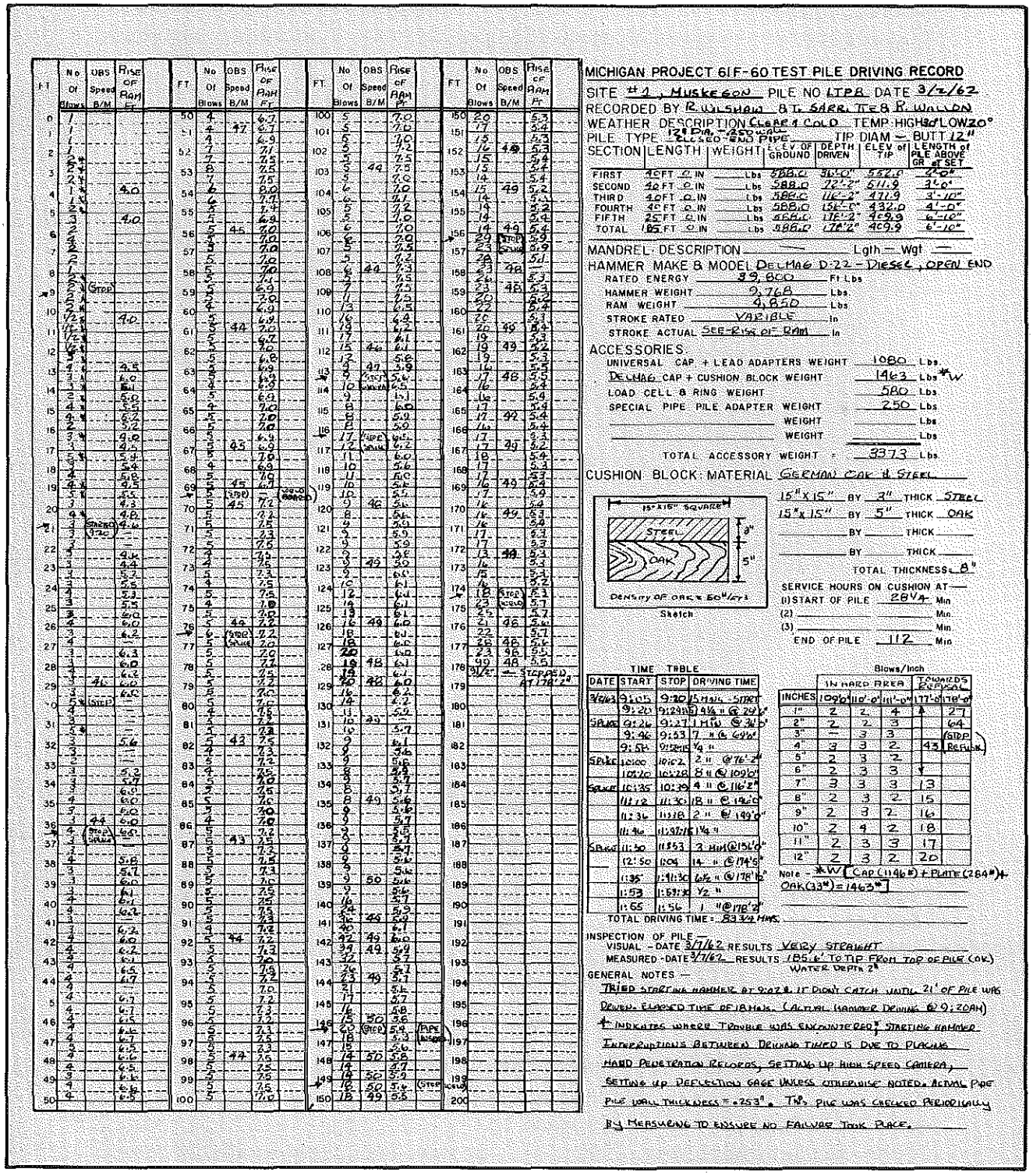

MICHIGAN PROJECT 61F-60 TEST PILE DRIVING RECORD

SITE #1, MUSKEGON PILE NO LTP8 DATE 3/2/62

RECORDED BY R. WILSHAW & T. SARR. TF & R. WALDEN

WEATHER DESCRIPTION CLEAR & COLD TEMP HIGH 30° LOW 20°

PILE TYPE 12¾ DIA. - .250 WALL - CLOSED - END PIPE TIP DIAM — BUTT 12"

SECTION	LENGTH	WEIGHT	ELEV OF GROUND	DEPTH DRIVEN	ELEV OF TIP	LENGTH of PILE ABOVE GR AT SET
FIRST	40 FT 0 IN	Lbs	586.0	360"	562.0	24'0"
SECOND	40 FT 0 IN	Lbs	588.0	72'2"	511.9	3'0"
THIRD	40 FT 0 IN	Lbs	588.0	116'2"	471.9	3'-10"
FOURTH	40 FT 0 IN	Lbs	588.0	156'2"	432.0	4'-0"
FIFTH	25 FT 0 IN	Lbs	466.0	176'2"	409.9	6'-10"
TOTAL	185 FT 0 IN	Lbs	586.0	176'2"	409.9	6'-10"

MANDREL DESCRIPTION — Lgth — Wgt —

HAMMER MAKE & MODEL DELMAG D-22 - Diesel, OPEN END

RATED ENERGY 39,800 Ft Lbs

HAMMER WEIGHT 2,768 Lbs.

RAM WEIGHT 4,850 Lbs.

STROKE RATED VARIBLE In

STROKE ACTUAL SEE-RISE OF RAM In

ACCESSORIES.

UNIVERSAL CAP + LEAD ADAPTERS WEIGHT	1080	Lbs.
DELMAG CAP + CUSHION BLOCK WEIGHT	1463	Lbs *W
LOAD CELL & RING WEIGHT	580	Lbs
SPECIAL PIPE PILE ADAPTER WEIGHT	250	Lbs
WEIGHT		Lbs
WEIGHT		Lbs
TOTAL ACCESSORY WEIGHT =	3373	Lbs

CUSHION BLOCK: MATERIAL GERMAN OAK & STEEL

Sketch

15"x15" BY 3" THICK STEEL

15"x15" BY 5" THICK OAK

— BY — THICK —

— BY — THICK —

TOTAL THICKNESS 8"

SERVICE HOURS ON CUSHION AT —

(1) START OF PILE 28V4 Min

(2) — Min

(3) — Min

END OF PILE 112 Min

TIME TABLE

DATE	START	STOP	DRIVING TIME
3/2/62	9:05	9:20	15 MIN. START
	9:20	9:29½	4½" @ 29½'
SPLICE	9:26	9:27	1 MIN @ 36½'
	9:46	9:53	7 " @ 49½'
	9:54	9:58½	¼ "
SPLICE	10:00	10:02	2 " @ 76'2"
	10:20	10:28	8 " @ 109'0"
SPLICE	10:35	10:39	4 " @ 116'2"
	11:18	11:30	18 " @ 134'0"
	11:36	11:38	2 " @ 149'0"
	11:46	11:57½	11¾ "
SPLICE	11:50	11:53	3 MIN @ 154'0"
	12:50	1:04	14 " @ 174'9"
	1:35	1:41:30	6½ " @ 178'6"
	1:53	1:53:30	½ "
	1:55	1:56	1 " @ 178'2"

TOTAL DRIVING TIME = 83 3/4 MIN.

Blows/Inch

INCHES	IN HARD AREA 109'0"	110'-0"	111'-0"	TOWARDS REFUSAL 177'-0"	178'-0"
1"	2	2	4	4	27
2"	2	2	3		64
3"	—	3	3		(STOP
4"	3	3	2	43	RESUME)
5"	2	3	2		
6"	2	3	3	1	
7"	3	3	3	13	
8"	2	3	2	15	
9"	2	3	2	16	
10"	2	4	2	18	
11"	2	3	3	17	
12"	2	3	2	20	

Note - *W [CAP (1146#) + PLATE (284#) + OAK (33#) = 1463#]

INSPECTION OF PILE —

VISUAL - DATE 3/7/62 RESULTS VERY STRAIGHT

MEASURED - DATE 3/7/62 RESULTS 185.6' TO TIP FROM TOP OF PILE (OK)

WATER DEPTH 2'

GENERAL NOTES —

TRIED STARTING HAMMER AT 9:02 & IT DIDN'T CATCH UNTIL 21' OF PILE WAS DRIVEN. ELAPSED TIME OF 18 MIN. (ACTUAL HAMMER DRIVING @ 9:20AM)

† INDICATES WHERE TROUBLE WAS ENCOUNTERED. STARTING HAMMER INTERRUPTIONS BETWEEN DRIVING TIMES IS DUE TO PLACING HAND PENETRATION RECORDS, SETTING UP HIGH SPEED CAMERA, SETTING UP DEFLECTION GAGE UNLESS OTHERWISE NOTED. ACTUAL PIPE PILE WALL THICKNESS = .253". THIS PILE WAS CHECKED PERIODICALLY BY HERSCHEDE TO ENSURE NO FAILURE TOOK PLACE.

Figure 41. Typical field pile-driving record sheet.

operator. It was an excellent-performing, trouble-free system, and with the direct writing provision it was possible to examine the dynamic records immediately, ensuring that the desired data had been obtained.

Other Recording Procedures

1. Blow Count with Penetration. Total blows per 6-in. increment of penetration for the entire pile length were recorded manually and automatically, the pile having been measured and marked before driving. At or near the target blow count or elevation, the recording increment was decreased to blows per inch. Manual counts were obtained using a hand-held counter, with the results entered on log sheets of the type shown in Fig. 41 (these logs are tabulated and plotted in App. A, along with log notations of significant occurrences during driving). A continuous automatic record of blow count was taken by a Brush oscillographic recorder (Fig. 42). A technician located near the pile actuated an event marking switch, placing an event mark on the trace record each time a pile increment mark passed into the ground.

2. Blow Count with Time. Blows per minute were recorded manually and automatically, with start and stop times noted so that net driving time and hammer speed could be determined. Occasional spot checks on hammer speed were made manually using a stop watch, and all intervals of actual driving time were noted, with entries for both being made on pile log sheets. The Brush oscillographic recorder traces included a known time base line for continuous determination of blow frequency.

3. Other Trace Notation. In addition to time, penetration, and speed notation on the Brush oscillographic traces (Fig. 42), event marks were also entered to indicate each time that a permanent force-acceleration-deflection record was made on the other oscillographic recording system (Hathaway or Visicorder). Other significant events during operations for each pile were also noted on its trace at the time of occurrence.

4. Pile Deflection. Pile deflections were recorded manually as well as automatically throughout driving. At selected penetrations, driving was stopped so that the manual and automatic deflection recording equipment could be secured to the pile. The manual device used (Fig. 43) consisted of a 1 by 2 ft thin sheet metal backing board attached to the pile, covered with a sheet of pressure sensitive paper, and protected in turn by a transparent acetate cover. A horizontal board positioned in front of this recording sheet was clamped to stakes driven into the ground, and a technician obtained the record by placing a pointed stylus against

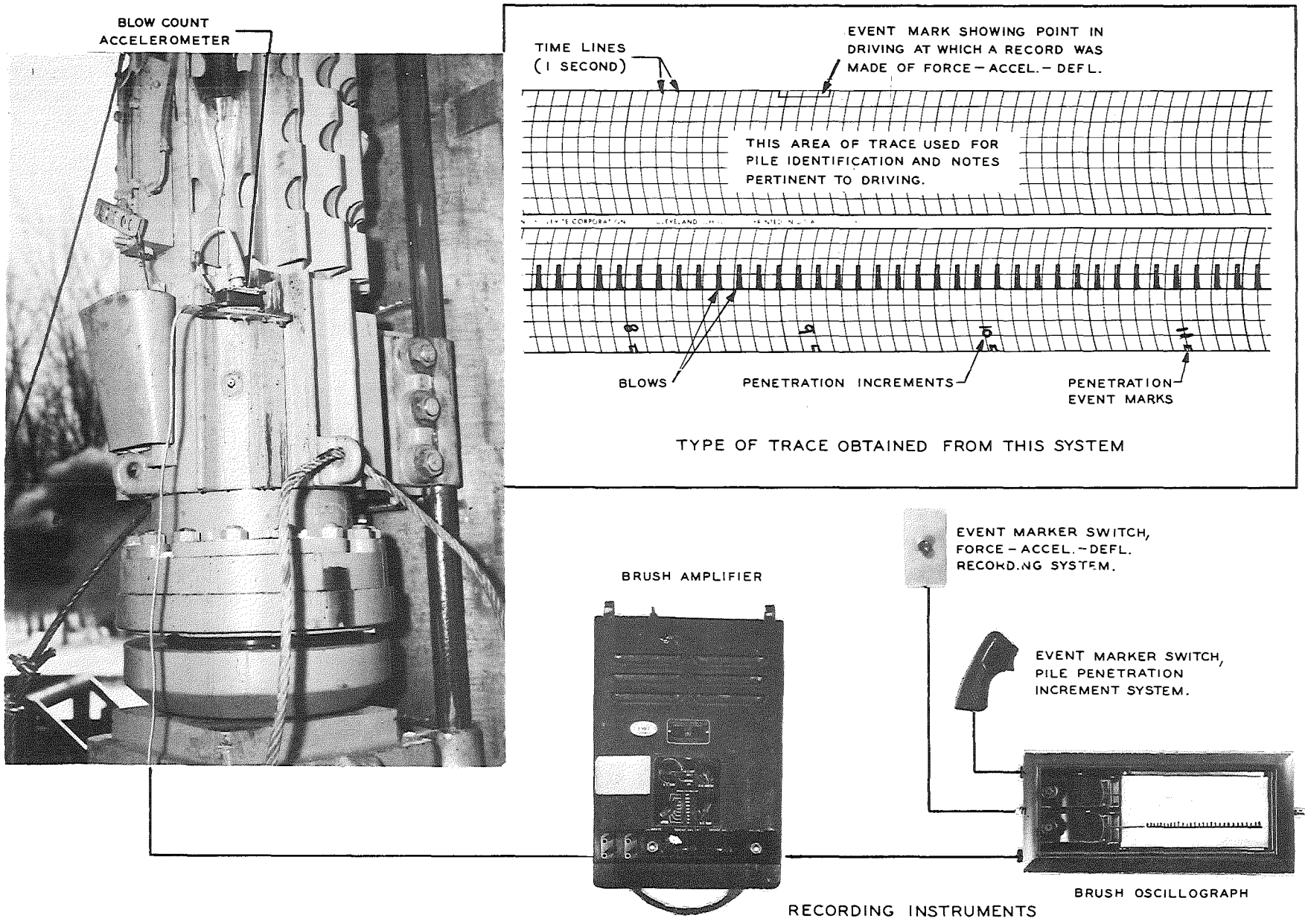

Figure 42. Recording system for blow count in relation to driving time and penetration.

the sheet, resting this stylus on the board, and drawing it slowly from left to right as the pile moved downward. These manual deflection traces included notation of the duration of automatic recording operations.

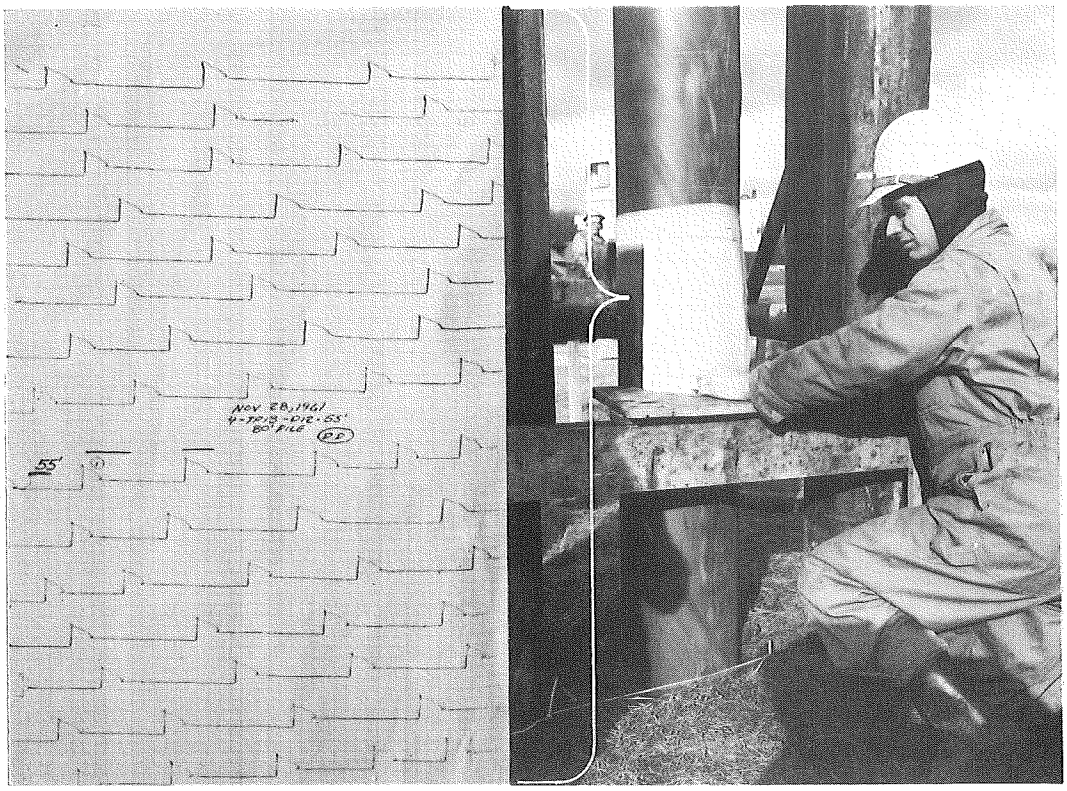

Figure 43. Operator using trace recording assembly for manual deflection record, with resulting trace. The 1 noted on the trace indicates first hammer blow recorded by the automatic recording system. Horizontal bars near 1 indicate simultaneous automatic records.

5. Air or Steam Pressure. Air pressure for the Vulcan No. 1 and steam pressure for the Vulcan 50C, Vulcan 80C, and Raymond 15-M hammers, were recorded from visual observation of a pressure gage mounted on the air or steam receiver. No internal cylinder operation pressures were recorded. In the case of the closed-top diesel hammers, pressure in the bounce chamber was recorded as observed on a positive-acting gage, located at ground elevation and connected to the chamber by an air hose. A gage and a typical chart of bounce chamber pressure vs. equivalent WH energy are shown in Fig. 44.

6. Ram Rise. For the open-top diesel hammers, a continuous record of ram rise was kept by observing movement along an indicator rod mounted on the top of the hammer and marked off in 6-in. increments

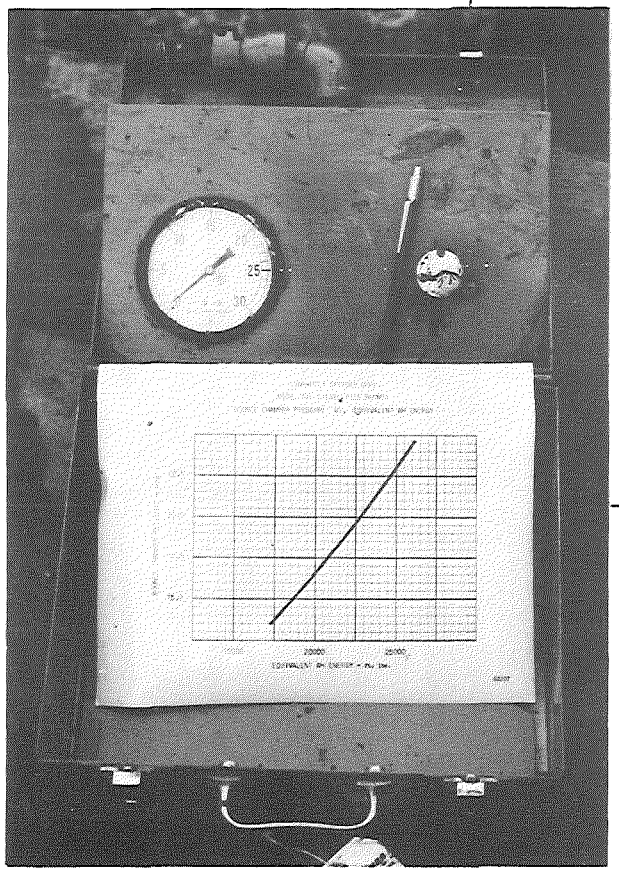

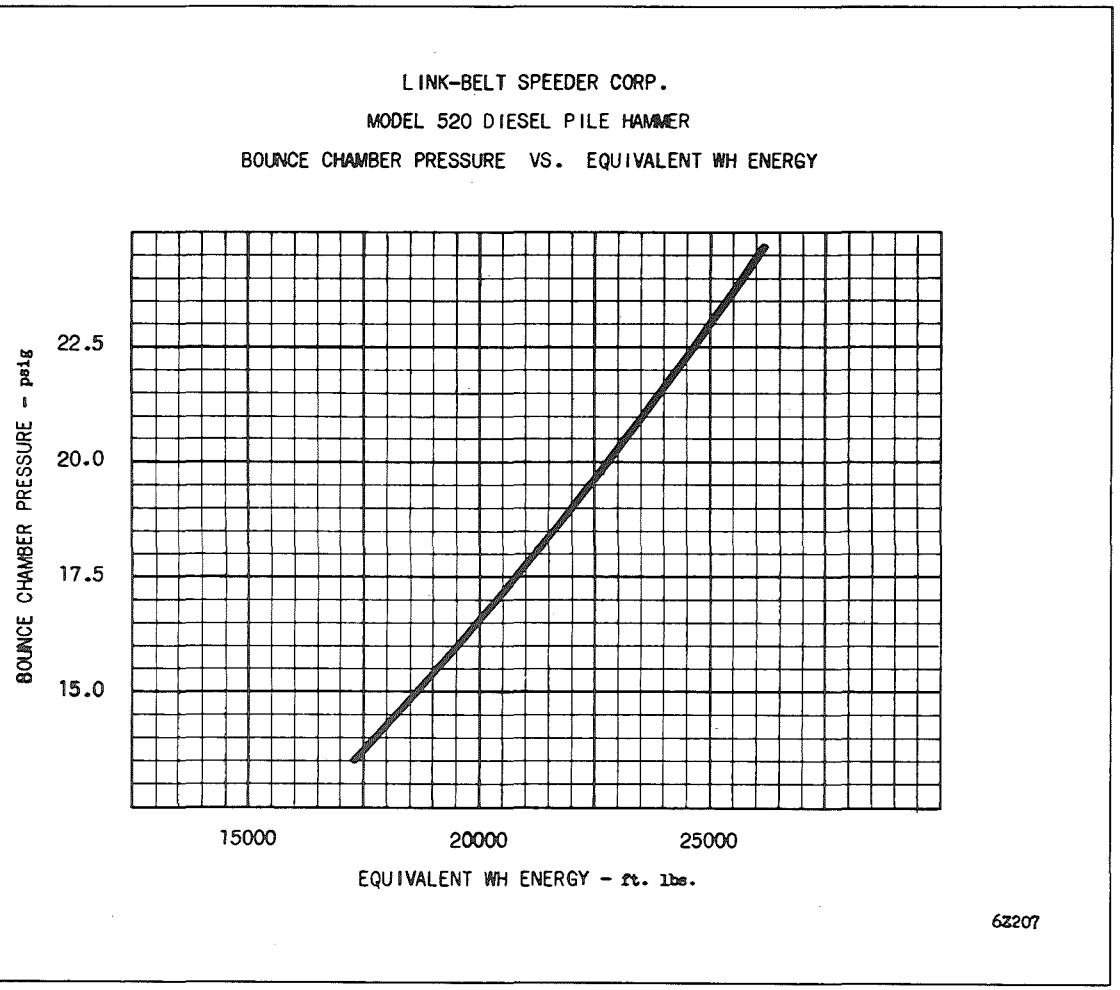

Figure 44. Positive acting gage, with manufacturer's energy chart.

(Fig. 45). The observer verbally relayed this ram rise, through a sound-powered phone system, to a technician or to a tape recorder located in the instrumentation van. These records were later tabulated for each pile driven (App. A).

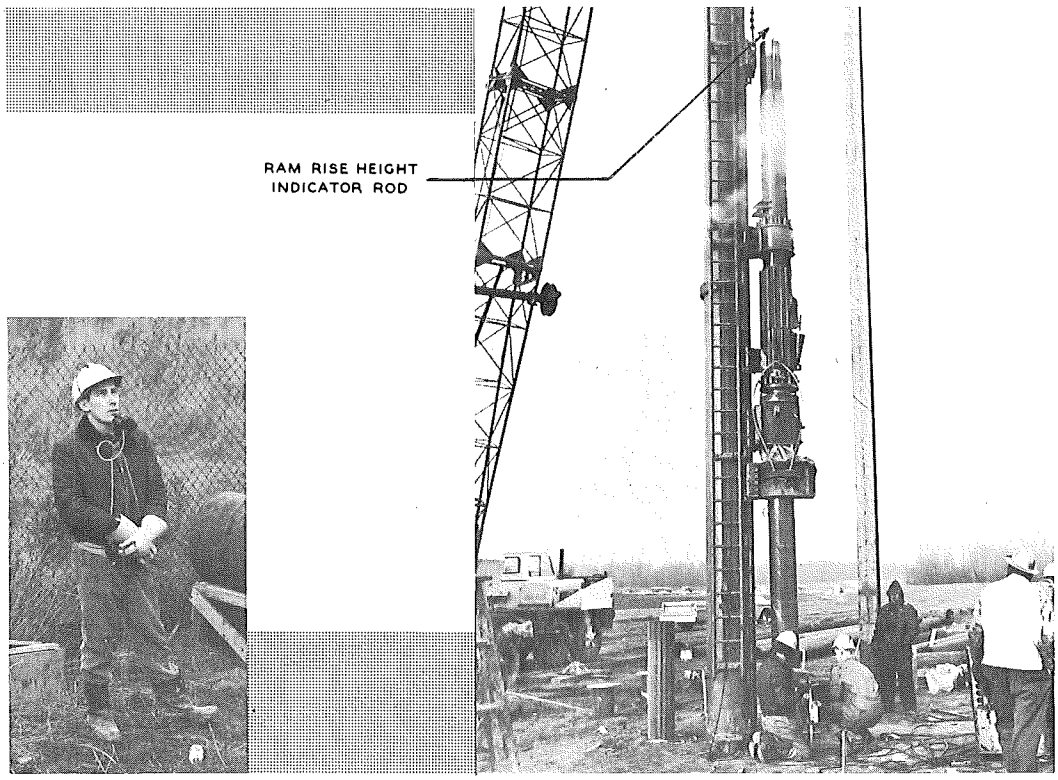

Figure 45. Technician observing and verbally relaying ram rise height to tape recorder.

High Speed Motion Pictures

In conjunction with field operations, arrangements were made to take high speed motion pictures (2200 frames a second) of one hammer, the Vulcan 50C, at Belleville in order to determine, if possible, the causes for the high frequency force peaks shown in this hammer's oscillographic record. It was also hoped that ram velocity might be obtained. However, the limited field of vision and difficulty in obtaining a permanent reference in this field due to operational movement and vibration (in addition to vibration of the ground supporting the camera) gave results that were too erratic to accept quantitatively. Another type of high speed camera operating at either 380 or 550 frames per second was used at Muskegon for six pile hammers, but again the resulting films were unsatisfactory.

CHAPTER FIVE

HAMMER BLOW COUNT

In the following four chapters, hammer characteristics are discussed in terms of the following four successive analytical steps:

1. Hammer blow count per foot of penetration (Chapter 5)
2. Hammer speed in blows per minute (Chapter 6)
3. Pile penetration rate in feet per minute (Chapter 7)
4. Hammer energy as rated by direct measurement during driving (Chapter 8).

Of these, blow count and penetration rate may be considered the major criteria for evaluation of hammer performance. Hammer speed and hammer energy, however, are also important characteristics of hammer performance. Evaluation for the first of these steps involved statistical analysis of automatic (oscillographic) trace records and manual count records. For the second, trace records were interpreted graphically. For the third, statistical analysis was performed on data resulting from the measurements for blow count and speed. In the fourth, load cell force traces and accelerometer traces were analyzed mathematically.

Selection of Usable Blow Count Data

An intial problem in preparing for these analyses was identification of those particular increments of time and penetration during test operations when data were unavailable or certain conditions rendered the data questionable, because of: 1) hammer operational factors (usually starting problems in soft soils and cold weather), 2) incomplete or unsatisfactory records of pile and hammer performance, or 3) the absence of driving records for the initial depth of soil pre-excavation (as at Belleville). Fig. 46 for H-piles at two sites and Fig. 47 for pipe piles at all sites, indicate those penetration ranges for each pile where data could reasonably be sampled and evaluated for Chapters 5, 6, and 7. It should be noted, however, that data for analysis of hammer energy was selected on a different basis, as is discussed in Chapter 8.

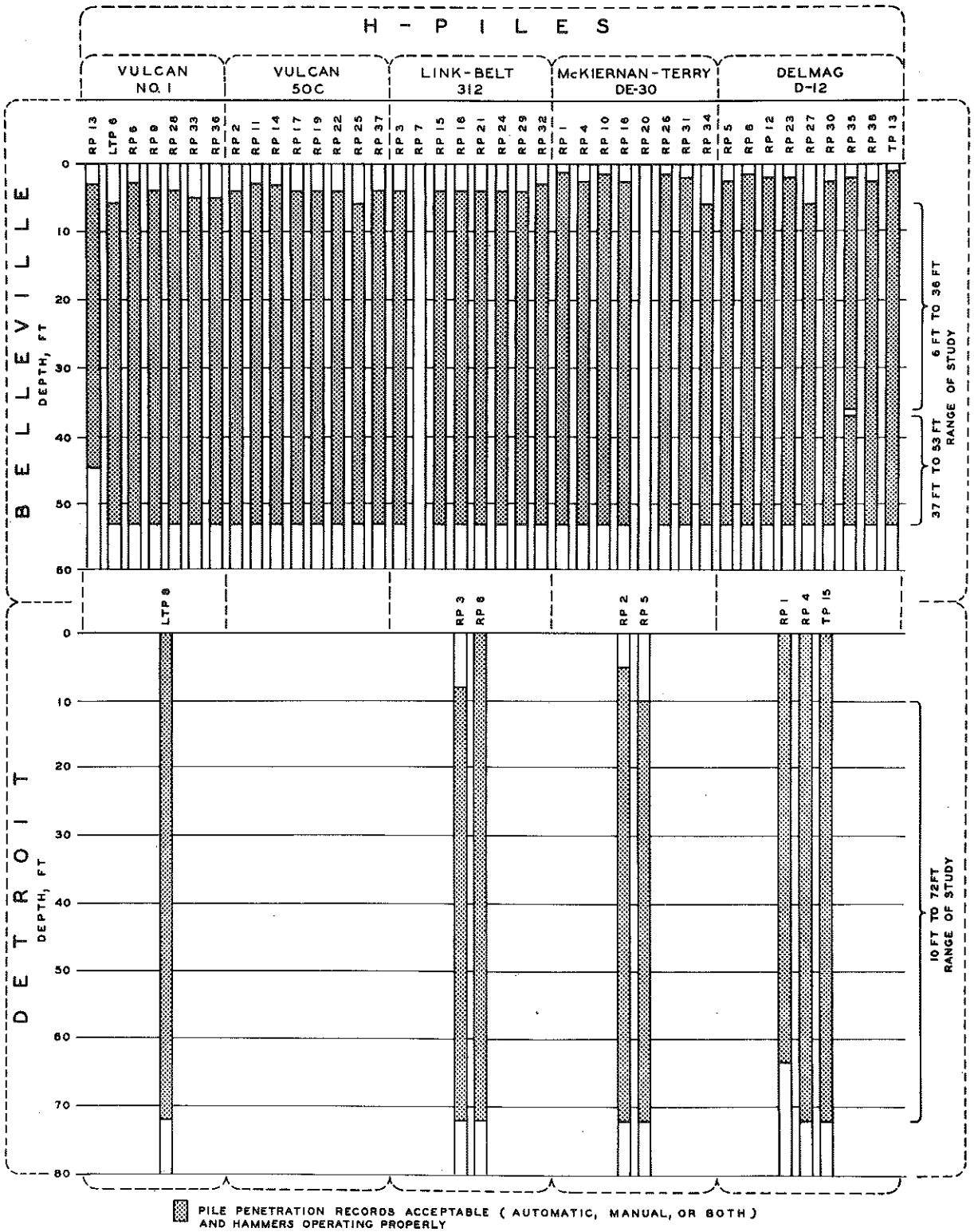

Figure 46. H-pile penetration increments used for hammer performance analysis. Omission of penetration increments in most cases indicates faulty operation of hammers, and less frequently, incomplete driving records. Note arbitrary data cutoff at 53 and 72 ft for Belleville and Detroit, respectively, due to unequal final penetrations.

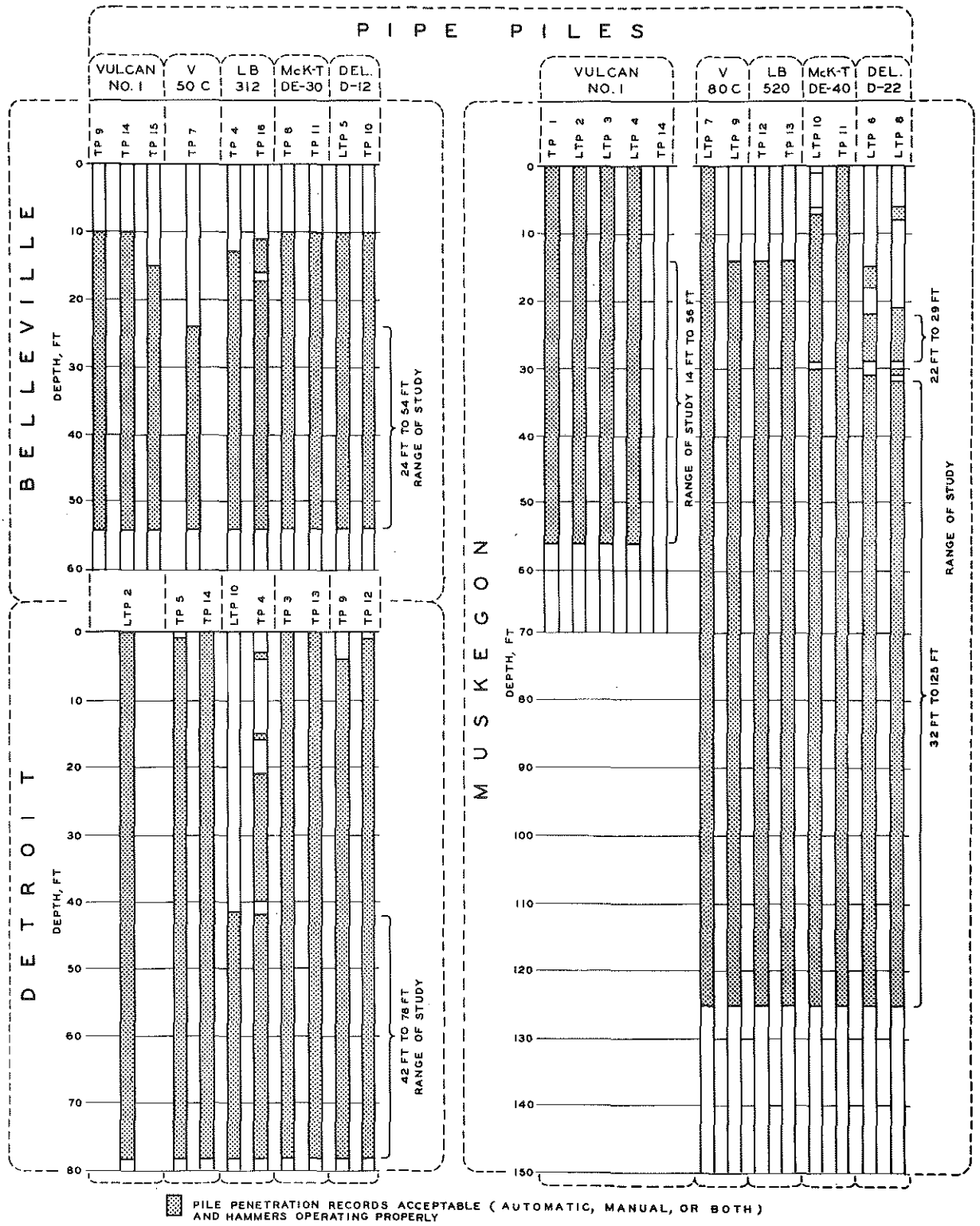

Figure 47. Pipe pile penetration increments used for hammer performance analysis. Omission of penetration increments in most cases indicated faulty operation of hammers, and less frequently, incomplete driving records. Note omission of top 10 ft for all Belleville pipes (soil pre-excavated), and arbitiary data cutoff at 54, 56, 78, and 125 ft at various sites, due to unequal final penetrations.

Blow count is an easily obtained and readily handled index of hammer driving ability. Moreover, it is used in estimating set during the last increment of pile penetration and provides a key term for most dynamic pile capacity formulas. However, if the energy used in such formulas does not parallel actual hammer energy performance as determined by blow count, then computation of pile capacity by a dynamic formula will depend on which hammer is used to penetrate to a given depth. For example, using blow counts for two hammers with nearly the same manufacturer's rated energy, at the same pile penetration level in Belleville soil, the following data would be obtained:

Hammer	H-Piles	Avg. Blow Count* (52 to 53 ft)
Vulcan No. 1 (15,000 ft-lb)	LTP 6, RP 6, RP 9, RP 28, RP 33, RP 36	123 blows/ft
Vulcan 50C (15,100 ft-lb)	RP 2, RP 11, RP 14, RP 17, RP 19, RP 22, RP 25, RP 37	79 blows/ft

* Averaged across the site to eliminate biasing due to soil differences.

Then, assuming the Engineering News Formula to be applicable,

$$R_d = \frac{2\ E_n}{S + 0.1}$$

where

E_n = manufacturer's rated energy (ft-lb)
S = set or final average penetration per blow (in. per blow)
R_d = computed design pile load capacity (lb)

the capacity computation for the Vulcan No. 1 using this formula would be:

$$R_d = \frac{30,000}{0.0974 + 0.1} = 152,000 \text{ lb}$$

and the capacity computation for the Vulcan 50C also using this formula would be:

$$R_d = \frac{30,200}{0.152 + 0.1} = 120,000 \text{ lb}$$

This example was chosen for its simplicity to illustrate the importance of differences in hammer performance when computing pile capacity by dynamic formulas.

To assess the relationship between rated energy and actual performance, as established by blow count records, some statistical manipulation of the field data was necessary to eliminate the unwanted effects of such extraneous variables as soil variation, hammer and operator performance, cushion block deterioration, and driving procedure.[1] Indeed, at the outset of the analysis it was not known whether hammer and pile type differences would be significant in view of the magnitude of uncontrolled variation encountered.[2]

Ideally, the project objectives would best be answered by statistical tests collectively analyzing the important variables (penetration rate, blow count, hammer type, pile type) to provide estimates of their differences, both singly and in combination.[3] Numerous difficulties were encountered in testing the data and several types of analysis were attempted. Only after considerable effort were adjustments of technique made which allowed satisfactory inferences concerning hammer performance comparisons. In analyzing test performance in terms of blow count, particularly where large-scale testing occurs over a large site area, soil variation (both laterally and with depth) presents considerable problems.

---

1 "Extraneous" in the sense that their contribution to the variable under study (blow count) is of no experimental interest.

2 Uncontrolled variation is inherent in all empirical work and is usually referred to as experimental error. If large enough, this error can obscure differences in the variables under examination. For statistical purposes the variables were presumed to be random even though successive observations were not always independent.

3 Statistical tests most efficiently providing this information are generally termed "analysis of variance tests." For the present case, a three-factor design (designating hammer make, pile type, and penetration as factors) would be appropriate if certain assumptions of the statistical model could be met. These assumptions are usually identified as: independence of errors, additivity of effects, normality of error distributions, and equality of variance of error distributions. In practice, these assumptions are rarely met exactly, and some approximation is within the limits of good practice, although the consequences of violating these assumptions are not entirely known. Early in analysis, it was obvious that pile driving projects would violate the assumptions of the proposed model to a considerable degree. Blow counts were definitely not independent--being correlated serially and between hammers for the penetration range. Interaction charts revealed that the hammer effects were not always additive and error charts indicated a direct functional relationship between blow count magnitude and error variance. By the use of transformations, attempts were made to improve the situation, but with limited success. Another approach (analysis of covariance) was considered, but in addition to the assumptions already mentioned an additional one was violated, namely the equality of regression line slopes. Blow counts and hence R-values increased at different rates for the various hammers, and often for the various piles driven with the same hammer. Another alternative not considered in this project would make use of recent developments in computer programs which provide a regression solution to the problem of unequal cell numbers. However, several of these assumptions are still required.

If sufficient data are available, less powerful non-parametric tests probably provide the best test method by requiring only the assumptions of independence and occasionally distribution symmetry. There is currently no completely satisfactory way to estimate interactions using these methods, but under certain conditions they will estimate differences in major effects with a power-efficiency of about 60 to 95 percent against the more common alternatives. In the present case, sufficient additional data were available because the freedom from restraining assumptions allowed a greater sampling range.

When an overall test of differences cannot be performed due to unequal variances for the several hammers, occasionally the problem can be broken down into several smaller ones involving "t" tests. However, these tests also require the usual parametric assumptions.

It inevitably complicates comparisons among hammers and piles of different types. The situation becomes even more complicated when a single study includes several sites representing a variety of soil conditions. Consequently, any generalization about other pile driving situations that is based on information obtained under these circumstances must be made with great care.

It has already been noted that some increments of pile penetration were omitted from analysis because of unsatisfactory hammer operation or inadequate field records. For such increments (as shown in Figs. 46 and 47) data were omitted to prevent biasing the analysis. However, in addition to such omissions, in other cases data were eliminated from analysis for all piles throughout a particular range of penetration because assumptions required for statistical tests could not be met. Thus, the most powerful statistical tests could not be used when blow count variations differed greatly from pile to pile for a given hammer or hammers. The usable depth ranges are indicated in Figs. 49 through 51. More extensive ranges of depth allowing use of less powerful tests are presented in Tables 10 and 14. Often graphs alone are used to emphasize differences among important variables. However, in this study blow count data scattered considerably, and thus statistical methods were desirable in assessing the significance of differences found in the graphical comparisons. These differences result from characteristic responses of hammers and cushion blocks to field variables.

Selection of a Standard Measure for Analysis (R)

Because blow count and pile set vary with depth, in analyzing field test data it was necessary for comparative purposes to select some unit of measure that would be independent of the effects of increasing depth, and yet accurately reflect hammer proficiency, preferably indicating relative hammer sensitivity to changes in soil qualitites.

Several experiments were made with the data until the most satisfactory procedure was found, consisting of dividing the total penetration of each pile driven into 1-ft increments, starting from ground elevation. This 1-ft increment was selected because it provided sufficient data (particularly important where only one or two piles could be analyzed for a given hammer at a given site), yet was usually large enough to permit some smoothing out of variations in blow count. Blow count for each 1-ft increment was tabulated from manually and automatically obtained records, and used throughout the analysis of Belleville, Detroit, and Muskegon data. While increments greater than 1 ft could have been

selected at Muskegon, because of much greater penetrations, an increment common to all sites was chosen to facilitate comparisons between sites.

Perhaps the most important advantage of dealing with total penetration range in terms of smaller increments, however, is that the effects of isolated data inconsistent with general trends may be confined, without affecting more general evaluation. Thus, when only a few piles encounter a hard layer in a given increment, and only that penetration range requires a high blow count, the incrementing procedure confines this effect to only the range involved. If total pile blow count for full penetration is used rather than incremented blow count, the effects of the unrepresentative increment could weaken comparisons with other piles and hammers. The incrementing procedure is not wholly satisfactory in clarifying performance differences, since an increment of extreme blow count (which could be of particular interest if it should affect all piles involved), may not be given the special attention it may require. Thus, special attention must be given to soil changes affecting all hammers and piles under comparison, as in Fig. 51 at about 110 ft. Plots of blow count such as those shown in Figs. 49, 50, and 51 are used for this purpose. It must also be remembered that the hammers compared differed in size and operating characteristics.

Blow counts for each increment at the same penetration were averaged for all hammers driving the same pile type (H or pipe) at each site,[4] and combined with the individual blow count for that increment to form the following ratio:

$$\underline{R}\ \text{(blow count ratio)} = \frac{\text{blow count for a specific hammer and specific pile}}{\begin{array}{c}\text{unweighted average blow count}\\ \text{for all hammers driving this specific pile type}\\ \text{for the same increment of penetration}\end{array}}$$

Other terms used in the blow count analysis include the following:

$\overline{R_i}$ = mean or average blow count ratio for a given 1-ft penetration increment i

$\overline{R_p}$ = mean or average blow count ratio for a given pile p

s_i = R-value standard deviation of all piles of a given type for a given hammer and given increment i

[4] Because most hammers drove an unequal number of piles, an unweighted average was necessary to prevent biasing of the ideal "normal performance." This was accomplished by averaging the piles for each hammer at a specified depth increment and then taking the average of the hammer averages.

s_p = R-value standard deviation for a given pile p

$\bar{\bar{R}}$ = grand arithmetic mean of all depth increments and all piles of a given type driven with a given hammer

r = briefly, one of the measures of statistical association; i.e. the degree to which the relationship between two variables can be represented by a straight line (called correlation coefficient).

Summarizing of Blow Count Ratios (R's)

After dividing the pile's usable range of penetration into 1-ft increments and forming the ratio R, frequency distributions were plotted for visual indication of performance differences among the air, steam, and diesel hammers. Because these distributions overlapped in patterns that complicated comparison of the hammers, it was decided to present the data instead in relative cumulative frequency distributions, or "ogives" (Fig. 48), using normal probability paper.[5] The vertical scale on this paper is such that a cumulative plot of an exact normal distribution appears as a straight line, facilitating interpretation without sacrificing accuracy.

The Fig. 48 hammer graphs include a "par intercept" shown as a heavy vertical line, to indicate the point at which the R-ratio equals 1. The various ogives intercept par at different points and are generally curved or skewed to the right, in the direction of increasing R. These skews result from hammer driving characteristics rather than from any mathematical properties of R. The hammers with ogives appearing farthest left are those which generally drove with the least blows. Those hammers with ogives closest to straight-line verticality produced the most consistent driving ratios, suggesting fairly uniform hammer output. For example, the Delmag D-12 at Belleville drove pipe piles from 24 to 54 ft with the smallest overall blow count ratios (line farthest left), least variability (greatest angle with the horizontal), and best approximation to the "normal" distribution (least skew). This indicates least relative susceptibility to changes in penetration resistance, and may be contrasted with the Vulcan No. 1 which showed greatest relative susceptibility to variations in penetration resistance for the same conditions. Hammer ogives as a group tend to have the least skew and are most nearly verical at Detroit (reflecting greatest soil uniformity and least variable driving

[5] This method of statistical presentation is often desirable because it not only facilitates calculation of the total frequency above or below a given value, but also facilitates comparison with the "normal" or Gaussian distribution.

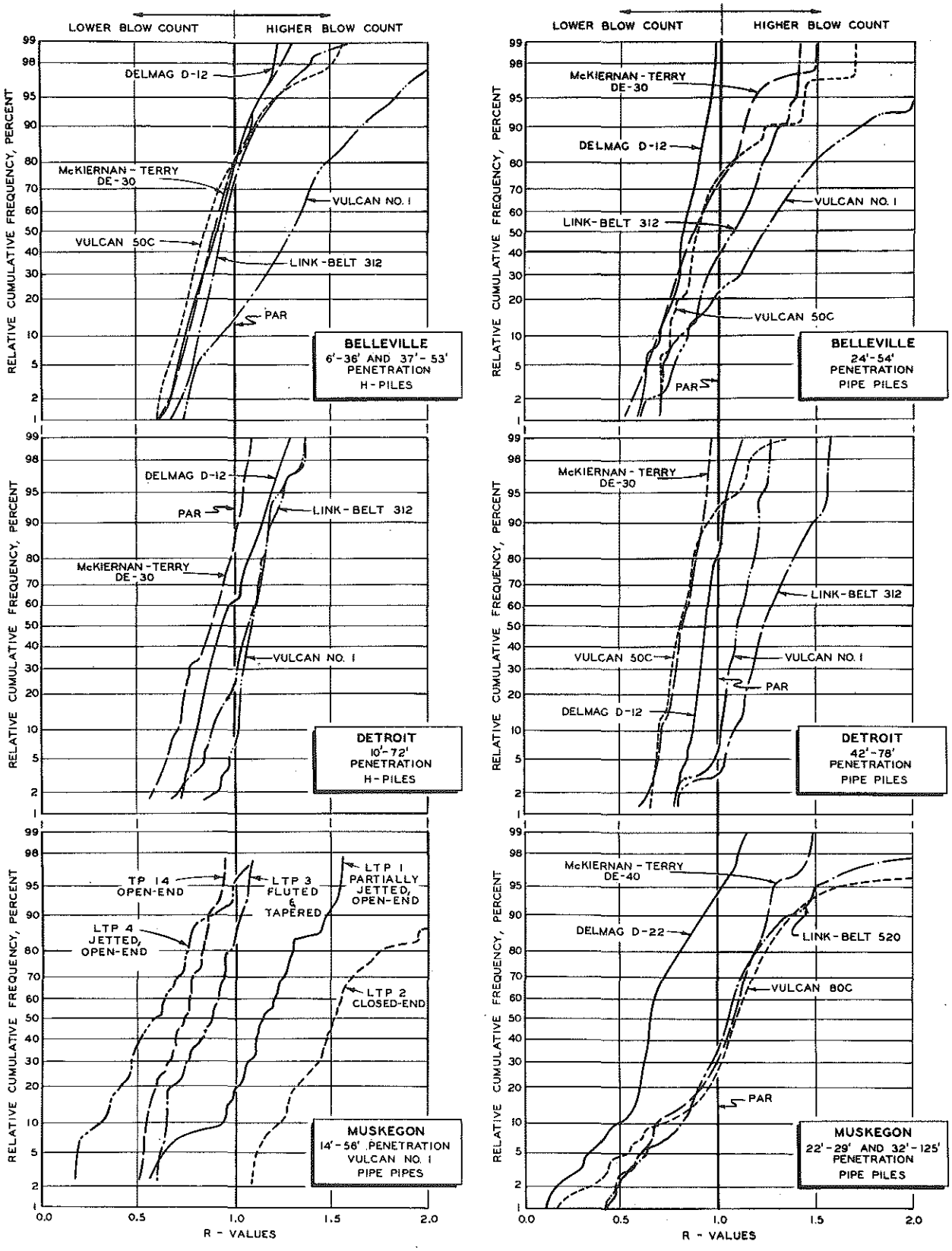

Figure 48. Hammer performance comparison using cumulative frequency distributions of R-values. All pipes closed-end except where noted for Muskegon Vulcan No. 1.

of the sites), more skew and somewhat less verticality at Belleville, and most skew as well as least verticality at Muskegon (reflecting least soil uniformity and most variable driving resistance).

In addition to the regular analysis of performance of the heavier hammers at Muskegon, a special study was conducted for various pile types driven there with the lighter Vulcan No. 1 hammer (Fig. 48, lower left). As would be expected, for the piles and techniques used, best blow count ratios were obtained by jetting open-end pipes, followed in order by unjetted open-end, fluted-tapered, and closed-end pipes.

These ogives indicate hammer ability to drive consistently above or below par ($\underline{R} = 1$), as defined for this study. However, in dealing with the Fig. 48 graphs one must take into account the soil conditions and other physical factors unique to the penetration increments shown.[6] In some cases, as at Muskegon, the data were limited both by the relatively small number of piles and by the relatively shallow depths to which some were driven. At Belleville and Detroit, only H-piles and closed-end pipe piles were driven in sufficient numbers to allow analysis. Of these, three Belleville H-piles (RP 7, RP 13, RP 20) and one Detroit H-pile (RP 1) were omitted for lack of satisfactory data.[7] Finally, Raymond piles and hammers are excluded from all performance analysis, since only two Raymond piles were driven and Raymond hammer design prevented taking records comparable to those for other hammers.

Comparing Belleville and Detroit data, Fig. 48 and Table 5 show that relative hammer performance was appreciably affected by soil conditions (Vulcan No. 1 and Link-Belt 312) and by pile type (Link-Belt 312). Further, some hammers generally drove better than par (Vulcan 50C, McKiernan-Terry DE-30, Delmag D-12), and others generally below par (Vulcan No. 1). Another indication of hammer performance also given in Table 5 is the grand arithmetic mean $\underline{\underline{R}}$ which is computed from all $\underline{R}$-values for a given hammer driving all piles of a single type. It must be remembered that the blow count ratio $\underline{R}$ is a relative value and that comparison of hammer performance among sites is possible only in terms of

---

[6] Tests of randomness failed where performed (on all hammers driving Belleville H-piles), and some cases such as the McKiernan-Terry DE-30 showed highy significant serial correlation. Thus, the $\underline{R}$-transformation was not entirely successful in providing independent samples, and statistical examination of these data is approximate.

[7] Extreme variation in bounce chamber pressure was encountered with the Link-Belt 312 while driving RP 7. RP 20 was the first pile driven with the McKiernan-Terry DE-30 and the factory representative considered hammer performance unsatisfactory. A replacement model of the same hammer continued to drive RP 20 and the other piles assigned to the DE-30. Also, TP 7 driven with the Vulcan 50C yielded questionable data for the first 24 ft of penetration because of inadequate air pressure. For the remainder of driving the air compressor was replaced with a steam boiler which gave satisfactory pressure.

the same hammers driving the same pile type. For example, no H-piles were driven with the Vulcan 50C at Detroit, and consequently all Belleville-Detroit hammer comparisons are only approximate for H-piles. Also, a marked improvement in blow count performance of one hammer with a given pile type or at a given site, will result in some

TABLE 5
COMPARISONS OF DRIVING PERFORMANCE
BY RELATIVE BLOW COUNT

	Hammer	Percent R-Values Better Than Par (R less than 1)				
		Belleville		Detroit		Muskegon
		H-Piles 6 to 36 ft 37 to 53 ft	Pipe Piles 24 to 54 ft	H-Piles 10 to 72 ft	Pipe Piles 42 to 78 ft	Pipe Piles 22 to 29 ft 32 to 125 ft
Lighter Hammers	Vulcan No. 1	13	22	8	6	--
	Vulcan 50C	81	77	--	92	--
	Link-Belt 312	73	41	23	3	--
	McKiernan-Terry DE-30	77	74	82	100	--
	Delmag D-12	75	100	63	82	--
Heavier Hammers	Vulcan 80C	--	--	--	--	26
	Link-Belt 520	--	--	--	--	34
	McKiernan-Terry DE-40	--	--	--	--	31
	Delmag D-22	--	--	--	--	94

	Hammer	Grand Arithmetic Mean R-Values ($\bar{R}$)				
		Belleville		Detroit		Muskegon
		H-Piles 6 to 36 ft 37 to 53 ft	Pipe Piles 24 to 54 ft	H-Piles 10 to 72 ft	Pipe Piles 42 to 78 ft	Pipe Piles 22 to 29 ft 32 to 125 ft
Lighter Hammers	Vulcan No. 1	1.304	1.269	1.097	1.110	-----
	Vulcan 50C	0.893	0.956	-----	0.853	-----
	Link-Belt 312	0.972	1.062	1.067	1.266	-----
	McKiernan-Terry DE-30	0.916	0.901	0.870	0.824	-----
	Delmag D-12	0.914	0.812	0.966	0.947	-----
Heavier Hammers	Vulcan 80C	-----	-----	-----	-----	1.145
	Link-Belt 520	-----	-----	-----	-----	1.122
	McKiernan-Terry DE-40	-----	-----	-----	-----	1.052
	Delmag D-22	-----	-----	-----	-----	0.680

apparent decline of performance for all other hammers. This relationship, however, follows from the definition of R. If hammer differences are to be interpreted in terms of experience with a given hammer (such as the Vulcan No. 1) appropriate ratios can be formed from the data in Table 5. Such hammer comparisons assume that relative performance does not vary appreciably with penetration level. Where this assumption could be evaluated statistically (for small penetration ranges) it usually proved

tenable. However, significant changes were noted in relative blow count performance with increasing penetration (as shown graphically in Figs. 49, 50, and 51) for the following hammers:

Hammer	Site	Pile Type	Range, ft
Vulcan No. 1	Belleville	H	45 to 53
Vulcan No. 1	Belleville	Pipe	50 to 54
Vulcan No. 1	Detroit	Pipe	54 to 72
Link-Belt 312	Belleville	Pipe	42 to 65
Link-Belt 312	Detroit	Pipe	58 to 70
Link-Belt 520	Muskegon	Pipe	93 to 112
McKiernan-Terry DE-30	Belleville	Pipe	50 to 61
All hammers (except Link-Belt)	Muskegon	Pipe	107 to 112

In any experiment where statistical techniques have been used for inferential purposes, one must be aware of the practical aspects of statistically significant findings. If there are enough data, small differences in hammer performance can be statistically significant, yet not large enough to be of any practical importance. Consequently, statistical significance is not a sufficient condition for action; the magnitude or extent of the finding, together with its implication, must be considered as well. On the other hand, presumed differences in performance based on relatively small samples can be very misleading, particularly if not backed up by statistical tests utilizing information about the uncontrolled variation inherent in all experimental work.

In the present case, statistically significant differences in hammer performance are to be expected in view of the diversity of hammer sizes and types. However, in this experiment, it was not assumed that these differences would follow from hammer design information. Consequently, statistical tests were used to determine hammer groups based on comparable performance irrespective of other factors. Proper evaluation of among-group differences requires consideration of the extent to which the size of these differences is really important.

To re-emphasize a point mentioned earlier, one must also be aware of the representativeness of the penetration range sampled. Statistical tests based on data sampled from small ranges of penetration do not hold for regions not available for sampling. This consideration was of special importance in this project, since small regions of high penetration resistance were generally excluded from the tests because of program limitations and analytical difficulties. Moreover, at the greater penetrations,

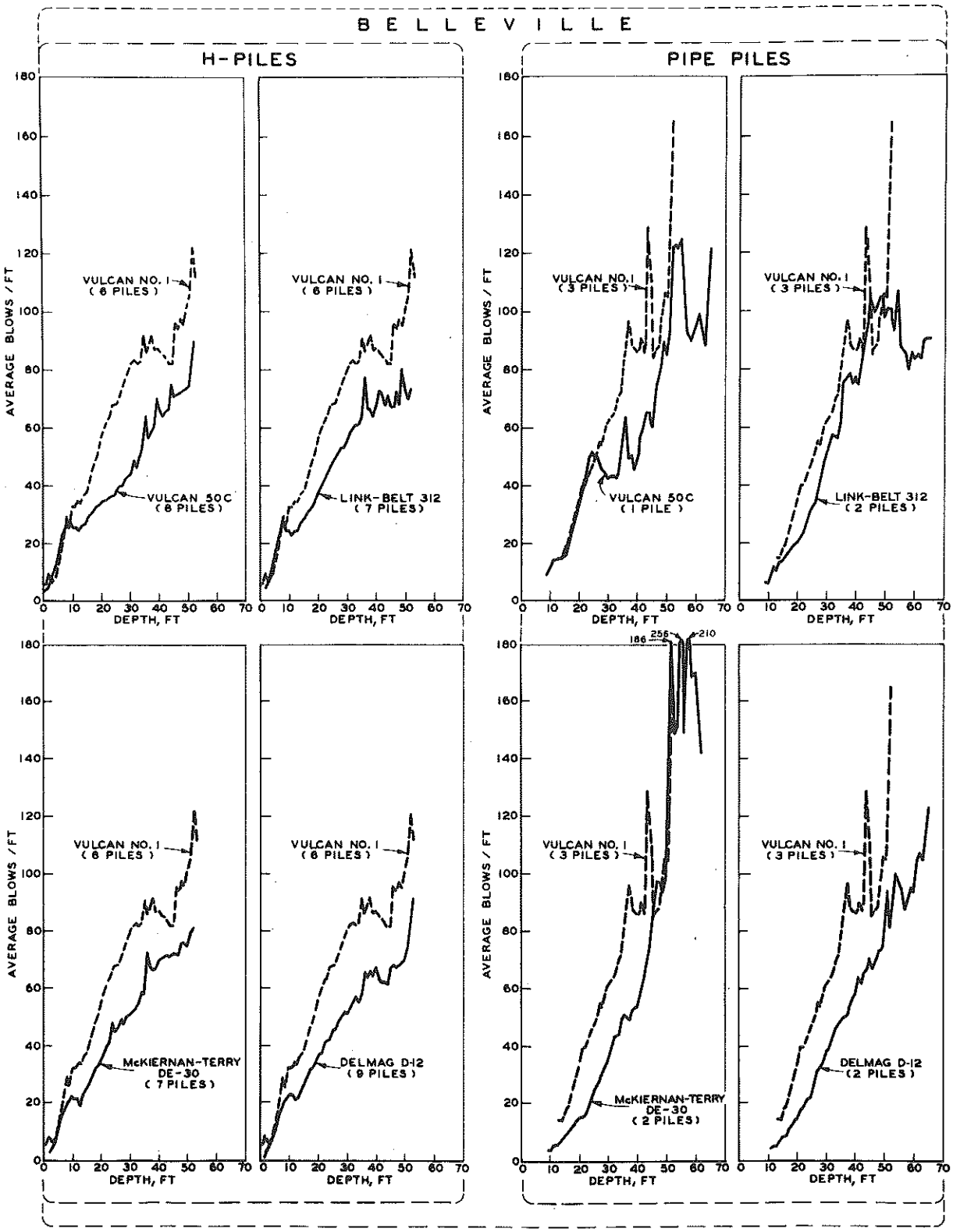

Figure 49. Relationships of blow count with increasing penetration, comparing each hammer with the Vulcan No. 1 (range of analysis of variance = 24 to 54 ft).

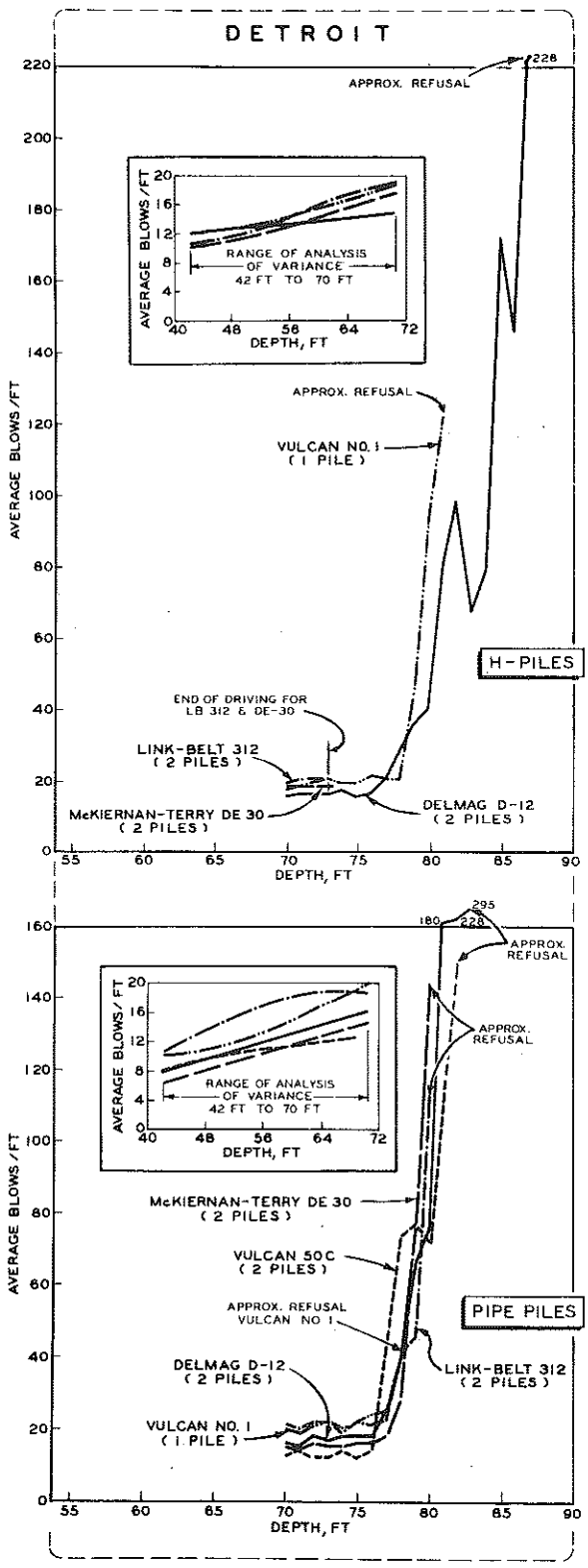

Figure 50. Relationships of blow count with increasing penetration, with details (plotted using "moving averages") for actual range of analysis of variance.

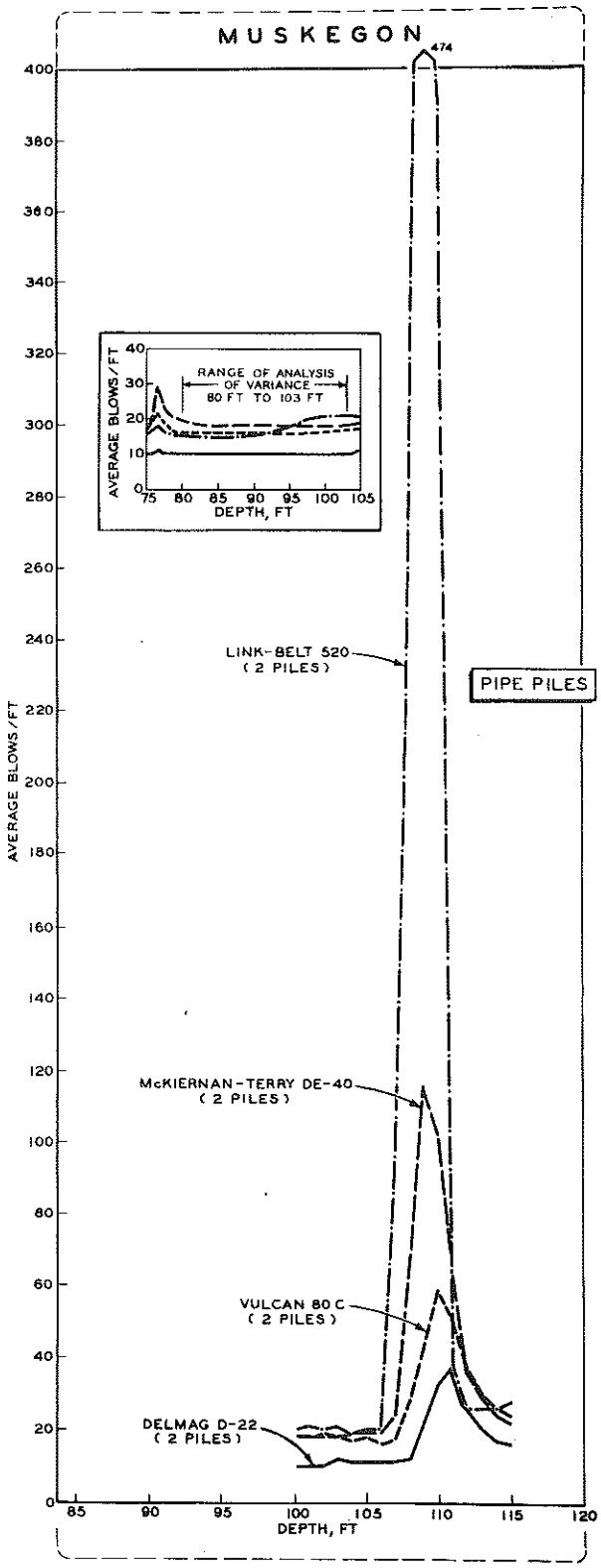

Figure 51. Relationships of blow count with increasing penetration, with details (plotted using "moving averages") for actual range of analysis of variance.

relative hammer performance often changed considerably. For instance, at Belleville marked improvement can be seen in Fig. 49 in relative performance of the Link-Belt 312 driving pipes deeper than about 54 ft (terminal depth for this analysis). For Detroit and Muskegon, even if appropriate statistical examinations could have been made for greater penetrations, only incomplete and very imprecise comparison could have been made because so few piles were driven to the greater depths. If such tests had been made, however, relative hammer performance probably would have been different. For example, Fig. 52 shows that at Muskegon the Delmag D-22 had a peak resistance of 85 blows per foot while other hammers varied from 293 to 767 blows per foot. At Detroit, fragmentary data below the maximum depth of analysis for pipes (78 ft) indicate the terminal depths for the various hammers in stiff clays (Fig. 50); the Delmag D-12 (which did not generally drive with the least blows per foot above hardpan) was the only hammer capable of penetrating to 84 ft.

Significance of Differences in Sampled Data

Much greater variability in blow count was recorded among piles driven by steam and air hammers than by diesels. This performance factor was of a magnitude that had not been anticiapted at the outset of the data analysis, and was sufficient to change the course of that analysis.

Differences among hammer variabilities became increasingly apparent in detecting meaningful differences in summarizing measures (such as the means of Table 5) derived from frequency distributions. This meaningfulness of observed differences can be rigorously established by statistical testing,[8] provided that the assumptions of the tests are reasonably well met. The use of R-values rather than blow count, resulted in in closer agreement with the statistical assumptions, although R-values for successive penetration increments were still interdependent.[9] However, each hammer still retained its own characteristic variability among the piles it drove. An indication of this variability for specified driving conditions can be seen in Table 6; diesels generally exhibit less variability than either air or steam hammers. Also, with reference to Vulcan No. 1 performance for Belleville pipe piles, a reservation must be made with regard to the figure given in Table 6 for average maximum range

[8] Analysis of variance with factors of hammer and depth.

[9] Because R-values were computed from blow count data in sets (each set belonging to a particular pile) the usual statistical assumption of independence can be only approximated.

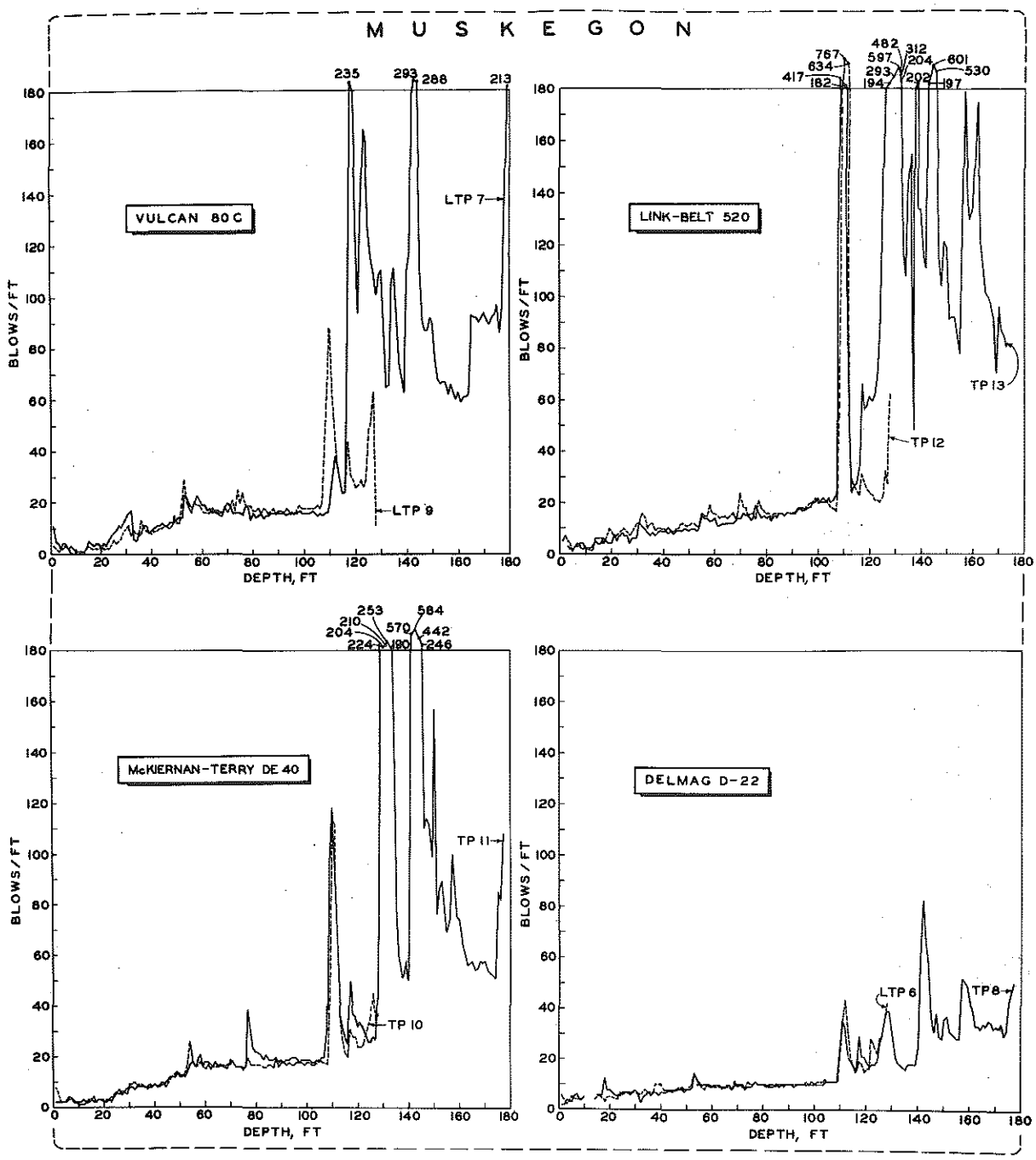

Figure 52. Relation of blow count to penetration for individual piles, covering total driving range, showing relative susceptibility of hammers to changing soil conditions.

between two piles. Upon examination of field data, the 54.10 blows per ft range (highest value in Table 6) results from a high count for one pipe which happened to be driven at a location where three other piles had already been driven within a radius of 6 ft. The possible biasing effect of driving piles in close proximity is discussed later in this chapter.

TABLE 6
HAMMER BLOW COUNT VARIABILITY
FOR VARIOUS DRIVING CONDITIONS
Showing Exclusions from Analysis of Variance Study (Parenthesized)
Due to Excessive Variability

	Hammer	Avg. Standard Deviation, blows per ft	Avg. Max Range Between Two Piles, blows per ft
		H-Piles (24 to 36 ft, 37 to 53 ft)	Pipe Piles (24 to 54 ft)
Belleville	Vulcan No. 1	(17.40)	(54.10)
	Vulcan 50C	8.04	-----
	Link-Belt 312	7.10	(19.43)
	McKiernan-Terry DE-30	7.60	(15.43)
	Delmag D-12	6.65	4.60

	Hammer	Average Range Between Two Piles, blows per ft		
		H-Piles (42 to 72 ft)	Pipe Piles (42 to 72 ft)	H & Pipe Piles (42 to 72 ft)*
Detroit	Vulcan No. 1	----	----	1.43
	Vulcan 50C	----	1.26	----
	Link-Belt 312	1.63	(2.25)	----
	McKiernan-Terry DE-30	1.33	1.10	----
	Delmag D-12	1.83	0.70	----

	Hammer	Average Range Between Two Piles, blows per ft	
		Pipe Piles (22 to 29 ft, 32 to 123 ft)	Pipe Piles (80 to 103 ft)
Muskegon	Vulcan 80C	(14.00)	1.38
	Link-Belt 520	(21.26)**	0.86
	McKiernan-Terry DE-40	3.30	1.38
	Delmag D-22	1.32	0.56

* Range between one pipe and one H-pile.

** Abnormally large blow count due to extreme difference between piles at 107 ft, probably because of slightly different sand elevations.

This effect also is reflected in the Vulcan No. 1 pipe pile curve in Fig. 49. The same effect can be observed for other hammers driving pipe piles at Belleville.

The problem posed by each hammer having its own characteristic between-pile variability was accentuated when unequal numbers of piles were driven. This was particularly true at Belleville where acceptable

H-piles varied from six for the Vulcan No. 1 to nine for the Delmag D-12. To reduce the effects of unequal pile quantities, an approximate two-phase analysis was planned to determine not only hammer differences, but whether depth of penetration affected hammers differently.[10,11] Approximate relationships of blow count performance with increasing penetration are shown in Figs. 49, 50, and 51.

It soon became apparent that the penetration ranges where the assumptions of the proposed analysis could be met were not large enough to be of practical value. The main difficulty arose from the comparatively high variability of air and steam hammers, as compared to diesels, particularly the Delmags and McKiernan-Terrys. Because comparison of air, steam, and diesel hammers was a primary objective of the project, and because of the analytical difficulties encountered, it was decided to use another mode of analysis. Although this was less powerful (less sensitive) from a statistical point of view, it was equally valid and did not require comparable hammer variabilities, thereby allowing a greater range of data to be used.[12] Results of these tests of relative hammer performance are presented later in Table 10.

---

[10] Phase 1 of the analysis consisted of taking the means of each cell (the R-values of all acceptable piles for a given hammer, pile type, and depth increment) and conducting a conventional two-way analysis of variance. Phase 2 consisted of a similar analysis on individual cells, thus providing an estimate of experimental error which was converted by the harmonic mean to a variability estimate for means. With this estimate, Phase 1 could be completed. For more detail on two-phase analyses, see F. Yates' "The Principles of Orthogonality and Confounding in Replicated Experiments" (Journal of Agricultural Science, Vol. 23 (1933), p. 108), and "The Analysis of Multiple Classifications with Unequal Numbers in the Different Classes" (Journal of the American Statistical Association, Vol. 29 (1934), p. 51).

[11] This is known as "interaction" and if statistically significant makes interpretation difficult because the treatments (hammers) are affected differently by the various penetration levels. Where overall "F" tests were not possible because of unequal hammer variables, comparisons were to be made using "t" tests of individual hammer pairs. In applying the t-tests, the pairing technique would be used when correlation exists between the variables being compared. Pairing would be necessary in this analysis because driving ratios of the various hammers are often directly (+) or inversely (-) related (or correlated) due to similar performance characteristics. The pairing technique here involves testing the mean of a distribution composed of the algebriac differences of R-values for corresponding depth increments, for significant deviation from zero. Thus, where correlation exists between the hammers under study, a cumulative sample difference between corresponding increments may be a more sensitive index of real difference than is the difference in means of the respective distributions. This is to be expected when the correlation is positive (+ or direct), as between the McKiernan-Terry DE-30 and Delmag D-12 for Belleville pipe piles. If, on the other hand, a negative correlation (- or inverse) is present (as for the Vulcan No. 1 and McKiernan-Terry DE-30 for Belleville pipe piles), exaggeration of the significance of sample differences of means will result unless pairing is used. Because the assumption is warranted on a logical basis--i.e., each penetration sampled yielded values for each of the two hammers compared--it is concluded that without the assumption of inherent pairing, the real difference between the hammers would be under- or over-estimated for all possible hammer pairs depending on the kind and degree of correlation present. The results or t-tests, conducted where the data permitted, agree with those of their non-parametric counterparts.

[12] These tests are classified under the generic term "non-parametric" or distribution-free methods. For the present analysis, the Friedmann rank test of homogeniety was used first to test for hammer group consistency analogous to the "F" test for the conventional analysis of variance. For specific tests of hammer differences by pairs, the Wilcoxon Signed Rank test was thought to be the most powerful for the alternatives considered of the non-parametric methods available. The asymoptotic power-efficiency of this test near the null hypothesis H_0 is $3/\pi$ when the assumptions of the parametric "t" test are met. Because the "t" test assumptions very likely were not met, the power-efficiency of the Wilcoxon test is probably greater than it would otherwise be. For more detail on these tests, see Milton Friedmann's "The Use of Ranks to Avoid The Assumption of Normality Implicit in the Analysis of Variance" (Journal of the American Statistical Association, Vol. 32 (1937), p. 675), and Frank Wilcoxon's "Individual Comparisons of Ranking Methods" (Biometrics, Vol. 1 (1945), p. 80).

Control Chart Techniques Applied to Sampling at Various Penetrations[13]

Only at Belleville were piles driven by each hammer in a quantity sufficient to allow use of control chart techniques. Control charts are often employed when samples are ordered sequentially in time or space, to spot trends or excessive deviations indicating marked changes uncharacteristic of the expected random fluctuation. Such trends are especially detectable by this technique because it produces visual as well as statistical evidence. In the case of hammer performance data, it was hoped that any notable relationship of blow count ratio $\underline{R}$ to increasing penetration would be readily apparent.

Penetration control charts for successive sample $\underline{R}$-values are shown in Figs. 53 and 54 for both the means and standard deviations (the latter being a mathemetically convenient measure of spread or dispersion) of all hammers driving Belleville H-piles. The circled numerals in these ten charts indicate the lengths of piling spliced to previously driven sections (at the penetrations indicated). The $\underline{R}$-value sample mean and standard deviation of all H-piles for each hammer and depth increment ($\bar{\underline{R}}_i$ and s_i) were plotted against depth to show any variations or trends in relative hammer performance. Upper control limits (99 percent) are included to indicate regions of excessive variability of sample $\underline{R}$-value means or standard deviations for sample sizes of six to nine piles. If at any penetration a mean or standard deviation exceeded an upper control limit it would be concluded that sampling error was not responsible, and that non-random factors such as gradual change in soil resistance (across the site) or change in quality of driving performance caused an abnormally large blow count. If trends are found in this type of analysis, one would have good evidence that the relative performance of the hammer-pile combination was functionally related to penetration level.

If relative performance of a given hammer is not a function of penetration, a random fluctuation of mean $\underline{R}$-values ($\bar{\underline{R}}_i$) will scatter around the grand mean ($\bar{\bar{\underline{R}}}$) for all depth increments studied. In Fig. 53, fairly good statistical control (lack of extreme variations or trends) is characteristic of the Delmag D-12 and the Link Belt 312. The Vulcans No. 1 and 50C are questionable, because their curves definitely do not fluctuate randomly around their means. The McKiernan-Terry DE-30, however, shows a definite trend toward increasing $\bar{\underline{R}}_i$-values with increasing depth.

---

[13] Techniques described here are those recommended in "ASTM Manual on Quality Control of Materials" (January 1951).

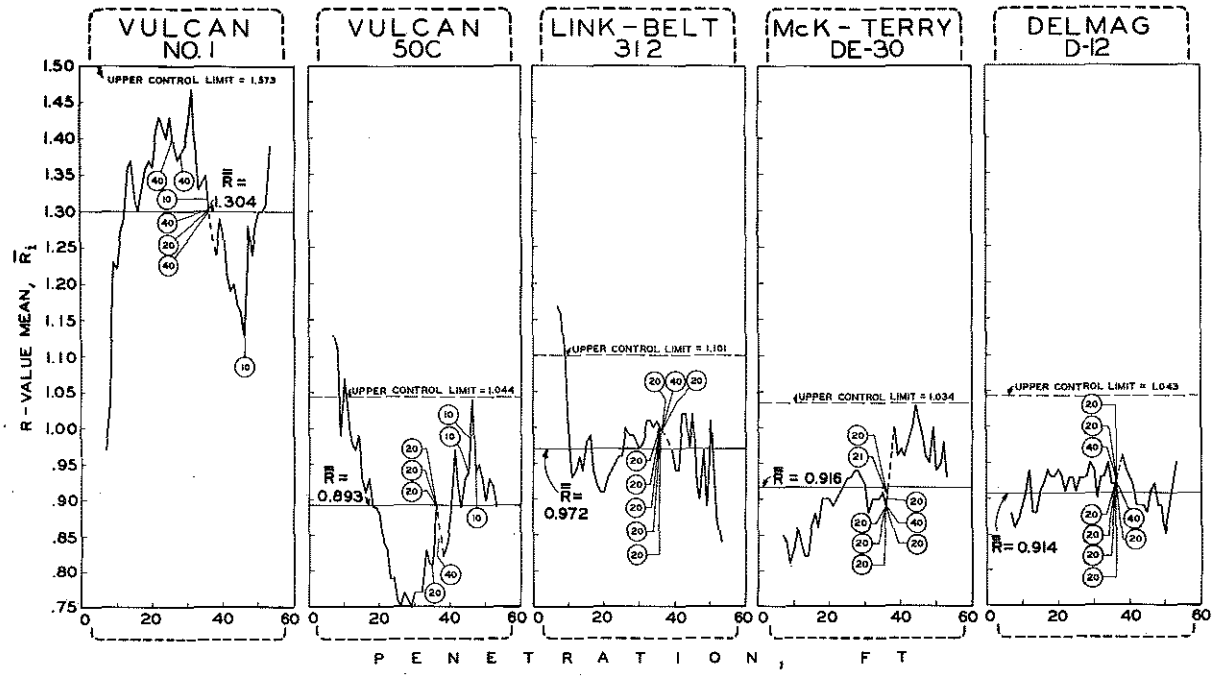

Figure 53. Belleville H-pile penetration control charts, for R-value means ($\bar{R}_i$) for the penetration increments given. Circled numerals indicate length of additional piling spliced to first pile section at indicated penetration.

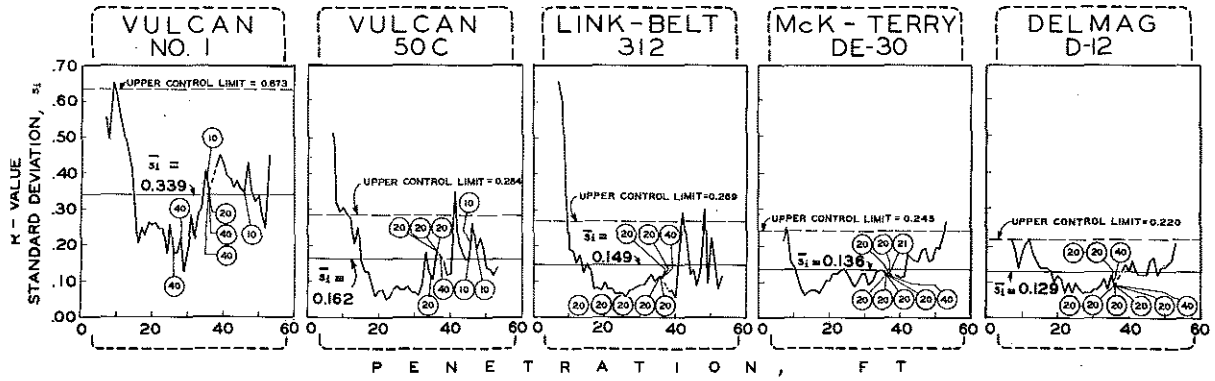

Figure 54. Belleville H-pile penetration control charts, for R-value standard deviations (s_i) for the penetration increments given. Circled numerals indicate length of additional piling spliced to first pile section at indicated penetration.

Thus, while this hammer performs better than its average at penetrations down to about 23 ft, it performs poorer than its average after splicing (at 36 ft). It was noted in Fig. 54 that deeper than about 20 ft all hammers show increasing variability with increasing penetration. These depth control charts indicate that hammers vary somewhat in their ability to perform independently of depth; all points above the control limits are examined in Table 7.

Pile Proximity as a Factor in Blow Count Variation

Examination of control charts and variability data (Table 6) revealed wide variations in blow counts for piles driven by the same hammer. Thus an attempt was made to investigate the possibility of adjacent pile influence. It was impossible to assess this very accurately with the available data, but a very rough approximation was developed by counting the number of piles previously driven within a circle of 6-ft radius around each Belleville H-pile. The number so determined was called "rank." Thus, a rank of 3 indicates that three piles had been driven within the circle prior to the pile in question.

Rank control charts for $\bar{R}_p$ and s_p demonstrate the effect, if any, of rank on blow count (Figs. 55 and 56). Upper control limits of 99 percent were computed, erratic points examined (Table 8), and statistical relationships among the R-values used to continue the study.[14] Fig. 57 summarizes the effects of rank independently of individual hammer performance and indicates that there is some relationship between quantity of previously driven adjacent piles and relative blow count performance. The extent to which this might affect the various hammers is demonstrated in Table 9, which shows, for example, that an average of about 3.2 piles had already been driven within a 6-ft radius before any Delmag D-12 began driving, while an average of about 0.9 pile had been driven before any Vulcan 50C test.

Site Soil Variation as a Factor in Blow Count Variation

Standard deviation control charts for penetration at Belleville (Fig. 54) show large variations for all hammers in the shallow penetration range (down to 10 ft). In addition, mean R-values per pile were notably greater at the west end of the test site than the east end (Table 9). To evaluate

[14] Regression lines were fitted by the "least squares" technique to the R-value rank scatter plots (Fig. 56). The slopes of these lines were then averaged for the ranks bounded by the data, thereby providing an estimate of the presumed linear relationship between ranks.

TABLE 7
HAMMERS DRIVING BELLEVILLE H-PILES
Explanation of Extreme $\bar{R}_i$ (Fig. 53) and s_i (Fig. 54) Values From Penetration Control Charts

Chart Showing Extreme Value		Penetration Increment, ft	Probable Explanation
VULCAN NO. 1	s_i	8-9	Variation in penetration resistance across site as follows:

Piles at W. Side	Penetration Increment, ft	R-Value	Piles at E. Side	Penetration Increment, ft	R-Value
RP 9	8-9	1.572	LTP 6	8-9	0.993
RP 33	8-9	2.399	RP 6	8-9	0.745
			RP 28	8-9	0.827
	Avg.	1.986	RP 36	8-9	0.786
				Avg.	0.838

Chart Showing Extreme Value		Penetration Increment, ft	Probable Explanation
VULCAN 50C	$\bar{R}_i$ s_i	6-7	Variation in penetration resistance across site as follows:
	$\bar{R}_i$ s_i	7-8	
	s_i	8-9	
	$\bar{R}_i$ s_i	9-10	
	s_i	10-11	

Piles at W. Side	Penetration Increment, ft	R-Value	Piles at E. Side	Penetration Increment, ft	R-Value
	6-7	1.564		6-7	0.753
	7-8	1.692		7-8	0.967
RP 2	8-9	1.489	RP 14	8-9	0.744
	9-10	1.545		9-10	0.911
	10-11	1.538		10-11	0.808
	6-7	1.042		6-7	0.753
	7-8	1.160		7-8	0.773
RP 11	8-9	1.075	RP 17	8-9	0.744
	9-10	1.505		9-10	0.951
	10-11	1.231		10-11	0.846
	6-7	1.216		6-7	0.985
	7-8	1.257		7-8	0.918
RP 22	8-9	1.282	RP 19	8-9	0.827
	9-10	0.990		9-10	0.792
	10-11	1.154		10-11	0.769
	6-7	2.143		6-7	0.579
	7-8	1.353		7-8	0.773
RP 25	8-9	1.075	RP 37	8-9	0.662
	9-10	1.149		9-10	0.753
	10-11	1.154		10-11	0.731
Avg.	6-7	1.491	Avg.	6-7	0.768
Avg.	7-8	1.366	Avg.	7-8	0.858
Avg.	8-9	1.230	Avg.	8-9	0.744
Avg.	9-10	1.297	Avg.	9-10	0.852
Avg.	10-11	1.269	Avg.	10-11	0.788
	Grand Avg.	1.331		Grand Avg.	0.802

VULCAN 50C	s_i	40-41	High blow count for RP 22 (R = 1.766) caused by 120-hr set-up time after splice.

TABLE 7 (cont.)
HAMMERS DRIVING BELLEVILLE H-PILES
Explanation of Extreme $\bar{R}_i$ (Fig. 53) and s_i (Fig. 54) Values From Penetration Control Charts

<table>
<tr><th colspan="2">Chart Showing Extreme Value</th><th>Penetration Increment, ft</th><th colspan="6">Probable Explanation</th></tr>
<tr><td rowspan="6">LINK-BELT 312</td><td rowspan="3">$\bar{R}_s$ s_i
$\bar{R}_s$ s_i
$\bar{R}_s$ s_i</td><td rowspan="3">6-7
7-8
8-9</td><td colspan="6">Variation in penetration resistance across site as follows:</td></tr>
<tr><td>Piles at W. Side</td><td>Penetration Increment, ft</td><td>R-Value</td><td>Piles at E. Side</td><td>Penetration Increment, ft</td><td>R-Value</td></tr>
<tr><td>RP 21</td><td>6-7
7-8
8-9
Avg.</td><td>2.490
2.368
1.778
2.212</td><td>RP 18

RP 29

RP 32

Avg.
Avg.
Avg.</td><td>6-7
7-8
8-9
6-7
7-8
8-9
6-7
7-8
8-9
6-7
7-8
8-9</td><td>0.637
0.677
0.827
0.811
0.822
0.993
0.695
0.725
0.744
0.714
0.741
0.854</td></tr>
<tr><td colspan="5"></td><td>Grand Avg.</td><td>0.770</td></tr>
<tr><td>s_i</td><td>41-42</td><td colspan="6">Very high blow count on RP 21 (R = 1.598). Cause unknown.</td></tr>
<tr><td>s_i</td><td>47-48</td><td colspan="6">Very high blow count on RP 32 (R = 1.634). Field records state that the hammer sputtered and stalled out between 47.5 and 48 ft.</td></tr>
<tr><td rowspan="3">McKIERNAN-TERRY DE-30</td><td rowspan="2">s_i</td><td rowspan="2">7-8</td><td colspan="6">Variation in penetration resistance across site as follows:</td></tr>
<tr><td>Piles at W. Side</td><td>Penetration Increment, ft</td><td>R-Value</td><td>Piles at E. Side</td><td>Penetration Increment, ft</td><td>R-Value</td></tr>
<tr><td>RP 1
RP 10
RP 34
</td><td>7-8
7-8
7-8
Avg.</td><td>1.305
0.967
0.918
1.063</td><td>RP 4
RP 16
RP 31
</td><td>7-8
7-8
7-8
Avg.</td><td>0.725
0.677
0.532
0.645</td></tr>
<tr><td>s_i</td><td>52-53</td><td colspan="6">Due to extreme effects of RP 31,(1.415) and RP 34,(0.622) RP 31 had the largest mean R (1.046) for this hammer while RP 34 had the smallest (0.790). Furthermore, the R-values for RP 31 were very low initially, but increased steadily with increased depth. RP 34, however, produced somewhat the opposite driving record (decreasing with depth). Similar negative correlation was found between RP 1 and RP's 4, 16, and 26. Variation in penetration resistance across the site would explain these correlations down to about only 25 ft.</td></tr>
<tr><td rowspan="3">DELMAG D-12</td><td rowspan="2">s_i</td><td rowspan="2">11-12</td><td colspan="6">Variation in penetration resistance across site as follows:</td></tr>
<tr><td>Piles at W. Side</td><td>Penetration Increment, ft</td><td>R-Value</td><td>Piles at E. Side</td><td>Penetration Increment, ft</td><td>R-Value</td></tr>
<tr><td>TP 13
RP 8
RP 23
</td><td>11-12
11-12
11-12
Avg.</td><td>0.855
0.933
1.477
1.088</td><td>RP 5
RP 27
RP 30
RP 38
</td><td>11-12
11-12
11-12
11-12
Avg.</td><td>0.699
0.816
0.972
0.777
0.816</td></tr>
</table>

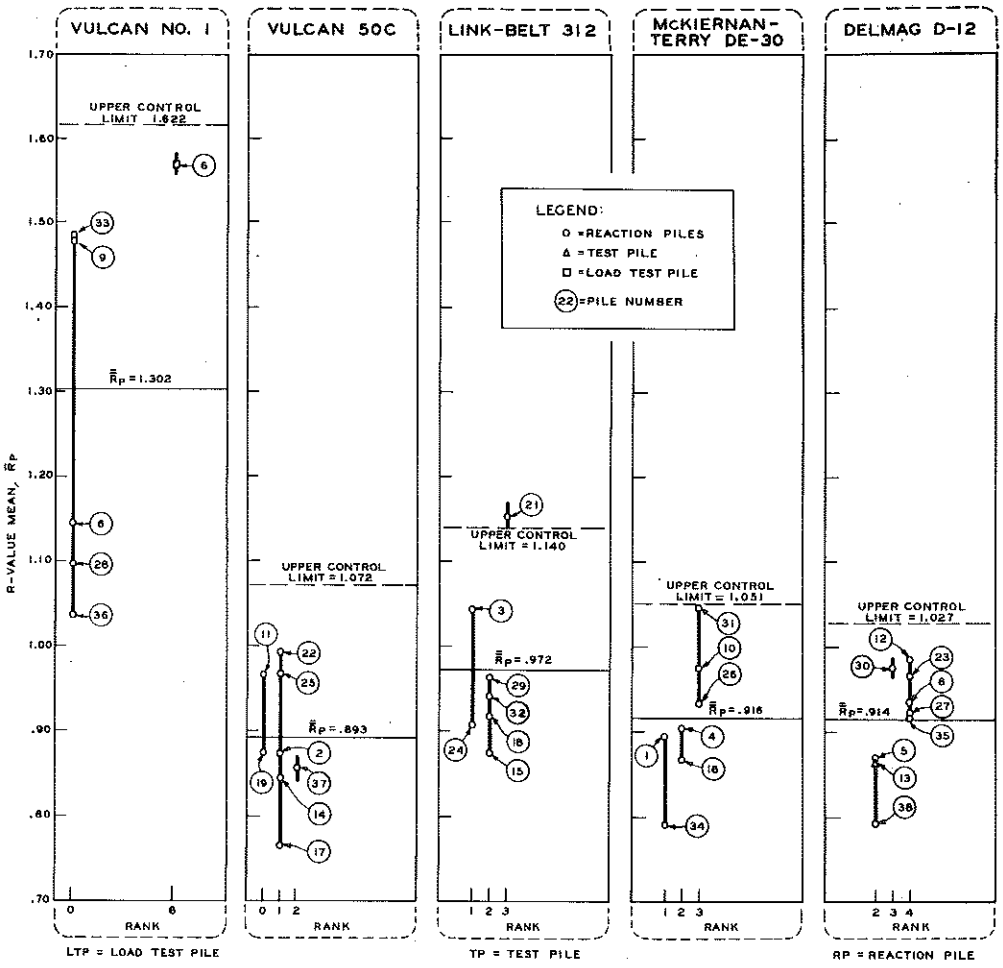

Figure 55. Belleville H-pile rank control charts, for R-value means ($\bar{R}_p$); "rank" defined as total piles previously driven within a 6-ft radius.

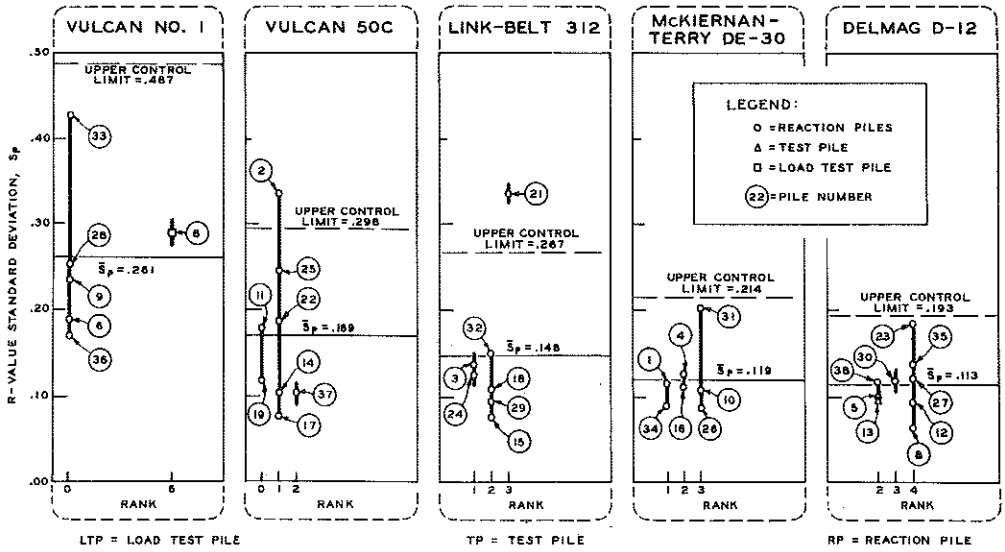

Figure 56. Belleville H-pile rank control charts, for R-value standard deviations (s_p); "rank" defined as total piles previously driven within a 6-ft radius.

TABLE 8
EXTREME $\bar{R}_p$ AND s_p VALUES FOR BELLEVILLE H-PILES
Explanation of Erratic Points from Rank Control Charts

Hammer	Pile No.	Chart Where Point is Out of Control	Probable Explanation
Vulcan 50C	RP 2	s_p (Fig. 54)	Variation in penetration resistance across site. Pile rank = 1, and was 20.5 ft from west end of site.
			Depth Range, ft: R 10-20: 1.214 20-30: 0.698 30-40: 0.612 40-50: 0.701
Link-Belt 312	RP 21	$\bar{R}_p$ and s_p (Figs. 53-54)	Variation in penetration resistance across site. Pile rank = 3, but was first pile driven by this hammer, 12.5 ft from west end of site.
			Depth Range, ft: R 10-20: 1.165 20-30: 1.084 30-40: 1.101 40-50: 1.028

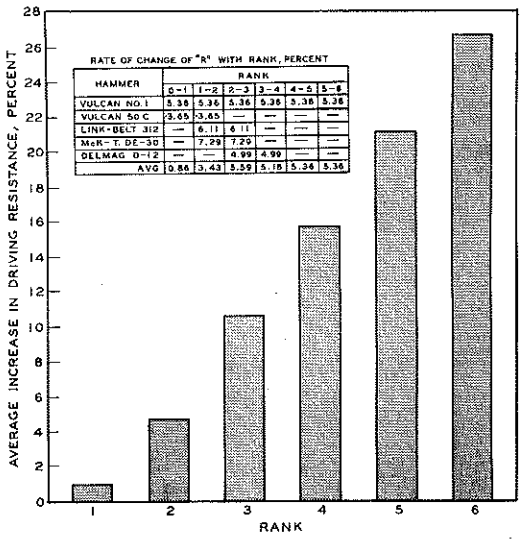

Figure 57. Relation between pile proximity (rank) and penetration resistance.

the influence of this variation on hammer performance, blow count for each Belleville H-pile was plotted against pile distance from a common north-south reference line, drawn through Boring No. 1 (at the site's west end).

Because variation across the site appeared to decrease with penetration, three successive depth intervals (3.5 to 10 ft, 10 to 20 ft, 20 to 40 ft) were selected and plotted (Fig. 58). Best-fit lines are shown for each hammer and depth interval, illustrating the degree of linear relationship present. For the first interval, the visual evidence, confirmed by statistical tests, clearly indicates that penetration resistance decreased across the site. [15] For the next depth interval, the slopes and degree of correlation are less pronounced, being statistically significant for only the Vulcan 50C. The third interval shows practically no consistent pattern across the site.

To minimize this effect of Belleville across-site variation in uppermost soils, the overall comparison of hammer performance on H-piles (Table 10 was limited to penetrations greater than 24 ft. H-pile blow count ogives (Fig. 48) and summaries (Table 5) were

[15] All slopes and correlation coefficients for this interval are considered significant at the 5-percent level.

TABLE 9
SUMMARY OF SOIL FACTORS AFFECTING BELLEVILLE H-PILE PERFORMANCE

Vulcan No. 1					Vulcan 50C				
Pile No.	$\bar{R}_p$	s_p	Rank	Distance from West End of Site, ft	Pile No.	$\bar{R}_p$	s_p	Rank	Distance from West End of Site, ft
LTP6	1.570	0.291	6	68.5	RP2	0.873	0.336	1	20.5
RP6	1.144	0.188	0	68.5	RP11	0.967	0.179	0	28.5
RP9	1.479	0.235	0	16.5	RP14	0.844	0.103	1	48.5
RP28	1.099	0.253	0	52.5	RP17	0.765	0.076	1	64.5
RP33	1.481	0.429	0	8.5	RP19	0.877	0.120	0	76.5
RP36	1.037	0.171	0	44.5	RP22	0.993	0.187	1	16.5
					RP25	0.968	0.245	1	36.5
					RP37	0.857	0.103	2	56.5
Avg.	1.302	0.261	1.0	43.2	Avg	0.893	0.169	0.9	43.5

Link-Belt 312					McKiernan-Terry DE-30				
Pile No.	$\bar{R}_p$	s_p	Rank	Distance from West End of Site, ft	Pile No.	$\bar{R}_p$	s_p	Rank	Distance from West End of Site, ft
RP3	1.045	0.138	1	32.5	RP1	0.896	0.114	1	8.5
RP15	0.876	0.076	2	52.5	RP4	0.905	0.126	2	44.5
RP18	0.919	0.109	2	72.5	RP10	0.974	0.107	3	24.5
RP21	1.153	0.339	3	12.5	RP16	0.868	0.110	2	60.5
RP24	0.909	0.126	1	28.5	RP26	0.934	0.085	3	40.5
RP29	0.963	0.096	2	60.5	RP31	1.046	0.204	3	72.5
RP32	0.941	0.150	2	76.5	RP34	0.790	0.090	1	20.5
Avg	0.972	0.148	1.9	47.9	Avg	0.916	0.119	2.1	38.8

Delmag D-12				
Pile No.	$\bar{R}_p$	s_p	Rank	Distance from West End of Site, ft
TP13	0.866	0.096	2	16.5
RP5	0.868	0.096	2	56.5
RP8	0.936	0.062	4	12.5
RP12	0.986	0.091	4	36.5
RP23	0.967	0.184	4	24.5
RP27	0.923	0.120	4	48.5
RP30	0.974	0.118	3	64.5
RP35	0.918	0.136	4	32.5
RP38	0.791	0.115	2	68.5
Avg	0.914	0.113	3.2	40.1

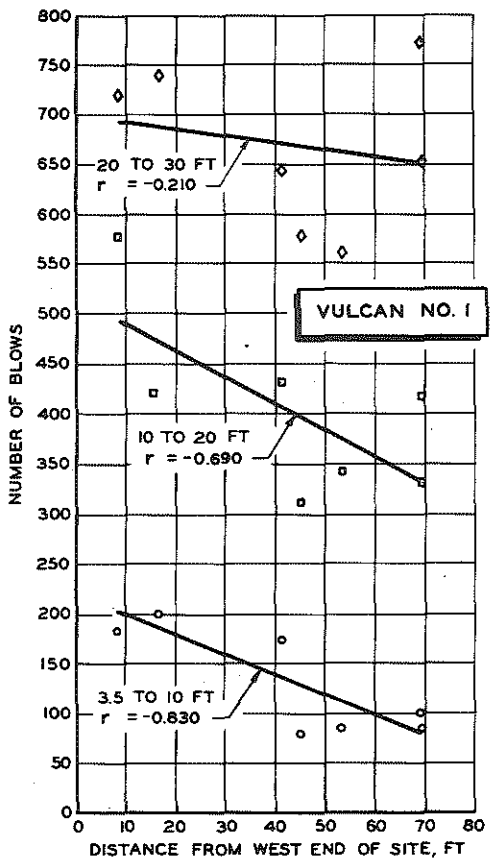

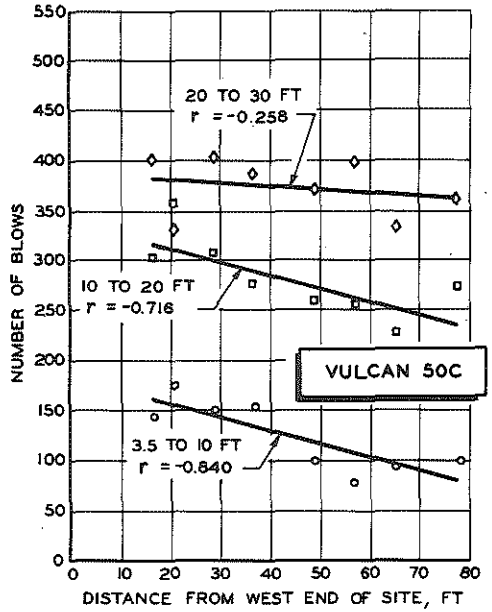

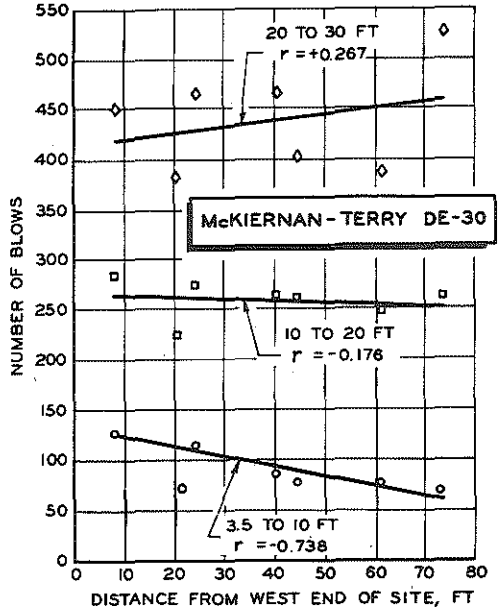

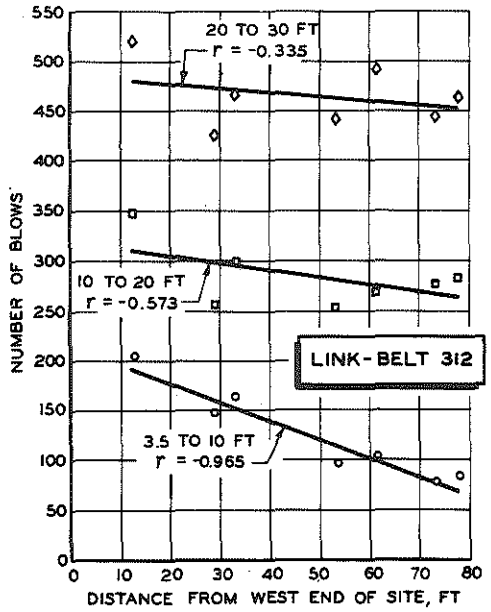

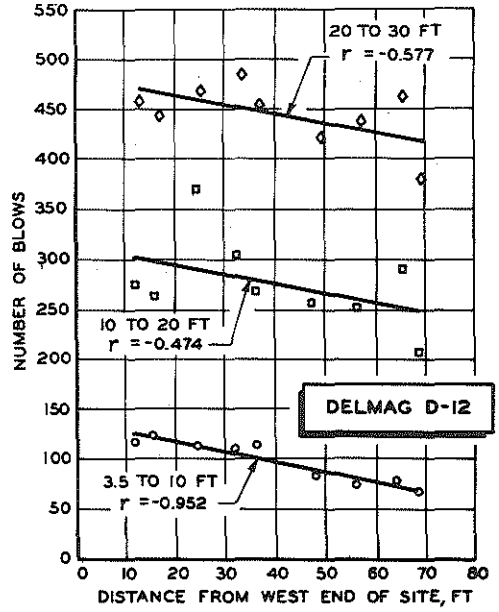

Figure 58. Variation in penetration resistance from west to east ends of Belleville site, at three ranges of penetration (r = correlation coefficient).

computed, however, using data from the 6 to 36 and 37 to 53 ft ranges originally planned for the analysis. Soil variations in this range detected late in analysis did not notably affect hammer comparisons.

Summary

On the basis of blow count, graphical and statistical evaluation of respective R-distributions permitted some general conclusions regarding hammer performance for particular combinations of site and pile type. In Table 10, hammers are listed from left to right in order of increasing mean R-values. Hammer groups are underscored to indicate minor differences within groups and major differences between groups on the basis of the statistical significance test described. The differences within groups are considered to be products of uncontrolled variations in soil or hammer operation, and thus are of relatively minor importance, even though R-values may differ somewhat within a group. Table 10 clearly shows that very little correlation exists between rated energy and relative blow count performance.

It must be borne in mind that these findings are meaningful only in the context and under the conditions of this research project. Any major change in the principal variables (such as cushion blocks, penetration resistances, or pile types) could seriously affect the hammer comparisons. Nevertheless, while some judgment was necessary in selecting significance levels, in classifying performance, and in choosing statistical techniques, it is considered that the Table 10 rankings are a valid index of real differences to be found in the field.

TABLE 10
RELATIVE HAMMER PERFORMANCE
BASED ON BLOW COUNT PER FOOT OF PENETRATION
Ordered by Increasing $\underline{\bar{\bar{R}}}$-Values (lowest relative blow count at left, highest at right)

Site, Pile Type, and Range		Hammer, Rated Energy, and $\underline{\bar{\bar{R}}}$-Value				
Belleville	H-Piles (24 to 36 ft, 37 to 53 ft)	Vulcan 50C 15,100 ft-lb $\bar{\bar{R}} = 0.893$	Delmag D-12 22,500 ft-lb $\bar{\bar{R}} = 0.914$	McKiernan-Terry DE-30 16,800 ft-lb mean 22,400 ft-lb max $\bar{\bar{R}} = 0.916$	Link-Belt 312 15,000 ft-lb max equiv. WH gage 18,000 ft-lb max mfr's rating $\bar{\bar{R}} = 0.972$	Vulcan No. 1 15,000 ft-lb $\bar{\bar{R}} = 1.304$
	Pipe Piles (24 to 54 ft)	Delmag D-12 22,500 ft-lb $\bar{\bar{R}} = 0.812$	McKiernan-Terry DE-30 16,800 ft-lb mean 22,400 ft-lb max $\bar{\bar{R}} = 0.901$	Vulcan 50C 15,100 ft-lb $\bar{\bar{R}} = 0.956$	Link-Belt 312 15,000 ft-lb max equiv. WH gage 18,000 ft-lb max mfr's rating $\bar{\bar{R}} = 1.062$	Vulcan No. 1 15,000 ft-lb $\bar{\bar{R}} = 1.269$
Detroit	H-Piles (10 to 72 ft)	McKiernan-Terry DE-30 16,800 ft-lb mean 22,400 ft-lb max $\bar{\bar{R}} = 0.870$	Delmag D-12 22,500 ft-lb $\bar{\bar{R}} = 0.966$	Link-Belt 312 15,000 ft-lb max equiv. WH gage 18,000 ft-lb max mfr's rating $\bar{\bar{R}} = 1.067$	Vulcan No. 1 15,000 ft-lb $\bar{\bar{R}} = 1.097$	
	Pipe Piles (42 to 78 ft)	McKiernan-Terry DE-30 16,800 ft-lb mean 22,400 ft-lb max $\bar{\bar{R}} = 0.824$	Vulcan 50C 15,100 ft-lb $\bar{\bar{R}} = 0.853$	Delmag D-12 22,500 ft-lb $\bar{\bar{R}} = 0.947$	Vulcan No. 1 15,000 ft-lb $\bar{\bar{R}} = 1.110$	Link-Belt 312 15,000 ft-lb max equiv. WH gage 18,000 ft-lb max mfr's rating $\bar{\bar{R}} = 1.266$
Muskegon	Pipe Piles (22 to 29 ft, 32 to 125 ft)	Delmag D-22 39,700 ft-lb $\bar{\bar{R}} = 0.680$	McKiernan-Terry DE-40 24,000 ft-lb mean 32,000 ft-lb max $\bar{\bar{R}} = 1.052$	Link-Belt 520 26,300 ft-lb max equiv. WH gage 30,000 ft-lb max mfr's rating $\bar{\bar{R}} = 1.122$	Vulcan 80C 24,450 ft-lb $\bar{\bar{R}} = 1.145$	

Underscored groups have differences of $\bar{\bar{R}}$ not large enough to suggest consistent performance diffferences; differences are on a per-comparison basis for the 5-percent confidence level. Overlapping of underscores here indicates indeterminate grouping for hammers in given pile type-site-range condition. More data would be required for definite determination of correct grouping.

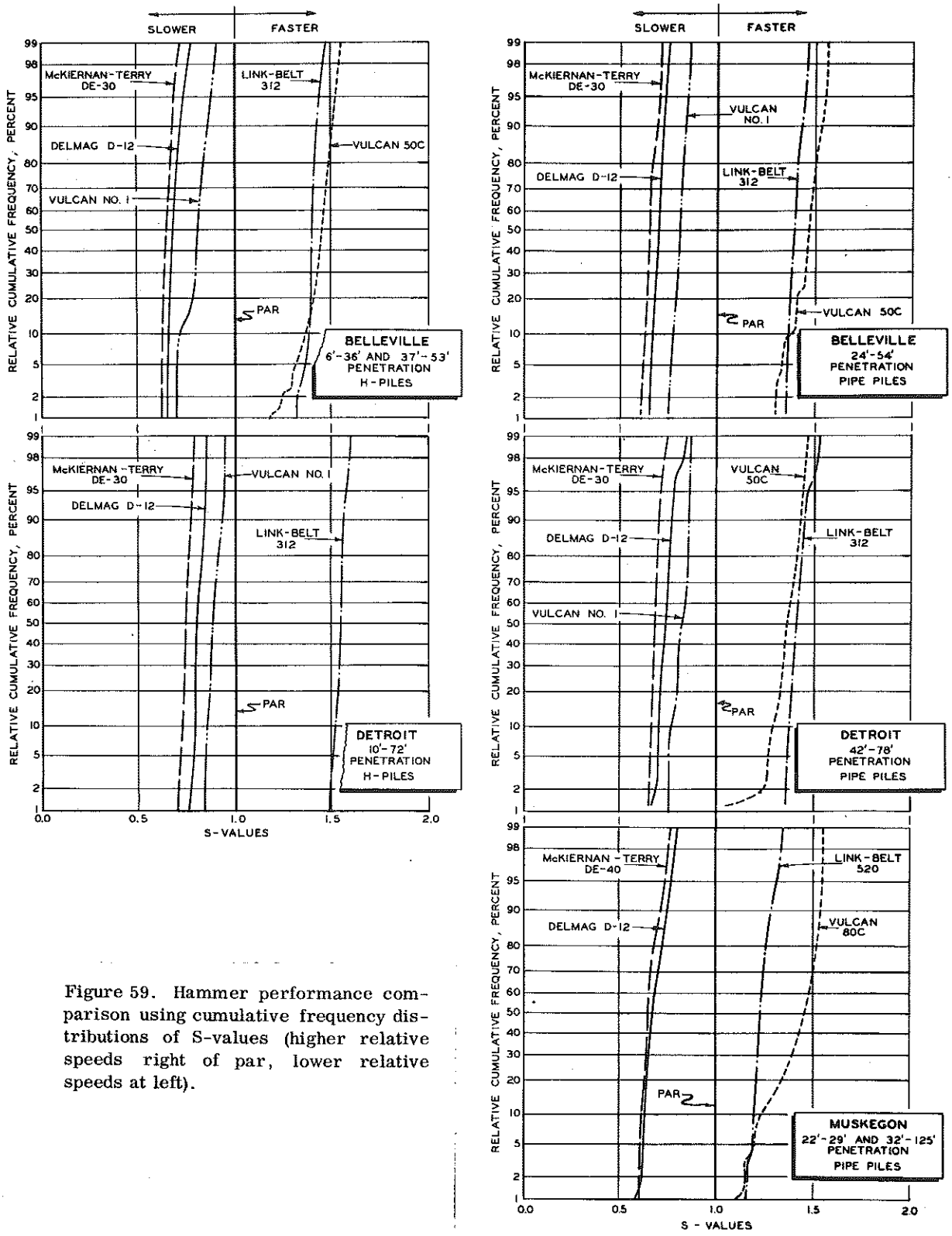

Figure 59. Hammer performance comparison using cumulative frequency distributions of S-values (higher relative speeds right of par, lower relative speeds at left).

CHAPTER SIX

HAMMER SPEED

Because hammer speed (expressed in blows per minute) is of interest for purposes of this study only insofar as it affects pile penetration rate, statistical testing of hammer differences was not required. However, soil and pile type do appear to cause small differences in hammer speed. Because speed data were necessary for penetration rate determinations (Chapter 7), this information was readily available for use with the computer program designed for the R-study (Chapter 5). Thus, an S-value analogous to R was computed for the same 1-ft depth increments:

$$S \text{ (speed ratio)} = \frac{\text{speed for a specific hammer and specific pile}}{\text{unweighted average speed for all hammers driving this specific pile type for the same increment of penetration}}$$

Cumulative relative frequency distributions of S similar to those for R are plotted in Fig. 59, although in this case values higher than par (greater than 1) are desirable. Fig. 59 shows that while relative hammer speed is more or less constant throughout the project sites, it is not entirely independent of pile type and soil conditions. Thus, although the Vulcan 50C was somewhat faster than the Link-Belt 312 at Belleville for both H-piles and pipe piles, the reverse situation was true for pipe piles at Detroit. Because no H-piles were driven with the Vulcan 50C at Detroit, it would be difficult to say whether soil or pile type made the difference. However, Fig. 60 shows that at Detroit all hammers responded to the pipe pile-soil system with a slight increase of blow frequency.

Comparisons using a numerical summarizing measure of hammer speed data can be made with the term $\bar{\bar{S}}$ for the grand arithmetic mean of all depth increments and all piles of given type driven with a given hammer. $\bar{\bar{S}}$ values for all hammer and site conditions are presented in Table 11.

Charts of hammer speed versus depth for Belleville, Detroit, and Muskegon (Figs. 60 and 61) show that the air and steam hammers generally operated faster with increasing penetration resistance, while the

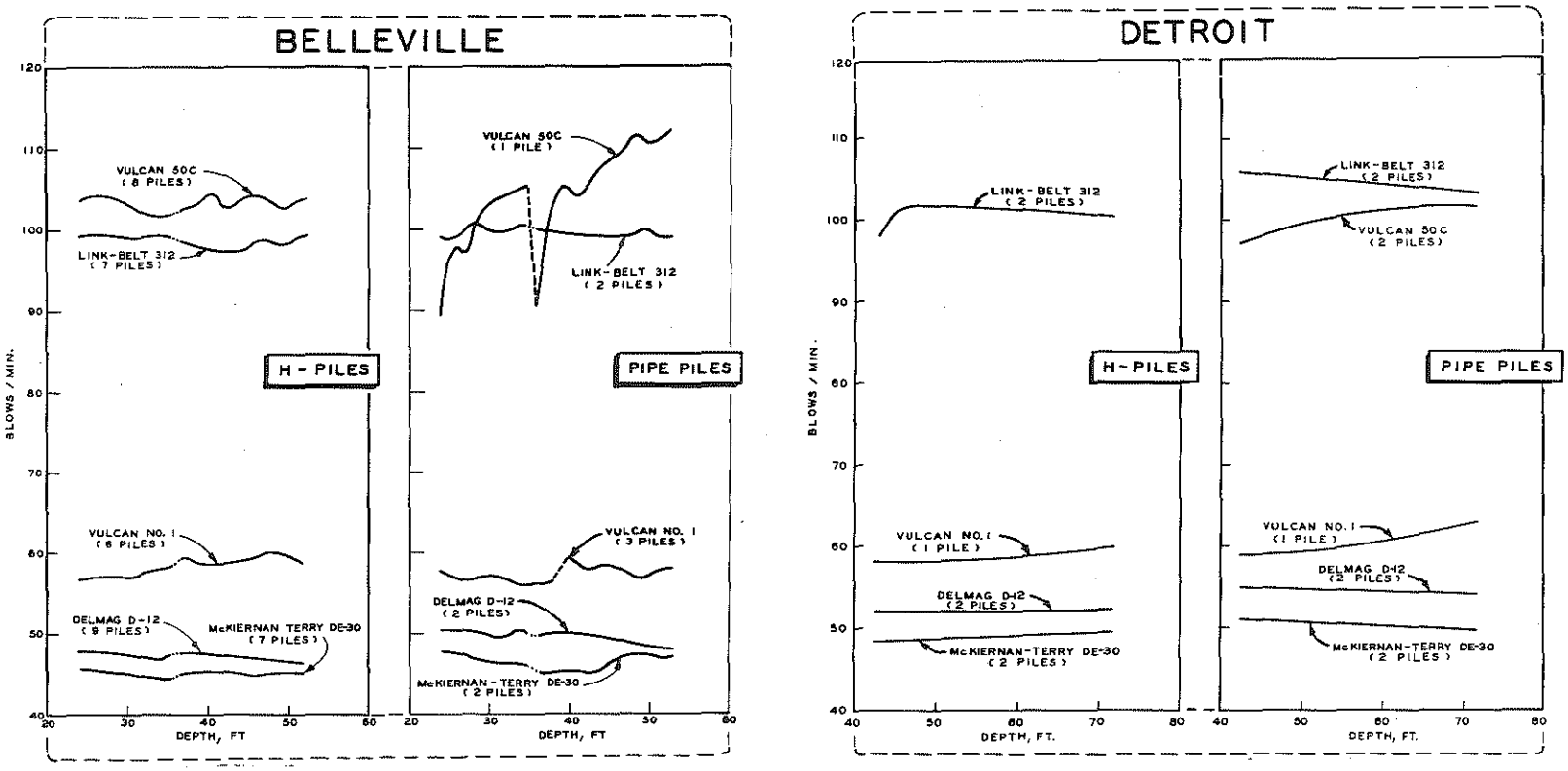

Figure 60. Approximate relationships of hammer speeds with increasing depth of pile penetration.

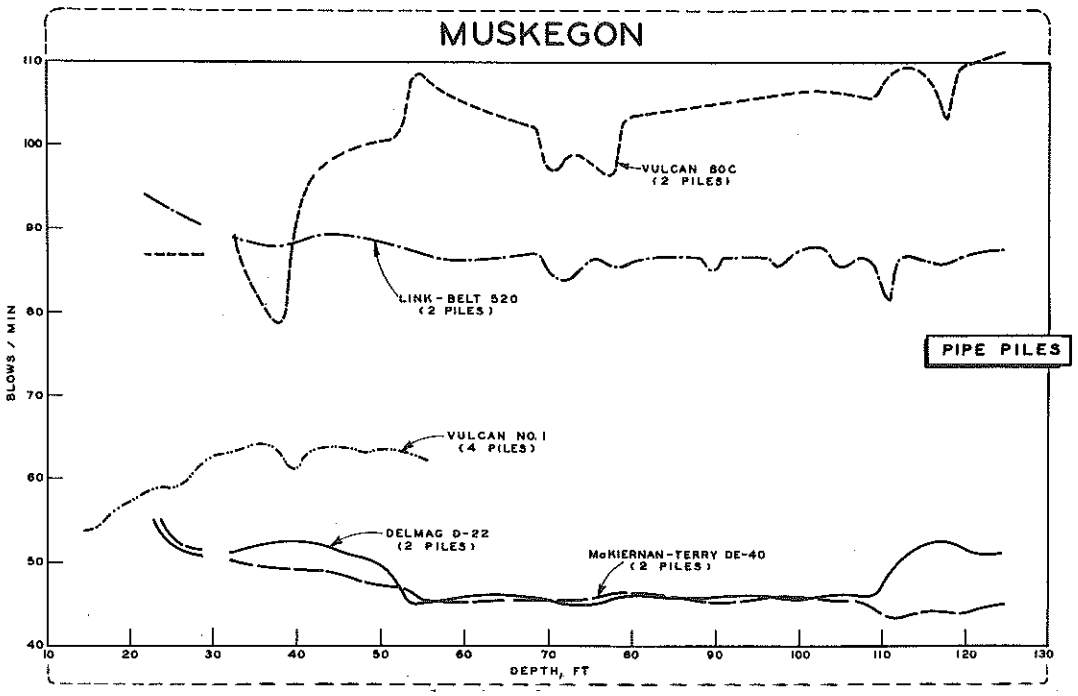

Figure 61. Approximate relationships of Muskegon hammer speeds with increasing depth of pile penetration.

diesels were relatively constant. It may be noted that at Muskegon one of the two slower diesels (Delmag D-22) increased in operating speed (to about 55 blows per min) upon entering a more resistant stratum at about 107 ft, while the other (McKiernan-Terry DE-40) decreased slightly (to 44 blows per min). In addition, at Belleville the Vulcan No. 1 produced a

TABLE 11
COMPARISON OF DRIVING PERFORMANCE BY RELATIVE SPEED

	Hammer	Grand Arithmetic Mean S-Values ($\bar{S}$)				
		Belleville		Detroit		Muskegon
		H-Piles 6 to 36 ft 37 to 53 ft	Pipe Piles 24 to 54 ft	H-Piles 10 to 72 ft	Pipe Piles 42 to 78 ft	Pipe Piles 22 to 29 ft 32 to 125 ft
Lighter Hammers	Vulcan No. 1	0.808	0.803	0.892	0.820	-----
	Vulcan 50C	1.444	1.460	-----	1.352	-----
	Link-Belt 312	1.408	1.394	1.551	1.413	-----
	McKiernan-Terry DE-30	0.653	0.650	0.748	0.680	-----
	Delmag D-12	0.687	0.694	0.808	0.734	-----
Heavier Hammers	Vulcan 80C	-----	-----	-----	-----	1.427
	Link-Belt 520	-----	-----	-----	-----	1.236
	McKiernan-Terry DE-40	-----	-----	-----	-----	0.658
	Delmag D-22	-----	-----	-----	-----	0.679

higher speed after pipe pile splicing although the cause is unknown. This sensitivity to increased length was not observed for any other hammer-pile-site combination. Also, the Vulcan No. 1 achieved its greatest measured speed at Muskegon.

TABLE 12
HAMMER SPEED VARIABILITY
FOR VARIOUS DRIVING CONDITIONS

	Hammer	Avg. Standard Deviation, blows per min.	Average Range Between Two Piles, blows per min
		H-Piles (24 to 36 ft, 37 to 53 ft)	Pipe Piles (24 to 54 ft)
Belleville	Vulcan No. 1	2.61	1.74
	Vulcan 50C	3.36	----
	Link-Belt 312	1.20	0.80
	McKiernan-Terry DE-30	1.15	1.90
	Delmag D-12	0.87	1.39

	Hammer	Average Range Between Two Piles, blows per min		
		H-Piles (42 to 72 ft)	Pipe Piles (42 to 72 ft)	H & Pipe Piles* (42 to 72 ft)
Detroit	Vulcan No. 1	----	----	3.34
	Vulcan 50C	----	7.41	----
	Link-Belt 312	1.47	0.76	----
	McKiernan-Terry DE-30	1.93	0.67	----
	Delmag D-12	0.69	3.78	----

	Hammer	Average Range Between Two Piles, blows per min	
		Pipe Piles (22 to 29 ft, 32 to 123 ft)	Pipe Piles (80 to 103 ft)
Muskegon	Vulcan 80C	5.85	8.04
	Link-Belt 520	2.07	1.23
	McKiernan-Terry DE-40	0.89	0.53
	Delmag D-22	2.92	2.35

* Range between one pipe and one H-pile.

Speed variability tabulations in Table 12 indicate that diesels generally operated at less variable speeds than either air or steam hammers; however, in the curves of hammer speed variability, the erratic speed of the Vulcan 50C for Belleville pipe piles actually represents experience in driving only one pile, while the smoother curves for other hammers were drawn by averaging records for two or more piles. Thus, Fig. 60 exaggerates variability for one hammer where only one pile was involved; consequently, comparisons of variability given in Table 12 are more meaningful for any site if unequal pile quantities are to be compared.

CHAPTER SEVEN

PILE PENETRATION RATE

Penetration rate is more an economic than a purely technical concern, since it bears directly on time required to achieve a specified pile depth. As defined here, it is the quotient of blows per minute and blows per foot required to penetrate a given 1-ft increment, or the feet per minute at some depth of penetration. In effect, the results of analyses presented in Chapters 5 and 6 are combined in the following discussion, since it could not be assumed that blow count and speed are independent for all hammers. Originally, it was thought that for a given hammer, the penetration rate would be calculated by dividing average speed by blow count. However, examination of data revealed some speed variation (particularly at Muskegon, as shown in Fig. 61); therefore, it was decided to compute penetration rates directly from the data.

Relative penetration rate values $\underline{P}$ which were independent of the effects of penetration level were computed in the same manner as the blow count ratios $\underline{R}$ of Chapter 5:

$$\underline{P}\ \text{(penetration rate ratio)} = \frac{\text{penetration rate for a specific hammer and specific pile}}{\text{unweighted average penetration rate for all hammers driving this specific pile type for the same increment of penetration}}$$

Other terms appearing in the penetration analysis are:

$\bar{\underline{P}}_i$ = mean or average penetration rate ratio for a given 1-ft penetration increment $\underline{i}$

$\bar{\bar{\underline{P}}}$ = grand arithmetic mean of all depth increments and all piles of a given type driven with a given hammer.

Handling the data for each pile in this way, as opposed to using total pile penetration time, confines any unusual soil effect to the depth increment where it occurs, so that the role of extraneous factors is substantially reduced. Cumulative relative frequency distributions (ogives) are plotted in Fig. 62, summarizing relative hammer penetration rates

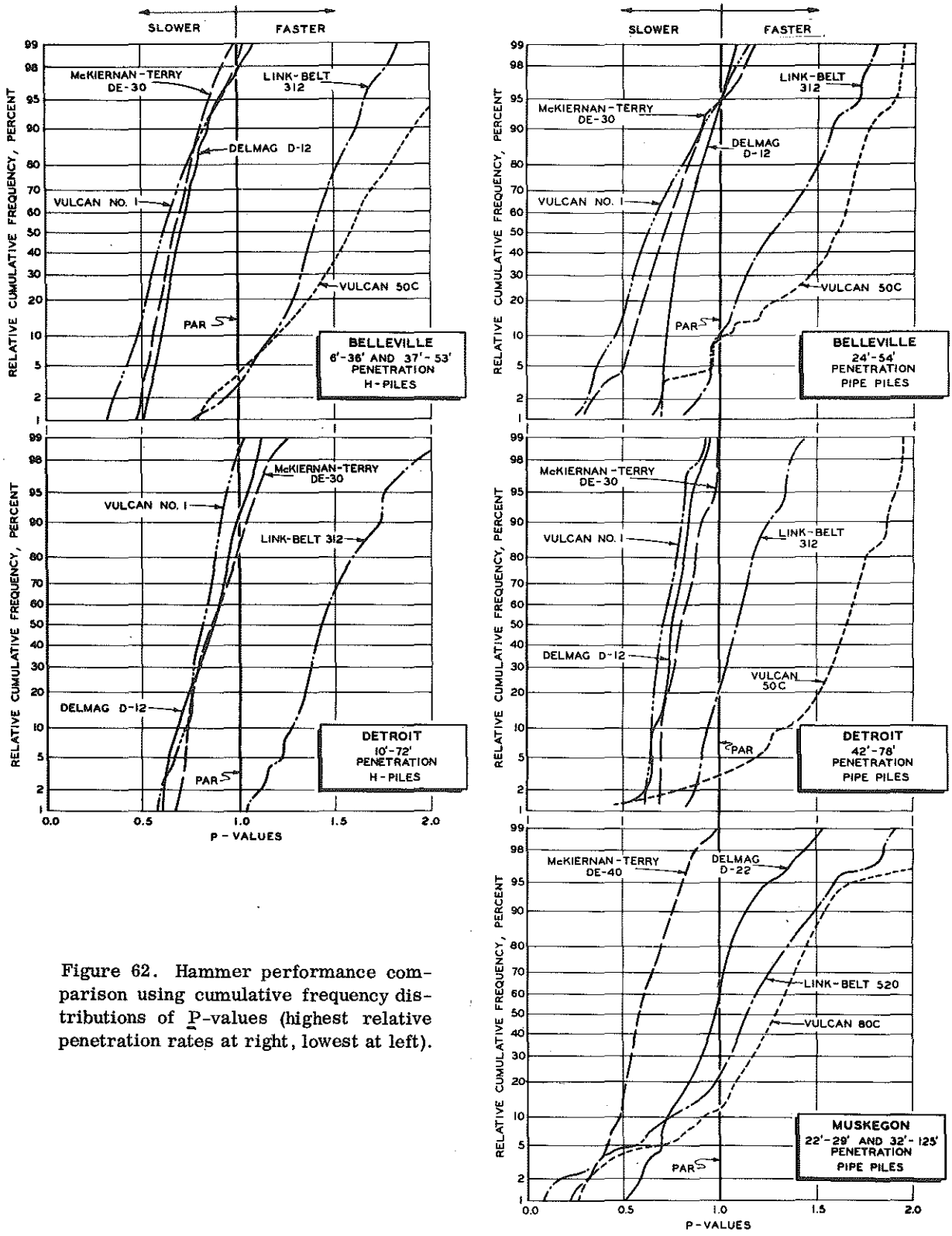

Figure 62. Hammer performance comparison using cumulative frequency distributions of P-values (highest relative penetration rates at right, lowest at left).

on a 1-ft depth increment basis. The descriptive remarks for Fig. 48 also apply to these distributions and need not be repeated here. It should be noted, however, that unlike the R-values of Chapter 5, P-values above 1 indicate above-average performance. Thus, the hammer delivering the highest overall penetration rates would be represented by a line farthest right in the Fig. 62 graphs. The combined effects of hammer blow count and speed performance can now be seen in terms of the time required to penetrate 1-ft depth increments.

It is evident that penetration rates for Delmag, Vulcan No. 1, and McKiernan-Terry hammers are quite similar at Belleville and at Detroit, with relative P-values ranging from 0.6 to 0.9 in about 50 percent of the cases. For the Link-Belt, penetration rates ranged from 1.1 to 1.4 in about 50 percent of the cases, and for the Vulcan 50C, rates ranged from 1.4 to 1.7 in about 50 percent of the cases. Fig. 62 also shows that the Vulcan 50C was somewhat more variable in its penetration rate at both sites, as evidenced by the smaller angle of the ogive relative to the horizontal, the Link-Belt 312 being intermediate in this regard. It may be noted that the relative rating of hammers by penetration rate (in feet per minute) over the depths considered parallels that based on blows per minute (Fig. 59). That is, the speed of hammer operation is a dominant factor in relative performance of the lighter hammers used at Belleville and Detroit, under soft-to-firm soil resistance conditions. The ability of a hammer to penetrate highly resistant layers (as at Muskegon) appears largely to be a function of hammer capacity (or abailable driving energy) and not hammer speed, as will be discussed subsequently in more detail.

Grand arithmetic means of penetration rates $\underline{\underline{P}}$ (similar to those of Tables 5 and 11) are given in Table 15. Detroit comparisons in Table 13 are only approximate, because no H-piles were driven with the Vulcan 50C, so that P-ratios for H-piles cannot be compared with those for pipe piles; Detroit pile penetration rate comparisons are shown in Fig. 63. At Belleville, however, all hammers drove both H-piles and pipes, allowing performance comparisons of the major pile types. If the faster hammers (Vulcan 50C and Link-Belt 312) responded to the greater elasticity of the pipe pile-soil system with slightly increased blow frequency, this was not sufficient to make a large improvement in penetration rate. At Belleville, the overall penetration rates of both these hammers were somewhat greater for pipes than for H-piles (Table 13). However, at Detroit the Link-Belt was able to drive H-piles faster than pipes, particularly in the shallow penetration ranges. This difference would be explained in part by an overall penetration rate improvement, characteristic of the diesels and the Vulcan No. 1 when pipe piles were driven. No comparative data are available for the 50C.

As in Chapter 5, penetration control charts (Figs. 65 and 66) were constructed to establish the areas of acceptable data, and mean penetration rate ratios $\bar{P}_i$ falling outside the specified limits[1] were examined. As would be expected, $\bar{P}_i$ and $\bar{R}_i$ values are out of control at about the

TABLE 13
COMPARISON OF DRIVING PERFORMANCE
BY RELATIVE PENETRATION RATE

	Hammer	Percent P-Values Better than Par (P more than 1)				
		Belleville		Detroit		Muskegon
		H-Piles 6 to 36 ft 37 to 53 ft	Pipe Piles 24 to 54 ft	H-Piles 10 to 72 ft	Pipe Piles 42 to 78 ft	Pipe Piles 22 to 29 ft 32 to 125 ft
Lighter Hammers	Vulcan No. 1	3	4	2	0	--
	Vulcan 50C	96	90	--	97	--
	Link-Belt 312	97	91	99	82	--
	McKiernan-Terry DE-30	1	6	19	0	--
	Delmag D-12	3	6	7	0	--
Heavier Hammers	Vulcan 80C	--	--	--	--	88
	Link-Belt 520	--	--	--	--	79
	McKiernan-Terry DE-40	--	--	--	--	1
	Delmag D-22	--	--	--	--	42

	Hammer	Grand Arithmetic Mean P-Values ($\bar{P}$)				
		Belleville		Detroit		Muskegon
		H-Piles 6 to 36 ft 37 to 53 ft	Pipe Piles 24 to 54 ft	H-Piles 10 to 72 ft	Pipe Piles 42 to 78 ft	Pipe Piles 22 to 29 ft 32 to 125 ft
Lighter Hammers	Vulcan No. 1	0.623	0.651	0.814	0.722	-----
	Vulcan 50C	1.579	1.518	-----	1.614	-----
	Link-Belt 312	1.392	1.289	1.467	1.110	-----
	McKiernan-Terry DE-30	0.694	0.720	0.892	0.809	-----
	Delmag D-12	0.722	0.822	0.846	0.757	-----
Heavier Hammers	Vulcan 80C	-----	-----	-----	-----	1.294
	Link-Belt 520	-----	-----	-----	-----	1.138
	McKiernan-Terry DE-40	-----	-----	-----	-----	0.599
	Delmag D-22	-----	-----	-----	-----	0.969

same penetration levels and probably for the same reasons. Therefore, explanations of erratic points given in Table 7 also are assumed to apply here.

[1] Set at three standard deviations as in Chapter 5.

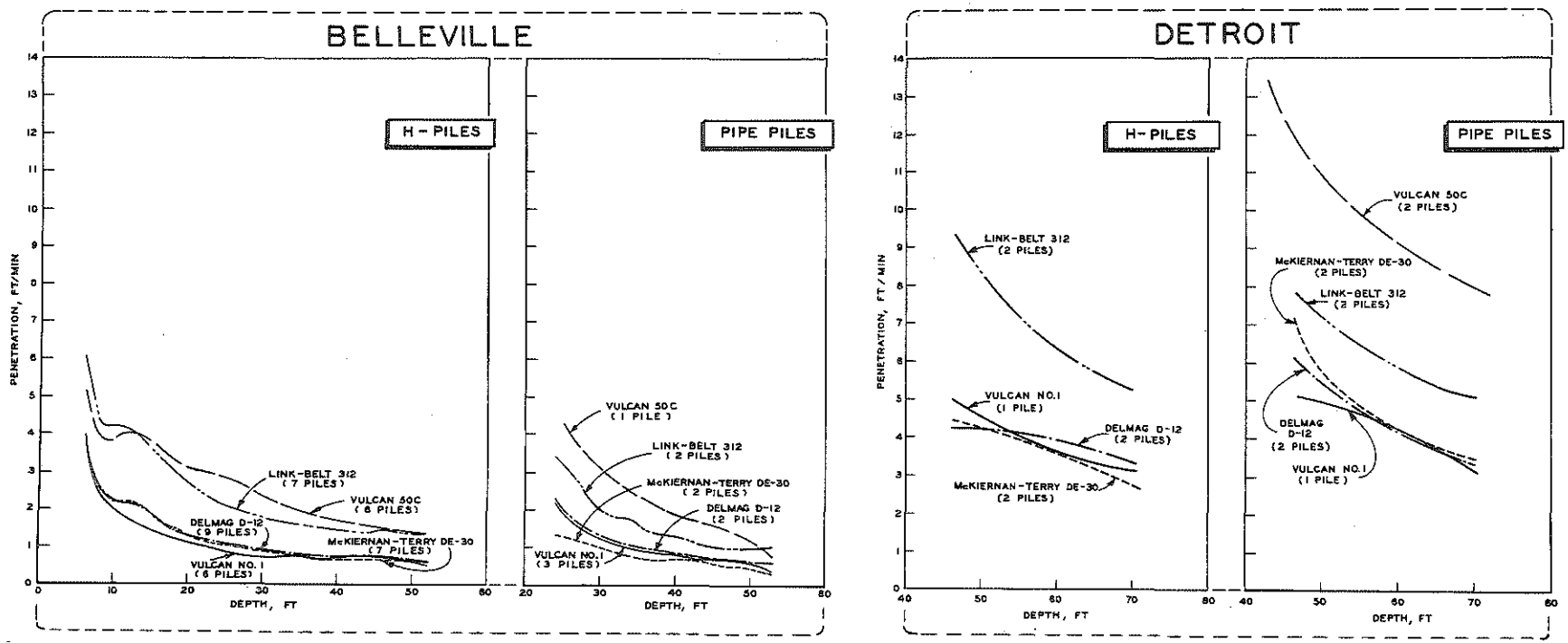

Figure 63. Approximate relationships of pile penetration rate with increasing depth (for Belleville pipe piles, first 33 ft for Vulcan 50C based on extrapolation of data, due to operating problems).

At Muskegon (Fig. 64) comparative penetration rates are shown for the depth range in which there was sufficiently small variability between the two pipe piles driven with each hammer. Also, hammer performance is shown in the first highly resistant stratum, encountered at about 107 ft. No statistical analysis was possible for this region because of its short depth and excessive variability among piles (Table 14); however, Fig. 64 indicates relative effects of the hammers in highly resistant sand soils.

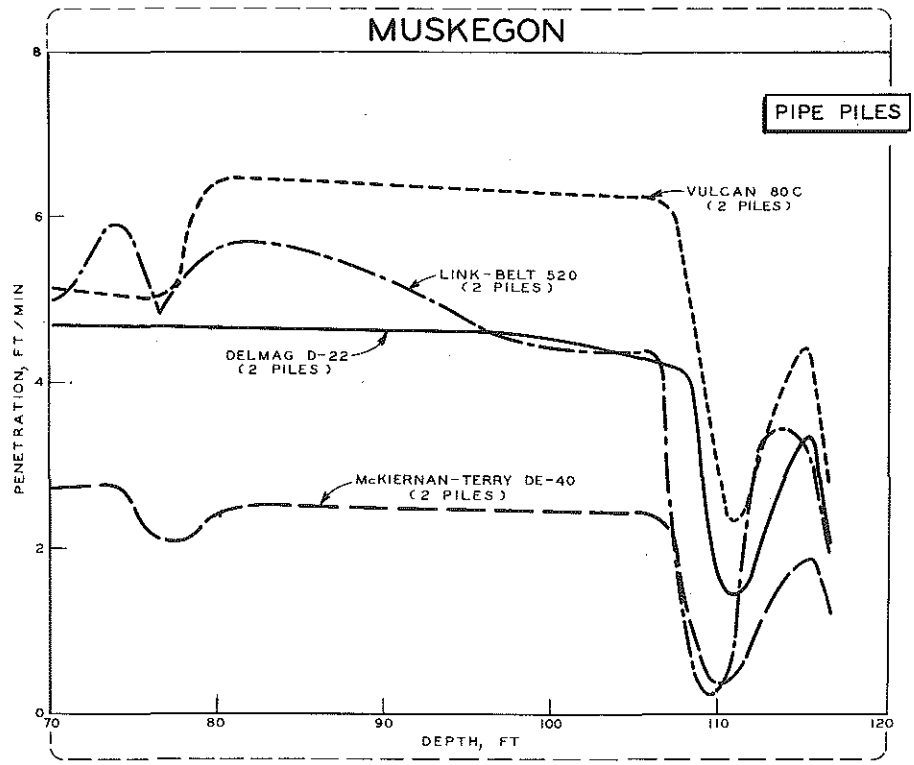

Figure 64. Approximate relationships of pipe penetration rate with increasing depth.

For example, the Delmag D-22, driving at a fairly constant speed of 45 to 50 blows per min (Chapter 6), did not penetrate soft soil (down to about 90 ft) as fast as the Link-Belt 520 driving with about the same speed variability (Table 12) at 95 to 105 blows per min. However, in the highly resistant intermediate strata encountered at various penetrations at Muskegon (i.e., 107 ft), the Delmag D-22 despite slower speed is able to penetrate more rapidly than the Link-Belt 520. This is because the Delmag was a larger hammer, and indicates that in this case, the "light, fast" Link-Belt hammer (a smaller-output design) had reached or exceeded its practical driving capacity. Thus, comparatively high usable energy as

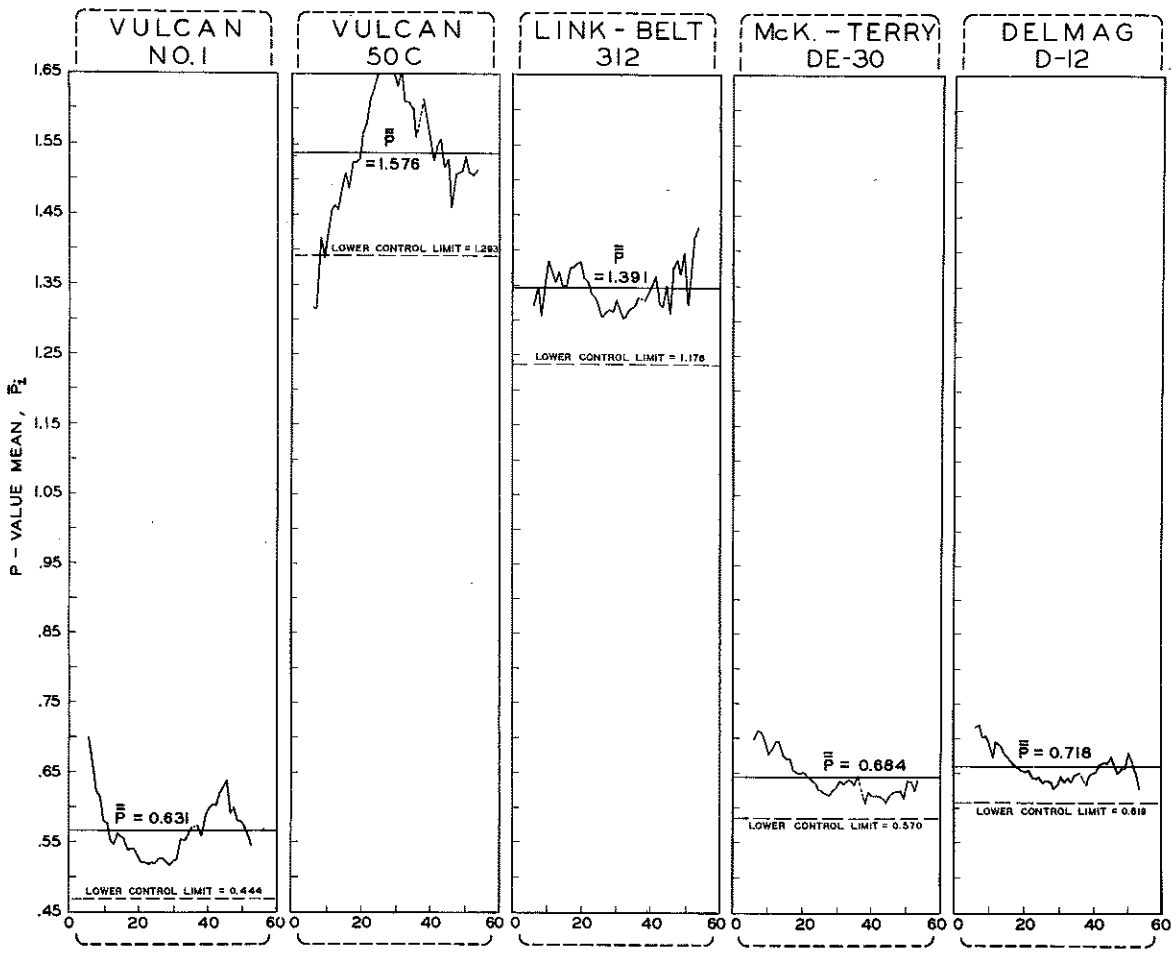

Figure 65. Belleville H-pile penetration control charts, for P-value means $\bar{P}_i$, for the penetration increments given.

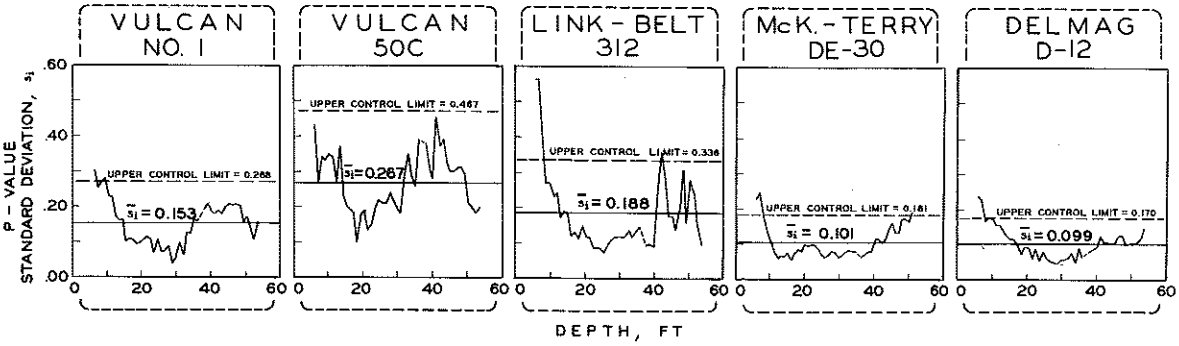

Figure 66. Belleville H-pile penetration control charts, for P-value standard deviations s_i, for the penetration increments given.

indicated by blow count performance (Table 10) can, under conditions of hard driving, make up for slower hammer speed and can become the limiting factor in penetration rate. In fact, at Muskegon under conditions of easy driving (0 to about 70 ft), the Link-Belt 520 delivered the highest

TABLE 14
VARIABILITY OF PILE PENETRATION RATES
FOR VARIOUS DRIVING CONDITIONS
Showing Exclusions from Analysis of Variance Study (Parenthesized)
Due to Excessive Variability

	Hammer	Avg. Standard Deviation, ft per min	Average Range Between Two Piles, ft per min
		H-Piles (24 to 36 ft, 37 to 53 ft)	Pipe Piles (24 to 54 ft)
Belleville	Vulcan No. 1	0.14	(0.17)
	Vulcan 50C	(0.30)	----
	Link-Belt 312	0.16	(0.18)
	McKiernan-Terry DE-30	0.10	(0.11)
	Delmag D-12	0.09	0.04

	Hammer	Average Range Between Two Piles, ft per min		
		H-Piles (42 to 72 ft)	Pipe Piles (42 to 72 ft)	H & Pipe Piles (42 to 72 ft)*
Detroit	Vulcan No. 1	----	----	4.68
	Vulcan 50C	----	(14.00)	----
	Link-Belt 312	(8.28)	(7.24)	----
	McKiernan-Terry DE-30	3.32	5.24	----
	Delmag D-12	4.20	3.28	----

	Hammer	Average Range Between Two Piles, ft per min	
		Pipe Piles (22 to 29 ft, 32 to 123 ft)	Pipe Piles (80 to 103 ft)
Muskegon	Vulcan 80C	(22.60)	3.44
	Link-Belt 520	(14.44)	2.70
	McKiernan-Terry DE-40	5.53	3.22
	Delmag D-22	6.17	3.09

* Range is between one pipe and one H-pile.

penetration rates of the four hammers compared.[2] However, under very hard driving conditions from 109 to 110 ft, the Link-Belt 520 delivered the lowest penetration rate of these hammers. The effects of extreme soil

[2] This was by a thin margin over the Vulcan 80C. The differences between piles were too great for detailed examination.

conditions (compact sand) were as follows, ranking hammers in order of penetration rate from highest to lowest:

Easy Driving (0-70 ft)	Hard Driving (109-110 ft)
Link-Belt 520	Vulcan 80C
Vulcan 80C	Delmag D-22
Delmag D-22	McKiernan-Terry DE-40
McKiernan-Terry DE-40	Link-Belt 520

The first statistical analysis was performed on the data obtained from 80 to 103 ft. In this region, hammer variability was no problem and the relative effects of some change in soil conditions could be determined. Statistical tests[3] established the significance of differences in hammer penetration rates for this soil region and substantiate the graphic indications (Fig. 64) that changing soils do affect the hammers unequally (note the Link-Belt 520). Because of the small penetration range for which this type of examination was possible, more flexible statistical tests were performed on the larger ranges of 22 to 29 and 32 to 125 ft.[4] These tests agree, in every case, with the results of the earlier analysis, but provide a more extensive basis for conclusions. Overall penetration rates for all hammers and sites are presented in Table 15, using a format similar to Table 10 but with greatest penetration rates at right, and lowest at left.

---

[3] Two-factor analysis of variance on penetration rates using a significance level of 0.05.

[4] Non-parametric Friedmann and Wilcoxon Signed Rank Tests (see footnote 12, Chapter 5) at the 0.05 level. These tests are somewhat less powerful than the F-tests used with the analysis of variance when the assumptions of the F-test are met. Also, the non-parametric tests do not assess the significance of interactions (the different effects changing soil conditions have on the penetration rates of the various hammers).

TABLE 15
RELATIVE HAMMER PERFORMANCE
BASED ON PILE PENETRATION RATE IN FEET PER MINUTE
Ordered by Increasing $\bar{\bar{P}}$-Values (lowest relative penetration rate at left, highest at right)

Site, Pile Type, and Range		Hammer, Rated Energy, and $\bar{\bar{P}}$-Value				
Belleville	H-Piles (24 to 36 ft, 37 to 53 ft)	Vulcan No. 1 15,000 ft-lb $\bar{\bar{P}} = 0.614$	McKiernan-Terry DE-30 16,800 ft-lb mean 22,400 ft-lb max $\bar{\bar{P}} = 0.686$	Delmag D-12 22,500 ft-lb $\bar{\bar{P}} = 0.723$	Link-Belt 312 15,000 ft-lb max equiv. WH gage 18,000 ft-lb max mfr's rating $\bar{\bar{P}} = 1.395$	Vulcan 50C 15,100 ft-lb $\bar{\bar{P}} = 1.582$
	Pipe Piles (24 to 54 ft)	Vulcan No. 1 15,000 ft-lb $\bar{\bar{P}} = 0.651$	McKiernan-Terry DE-30 16,800 ft-lb mean 22,500 ft-lb max $\bar{\bar{P}} = 0.720$	Delmag D-12 22,500 ft-lb $\bar{\bar{P}} = 0.822$	Link-Belt 312 15,000 ft-lb max equiv. WH gage 18,000 ft-lb max mfr's rating $\bar{\bar{P}} = 1.289$	Vulcan 50C 15,100 ft-lb $\bar{\bar{P}} = 1.518$
Detroit	H-Piles (10 to 72 ft)	Vulcan No. 1 15,000 ft-lb $\bar{\bar{P}} = 0.814$	Delmag D-12 22,500 ft-lb $\bar{\bar{P}} = 0.846$	McKiernan-Terry DE-30 16,800 ft-lb mean 22,500 ft-lb max $\bar{\bar{P}} = 0.872$	Link-Belt 312 15,000 ft-lb max equiv. WH gage 18,000 ft-lb max mfr's rating $\bar{\bar{P}} = 1.467$	
	Pipe Piles (42 to 78 ft)	Vulcan No. 1 15,000 ft-lb $\bar{\bar{P}} = 0.722$	Delmag D-12 22,500 ft-lb $\bar{\bar{P}} = 0.757$	McKiernan-Terry DE-30 16,800 ft-lb mean 22,400 ft-lb max $\bar{\bar{P}} = 0.809$	Link-Belt 312 15,000 ft-lb max equiv. WH gage 18,000 ft-lb max mfr's rating $\bar{\bar{P}} = 1.098$	Vulcan 50C 15,100 ft-lb $\bar{\bar{P}} = 1.614$
Muskegon	Pipe Piles (22 to 29 ft, 32 to 125 ft)	McKiernan-Terry DE-40 24,000 ft-lb mean 22,400 ft-lb max $\bar{\bar{P}} = 0.599$	Delmag D-22 39,700 ft-lb $\bar{\bar{P}} = 0.969$	Link-Belt 520 26,300 ft-lb max equiv. WH gage 30,000 ft-lb max mfr's rating $\bar{\bar{P}} = 1.138$	Vulcan 80C 24,450 ft-lb $\bar{\bar{P}} = 1.294$	

Underscored groups have differences of P not large enough to suggest real performance differences; differences are on a per-comparison basis for the 5-percent confidence level.

CHAPTER EIGHT

HAMMER ENERGY

Pile driving hammers are usually rated on the basis of maximum kinetic energy developed prior to impact. However, it is recognized that a significant portion of this energy is lost by mechanical friction within the hammer, and during the inelastic compression of the cushion and/or cap located between the hammer and the top of the pile. One might consider these losses as work done incidental to the pile driving, dissipated as non-recoverable heat. Certain of the pile driving formulas attempt to account for this loss by reducing the energy considered to be delivered into the top of the pile, available for compressing and advancing the pile through the ground.

One of the objectives of the pile hammer study was development of a method for direct measurement of the net energy delivered into the top of the pile. The procedure selected was based on measuring simultaneously the force $\underline{F}$ and associated movement $\underline{\Delta S}$, measured at a load cell located at the top of the pile, and then summing the successive increments:

$$\text{Work} = \sum_{i=1}^{i=N} \left[F\ (i) \times \Delta S\ (i) \right]$$

It is assumed that this work is numerically equal to the net delivered energy. It is implicit in this method of measuring net delivered energy that there be no significant energy losses in transmitting the hammer blow's kinetic energy through the load cell to the top of the pile. This work is analogous to that which would be recorded in each of a series of adjoining billiard balls when struck by the cue ball. In this classic example only the end ball would appear to react, ideally having a kinetic energy equal to that of the impinging cue ball. However, the successive contact forces and compression strain in each of the intermediate balls would again ideally yield a peak work figure exactly equal to the original kinetic energy, with a final work value equal to zero after the end ball has left the row. Thus, the intermediate balls could be considered to transmit the kinetic energy by being "worked" upon by balls preceding and in turn "working" upon succeeding balls.

Similarly, the load cell (if of sturdy enough construction) would absorb essentially no energy, although being "worked" upon by the hammer. Such "work" is essentially the same as in the billiard ball analogy. To avoid any possibility of confusion, the coined term ENTHRU is used to identify net transmitted energy, or more specifically the work done on the load cell. It had been planned at first to measure displacements of the pile at the ground surface. However, as a consequence of instrumentation difficulties at the first two sites, the only valid displacement measurements were taken at Muskegon, the last test site. A high-capacity accelerometer was also provided at the load cell flange during most of the test program, and acceleration measurements were taken in conjunction with most force traces obtained. Subsequent analysis involved double integrating the acceleration trace data to obtain deflection values, and then taking a summation of $F \times \Delta S$ increments, as expressed in the preceding equation. However, the necessity of deriving deflection curves from acceleration traces generated its own problems, and considerable experimentation and crosschecking were required to reconcile the deduced results. Because some of the data reduction techniques and the manner of analysis were dictated by the circumstances of this particular project, this aspect of the analysis will be discussed in some detail.

Data Reduction

The basic dynamic test data consisted of continuous trace lines recorded by a high-speed oscillograph, showing the load cell and accelerometer output against a common time base. Typical trace records are shown in Fig. 32. These records were generally obtained for a succession of two to five hammer blows at depth intervals of 5 ft. Not all the hammer-pile combinations studied were thus measured because of various experimental difficulties; still a formidable volume of data was acquired (in excess of 1500 blows).

A general review of the trace data indicated that accelerometer and load cell output varied over a wide range, and often displayed a high frequency of fluctuations. Nonetheless the trace records obtained from successive blows were almost identical and indicated that response of the measuring system was relatively stable. It was apparent, however, that several dozen digital readings were required just to locate the inflection points to even approximate a single trace in all its complexities. These readings, in conjunction with the associated time values, aggregated in the tens of thousands.

To facilitate the data reduction, a Benson-Lehner oscillographic trace reader was used. Details of its operation are described in App. B.

Briefly, the trace data were read as a succession of point values from arbitrary base lines to a 0.01-in. accuracy. Appropriate scale factors and correction values were also determined in order to convert inches measured into force, acceleration, and time values. These data were then transcribed onto punch cards for eventual processing in a high-speed electronic computer.

About 10 percent of all the traces were rejected for various reasons; some traces were distorted in photographic development, causing time lines to appear bent or curved, and in some cases traces were too faint to be readable. Blows were rejected if the recording paper had undergone acceleration, or after changes in velocity during a given hammer blow (primarily a problem with the older recorder used at Belleville and Detroit). Certain other malfunctions were also evident and were the bases for omitting traces from further consideration.

In the case of high-frequency response of small amplitudes, faithful transcription of all trace fluctuations was impossible or impractical. It was decided to average the values over small time increments. Because this small amplitude "hash" generally occurred beyond the time of peak displacement or ENTHRU development, averaging resulted in negligible errors in the final curves computed for displacement and ENTHRU. This was considered a practical device for digitizing data necessary for the computer program used.

Computation of Displacements and ENTHRU

A high-speed electronic computer was used to facilitate determination of time-displacement and ENTHRU over the period of significant forces and accelerations for single hammer blows. Program details are presented in App. B (Plates 2-8). Essentially, it involved successive velocity and displacement determinations, based on linear interpolations and numerical integration of input acceleration values $\underline{A}$, at 0.0001-sec intervals (300 to 700 or more intervals). ENTHRU was then computed as the sum of a succession of force x displacement at 0.0001-sec intervals, based on interpolated average force values and associated displacement increments.

The displacement computation was essentially a numerical evaluation of the basic double integral:

$$S = \iint_{t=0}^{t=T} A \, d_t d_t$$

Therefore it was to be expected that the final answer would be extremely sensitive to small variations (from whatever source) in the acceleration-time values used. This indeed proved to be the case, and it was necessary to incorporate certain controls and adjustments to process and evaluate the trace data.

The first control was the series of manually recorded deflection trace values, obtained during most of the driving program (Chapter 4). Each consisted of an independent record of peak and terminal displacement of a pile under a single hammer blow, measured near the ground surface. The peak values then were a direct measure of maximum displacement, and should have closely matched associated vertical movements at the top of the pile (at the accelerometer location). The peak manually recorded deflection, with a small correction for deflection of pile stub length, is designated "limset." This value was set as a target point through which the companion double-integrated trace should pass at peak value.

A further restriction on the computed displacement trace was that it should look like a true time-displacement trace; that is, it should proceed to a maximum and ideally then return to a terminal displacement about equal to the permanent set recorded for that hammer blow. However, the latter goal depended on achieving very great accuracy of detail or compensating error in acceleration data, and this could be achieved completely in only some instances (e.g., Belleville TP 14, Plate 185, App. B).

The most straightforward way of adjusting the computed deflection curve was by making small positive or negative corrections in the acceleration values. By a series of trial computations, varying the size and sign of the correction factor and comparing results, it was possible to pass the peak of the computed deflection curve through or close to the limset value. It was noted that the general character of the computed curves was sometimes improved after adjustment, particularly the portion of the curve after peak displacement.

In considering the possible data errors which might necessitate corrections, the following factors were noted:

1. Small errors in the base line assigned to the acceleration data would be constant and would have a cumulative effect with increasing time.

2. Peaks combining high amplitudes and frequencies were generally more difficult to record and/or read accurately.

For these reasons it was decided to make a small percentage adjustment on all acceleration readings, in either a positive or negative direction. This would in effect give a maximum adjustment to the generally less certain high peak values of acceleration. Also, it would have roughly the same effect on the computed displacement as raising or lowering the zero base line of the acceleration record.

The effect of increasing or decreasing the acceleration values is illustrated in Figs. 67 through 69, where the computed displacement and associated ENTHRU curves have been plotted for the range of correction

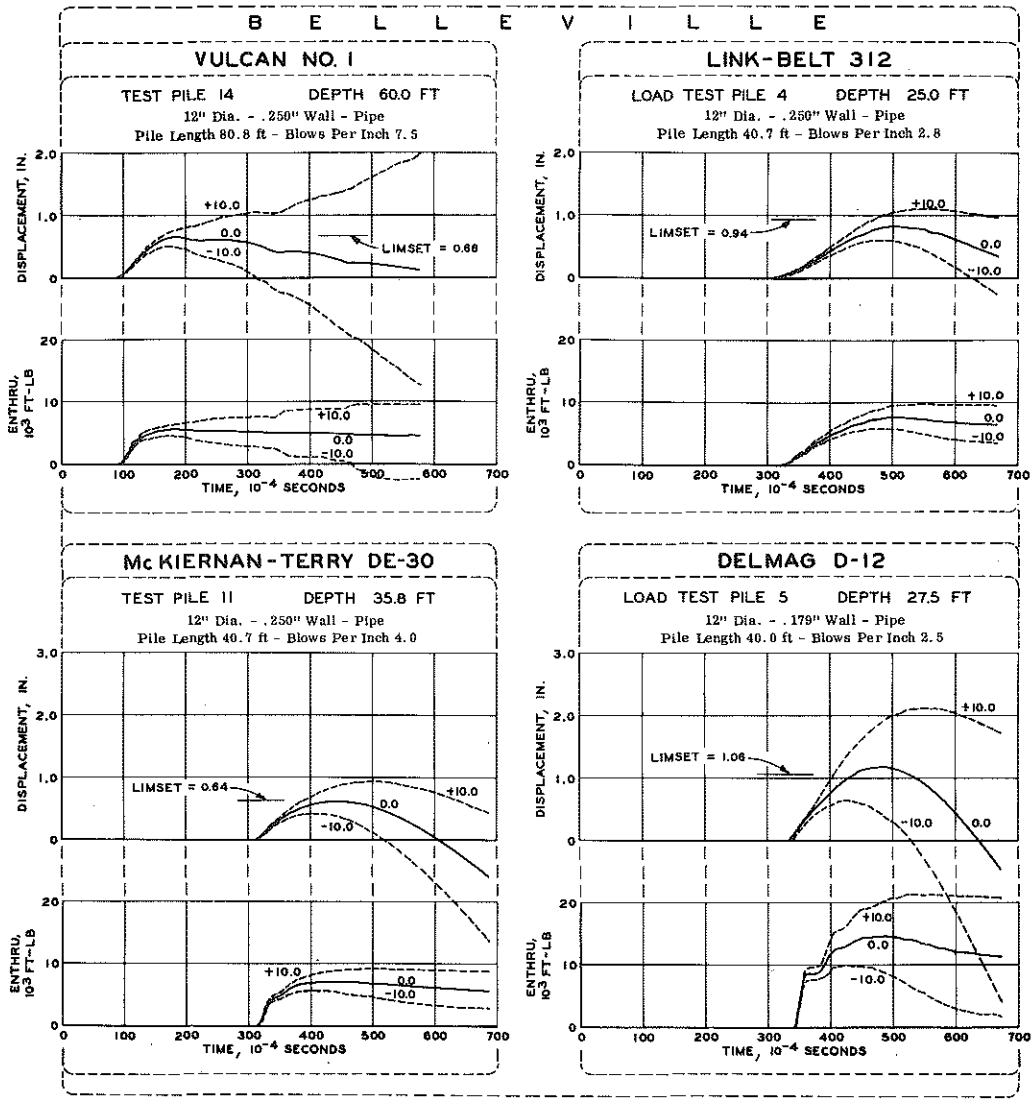

Figure 67. Effect of varying the percent adjustment of acceleration.

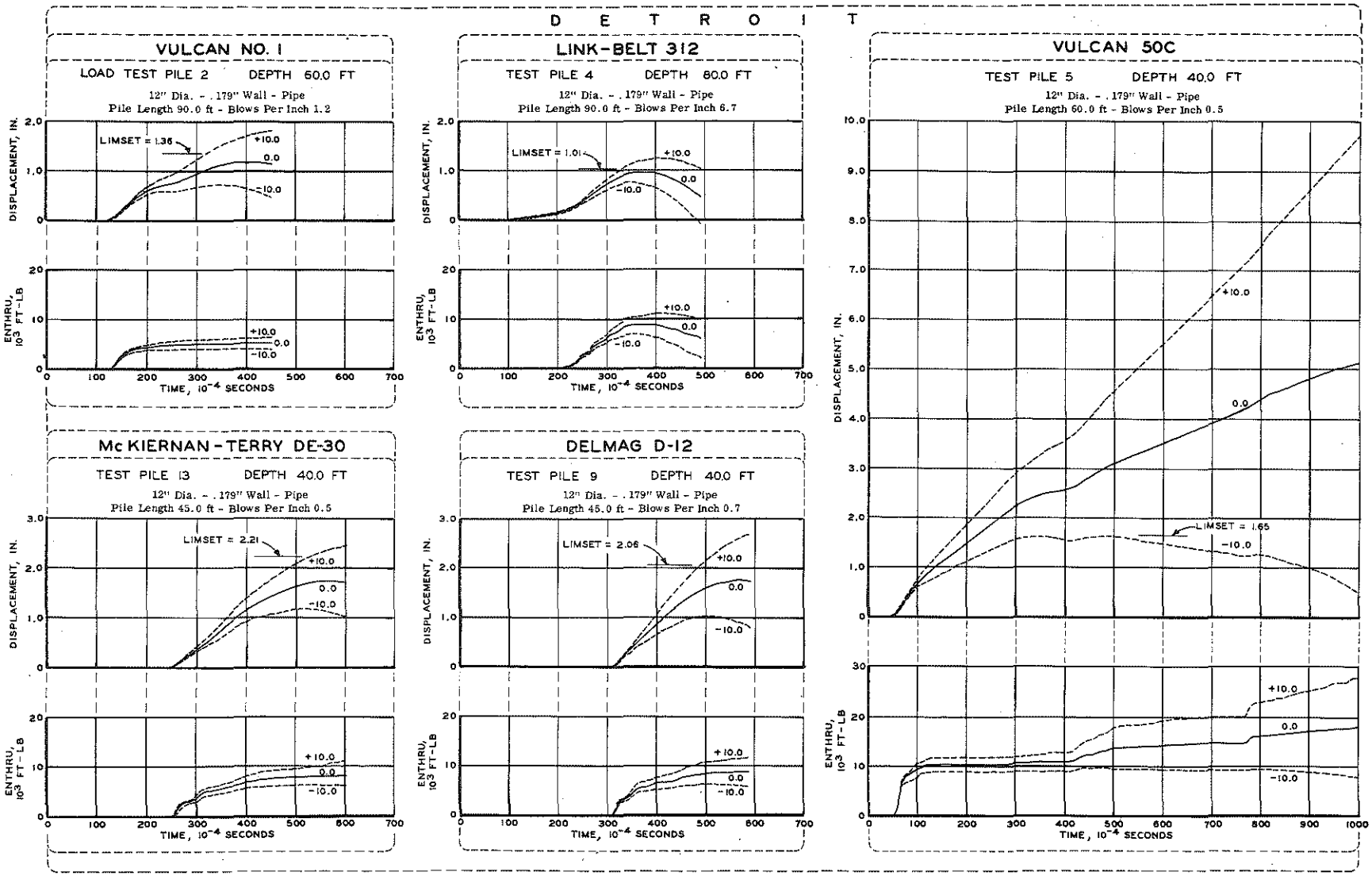

Figure 68. Effect of varying the percent adjustment of acceleration.

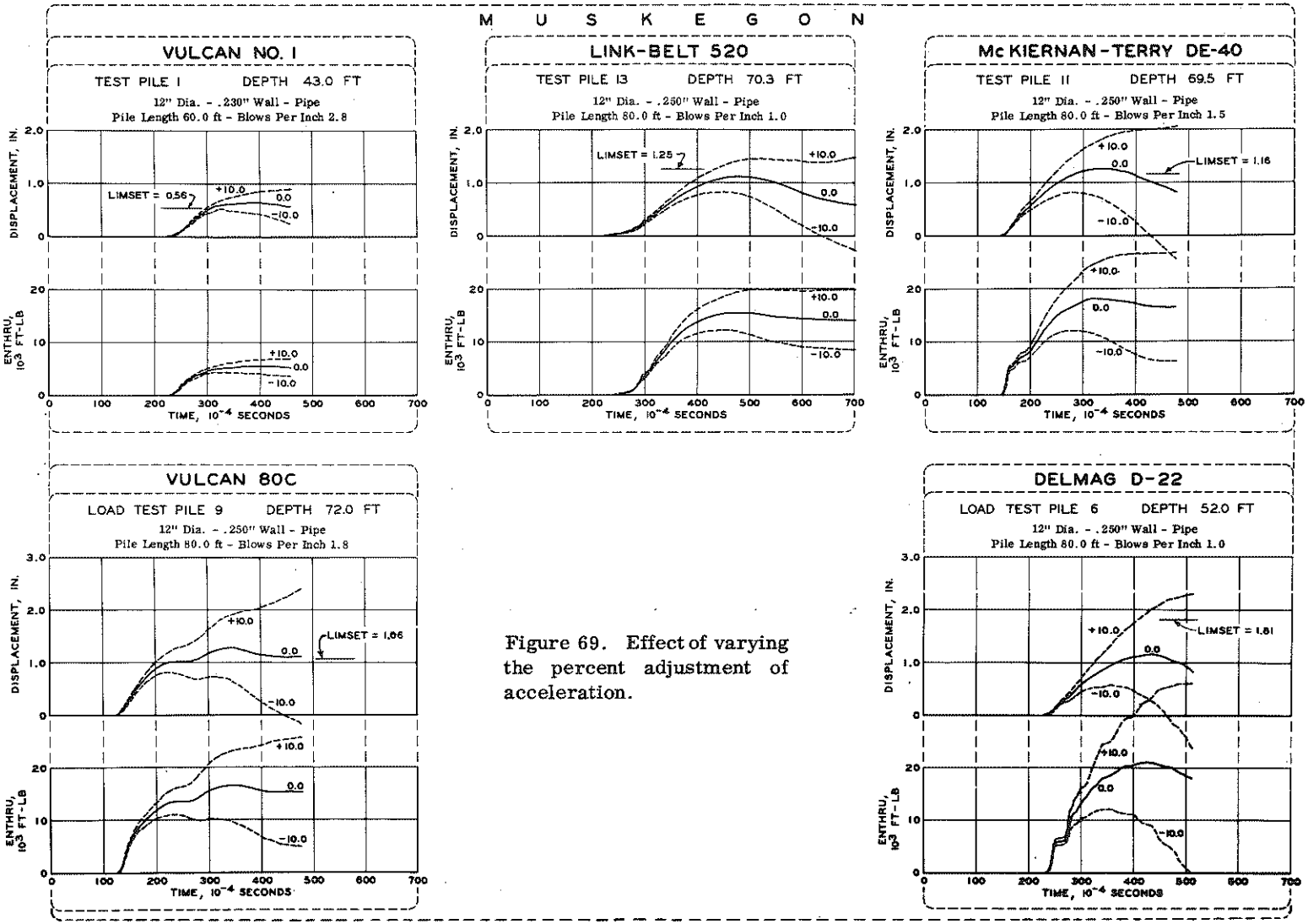

Figure 69. Effect of varying the percent adjustment of acceleration.

factors ± 10 percent. The general character of the initial portion of the computed curves is not greatly changed by adjustments of this range. However, the peak values of both computed deflection and ENTHRU can differ by over 100 percent, and the trend of the terminal portion of the curve is radically altered. Limset values are also indicated, and for the traces shown, only a small correction would be required to bring the computed deflection curve through this target. In addition, the peak ENTHRU coincides with the peak deflection, as is mathematically required. Thus, the fact that the terminal portion of the deflection curves may drift away from the true asymptotic level deduced from penetration resistance at a given depth, has no influence on the peak ENTHRU value computed.

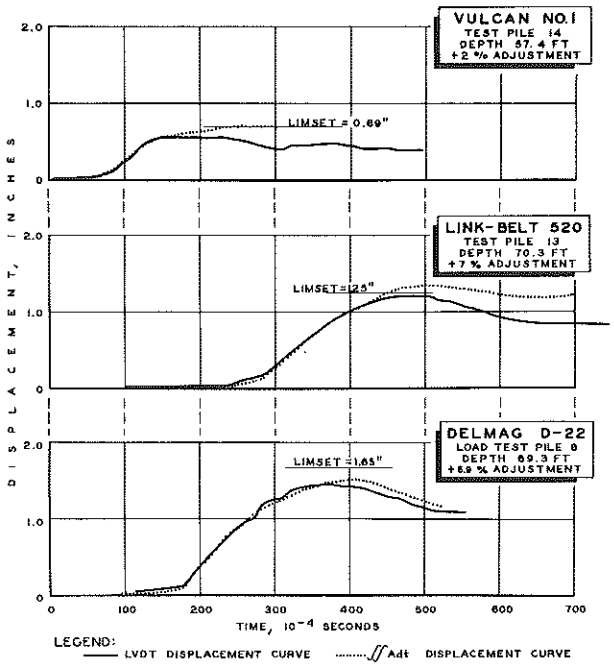

Figure 70. Comparison of measured and computed displacements (Muskegon). Percent adjustments shown are for acceleration.

More directly, the computed deflection curves can be compared with the few available LVDT traces (directly measured) obtained at Muskegon, some of which are shown in Fig. 70. A remarkable similarity may be noted over the significant portion of the traces (up to peak values), even though corrections up to 7 percent are required to bring the calculated deflection near the target limset. Validity of the double integration method can also be gaged by comparing ENTHRU based on the LVDT and the acceleration data at Muskegon, given in Table 16. Plotting these values in Fig. 71 indicates a fairly good correlation between ENTHRU by the two methods, except that the double-integrated acceleration generally gives the higher ENTHRU values. In part, this discrepancy appears to be due to the time lag (function of stub length and velocity of elastic compression in steel), causing displacement measurements by LVDT method to lag behind force measurements at the load cell. If a time adjustment is introduced so as to simulate this time lag into the double-integrated data, there is a significantly better agreement between

TABLE 16
COMPARISON OF MEASURED AND COMPUTED PILE DEFLECTIONS AND THEIR ASSOCIATED ENTHRU VALUES (MUSKEGON)

	Line	Subject	Vulcan No. 1			Link Belt 520						McKiernan-Terry DE-40					Delmag D-22						
			TP 14			TP 12			TP 13					TP 10			TP 11		LTP 6		LTP 8				
Pile Driving Information	1	Depth, ft	40.5	49.3	57.4	70.8	109.3	125.5	70.3	108.8	135.3	156.1	173.0	69.5	109.8	127.5	69.5	150.0	52.0	109.8	69.3	109.5	149.5	176.9	178.0
	2	Blows per Inch	2.2	2.3	3.2	1.3	100.0	2.7	1.0	31.0	14.0	17.7	6.8	1.7	11.0	2.0	1.5	18.5	1.0	1.8	0.8	1.8	3.0	4.7	27.0
	3	Deflection Measured by Manual Trace Method, in.	0.69	0.68	0.68	1.01	1.12	1.11	1.21	1.25	1.20	1.30	1.40	0.94	1.28	1.13	1.09	1.37	1.66	1.24	1.59	1.41	1.35	1.69	1.67
Associated Data and Computed Enthru Values	4	Deflection Measured from LVDT Trace, in.	0.61	0.62	0.56	1.09	0.96	1.12	1.21	1.25	1.23	1.22	1.36	0.99	1.28	1.10	1.11	1.27	1.49	1.26	1.47	1.31	1.09	1.48	1.61
	5	Computed Enthru Using Deflections from LVDT Trace, ft-lb	5055	6165	5966	14333	11204	18798	17450	20021	18056	15275	16060	13107	16571	13765	13673	14224	27207	16880	23134	16549	10183	16305	16925
	6	Deflection Computed by // Adt Method, in.	----	0.69	0.71	0.95	----	0.99	1.36	----	1.29	1.36	1.30	----	1.42	1.15	1.16	1.35	1.76	1.27	1.51	1.37	1.40	1.55	1.51
	7	Computed Enthru Using Deflections from // Adt Method, ft-lb	----	6843	7199	13136	----	18222	18412	----	19938	17770	15922	----	20795	16895	16764	17897	29227	21655	24892	23399	20960	23270	22054
	8	Percent Adjustment to Acceleration Data	----	4.0	2.0	10.0	----	-5.0	7.0	----	6.0	8.0	10.0	----	-9.0	1.9	-1.9	0.0	6.0	0.0	6.9	6.0	-1.0	9.0	10.0
	9	Stub Length, ft	4.5	13.7	5.6	9.2	10.7	4.5	9.7	11.2	24.7	33.9	17.0	10.5	10.2	7.5	10.5	10.0	28.0	10.2	10.7	10.5	10.5	8.1	7.0
	10	Time Differential Between Point of Acceleration Measurement and LVDT Trace Measurement, sec x 10^{-4}	0	6	2	4	5	1	4	5	13	18	8	5	4	3	5	4	15	4	5	4	4	4	2
	11	Computed Enthru Using Deflections from // Adt Method including Time Differential Adjustment, ft-lb*	----	6404	7070	13057	----	18053	18124	----	18942	17374	15718	----	19081	15747	14877	15762	26336	18007	21635	19227	17582	19888	19827
Ratios	12	Ratio of Deflections Measured by Manual Trace and LVDT Trace Methods, $\left(\frac{\text{Line 3}}{\text{Line 4}}\right)$	1.13	1.10	1.21	0.93	1.17	0.99	1.00	1.00	0.98	1.07	1.03	0.95	1.00	1.03	0.98	1.08	1.12	0.98	1.08	1.08	1.24	1.14	1.04
	13	Ratio of Enthru Computed Using Deflections from // Adt and LVDT Trace Methods, $\left(\frac{\text{Line 7}}{\text{Line 5}}\right)$	----	1.11	1.21	0.92	----	0.97	1.06	----	1.10	1.16	0.99	----	1.25	1.23	1.23	1.26	1.07	1.28	1.08	1.41	2.06	1.43	1.30
	14	Ratio of Enthru Computed Using Deflections from // Adt Method, Including Time Differential Adjustment and LVDT Trace Method, $\left(\frac{\text{Line 11}}{\text{Line 5}}\right)$	----	1.19	1.19	0.91	----	0.96	1.04	----	1.05	1.14	0.98	----	1.15	1.14	1.09	1.11	0.97	1.07	0.94	1.16	1.73	1.22	1.17

* For convenience in computations the time differential was added in the // Adt deflection method rather than subtracted in the LVDT trace deflection method.

ENTHRU's computed by the two methods (Fig. 72). Note, however, that the time lag adjustment actually introduces an error into the double-integrated ENTHRU values, and has been used here merely to facilitate a comparison of the two ENTHRU values on a common basis. Figs. 71 and 72 also show values for differences between manual trace deflection values (used as target values in the double-integration ENTHRU), and peak displacement values by the LVDT method. These differences are mostly positive, varying up to 0.26 in., and this fact would also tend to make the ENTHRU values computed by double-integration somewhat larger.

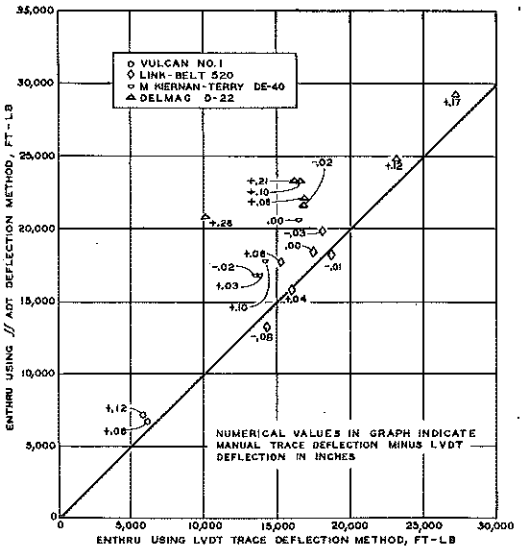

Figure 71. Comparison of Muskegon ENTHRU's.

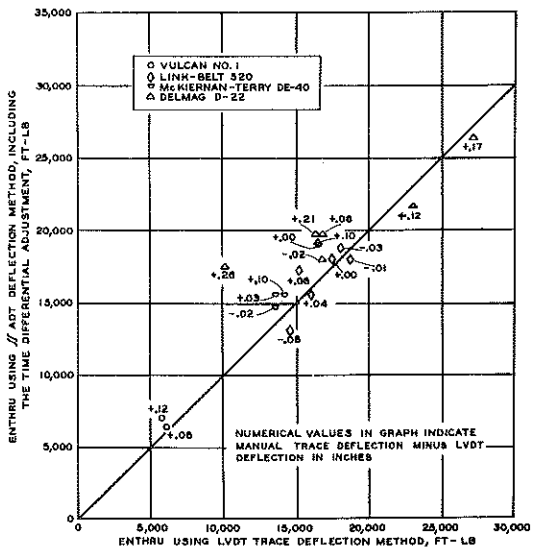

* ALL LVDT ENTHRU'S ARE BASED ON DEFLECTIONS MEASURED FROM 1 TO 25 FT FROM LOAD CELL

Figure 72. Comparison of Muskegon ENTHRU's with time differential adjustments.

These observations suggest that in spite of inherent difficulties in executing the double-integration method, this procedure gives displacements over the ascending range comparable to those based on LVDT data, and that computed ENTHRU values are somewhat larger and apparently more appropriate than those based on LVDT traces without time lag corrections.

Trial Computations

Over a period of several months, force and acceleration data were accumulated for a total of 577 hammer blows, of which 440 were processed through the computer, involving about 1,000 separate trial computations (summarized in App. B, Plates 15-63). As has been mentioned, it was

only after a period of experimentation that certain criteria were established for accepting, adjusting, and interpolating trace data, which may be summarized as follows:

1. Before Processing

   a. Force and acceleration readings were required for at least 0.0300 sec beyond first significant trace movement.

   b. Peak displacement values were selected by the following method, in the enumerated priority:

      (1) Directly related manual trace values.

      (2) Interpolated manual trace values for the same pile, based on least squares.

      (3) Interpolated manual trace values from comparable piles.

2. After Processing

   a. Adjustment of acceleration trace data was not to exceed $\pm$ 10 percent.

   b. Limset deflection was to match peak value of computed deflection with a maximum deviation of 0.20-in. or 20 percent, whichever was less.

   c. Terminal deflection, when force and acceleration are no longer significant, was to be between peak deflection and zero.

   d. ENTHRU was to be reviewed for consistency with comparable traces; also magnitudes of force and acceleration were to be checked for inconsistencies.

   e. The number of traces for a given hammer meeting these criteria was to be considered in relation to the total number of traces processed for the site.

In this connection, most data not processed lacked accompanying manual trace records. The limset values, which were the primary target points to which the computed displacement curves were adjusted by the trial computations, were selected from the most representative

values available. This is indicated in the trial computation summary (App. B).

The 20-percent or 0.20-in. range of acceptable variation between actual target and computed peak displacement reflects the observed discrepancy between comparable LVDT and manual trace displacements, and the requirement to limit numbers of trial computations to about three attempts for a given hammer blow. Actually, in most cases, the achieved agreement was better than $\pm$ 10 percent.

Turning now to the summary of trial computations for each pile (App. B), hammer blows analyzed are arranged in descending order, showing depth and estimated penetration resistance (blows per inch) obtained from the pile driving records (App. A).

Under the general heading "Adjusted Pile Movement" on the App. B trial computation plates, are shown the "manual trace values" of deflections recorded near ground surface by the "pencil and board" method described in Chapter 4. The indicated stub length is used in conjunction with an "equivalent constant force" (average force recorded in the period required to reach peak displacement) obtained from the force-time trace, to determine the "limset."

The data summarized in the columns headed "Trial Computations," were obtained or derived from the actual computer output sheets (such as those shown in App. B Plates 9-14). Columns 9 through 24 have headings defined as follows:

1. Limset is the peak deflection value based on manual trace data, with a correction for deflection of the stub length.

2. Δ Max is the peak deflection value of the computed curve.

3. % Adj is the value of the multiplication factor used in adjusting all input acceleration data.

4. Δ NBAR is the computed deflection at the time designated NBAR, which always equals or exceeds the time required to achieve peak deflection. The time NBAR is either:

   a. The time associated with the last input value of acceleration and force, or

   b. The time at which the velocity of movement is zero.

5. $\frac{\Delta \text{ NBAR}}{\Delta \text{ Max}}$ is the ratio of terminal-to-peak deflection values, and by definition ranges downward from a value of 1.

6. ENTHRU is the computed peak value of work performed on the load cell for the specific input in terms of measured force and acceleration, the latter being adjusted when necessary.

Under the subheading "Accepted Deflection-ENTHRU Determinations" are grouped the trial computations which meet the "After Processing" criteria just outlined, particularly the following:

1. Computed maximum deflections, Δ Max, are within either 20 percent or 0.20 in. of the limset, whichever is less.

2. Required "% Adj" is within $\pm$ 10 percent.

3. The shape factor $\frac{\Delta \text{ NBAR}}{\Delta \text{ Max}}$ lies between one and zero, indicating that the terminal deflection lies in a proper relationship to the maximum deflection.

There was one significant departure from this standard, involving data for the Vulcan 50C hammer at Belleville. None of the determinations for this hammer are designated as acceptable, although 18 out of the 53 hammer blows do meet the conditions required. Closer examination suggests that this entire body of data was significantly less reliable than that collected for other Belleville hammers. Note that in contrast to less than 35-percent success in meeting the criteria with the Vulcan 50C, the data derived from the other four hammers indicated 52- to 64-percent success for comparable circumstances. Also, with the 50C hammer a disproportionately large amount (80 percent) of the limset values had to be estimated, leaving a considerable uncertainty regarding the target deflection in these instances. In a more subjective vein, it was noted that the data led to widely divergent results; that is, computed deflections for the same piles became widely erratic for progressively greater depths (for example, see RP's 11 and 14, Plates 24 and 25, App. B). The reason for this unsatisfactory situation is not known.

Another exception to the general criteria was rejection of trial computations for TP 10 at Belleville driven by a Delmag D-12 (Plates 43-44, App. B). Study of the force trace data after processing by the computer showed that the initial peak forces were far out of line with data from other comparable piles, and resulted in relatively low ENTHRU values. It appears that there is about a 100-percent discrepancy in the peak force readings in these instances, and the data were not considered further.

It appears that there is about a 100-percent discrepancy in the peak force readings in these instances, and the data were not considered further.

Compilation of Acceptable ENTHRU Calculations

All acceptable force and acceleration values were tabulated, as shown in Appendix B Plates 64-179. These values were also charted, along with their corresponding displacement values and resulting ENTHRU values as shown in Appendix B Plates 180-253, drawn to a common time scale. Associated "limsets" are also indicated. The somewhat simplified graphical representation of forces and accelerations is a compromise between an exact and literal presentation of the oscillographic trace data (Fig. 32) which were complicated by a variety of scale factors and relatively poor legibility, and a simple compilation of peaks and associated time values from which it would be difficult to obtain a concept of the interrelation of the dynamic responses. Thus, certain of the acceleration and force traces plotted must not be taken literally, as there was some averaging and cutting off of nonessential details, when these were of no influence insofar as ENTHRU computations were concerned. However, an attempt was made to include at least a few detailed and extended trace plots for each hammer-site combination in this presentation. They generally can be identified by the abundance of oscillations in the acceleration and force traces; for example in Plate 182, App. B (LTP 6 at 20 ft), note the high-frequency acceleration fluctuations occurring after the peak displacement, consisting of alternating positive and negative values of about equal magnitude.

Relation Between ENTHRU and Impact Loss Factor

Results of the acceptable ENTHRU data summarized in App. B have been assembled for the respective sites in Figs. 73 through 75. Values of ENTHRU are shown on a series of profile charts, spanning the driving depths, in association with peak acceleration values and peak and equivalent constant force values. The data are assembled by specific site, hammer, and where possible by pile type. Representative ENTHRU values and other hammer blow characteristics have been compiled in Tables 17 and 18. Related $\underline{E}_n$ values (manufacturer's maximum rating) are obtained from Table 1. Also shown in Table 18 are values of impact loss factor, $\frac{W_r + e^2 W_p}{W_r + W_p}$, for half and full pile lengths, based on designated $\underline{e}$-values (coefficient of restitution) and pile and ram weights shown in Tables 1

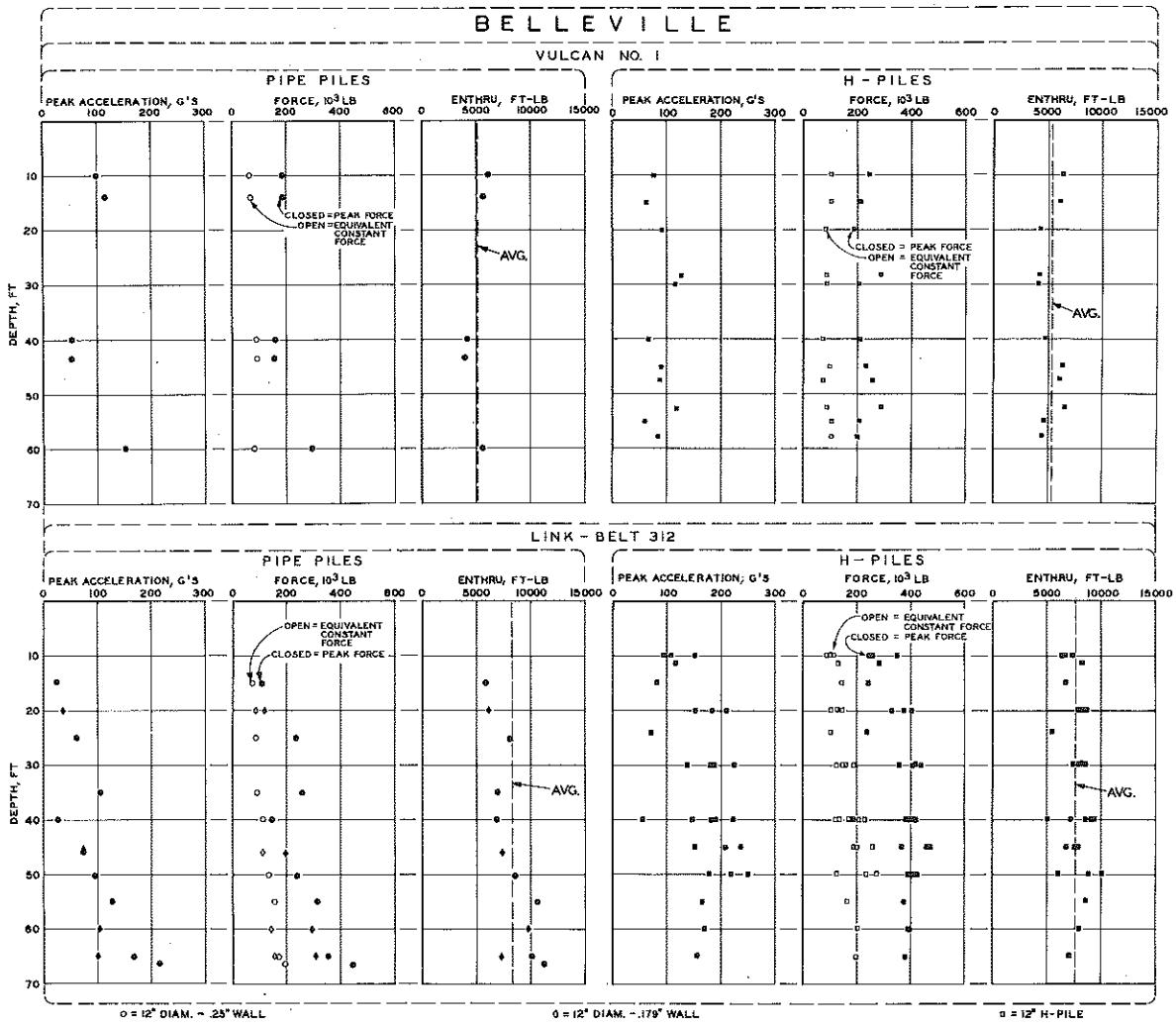

Figure 73. Hammer blow characteristics for Belleville hammers.

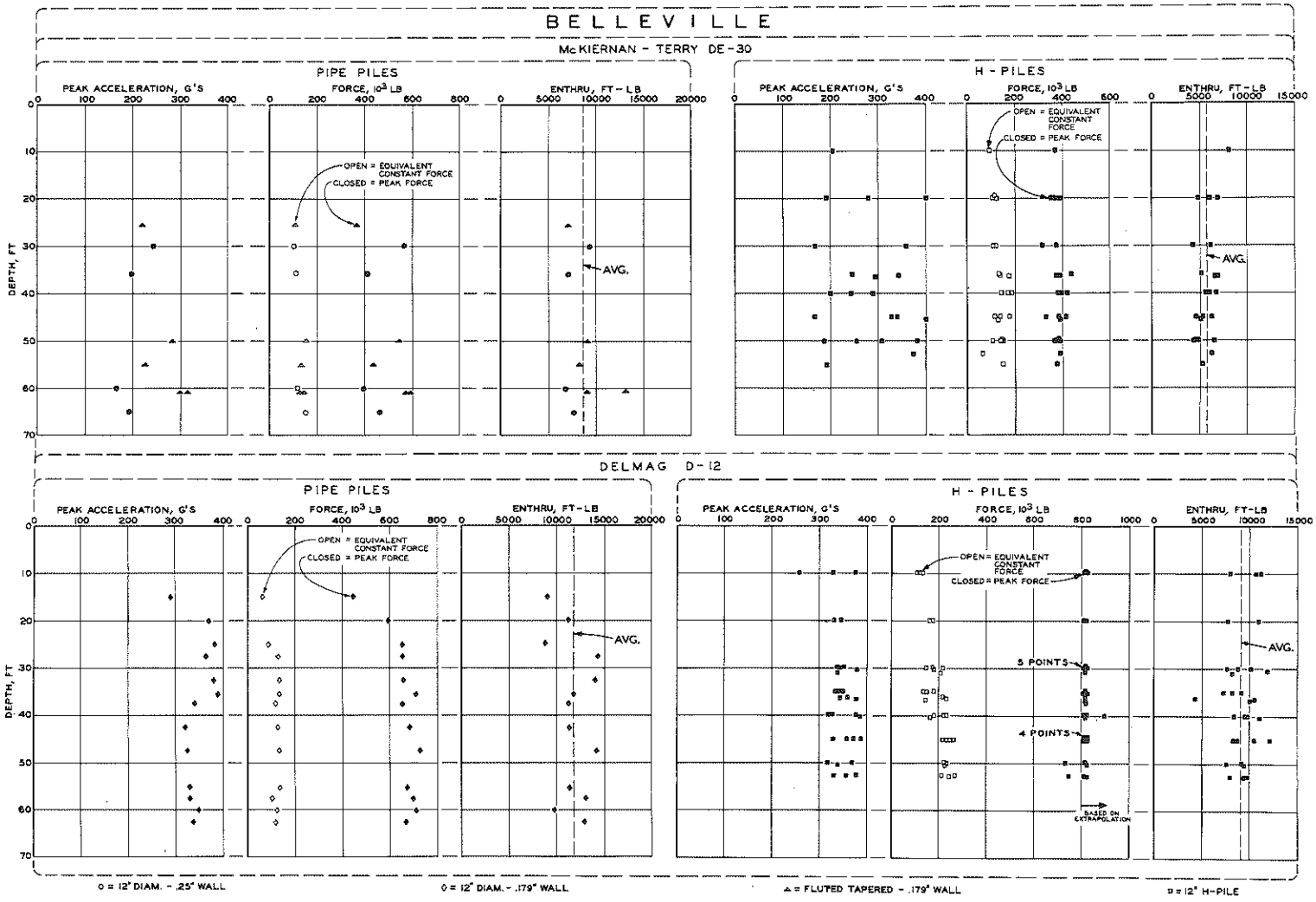

Figure 73 (cont.). Hammer blow characteristics for Belleville hammers.

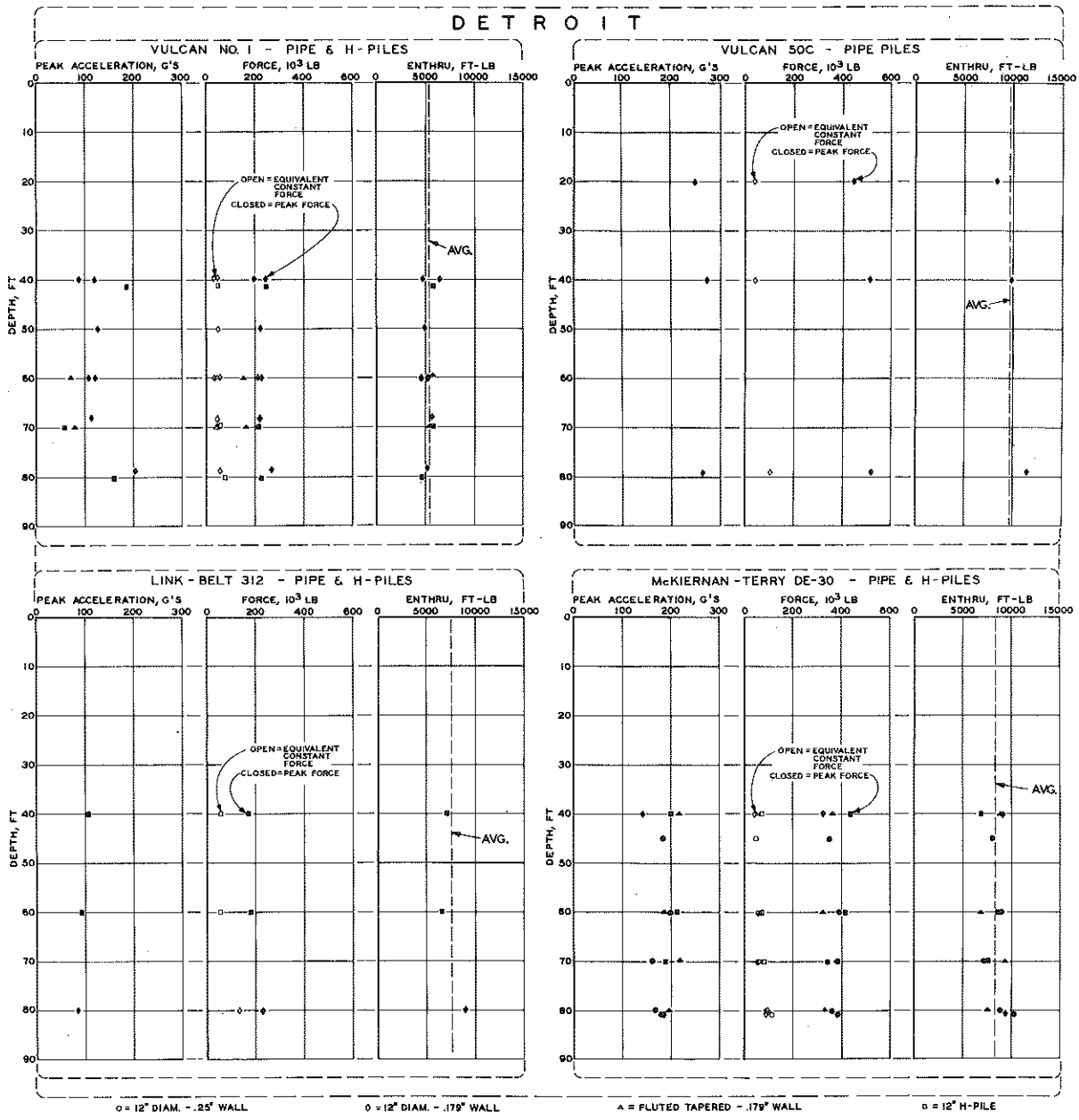

Figure 74. Hammer blow characteristics for Detroit hammers.

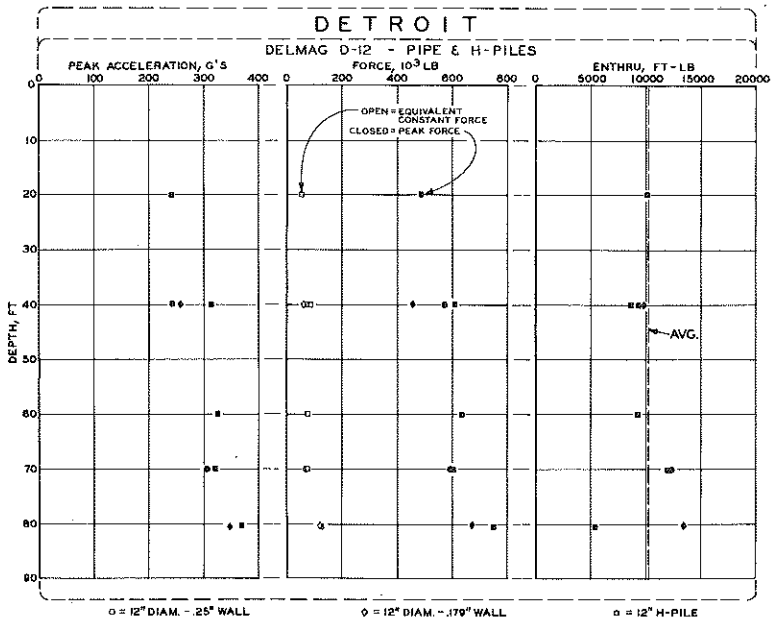

Figure 74 (cont.). Hammer blow characteristics for Detroit hammers.

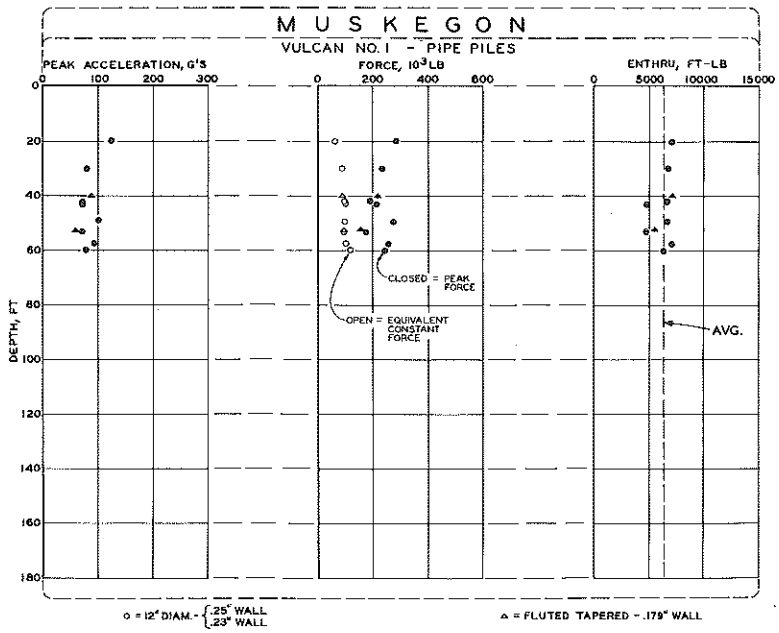

Figure 75. Hammer blow characteristics for Muskegon hammers.

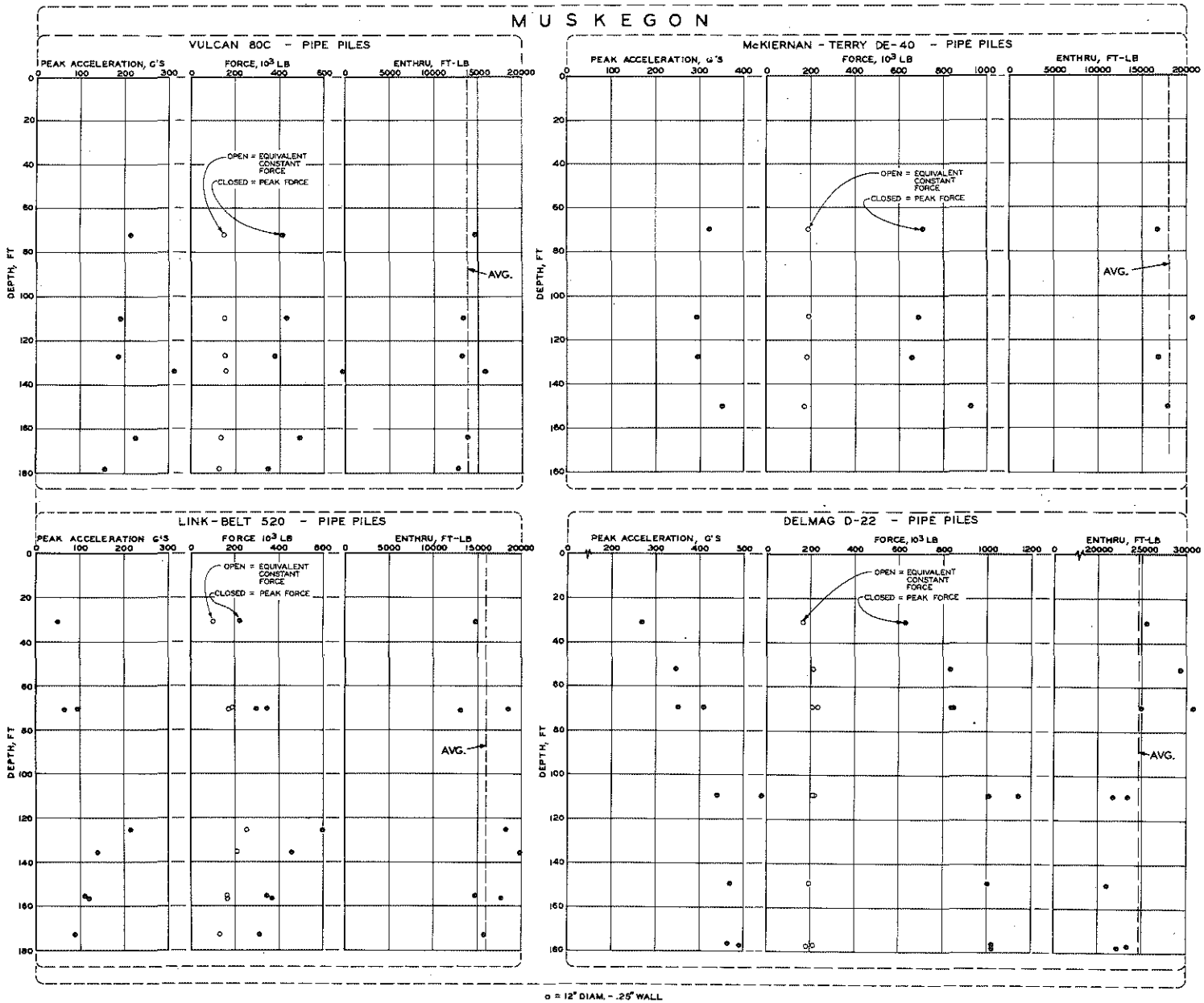

Figure 75 (cont.). Hammer blow characteristics for Muskegon hammers.

TABLE 17
SUMMARY OF REPRESENTATIVE HAMMER BLOW CHARACTERISTICS

Site	Hammer	Pile Type	① Peak Acceleration, g's	② Equivalent Constant Force, kips	③ Peak Force, kips	④ ENTHRU, ft-lb	⑤ Force Acceleration Index $\sqrt{① \times ③}$
Belleville	Vulcan No. 1	Pipe	75	80	180	5,094	116
		H	90	80	230	5,283	144
	Link-Belt 312	Pipe*	210	---	440	-----	304
		Pipe	100	130	270	8,226	164
		H	170	170	380	7,726	254
	McKiernan-Terry DE-30	Pipe	240	120	490	8,682	343
		H	270	140	390	5,769	325
	Delmag D-12	Pipe	350	120	690	11,870	491
		H	360	200	800	9,123	537
Detroit	Vulcan No. 1	Pipe & H	110	40	200	5,339	148
	Vulcan 50C	Pipe	270	50	490	9,822	364
	Link-Belt 312	Pipe & H	100	70	200	7,564	141
	McKiernan-Terry DE-30	Pipe & H	190	70	370	8,417	265
	Delmag D-12	Pipe & H	320	90	600	10,033	438
Muskegon	Vulcan No. 1	Pipe	80	100	220	6,359	133
	Vulcan 80C	Pipe*	310	160	650	16,000	449
		Pipe	220	160	410	13,872	300
	Link-Belt 520	Pipe*	150	210	560	18,500	290
		Pipe	110	160	350	16,637	196
	McKiernan-Terry DE-40	Pipe	310	200	700	18,088	466
	Delmag D-22	Pipe**	470	200	1050	22,500	702

* Representative of hard driving.
** Representative of moderate-to-hard driving.

TABLE 18
SUMMARY OF AVERAGE MEASURED AND COMPUTED IMPACT LOSS CHARACTERISTICS

Site	Hammer	Pile Type	ENTHRU, ft-lb	① ENTHRU / E_n	W_r, lb	e*	Intermediate Length L_1, ft	Intermediate Length W_{p1}, lb	Intermediate Length ②	Long Length L_2, ft	Long Length W_{p2}, lb	Long Length ②	③ 2 x ① / (② + ②)
Belleville	Vulcan No. 1	H	5,283	0.35	5000	0.15	30	4250	0.55	60	5,840	0.47	0.69
		Pipe	5,094	0.34			40	4160	0.55	80	5,420	0.49	0.65
	Vulcan 50C	H	-----	----	5000	0.60	30	4250	0.72	60	5,840	0.67	
		Pipe	-----	----			40	4160	0.73	80	5,420	0.68	
	Link-Belt 312	H	7,726	0.43	3855	0.65	30	5819	0.65	60	7,409	0.62	0.68
		Pipe	8,226	0.46			40	5731	0.66	80	6,984	0.63	0.71
	McKiernan-Terry DE-30	H	5,769	0.26	2800	0.50	30	5424	0.50	60	7,014	0.47	0.54
		Pipe	8,682	0.39			40	5330	0.51	80	6,580	0.47	0.80
	Delmag D-12	H	9,123	0.41	2750	0.60	30	5089	0.59	60	6,679	0.55	0.72
		Pipe	11,870	0.53			40	5000	0.60	80	6,253	0.56	0.91
Detroit	Vulcan No. 1	Pipe & H	5,339	0.36	5000	0.25	45	4610[b]	0.55	90	6,310	0.48	0.70
	Vulcan 50C	Pipe	9,822	0.65	5000	0.60	45	3930[c]	0.72	90	4,950	0.68	0.93
	Link-Belt 312	Pipe & H	7,554	0.42	3855	0.65	45	6179[b]	0.65	90	7,879	0.61	0.67
	McKiernan-Terry DE-30	Pipe & H	8,417	0.38	2800	0.50	45	5780[b]	0.50	90	7,480	0.46	0.79
	Delmag D-12	Pipe & H	10,033	0.45	2750	0.60	45	5449[b]	0.58	90	7,149	0.54	0.80
Muskegon	Vulcan No. 1	Pipe	6,359	0.42	5000	0.25	30	3685[a]	0.60	60	4,460	0.56	0.72
	Vulcan 80C	Pipe	13,872	0.57	8000	0.60	90	6870[d]	0.71	180	9,590	0.65	0.84
	Link-Belt 520	Pipe	16,637	0.55	5070	0.65	90	7290[d]	0.66	180	10,110	0.62	0.86
	McKiernan-Terry DE-40	Pipe	18,088	0.57	4000	0.50	90	8980[d]	0.48	180	11,800	0.44	1.24
	Delmag D-22	Pipe	24,660	0.62	4850	0.60	90	7325[d]	0.62	180	10,145	0.57	1.04

② $\frac{W_r + e^2 W_p}{W_r + W_p}$ Computed impact loss factor.

③ Percent correlation between measured and computed impact loss factor.

* e is estimated between 0.15 (Vulcan No. 1 at Belleville using unconfined oak cushion block, possibly with wood chips added), and 0.65 (Link-Belt 312 at Belleville using aluminum-micarta cushion block).

(a) Based on average for 7-gage and 0.23 in. pipes.
(b) Based on average for 7-gage pipe piles and H-piles.
(c) Based on 7-gage pipes.
(d) Based on 0.25-in. pipes.

and 2. ENTHRU and impact loss factors are also shown in Fig. 76 for ease of reference and comparison. A general review indicates that:

1. There is no consistent change in ENTHRU over the depths driven, with the possible exception of the Link-Belt 312 hammer-pipe pile combination at Belleville (Fig. 73) which shows a rise in ENTHRU with depth driven, and the Delmag D-22 hammer-pipe pile at Muskegon (Fig. 75) which shows a drop in ENTHRU below 80 to 100 ft depth.

2. ENTHRU's delivered to the top of the pile are expressed as percentages of the corresponding E_n values and for the hammers studied ranged from an average of 26 to 53 percent at Belleville, from 36 to 65 percent at Detroit, from 42 to 62 percent at Muskegon, and were generally from 10 to 50 percent less than comparable impact loss factors.

3. With the exception of the Vulcan No. 1 hammer, the values of ENTHRU for pipe piles exceeded the ENTHRU's delivered into comparable H-piles (see particularly McKiernan-Terry and Delmag graphs in Fig. 73).

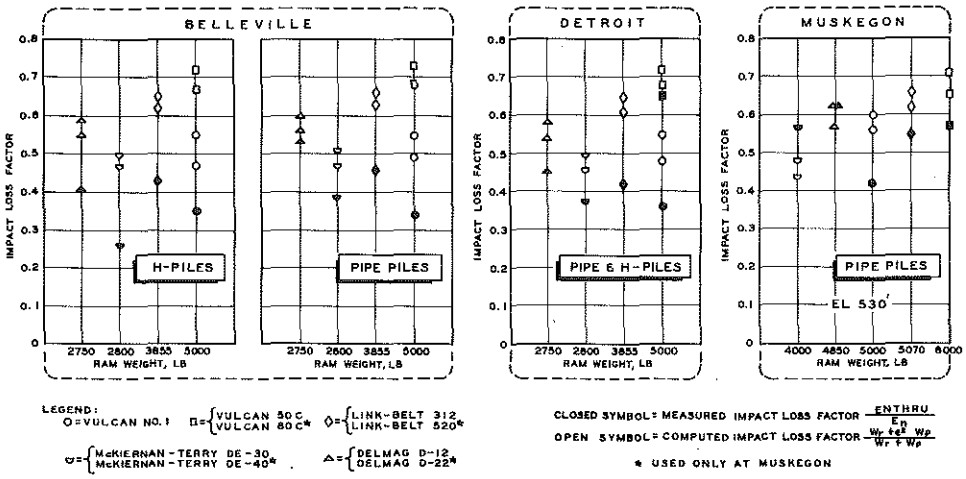

Figure 76. **Relationship between impact loss factor and ram weight.**

Concerning the lower ENTHRU values for the Link-Belt pipe piles at Belleville, one may note that corresponding peak forces and accelerations are also lower in early driving (Fig. 73). An examination of Plates 23 and 24 of App. A shows: 1) that bounce chamber pressures for the first 20 ft of pile penetration are less than 15 psi, and 2) that temporary compression increases significantly for the first 40 ft of penetration. This was not generally observed for other hammers driving pipe piles in this depth range. It may be pointed out, however, that the same trends in

Link-Belt operating characteristics, though less marked, were noted for the H-piles (Fig. 73), but there was no comparable trend in ENTHRU values.

In constrast, for the Delmag D-22 hammer at Muskegon the high ENTHRU's recorded down to 80 ft depth are associated with low peak forces and accelerations. Here, however, the pile was penetrating between 1.5 and 2.0 in. per blow (Plates 93 and 95, App. A) and it may be that this inordinately large movement accounts for the relatively large ENTHRU values (Fig. 75).

It is fairly well established by Table 18 that ENTHRU values represent a relatively small fraction of the manufacturer's maximum rated energy at impact, e.g., less than 40 percent of the Vulcan No. 1 and McKiernan-Terry DE-30 at Detroit and Belleville. Such percentages seem at first glance inordinately low, and on the face of it, indicate that effective hammer energies are being generally overestimated in the conventional dynamic formulas. Bearing in mind that ENTHRU is construed to be the "work" done on the load cell, its value should be closely related to the energy delivered into the top of the pile expressed as the maximum available energy at impact reduced by hammer friction and cushion block compression losses. The effect of the latter losses are usually expressed as follows:

$$\text{Net energy delivered into pile} = (E_n - \text{Hammer Friction}) \times \frac{W_r + e^2 W_p}{W_r + W_p}$$

where e is the coefficient of restitution of the combined cushion cap block, adapters, etc., and the weight of hammer ram W_r and pile-driving assembly W_p are considered to be concentrated masses (point sources). Representative values of the impact loss factor have been compiled in Table 18 and are compared to related ENTHRU values, expressed as percent of manufacturer's maximum energy rating E_n (Fig. 76). For each hammer, the higher values of the impact loss factor represent the half-pile-length values (smaller values of W_p) and lower factors correspond to maximum or full lengths driven. The ENTHRU's tabulated represent average values based on individual determinations, ranging over the entire length of driving, and these should be compared to the average of corresponding impact loss factor values. The discrepancy between the ENTHRU and corresponding impact factors is indicated at the right hand column in Table 18. As shown, the ratio of ENTHRU/E_n ranges from 0.54 to 1.25 of related computed impact loss factor. Also, for 16 out of 18 instances, the comparative ratios ranged from 0.65 to 1.04.

Fig. 76 also shows that hammers striking ordinary oak cushion blocks (i.e., Vulcan No. 1 and McKiernan-Terry DE-30) gave the lowest ENTHRU/E_n ratios. This priority in relative values is also reflected by associated values of $\frac{W_r + e^2 W_p}{W_r + W_p}$, but to a less pronounced degree. The differences between the ENTHRU/E_n ratio and impact loss factor is shown graphically in Fig. 77 based on Table 18 data. Holding ENTHRU values constant, there are various alternatives for adjusting factors so as to bring the several points shown onto the 45° line. For example, a 20-percent reduction in E_n value for the McKiernan-Terry hammer with pipe piles, a 50-percent reduction for the H-piles, and a 20-percent increase for pipe piles at Muskegon, brings the ENTHRU/E_n into agreement with the corresponding impact factor. There is no apparent reason to justify such varying adjustments, nor is this in line with experience with other hammers. Certainly a 50-percent reduction in assigned energy at impact is far more than now seems reasonable. Thus, the arbitrary adjustment of E_n values alone, in amounts sufficient to bring results into agreement, is not justified on the basis of current data.

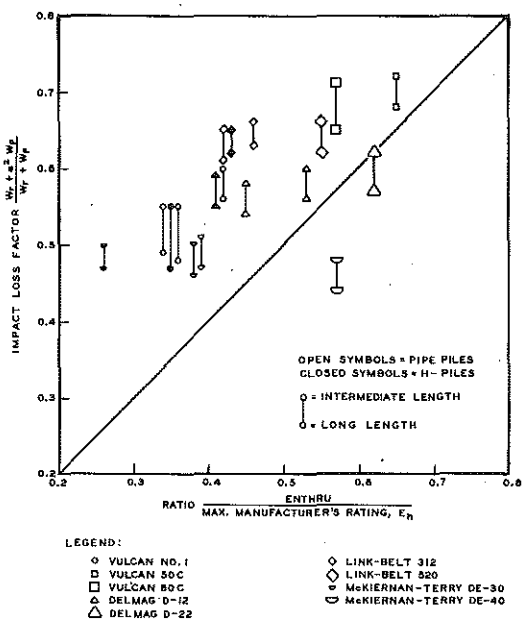

Figure 77. Comparison of impact loss factors.

Similarly, re-assignment of e - factors (generally reducing them) would improve the agreement between ENTHRU/E_n and impact loss factors. However, such adjustments do not follow a rational pattern. For example, the e-factor for the oak block and plywood plates used with the McKiernan-Terry hammer at Muskegon would have to be increased from the assigned value of 0.50. Yet, the assigned e for comparable oak blocks at Belleville and Detroit would have to be significantly reduced from the estimated value of 0.50. In fact, the deduced e for the Vulcan No. 1 oak block is less than zero, a physical impossibility.

ENTHRU values appear significantly affected by the pile type considered, with H-piles yielding the lower values at Belleville, with the

exception of the Vulcan No. 1 hammer, where ENTHRU values are approximately equal (Fig. 76 and Table 18). There is an indication that the lighter-ram hammers are more affected than the heavier-ram hammers. Note that the combined weights of the pile and driving head W_p do not differ greatly between pipe and H-piles at Belleville, and thus this factor alone does not correlate with the observed ENTHRU differences. However, an H-pile's perimeter is about 6 ft, while the perimeter of a 12-in. pipe pile is 3.14 ft, and thus, one may speculate that a significantly greater weight of soil could adhere to the H-pile and act with the pile during driving. The consequent increase in effective mass of the pile would result in less energy transference at impact. This inference would also explain the fact that the transferred energy (ENTHRU) decreases most for the lighter-ram hammers.

Qualifications to ENTHRU Values Presented

The preceding observations involve only a few of the more obvious relationships which can be constructed from the extensive and diverse data presented. As has been noted, it might be possible to determine the values of $\underline{e}$ and assigned $\underline{E_n}$ required to bring the percent delivered energy computed by the impact factor into agreement with the specific average ENTHRU values. Also, estimates could be made of the equivalent weight of soil trapped in the flanges of H-piles (Chapter 9), or its equivalent effect due to augmented perimeter contact,and the consequent effect on the impact factor could be evaluated.

However, before drawing further conclusions, the reader should not lose sight of the essentially exploratory nature of most of the electronic measurements taken on this project. Some experimental variations, breakdowns, and correcting adjustments occurred throughout this phase of the program, and are reflected in certain of the displacement and ENTHRU values reported. Although an attempt was made to distribute the hammer-pile combinations uniformly over the sites, field conditions necessitated that all the piles for a given hammer be driven in succession before proceeding with another hammer. Thus, some possible biasing of data must be recognized.

Another important and problematical aspect of the ENTHRU data is the relatively large range of values computed for similar field conditions. It cannot now be determined whether this scatter reflects actual variations in ENTHRU, or stems from a combination of variations in the data and approximations in computation methods. It is perhaps significant that the peak forces and comparable peak accelerations both appear to range

over wide limits (Link-Belt and McKiernan-Terry graphs in Fig. 73), suggesting that there may well be variation in hammer-pile-soil interaction in the course of normal driving.

Similarly, there is generally a wide range of required adjustments to the accelerations, as is shown in Figs. 78 through 80. In about half the cases, these graphs show a random distribution and indicate that the ENTHRU's are not overly biased from this standpoint. But the data are actually insufficient to establish this fact with certainty. These and many other aspects need to be explored in much greater detail before actual ENTHRU values reported can be viewed with the desired confidence.

Relation Between ENTHRU and Driving Resistance

With these qualifications in mind, note the relation between average computed ENTHRU, maximum manufacturer's rated energy, and measured driving resistance, shown for various circumstances in Figs. 81 through 83, along with companion charts relating equivalent constant driving force and resistance. The equivalent constant force is defined as the total impulse ($\int F \times dt$) to maximum displacement, divided by the time to maximum displacement. This factor has the advantage that it may be evaluated without the double integration and adjustments required to determine ENTHRU, and thus may make a convenient index to hammer performance.

First, Fig. 81 shows ENTHRU vs. driving resistance at Belleville for H-piles and pipe piles. Correlation is generally poor between ENTHRU and driving resistance in both instances, although based on the limited data there appears to be some correlation for pipe piles at 15- and 35-ft depths. At this site, the maximum manufacturer's energy also shows a poor correlation with driving resistance. Equivalent constant force and blow count have a somewhat better correlation, suggesting that hammers developing relatively high equivalent constant forces are more capable of advancing the H-piles. Also, the equivalent constant force for a given hammer generally increases as driving resistance increases with depth. A similar but less pronounced correlation is shown for comparable pipe piles.

Fig. 82 shows the correlation between depth of pipe pile penetration into the Detroit bearing stratum and the hammer's ENTHRU value. Here the correlation is excellent and has the expected trend. The top of the bearing stratum for this purpose was located at the elevation where hammer blow count doubled. In contrast, the maximum manufacturer's rating shows

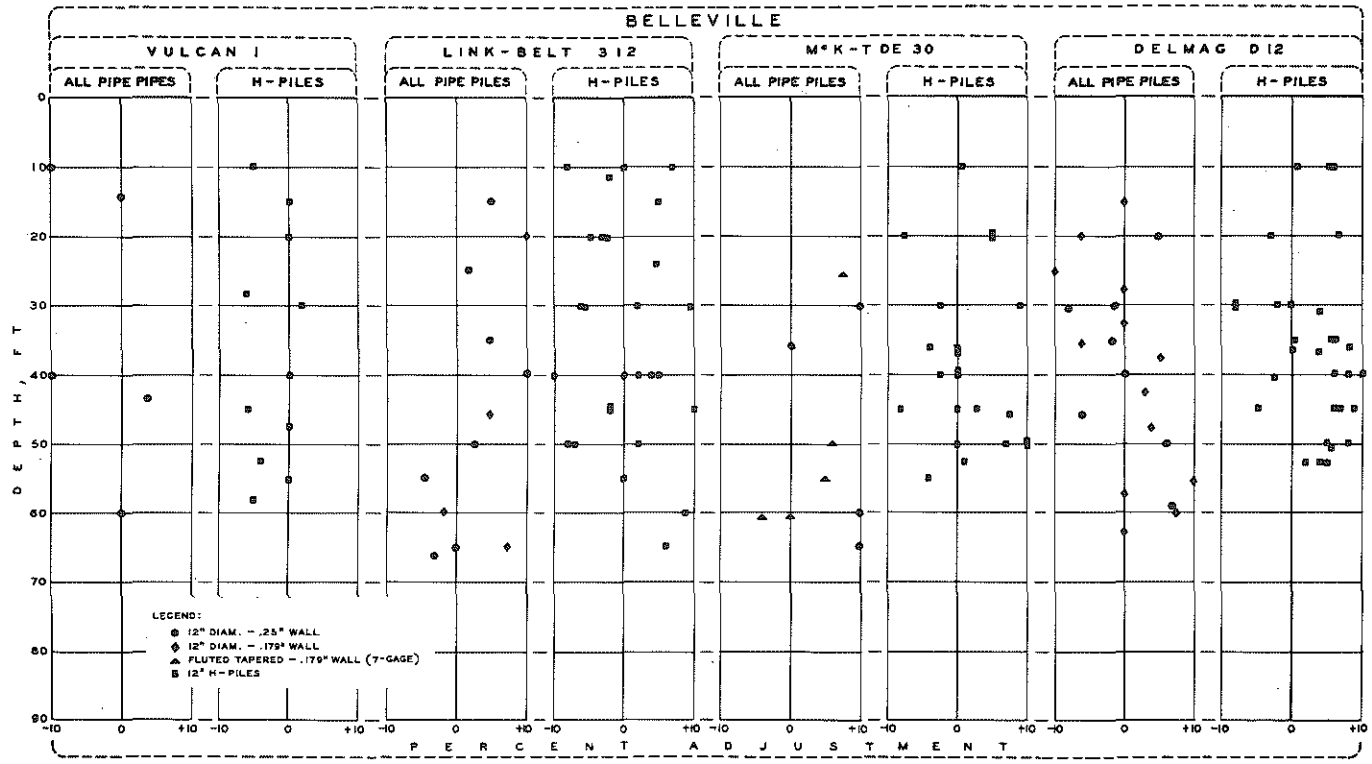

Figure 78. Percent acceleration adjustment of acceptable traces.

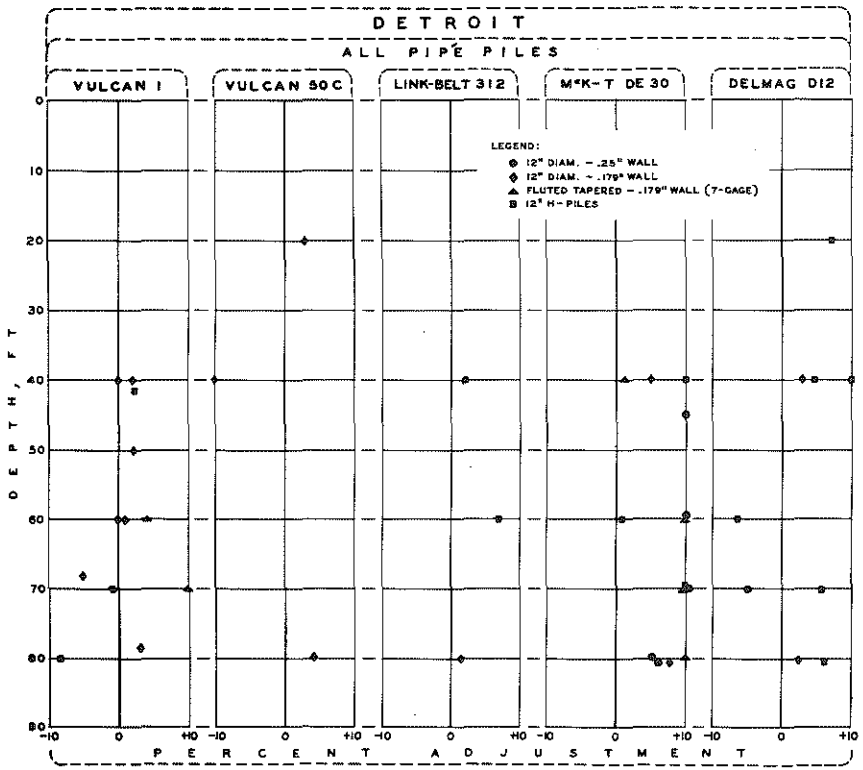

Figure 79. Percent acceleration adjustment of acceptable traces.

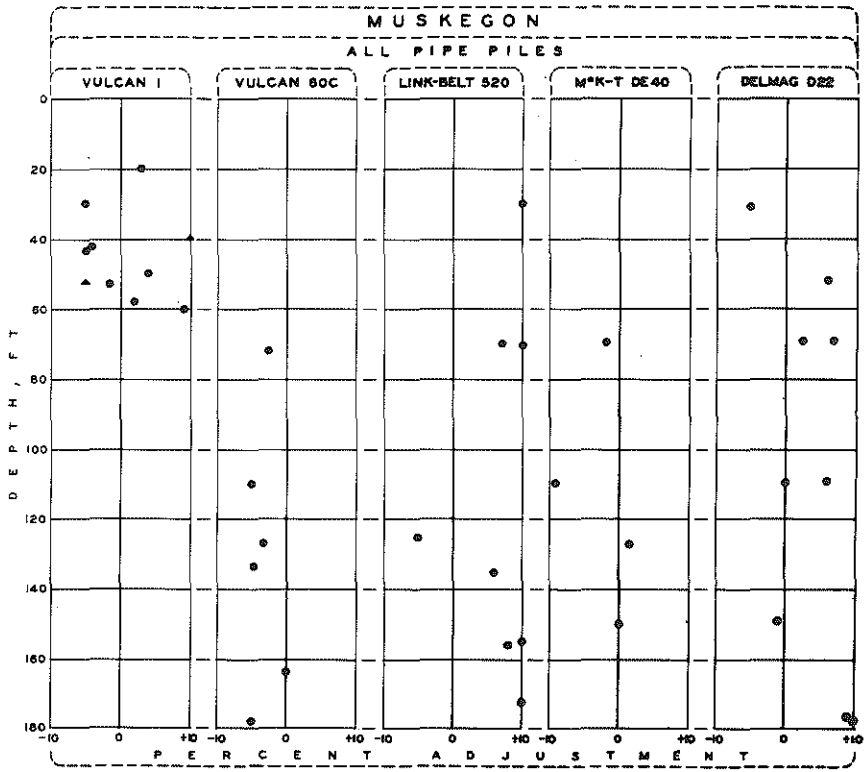

Figure 80. Percent acceleration adjustment of acceptable traces.

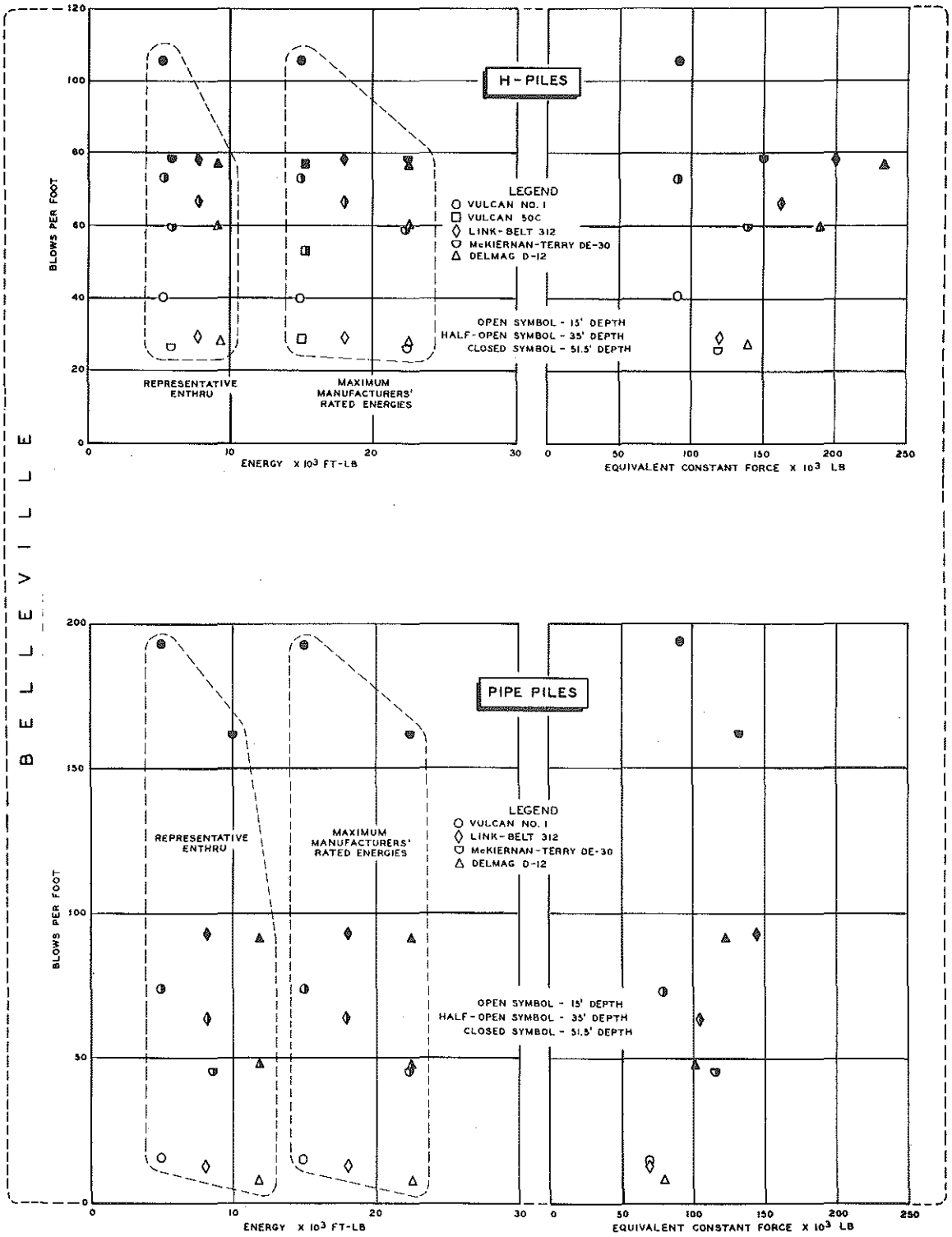

Figure 81. Correlation of driving resistance with hammer energy and equivalent constant driving force for piles at various depths.

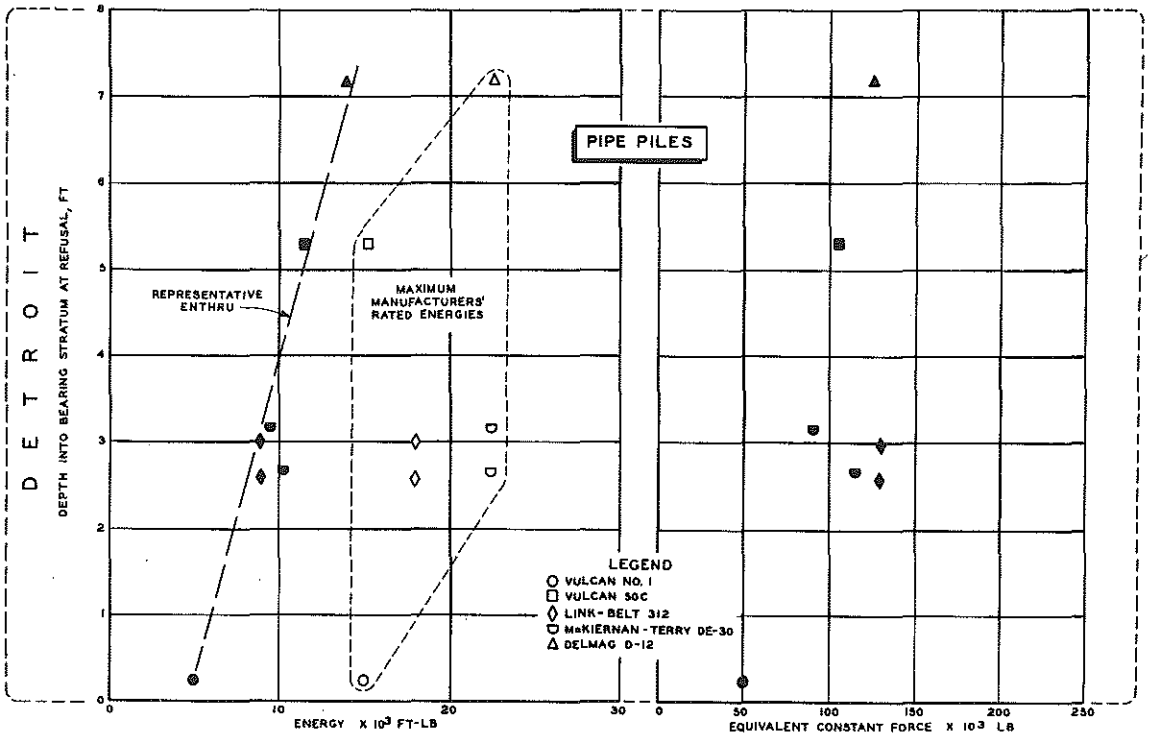

Figure 82. Correlation of driving resistance with hammer energy and equivalent constant force for piles at various depths.

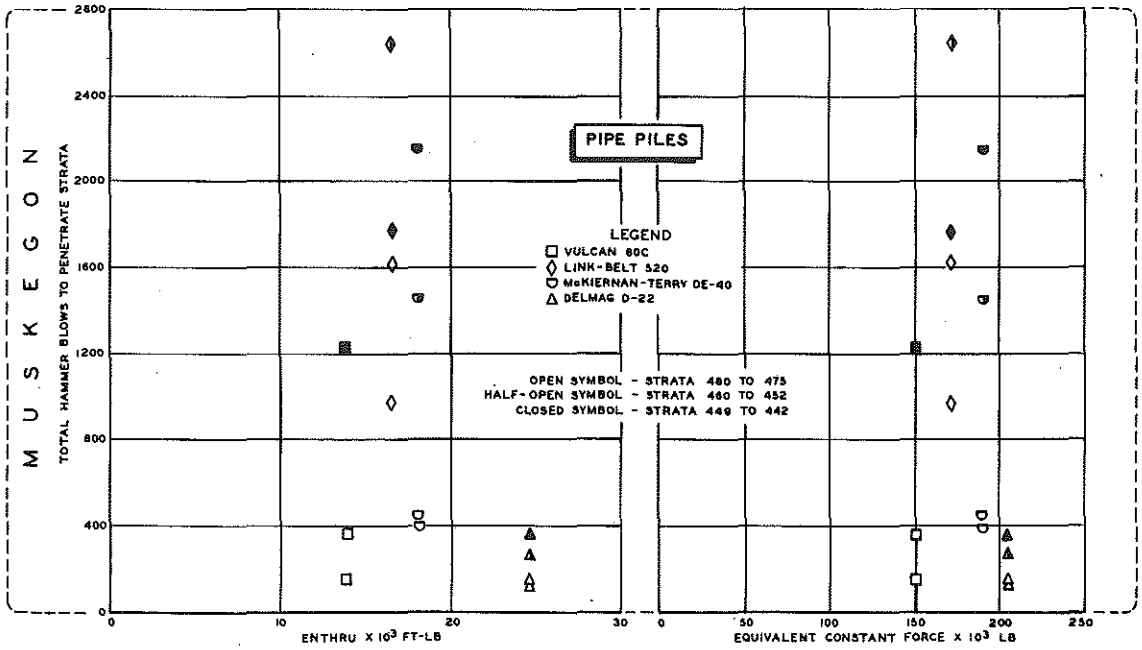

Figure 83. Correlation of driving resistance with ENTHRU and equivalent constant force for piles at various depths.

essentially no correlation. The relationship between driving depths and ENTHRU is based on only seven piles, although remarkably close agreement between the similar piles lends added confidence to the specific data presented. On the other hand, a less defined correlation appears between equivalent constant force and bearing stratum penetration.

Finally, the relation is shown between ENTHRU (and equivalent constant force) and ability to penetrate three of the more resistant strata at Muskegon (Fig. 83). The correlations are poor, the only clear indication being that the heavier Delmag hammer is significantly more capable of penetrating the two deeper strata, than the other hammers tested.

Relation Between ENTHRU, Peak Driving Force, and Peak Acceleration

Table 17 presents representative values of peak force and peak acceleration obtained from Figs. 73 through 75. These are related to hammer performance in a general way and have the advantage that they can be obtained directly from the load cell and accelerometer measurements. The values were examined for correlation with driving ability. From this evolved a combined factor designated Force-Acceleration Index (F-AI), equal to the square root of the product of associated peak force and peak acceleration values. Fig. 84 shows the correlation of the F-AI with associated ENTHRU values, indicating a fair correlation, separated by hammer size and pile type. It is recognized that the heavier hammers were all tested at Muskegon and thus the site itself might be the controlling factor in this separation. However, the Vulcan No. 1 hammer F-AI value at Muskegon grouped with Vulcan No. 1 values at Detroit and Belleville. Thus, in this instance, the relation between F-AI and ENTHRU is a function of hammer size. At Belleville, the H-piles generally gave lower values of ENTHRU than did the associated pipe piles, indicating that pile type also may influence the ENTHRU vs. F-AI relation.

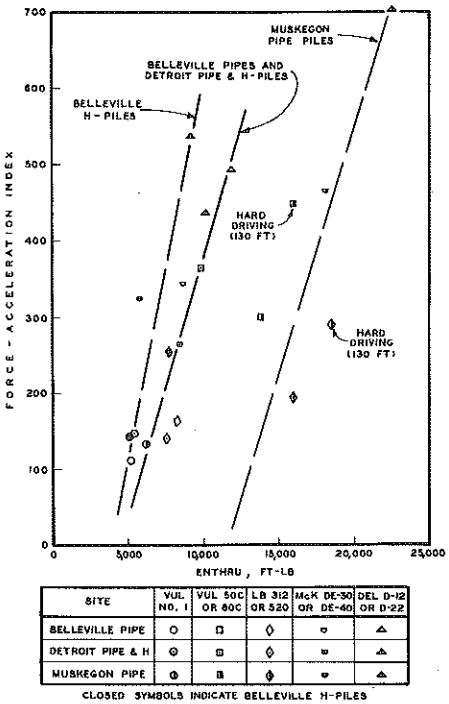

Figure 84. Correlation of ENTHRU and Force-Acceleration Index.

The relation between F-AI and driving effort is shown in Fig. 85. For Belleville H-piles, there is a good and rational correlation, with the required blow counts rising for decreasing values of F-AI. Further, for Belleville pipe piles, and for driving resistances up to 75 blows per foot, there is the expected relationship. However, under very heavy driving (more than 150 blows per foot for the Vulcan No. 1) the relationship breaks down. Likewise, at Muskegon (Fig. 86) the correlation is fair for the upper stratum (elevation 475 to 480), noting that there is a sharp increase in the required number of blows at greater depth and under harder driving, when the F-AI becomes less than 400. The relation is erratic and also complicated here by failure of one of the piles.

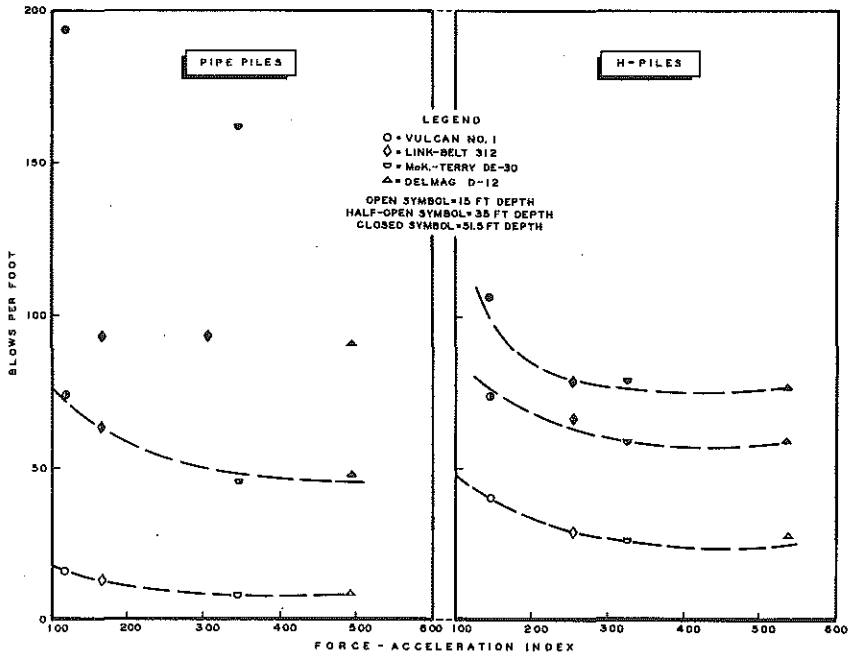

Figure 85. Correlation of driving effort and Force-Acceleration Index for Belleville piles.

The relation between F-AI and depth of penetration to refusal at Detroit (Fig. 87) appears less consistent than between ENTHRU and penetration depth (Fig. 83). Specifically, the Link-Belt 312 results fall out of line, having F-AI values of only about 140, equal to those of the Vulcan No. 1 hammer at this site. However, these Detroit F-AI values were based on an average of only three determinations (Link-Belt graph in Fig. 74) and actually only one specific measurement was made in the bearing stratum for the Link-Belt. By contrast, the Link-Belt 312 had an average Belleville F-AI value about twice that observed for the Vulcan No. 1. Additional test results would be required to clarify this point.

Data so far considered show that F-AI's are related to associated ENTHRU's and appear to depend on pile type and hammer size. The F-AI values correlate at least as well as do ENTHRU's with hammer driving ability, and are obtained directly from force cell and accelerometer measurements. However, hammer size, pile type, and possibly soil conditions, all influence the correlation between ENTHRU, F-AI, and driving ability. Considerably more test data must be obtained for

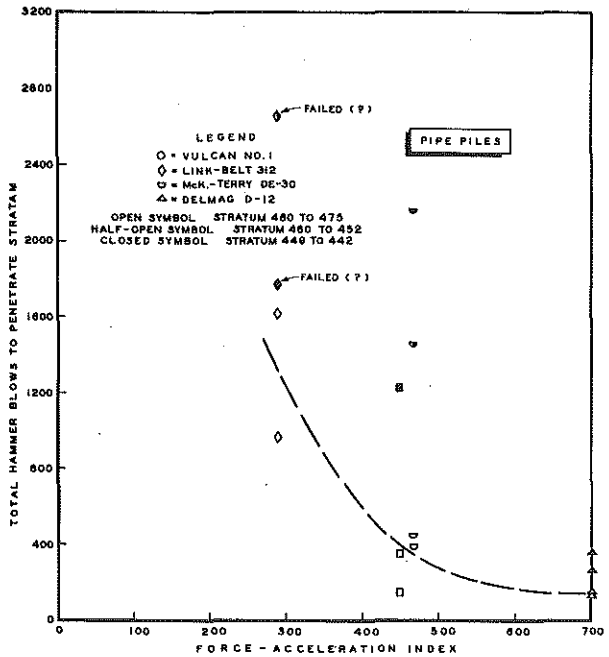

Figure 86. Correlation of Force-Acceleration Index and Muskegon hammer driving effort.

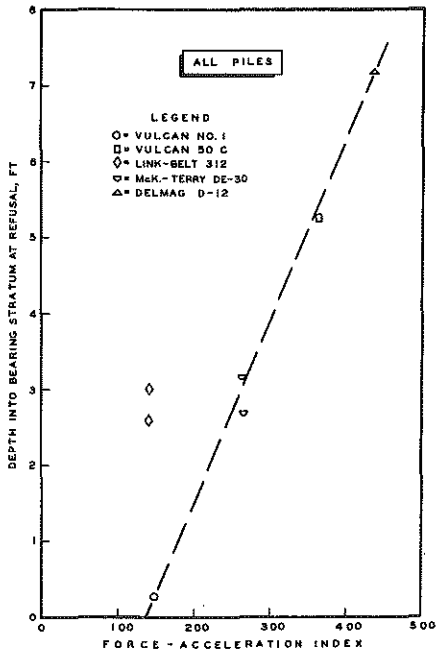

Figure 87. Correlation of Force-Acceleration Index and Detroit depth of refusal penetration.

adequate definition of the significance and range of their influence. Finally, the F-AI factor, as defined, might also be improved from a theoretical basis since it is purely empirical in its current form.

Other Correlations

The following general relationships were also studied:

1. Blow Count vs. ENTHRU. Penetration resistance measured as blow count generally increased with depth, and since ENTHRU did not show a parallel increase, it may be concluded that no correlation exists between blow count and ENTHRU. Fig. 88 indicates this absence of correlation. Certain exceptions may be noted (e.g., the Link-Belt at

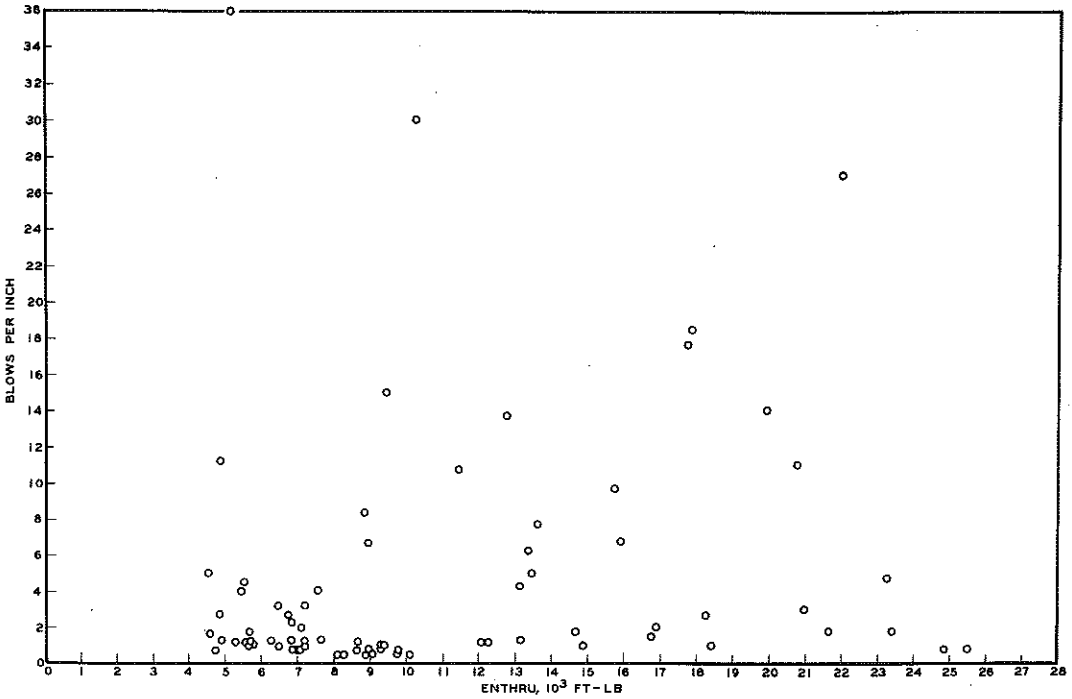

Figure 88. Attempted correlation of ENTHRU and blow count.

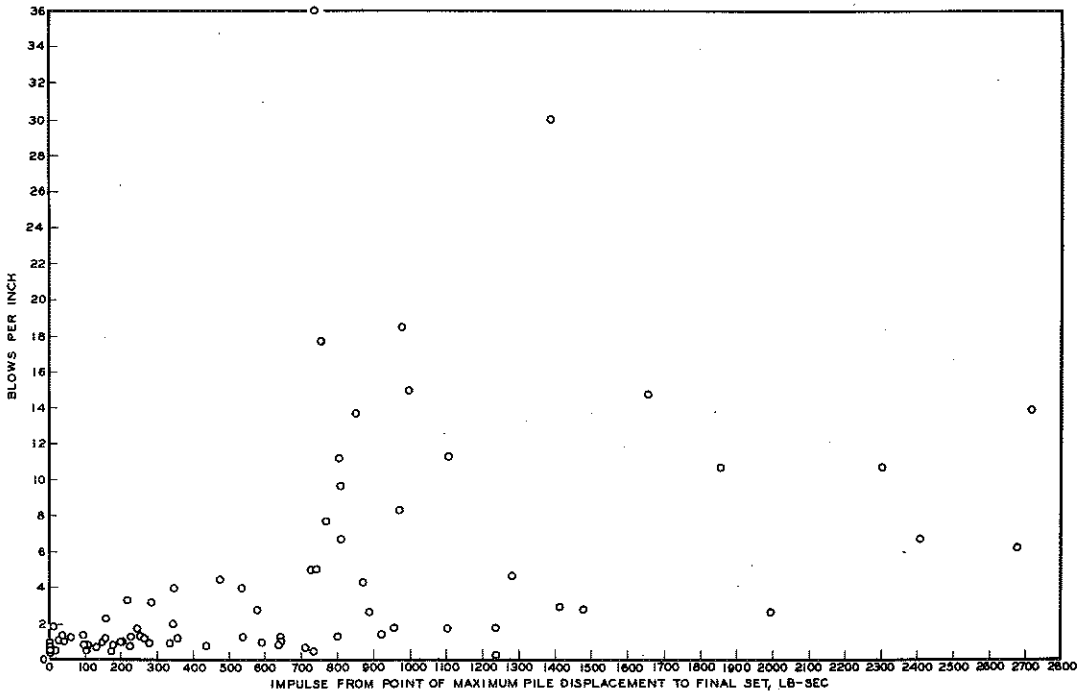

Figure 89. Attempted correlation of blow count with Muskegon-Detroit impulse.

Belleville, Delmag at Muskegon), and the correlating factors were discussed earlier.

2. Blow Count vs. Impulse (Muskegon and Detroit). Fig. 89 shows no evidence of correlation. Impulse is defined here as the summation of products of load cell force and corresponding time increments beyond time for maximum displacement.

3. ENTHRU vs. Impulse (Belleville). As shown in Fig. 90, there is a very poor correlation although there is the expected parallel increase. Certainly in the present form, such a correlation would be of only limited use.

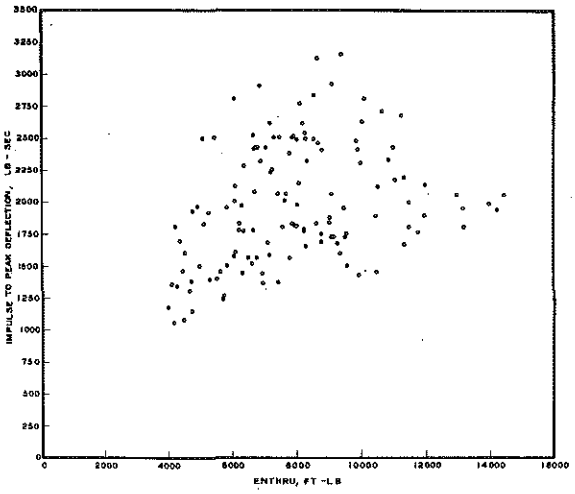

Figure 90. Attempted correlation of Belleville impulse and ENTHRU.

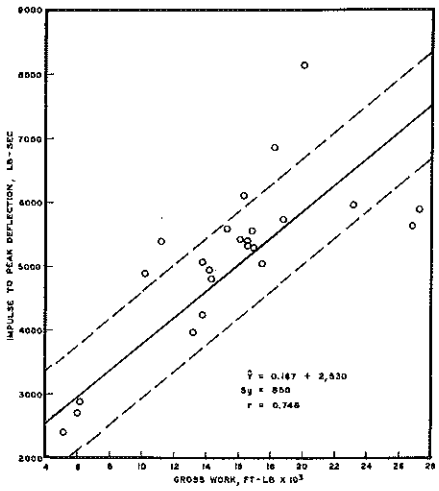

Figure 91. Correlation of gross work of Muskegon hammers with impulse.

4. Gross Work vs. Impulse (Muskegon). It should be noted that in this case both gross work and impulse, as shown in Fig. 91, were obtained somewhat differently than for data obtained up to this point. The pile penetration trace was obtained directly by using the linear variable differential transducer, rather than by using a pile penetration curve obtained by double integration of the acceleration trace as was discussed earlier. In addition, the energy was obtained as the cross-product of the average force during a short time increment, multiplied by the difference in pile displacement during the same increment, and these cross-products were summed algebraically from initial displacement of the pile to peak displacement. The impulse value shown was the area under the force-time trace to peak deflection. Fig. 91 shows a fairly good correlation, based on the limited data available. However, the three points at about 6000 ft-

lb are for the Vulcan No. 1 hammer, and when these are excluded from the data considered, the correlation is much less defined for the remaining heavier hammers.

5. Effect of Cushion Block. Although a basic objective of this program was to evaluate pile hammers over a range of probable field conditions, it was also recognized that the character of the cushion block was an important variable in hammer performance. Therefore, a brief study of cushion block effect was designed and performed at the end of the field work (at Muskegon).

First, for a Vulcan No. 1 test, the cushion block and cap assembly were removed from the load cell and a 2-in. thick steel block was inserted between the ram and the load cell. The assembly was placed on TP 12, a 1/4-in. wall, closed-end pipe, previously driven to 128 ft (5 blows for the last half-inch) with a Link-Belt 520 hammer. Several force and LVDT deflection readings were taken without the cushion block and cap. Unfortunately, no companion force deflection records were made on this pile with the cushion and load cell in place. However, a Vulcan No. 1 blow was recorded with a cushion, under similar circumstances, specifically for LTP 2 at Muskegon on a .230-in. wall pipe at 53 ft penetration driven to 11.2 blows per inch (Fig. 92).

TABLE 19
FORCE-TRACE COMPARISON

Observation	Vulcan No. 1		McKiernan-Terry DE-40	
	With Cushion**	Without Cushion	With Cushion	Without Cushion
Form of force trace	Relatively low frequency, low amplitude, long-duration curves.	Relatively high frequency, high amplitude, short-duration spikes.	Relatively low frequency, high amplitude, long-duration curves.	Relatively high frequency, high amplitude, short-duration spikes.
Peak initial force, lb	175,000	880,000	640,000	1,505,000
Impulse, lb-sec	1,373	1,565	3,621	3,178
Time, 10^{-4} sec*	171	129	212	202

* Time from initial force to maximum deflection.
** Derived from a blow on Muskegon LTP 2 at 53 ft.

Second, the entire cushion and cap assembly was removed for a McKiernan-Terry DE-40 test, so that the hammer anvil rested directly on the load cell (Fig. 93). Force and deflection for several blows on TP 11, a 1/4-in. wall closed-end pipe pile, were recorded at a 175.3-ft penetration (driven at 65 blows per inch). A force and deflection record was then made on the same pile at 175.3 ft penetration with the cap and cushion assembly in place (Fig. 92).

Significant factors are compared in Table 19. Initial peak forces are much greater when the cushions are removed, and for the 1/4-in. wall pipe these would give unit compressive stresses of 100,000 psi or more.

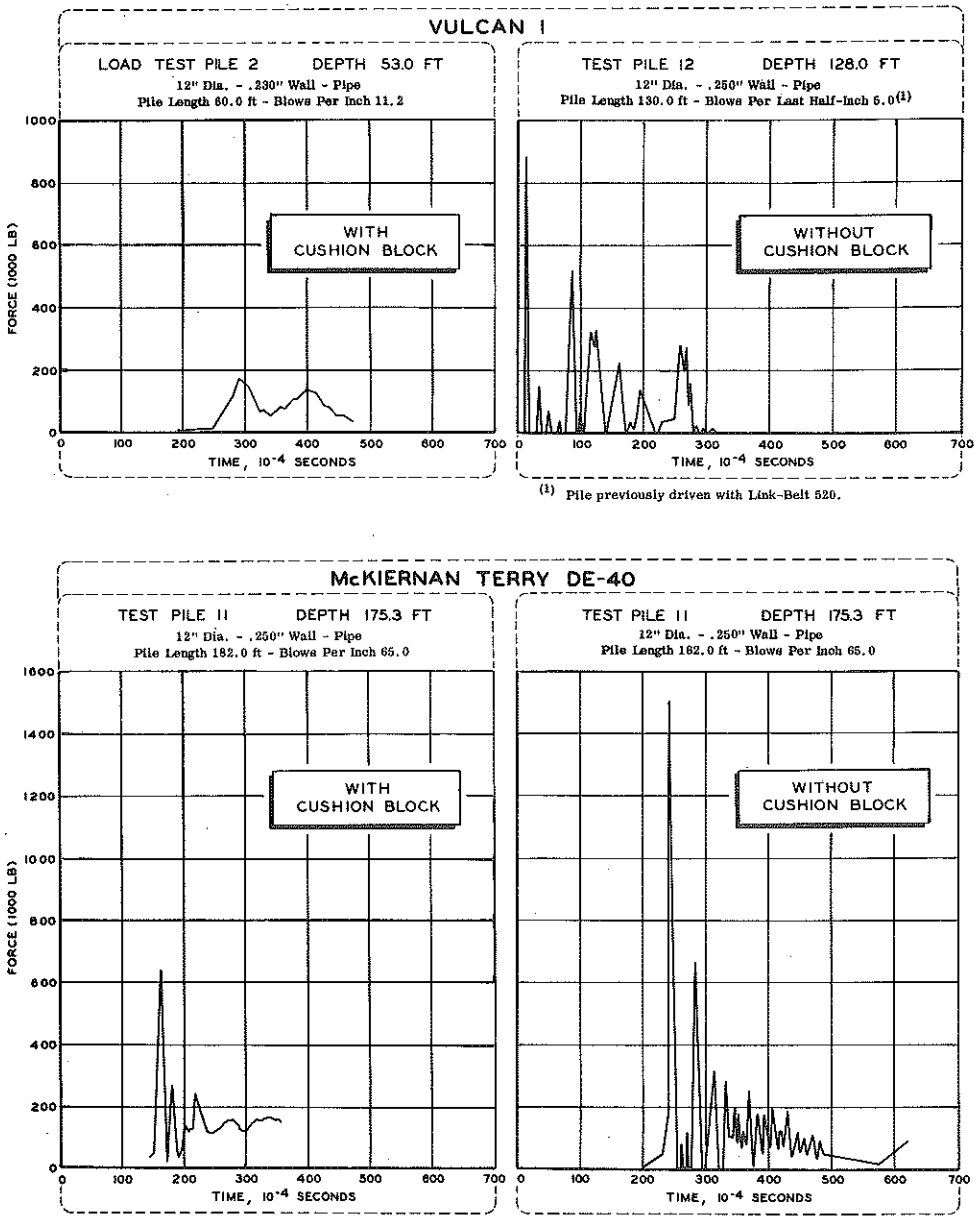

Figure 92. Force traces with and without cushion block (Muskegon).

On the other hand, the impulse values are roughly comparable. It was not possible to make the desired ENTHRU comparison, however, because of the time lag in LVDT displacement measurements discussed previously.

From a practical standpoint, the question of relative ENTHRU is of less significance than the large difference in peak stresses. Because peak stress is probably a major factor in the onset of pile collapse under hard driving, some cushion is generally necessary. Also, the hammer itself might be damaged due to repeated high stresses accompanying uncushioned driving.

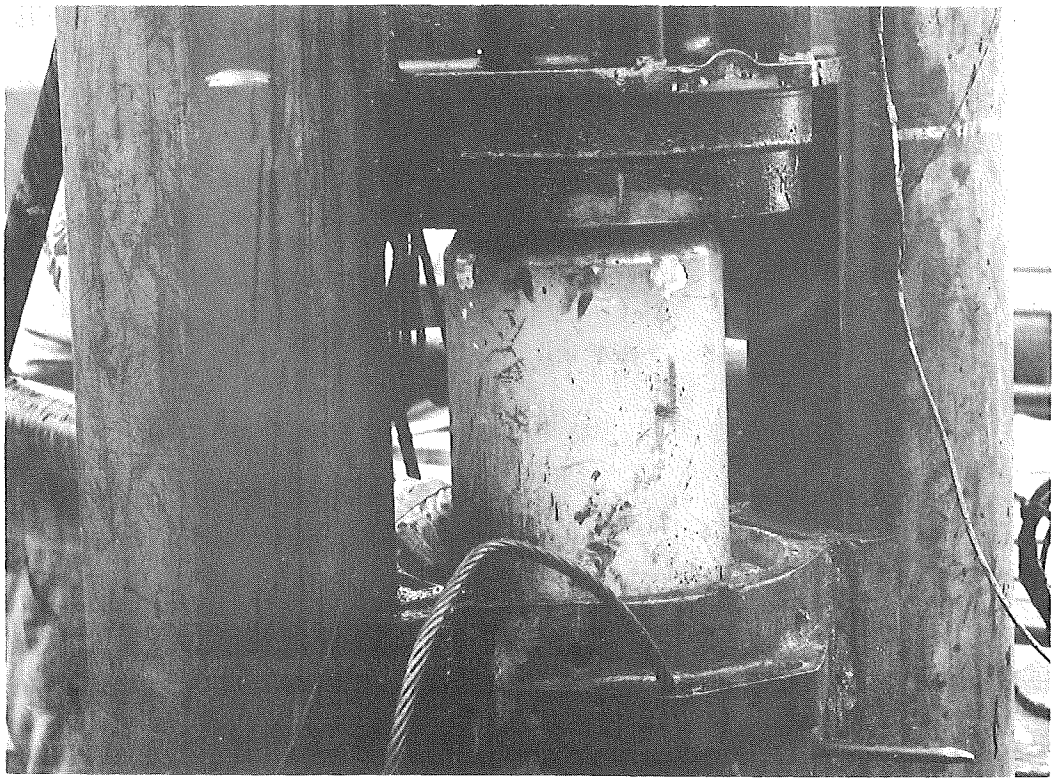

Figure 93. McKiernan-Terry DE-40 positioned directly on load cell.

Summary

A procedure was developed to estimate net energy delivered into the top of a pile under hammer impact, based on the analysis of oscillographic records from the load cell and accelerometer obtained during the hammer test program. This energy is actually the work performed on the load cell and is designated ENTHRU. Results compare favorably with

ENTHRU values based on limited data on force and direct measurements of pile displacements at Muskegon by the LVDT method. A total of 440 hammer blows were analyzed involving examples of all nine hammer types and three basic pile types at all sites. Compilation of ENTHRU values indicated:

1. ENTHRU's delivered to the pile top expressed as percentages of the corresponding manufacturer's rated maximum energy ranged from an average of 26 to 53 percent at Belleville, 36 to 65 percent at Detroit, and 42 to 62 percent at Muskegon, generally being lowest for hammers striking unconfined oak cushion blocks.

2. ENTHRU values for pipe piles generally exceeded comparable H-pile values.

3. For the normal range of hammer performance, no consistent change in ENTHRU was observed over the depths and varying driving resistances encountered.

There is a rough correlation between ENTHRU and penetration resistance for the shallower depths at Belleville. At Detroit, there is an excellent correlation between a hammer's ability to penetrate the bearing stratum and its ENTHRU value. At Muskegon, the relation between a hammer's ability to penetrate resistant layers, measured as total blows per layer, and its ENTHRU is erratic. However the single large hammer that was capable of advancing the pile for its entire depth at Muskegon, under a reasonable number of hammer blows, had an ENTHRU 35 percent greater than the next largest hammer tested.

Other correlations indicate that a Force-Acceleration Index (i.e., the square root of the product of peak force and peak acceleration values) would be a useful measure of hammer driving ability up to a resistance of about 150 blows per foot with a correlation equal to that with ENTHRU. Its principal advantage is that it does not require a time base for either acceleration or force measurements.

Removing the cushion block can cause an increase of 300 percent or more in peak force at impact, without a significant increase of delivered impulse.

CHAPTER NINE

PILE PERFORMANCE DURING DRIVING

The influence of pile type on hammer performance has already been discussed in some detail in Chapters 5 through 8. This chapter presents a direct comparison, where possible, of driving characteristics for differing pile types for the same site and pile hammer. The effects of pile cross-section and surface configuration, pipe wall thickness, displacement and/or jetting, soil set up, and soil drag-down in H-pile flanges, are considered specifically. The relation of driving effort and soil conditions to structural failure of piles during driving is also discussed.

Effect of Cross-Section and Surface Configuration on Blow Count

Considering the Belleville site first, Fig. 94 shows the required driving effort in the range of 24 to 52 ft of pile penetration, comparing H-piles and pipe piles driven by the Vulcan No. 1 and the three diesel hammers. It is apparent that initially (at 24 ft) H-piles required between 50 to 100 percent greater driving effort, but beyond about 40 ft, pipe pile penetration resistance became larger. This is consistent with the fact that during initial driving both developed relatively small end-bearing resistance, but the H-pile developed the larger side soil contact and thus greater driving resistance. Load tests reflect the larger side friction developed by the H-pile at relatively shallow penetration (compare bearing capacities of LTP 3 and LTP 6 at Belleville in Table 21).

For the Detroit site, Fig. 95 shows H-piles developing the higher penetration resistance for most of the depth, with one notable exception. For the Link-Belt 312 hammer, the pipe pile required a small but consistently greater driving effort than companion H-piles. The reason for this reversal is not clear.

Effect of Wall Thickness on Blow Count

Results of an analysis correlating wall thickness of pipe piles with driving resistance is given in Table 20. For both Belleville and Detroit, four hammers are listed where companion 1/4-in. and 7-gage pipe piles

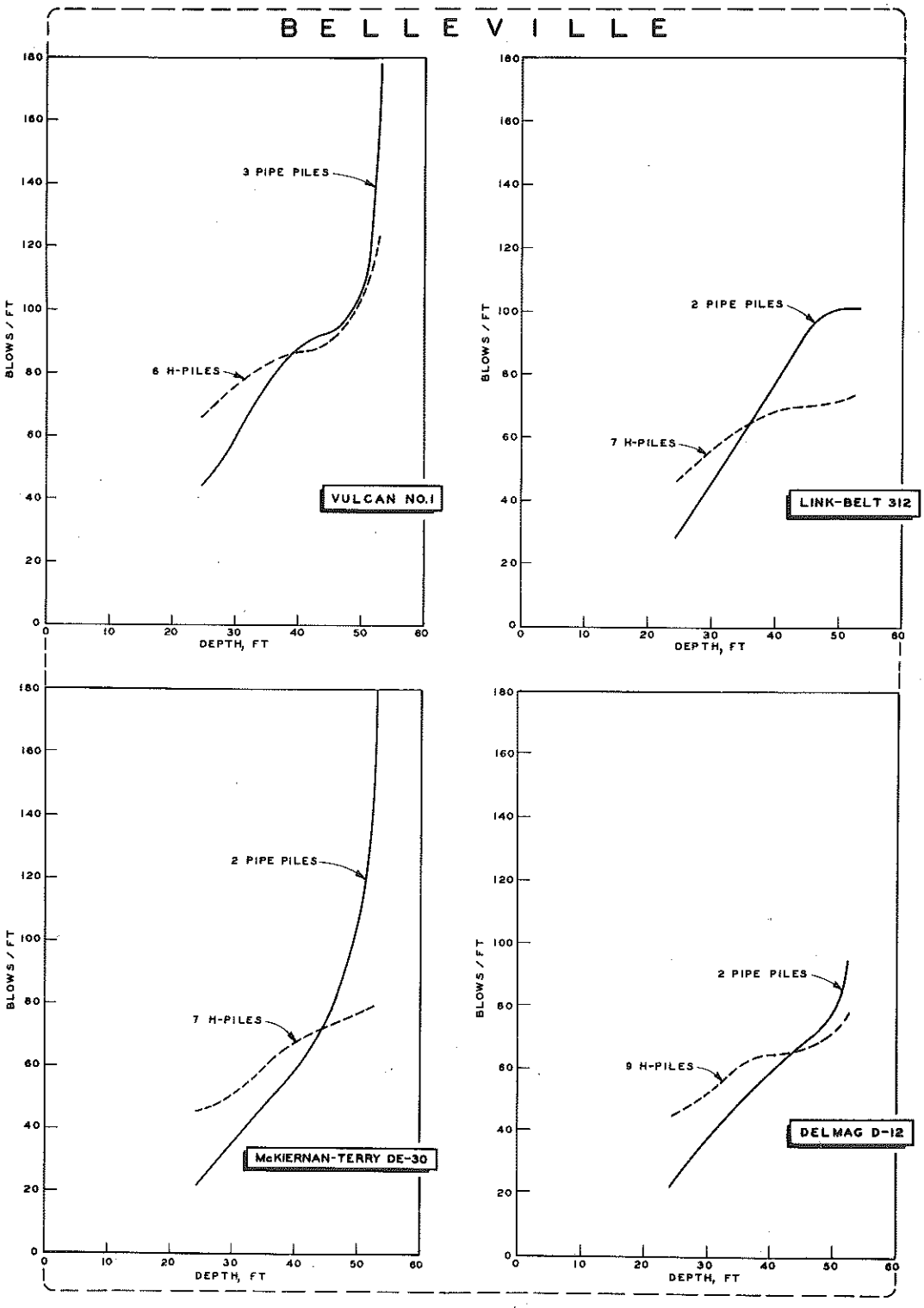

Figure 94. Approximate relationship of driving effort required in penetrating Belleville soil range of 24 to 53 ft.

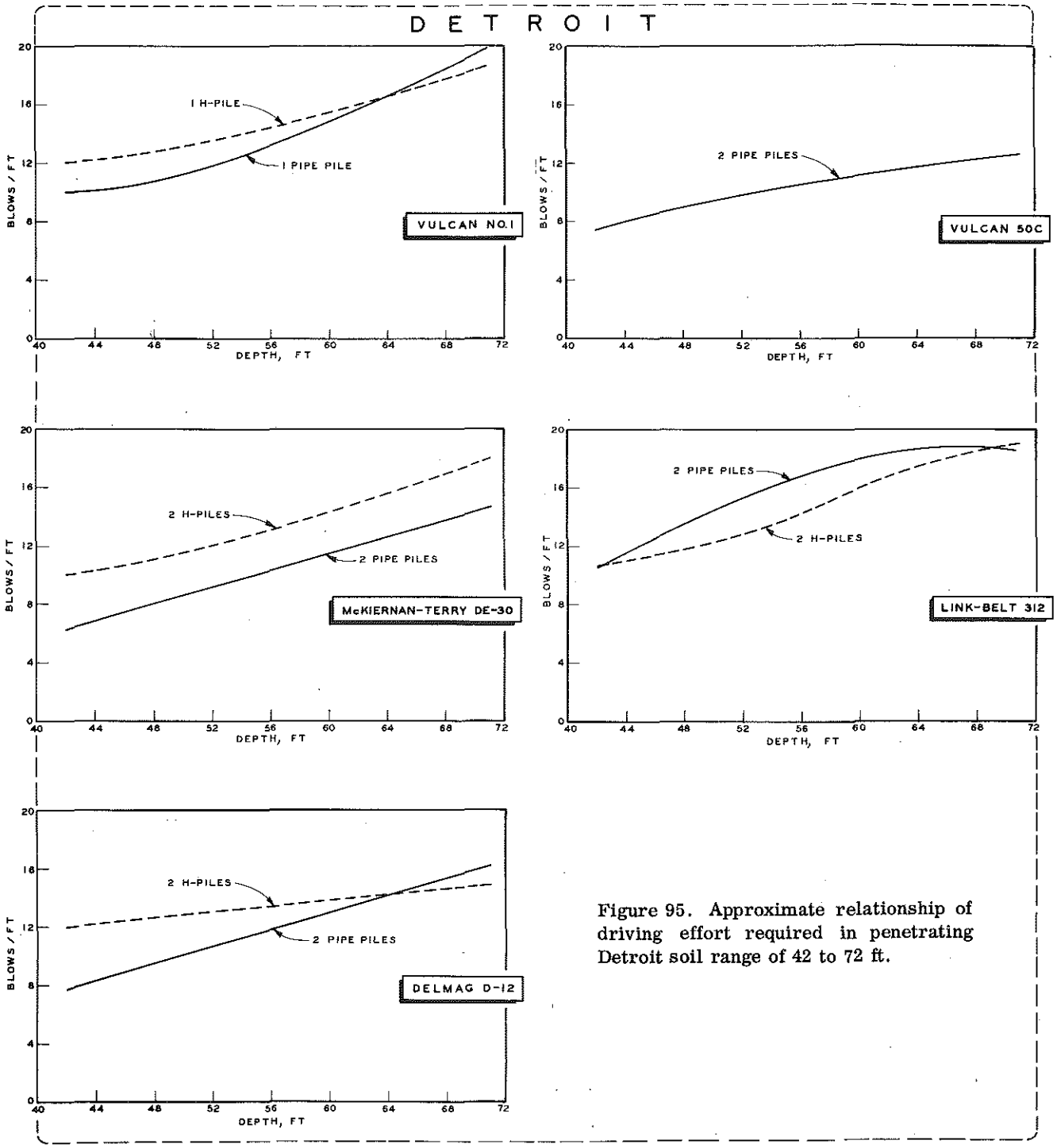

Figure 95. Approximate relationship of driving effort required in penetrating Detroit soil range of 42 to 72 ft.

were driven over an equal depth interval, showing the total hammer blows and the statistical significance of differences reported. It was also observed that the pile having the higher blow count in each instance, also generally took the higher blow count for the entire depth of driving, and thus the relative ranking was consistent over that depth.

TABLE 20
STUDY OF 7-GAGE AND 1/4-IN. PIPE PILES

Site	Hammer	Blow Count for Interval Sampled				Pile Taking Most Blows	Significant Difference Between Driving Ratios[2]
		Pile No.	7-Gage	Pile No.	1/4-in.[1]		
Belleville (24 to 54 ft)	Vulcan No. 1	TP 9	3397	TP 15 TP 14	2198 2157	7-gage	Yes
	Link-Belt 312	TP 16	1864	TP 4	2465	1/4-in.	Yes
	McKiernan-Terry DE-30	TP 8	2192	TP 11	1763	7-Gage	Yes
	Delmag D-12	TP 5	1621	TP 10	1701	1/4-in.	Yes
Detroit (42 to 77 ft)	Vulcan 50C	TP 5	398	TP 14	377	7-Gage	Yes
	Link-Belt 312	TP 4	628	LTP 10	562	7-Gage	Yes
	McKiernan-Terry DE-30	TP 13	380	TP 3	408	1/4-in.	Yes
	Delmag D-12	LTP 9	450	TP 12	445	7-gage	---

(1) Nominal 1/4-in. wall pipe varies from 0.23 to 0.25 in.

(2) Significance of difference in increment blow counts, based on pairing technique outlined in footnote 11, Chapter 5.

There were four instances where the 7-gage pile was more resistant and three instances where the 1/4-in. pile took a greater blow count. There are, however, no logical or consistent trends. For the Link-Belt 312 hammer, the 1/4-in. pile developed the greater penetration resistance at Belleville, whereas the 7-gage showed the greater resistance at Detroit. Just the reverse relationship was observed for the McKiernan-Terry DE-30 hammer at these two sites. One must conclude that factors other than pile wall thickness exercised an equal or greater effect on penetration resistance for the hammers and sites studied. In this regard, it has already been noted that the west side of the Belleville site was more resistant for the upper 20 ft. This would explain why TP 8 (7-gage) and TP 10 (1/4-in.) required more hammer blows than companion piles TP 11 (1/4-in.) and TP 5 (7 gage), with the former two piles located from 10 to 15 ft west of the latter two. Note also that under the relatively uniform, soft driving conditions at Detroit, driving resistance of the so-called "light" and "heavy" wall pipes differed only 12 percent or less for any given hammer.

Recognizing the scarcity of data and limited conditions of the test program, one can still make the following generalizations:

1. Pipe pile wall thickness in a range from 1/4-in. to 7-gage has a relatively small effect (12 percent or less) on driving resistance in soft deep clays, as at Detroit.

2. Variations in such factors as hammer performance, soil conditions, driving sequence, and possibly other influences, have as much if not more effect on observed driving resistance as does pipe wall thickness selected in the range of 7-gage to 1/4-in., in firm-to-stiff clays and silts, as at Belleville.

It appears that a statistically designed experiment to define the differences in driving resistance as a function of pile wall thickness would require a rather extensive pile driving program.

Pile Failures During Driving

A critical aspect of pile type selection for a given job is the ability to sustain the required driving without suffering structural damage. Some insight into this problem was gained in the test program, since six pipe piles were damaged structurally. These may be listed as follows, by site, wall thickness, hammer type, and character and location of the upper boundary of distress:

Site	Pile No.	Wall Thickness	Hammer	Remarks
Belleville	TP 7	7-gage	Vulcan 50C	Collapsed 21 ft from tip
	TP 8	7-gage	McKiernan-Terry DE-30	Collapsed 12 ft from tip
Detroit	TP 5	7-gage	Vulcan 50C	Collapsed 3 ft from tip; probable split
	TP 9	7-gage	Delmag D-12	Collapsed 21 ft from tip
	TP 14	1/4 in.	Vulcan 50C	Collapsed at tip; probable split 16 ft from tip
Muskegon	TP 13	1/4 in.	Link-Belt 520	Collapsed 40 ft from tip; probable split

As might be expected, the 7-gage pile was more susceptible to wall collapse. At Belleville, only the upper limit of the crimping could be verified visually although it was possible to plumb to the bottom confirming that the tip was at the correct elevation. Similarly, Detroit TP 9 showed a wall collapse above the tip. On the other hand TP 5 indicated crumpling

at the tip, but it was not possible to reach the tip elevation. TP 14 indicated a localized inward buckling of the pipe at the shoulder of the concial tip; this could possibly have been due to caving of the tip due to impinging on a boulder or bedrock. Concerning Muskegon TP 13, it is significant that it was subjected to about 12,000 blows, more than twice the total delivered to any other pile on this project; this represents unusually severe treatment and thus falls outside the slope of this discussion.

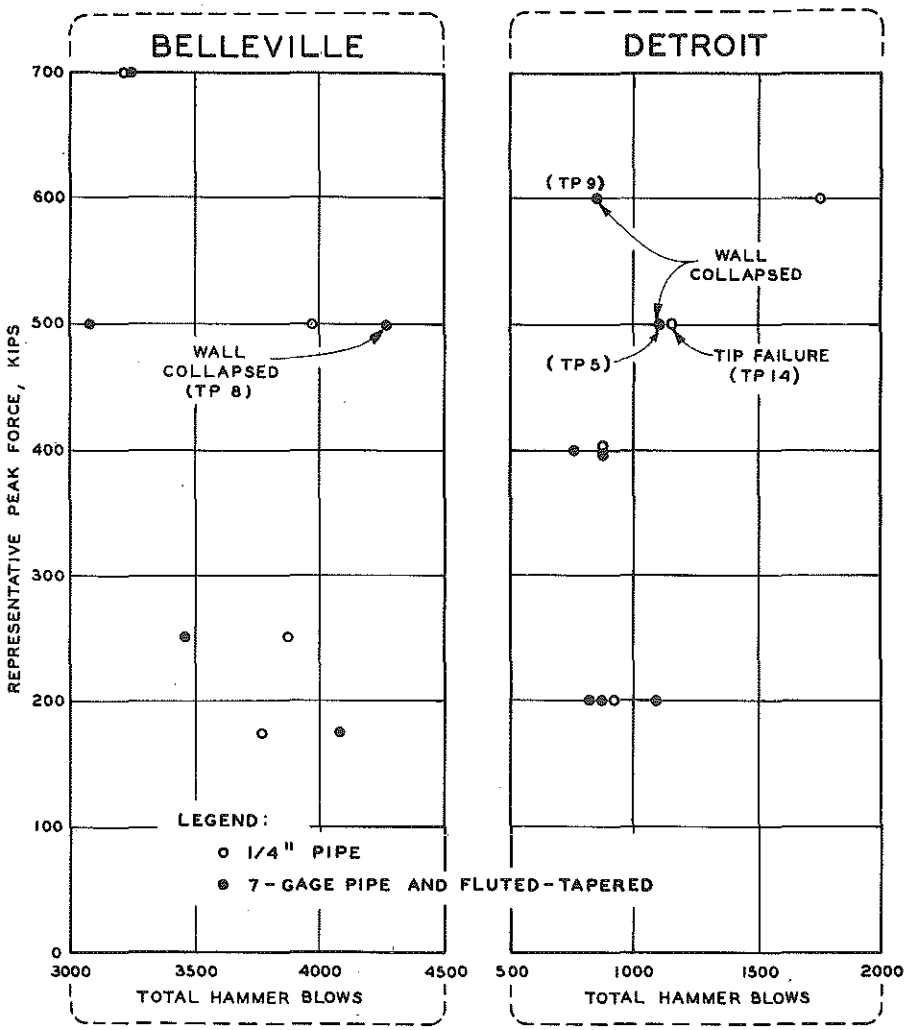

Figure 96. Correlation of representative peak force, hammer blows, and incidence of pile structural failure.

Based on the limited data, the correlation between representative driving force (Figs. 73, 74, 75), total blows, and absence or presence of failure is shown for comparable pipe piles at Belleville and Detroit in Fig. 96. There is some indication that the combined effect of peak force

and number of blows is related to the onset of collapse for the 7-gage pipe piles. It may also be noted that at least one 1/4-in. wall pipe was successfully driven for a significantly greater number of blows of high peak force than the two 7-gage piles which collapsed at Detroit.

More striking is the large difference in tolerable blow count between sites. Whereas pipes were damaged after about 1,000 blows at Detroit; at least 4,000 blows could be sustained for the same hammer and pile type at Belleville without evident damage. Since the piles were driven to about the same depth and penetration resistance, soil conditions appear to be of primary importance in their influence on the safe limit for combined peak force-blow count. It would seem that the relatively hard end bearing, and soft overlying soil strata at Detroit represent relatively severe driving conditions. Although peak driving stress at the top of the piles was comparable for the same hammer at the two sites, it is probable that more intense compression waves reached the bottom of the pile at Detroit. Here the effect of high end-bearing resistance would reinforce the wave stress at the bottom.[1] Theoretically, this might double the maximum compressive stress at the bottom of a free standing end-supported pile. On the other hand, the considerable side friction developed at Belleville must have absorbed a proportionately larger amount of energy and thus reduced the compressive stresses at the pile tip.

Effects of Open-End Driving and Internal Jetting

It has become standard practice where intermediate layers of compact sand must be penetrated below the water table, to use external water jets to loosen and/or displace such sands along the sides or ahead of the piles. There is uncertainty regarding the suitability and amount of disturbance caused by this method, making questionable the final pile side friction to be assigned for design calculations. Muskegon borings showed the upper sand to be of variable resistance with some indication of a moderately compact zone about 50 to 55 ft. It was decided to investigate the effectiveness of controlled internal jetting of an open-end pile, and to compare its driving resistance to other types of unjetted piles, during Muskegon operations.

In the first attempt, a 15-ft open-end pipe section was driven to 12 ft (TP 1). Then, a 45-ft extension with an attached 4-ft jet follower assembly was spliced to the 15-ft section already driven (Fig. 97, upper right).

---

[1] Samson, C. H., Jr.; Hirsch, T. J.; and Lowery, L. L. Jr. "Computer Study of Dynamic Behavior of Piling." Journal of the Structural Division, ASCE Proc, Vol. 89, No. ST4 (August 1963, Part 1), pp. 413-449.

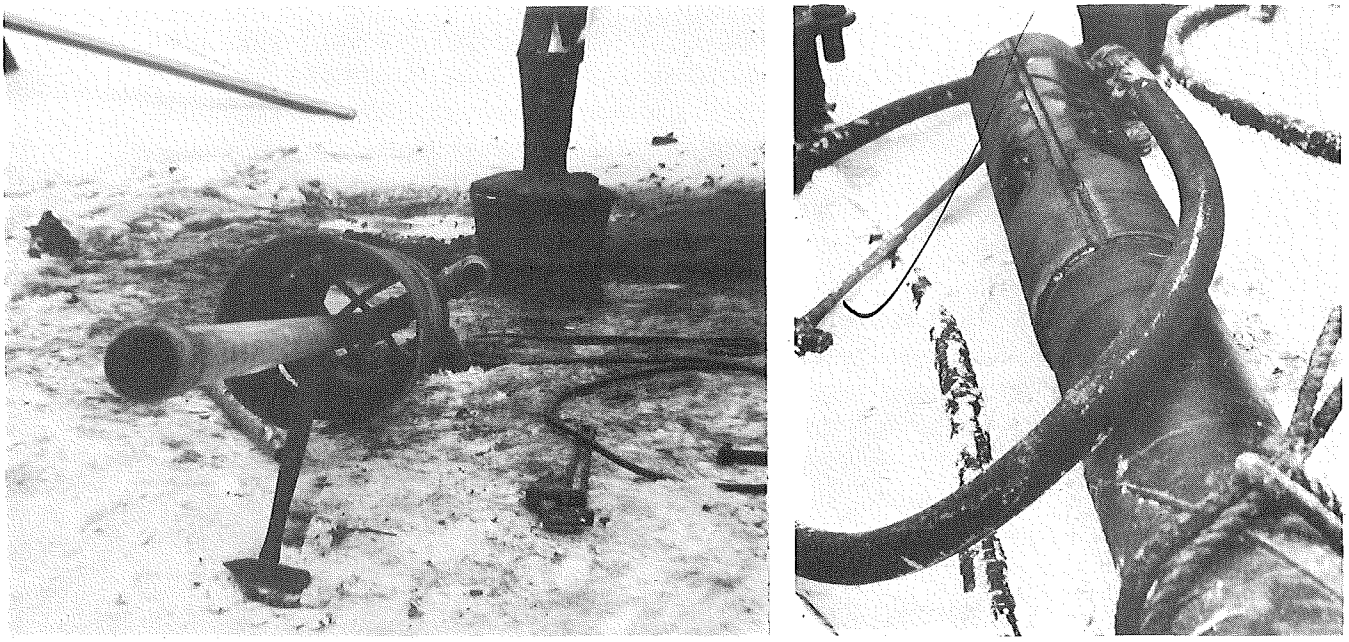

Figure 97. Internal jetting of open-end pipe piles during driving originally involved a system having a jet pipe fixed in the follower (upper left) with an inlet connection elbow fixed by welding; this follower assembly was then welded to the pile (upper right). The second system fabricated (lower left) had a floating, non-fixed jet pipe, allowed to protrude through an open port in the follower side; spoil flowed through ports when the assembly was in operation (lower right).

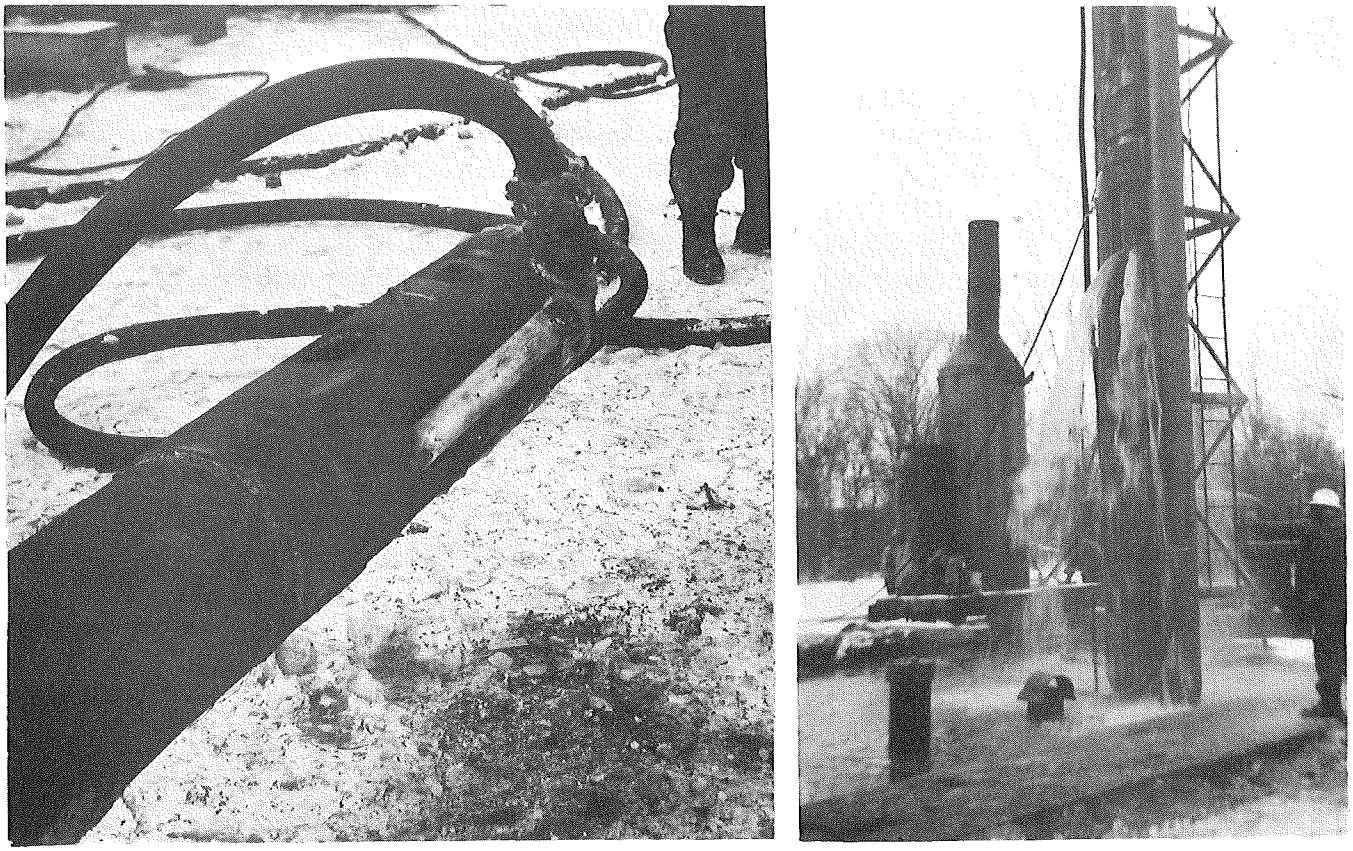

The jet pipe was rigidly connected to the follower at the top and extended to within 1.5 ft of the soil plug (Fig. 97, upper left). Before driving, the jet assembly was to run for 2 minutes, powered by a pump with a capacity of 700 gpm at 250 psig. Shortly after driving commenced it was evident that the jet was not functioning properly. Examination revealed that the jet pipe had broken at the 90° rigid elbow connection. Driving was suspended at 43.5 ft of penetration.

It was decided to bend the jet rod to protrude through a port in the side of the follower and allow it to hang free during driving and jetting (Fig. 97, lower left). This proved to be successful while driving LTP 4 for 58 ft (elevation 530). At completion of driving, about 8 ft of sand settled out above the pile tip and this soil was washed out subsequently. There was no evidence that the jet water penetrated beyond the open end and up along the outside of the pile.

Three other pipe piles were driven to 58-ft depth with the Vulcan No. 1 hammer at Muskegon and the penetration blow count records are summarized in Fig. 98. It is apparent that the closed-end pipe pile required by far the highest blow count and the internally jetted pile the lowest. Unjetted open-end TP 14 required more than twice the blow count in the resistant layer at about 50-ft depth. Rather surprising was the relatively low driving resistance of the closed-end fluted-tapered pile. Although this pile had only an 8-in. tip compared to the 12-in. diam straight-sided pipe, one would not expect as large a difference in blow count as is indicated.

Again, results are merely indicative, but do show that internal jetting results in a significant decrease in required driving effort. Moreover, field experience indicates that the procedure is practical.

Side Friction Set-Up

Another factor which can exert a significant influence on pile driving resistance is so-called "set-up." This is indicated by an increase over initial blow count when commencing to redrive a pile after some period of time has elapsed. It is particularly noticeable in cohesive soils and is thought due to a "thixotropic" strength gain stemming from molecular reorientation of the water-clay system after the disturbing effects of driving are dissipated. This strength gain will also be discussed in connection with Belleville and Detroit set-up piles in Chapter 11.

Although the test program was not specifically designed to evaluate this phenomenon, some data were available and are summarized in Fig. 99.

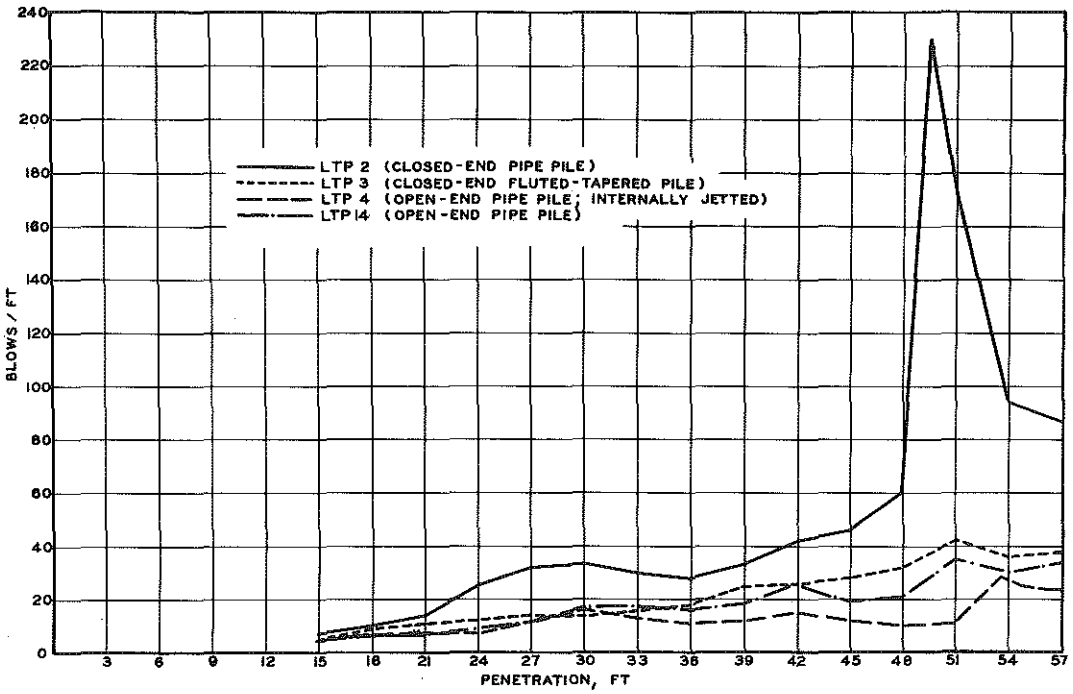

Figure 98. Effect of jetting on Muskegon hammer driving performance.

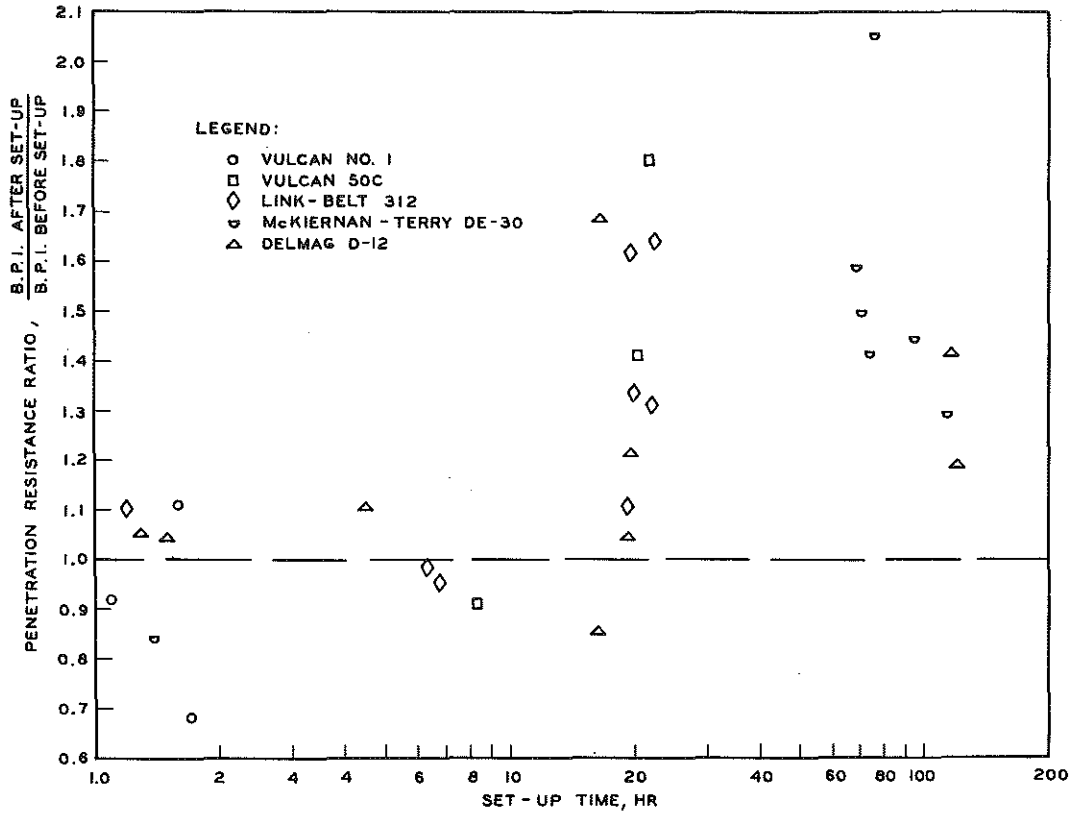

Figure 99. Effect of hammers and set-up time on penetration resistance (Belleville H-piles at 36-ft penetration; 40-ft long before set-up, 60-ft after).

Shown are the ratios of penetration resistance, expressed as blows per inch immediately after and before the period of set-up, related to duration of this period in hours. Although the penetration resistance shows a definite increase with increasing time, the specific values presented must be qualified. The set-up period was used to add about 20 ft of additional pile length, and often other piles were driven in adjoining areas. Thus, the increase in blow counts cannot be ascribed to the set-up alone, and to some degree may reflect effects of greater mass and elastic deformation of the longer piles, as well as possible compaction effects of adjoining piles. There is evidence that set-up time is the more important factor, noting there is only a small increase in blow count after 1 to 2 hours although 20 ft of pile was added during that period. Also, hammer performance and cushion block condition may exert an effect on driving resistance as important as set-up time, for the test conditions of this study.

Soil Displacement in H-Pile Flanges

When it was noted at Belleville that soil adhering within H-pile flanges was being dragged down, measurements were made to determine the extent of this displacement. The soil was generally adhering in both sides of the pile web (designated "west" and "east" below, in terms of directions shown in Fig. 22, and with few exceptions did not exceed 16 in. in depth. No measurements were made for H-piles driven by the Delmag D-12, but average displacements for other hammers were 5 in. for the Vulcan No. 1 (six piles, excluding LTP 6), 12 in. for the Vulcan 50C (eight piles), and 9 in. for the McKiernan-Terry DE-30 (eight piles). Drag-down for the Link-Belt 312 (eight piles) was notably greater than for the other hammers, with an average depth of 7 ft 2 in. Further, although drag-down in piles driven by other hammers was generally equal in both flanges, for the Link-Belt the depths often varied considerably from one side to the other. For the following piles, displacements greater than 16 in. were recorded in at least one flange:

Hammer	Pile No.	Depth of Soil Displaced			
		West		East	
		ft	in.	ft	in.
Vulcan No. 1	RP 37	0	8	5	0
Link-Belt 312	RP 3	1	0	6	6
	RP 7	0	8	9	0
	RP 18	15	0	15	0
	RP 21	5	0	9	0
	RP 24	9	0	0	0
	RP 29	15	0	15	0
McKiernan-Terry DE-30	RP 31	0	4	3	6

CHAPTER TEN

PILE LOAD TESTS

A comprehensive program of static load tests was undertaken at all three test sites, to determine bearing capacity and relate it to penetration resistance of piles driven with the various hammers, and also to soil resistance as determined by borings and laboratory tests. Selected piles were loaded to failure or to the capacity of the load reaction system. The pile lengths tested varied from 44 to 67 ft at Belleville (with loads of 55 to 400 tons), 69 to 81 ft at Detroit (with loads of 22 to 270 tons), and 58 to 178 ft at Muskegon (with loads of 50 to 370 tons).

A total of 19 piles were load tested, and are identified as LTP's in Figs. 22, 23, and 24. Two were open-end pipes, driven in clay soils purely as side shear piles, to determine the set-up or change in shearing resistance developed with time, from initial driving over an extended period. A third open-end pile, internally jetted during driving, was tested to determine side shear in granular soil. Fourteen were pipe piles filled with concrete, and had 1/4-in. "tell-tale" rods (Fig. 100) installed to float freely within a 1/2-in. oil-filled pipe extending to the bottom of the pile. These tell-tales were used to record settlement and permanent set of the tip during test loading, pile shortening due to compression, and elastic rebound after unloading. The remaining two piles were H-sections.

Pile Preparation for Load Testing

Each closed-end pipe pile was instrumented with its tell-tale device before being filled with 7-sack, 1-percent calcium chloride, high early strength, Class AA concrete. All pile tops were covered with straw and polyethylene sheets while curing. Core samples for testing of concrete compressive strength were taken from a 10-ft specimen of Belleville LTP 3, after 303 days of curing. Compressive strengths of six samples varied from 6460 to 7660 psi. For further information on compressive strength and modulus of elasticity, a laboratory mix was prepared dupli-

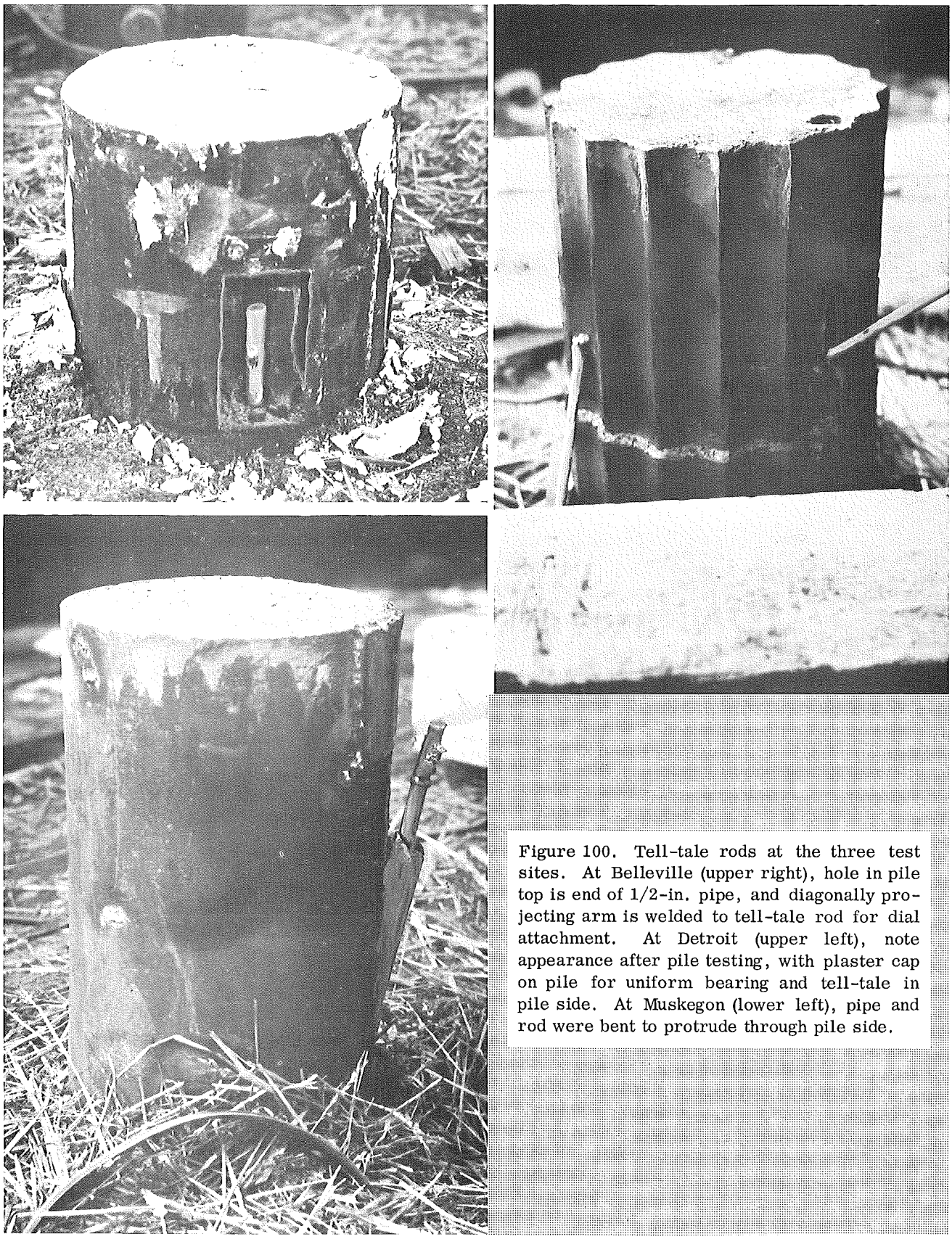

Figure 100. Tell-tale rods at the three test sites. At Belleville (upper right), hole in pile top is end of 1/2-in. pipe, and diagonally projecting arm is welded to tell-tale rod for dial attachment. At Detroit (upper left), note appearance after pile testing, with plaster cap on pile for uniform bearing and tell-tale in pile side. At Muskegon (lower left), pipe and rod were bent to protrude through pile side.

cating that used at Belleville and Detroit with the following results:

Days Cured	Compressive Strength, psi	Modulus of Elasticity, psi	
		Secent Method	Tangent Method
7	5040	3.50×10^6	3.89×10^6
14	5620	3.80×10^6	4.00×10^6
28	5900	4.05×10^6	4.76×10^6
35	6380	3.79×10^6	4.49×10^6
35	6380	---	---

Test cylinders also were made during concreting of load test piles at Muskegon. Concrete used in LTP's 6, 7, 8, and 9 had average compressive strengths of 4540 and 5255 psi after 14 days and 28 days, respectively. Concrete used in LTP's 2, 3, and 5 was tested after 14 and 28 days of curing with average strengths of 4595 and 5805 psi, respectively.

Load Reaction Assemblies

The test reaction systems used are shown schematically in Fig. 101. Load reaction at Belleville, totaling 400 tons, was obtained primarily from anchor reaction piles connected to a steel load frame supporting 100 tons of steel slabs. Short sections of pipe were welded to these reaction piles to support the frame and steel slabs (Fig. 102). At Detroit, the reaction was obtained from 300 tons of steel slabs placed on steel framing supported on timber cribbing, so designed that the assembly could be moved along tracks over the test row (Fig. 103). Load reaction for the Detroit open-end friction pile was obtained entirely from six reaction piles. At Muskegon (Fig. 104), 370 tons of sand were used for load reaction, supported in a load box that could be moved in the same manner as at Detroit.

Test Procedure

The basic test procedure involved measuring pile settlement using a constant time interval for application of equal load increments.[1] Each increment was about one-eighth the estimated load required to cause initial progressive settlement of the pile. The constant time interval was 60 min. This procedure usually provided five settlement points for plotting in the elastic range, and two to three points in the range of progressive settlement of the pile.

[1] Housel, William S. "Field and Laboratory Correlation of Bearing Capacity of Hardpan for Design of Deep Foundation." ASTM Proc., Vol. 56 (1956), pp. 1320-50.

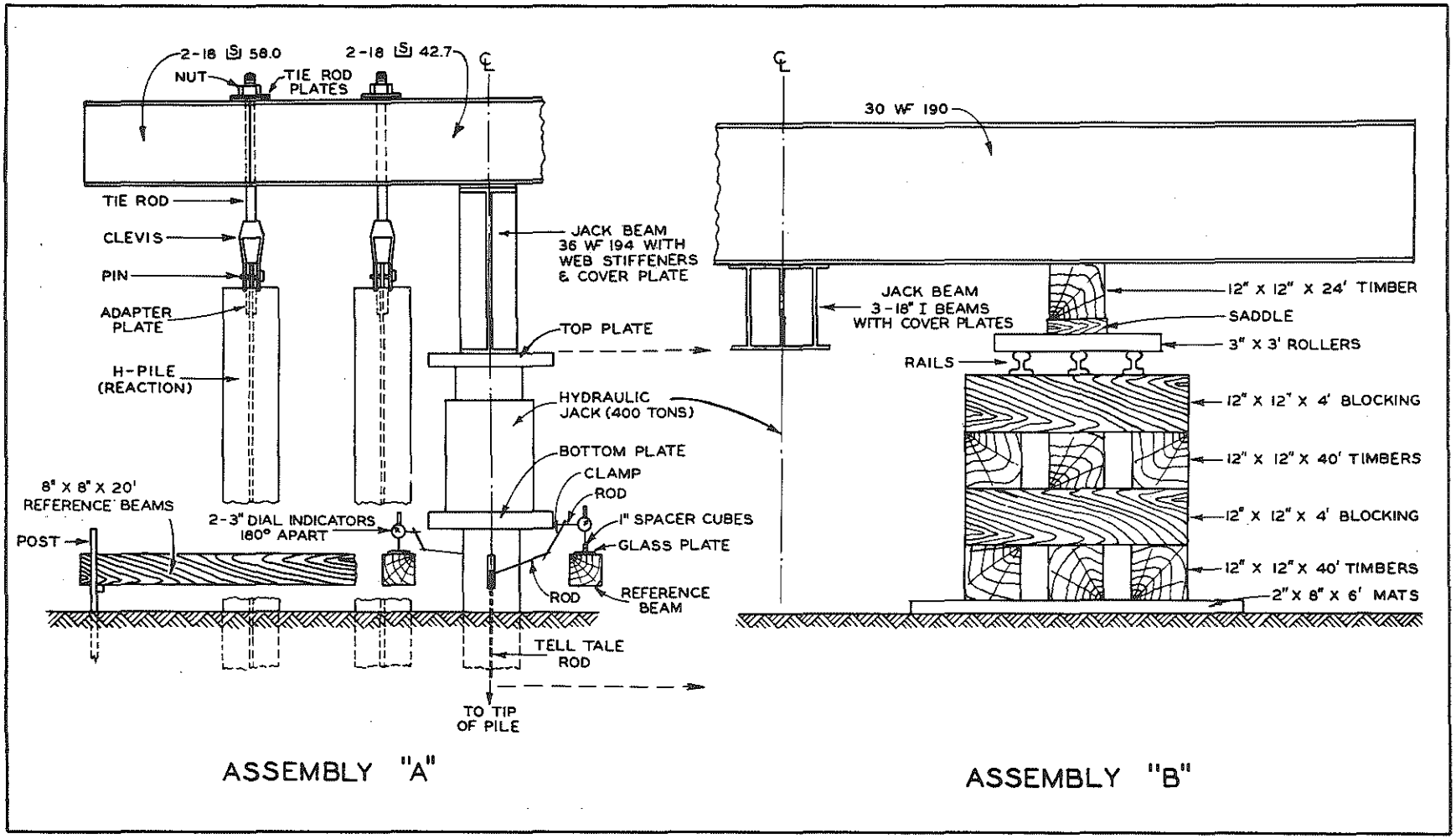

Figure 101. Pile load test reaction assemblies; assembly "A" used at Belleville and Detroit, and assembly "B" at Detroit and Muskegon. Assemblies are symmetrical about the centerline of the jack beam.

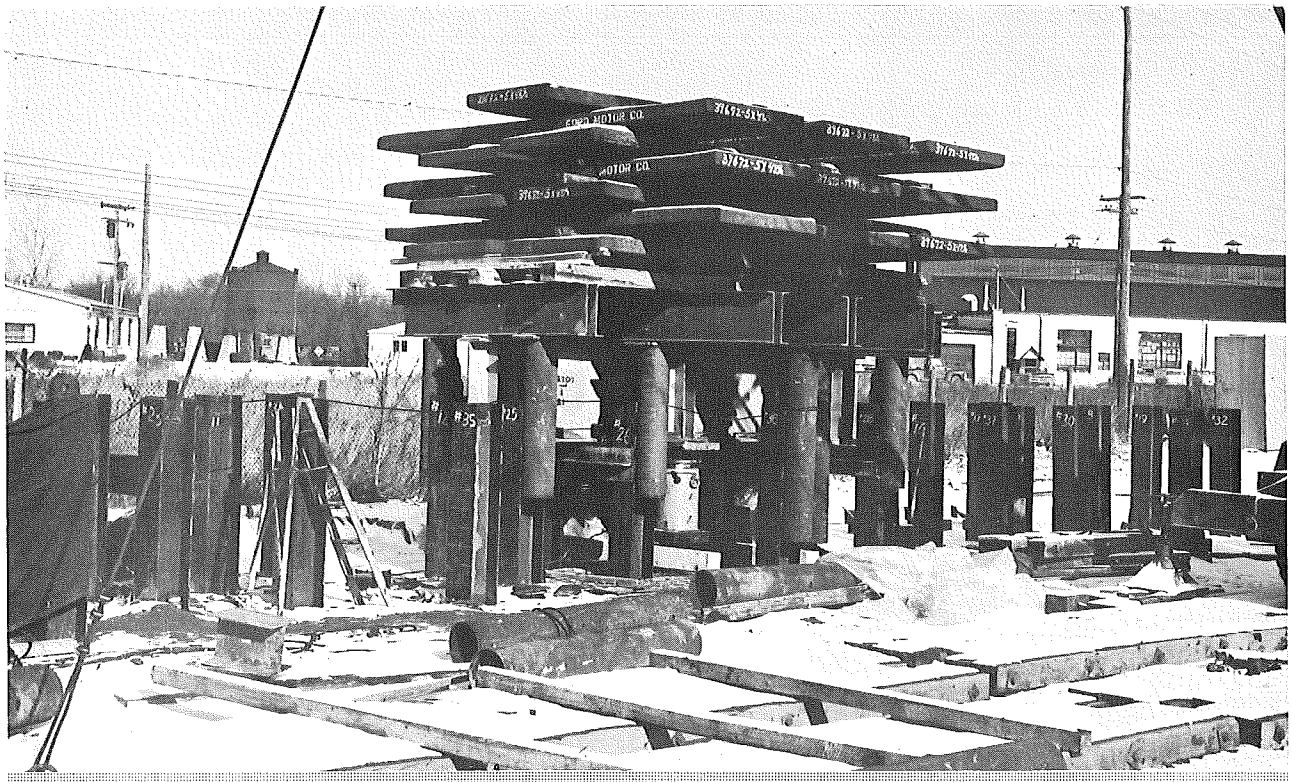

Figure 102. Belleville load reaction assembly, showing reaction frame with 100 tons of steel slabs in place (top), and reaction beam and jack in place (bottom). Note spacing of reaction piles.

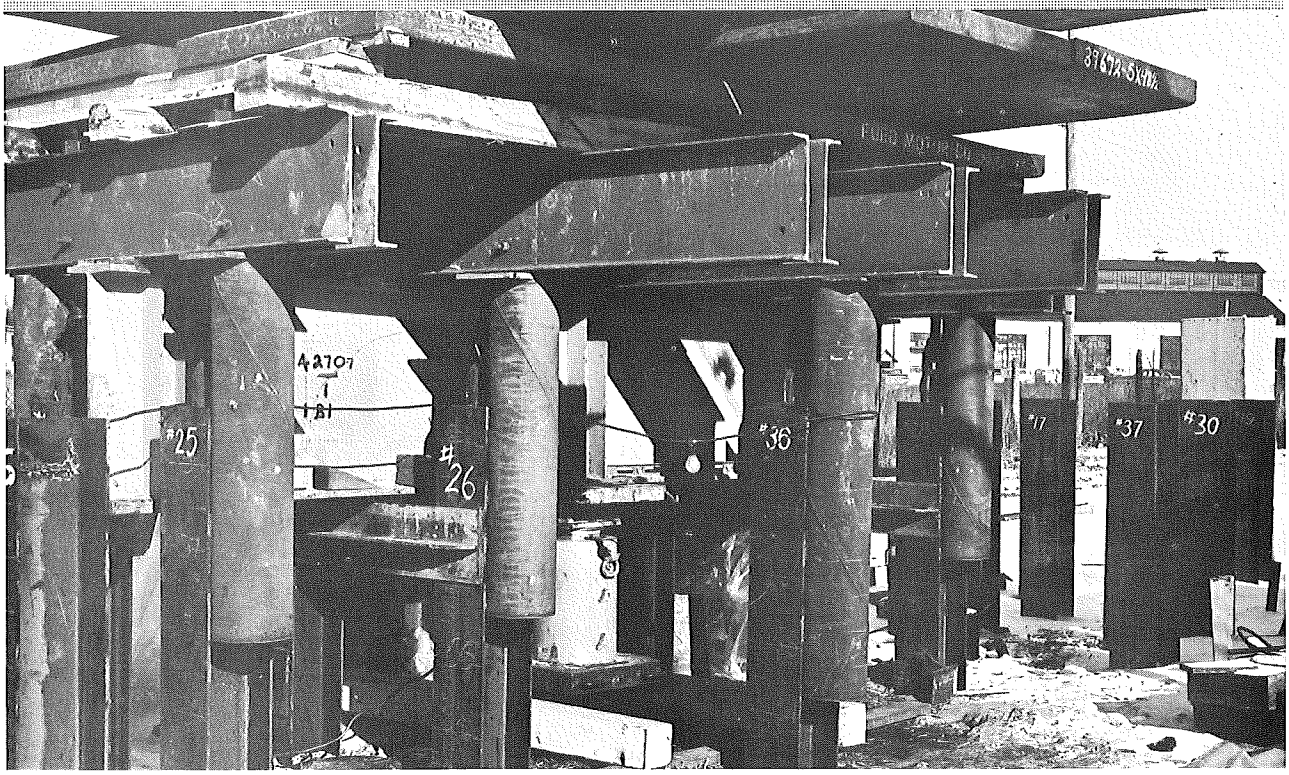

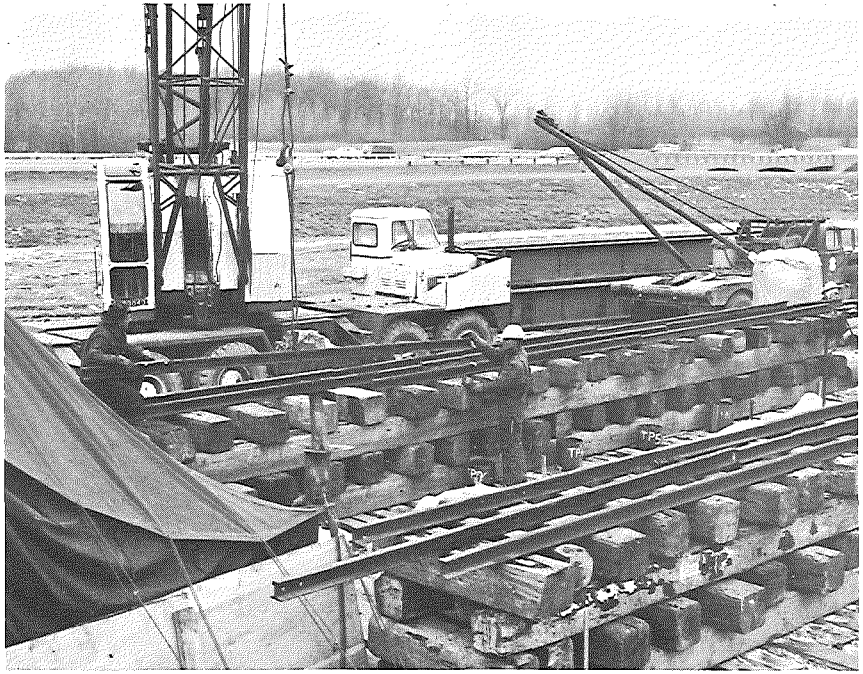

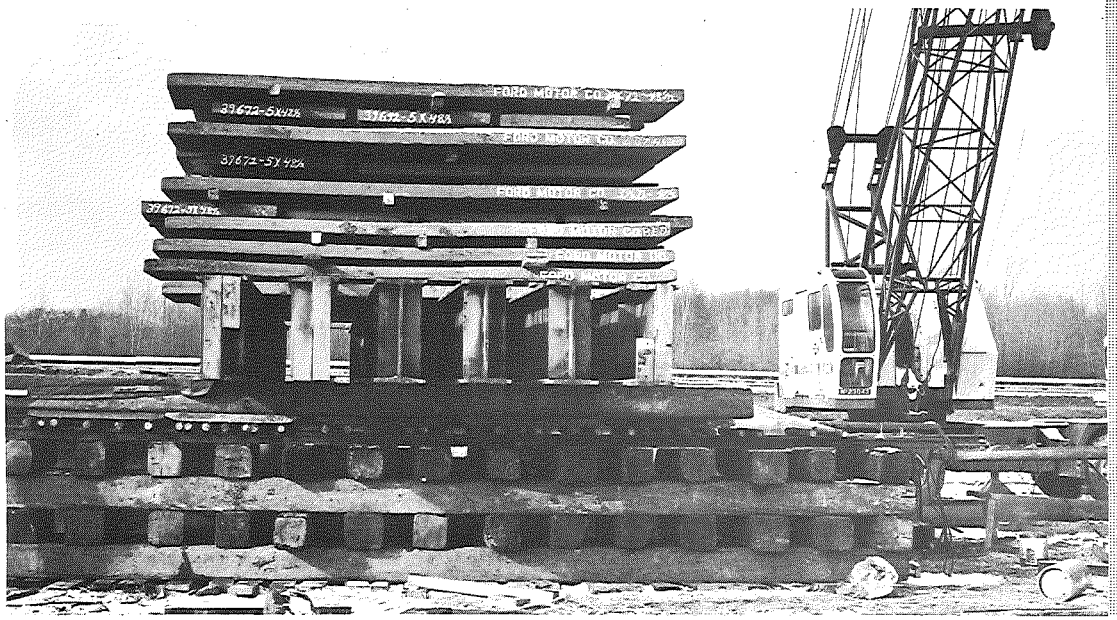

Figure 103. Movable load-reaction box at Detroit, showing rails being placed on timber cribbing foundation (upper left), view along test row (upper right), and reaction box in position (lower left).

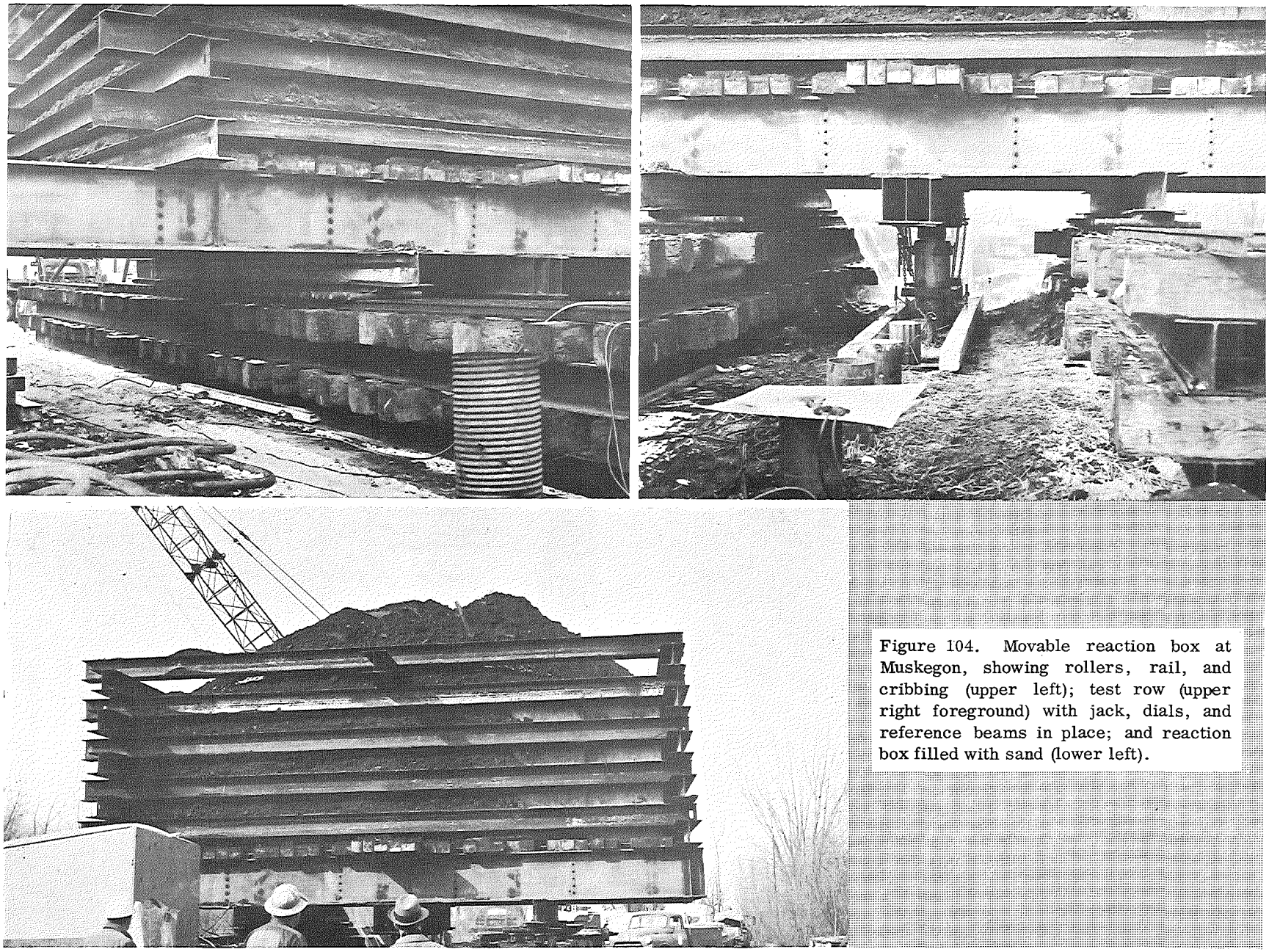

Figure 104. Movable reaction box at Muskegon, showing rollers, rail, and cribbing (upper left); test row (upper right foreground) with jack, dials, and reference beams in place; and reaction box filled with sand (lower left).

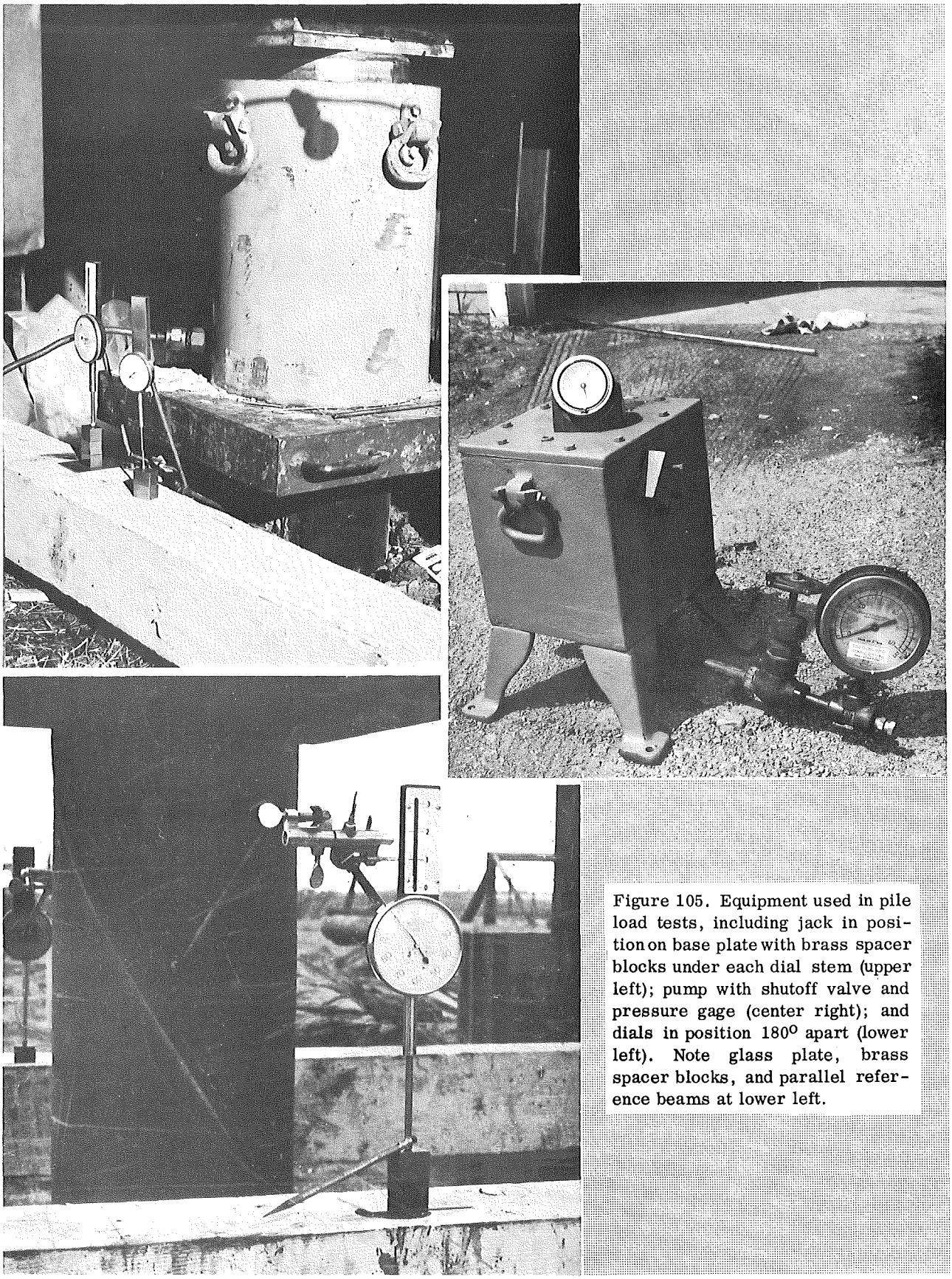

Figure 105. Equipment used in pile load tests, including jack in position on base plate with brass spacer blocks under each dial stem (upper left); pump with shutoff valve and pressure gage (center right); and dials in position 180° apart (lower left). Note glass plate, brass spacer blocks, and parallel reference beams at lower left.

The test procedure and program consisted of the following three phases:

1. Initial Loading (Cycle 1). Application of the first load increment was usually completed within the first minute of the 60-min. interval. Settlement readings were taken at 1 min, and every 10 min of the 60-min interval, using the equipment shown in Fig. 105. Then, at the end of the 60-min interval, the next load increment was applied, and the same sequence repeated for each load increment until the pile was loaded well into the range of progressive settlement.

2. Unloading or Rebound. After the final reading for the last load increment of the loading cycle, the maximum load was released in successive increments of 25 percent of the total load at 30-min intervals. Readings were taken 1 min after each release and at the end of each 30-min interval. One minute after complete removal of all load, an elastic rebound reading was taken, with additional readings every 10 min until pile movement was less than 0.001 in.

3. Recycling or Repetitive Load (Cycle 2). A second cycle of loading was performed on each test pile, immediately following the first, as illustrated in Fig. 106. This was done to assist in establishing the character of the permanent deformation or set, however small, that took place upon application and removal of load in each loading cycle. In

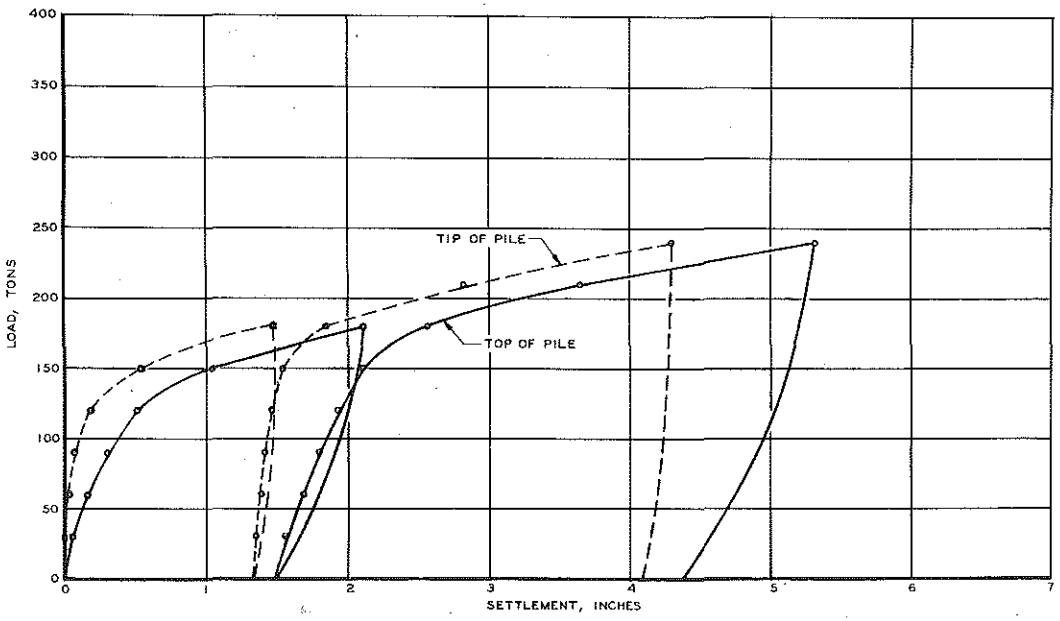

Figure 106. Repetitive loading cycles for a typical pile load test.

addition, at Belleville, the open-end pipe pile underwent six loading cycles, the first cycle immediately following driving and the five other tests at selected time intervals, the last being completed 1224 hr or 51 days later (Fig. 107). At Detroit, the open-end pipe pile had four loading cycles, the first performed immediately after driving and the last 300 hr later (Fig. 113). At Muskegon, one closed-end pipe pile had three successive loading cycles (Fig. 118). In every case where a tell-tale rod was installed, it was checked for free movement at the completion of each load test to assure accurate tip measurement.

Treatment of Test Data

The pile load test data furnished information for plotting of the following four graphs as shown in Figs. 107 to 125:

Repetitive loading
Load-settlement
Yield-value
Time-settlement

The Repetitive Loading Graph shows the combined series of load-settlement curves for settlement as measured at the top of each pile. In addition, tip (bottom) settlement is shown for all closed-end piles where tell-tale rods were installed.

The Load-Settlement Graph shows loading and unloading (rebound) curves for each loading cycle. Elastic behavior of the pile and soil system is normally indicated in the lower portion of the loading curve, which shows a uniform (straight-line) relationship between load and settlement. When the load exceeds the elastic limit, settlement increases more rapidly with small increases of load. The elastic limit is defined as the load carried at a settlement equal to the measured rebound or elastic deformation.

The Yield-Value Graph is a plot of the terminal rate of settlement for the last 30 min of each time interval versus the applied increment loads. The intersection of the best straight line through the points showing elastic behavior (settlement approaching equilibrium), with the best straight line through points showing progressive settlements, is defined as the true yield value of the pile for cohesive soils. The corresponding load ordinate on a similar graph of a pile test in cohesionless soils, is identified as the equivalent yield value. Thus, the yield value is the load at which progressive settlement begins, as determined by extrapolation of the rates of settlement for each load increment.

When test data were not adequate to establish a well-defined line representing progressive settlement, the method of determining load capacities from the yield-value graph in conjunction with the time settlement graph was as follows:

a. The Minimum Yield Value (cohesive soil) or Minimum Failure Load (cohesionless soil) is the highest load increment plotted on the steep straight line through the points in the range of elastic behavior.

b. Maximum Yield Value (cohesive soil) or Maximum Failure Load (cohesionless soil) is the next succeeding load increment above the minimum yield value or minimum failure load. This load usually results in or precedes complete failure, or progressive settlement beyond the range of the testing equipment.

c. Estimated Yield Value (cohesive soil) or Estimated Failure Load (cohesionless soil) is the average of the minimum yield value or minimum failure load and the maximum yield value or maximum failure load, respectively.

The Time-Settlement Graph is a plot of a family of curves showing the pile settlement during each 60-min time interval for successive increments of load for each loading cycle. For initial loads, within the elastic range, the terminal slope of the curves is almost horizontal, indicating static equilibrium. As loads exceed the limit of static equilibrium, the incremental time-settlement curves show a significant increase in terminal rate of settlement. A high rate of terminal settlement indicates that the pile is in progressive settlement.

Belleville Load Test Results (stiff-to-firm cohesive subsoils)

Table 21 includes pile characteristics, driving and load test information, and static load capacities for LTP's 1 through 6. Pile capacities are given in terms of "true" yield value and elastic limit. In cases where data were insufficient to establish "true" yield value, "minimum" and "estimated" yield values capacities are given.

LTP 1 was an open-end 12-in. pipe pile, supported by friction or side shear, tested as shown in Fig. 107 in six successive loading cycles. Maximum applied loads at various time periods after driving varied from 55 to 105 tons with a total settlement of 14.32 in. at the top of the pile.

TABLE 21
BELLEVILLE PILE LOAD TESTS

Pile	Hammer (Mfr's Rated Energy)	Final Driving Resistance, blows	Net Driving Time, min	Pile Type	Embedded Length and Tip Elevation, ft	Date Driving Completed	Date Load Test Started	Load Cycle No.	Time, hr[(a)]	Soil Plug Length Before Loading, ft	Maximum Test Load Applied, tons	Total Net Accumulated Pile Settlement, in.	Pile Load Capacity			
													Yield Value, tons			Elastic Limit, tons
													True	Minimum	Estimated	
LTP 1	Vulcan No. 1 (15,000 ft-lb)	11 (last 1 in.)	-----	12-in. OD pipe (.25-in. wall) driven open-end	44.4 607.0	12-5-61	12-5-61	1	4.1	3.1	55	3.4	37	--	--	34
							12-7-61	2	43.5	3.1	70	6.6	--	50	55	44
							12-9-61	3	101.3	3.1	80	9.7	--	60	65	56
							12-18-61	4	305.0	4.3	96	11.6	79	--	--	68
							12-18-61	5	316.0	4.3	90	12.4	--	80	85	78
							1-25-62	6	1228.8	4.3	105	14.3	--	80	90	79
LTP 2	Raymond 15-M (15,000 ft-lb)	36 (last 1 in.)	47.5	Step-taper shell 9-in. diam. with 1-in. step each 8 ft	67.1* 584.3	11-30-61	1-16-62	1	----	---	285	1.8	237	--	--	200
								2**	----	---	330	3.6	265	--	--	275
LTP 3	McKiernan-Terry DE-30 (16,800 ft-lb mean 22,400 ft-lb max)	29 (last 1/2 in.)	71.5	Fluted-tapered 12-in. ND pipe #7 gage wall (.179 in.)	60.9* 590.5	11-30-61	1-18-62	1	----	---	195	1.6	---	150	165	160
								2**	----	---	210	3.3	171	---	---	169
LTP 4	Link-Belt 312 (up to 18,000 ft-lb)	30 (last 1/2 in.)	40.0	12-in. OD pipe (.25-in. wall)	66.5* 584.9	12-1-61	1-19-62	1	----	---	360	0.3	---	330	345	318
								2**	----	---	390	0.5	345	---	---	352
LTP 5	Delmag D-12 (22,600 ft-lb)	34 (last 1 in.)	70.0	12-in. OD pipe #7 gage wall (.179-in.)	66.7* 584.7	11-27-61	1-22-62	1	----	---	360	0.3	---	320	340	310
								2**	----	---	400	1.0	346	---	---	345
LTP 6	Vulcan No. 1 (15,000 ft-lb)	49 (last 1 in.)	40.0	12 by 12 in. H-section	58.0 593.4	12-4-61	1-24-62	1	----	---	225	1.6	200	---	---	183
								2**	----	---	240	3.2	206	---	---	202

(a) Hours from completion of driving to start of load cycle.
* Pre-excavated 10 ft before driving.
** No time lapse between load cycles.

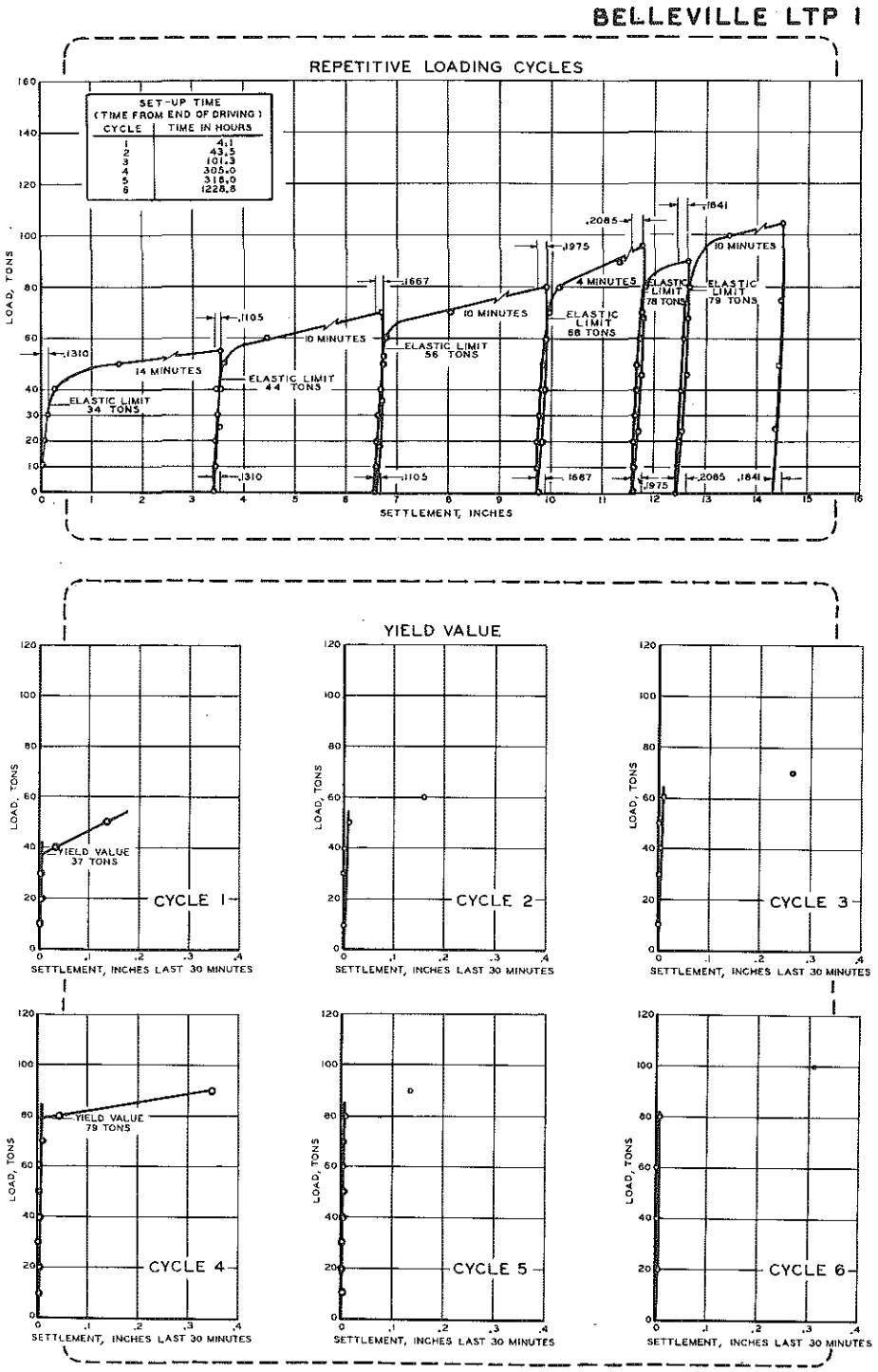

Figure 107. Load test results for Belleville LTP 1.

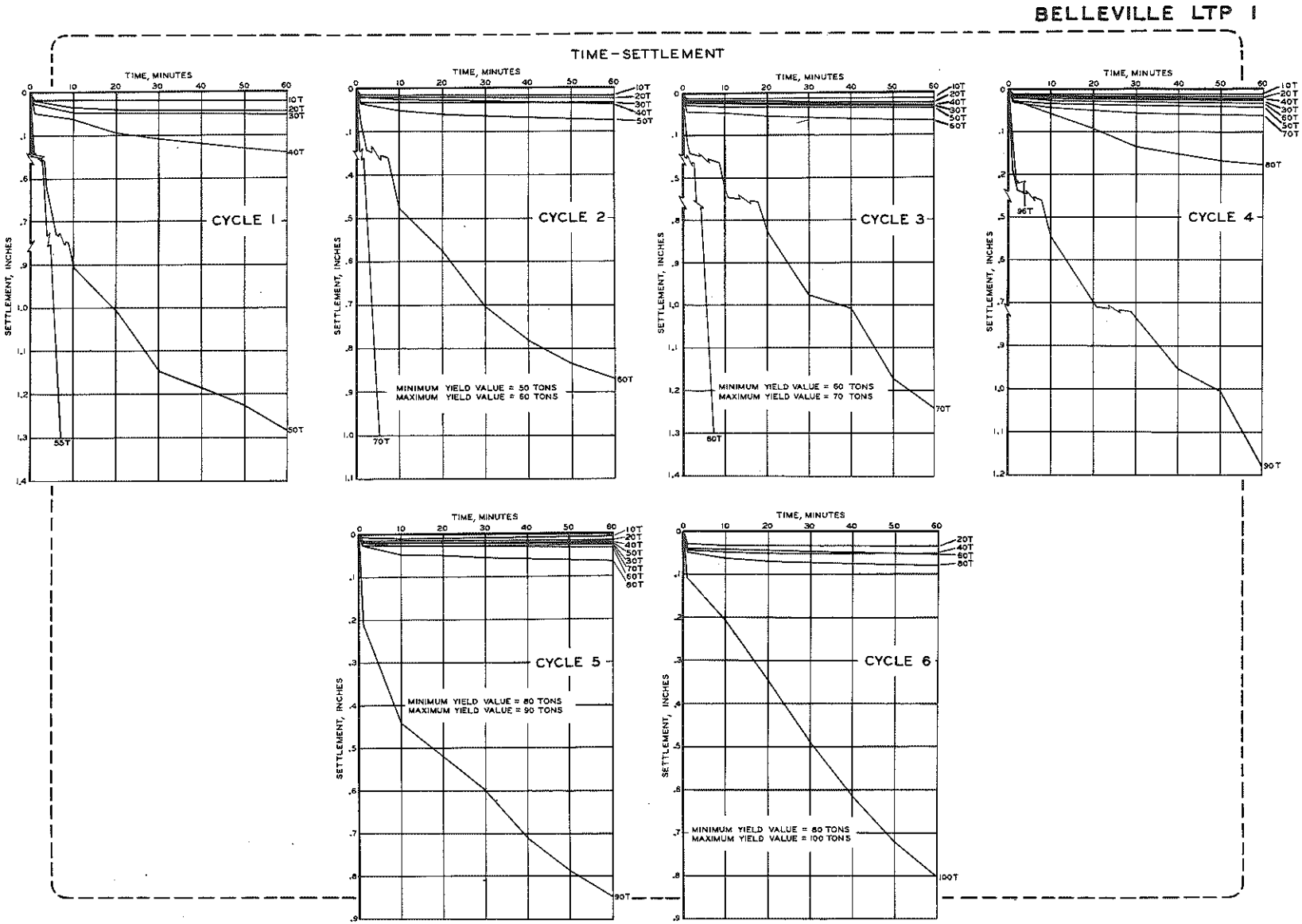

Figure 107 (cont.). Load test results for Belleville LTP 1.

LTP 2 was a step-taper shell, pre-excavated 10 ft and driven the greatest depth into hard till clay or "hardpan" (estimated tip penetration of 2.1 ft). The repetitive loading curve in Fig. 108 shows second-cycle tip settlement of about 0.27 in., while the top of pile moved 1.80 in., indicating a pile shortening of 1.54 in. under a load of 330 tons. Tip measurement was not completed in the first cycle because of a gage malfunction above the applied load of 240 tons.

LTP 3 was a fluted-tapered pile, pre-excavated 10 ft, driven through the upper firm-stiff clay and stopping in the 14-ft zone of sand and silt without reaching hardpan, where it developed a maximum load of 210 tons. The repetitive loading cycle graph (Fig. 109) shows that in the first cycle the pile tip moved in a pattern similar to its top. Tip measurement was lost in the second cycle because of malfunctioning of the settlement gage.

LTP 4 was a closed-end 12-in. pipe, pre-excavated 10 ft and driven to an estimated tip penetration of 1 ft into hardpan. Fig. 110 shows that pile behavior was almost identical during the first and second loading cycles at a maximum applied load of 390 tons. Total set at the pile top and tip at the ends of the two loading cycles was 0.53 in. and 0.43 in., respectively, indicating a permanent 0.10-in. shortening of the pile.

LTP 5 was a closed-end 12-in. pipe, pre-excavated 10 ft and driven to an estimated tip penetration of 1.2 ft into hardpan. Graphs of pile behavior (Fig. 111) are similar to those for LTP 4. The maximum applied load was increased to 400 tons in the second cycle and resulted in increased tip penetration of 0.67 in., in addition to the first cycle tip penetration of 0.23 in.

LTP 6 was an H-pile driven through the upper firm-stiff clay, penetrating an estimated 9 ft into the silt and very fine sand. The tip did not reach the hardpan. The two cycles of loading produced almost identical load-settlement curves (Fig. 112) with maximum test loads of 225 and 240 tons causing progressive settlement. Extra steel plates were welded to the pile top flanges to aid in distribution of concentrated stresses.

Detroit Load Test Results (soft cohesive subsoils)

Table 22 presents pile load test results for LTP's 1, 2, 7, 8, and 10.

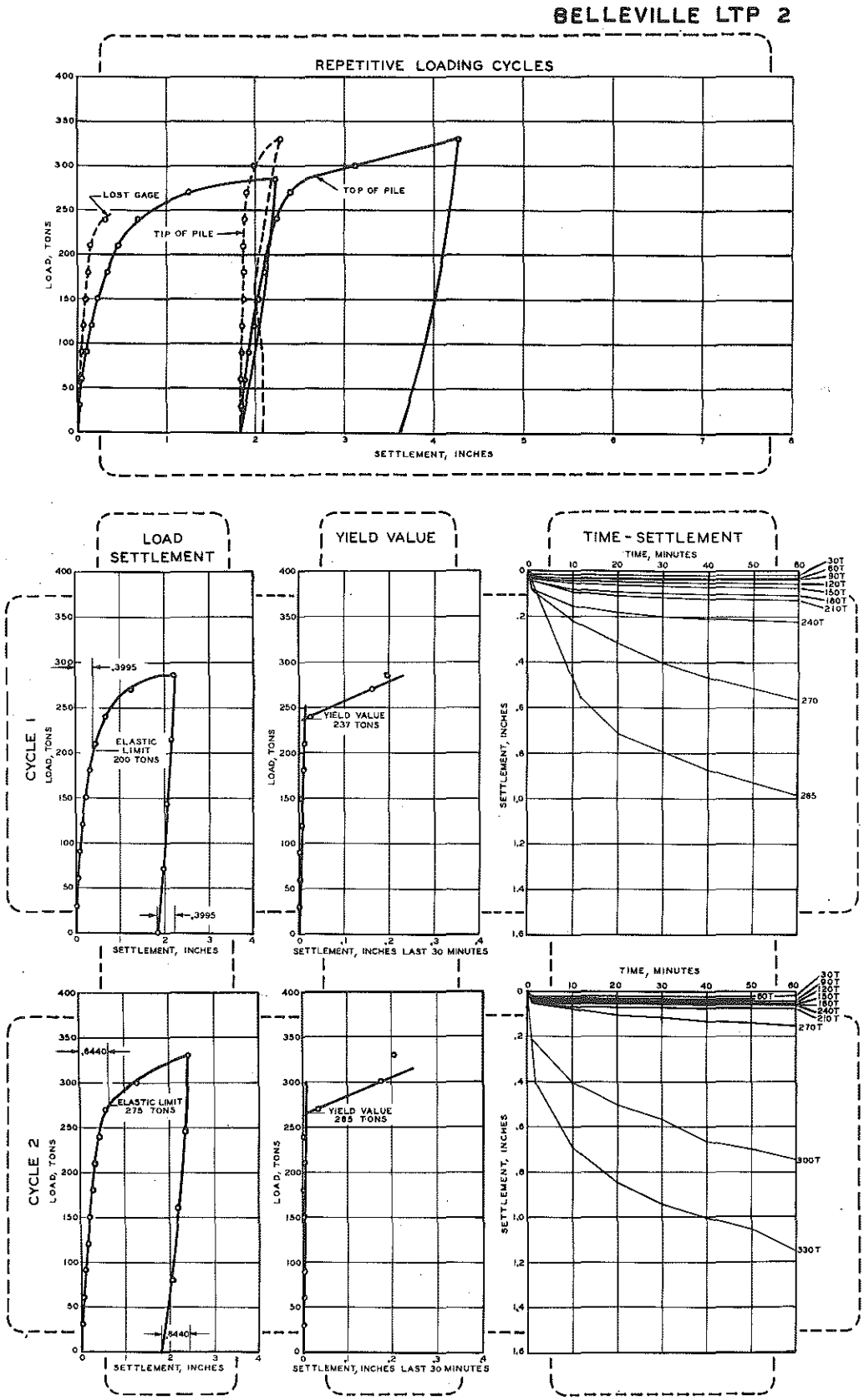

Figure 108. Load test results for Belleville LTP 2.

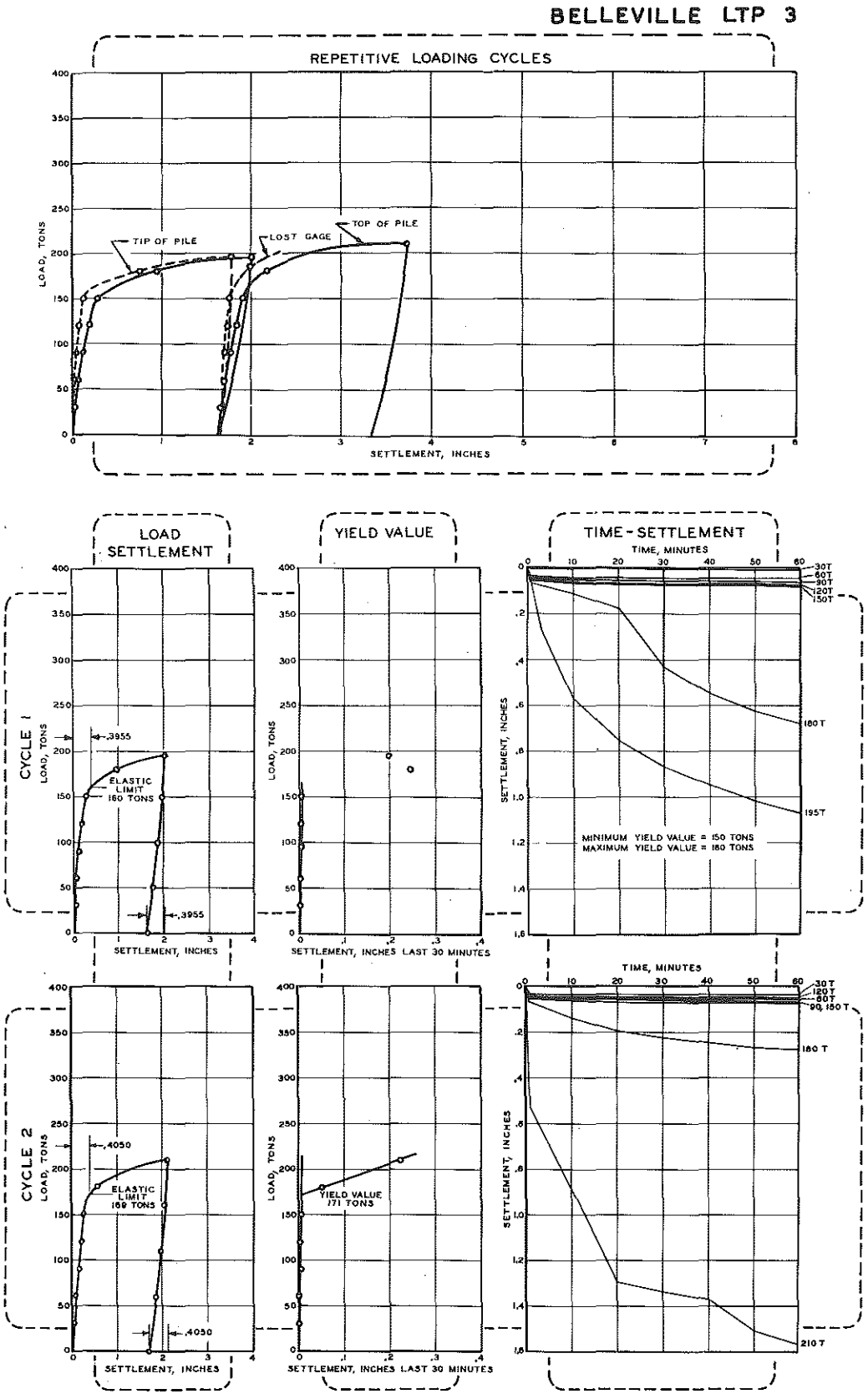

Figure 109. Load test results for Belleville LTP 3.

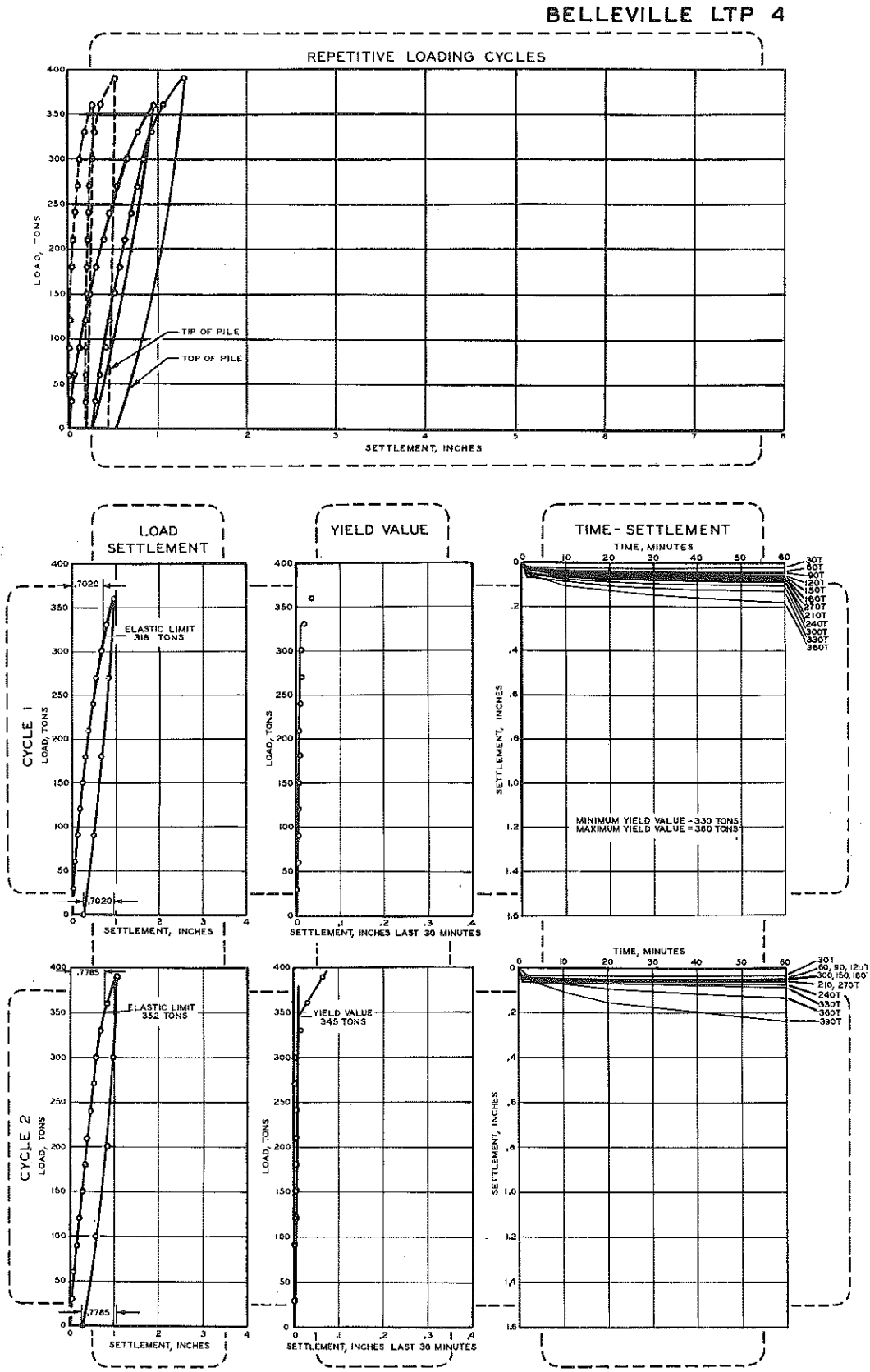

Figure 110. Load test results for Belleville LTP 4.

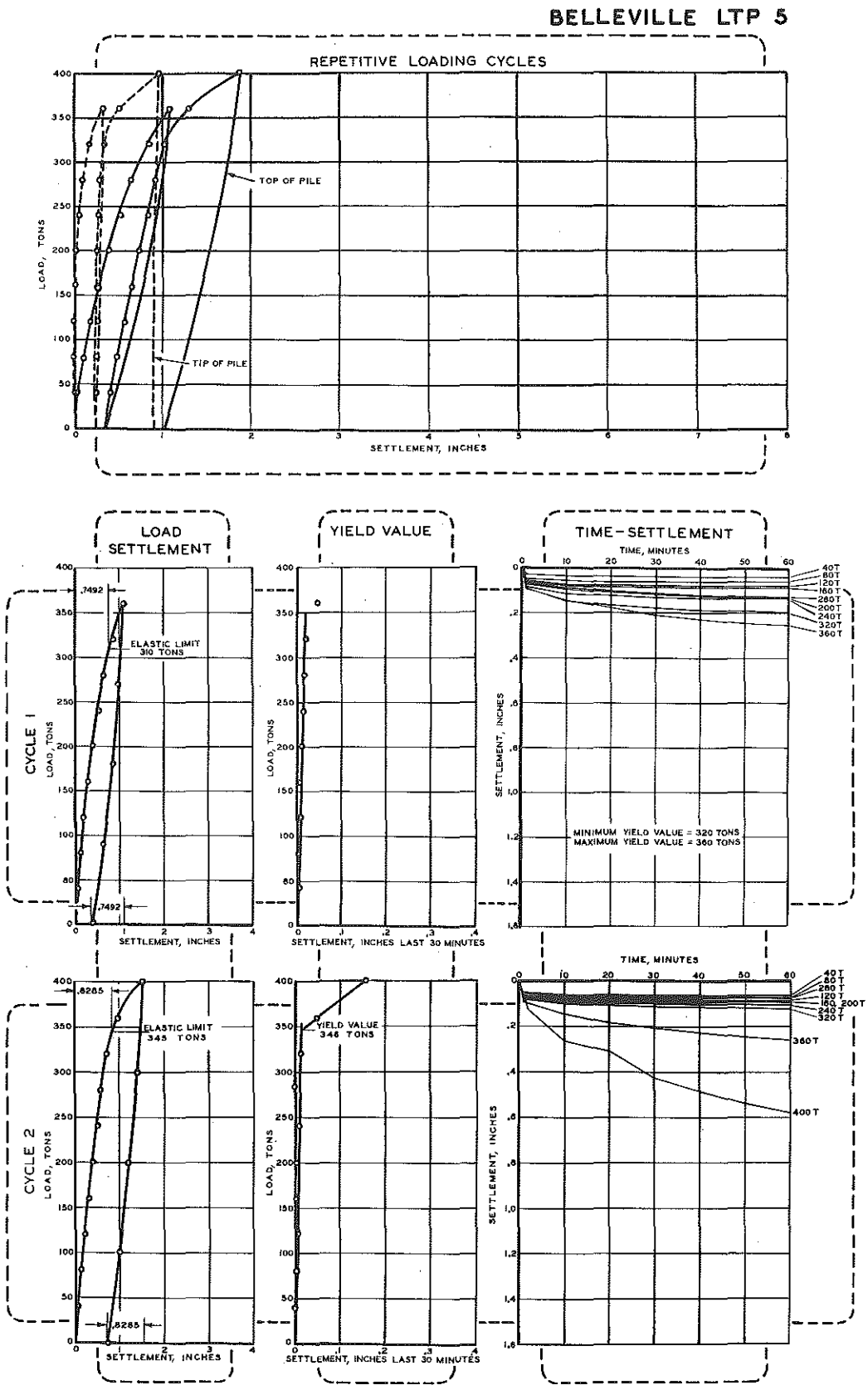

Figure 111. Load test results for Belleville LTP 5.

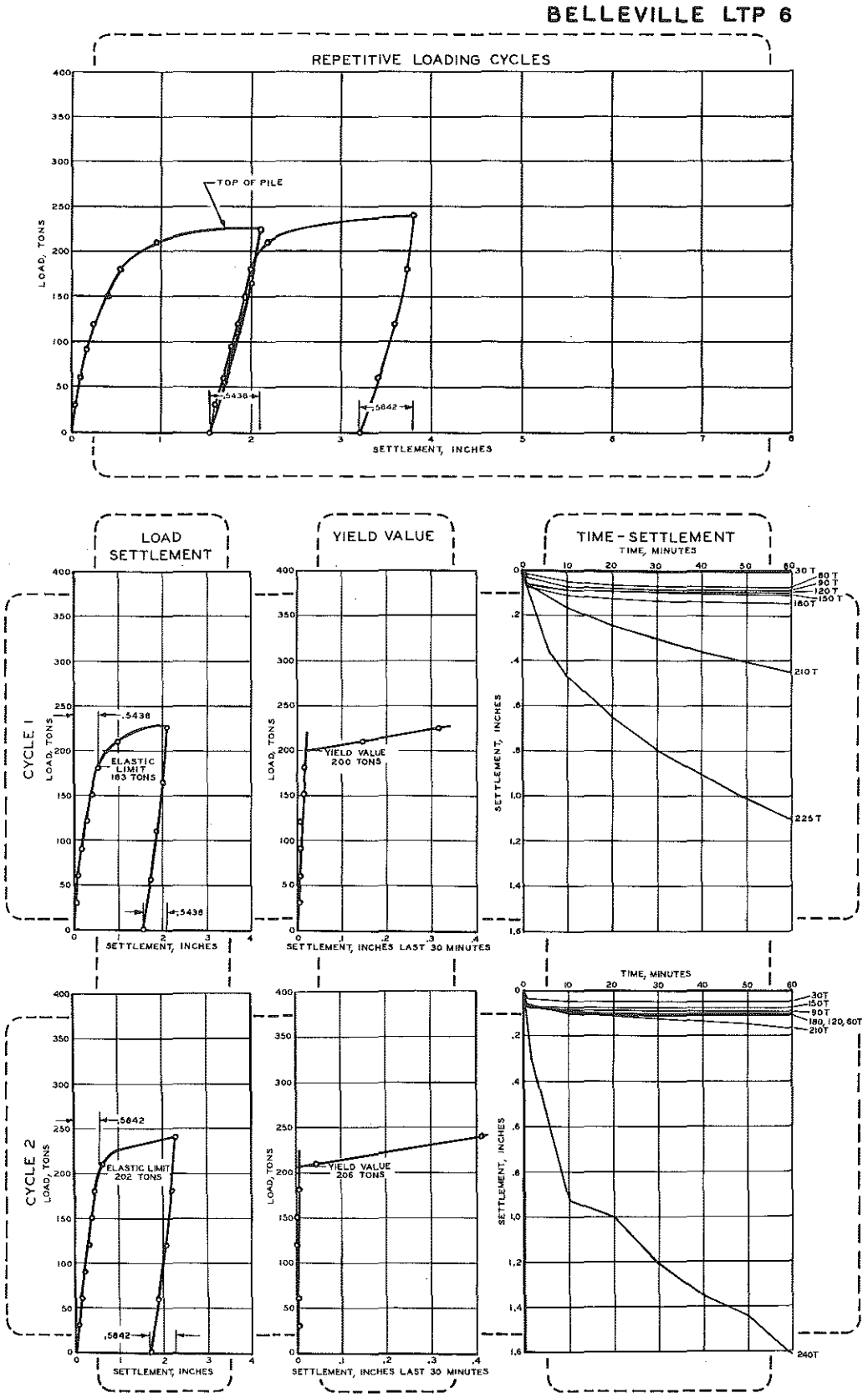

Figure 112. Load test results for Belleville LTP 6.

TABLE 22
DETROIT PILE LOAD TESTS

Pile	Hammer (Mfr's Rated Energy)	Final Driving Resistance, blows	Net Driving Time, min	Pile Type	Embedded Length and Tip Elevation, ft	Date Driving Completed	Date Load Test Started	Load Cycle No.	Time, hr[a]	Soil Plug Length Before Loading, ft	Maximum Test Load Applied, tons	Total Net Accumulated Pile Settlement, in.	Pile Load Capacity			
													Yield Value, tons			Elastic Limit, tons
													True	Minimum	Estimated	
LTP 1	Vulcan No. 1 (15,000 ft-lb)	11 (last 6 in.)	--	12-in. OD pipe, #7 gage wall (.179-in.) driven open end	69.5 519.9	12-21-61	12-21-61	1	3.7	33.7	22	3.5	---	15	17.5	14.5
							12-23-61	2	46.6	33.7	24	5.5	---	20	22.0	19.5
							12-26-61	3	119.0	33.7	28	9.2	---	20	22.0	20.0
							1-2-62	4	286.8	33.7	32	10.7	---	28	30.0	----
LTP 2	Vulcan No. 1 (15,000 ft-lb)	36 (last 1 in.)	18	12-in. OD pipe #7 gage wall (.179-in.)	78.6 510.8	12-20-61	12-28-61	1	----	----	180	1.5	113	---	----	130
								2*	----	----	240	4.4	165	---	----	172
LTP 7	McKiernan-Terry DE-30 (16,800 ft-lb mean 22,400 ft-lb max)	30 (last 1 in.)	18	Fluted-tapered 12-in. ND pipe #7 gage wall (.179-in.)	81.1 508.3	12-13-61	1-4-62	1	----	----	180	3.2	148	---	----	141
								2*	----	----	190	5.6	159	---	----	155
LTP 8	Vulcan No. 1 (15,000 ft-lb)	37 (last 1 in.)	20	12- by 12-in. H-section	81.1 508.3	12-20-61	1-3-62	1	----	----	220	2.2	---	160	180	163
								2*	----	----	200	2.7	---	160	180	180
LTP 10	Link-Belt 312 (up to 18,000 ft-lb)	20 (last 1 in.)	10**	12-in. OD pipe (.23-in. wall)	81.0 508.4	12-11-61	1-2-62	1	----	----	240	2.1	194	---	----	171
								2*	----	----	270	5.6	225	---	----	208

(a) Hours from completion of driving to start of load cycle.
* No time lapse between load cycles.
** Recorded only from 41 ft 7 in. to 81 ft 1 in. penetration.

LTP 1 was an open-end 12-in. pipe driven as a friction or shear pile, (Fig. 113), load tested at four successive time periods following driving in deep soft clay. Note that non-uniform loading increments were used during the fourth cycle, which came from misinterpretation of the hydraulic pump gage readings. This resulted in load applications of 2 tons for the first six intervals, 8 tons for the seventh interval, and 4 tons for the last three time intervals to the maximum test load applied. This differs from the uniform loads of 5 and 4 tons used in the first three cycles. The fourth cycle rebound measurement was 0.075 in., considerably less than for the second and third cycles. This value was considered unsatisfactory for determination of the elastic limit due to an accidental disturbance of the measuring equipment (as recorded in the field notes). The pile settled a total of 10.72 in. during the test.

LTP 2 was a closed-end 12-in. pipe, driven through the deep soft clay deposit to an estimated tip penetration of 0.3 ft into Detroit hardpan. Pile tip settlement shown in Fig. 114 followed pile top movement during the entire loading period. Because of the weak upper soil, most of the pile support was obtained from point bearing in the Detroit hardpan. Loading the pile into the range of progressive settlement caused an additional pile tip penetration of 4.09 in. into hardpan, with a simultaneous sharp increase in capacity. This is reflected in the "true" yield values which increased from 113 to 165 tons from the first to the second cycle.

LTP 7 was a closed-end 12-in. fluted-tapered pile, driven through the deep soft clay to an estimated tip penetration of 1.9 ft into Detroit hardpan. Boring No. 3 soil analysis (closest to this pile) suggests that the tip may have been on top of a compact sand-gravel lens with a standard penetration resistance $\underline{N}$ of 44. During the load test (Fig. 115) tip settlement followed pile top settlement, and maximum applied loads of 180 and 190 tons caused progressive pile settlement, but in this case additional tip penetration of 5.53 in. produced only a small increase in capacity.

LTP 8 was an H-pile driven through the deep soft clay deposit to an estimated tip penetration of 2.3 ft into Detroit hardpan. Although the pile top moved nearly 3 in. in the first cycle (Fig. 116) no significant increase in load support is indicated by the second loading cycle time-settlement curve. In the first cycle, after application of 200 tons the flange bulged slightly and the pile developed a slight twist, resulting in an eccentric load effect which left 1/8-in. clearance at one corner of the pile top. The next load increment of 20 tons was applied only 10 min. and then released because of continued structural damage. The second cycle was carried to only 200 tons, without further structural damage to the pile being evident.

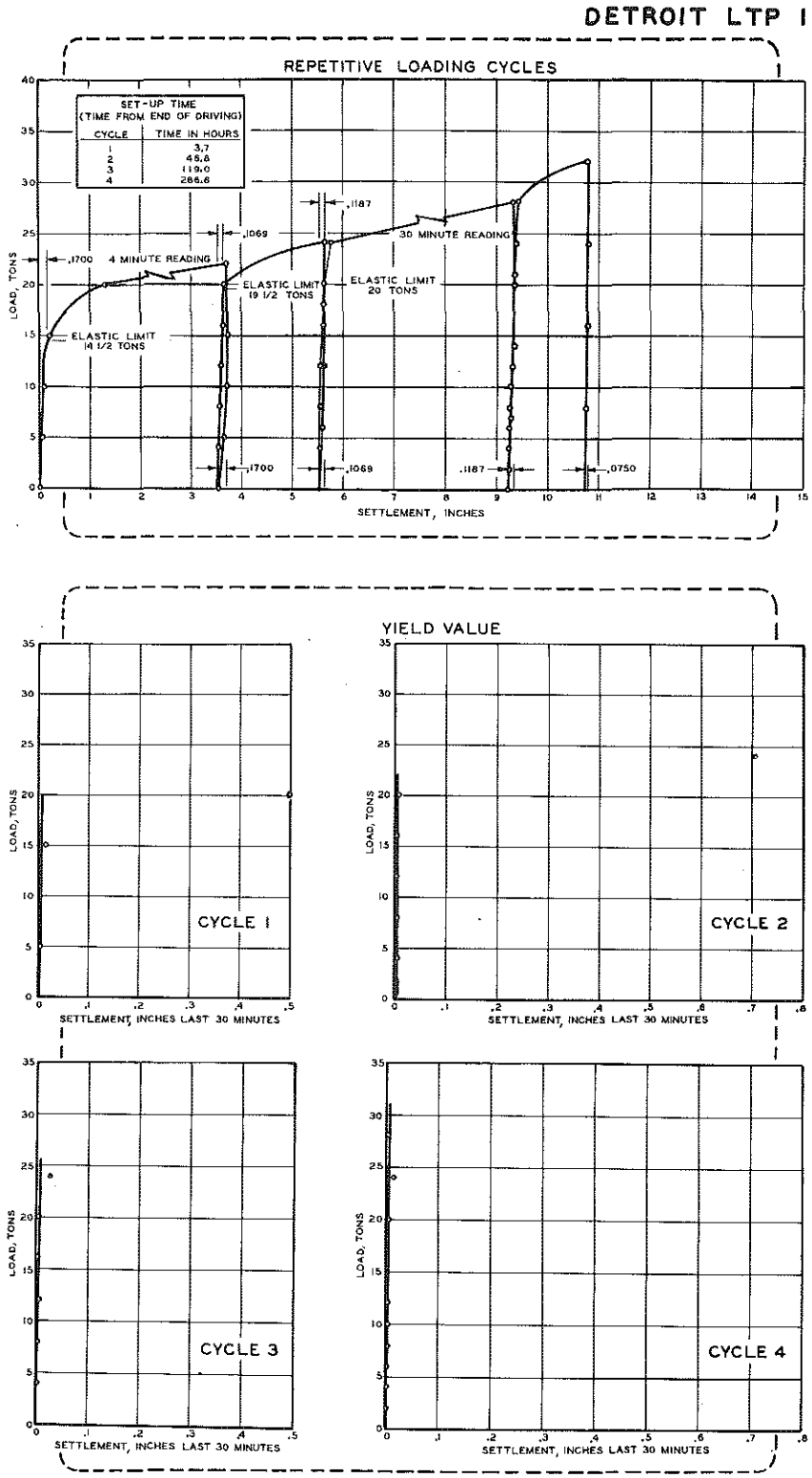

Figure 113. Load test results for Detroit LTP 1.

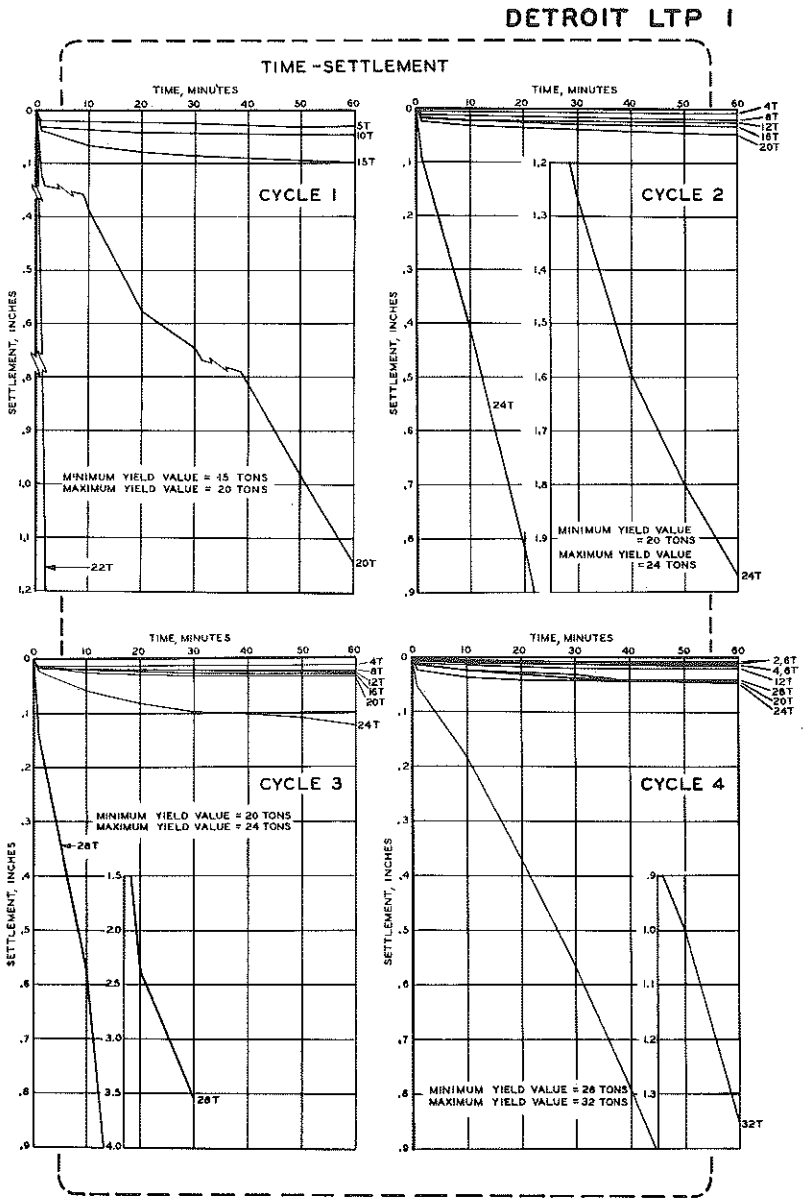

Figure 113 (cont.). Load test results for Detroit LTP 1.

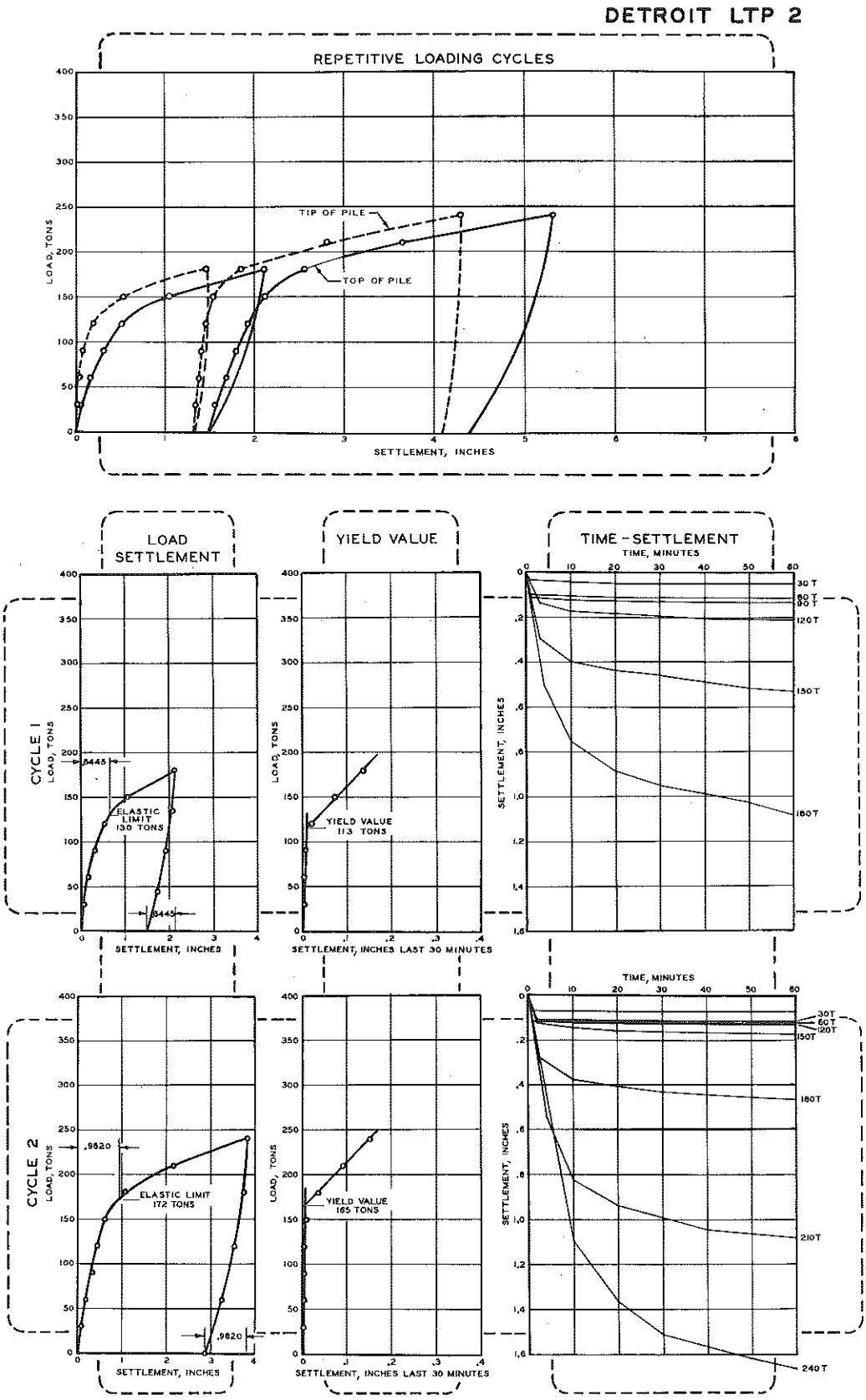

Figure 114. Load test results for Detroit LTP 2.

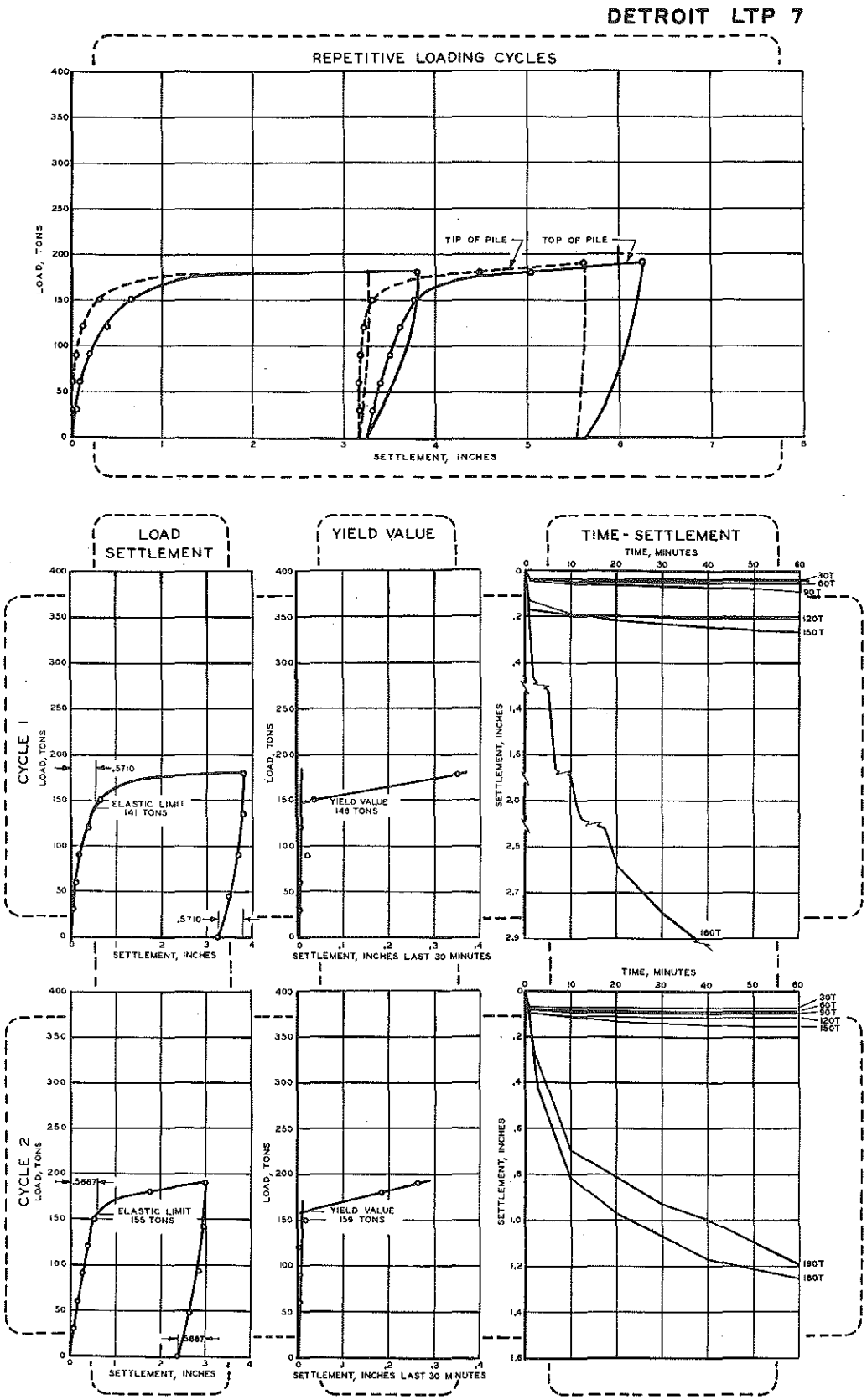

Figure 115. Load test results for Detroit LTP 7.

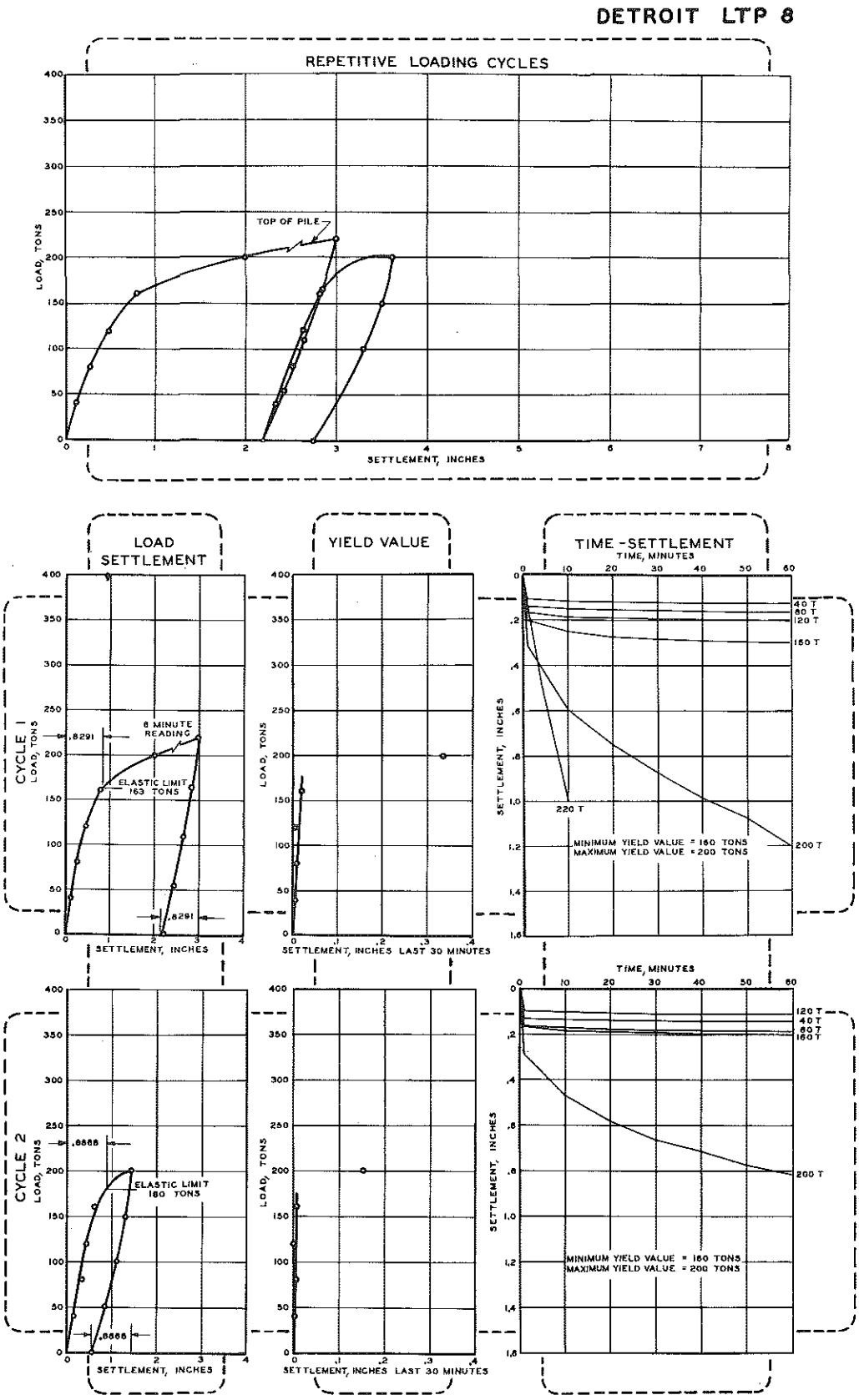

Figure 116. Load test results for Detroit LTP 8.

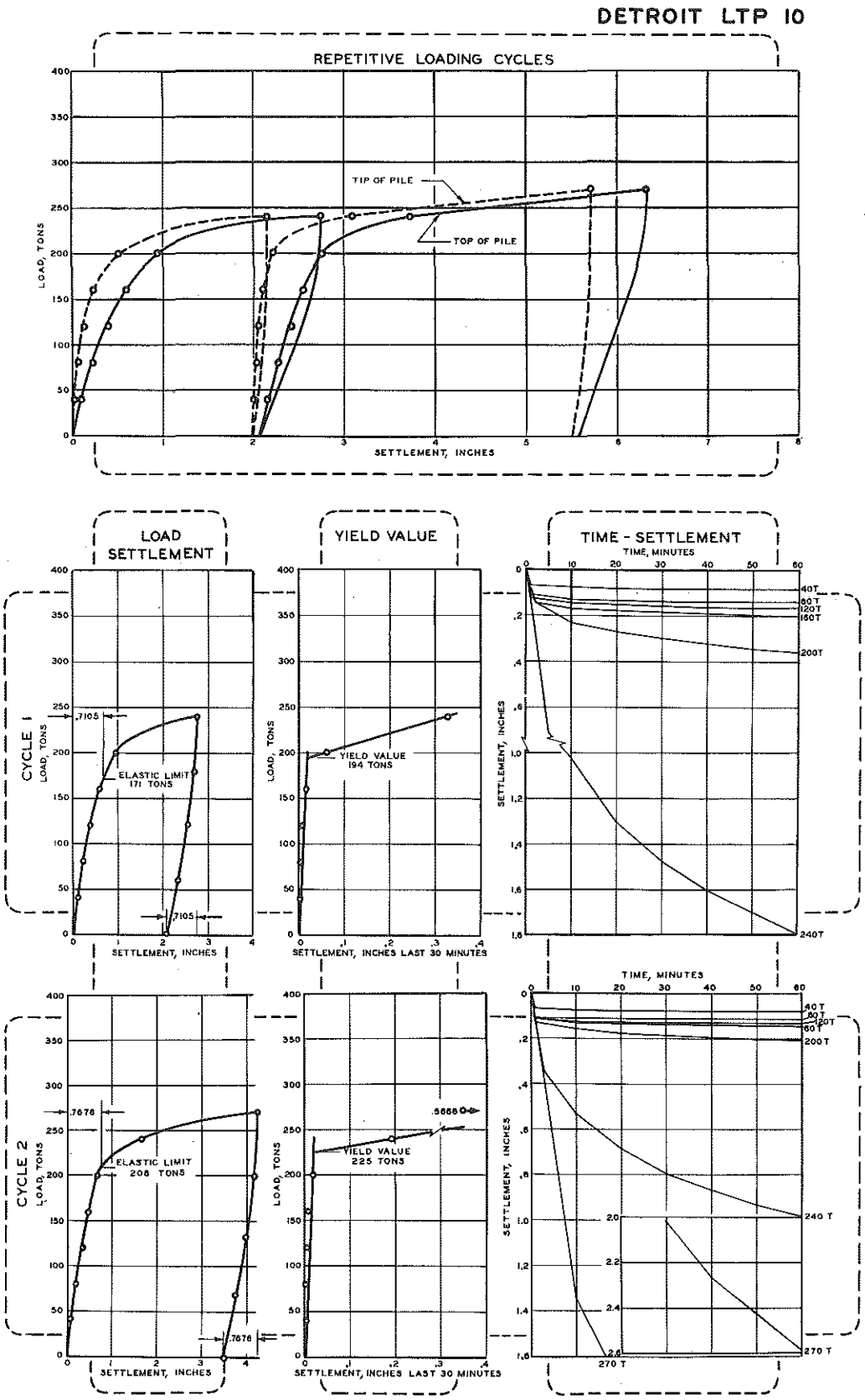

Figure 117. Load test results for Detroit LTP 10.

LTP 10 was a closed-end 12-in. pipe, driven through the deep soft clay to an estimated tip penetration of 2.5 ft into Detroit hardpan. Fig. 117 shows that during the load tests, tip settlement followed top settlement closely during each loading cycle. The maximum loads of 240 and 270 tons in the first and second loading cycles caused increases in tip penetration into hardpan of 2.07 in. and 3.51 in., respectively (total tip penetration 5.58 in.). Additional tip settlement of 3.51 in. between the first and second loading cycles was accompanied by an increase in "true" yield value of 31 tons (from 194 to 225 tons). Although LTP's 7, 8, and 10 were comparable in tip elevations they differed in pile driving resistance as measured by blow count. However, it should be noted that these piles were of different types, driven with different hammers.

Muskegon Load Test Results (granular subsoils)

Table 23 summarizes test data for the following eight load test piles: LTP's 2, 3, 4, and 5 driven to 58 ft; LTP's 6 and 9 driven to 128 ft; and LTP's 7 and 8 driven to 178 ft. Pile load capacities are given in terms of "equivalent" yield value and elastic limit for each loading cycle, except where insufficient data were available to establish these capacities. For loading cycles where it was impossible to determine "equivalent" yield value, the elastic limit is supplemented by "minimum" and "estimated" failure loads. Pile settlement in the cohesionless soil was observed to be a series of small sharp movements, suggesting a build-up of resistance and sudden adjustment, frequently observed in loading granular materials.

LTP 2 was a closed-end 12-in. pipe, driven through 58 ft of loose sand. In each loading cycle, tip movement corresponded closely to that of the pile top, with marked progressive settlement occurring during the 120-ton load increment of the third loading cycle (Fig. 118). The pile tip moved 1.57, 0.58, and 1.71 in. in the three successive cycles.

LTP 3 was a closed-end fluted-tapered pile driven 57.8 ft in loose sand. Test results shown in Fig. 119 indicate that the 20-ton load increments applied during the first loading cycle were excessive and the third load application produced progressive settlement. Consequently, load increments in the second cycle were reduced to 10 tons, providing five settlement points in the elastic range and two points in the progressive settlement range. Pile tip and pile top settlements were parallel, both showing only negligible elastic rebound after a maximum applied load of 70 tons.

TABLE 23
MUSKEGON PILE LOAD TESTS

Pile	Hammer (Mfr's Rated Energy)	Final Driving Resistance, blows	Net Driving Time, min	Pile Type	Embedded Length and Tip Elevation, ft	Date Driving Completed	Date Load Test Started	Load Cycle No. (a)	Maximum Test Load Applied, tons	Total Net Accumulated Pile Settlement, in.	Pile Load Capacity			
											Equivalent Yield Value, tons	Minimum Failure Load, tons	Estimated Failure Load, tons	Elastic Limit, tons
LTP 2	Vulcan No. 1 (15,000 ft-lb)	8 (last 1 in.)	40.0	12-in. OD pipe (.23-in. wall)	58.0 530.0	2-15-62	3-13-62	1 2 3	110 110 120	1.5 2.0 3.7	--- --- ---	60 100 100	70 105 110	70 90 88
LTP 3	Vulcan No. 1 (15,000 ft-lb)	2 (last 1/2 in.)	16.8	Fluted-tapered 12-in. ND pipe #7 gage wall (.179 in.)	57.8 530.2	2-16-62	3-14-62	1 2	60 70	1.3 3.7	--- 55	40 ---	50 ---	40 50
LTP 4*	Vulcan No. 1 (15,000 ft-lb)	13 (last 6 in.)	10.5	12-in. OD pipe (.23-in. wall)	58.0 530.0	2-20-62	3-15-62	1 2	50 55	2.3 7.4	--- 42.5	30 ---	35 ---	32 43
LTP 5	Raymond 15-M (15,000 ft-lb)	36 (last 6 in.)	19.5	Step-taper shell 9-in. diam. with 1-in. step each 8 ft	58.0 530.0	2-22-62	3-16-62	1 2	120 120	2.3 3.5	--- ---	80 100	90 110	76 96
LTP 6	Delmag D-22 (39,800 ft-lb)	3 (last 1 in.)	28.3	12-in. OD pipe (.25-in. wall)	128.0 460.0	3-1-62	3-19-62	1 2	290 300	3.0 5.1	270 273	--- ---	--- ---	220 246
LTP 7	Vulcan 80C (24,450 ft-lb)	213 (last 5 in.)	79.0	12-in. OD pipe (.25-in. wall)	178.4 409.6	2-23-62	3-20-62	1 2	370** 350**	0.4 0.5	--- ---	>370 >350	--- ---	320 340
LTP 8	Delmag D-22 (39,800 ft-lb)	64 (last 1 in.)	83.8	12-in. OD pipe (.25-in. wall)	178.2 409.9	3-2-62	3-21-62	1 2	370** 350**	0.5 0.5	--- ---	>370 >350	--- ---	312 ---
LTP 9	Vulcan 80C (24,450 ft-lb)	11 (last 2 in.)	21.8	12-in. OD pipe (.25-in. wall)	128.2 459.8	2-26-62	3-23-62	1 2	260 275	1.6 3.5	235 230	--- ---	--- ---	205 225

(a) No time lapse between cycles.
* Internally jetted; tested open-end with 1.4-ft soil plug.
** Limit of load reaction = 370 tons.

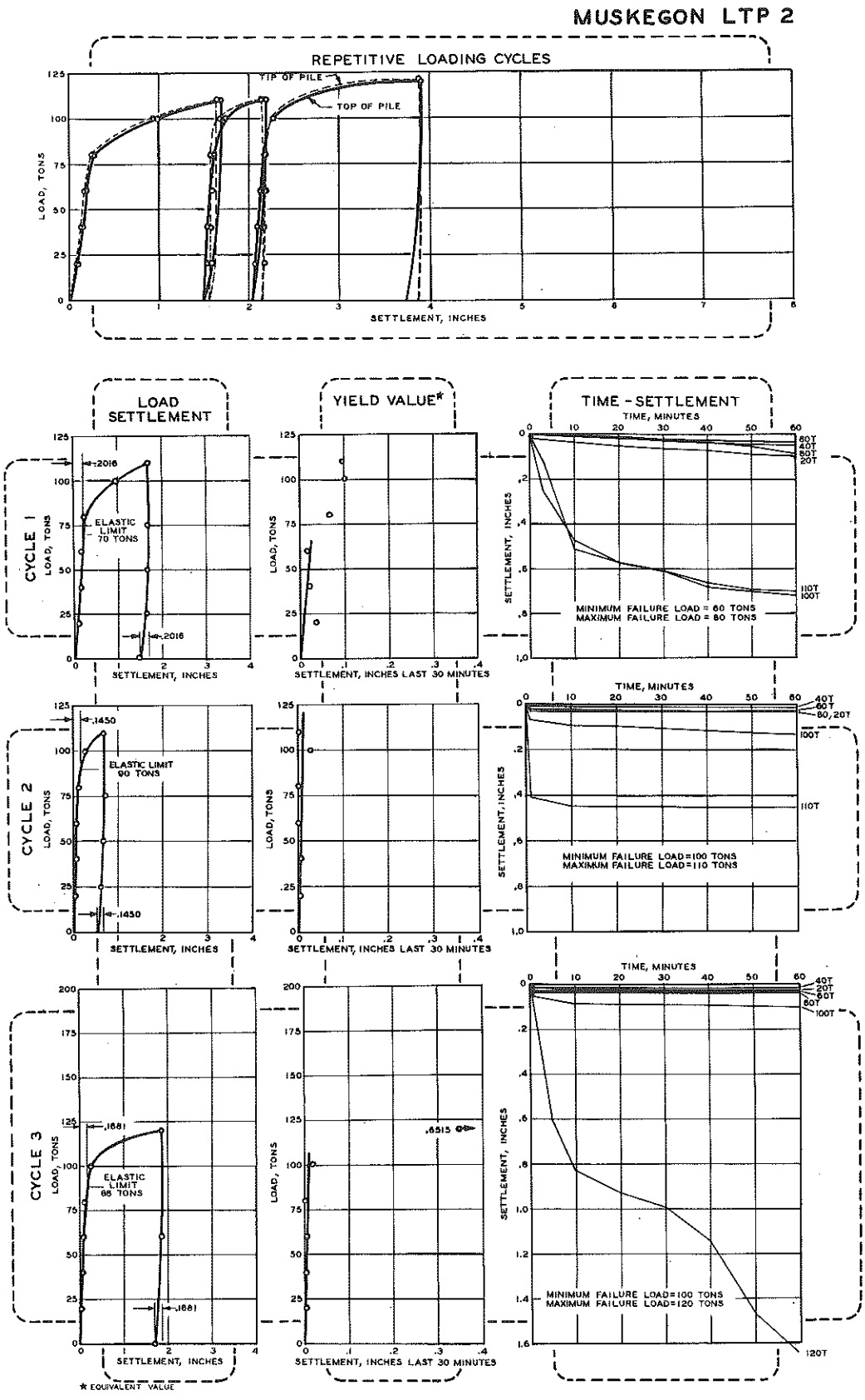

Figure 118. Load test results for Muskegon LTP 2.

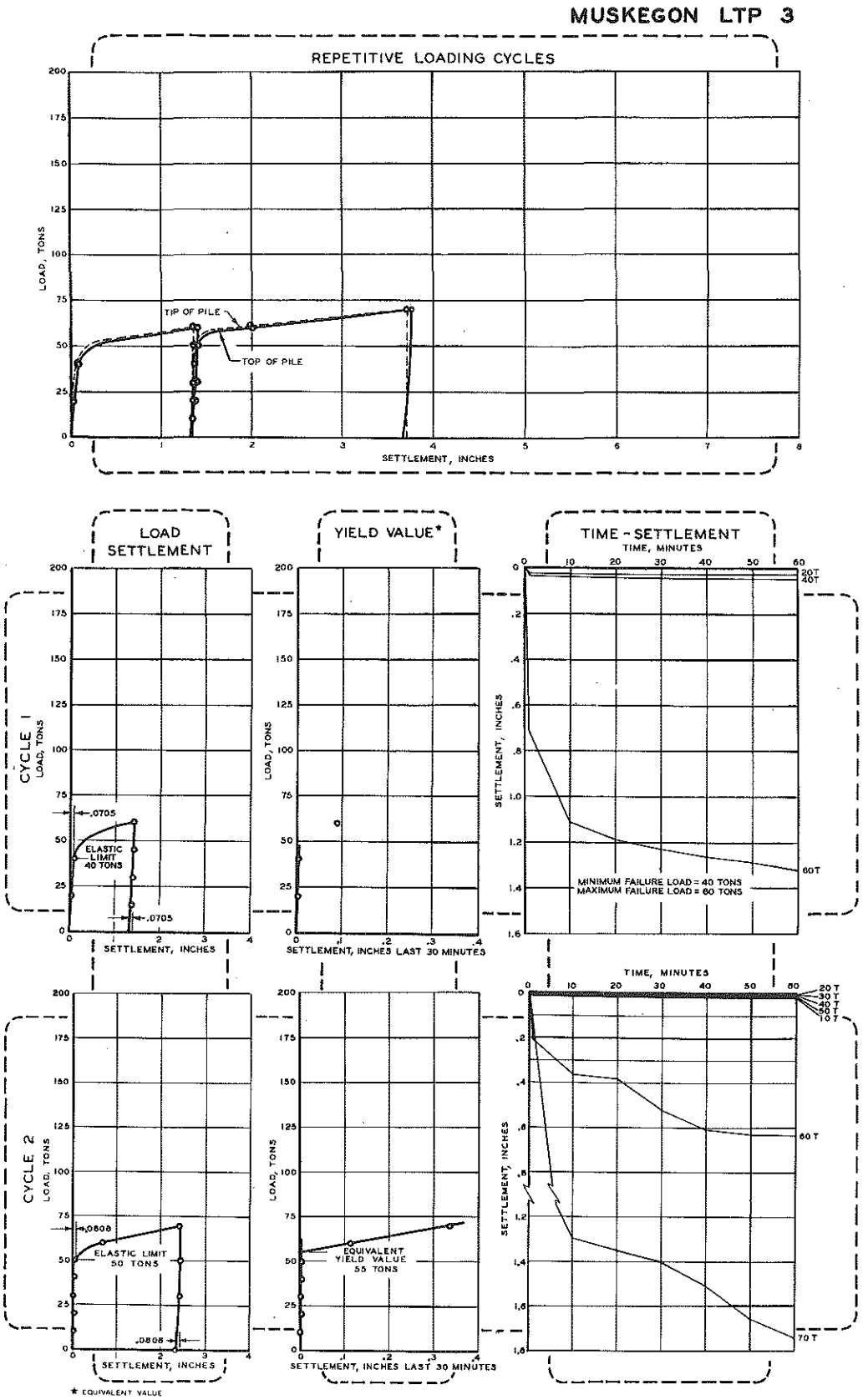

Figure 119. Load test results for Muskegon LTP 3.

LTP 4 was an open-end 12-in. pipe, internally jetted during driving in 58 ft of loose sand. When tested, the pile had a 1.4-ft soil plug and was full of water. In the first and second loading cycles (Fig. 120) the pile sustained a load of 40 tons without excessive settlement, but increased load in both cycles caused large settlements (total set of 7.42 in. after the second cycle).

LTP 5 was a step-taper shell, driven in 58 ft of loose sand. The time-settlement graphs (Fig. 121) show that 100-and 120-ton increments of the first loading cycle, and the 120-ton load increment of the second cycle, were sustained after large initial settlement, indicating re-adjustment of resistance within the cohesionless soil. The tip and top of the pile moved together through both loading cycles; elastic rebound of the top was 0.15 and 0.17 in., but only negligible elastic rebound was indicated at the tip.

LTP 6 was a closed-end 12-in. pipe driven 128 ft (elevation 460). At that elevation Muskegon Soil Borings 1 and 2 indicated standard penetration resistance $\underline{N}$ of 30 to 40 blows per foot. In both loading cycles, loads of over 240 tons were required to produce substantial tip settlements (Fig. 122).

LTP 9 was another closed-end 12-in. pipe, driven to 128.2 ft (elevation 559.8) with the same soil conditions as for LTP 6. In each load cycle (Fig. 125) only slight tip settlement was obtained up to 200 tons, but at 240 tons the pile tip began to move. At loads of 260 and 275 tons, pile compression reached 0.72 and 0.65 in., respectively, and the tip was in progressive settlement. Although the tip moved 1.52 in. between the first and second cycle, there was no significant change in capacity.

LTP 7 was a closed-end 12-in. pipe, driven to 178.4 ft (elevation 409.6). The tip penetrated an estimated 1.4 ft into a compact-to-very-compact sand layer. Soil borings indicated that this compact sand layer was very difficult to penetrate. The available test load of 370 tons was insufficient to determine elastic limit values, since that load was not enough to reach the range of progressive settlement (Fig. 123). Maximum tip settlements in the two loading cycles were 0.15 and 0.16 in., with a tip rebound in the first cycle of about 0.21 in. It may be noted that the 0.41-in. permanent settlement of the pile top in the first loading cycle was due to permanent compression or set in the pile rather than pile displacement. This was confirmed by the tell-tale measurement which showed negligible movement at the tip. In the second cycle of loading and unloading, set at the tip and top of the pile was only 0.04 and 0.05 in., respectively, confirming that the ultimate capacity of the pile had not been reached.

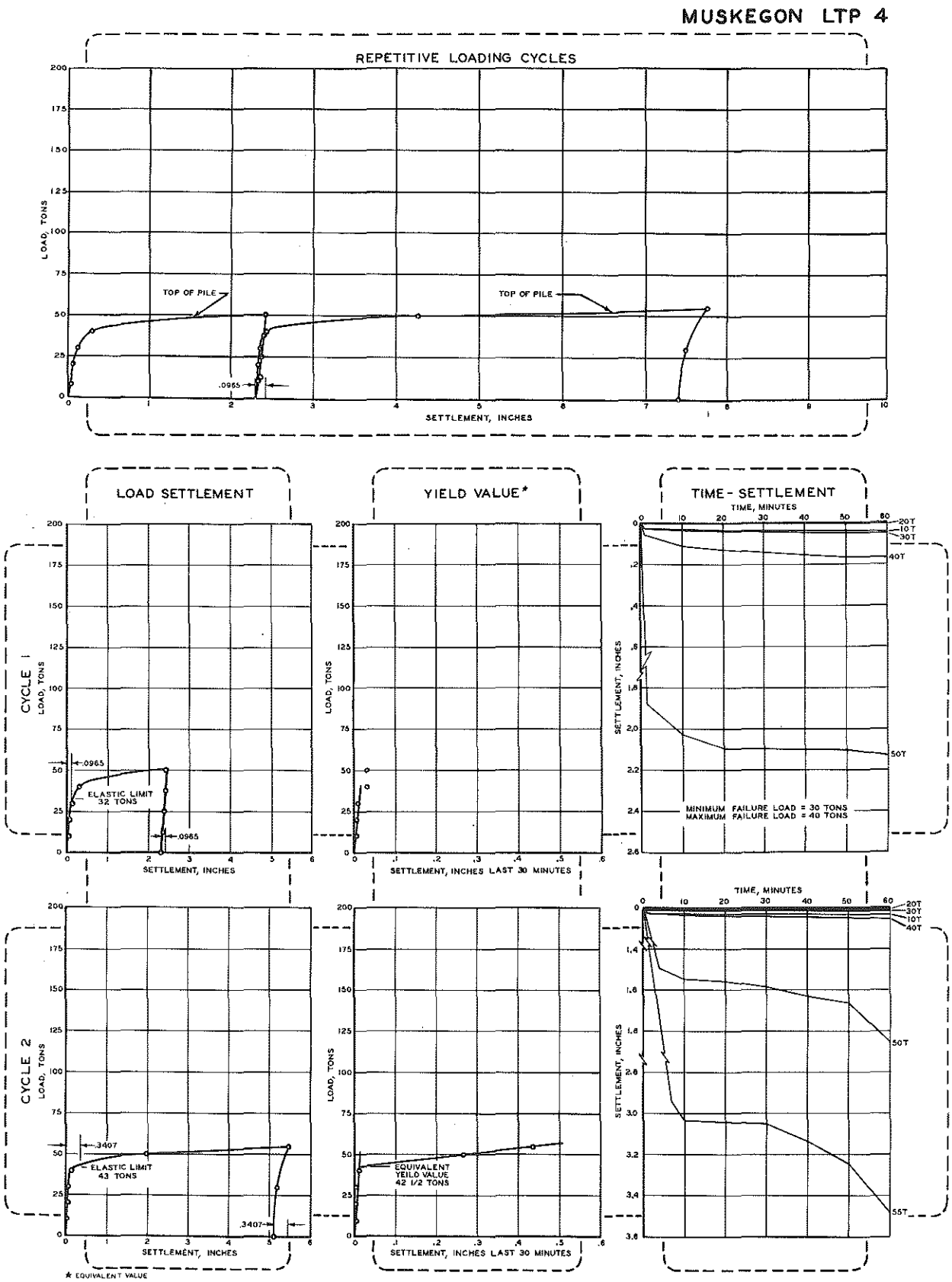

Figure 120. Load test results for Muskegon LTP 4.

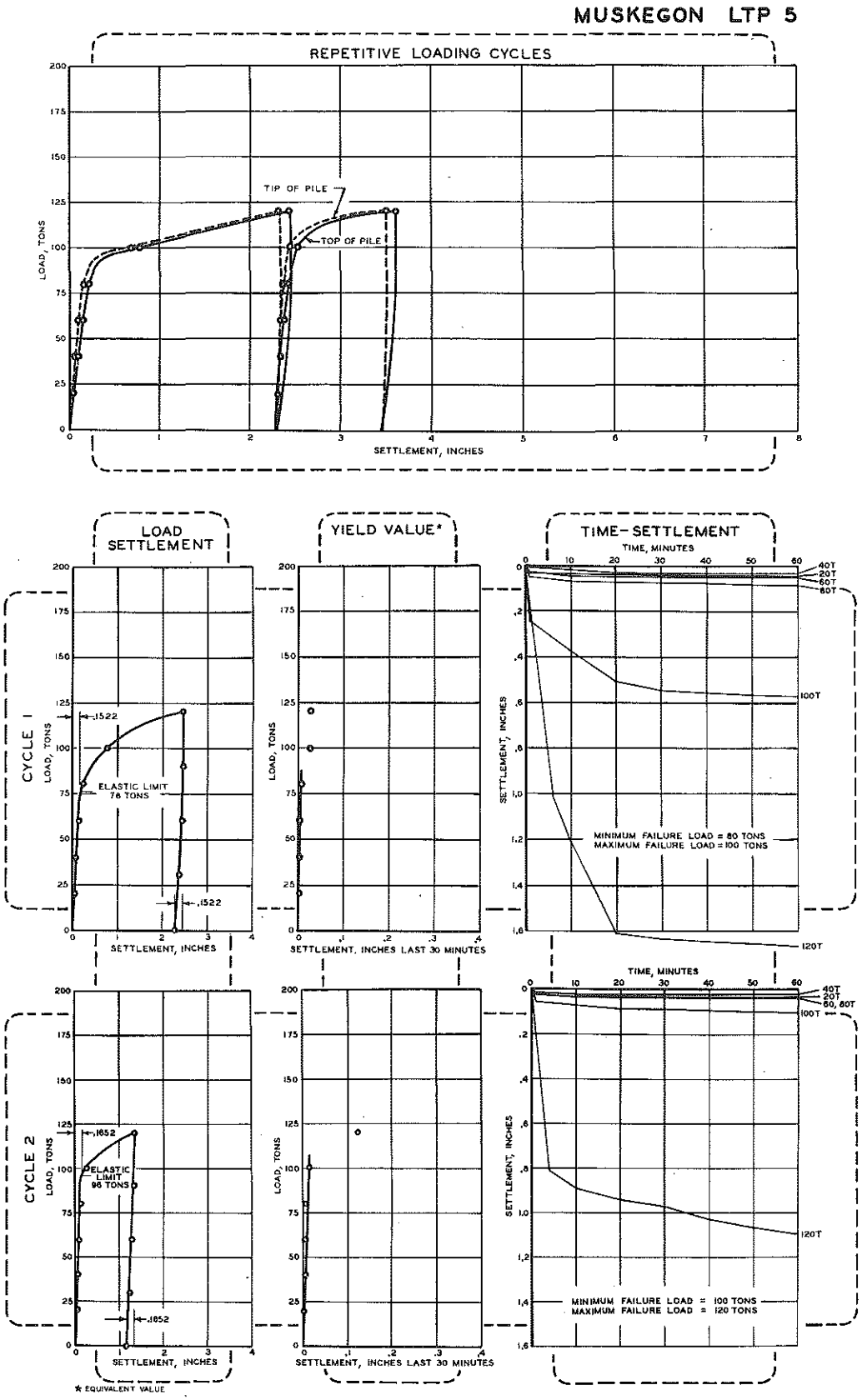

Figure 121. Load test results for Muskegon LTP 5.

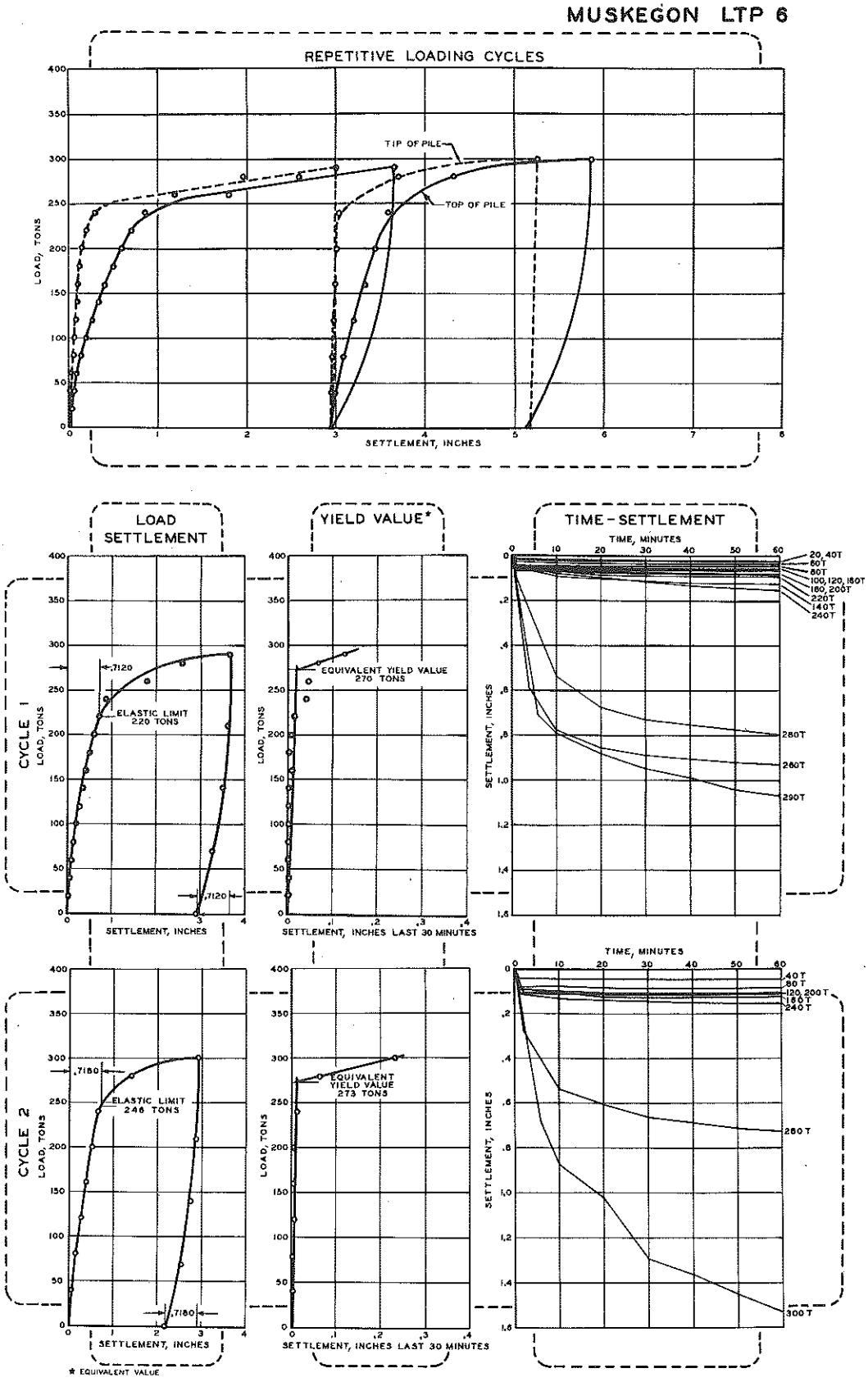

Figure 122. Load test results for Muskegon LTP 6.

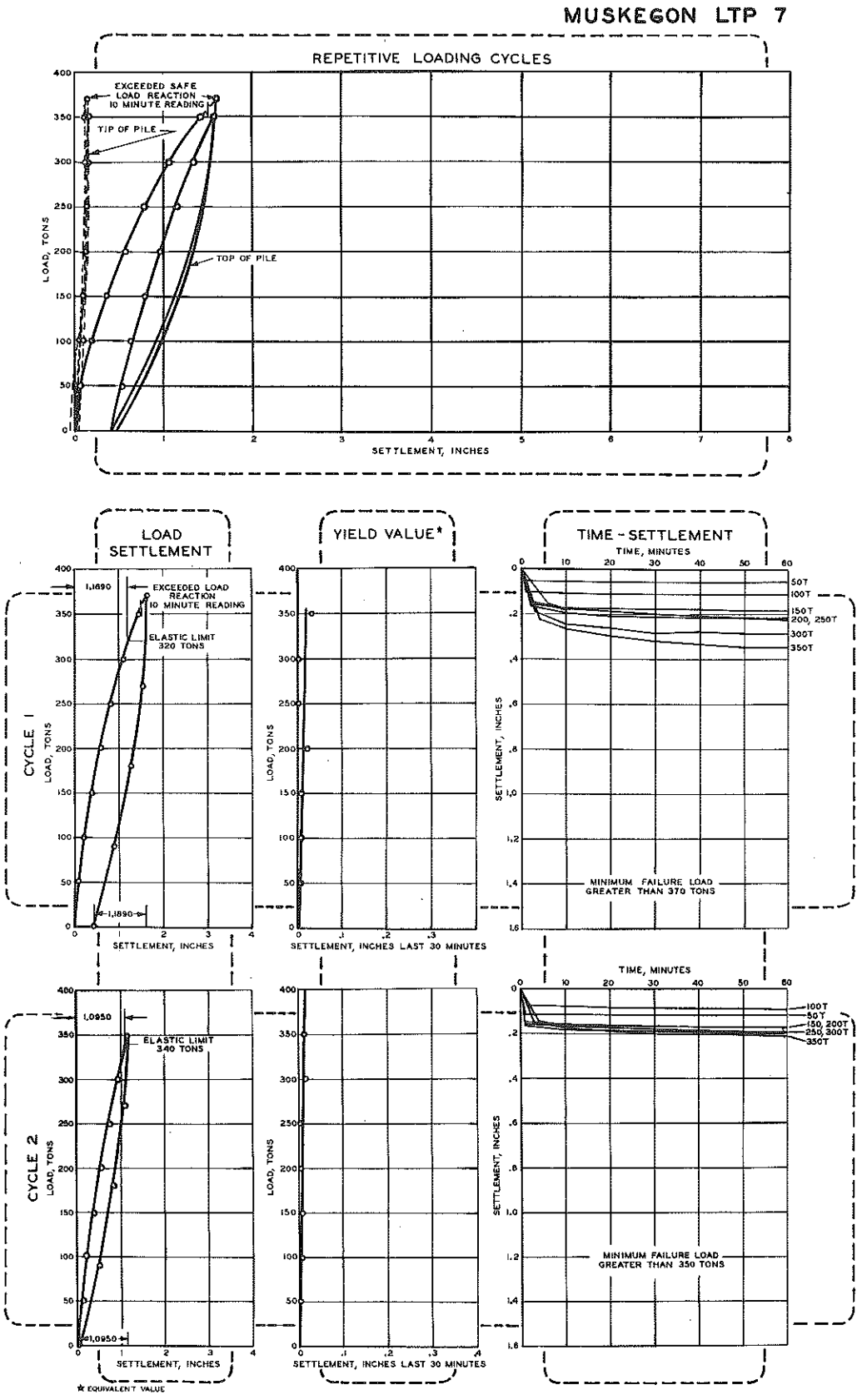

Figure 123. Load test results for Muskegon LTP 7.

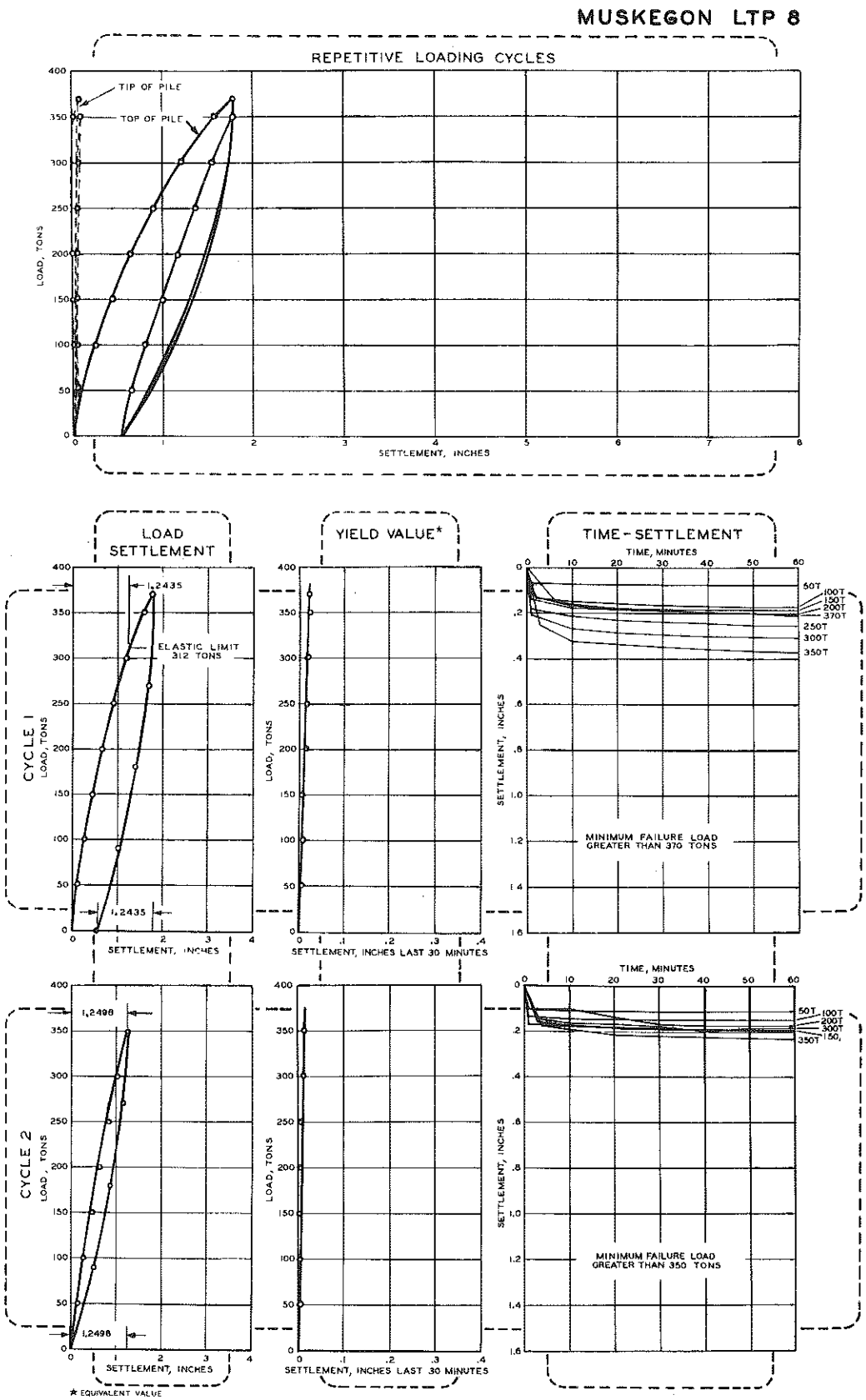

Figure 124. Load test results for Muskegon LTP 8.

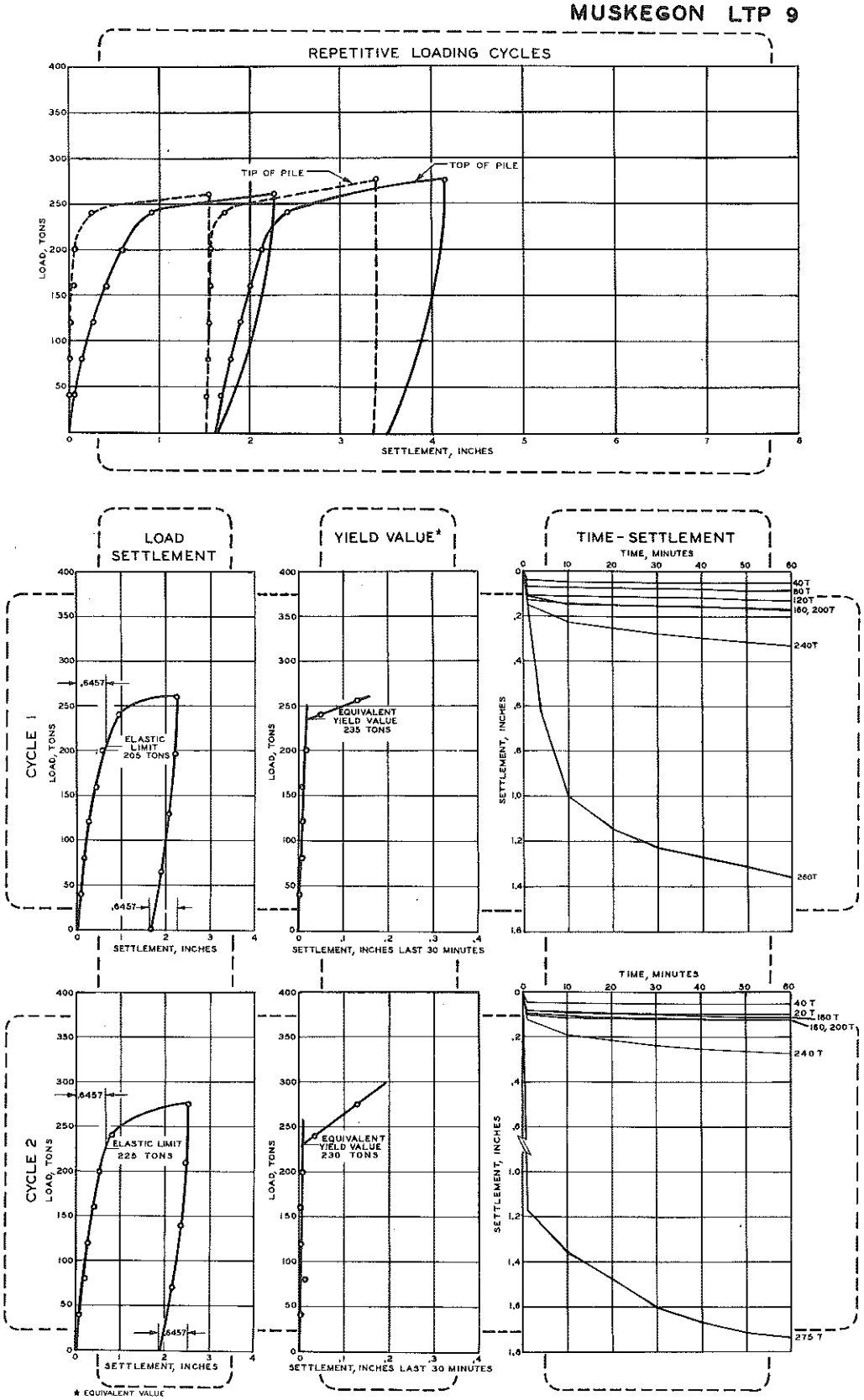

Figure 125. Load test results for Muskegon LTP 9.

LTP 8 was a closed-end 12-in. pipe also driven to 178.1 ft (elevation 409.8). The tip penetrated an estimated 1.2 ft into the compact-to-very compact sand layer. Subsoil conditions were substantially the same as for LTP 7. In the two loading cycles (Fig. 124), settlement at the tip was negligible at the maximum load of 370 tons. Maximum settlement at the top of the pile was 1.79 in., rebound was 1.25 in., and the permanent shortening was 0.54 in. in the first cycle with an applied load of 370 tons. In the second cycle the pile showed elastic behavior (100-percent rebound) indicating that the ultimate capacity of the pile had not been reached.

CHAPTER ELEVEN

ANALYSIS OF LOAD TEST RESULTS

A major goal of this investigation was correlation of bearing pile capacity as measured by field loading tests with soil resistance as determined by borings and laboratory tests. The intent was to determine whether data obtained from a routine soil investigation provided an accurate and reliable basis for designing a pile foundation, in terms of a predetermined pile length and predicted load bearing capacity. This correlation may be contrasted with the common practice of driving test piles and using only penetration resistance in well known dynamic formulas to determine static load capacity and length of piles.

Soil investigation results and other site conditions were discussed in Chapter 1, and results of the static load tests were presented in Chapter 10 with an outline of test procedure as well as those test details that may have affected pile capacity. With these presentations of basic data, attention in Chapter 11 may focus on correlation of pile load test and soil test results, pointing out the more significant findings and emphasizing essential elements of test procedure.

Discussion of Site Conditions

The Belleville site is representative of large areas in Michigan, outside the lake beds, where clay till predominates but is frequently combined with other deposits of glacial and post-glacial origin. These clays and related soils are better consolidated and more highly resistant. They often provide adequate support for spread foundations, but heavier structures and some bridge foundations may require pile support. Friction or shear piles are adequate in many cases, but bearing piles delivering loads to underlying hardpan or rock may still be more practical and economical under certain conditions.

At the Detroit site, soil conditions are typical of shoreline deposits bordering the Great Lakes, tributary rivers, and navigable channels. Lacustrine clay, ranging in depth from a few feet to a maximum of about 200 ft, is soft or plastic and may be characterized as an essentially

cohesive saturated clay. Friction or shear piles may be used infrequently but bearing piles are generally required to carry loads of larger structures to underlying hardpan or rock.

In describing the soils encountered, particularly at Detroit and Belleville, there has been frequent mention of a material variously described as hardpan, hard clay, hard till clay, or "Detroit hardpan." This material, well known in the Detroit metropolitan area, is predominantly a highly consolidated mixture of sand, gravel, and sometimes boulders, bound in a matrix of stiff, tenacious, blue-gray clay. It is identified geologically as of Pre-Wisconsin origin, a remnant of an older till not cut away by the last or Wisconsin invasion of the glaciers in the Great Lakes area. This hardpan is frequently replaced by sand, gravel, and boulders, usually water bearing, making a soil complex that in undisturbed state, with rare exceptions, has been highly consolidated under tremendous pressure. More precisely described as a claypan, this deposit is of generally high bearing value and is the bearing stratum on which caissons and bearing piles are normally landed in the Detroit area.

Soil conditions at the Muskegon site are common to the Lake Michigan shoreline on the western side of the lower peninsula. Deep glacial valleys have filled with alluvial deposits of sand and some gravel, interspersed with buried peat and soft swamp deposits. Bodies of sand in the upper soil profile are sometimes moderately compact and difficult to penetrate, but underlying peat and poorly consolidated soils preclude use of the shallow sand deposits as foundations for important structures. The depth to sound bearing materials may range from 150 to 200 ft, requiring unusually long piles and heavy driving to reach reliable bearing.

PILE LOAD TESTS

The pile loading test procedures described in Chapter 10 were developed over the past 30 years in a cooperative research program at the University of Michigan, supported by the Michigan State Highway Department and many other agencies, both public and private. During this time, the effectiveness of these procedures in producing consistently reliable and precise results has often been demonstrated.[1] [2] Test results in the

[1] Housel, W. S. "Dynamic and Static Resistance of Cohesive Soil: 1846-1958." ASTM Spec. Tech. Pub. No. 254 (1959), pp. 4-35.

[2] Housel, W. S. "Field and Laboratory Correlation of the Bearing Capacity of Hardpan for Design of Deep Foundations." ASTM Proc., Vol. 56 (1956), pp. 1320-1346.

current investigation as presented in Chapter 10 are quite representative and serve as an excellent example of the definitive character of these procedures.

Discussion of Test Procedures

The repetitive loading cycle plotted in Fig. 106 illustrates several features important in evaluating pile load bearing capacity. To obtain a measure of the ultimate capacity of a pile and its supporting soil, loading must be carried well into the stage of progressive settlement. The settlement due to permanent deformation will then be considerably beyond the range permissible in foundation design, but includes stress-conditioning of both the soil and pile that must be developed before ultimate capacity of the combination is reached.

The resulting increase in capacity, particularly for bearing piles, is largely due to consolidation under the tip. It is characterized in Fig. 106 by absence of a linear portion or elastic range in the first cycle of loading, and a marked increase in load and improvement in elastic characteristics in the second cycle. Repetitive loading and measurement of the settlement at both the pile top and the tip or bottom are a most effective means of evaluating such stress conditioning and defining the pile's related elastic characteristics. In Figs. 106 and similar load-settlement diagrams (Fig. 110, 111), it is notable that settlement at the tip is preceded by compression in the pile, while elastic rebound at the tip is generally negligible. The fact that settlement at the tip is largely permanent deformation or consolidation is consistent with the concept of stress conditioning that produced the increased bearing capacity and improved elastic characteristics.

From the standpoint of a reliable test procedure and results in terms that may be used with confidence under practical field conditions, the method of controlling primary variables is of fundamental importance. Without becoming involved in secondary considerations that might complicate and confuse the main objective of the test, these variables are three in number--time, load, and settlement. It is a simple but often neglected rule that to measure the relation between three variables, the direct approach is to hold one constant and observe the variation in the other two. Following this rule, the most important factor in success of the test procedures under discussion is the use of equal load increments at constant time intervals. This procedure is basic, and when followed without deviation, experience has shown that it provides accurate and reliable measures of pile bearing capacity in terms of resistance developed in both the elastic and plastic ranges.

Strength Criteria--Elastic Limit and Yield Value

The direct relationship between time, load, and settlement is illustrated in the typical graphs shown in Fig. 126.

The load-settlement curve provides the essential information for determining the pile's elastic limit, which is one of two basic measures of the ultimate capacity. The elastic limit is defined as the load carried at a settlement equal to the total elastic deformation, which is generally taken as the elastic rebound. Another determination of the total elastic deformation shown in Fig. 126 is the settlement ordinate at the intersection of two tangents to the load-settlement diagram, one representing the elastic range and the other the range of progressive settlement.

These two determinations of elastic deformation usually check quite well in shear piles, such as Belleville LTP 1 (Fig. 107) and Detroit LTP 1 (Fig. 113), with an extended elastic range and an abrupt transition to plastic displacement. However, in bearing piles where consolidation under the tip and increased bearing is a measurable part of the ultimate capacity, the rebound reflects the improvement due to stress conditioning, while the intersection of the tangents does not. Consequently, rebound is generally preferred as the basis for determining the elastic limit, as an index to ultimate capacity in terms of load.

Yield value, as determined by extrapolation of the terminal rates of settlement from the time-settlement curves, is the other of the two basic measures of a pile's ultimate capacity. It is quite independent of the elastic limit, being derived from settlement rates in the plastic range at higher loads, in contrast to load-settlement relations in the elastic range at lower loads. There is nothing complex or difficult in interpreting the relation of time, load, and settlement in the range of plastic displacement. The time-settlement curves in Fig. 126 for 1-hr time intervals show quite clearly that loads up to 150 tons produced terminal slopes or settlement rates at or near zero. These terminal settlement rates are shown on the yield value curve as settlement in the last 30 min of each time interval. The definite change to progressive settlement at loads of 180 to 210 tons is equally clear in both graphs.

It may be noted in Fig. 126 that there is a close correlation between the elastic limit and yield value even though they represent two different approaches for determining ultimate supporting capacity. Such correlation has also generally been found in previous test series.[1] [2] Results from the current tests shown in Fig. 127 confirm previous evidence sup-

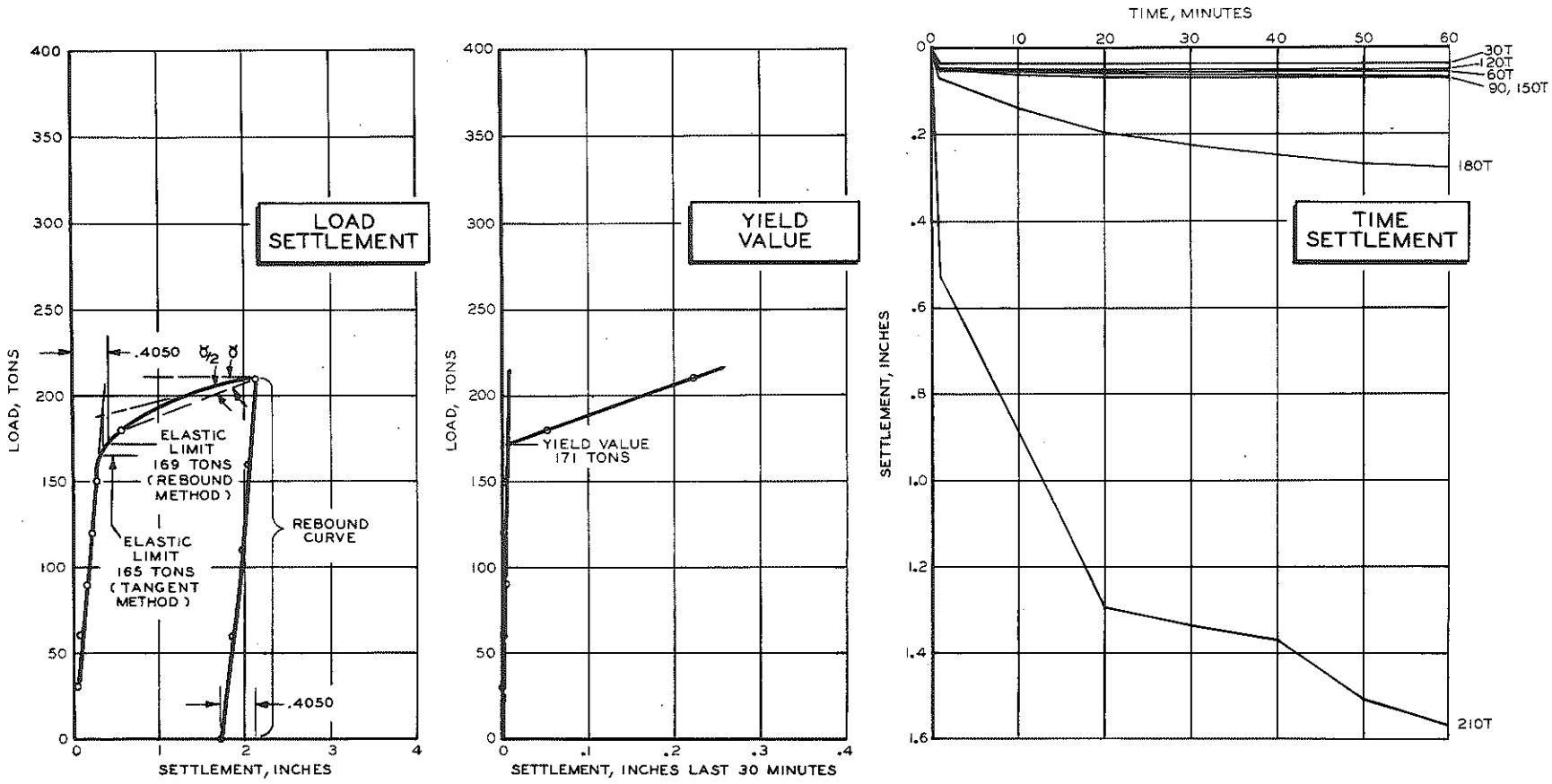

Figure 126. Typical graphs derived from a pile load test.

porting the reliability of the test procedure and validity of the load-settlement relations on which the determinations are based.

Some additional discussion of data in Fig. 127 may be helpful. The agreement between the yield value and the elastic limit is good, with the majority of plotted points falling within lines representing 10-percent deviation from perfect agreement (the 45° line). However, most points deviating from this line show the elastic limit as less than the yield value.

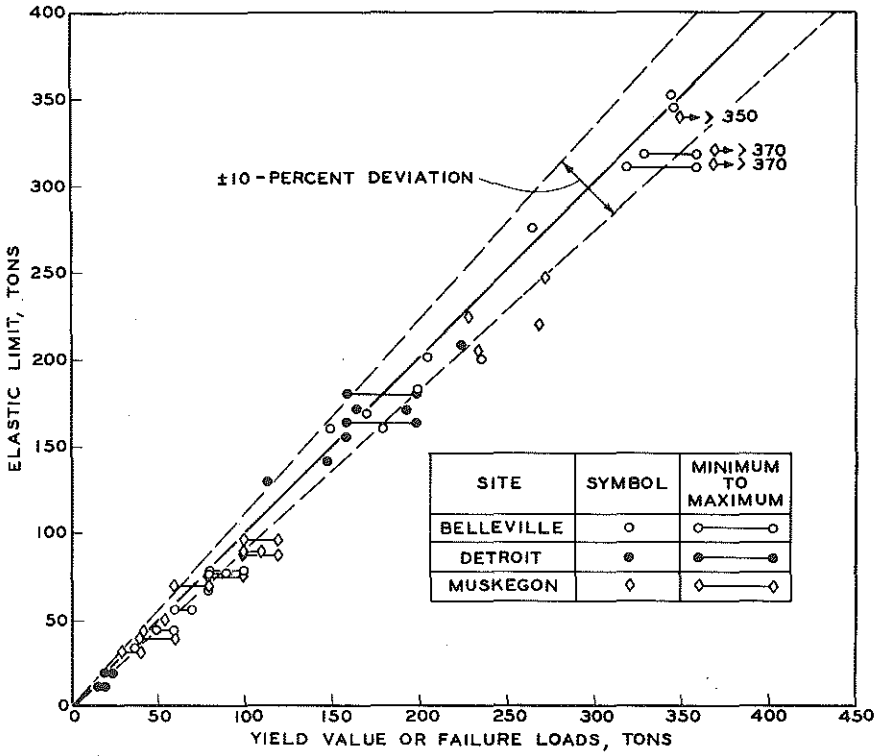

Figure 127. Correlation between elastic limit and yield value or failure load.

There is valid reason for this in that the load at elastic limit is determined from the load-settlement diagram in the range that does not fully account for the increase in capacity due to stress conditioning in any single loading cycle. Consequently, the yield value will generally be higher and is considered to provide a better measure of ultimate capacity under all test conditions.

Some attention should also be directed to the "true" and "equivalent" yield value or failure load as defined in Chapter 10 (and given in Tables 21, 22, and 23). By definition and the generally accepted concept of a plastic solid, the yield value is associated with cohesive materials having the

basic property of plasticity. When dealing with confined granular materials, it is a matter of common knowledge that their response to load application has some of the characteristics of a yielding material even though they are non-cohesive. Thus, in this investigation's loading tests on piles in granular materials, the transition from static equilibrium with some elastic response to the range of progressive settlement is often quite similar to that observed in cohesive materials. It is then possible to determine the load limit used to define the ultimate capacity by extrapolation of settlement rates in the stage of progressive settlement. The terms "true" or "equivalent" yield value were used to provide some distinction between the use of a yield value as a load limit for cohesive or granular materials, respectively.

Another series of Chapter 10 terms requiring some explanation are the "minimum," "maximum," and "estimated" yield value or failure load. The yield value graphs, particularly for loading tests in granular materials, show that in a number of cases the transition from the elastic range to progressive settlement or failure is quite abrupt, so that there may be only one load increment in the range of progressive settlement for which a settlement rate could be observed. Determination of yield value as the intersection of two straight lines representing elastic and plastic ranges of applied stress is no longer possible or depends upon an arbitrary estimate.

It is obvious that the yield value will be greater than the highest load increment in the elastic range, and less than the next load increment causing excessive settlement or failure. Taking the estimated yield value midway between these two loads is the closest approximation possible under the circumstances. Designating it as the "estimated" yield value identifies it as an approximation conditioned by the procedure used in its determination. A number of pairs of plotted points are connected in Fig. 127 to show that they are "minimum" and "maximum" yield values or failure loads, which can also be identified in Tables 21, 22, and 23.

BEARING CAPACITY COMPUTATIONS

Details of computations of pile supporting capacity and their comparison with load test results will be presented so that the reader may reconstruct the various phases of the problem. Soil boring and laboratory test data from Chapter 1 and pile load test data from Chapter 10 are used

for incidental reference, but primary attention is focused on methods of predicting pile capacity from such data and on comparison of results.

Computations and comparisons have been assembled in a series of tables and graphs for each site with all quantities identified and generally self-explanatory. The equations for computing the several components of ultimate capacity, however, will require some discussion.

Comparisons of computed and measured pile capacity for Belleville are presented in Tables 24 and 25 and Figs. 128 to 133. In Table 24, side shear capacity has been computed for each of the three borings. This was done because soil properties varied considerably over the test area. It was felt that correlating between individual borings and nearby piles would probably be better than attempting to average shear values over the site. The combinations of individual borings and nearest piles are indicated in the three sections of Table 24. It was recognized that with so wide a range in soil resistance values as at Belleville, it would be optimistic to expect a close correlation between laboratory tests from a single boring and field loading on nearby test piles; however, the complete comparative analysis was made and is presented as a matter of record.

At Detroit, soil conditions were more uniform, so that computation of bearing capacity was based on the average of field and laboratory soil resistance values from the three borings. Computations of side shear and end-bearing capacities are given in Tables 26 and 27. Side shear capacity combined with minimum and maximum values of end bearing is correlated with measured pile capacity. The comparison of computed and measured pile capacity is most clearly shown in Figs. 134 through 138, which also show the several variable factors involved in pile capacity, in terms of their relative magnitude and general relationship to site soil conditions.

Muskegon soil conditions differ substantially from the other two sites, consisting of considerable depths of granular materials with some interbedded strata of soft organic soils, a compact sand layer, and one deeper layer of plastic clay. Laboratory shearing resistance tests were available for the cohesive materials, but for the granular materials soil resistance was evaluated in terms of standard penetration observations.[3] The two borings have been combined and a composite profile prepared which is

[3] "Tentative Method for Penetration Test and Split-Barrel Sampling of Soils" (ASTM Designation D 1586-63T). ASTM 1964 Book of Standards, Part 11, pp. 487-489.

TABLE 24
BELLEVILLE PILES - SIDE SHEAR COMPUTATION

BORING 1 DATA							Cumulative Capacity				
Subsoil	Elevation, ft Ground Surface 651.4	N Blows Per ft	θ deg	Soil Resistance Values, psf		Side Shear (each major stratum) tons per lin ft of Perimeter	Side Shear, tons			
							LTP 1 P = 3.14 ft		LTP 2 P = 4.24 ft	
							Min.	Max.	Min.	Max.
				Cohesive		Cohesive			(pre-excavated 10 ft)	
				Average Cumulative, S_c						
	651.4									
Stiff Clay	645.5			2052		6.1	19.2	19.2	0.0	0.0
	643.0			1566		6.6	20.7	20.7	0.0	0.0
	640.5			1326		7.2	22.6	22.6	0.6	0.6
	640.5									
	632.5			612		2.4	30.1	30.1	10.8	10.8
	630.0			616		3.2	32.6	32.6	14.2	14.2
	627.5			619		4.0	35.2	35.2	17.6	17.6
	625.0			635		4.9	38.0	38.0	21.4	21.4
	622.3			645		5.9	41.1	41.1	25.6	25.6
Firm	619.9			647		6.7	43.6	43.6	29.0	29.0
Clay	617.5			651		7.5	46.2	46.2	32.4	32.4
	615.0			656		8.4	49.0	49.0	36.2	36.2
	612.5			670		9.4	52.1	52.1	40.3	40.3
	610.0			685		10.4	55.3	55.3	44.7	44.7
	607.0			685		11.5	58.7	58.7	49.4	49.4
	605.0			670		11.9	60.0	60.0	51.1	51.1
	602.5			663		12.6			54.0	54.0
	602.0			666		12.8			54.9	54.9
				Granular[a]		Frictional				
				Active $wh \tan^2 \theta$	Passive $wh \cot^2 \theta$	Min. Max.				
	602.0									
Very	600.0	41	25.5	1503	28675	1.5 28.7			61.3	176.6
Fine	597.5	20	28.4	1966	23186	4.0 57.7			71.9	299.5
Sand	595.0	11	29.9	2328	21304	6.9 84.3			84.2	412.3
and	592.5	11	29.9	2419	22135	9.9 112.0			96.9	529.8
Silt	590.0	8	30.1	2586	22662	13.1 140.3			110.4	649.8
	589.0	8	30.1	2651	23235	14.4 151.9			115.9	699.0
Plastic Clay	589.0									
	587.5	7		210[b]		0.2			116.7	699.8
	586.0					0.3			117.2	700.3
Hard Clay (Hard-pan)	586.0	179[c]		5370[b]		2.7			128.6	711.7
	585.0									
	584.3					4.6			136.7	719.8

(a) Computed from boring blow count (N)
Assumed wet soil unit weights (w) as follows: Clay - 130 pcf, Sand - 110 pcf.
(b) Based on correlation between N and S_c (S_E = 30N)
(c) Based on average measured ASTM blow count in hard pan

TABLE 24 (Cont.)
BELLEVILLE PILES - SIDE SHEAR COMPUTATION

BORING 2 DATA						Cumulative Capacity		
Subsoil	Elevation, ft Ground Surface 651.4	N Blows Per ft	θ deg	Soil Resistance Values, psf		Side Shear (each major stratum) tons per lin ft of Perimeter	Side Shear, tons LTP 3, 4, 5 P = 3.14 ft	
							Min.	Max.
				Cohesive				
				Average Cumulative, S_c		Cohesive	(pre-excavated 10 ft)	
	651.4							
	642.1			778		0.0	0.0	0.0
	639.1			700		0.8	2.5	2.5
Firm Clay	639.1							
	637.1			583		0.6	4.4	4.4
	634.6			582		1.3	6.6	6.6
	632.1			593		2.1	9.1	9.1
Stiff Clay	627.1			586		3.5	13.5	13.5
	624.6			578		4.2	15.7	15.7
	622.1			562		4.8	17.6	17.6
	619.6			538		5.2	18.8	18.8
Firm Clay	617.1			518		5.7	20.4	20.4
	610.1			487		7.1	24.8	24.8
	607.6			489		7.7	26.7	26.7
	605.1			498		8.5	29.2	29.2
	603.0			507		9.2	31.4	31.4
				Granular[a]		Frictional		
				Active wh tan² θ	Passive wh cot² θ	Min.	Max.	
	603.0							
Very	602.6	18	28.8	1894	20890	0.4	4.2	32.7	44.6
Fine	600.1	17	28.9	1909	21791	2.8	31.4	40.2	130.0
Sand	597.6	20	28.4	2162	21201	5.5	57.9	48.6	213.2
and	595.1	9	30.1	2216	22445	8.3	86.0	57.5	301.4
Silt	592.6	7	30.4	2482	21745	11.4	113.2	67.2	386.8
	590.1	8	30.1	2575	22569	14.6	141.4	77.2	475.4
	587.5	8	30.1	2670	23405	17.9	170.7	87.6	567.4
Plastic Clay	587.5							
	585.5			94		0.1		87.9	567.7
Hard Clay (Hardpan)	585.5							
	584.9	179[c]		5370[b]		1.6		92.9	572.7
	584.7					2.1		94.5	574.3

(a) Computed from boring blow count (N)
Assumed wet soil unit weights (w) as follows: Clay - 130 pcf, Sand - 110 pcf
(b) Based on correlation between N and S_c (S_E = 30N)
(c) Based on average measured ASTM blow count in hardpan

BORING 3 DATA						Cumulative Capacity		
Subsoil	Elevation, ft Ground Surface 651.4	N Blows Per ft	θ deg	Soil Resistance Values, psf		Side Shear (each major stratum) tons per lin ft of Perimeter	Side Shear, tons LTP 6 P = 6.0 ft	
							Min.	Max.
				Cohesive				
				Average Cumulative, S_c		Cohesive		
	651.4							
	644.6			1026		3.5	21.0	21.0
	642.1			1071		5.0	30.0	30.0
	639.6			1026		6.1	36.6	36.6
	639.6							
	637.1			738		0.9	42.0	42.0
	634.6			628		1.6	46.2	46.2
	632.1			570		2.1	49.2	49.2
Firm Clay	629.6			531		2.7	52.8	52.8
	627.1			520		3.3	56.4	56.4
	624.6			525		3.9	60.0	60.0
	622.1			528		4.6	64.2	64.2
	619.6			530		5.3	68.4	68.4
	617.1			544		6.1	73.2	73.2
	609.6			550		8.3	86.4	86.4
	604.6			562		9.8	95.4	95.4
	602.0			584		11.0	102.6	102.6
				Granular[a]		Frictional		
				Active wh tan² θ	Passive wh cot² θ	Min.	Max.	
Very	602.0	45	25.1					
Fine	599.6	25	27.7	1642	26777	2.0	32.1	114.6	295.2
Sand	597.1	25	27.7	1911	24769	4.4	63.1	129.0	481.2
and	594.6	9	30.1	2413	21153	7.4	89.5	146.0	639.6
Silt	593.4	9	30.1	2482	21760	9.8	102.6	161.4	718.2

(a) Computed from boring blow count (N)
Assumed wet soil unit weights (w) as follows: Clay - 130 pcf, Sand - 110 pcf

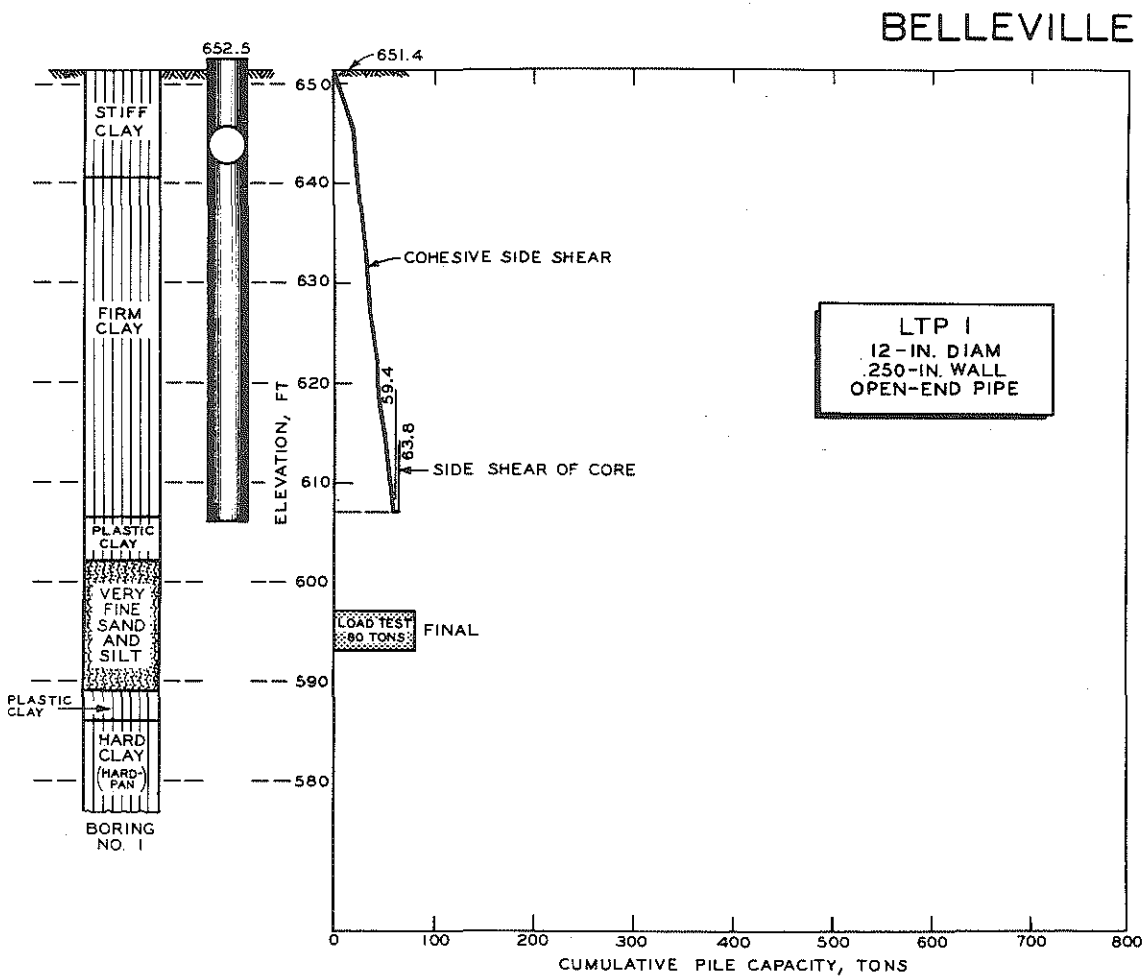

Figure 128. Comparison of computed and measured capacities for Belleville LTP 1.

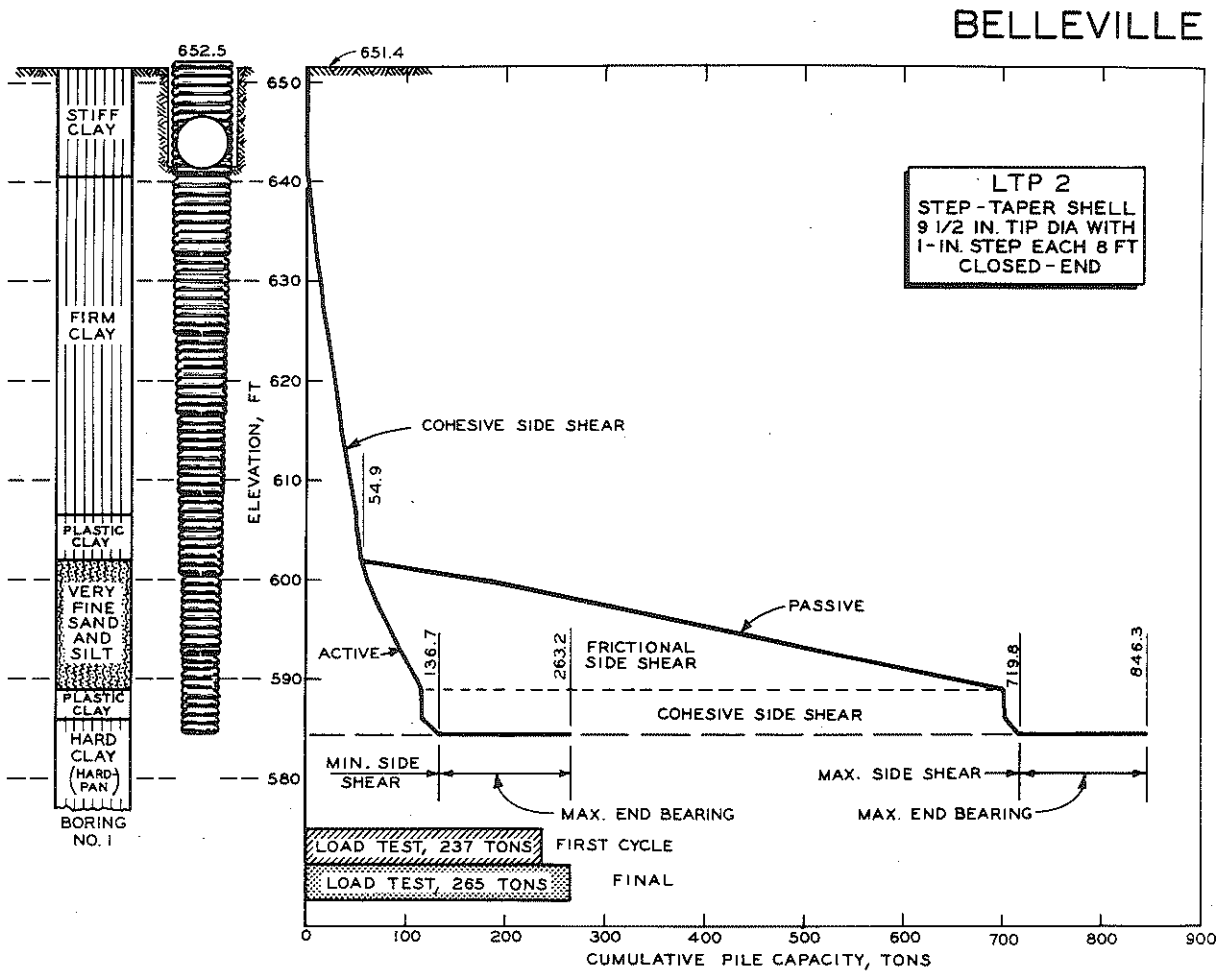

Figure 129. Comparison of computed and measured capacities for Belleville LTP 2.

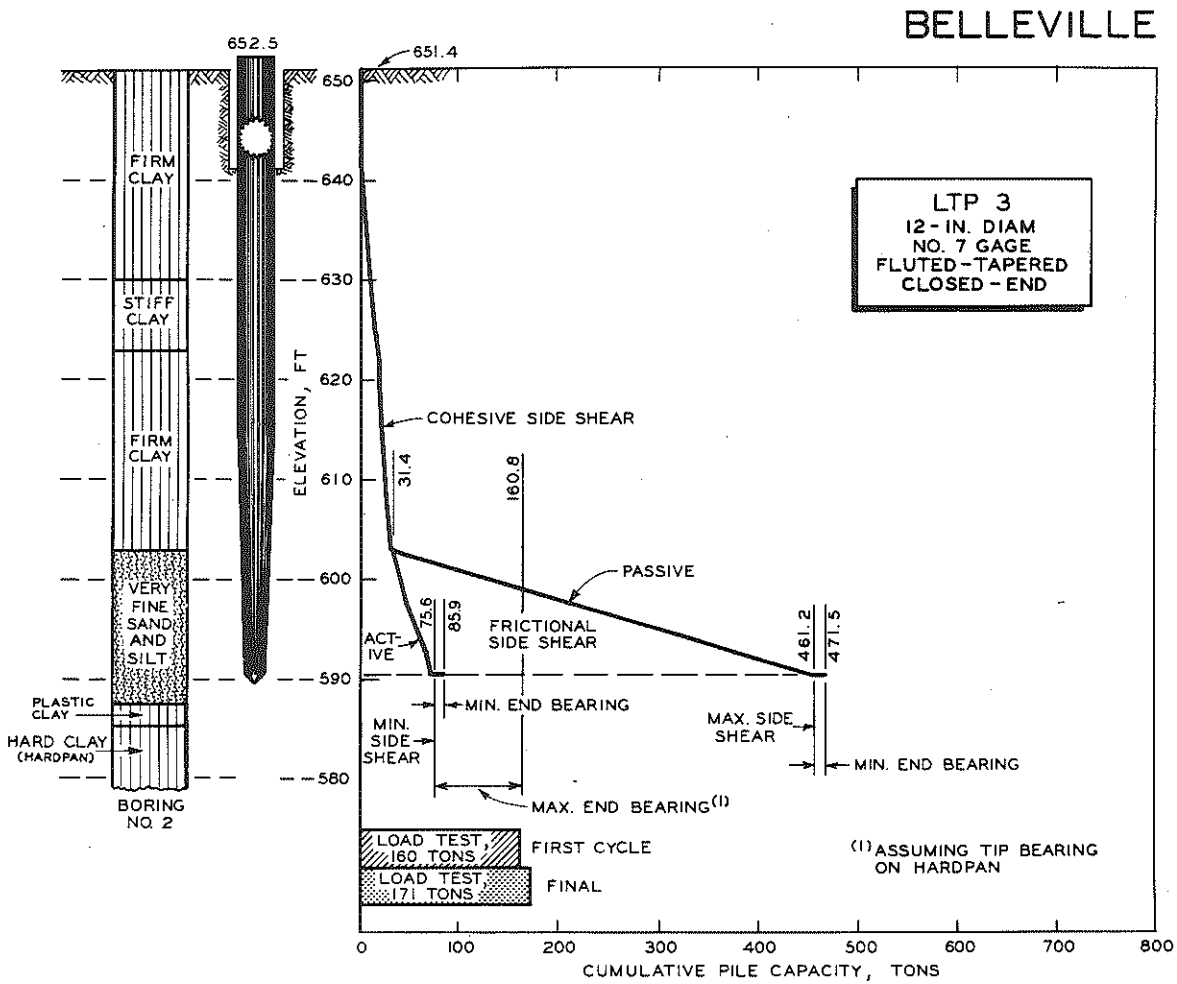

Figure 130. Comparison of computed and measured capacities for Belleville LTP 3.

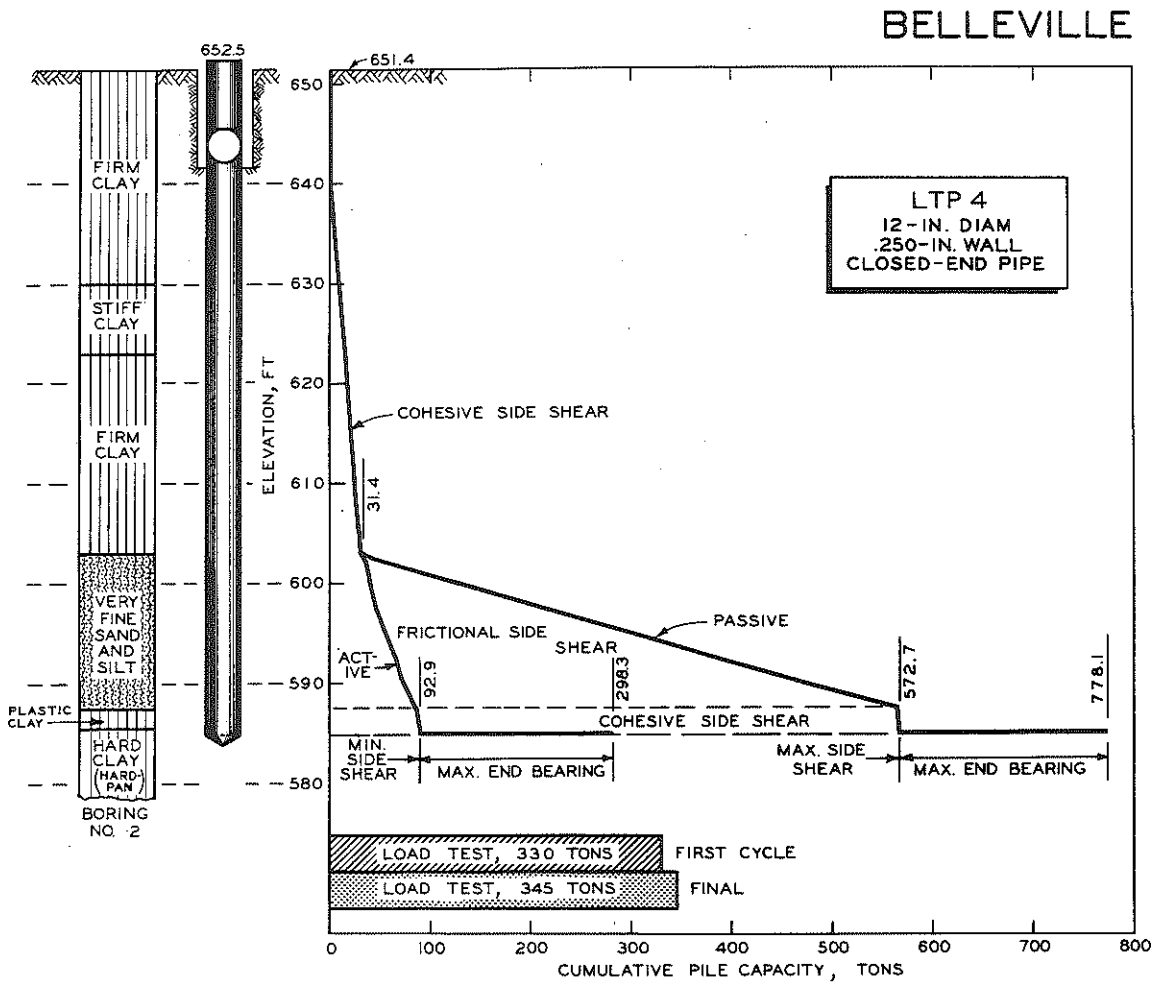

Figure 131. Comparison of computed and measured capacities for Belleville LTP 4.

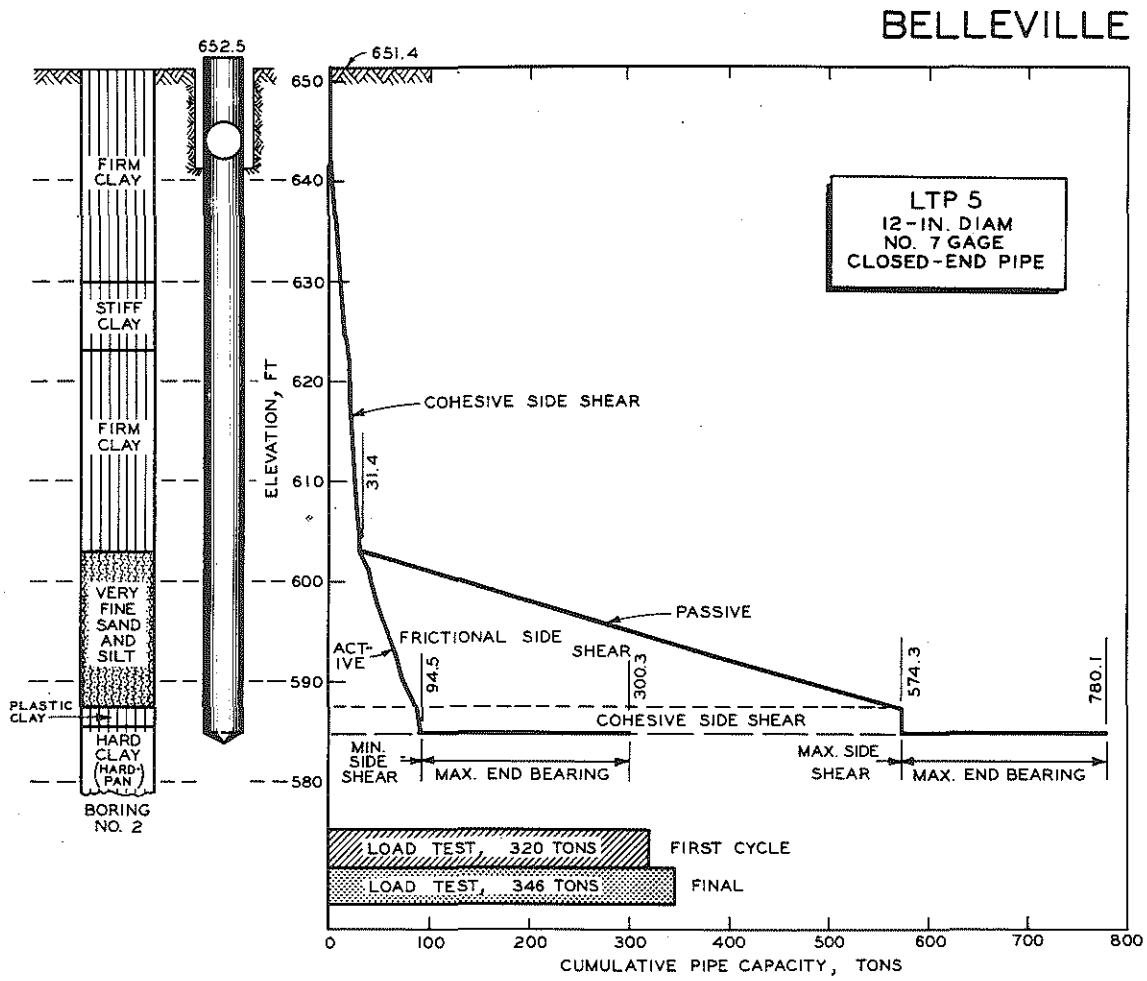

Figure 132. Comparison of computed and measured capacities for Belleville LTP 5.

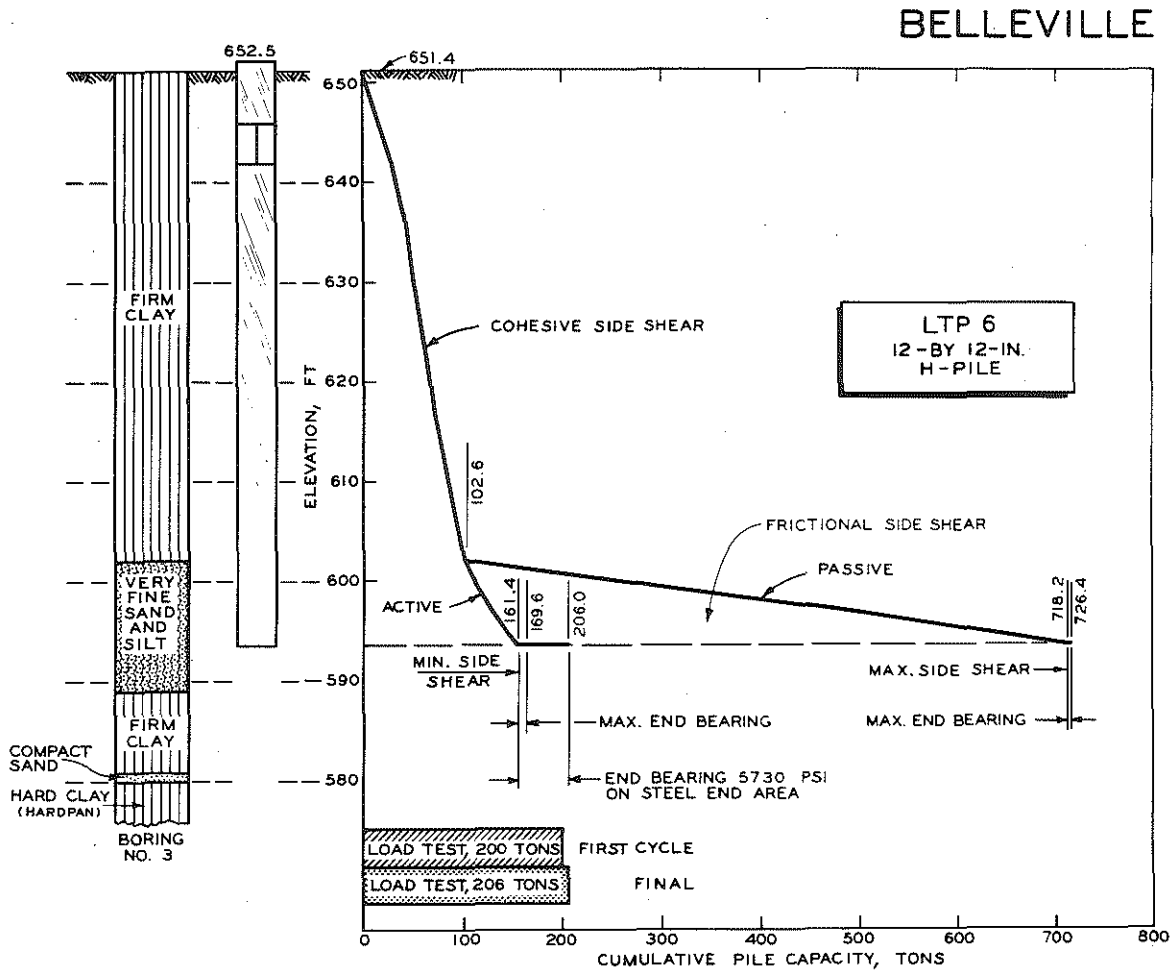

Figure 133. Comparison of computed and measured capacities for Belleville LTP 6.

TABLE 26
DETROIT PILES - SIDE SHEAR COMPUTATION

AVERAGE DATA FROM BORING 1, 2, 3			Cumulative Capacity		
				Side Shear, tons	
Subsoil	Elevation, ft Ground Surface 589.4	Soil Resistance Values, psf	Side Shear (each major stratum) tons per lin ft of Perimeter	Pipe LTP 1, 2, 7, 10 P = 3.14 ft	H-Pile LTP 8 P = 6.0 ft
		Cohesive Average Cumulative, S_c	Cohesive		
Fill	589.4 583.6	450	1.3	4.1	7.8
	583.6				
Plastic Clay	581.4	404	0.4	5.4	10.2
	578.4	398	1.0	7.2	13.8
	576.1	398	1.5	8.8	16.8
	576.1				
	573.5	266	0.3	9.8	17.6
	571.1	230	0.6	10.6	20.4
	568.4	179	0.7	11.0	21.0
	563.9	194	1.2	12.6	24.0
	558.7	179	1.6	13.8	26.4
	555.7	171	1.7	14.1	28.7
	552.7	161	1.9	14.8	28.2
	549.4	161	2.1	15.4	29.4
Soft Clay	546.9	156	2.3	16.0	30.6
	542.4	152	2.6	17.0	32.4
	540.0	150	2.7	17.3	33.0
	536.2	148	2.9	17.9	34.2
	533.7	147	3.1	18.5	35.4
	530.9	146	3.3	19.2	36.6
	529.6	146	3.4	19.5	37.2
	525.7	147	3.7	20.4	39.0
	523.2	148	3.9	21.0	40.2
	520.2	146	4.1	21.7	41.4
	517.7	150	4.4	22.6	43.2
	515.2	145	4.4	22.6	43.2
	510.8	145	4.7	23.6	45.0
Hard Clay (Hardpan)	510.8 508.4 508.3	2190[a]	2.6 2.7	31.8 32.1	60.6 61.2

(a) Based on correlation between N and S_c (S_E = 30N)
Average measured ASTM blow count was 73.0 blows/ft in hardpan

TABLE 27
DETROIT PILES - TIP CAPACITY COMPUTATION AND PILE SUMMARY

Driving Data				Pile Tip Capacity													Pile Capacity Summary						
Pile	Pile Type	Hammer Type and Manufacturer's Maximum Rated Energy, ft-lb	Final Driving Resistance (blows/last increment) at Tip Elevation, ft	General Equation for Tip Capacity in Granular-Cohesive Soil $R_{tip} = \frac{A}{2000}\left[\frac{1}{3} Kw \frac{B}{2} \cot^5\theta + \frac{2 S_c (1 + \cot^2\theta)}{\sin 2\theta} + wh (\cot^4\theta - 1)\right]$													Cumulative Side Shear Capacity, tons	Computed Capacity (shear + tip), tons		Load Test Capacity, tons		Computed Capacity, tons	Ratio of Load Test to Computed, percent	
				Min. and Max.	N	θ deg	A sq ft	K	w pcf	B ft	$\cot^5\theta$	S_c(a) psf	$\sin 2\theta$	$\cot^2\theta$	wh psf	$\cot^4\theta$	R_{tip} tons		Min.	Max.	Cycle First	Cycle Final	Most Probable	Cycle First	Cycle Final
LTP 1	12-in. diam. No. 7 gage open-end	Vulcan No. 1 15,000	4/last 6 in. 519.9	Min.	---	----	0.79	----	122	1.00	-----	----	----	----	----	-----	2.2*	22.3	24.5	36.2	15	28	24.5	61	114
				Max.	---	----	0.79	----	122	1.00	-----	----	----	----	----	-----	13.9**								
LTP 2	12-in. diam. No. 7 gage closed-end	Vulcan No. 1 15,000	36/last in. 510.8	Min.	40	30.6	0.79	9.7	122	1.00	13.93	1200	0.88	2.86	9589	8.24	32.7	23.6	56.3	157.8	130	165	157.8	82	105
				Max.	170	23.9	0.79	13.1	122	1.00	59.00	5100	0.75	5.11	9589	26.11	134.2								
LTP 7	12-in. diam. No. 7 gage fluted-taper closed-end	McKiernan-Terry DE-30 22,400	30/last in. 508.3	Min.	40	30.6	0.35	9.7	122	0.67	13.93	1200	0.88	2.86	9894	8.24	14.7	32.1	46.8	92.0	148	159	92.0	161	173
				Max.	170	23.9	0.35	13.1	122	0.67	59.00	5100	0.75	5.11	9894	26.11	59.9								
LTP 8	12 by 12 in. H-pile	Vulcan No. 1 15,000	37/last in. 508.3	Min.	40	30.6	0.11	9.7	122	1.00	13.93	1200	0.88	2.86	9894	8.24	4.7	61.2	65.9	80.3	163	180	80.3	203	224
				Max.	170	23.9	0.11	13.1	122	1.00	59.60	5100	0.75	5.11	9894	26.11	19.1								
LTP 10	12-in. diam. .230-in. wall closed-end	Link-Belt 312 18,000	20/last 1/4 in. 508.4	Min.	40	30.6	0.79	9.7	122	1.00	13.93	1200	0.88	2.86	9882	8.24	33.6	31.8	65.4	169.1	194	225	169.1	115	133
				Max.	170	23.9	0.79	13.1	122	1.00	59.00	5100	0.75	5.11	9882	26.11	137.3								

* LTP 1 driven open-end; earth core 33.7 ft long; end-bearing: $R_{tip} = \frac{A}{2000}(8 S_c + wh) = \frac{.79}{2000}(8 \times 148 + 36 \times 122) = 2.2$ tons.

** LTP 1 driven open-end; earth core 33.7 ft long; end-bearing due to earth core: $R_{tip} = \frac{S_c hP}{2000} = \frac{[(450)(5.8) + (398)(7.5) + 171\ (20.4)]3.06}{2000} = 13.9$ tons.

(a) Based on correlation data between S_c and N ($S_E = 30N$).

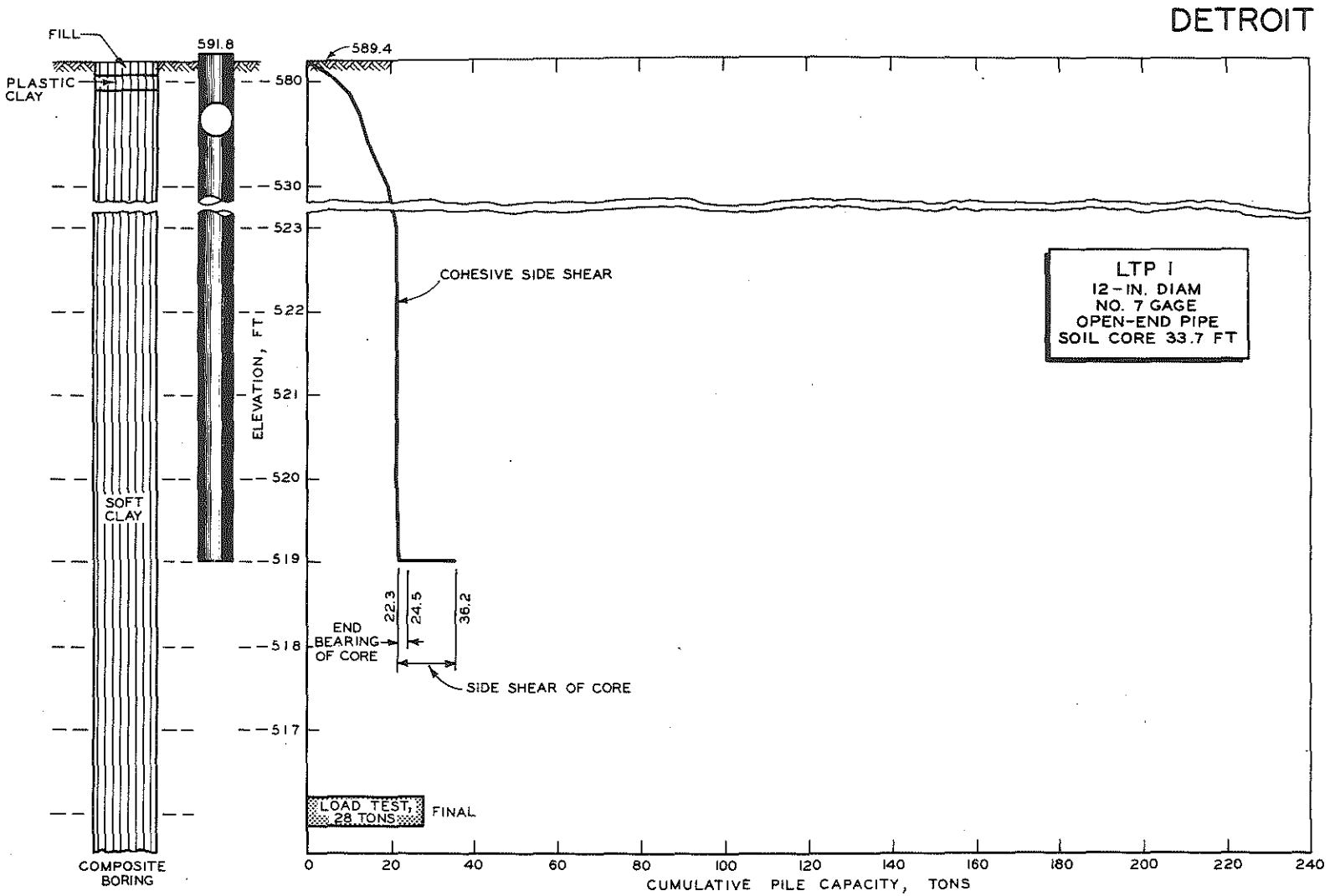

Figure 134. Comparison of computed and measured capacities for Detroit LTP 1.

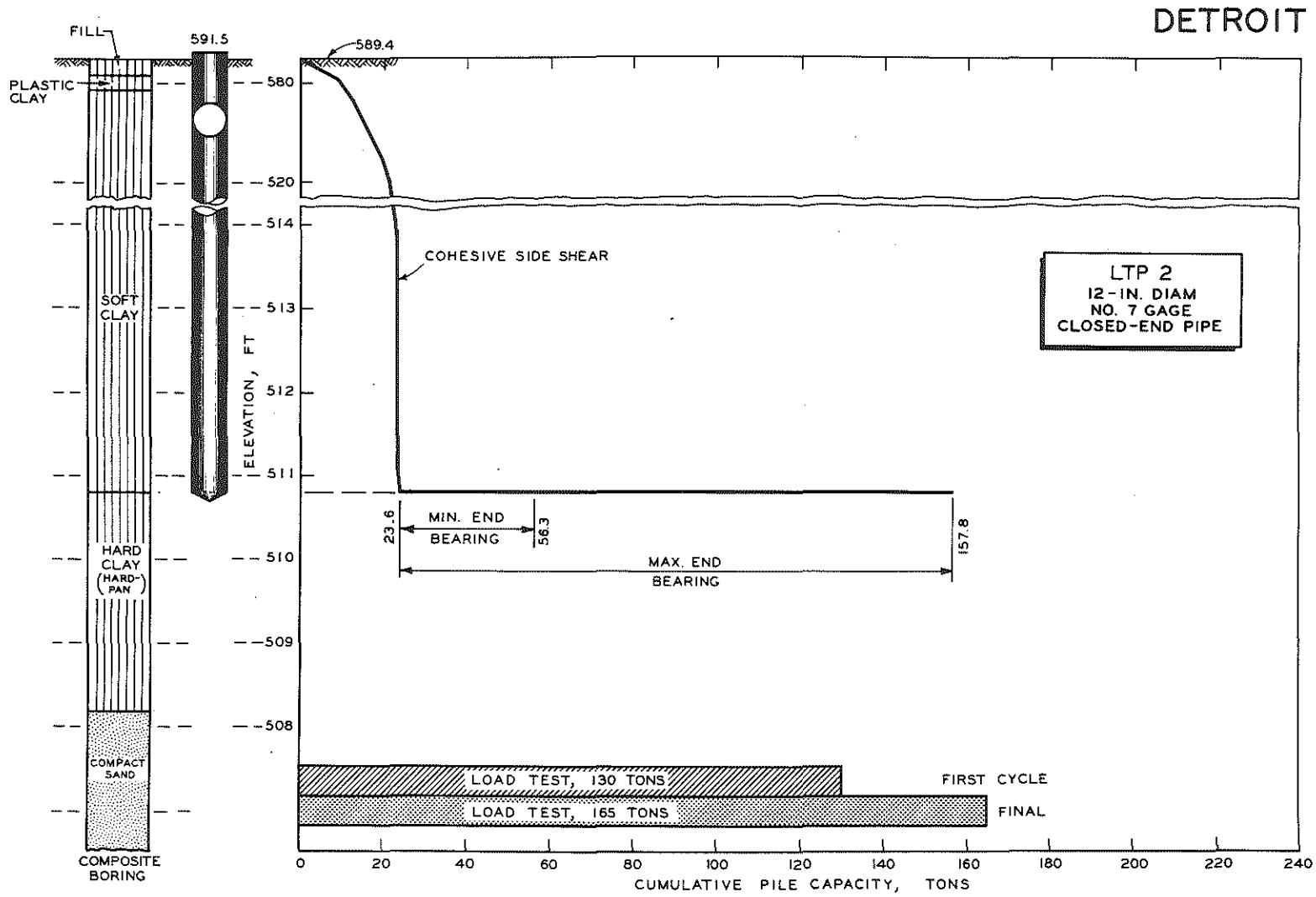

Figure 135. Comparison of computed and measured capacities for Detroit LTP 2.

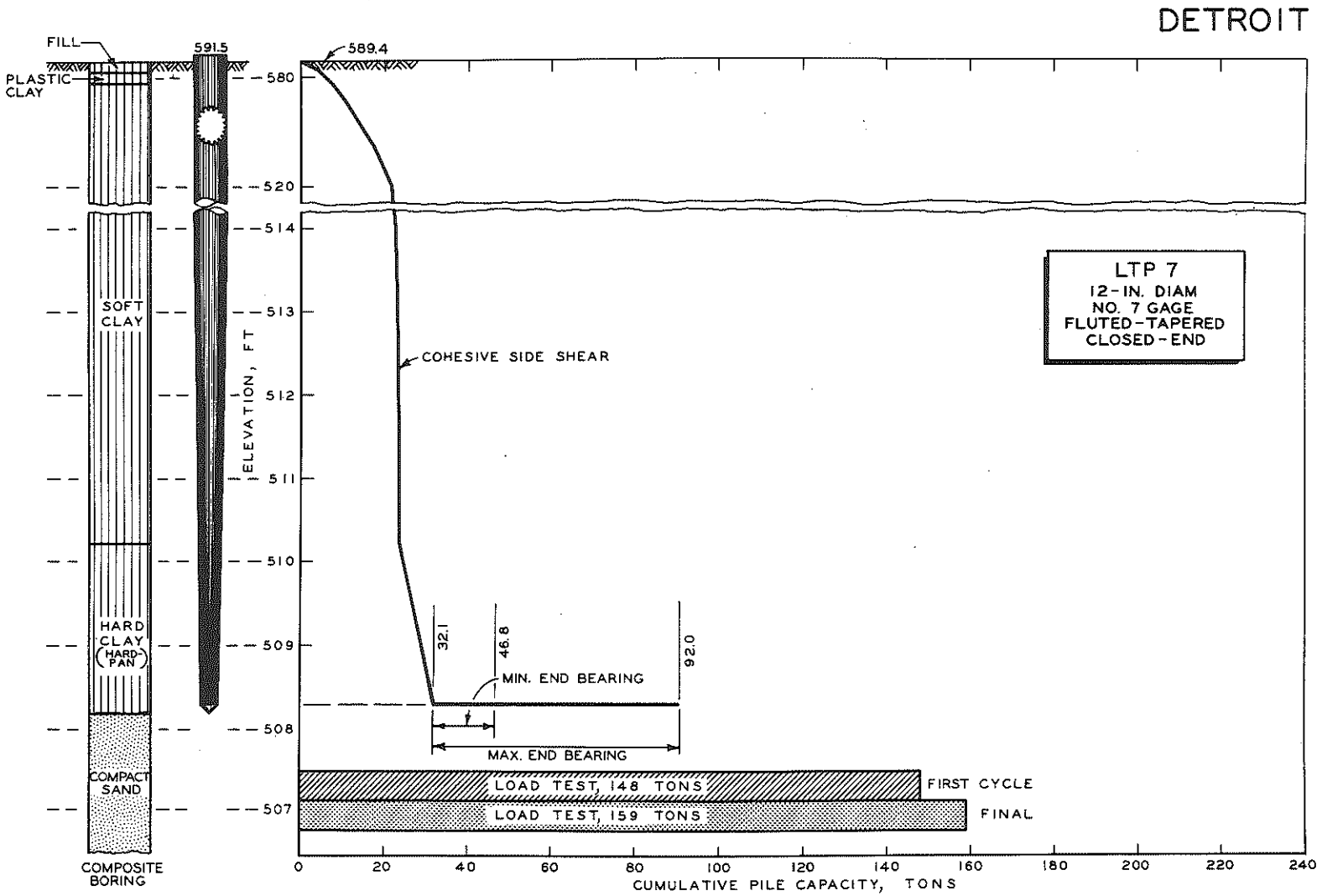

Figure 136. Comparison of computed and measured capacities for Detroit LTP 7.

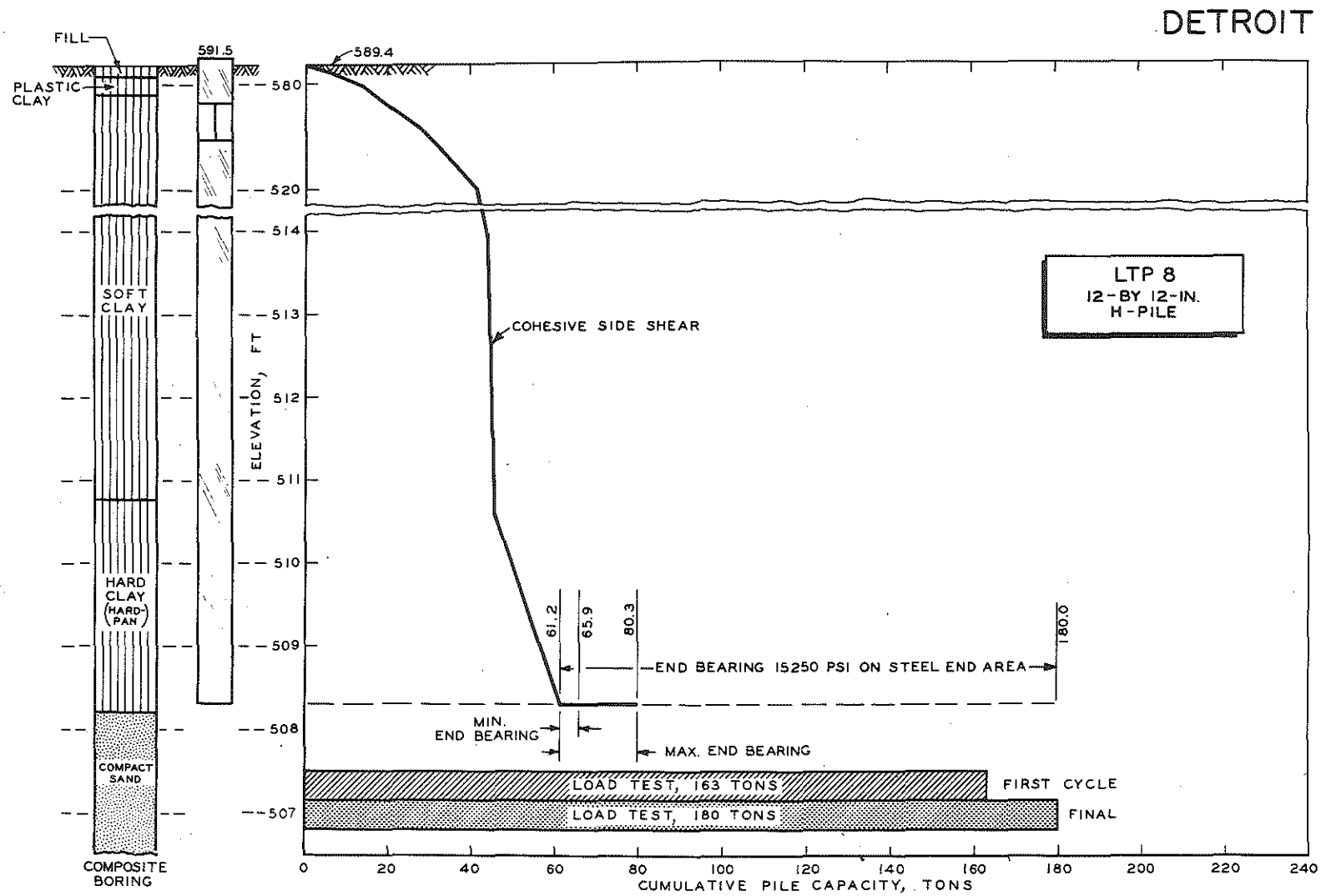

Figure 137. Comparison of computed and measured capacities for Detroit LTP 8.

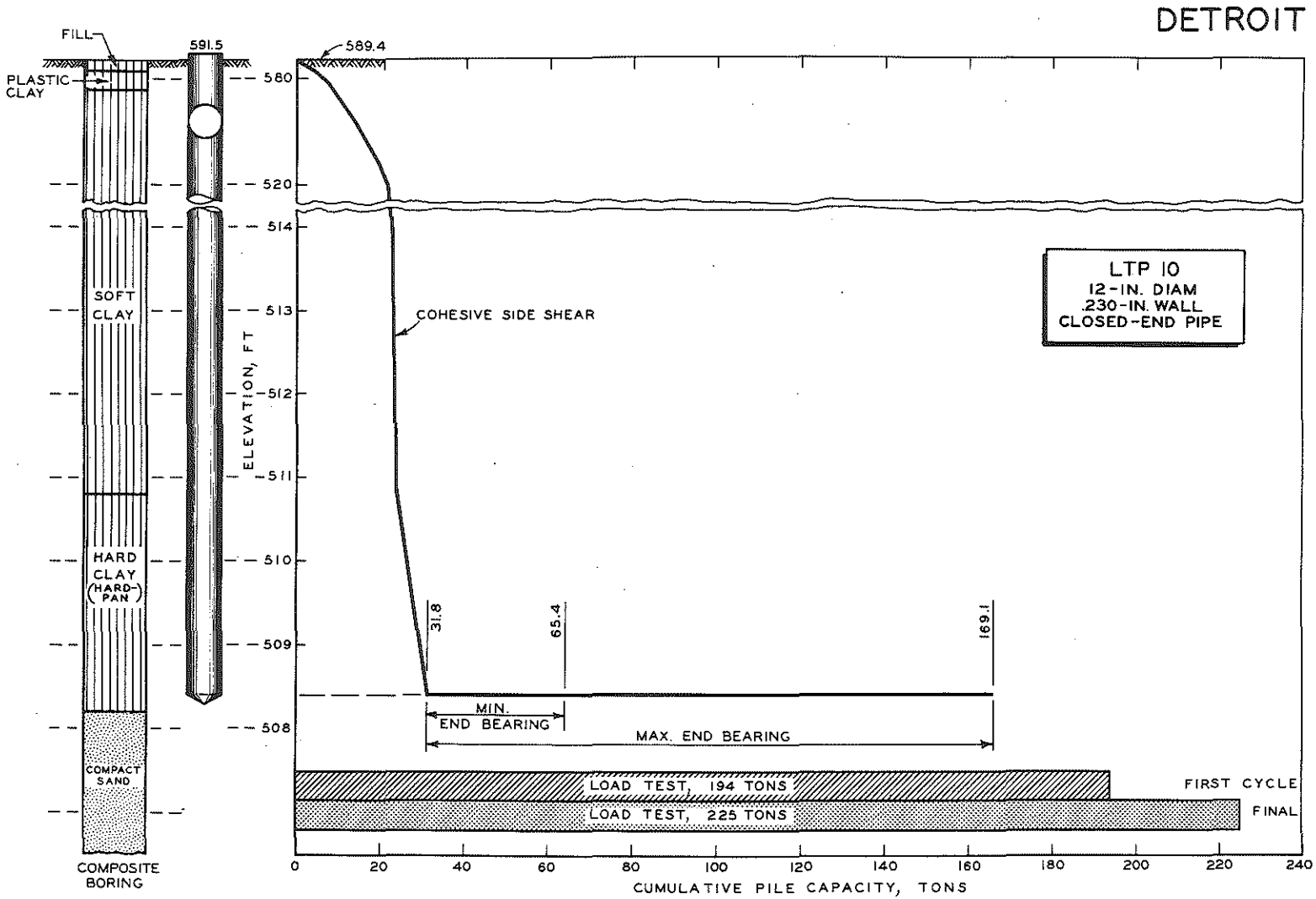

Figure 138. Comparison of computed and measured capacities for Detroit LTP 10.

taken to be representative of Muskegon soil resistance values. Computations of side shear through layers of both granular and cohesive materials are compiled in Table 28. The most important feature of this estimate is the computation of the range in frictional side shear, depending upon minimum and maximum values of lateral pressure acting normal to the shearing surface of the piles. Table 29 presents computations of total bearing capacity, including both the cumulative side shear reaction and the end bearing or tip capacity. End bearing or tip capacity is based on minimum and maximum values of standard penetration in the sand strata where the tips stopped. Comparison of computed and measured bearing capacity at Muskegon and the relationship between the several variable factors which enter into it, are shown in Figs. 139 through 146.

Side Shear--Cohesion and Friction

The reaction developed by the soil mass in side shear has been computed using shearing resistance values for each elevation at which samples were obtained. Total side shear from the highest point on the pile in contact with soil to any other elevation is the summation for major subdivisions of the soil profile of the products of the pile perimeter, embedded length, and cumulative average shearing resistance. Individual rather than cumulative shear values were used at Muskegon. Consecutive values of side shear in terms of total capacity at various strata elevations are given in the tables and graphs for each site.

In these computations clay soils were treated as cohesive, with side shear due entirely to cohesion and independent of normal pressure. Where laboratory test results were available, cumulative average shearing resistance was based on the yield value from the ring shear test. The comparable static yield value of one-fourth the shearing resistance from the rapid unconfined compression test (5-min loading period) was not used in the side shear computations, although this would have given comparable results. Normally, as illustrated in Figs. 7, 8, and 9 for the Detroit site, which is representative of a saturated clay behaving as a truly cohesive soil, there is a 1:4 ratio between the static yield value from the ring shear test and the shearing resistance from the rapid unconfined compression test. Based on thousands of comparative tests conducted over the past 25 years, it has been the practice to plot the compression shear to a scale four times that used for plotting the results of the ring shear test. This generally brings the equivalent shear values into close agreement.[1,2] Where laboratory tests were not available, as in the deeper clay strata, the estimated shearing resistance S_E was

TABLE 28
MUSKEGON PILES - SIDE SHEAR COMPUTATION

DATA FROM BORING 1, 2						Cumulative Capacity					
Subsoil	Elevation, ft Ground Surface 588.0[b]	N Blows Per ft	θ deg	Soil Resistance Values, psf		Side Shear (each major stratum) tons per lin ft of Perimeter		Side Shear, tons			
								LTP 2, 3, 4, 6, 7, 8, 9 P = 3.14 ft		LTP 5 P = 4.24 ft	
								Min.	Max.	Min.	Max.
				Granular[a]		Frictional					
				Active wh $\tan^2 \theta$	Passive wh $\cot^2 \theta$	Min.	Max.				
	588.0										
	579.6	3	31.0	170	1314	0.7	5.5	2.2	17.3	3.0	23.3
	577.7	2	31.2	368	2705	1.0	8.1	3.1	25.4	4.2	34.3
	574.6	4	30.9	408	3158	1.6	13.0	5.0	40.8	6.8	55.1
	572.7	8	30.3	432	3707	2.0	16.5	6.3	51.8	8.5	70.0
	569.6	6	30.6	493	4024	2.8	22.7	8.8	71.3	11.9	96.2
	567.7	6	30.6	541	4417	3.3	26.9	10.4	84.5	14.0	114.1
	564.6	6	30.6	589	4811	4.2	34.4	13.2	108.0	17.8	145.9
	562.7	13	29.5	582	5695	4.8	39.8	15.1	125.0	20.4	168.8
	559.6	10	30.0	665	5852	5.8	48.9	18.2	153.5	24.6	207.3
	557.7	17	29.0	629	6786	6.4	55.3	20.1	173.6	27.1	234.5
Loose	554.6	17	29.0	670	7232	7.4	66.5	23.2	208.8	31.4	282.0
Sand	552.7	10	30.0	806	7085	8.2	73.2	25.7	229.8	34.8	310.4
	549.6	6	30.6	878	7170	9.6	84.3	30.1	264.7	40.7	357.4
	547.7	8	30.3	899	7722	10.5	91.6	33.0	287.6	44.5	388.4
	544.6	4	30.9	1002	7762	12.1	103.6	38.0	325.3	51.3	439.3
	542.7	6	30.6	1022	8350	13.1	111.5	41.1	350.1	55.5	472.8
	539.6	10	30.0	1039	9141	14.7	125.7	46.2	394.7	62.3	533.0
	537.7	7	30.5	1118	9232	15.8	134.5	49.6	422.3	67.0	570.3
	534.6	17	29.0	1000	10795	17.4	151.2	54.6	474.7	73.8	641.1
	532.7	8	30.3	1180	10131	18.5	160.8	58.1	504.9	78.4	681.8
	529.6	3	31.0	1299	10064	20.5	176.4	64.4	553.9	86.9	747.9
	527.7	10	30.0	1273	11196	21.7	187.0	68.1	587.2	92.0	792.9
	524.6	3	31.0	1398	10831	23.9	203.8	75.0	639.9	101.3	864.1
				S_c		Cohesive					
	524.6										
	522.7			246		0.2		75.6	640.5		
	520.6			374		0.6		76.9	641.8		
	517.7			187		0.9		77.8	642.7		
	514.6			346		1.4		79.4	644.3		
	512.7			288		1.7		80.3	645.2		
	509.6			360		2.3		82.2	647.1		
	507.7			382		2.7		83.5	648.4		
Soft	504.6			259		3.1		84.7	649.6		
Seds	502.7			461		3.5		86.0	650.9		
Peat	499.6			350		4.0		87.6	652.5		
	497.7			403		4.4		88.8	653.7		
	494.6			360		5.0		90.7	655.6		
	492.7			490		5.5		92.3	657.2		
	489.6			259		5.9		93.5	658.4		
	487.7			389		6.3		94.8	659.7		
	482.7			187		6.8		96.4	661.3		
	479.6			288		7.2		97.6	662.5		
	477.7			432		7.6		98.9	663.8		

TABLE 28 (Cont.)
MUSKEGON PILES - SIDE SHEAR COMPUTATION

DATA FROM BORING 1, 2						Cumulative Capacity					
Subsoil	Elevation, ft Ground Surface 588.0[b]	N Blows Per ft	θ deg	Soil Resistance Values, psf		Side Shear (each major stratum) tons per lin ft of Perimeter		Side Shear, tons			
								LTP 2, 3, 4, 6, 7, 8, 9 P = 3.14 ft		LTP 5 P = 4.24 ft	
								Min.	Max.	Min.	Max.
	477.7										
	474.6	11	29.9	3943	35140	6.1	54.5	118.1	837.3		
	472.7	15	29.3	3638	37200	9.6	89.8	129.0	945.8		
	469.6	5	30.8	4274	33480	16.2	141.7	149.8	1108.7		
Compact Sand	467.7	18	28.8	3603	39753	19.6	179.5	160.4	1227.4		
	464.6	12	29.7	3887	37172	25.6	237.1	179.3	1408.3		
	462.7	41	25.5	2826	54177	28.3	288.6	187.8	1570.0		
	459.6	34	26.5	3105	50186	31.1	366.4	202.8	1814.3		
	457.7	35	26.5	3140	50742	36.1	414.6	212.2	1965.6		
	454.6	9	30.2	4317	37585	42.8	472.9	233.3	2148.7		
	454.6										
	451.7			518		0.8		244.6	2235.9		
	451.0			490		1.0		245.2	2236.5		
	445.6			374		2.0		248.4	2239.7		
	442.7			648		2.9		250.2	2242.5		
	440.6			317		3.2		252.1	2243.4		
	437.7			374		3.7		253.7	2245.0		
	435.6			288		4.0		254.7	2246.0		
Firm Clay	432.7			432		4.6		256.5	2247.8		
	430.6			403		5.0		257.8	2249.1		
	427.7			346		5.5		259.4	2250.7		
	425.6			317		5.8		260.3	2251.6		
	422.7			346		6.3		261.9	2254.2		
	420.6			288		6.6		262.8	2255.1		
	417.7			403		7.2		264.7	2256.0		
	415.6			288		7.5		265.7	2257.0		
	412.7			288		7.9		266.9	2258.2		
	411.0			288		8.1		267.5	2258.8		
	411.0										
Very Compact Sand	410.0	24	27.7	5148	66370	2.6	33.2	275.6	2363.0		
	409.0	103[c]	26.1	4426	76710	4.8	71.8	282.6	2484.3		
	408.0	103[c]	26.1	4439	76939	7.0	110.3	289.5	2605.1		

(a) Computed from boring blow count (N)
Assumed soil unit weights (w) as follows: Peat - 90 pcf, Sand - 115 pcf, Clay - 125 pcf, submerged sand - 55 pcf
(b) Water table elevation 580.0
(c) Based on average measured ASTM blow count in very compact sand

TABLE 29
MUSKEGON PILES - TIP CAPACITY COMPUTATION AND PILE SUMMARY

Driving Data				Pile Tip Capacity											Pile Capacity Summary							
Pile	Pile Type	Hammer Type and Manufacturer's Maximum Rated Energy, ft-lb	Final Driving Resistance (blows/last increment) at Tip Elevation, ft	General Equation for Tip Capacity in Granular Soil $R_{tip} = \frac{A}{2000}\left[\frac{1}{3} Kw \frac{B}{2} \cot^5\theta + wh\,(\cot^4\theta - 1)\right]$											Cumulative Side Shear Capacity, tons		Computed Capacity (shear + tip), tons		Load Test Capacity, tons		Computed Capacity, tons	Ratio of Load Test to Computed, percent	
				Min. and Max.	N	θ deg	A sq ft	K	w pcf	B ft	$\cot^5\theta$	wh psf	$\cot^4\theta$	R_{tip}, tons	Min.	Max.	Min.	Max.	Cycle		Most* Probable	Cycle	
																			First	Final		First	Final
LTP 2	12-in. diam. .230 in. wall closed-end	Vulcan No. 1 15,000	8.0/last in. 530.0	Min.	3	31.0	0.79	0.7	55	1.00	12.75	3670	7.66	9.7	63.6	547.6	73.3	557.3	70	100.0	75.6	93	132
				Max.	17	28.9	0.79	2.4	55	1.00	19.48	3670	10.76	14.2			77.8	561.8					
LTP 3	12-in. diam. No. 7 gage fluted-tapered closed-end	Vulcan No. 1 15,000	2/last 1/2-in. 530.2	Min.	3	31.0	0.35	0.7	55	0.67	12.75	3681	7.66	4.3	63.6	547.6	67.9	551.9	50	55.0	68.9	73	80
				Max.	17	28.9	0.35	2.4	55	0.67	19.48	3681	10.76	6.3			69.9	553.9					
LTP 4	12-in. diam. .230 in. wall open-end (jetted)	Vulcan No. 1 15,000	13/last 6 in. 530.0	Min.	3	31.0	0.06	0.7	55	1.00	12.75	3670	7.66	0.7	63.6	547.6	64.3	548.3	35	42.5	64.5	54	66
				Max.	17	28.9	0.06	2.4	55	1.00	19.48	3670	10.76	1.1			64.7	548.7					
LTP 5	step-taper shell 9-1/2 in. tip diam. with 1 in. step each 8 ft closed-end	Raymond 15M 15,000	36/last 6 in. 530.0	Min.	3	31.0	0.49	0.7	55	0.79	12.75	3670	7.66	6.0	85.8	739.4	91.8	745.4	90	100.0	93.2	97	107
				Max.	17	28.9	0.49	2.4	55	0.79	19.48	3670	10.76	8.8			94.6	748.2					
LTP 6	12-in. diam. .250 in. wall closed-end	Delmag D-22 39,700	3/last in. 460.0	Min.	9	30.1	0.79	1.5	55	1.00	15.50	12486	8.96	39.3	200.9	1782.8	240.2	1922.1	270	273.0	266.4	101	102
				Max.	41	25.5	0.79	5.2	55	1.00	40.84	12486	19.44	91.7			292.6	1874.5					
LTP 7	12-in. diam. .250 in. wall closed-end	Vulcan 80C 24,450	213/last 5 in. 409.6	Min.	24	27.9	0.79	3.2	55	1.00	24.12	19744	12.75	91.9	277.7	2399.6	369.6	2491.5	Greater than 370		495.2	---	---
				Max.	191	23.4	0.79	13.3	55	1.00	65.90	19744	28.47	217.5			495.2	2617.1					
LTP 8	12-in. diam. .250 in. wall closed-end	Delmag D-22 39,700	64/last in. 409.9	Min.	24	27.9	0.79	3.2	55	1.00	24.12	19744	12.75	91.9	276.3	2375.2	368.2	2467.1	Greater than 370		493.8	---	---
				Max.	191	23.4	0.79	13.3	55	1.00	65.90	19744	28.47	217.5			493.8	2592.7					
LTP 9	12-in. diam. .250 in. wall closed-end	Vulcan 80C 24,450	11/last 2 in. 459.8	Min.	9	30.1	0.79	1.5	55	1.00	15.50	12497	8.96	39.4	201.9	1799.6	241.3	1839.0	235	235.0	267.5	87	87
				Max.	41	25.5	0.79	5.2	55	1.00	40.84	12497	19.44	91.8			293.7	1891.4					

* Average of minimum and maximum tip capacity, plus minimum side shear for all piles except LTP's 7 and 8.

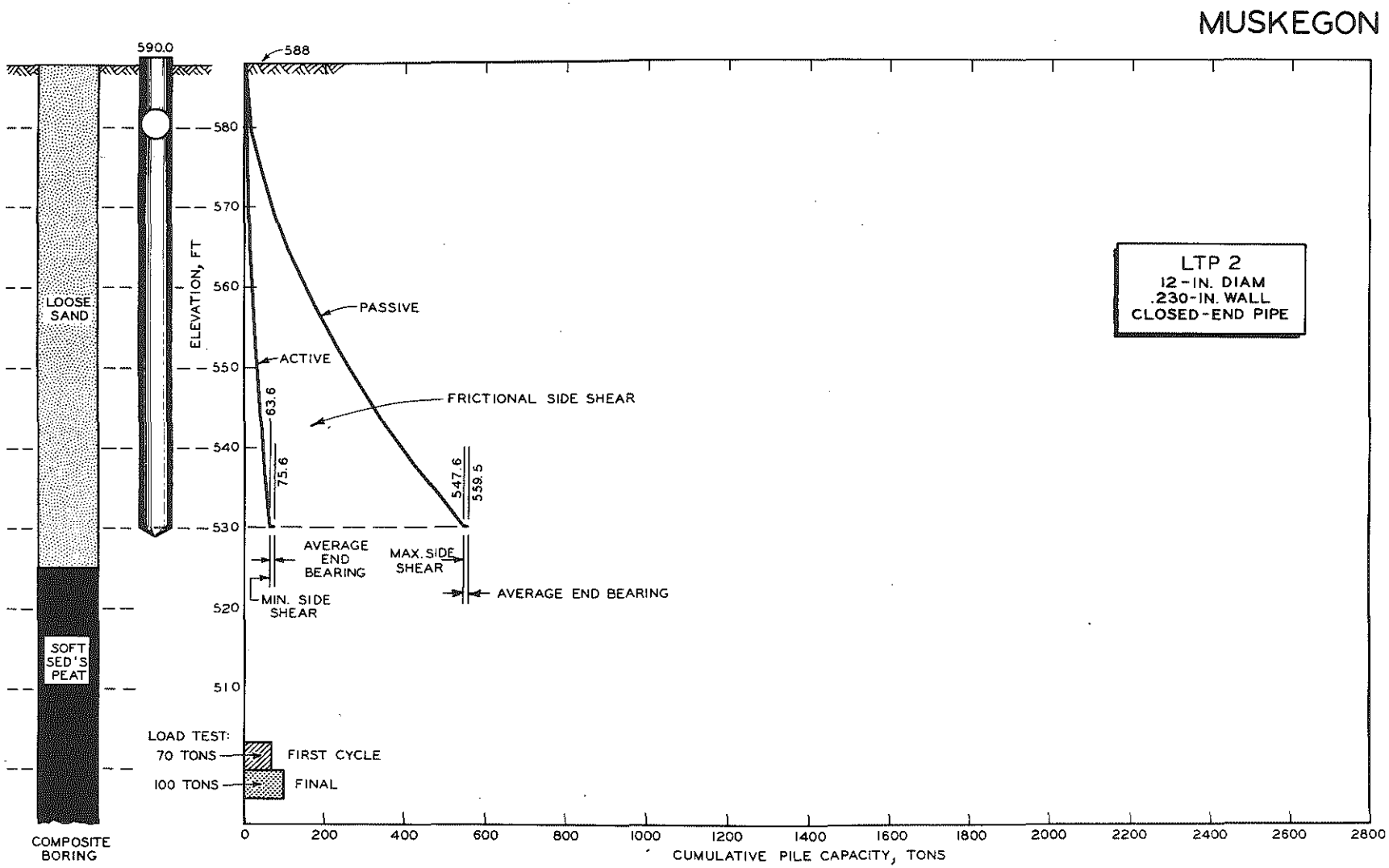

Figure 139. Comparison of computed and measured capacities for Muskegon LTP 2.

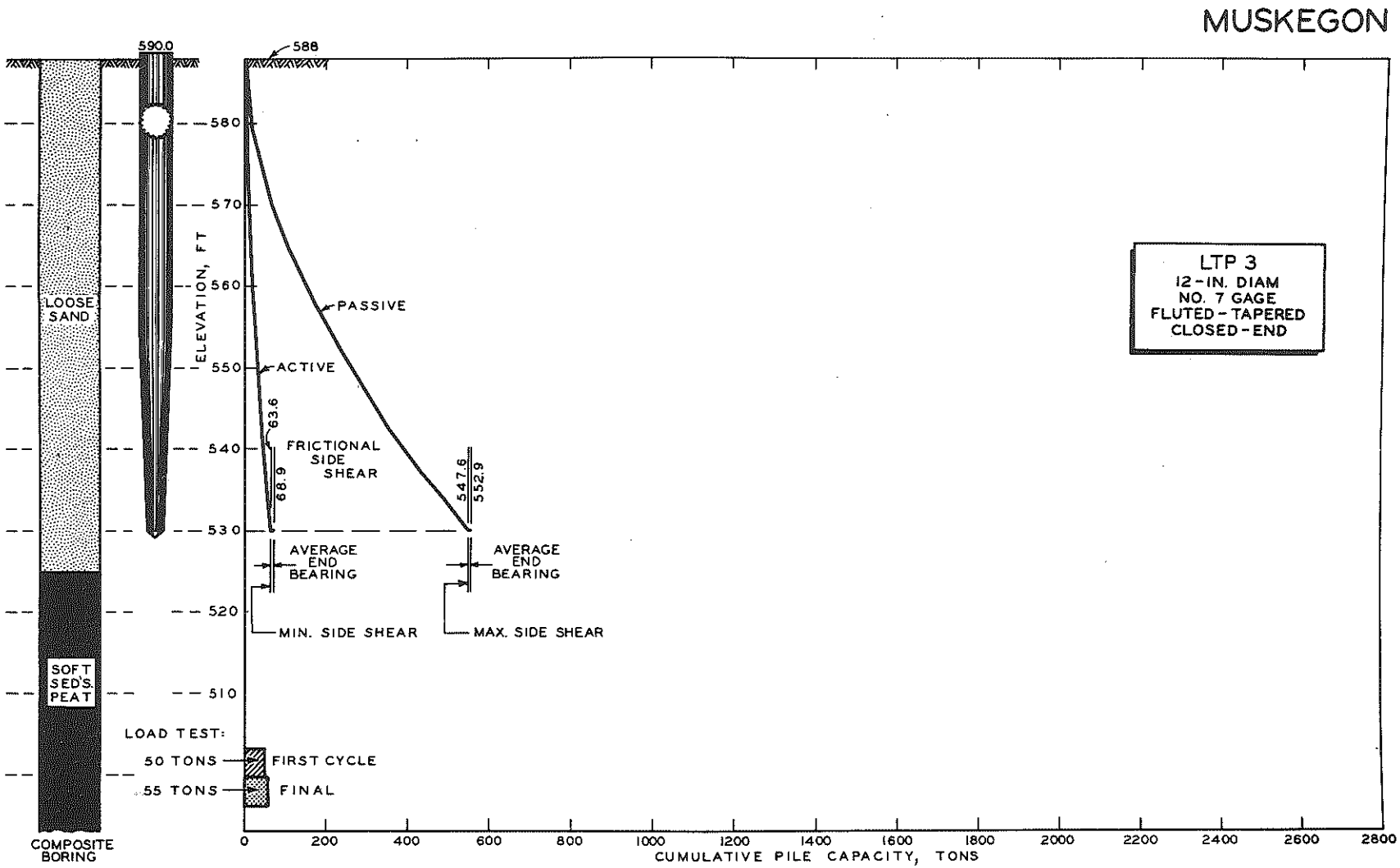

Figure 140. Comparison of computed and measured capacities for Muskegon LTP 3.

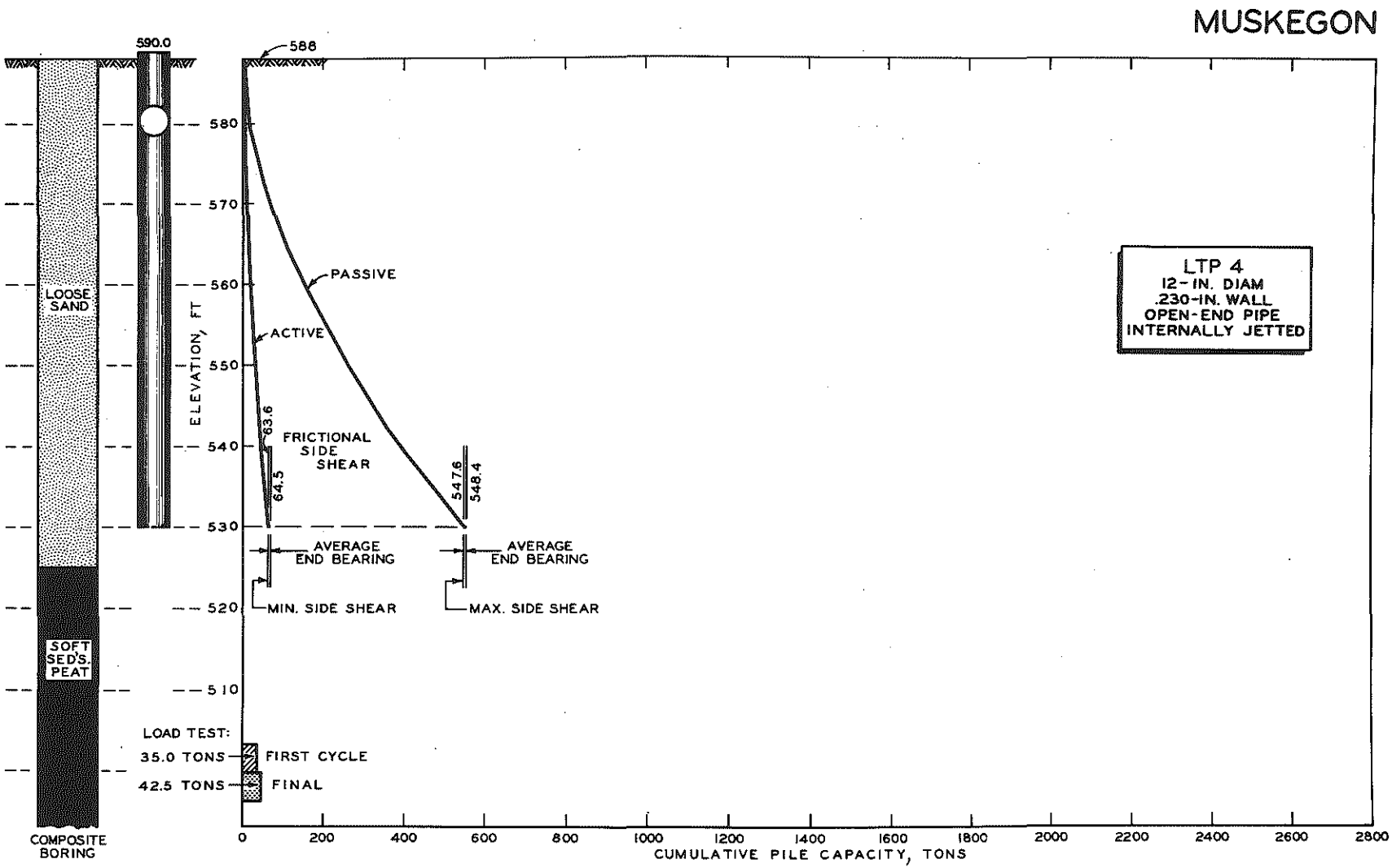

Figure 141. Comparison of computed and measured capacities for Muskegon LTP 4.

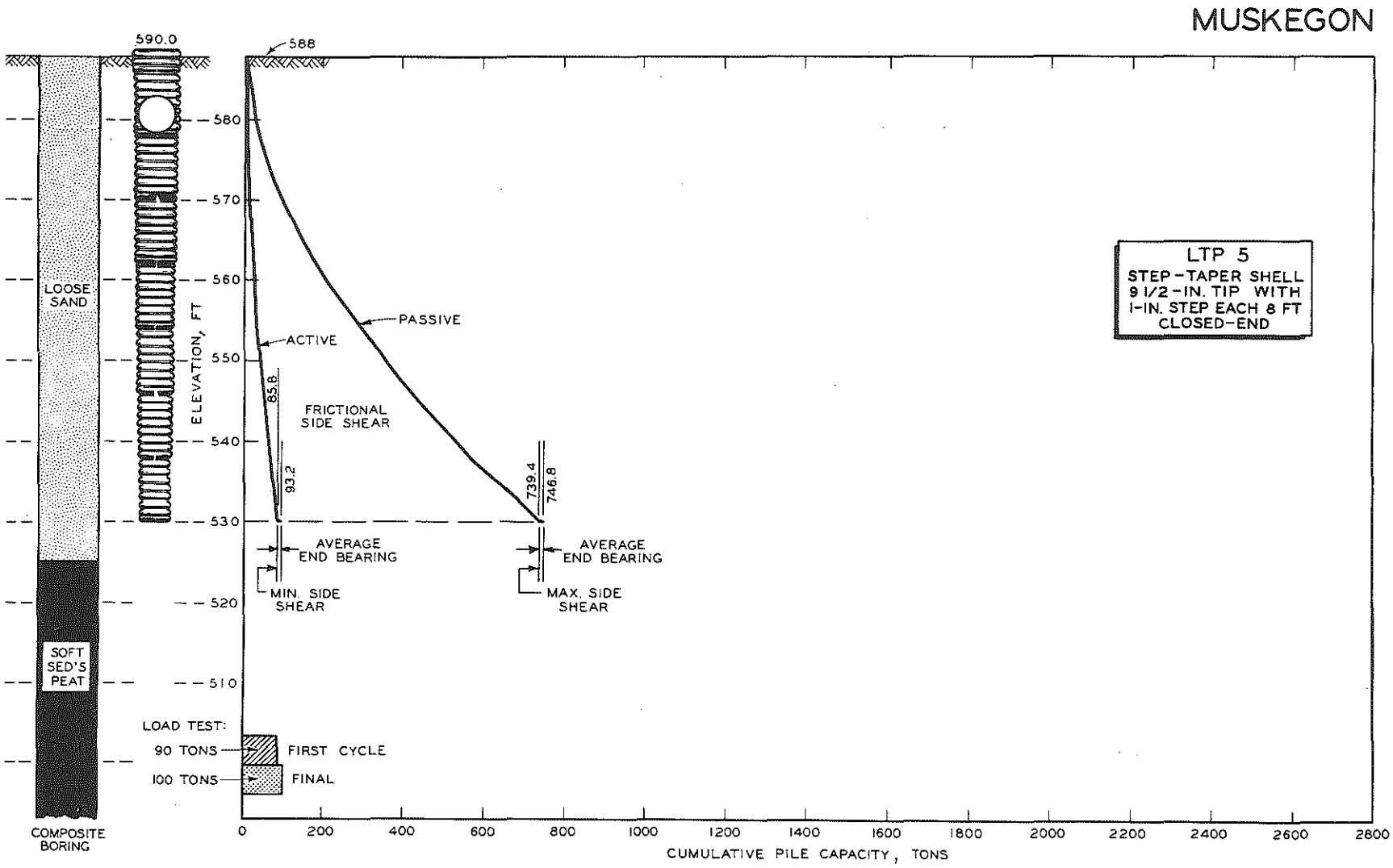

Figure 142. Comparison of computed and measured capacities for Muskegon LTP 5.

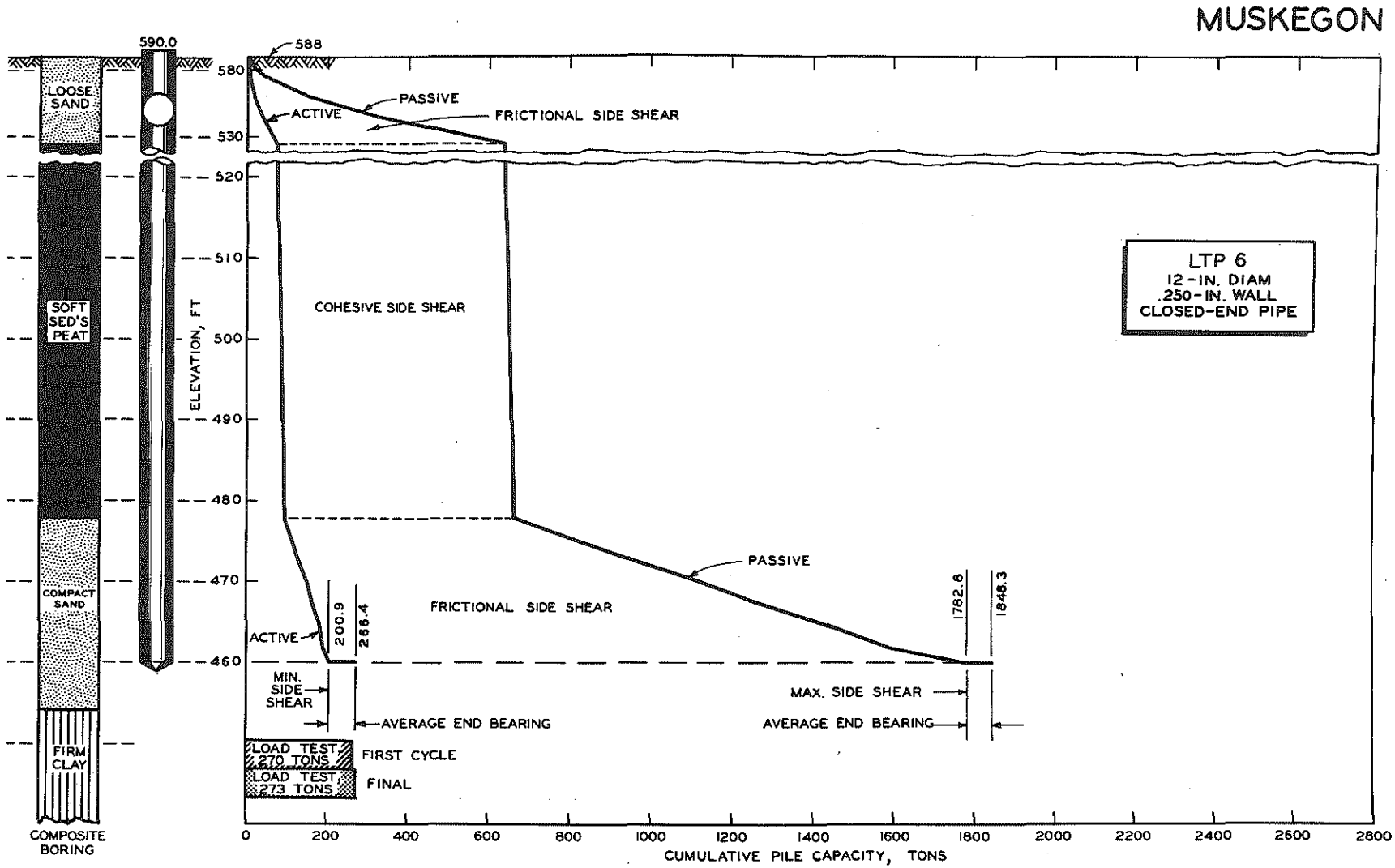

Figure 143. Comparison of computed and measured capacities for Muskegon LTP 6.

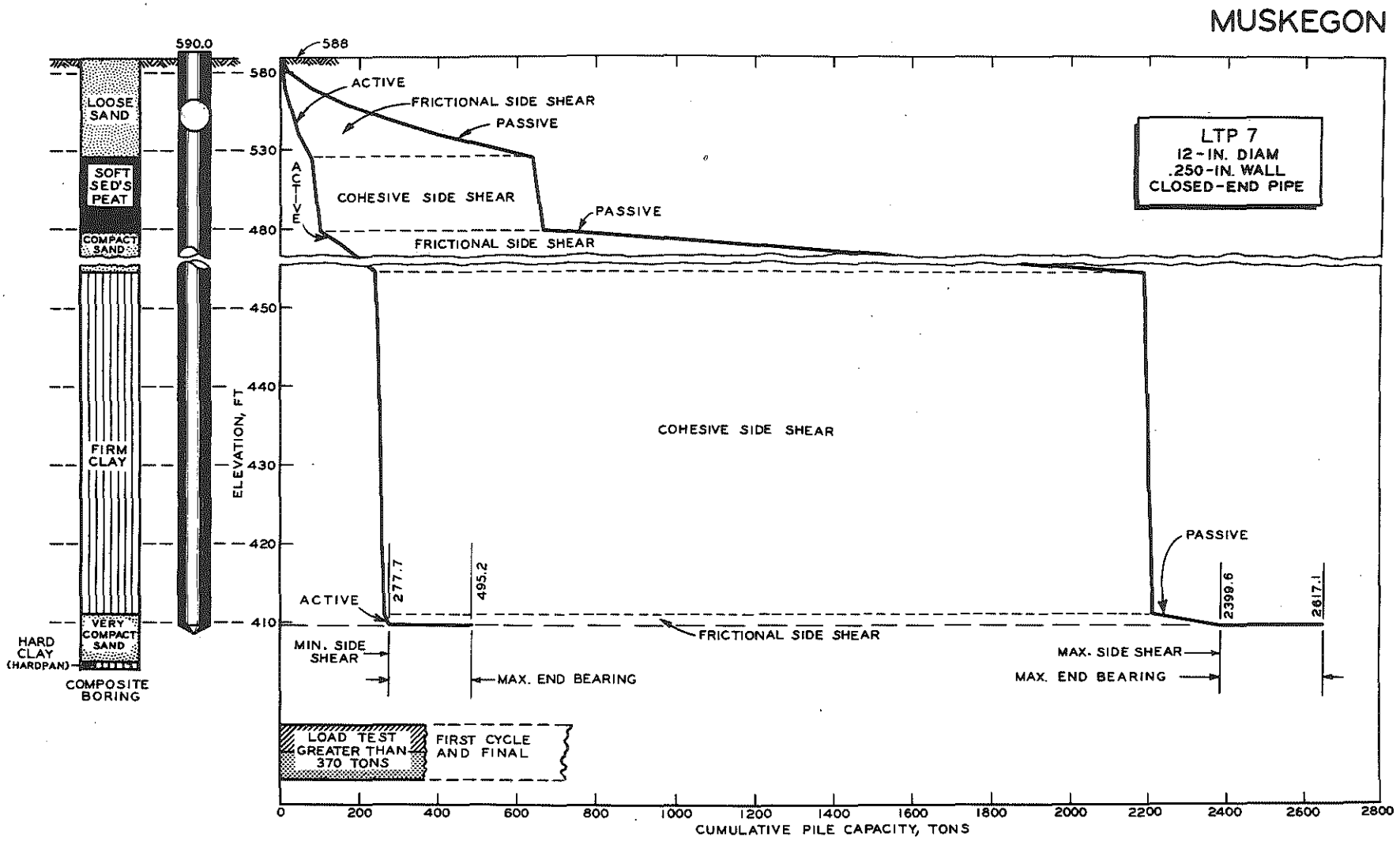

Figure 144. Comparison of computed and measured capacities for Muskegon LTP 7.

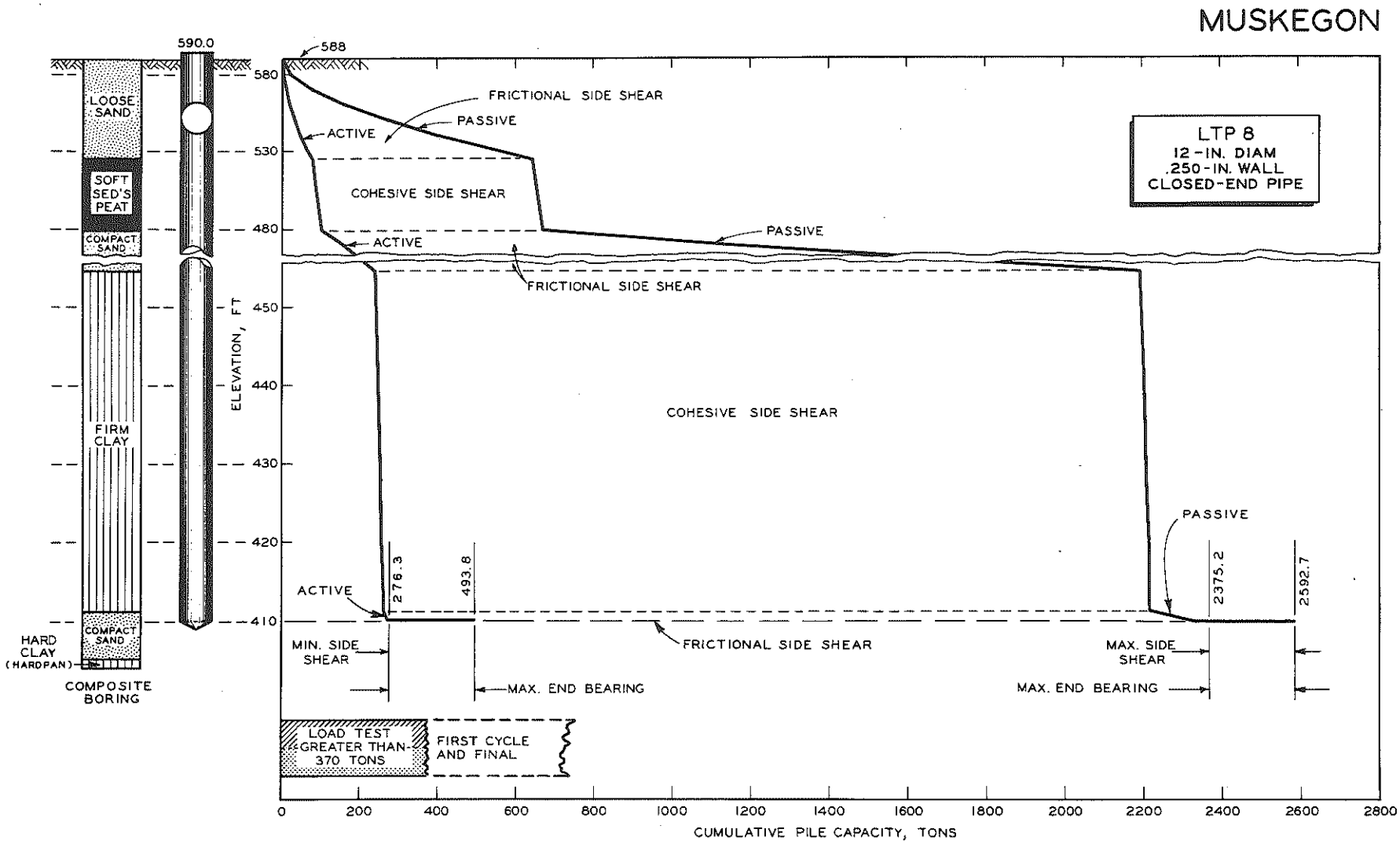

Figure 145. Comparison of computed and measured capacities for Muskegon LTP 8.

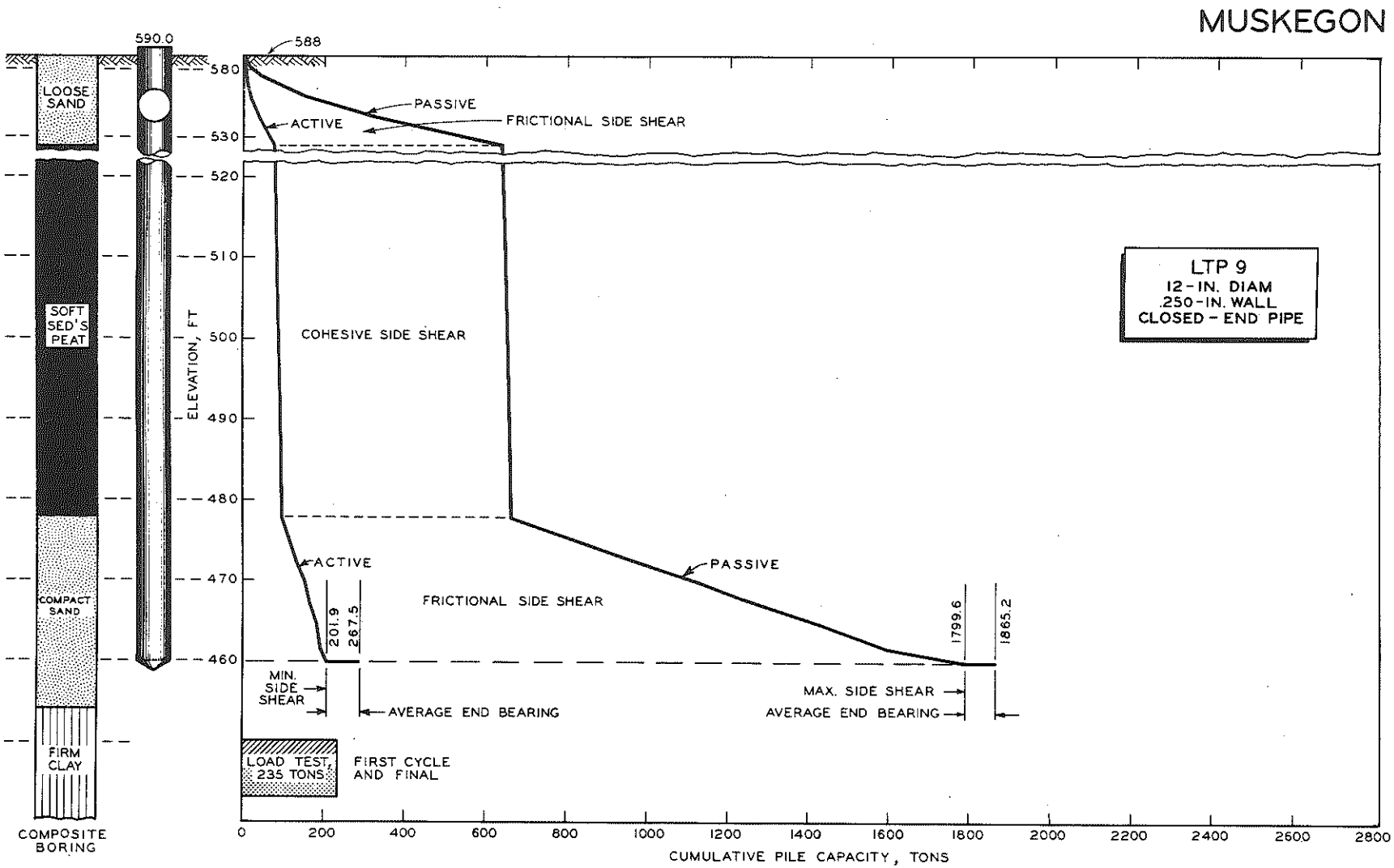

Figure 146. Comparison of computed and measured capacities for Muskegon LTP 9.

determined from the standard penetration blow count by an empirical relationship ($S_E = 30\ N$) developed in previous investigations.

In granular materials side shear results from friction and depends on two indeterminate factors that may vary with test conditions--the magnitude of lateral pressure acting normal to the shear surface of the pile, and the coefficient of friction. The range of lateral pressure from minimum or active pressure to maximum or passive pressure has been computed as the limits within which the normal pressure may vary. The equations for active and passive pressure are based on the theory of internal stability of granular materials developed during 30 years of research at the University of Michigan.[4] [5] This theory of internal stability, used by the Michigan State Highway Department,[6] is based primarily on triaxial compression tests dating back to 1934, but also includes field correlations. It is obviously impossible to elaborate on this development in the present discussion, but it is desirable to indicate the origin of relations used in the computations and to provide suitable references.

In evaluating granular materials, the basic concept of internal stability defines the relationship between principal pressures as a function of resistance to displacement in the soil mass, through mutual support between adjacent particles too large to be measurably affected by molecular forces. Quantitatively, internal stability is expressed by the angle of pressure transmission θ and functions of that angle.

Curves and tables for translating standard field penetration blow counts into angles of pressure transmission and their functions have been developed through a continuous process of refinement as field data have become available. The most recent correlations are given in the Department's "Field Manual of Soil Engineering"[6] and were used in the computations of pile capacity.

Pile Tip Capacity or Bearing on Hardpan

Detailed computations of pile tip capacity or point resistance for each test site are given in Tables 25, 27, and 29. Equations for com-

---

[4] Housel, W. S. "Internal Stability of Granular Materials." ASTM Proc., Vol. 36, Part II (1963), pp. 426-458.

[5] Housel, W. S. "Interpretation of Triaxial Compression Tests on Granular Mixtures." AAPT Proc., Vol. 19 (1950), pp. 245-260.

[6] "Field Manual of Soil Engineering" 4th Edition. Lansing: Michigan State Highway Dept. (1960).

puting tip capacity in terms of internal stability are provided for granular materials and for granular-cohesive mixtures. The general equation for tip capacity is as follows:

$$R_{tip} = \frac{A}{2000}\left[\frac{1}{3} K w \frac{B}{2} \cot^5 \theta + \frac{2 S_c (1 + \cot^2 \theta)}{\sin 2\theta} + w h (\cot^4 \theta - 1)\right]$$

where

R_{tip} = pile tip capacity, tons

A = pile tip area, sq ft

K = edge factor

w = soil unit weight at pile tip, pcf

B = pile tip minimum width, ft

θ = angle of pressure transmission, deg

S_c = transverse shearing resistance (ring shear yield value) at pile tip, psf

w h = surcharge pressure at pile tip, psf

h = pile length below ground surface, ft

The original development of these equations is given in the literature,[4] [5] and is only briefly discussed here. Tip capacity in granular materials is derived from two sources--internal stability or mechanical resistance to displacement in the loaded soil mass, and the passive resistance generated by surcharge. In granular-cohesive mixtures the difference in principal pressures due to cohesion is added to the two other sources of tip capacity.

In computing tip capacity by the stability equations under discussion, the angle of pressure transmission $\underline{\theta}$ is the quantitative control which translates the structural properties of the soil mixture into bearing capacity. In other words, $\underline{\theta}$ is the angle at which pressure is transmitted and is also the angle of potential displacement or failure. This angle is determined by the mechanical arrangement of the particles and is inherent in the material. With the angle of failure controlled by the granular structure, shearing resistance due to cohesion is presumed to act at that same angle, even though the failure surface at this angle is not the plane of maximum shearing stress.

COMPARISON OF COMPUTED AND MEASURED CAPACITY

Pile capacities at each site are summarized in Tables 25, 27, and 29, in which the three important factors in total pile capacity--cohesive side shear, frictional side shear, and point resistance or end bearing--are combined, and are also shown in the graphs supplementing these tables. Total computed capacity, in tons, is given in terms of a minimum and a maximum, and the actual capacity is expected to fall between these limits. In the tables and graphs, capacities from the load tests are given for the first and final loading cycles, selected from the several test determinations (Tables 21, 22, and 23) as the most reliable measure of capacity in each case. In general, those selected are the yield values determined by extrapolating the settlement rate. For piles driven to refusal in Belleville and Detroit hardpan and Muskegon compact sand, two values of tip capacity have been computed, based on the range of standard penetration N in the hardpan. The extent to which tip capacity is mobilized is indicated by comparison with these minimum and maximum values. It should be emphasized that most of these were primarily bearing piles, intentionally driven to practical refusal (33 blows per inch with a Vulcan No. 1 hammer or equivalent, with E_n of 15,000 ft-lb per blow) to develop this potential capacity to the fullest extent possible under field conditions. However, side shear due both to cohesion in the clay and to friction in granular material cannot be neglected, since these are substantial factors in total capacity.

The number of variable factors to be considered, and the fact that several must be estimated rather than measured, makes computation of pile capacity somewhat speculative. The only possible procedure is to evaluate these factors one at a time, preferably in the sequence in which they are developed. In doing so, soil resistance values that are measured can be separated from those that must be estimated, and both can be rated in terms of significance and reliability. Some judgment can then be made as to the acceptability of the final result.

Cohesive Side Shear

Side shear due to cohesion was the first soil resistance to be mobilized under static loading, and was developed by compression and displacement of the pile starting at the top. Special pile tests were conducted with Belleville LTP 1 and Detroit LTP 1, to measure cohesion as a separate factor in pile capacity. Repetitive loading tests (Figs. 107 and 113) were used to evaluate the "set-up" or recovery of clay from remolding along

the shearing surface of the pile, with the results shown in Fig. 147. At Belleville, in the firm cohesive clay, total pile capacity increased from 37 to 80 tons (or approximately 216 percent) in 13 days. At Detroit, in a soft plastic clay, the increase was from 15 to 28 tons (or approximately 186 percent) in 12 days. For Detroit, the evidence suggests the possibility of some additional increase in capacity over a longer period of time.

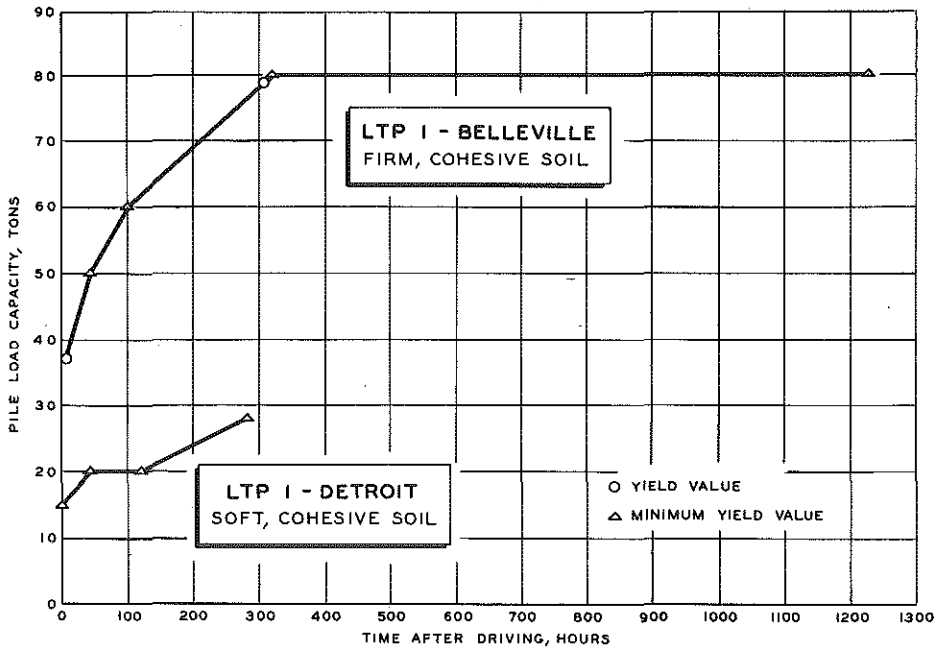

Figure 147. "Set-up" or recovery of strength after driving.

Set-up or recovery of about 200 percent in these two tests is somewhat less than reported for previous tests conducted in this same general area.[7] In the Detroit Edison Company tests in 1931, the increase in capacity was over 300 percent in about 14 days. However, the initial test was conducted about 1-1/4 hr after driving, compared to about 4 hr in the current test. The early recovery from the remolding effect is quite rapid, and could easily account for the greater percentage increase.

The primary objective of the current repetitive loading tests measuring set-up was to determine how soon after driving that loading tests could be conducted with reasonable expectation of developing the full

[7] Housel, W. S. Discussion of "Effect of Driving Piles into Soft Clay." ASCE Proc., Vol. 75, No. 10 (December 1949), pp. 1521-1528.

cohesive side shear. From the data obtained, a period of two weeks appears to be adequate and, with one exception, the elasped time before conducting load tests in this investigation was more than two weeks. That exception was Detroit LTP 2, for which the elasped time was eight days. If cohesive side shear as computed were adjusted for this time effect, the reduction would amount to about 4 tons of a total capacity of 157.8 tons (Fig. 135). No correction has been made for this time effect because it was such a relatively small proportion of total pile capacity, and also because the data available to support this adjustment were considered insufficient to justify such refinement.

The direct comparison between measured and computed pile capacity is summarized for Belleville in Table 25, and in Table 27 for Detroit, and is also shown graphically for the two sites in Figs. 128 through 138. In computing capacity, it is generally assumed that the yield value shearing resistance, based upon the laboratory ring shear test, is the most reliable basis for computing cohesive side shear as a factor in total pile capacity.

For the Belleville LTP 1 test (Fig. 128), designed specifically to measure side shear, measured pile capacity in the final loading cycle was 80 tons, which is 25-percent higher than the most probable computed capacity of 63.8 tons. At Detroit, measured capacity for the final loading cycle was 28 tons, which was 14-percent higher than the most probable computed capacity of 24.5 tons. As was previously pointed out, the Belleville comparison is based upon a single boring since soil resistance varied considerably over the test area, and it was felt that the difference between computed and tested capacity also might be considerable. Under the circumstances the correlation is considered quite acceptable. At Detroit, the correlation is based upon an average of three borings, and from previous experience, a correlation within 10 percent was expected.

While results of this correlation between measured and computed capacity for cohesive side shear are fairly good, some comment is probably desirable on several possible sources of the differences that were found. For example, at Belleville it was assumed that side shear would be entirely cohesive and computations were based upon laboratory tests at zero normal pressure. In the Belleville firm clay it would not be unreasonable to expect some frictional side shear in addition to the cohesion, and certainly enough to account for the 25 percent by which measured capacity exceeded computed capacity. In addition, there is always the presumption of some disturbance during sampling, resulting in lower shearing resistance test results in the laboratory than under natural, in-place conditions in the field. Previous experience in thou-

sands of tests and numerous field correlations indicates, however, that the effect of sampling disturbance has seldom been a significant factor in correlation of field and laboratory test results.

At Detroit, the soft or plastic clay soils have generally been treated as a purely cohesive material with little evidence of any significant internal friction. In this case, however, there is another factor that may have affected the results, involving an inside core some 34 ft long, and the point resistance which might be developed under repetitive loading. In the 1931 Detroit Edison tests,[7] it was found that under repetitive loading a dynamic point resistance was developed which while temporary in character took a considerable period of time for relaxation. Such dynamic resistance, observed in certain soils under driving and in other soils under repetitive loading, could very readily develop a substantial part of the side shear of the soil core. As Fig. 134 shows, this could have produced a total capacity of 36.2 tons. Thus, the final load test value of 28 tons could quite readily include a temporary supporting capacity exceeding the computed capacity by some 4 tons.

Frictional Side Shear

Attention may next be directed to frictional side shear in the deep granular layer at Belleville, as a source of pile capacity. In this case, the lateral pressure acting normal to the pile's vertical shearing surface can vary between the minimum or active pressure and maximum or passive pressure. In Figs. 129 through 133, the active and passive pressures have been plotted as the limits of potential capacity in the stratum of very fine sand and silt. What capacity will actually be developed under testing conditions may be deduced to some extent from the test results but becomes very largely a matter of judgment. This is further complicated by uncertainty as to the actual coefficient of friction value. In computing capacity, the coefficient of friction has not been indicated numerically, but left in the equation as one of the variables, which means in effect that it has been assigned a value of unity as shown in the graphs.

For Belleville LTP 2 (Fig. 129) frictional side shear under active lateral pressure has been combined with cohesive side shear in building up the minimum capacity of 136.7 tons. It may be noted that this is a step-taper pile with a corrugated metal shell so that the internal friction of the granular material itself is involved rather than friction between sand and steel. In previous laboratory tests of internal friction under direct shear, the minimum value of the coefficient of friction measured

in consolidated granular materials was approximately unity, corresponding to an angle of 45°. Thus, it is considered that a coefficient of friction of unity is a reasonable estimate of the minimum frictional side shear. When this minimum is combined with maximum end bearing (which will be discussed later) the total capacity of 263.2 tons compares very well with measured capacity from the loading test. In Table 25, the test load in the first cycle was 10-percent less than the computed capacity and only 1-percent more in the final cycle. The increase in ultimate capacity is due to stress conditioning under static load, creating a change in point resistance. With the excellent comparison between the tested and computed capacity, for this case there seems to be little justification for further speculation regarding passive or maximum pressure.

For Belleville LTP 3 (Fig. 130), which was fluted-tapered, there are some special conditions to be considered. Cohesive side shear has been combined with frictional side shear in the same way as for LTP 2, but there is some question how to evaluate end bearing. From boring data, it would appear that this pile was seated in very fine sand and silt of low end-bearing capacity. However, driving information and load tests indicate that this pile may possibly have been seated in hardpan or material of equivalent bearing capacity. If it is accepted that the pile was seated in fine sand and silt, total bearing capacity would be computed as 85.9 tons. Measured capacities of 160 and 171 tons in the first and second cycles, approach more than twice the computed capacity, suggesting that this assumption is not completely realistic and that this pile may have actually reached bearing in hardpan. This latter assumption appears plausible since resistance to penetration was 29 blows for the last half-inch (with a McKiernan-Terry DE-30 hammer). Thus, the final driving was substantially harder than originally set up for practical refusal. With the pile seated in hardpan, the computed maximum end bearing would produce a total bearing capacity of 160.8 tons. Measured capacity in the first cycle was 160 tons, agreeing closely with the computed capacity, while in the final cycle measured capacity of 171 tons was only 6 percent above that estimate.

While the combination of the cohesive side shear, frictional shear under active lateral pressure, and maximum end bearing in hardpan provides a very favorable comparison with capacity measured by the loading test, a second approach may reasonably be considered in computing pile capacity. It might be assumed that end bearing in the very fine sand and silt was no more than the computed minimum, and that the difference between that minimum capacity and the load test values could

be accounted for by frictional side shear generated by either the active or passive lateral pressure, with the coefficient of friction being considered variable. Following this approach, the coefficient of friction, with reference to active lateral pressure, varies from 2.9 to 3.1, or an average of 3.0 for both loading cycles. If it is assumed that the passive lateral pressure is mobilized, the coefficient of friction would vary from 0.3 to 0.33, or an average of 1/3. The latter coefficient is in a range quite comparable to conventional values for friction between sand and steel, and might be considered an acceptable assumption. Considering that the tapered piling had been driven some 12-1/2 ft into the very fine sand and silt, classified as compact, it would not be unreasonable to assume the possibility of mobilizing the passive lateral pressure in this case.

Driving data (App. A Plate 33) indicated a substantial increase in driving resistance for the final 4-1/2 in., supporting the first of these two possible approaches.

Point Resistance or End Bearing

Point resistance or end bearing, computed as tip capacity in Tables 25, 27, and 29, is the third and possibly most important factor in total pile capacity, inasmuch as most Belleville and Detroit piles were driven to refusal in the hardpan. Tip capacity computation follows a procedure formulated over a period of years in development of "high-capacity" bearing piles in the Detroit metropolitan area. In this procedure, standard penetration has been correlated with internal stability (as previously defined) and is applied to both granular materials and granular-cohesive mixtures.

Stability equations used in this computation are given in Tables 25, 27, and 29, with the computation set forth in successive steps. Because of the magnitude and importance of end bearing, the range of potential capacity has been computed, based on minimum and the maximum field penetration. This range of end bearing is shown in the graphs in combination with cohesive side shear, and also with frictional side shear for both active and passive pressure. This treatment of active and passive pressure applied to Belleville and Muskegon where strata of granular material are involved in side shear capacity. At Detroit, where piles were driven entirely through cohesive soils, maximum and minimum end bearing has been combined with cohesive side shear in making up total capacity.

Summary of Belleville Piles

Belleville LTP's 1, 2, and 3 have already been discussed in terms of total capacity, in connection with cohesive and frictional side shear as controlled by active and passive lateral pressure. For these three piles, it was indicated that with one possible exception combining of minimum side shear components with maximum end bearing provided the most probable combination of the several factors involved.

The same combination seems to hold true for the two other Belleville pipe piles (LTP's 4 and 5). Table 25 shows, however, that measured capacity is from 7 to 11 percent greater than computed capacity in the first loading cycle, and 15 to 16 percent greater in the second. This consistent margin of greater capacity from the load tests is characteristic of all the project's bearing piles. This indicates that driving bearing piles to practical refusal has not only accomplished its objective of developing maximum supporting capacity in the bearing strata, but has produced capacities exceeding those computed from the maximum values of standard penetration from the borings.

For Belleville H-pile LTP 6, combination of cohesive side shear, frictional side shear under active pressure, and minimum end bearing is the basis of the first attempt at computing pile capacity. With the H-pile's small volume displacement and straight-sided shearing surface, there seems to be little basis for developing more than a negligible amount in excess of active lateral pressure. The borings indicate that the pile was seated in very fine sand and silt. Table 25 shows that tested capacity varied from 18 to 22 percent greater than computed capacity, enough to suggest some additional source of supporting capacity. Fig. 133 shows that an end bearing of 5730 psi on the pile's steel end area would be required in addition to the previously computed capacity to account for the maximum load of 206 tons. Even higher stresses are required to account for the total capacity of H-piles in other tests. This subject will be discussed later in more detail.

Tested and computed capacity comparisons for all Belleville piles (Table 25) indicate acceptable results. The final load test capacity, including static stress conditioning varies from 1 to 25 percent greater than computed capacities, with an average of approximately 15 percent. As has been noted, the two highest differences (25 and 22 percent for LTP's 1 and 6, respectively) can probably be explained by factors of resistance not fully evaluated in the computed pile capacity.

Summary of Detroit Piles

All Detroit test piles were driven to refusal in hardpan (except LTP 1, discussed previously). The several factors in the capacity of these piles are cohesive side shear in the soft clay above hardpan, cohesive side shear in the hardpan itself for the depth of penetration involved, and end bearing in hardpan. Cohesive side shear in the soft clay was computed from yield value shearing resistance measured in the laboratory. Cohesive side shear in the hardpan was estimated from an empirical relation ($S_E = 30\ N$, as previously discussed). Average standard penetration blow counts were used in computing cohesive side shear, rather than minimum or maximum penetration values. End bearing was computed for both the minimum and maximum penetration values, to provide a range for comparison with capacity as measured by load tests.

In selecting the most probable combination of the variable factors for computing pile capacity, there are several conditions to be considered. First, the piles were driven to practical refusal, which means that they probably were seated in material approaching or even exceeding the maximum resistance of hardpan in its original state. This could be attributed to consolidation as a result of heavy driving. Another factor entering into ultimate capacity is the stress conditioning due to static loading, evident in practically all the tests. With this combination of conditions, it is not unreasonable to suppose that the end bearing ultimately developed in the hardpan could very well equal or possibly exceed the maximum resistance based on standard penetration values.

This, in effect, is what the load tests actually show, since in all cases measured capacity in the final cycle of loading (and in many cases the first cycle) exceeds the computed combination of cohesive side shear and maximum end bearing. This is shown very clearly in Figs. 135 through 138 in the graphical comparison between load test values and computed capacity. The results are also summarized in Table 27, which shows that measured capacity for all pipe piles exceeds the computed capacities in amounts varying from 5 to 73 percent.

The LTP 8 (H-pile) load test needs special consideration. End bearing, computed on the basis of maximum resistance of the hardpan acting on the steel end area, falls far short of accounting for the measured capacity. Fig. 137 shows that if the measured capacity of 180 tons in the final loading cycle is taken as this pile's maximum capacity, actual bearing on the steel end area would amount to 15,250 psi. This bearing pressure is comparable to the unconfined compressive strength obtained

in several investigations of Detroit area bedrock. From the high capacity developed by H-piles under these conditions, it would appear that they reached bearing on rock either by penetrating through the hardpan to bedrock, or accumulating rocks and boulders under the tip in sufficient quantity to develop rock bearing pressures over most of the steel end area. This hypothesis must be regarded as speculative, but it is not without precedent and there is no escaping the test results which show consistently that a reaction of this magnitude must have been realized.

In this connection, reference is made to two other sources of corroborating information. In the AASHO Bridge Specifications the maximum design load for steel piles in point bearing is given as 6,000 psi.[8] A second reference is provided by Chellis,[9] who recommends pressures for steel H-piles driven to bearing on rock of 3,000 to 6,000 psi in comparison with the crushing strength of rock ranging from 6,000 to 18,000 psi.

Summary of Muskegon Piles

As has been noted, Muskegon soil conditions differed notably from those at the other two sites, with alternating layers of granular and cohesive soils making evaluation of both cohesive and frictional side shear of major importance. Computations of cumulative capacity due to side shear are given in Table 28. Computations of total capacity are given in Table 29, along with comparisons of measured and computed capacity (these comparisons also being shown in Figs. 139 through 146). Minimum and maximum values of frictional side shear, corresponding to the active and passive lateral pressure, were computed and are plotted for all granular materials. Side shear in the cohesive materials was based on individual yield shear values obtained in the laboratory from the ring shear test. Two end-bearing values were computed corresponding to the range of standard penetration in the granular materials where pile tips were seated. It is re-emphasized that most Muskegon load test piles were driven to specific elevation rather than to refusal, and may not necessarily have developed maximum bearing. However, in the case of the two piles driven to refusal in the very compact sand (LTP's 7 and 8), it might be anticipated that maximum end bearing was mobilized.

---

[8] "Bearing Value of Piling" (Section 1.4.17). AASHO Standard Specifications for Highway Bridges, 8th Edition (1961), pp. 54-57.

[9] Chellis, Robert D. "Pile Foundations" 2nd Edition. New York: McGraw-Hill (1961), p. 315.

The first four load test piles (LTP's 2, 3, 4, 5) were about 58 ft long, driven to the same elevation in the upper stratum of loose sand. The direct comparison between computed and measured capacity in Figs. 139 through 142, indicates quite clearly that the mobilized frictional side shear falls in the range produced by active lateral pressure, as might be anticipated in loose sand. The results also indicate some interesting variations in the capacity of these four friction piles, related to their surface configuration and certain other conditions associated with driving. In comparing computed and measured capacities (Table 29), minimum side shear capacity has been combined with average end bearing. Side shear values are based upon an assumed coefficient of friction of unity, which may be modified by direct comparison with the measured capacity. As noted before, both minimum and maximum end bearing were computed, but in the loose sand even using the maximum values of standard penetration the range of end bearing was very small. Here, too, the piles have probably not developed maximum resistance to penetration.

In Table 29, the ratio between tested and computed capacity indicates that LTP 4 developed the smallest proportion of the computed capacity--54 and 66 percent in the first and second loading cycles, respectively. It is also significant in Fig. 120 that this pile in both loading cycles showed very high settlements, up to a total of 7-1/2 in. with little indication of improvement due to stress conditioning under static load. Without differentiating between end bearing (which was of minor importance) and frictional side shear, the coefficient of friction of sand and steel (based on active lateral pressure) varied from 0.54 to 0.66. The most significant condition in connection with LTP 4's low capacity was its internal jetting during driving, which left the pile water-filled with approximately 1-1/2 ft of sand core at the bottom.

Fluted-tapered LTP 3 developed the next lowest capacity under static loading, amounting to 73 to 80 percent of the computed capacity, in the first and second cycles, respectively. Its load-settlement characteristics (Fig. 119) were similar to the jetted pile (LTP 4), although the total settlement was substantially less. The fact that it was driven as a closed-end pile and involved considerable volume displacement, coupled with the advantage of taper, would indicate at least some consolidation of the loose sand, leading to a somewhat higher value of total supporting capacity. Based on active lateral pressure, this pile provided a coefficient of friction varying from 0.7 to 0.8 in the first and second cycles.

Step-tapered LTP 5, with the corrugated shell, had the highest computed capacity (93.2 tons) of any ot the four friction piles under consider-

ation. It developed 97 percent of this capacity in the first cycle and 107 percent in the second, showing that it mobilized the computed strength consistently in both cycles. A coefficient of friction close to unity is consistent with the fact that the shearing failure was forced to take place in the granular material itself rather than being conditioned by friction between sand and steel. Compared to the two weaker friction piles, greater volume displacement in this case appeared to produce some improvement due to preconsolidation of the loose sand. The increase in capacity of some 10 percent between the first and second cycles would indicate at least a small amount of improvement due to stress conditioning under static load, presumably resulting largely from consolidation under its tip.

LTP 2 is closely comparable to the step-tapered pile insofar as behavior is concerned, developing the same load capacity of 100 tons in the second cycle. Any difference in behavior stems from this straight-sided pipe's developing less capacity in the first cycle than the corrugated shell, indicating a somewhat lower coefficient of friction. At the same time, it showed a considerably higher increase in capacity in the second loading cycle (up to 132 percent of the computed capacity) indicating more improvement due to stress conditioning under static load. Again presuming this increase to be largely related to consolidation under the pile tip, and considering that a 12-in. pipe has a larger volume displacement than a step-tapered shell, the combination of conditions points to greater consolidation of loose sand as the major factor involved in the higher capacity.

The tips of LTP's 6 and 9, driven through the upper loose sand and soft sedimentary peat into the compact sand, penetrated approximately to elevation 460.0. Both minimum and maximum end bearing were computed corresponding to a range in standard penetration from 9 to 41 blows. However, the major factor in capacity is still side shear. Had these piles been driven to refusal in the compact sand, it might have been expected that the maximum point resistance would be mobilized. However, direct comparison between tested and computed capacity indicates that LTP 6's measured capacity was very close to its average computed capacity, while LTP 9's measured capacity was only 87 percent of the average computed capacity, and only 96 percent of the minimum computed capacity.

Finally, LTP's 7 and 8 were actually driven considerably harder than the nominal project requirement. LTP 7 was driven 42 blows to the last inch with a Vulcan 80C. LTP 8 was driven 74 blows to the last inch with a Delmag D-22. Both piles were driven to a depth of 178 ft

(elevation 410) and were anticipated to develop maximum available tip capacity. Figs. 144 and 145 show the computed capacity to be made up of minimum frictional side shear under active lateral pressure through the upper loose sand and intermediate sand, cohesive side shear through the soft sedimentary peat and firm clay overlying the bearing strata, and end bearing in the very compact sand, for minimum and maximum penetrations of 24 to 191 blows.

Combining total side shear with minimum end bearing (Table 29), results in a total capacity of approximately 369 tons for both piles, or less than the applied load of 370 tons in both cases. This applied load was the maximum possible with the available testing equipment, and in neither case did the results represent the pile's ultimate capacity. This is evident from Figs. 123 and 124, where there is no evidence of yielding and where both piles showed substantially elastic behavior with 100-percent rebound in the final loading cycle. With these two piles driven to refusal in a highly consolidated and highly confined granular material, it would be consistent with results from the other sites to combine minimum side shear capacity with maximum end bearing, as representing the ultimate capacity of these two piles. This would amount to approximately 495 tons, or about 125 tons over the capacity of the testing equipment. Because of the equipment's limitations, no further comparison can be made between computed and measured capacity.

LOAD SETTLEMENT AND PILE ELASTIC PROPERTIES

The compressive strength and modulus of elasticity of the concrete mixtures used in the test piles were reported in Chapter 10 and the physical properties of the piles in Table 2. This information can be combined with measurements of settlement at both the top and bottom of the cast-in-place concrete bearing piles for analysis of their elastic behavior. Through the use of tell-tales at the pile tip these settlement measurements, under full load and after removal of the load, permitted differentiation between elastic and permanent settlement at the tip and elastic and permanent compression of the pile. Previous investigations have shown that with these data available, it is possible to work out stress distribution along the pile side and at the tip in considerable detail.

Circumstances arising in connection with the current investigation have made it necessary to postpone a comprehensive analysis of this nature until some time when the research program can be extended.

However, it was felt that the settlement data should be made available in some convenient form so that anyone could make such analyses if he wished. Detailed settlement and rebound data are reported in Table 30 for all load test piles at the three test sites and will be commented upon briefly.

The load-settlement graphs (Figs. 107 through 125) and the settlement data in Table 30 indicate that the major part of permanent settlement or set is due to consolidation under the pile tip. Elastic rebound in the bearing piles is largely elastic compression of the pile, accompanied by equal elastic deformation in the surrounding soil. Rebound at the pile tip is generally negligible, ranging from 0.05 to 0.2 in. Permanent compression of the cast-in-place concrete piles, where the steel shell acts as vertical reinforcement, is of small magnitude, ranging from 0.02 to 0.2 in. with the exception of the two heavily loaded Muskegon piles (LTP's 7 and 8). For these two piles, due to the heavier load, permanent compression approached 0.5 in. at load applications of 370 tons, which is much less than the usual allowance of 0.01 in. per ton of load.

Two other piles (Belleville LTP 2 and Muskegon LTP 5) require special consideration because their settlement and compression differ from other test results. These are Raymond piles and the corrugated metal shell provides no determinate reaction to vertical compression. Consequently, for all practical purposes, the full load is carried by the concrete. As shown in Fig. 108 and Table 30, permanent pile compression in Belleville LTP 2's second cycle was 1.539 in., with a final settlement at the tip in this cycle of 0.265 in.

As reported in Chapter 10 (page 169), compressive strength of the concrete at 28 days was 5805 psi. LTP 2 was tested 47 days after casting and with some allowance for increasing strength, the ultimate strength would not exceed 6000 psi.

Compressive stress at the top of the Belleville step-taper pile (LTP 2) at maximum load was 2910 psi. Following the load distribution shown in Fig. 129, compressive stress at the bottom of the clay (elevation 602) was 5540 psi and at the tip (elevation 584.3) 5480 psi. Thus, the pile concrete was loaded close to its probable ultimate strength and the permanent compression may have crushed the concrete. At any rate, the pile was loaded far beyond its design capacity and this conclusion would be supported by the apparent lack of permanent settlement at the tip (as shown by the tip tell-tale). On the other hand, erratic behavior of the tip tell-tale was reported from the field; thus, the reliability of tip settlement as reported is subject to question. Under these conditions no positive

TABLE 30
SUMMARY OF LOAD TEST
SETTLEMENT MEASUREMENTS

	Pile No.	Load Cycle No.	Maximum Test Load Applied	Settlement Measurements, in.				Total Elastic Rebound, in.		Total Pile Compression, in.	
				At Maximum Test Load Applied		At Completion of Load Cycle (Set)				Temporary (elastic)	Permanent (set)
				Top	Tip	Top	Tip	Top	Tip		
Belleville	LTP 1	1	55	3.528	---	3.397	---	0.131	---	---	---
		2	70	3.287	---	3.176	---	0.111	---	---	---
		3	80	3.312	---	3.145	---	0.167	---	---	---
		4	96	2.060	---	1.862	---	0.198	---	---	---
		5	90	1.066	---	0.857	---	0.209	---	---	---
		6	105	2.068	---	1.884	---	0.184	---	---	---
		Total Set	---	---	---	14.321	---	---	---	---	---
	LTP 2	1[a]	285	2.228	---	1.828	---	0.400	---	---	---
		2	330	2.448	0.454	1.804	0.265	0.644	0.189	0.455	-1.539
		Total Set	---	---	---	3.632	---	---	---	---	---
	LTP 3	1	195	2.021	1.786	1.625	1.668	0.396	0.118	0.278	+0.043
		2[b]	210	2.120	---	1.715	---	0.405	---	---	---
		Total Set	---	---	---	3.340	---	---	---	---	---
	LTP 4	1	360	0.955	0.271	0.253	0.182	0.702	0.089	0.613	-0.071
		2	390	1.056	0.347	0.277	0.251	0.779	0.096	0.683	-0.026
		Total Set	---	---	---	0.530	0.433	---	---	---	-0.097
	LTP 5	1	360	1.093	0.327	0.344	0.231	0.749	0.096	0.653	-0.113
		2	400	1.545	0.721	0.716	0.669	0.829	0.052	0.777	-0.047
		Total Set	---	---	---	1.060	0.900	---	---	---	-0.160
	LTP 6	1	225	2.097	---	1.553	---	0.544	---	---	---
		2	240	2.263	---	1.679	---	0.584	---	---	---
		Total Set	---	---	---	3.232	---	---	---	---	---
Detroit	LTP 1	1	22	3.707	---	3.537	---	0.170	---	---	---
		2	24	2.103	---	1.996	---	0.107	---	---	---
		3	28	3.795	---	3.676	---	0.119	---	---	---
		4	32	1.590	---	1.515	---	0.075	---	---	---
		Total Set	---	---	---	10.724	---	---	---	---	---
	LTP 2	1	180	2.133	1.473	1.488	1.335	0.645	0.138	0.507	-0.154
		2	240	3.849	2.962	2.887	2.751	0.962	0.211	0.751	-0.136
		Total Set	---	---	---	4.376	4.086	---	---	---	-0.290
	LTP 7	1	180	3.817	3.265	3.246	3.169	0.571	0.096	0.475	-0.077
		2	190	2.980	2.454	2.391	2.360	0.589	0.094	0.495	-0.032
		Total Set	---	---	---	5.638	5.529	---	---	---	-0.109
	LTP 8	1	220	2.999	---	2.170	---	0.829	---	---	---
		2	240	1.446	---	0.559	---	0.887	---	---	---
		Total Set	---	---	---	2.729	---	---	---	---	---
	LTP 10	1	240	2.785	2.159	2.074	1.992	0.711	0.167	0.544	-0.082
		2	270	4.253	3.709	3.489	3.509	0.768	0.200	0.568	+0.025
		Total Set	---	---	---	5.558	5.501	---	---	---	-0.057

(a) Tell-tale rod bracket broke off (lost gage readings).
(b) Tell-tale rod hung up (lost gage readings).

TABLE 30 (Cont.)
SUMMARY OF LOAD TEST
SETTLEMENT MEASUREMENTS

	Pile No.	Load Cycle No.	Maximum Test Load Applied	Settlement Measurements, in.				Total Elastic Rebound, in.		Total Pile Compression, in.	
				At Maximum Test Load Applied		At Completion of Load Cycle (Set)					
				Top	Tip	Top	Tip	Top	Tip	Temporary (elastic)	Permanent (set)
Muskegon	LTP 2	1	110	1.698	1.643	1.497	1.565	0.201	0.078	0.123	+0.068
		2	110	0.696	0.590	0.551	0.583	0.145	0.007	0.138	+0.032
		3	120	1.871	1.762	1.703	1.712	0.168	0.050	0.118	+0.009
		Total Set	---	---	---	3.751	3.860	---	---	---	+0.109
	LTP 3	1	60	1.393	1.368	1.322	1.349	0.071	0.019	0.052	+0.027
		2	70	2.437	2.374	2.356	2.357	0.081	0.017	0.064	+0.001
		Total Set	---	---	---	3.678	3.706	---	---	---	+0.028
	LTP 4	1	50	2.409	---	2.312	---	0.097	---	---	---
		2	55	5.445	---	5.104	---	0.341	---	---	---
		Total Set	---	---	---	7.416	---	---	---	---	---
	LTP 5	1	120	2.446	2.337	2.294	2.304	0.152	0.033	0.119	+0.010
		2	120	1.327	1.209	1.162	1.165	0.165	0.044	0.121	+0.003
		Total Set	---	---	---	3.456	3.469	---	---	---	+0.013
	LTP 6	1	290	3.663	3.014	2.951	2.925	0.712	0.089	0.623	-0.026
		2	300	2.907	2.334	2.189	2.248	0.718	0.086	0.632	+0.059
		Total Set	---	---	---	5.140	5.173	---	---	---	+0.033
	LTP 7	1[a]	370	1.603	0.146	0.414	(>)-0.060[b]	1.189	0.206	0.983	(>)-0.474
		2	350	1.144	0.160	0.049	0.040	1.095	0.120	0.975	-0.009
		Total Set	---	---	---	0.463	(>)-0.020[b]	---	---	---	(>)-0.483
	LTP 8	1	370	1.787	0.085	0.543	0.006	1.244	0.079	1.165	-0.537
		2	350	1.245	0.087	-0.005[b]	0.009	1.250	0.078	1.172	+0.014
		Total Set	---	---	---	0.538	0.015	---	---	---	-0.523
	LTP 9	1	260	2.272	1.555	1.624	1.521	0.648	0.034	0.614	-0.103
		2	275	2.519	1.874	1.873	1.841	0.646	0.033	0.613	-0.032
		Total Set	---	---	---	3.497	3.362	---	---	---	-0.135

(a) Inadequate gage throw to record complete rebound at zero load.
(b) Negative value indicates that pile position is above starting reference point.

conclusion is possible as to whether this permanent deformation is pile compression, tip settlement, or a combination of both.

The second Raymond pile (Muskegon LTP 5) is among the piles that will be discussed in connection with positive values of permanent pile deformation. The difference between permanent deformation of the two Raymond piles under widely differing conditions is the main reason for devoting some attention to this subject. Actually, this difference in behavior lends some support to the hypothesis to be offered in explaining possible pile elongation in the Muskegon sands.

Positive and negative values of permanent compression or set are given in Table 30. Permanent compression, some of which would normally be expected in such load tests, is indicated by negative values. While neither the possibility of experimental error in gage readings nor malfunction of the recording system can be ignored, the consistent occurence of positive values of pile compression does suggest pile elongation. In such measurements, it is recognized that elastic compression of the pile must be accompanied by elastic compression of the adjoining soil. When side shearing resistance is exceeded, the pile will slip with respect to the soil, but elastic deformation in the surrounding soil generally is maintained during loading and recovered during unloading. Under certain conditions when the pile's elastic deformation exceeds that in the soil, the soil can exert some restraint in recovery of elastic compression by the pile. This restraint adds to the pile's permanent compression, and has been observed and accounted for in the analysis of elastic behavior of piles and surrounding soil.

The peculiar behavior of the shorter piles in loose sand at Muskegon and the consistent positive readings (or elongation) in terms of set or permanent deformation in all cycles for LTP's 2, 3, and 5 suggest a possible deformation mechanism of sufficient interest for brief discussion. Although these positive readings are within the range of experimental error, a possible alternate explanation may be suggested. It might be presumed that these piles developed dynamic point resistance during driving, frequently encountered in fine-grained soils, accompanied by negligible resistance along the side of the pile during driving. After driving, the residual dynamic point resistance could exert an upward force for which the reaction is provided by downward shear forces along the pile as a residual stress and a locked-in compressive strain.

During the testing of these piles under static load, the applied loads would first be carried at the pile tip, tending to neutralize the residual downward shear, as the ultimate tip capacity was being developed. As the applied load reached a maximum, sudden failure resulted, accompanied

by a sharp decrease in the load application and clearly audible and visible re-adjusting of the loading equipment and pile. This behavior suggests a sudden collapse of arching action built up in the granular structure at the pile tip, an equally sudden increase in tip settlement, and transfer of the remaining applied load to side shear, tending to reverse the downward direction of the shearing stress. Considering that pile deformation is measured as the difference between settlement at its tip and its top, the reversal in shear stress and loss of point resistance might result in net elongation of the pile to the extent indicated by the recorded positive values of set.

This hypothesis is offered for possible insight into behavior of piles driven in loose granular materials under the special conditions noted. It is not presumed that a pile can be elongated even the small amounts involved here by mere application of static load. As a first condition, there must be residual soil stresses and locked-in compression from the driving of the pile. Second, the granular material may have to be at a certain state of consolidation, probably not far from the critical density, in order to produce an irregular or jerky build-up and collapse of resistance developed at points of load concentration.

On the other hand, experimental error in gage operation is one of the problems to be overcome in loading tests under field conditions. Any tilting or lateral movement of the pile would affect gage readings, and experience indicates that lateral movements or tilting sufficient to produce settlement readings of the magnitude under discussion, are quite common in tests of this nature. Another source of such error arises from the fact that the reference beams supporting the gages cannot be entirely protected from ground movement associated with shifting the load from the timber cribbing to the pile during the loading process, and shifting it back again during unloading. While discrepancies of this kind cannot be completely avoided, they are comparatively small in relation to total settlement, both elastic and permanent, and do not destroy the value of including permanent compression of the pile in analysis of pile behavior.

PREDICTABILITY OF SUPPORTING CAPACITY FROM SOIL TEST DATA

In conclusion, a brief summary of the detailed analysis of pile load test results and the comparison of measured with computed capacity is desirable. In Fig. 148 ultimate supporting capacity as measured in the pile loading tests has been plotted against the most probable value of

computed capacity. These results are represented by pairs of plotted points showing the measured capacity for both the first and final loading cycles. Thus, the span between these points represents the improvement in bearing capacity due to stress conditioning under static load. The points are identified by test site and pile type for easy cross-reference to Tables 25, 27, and 29.

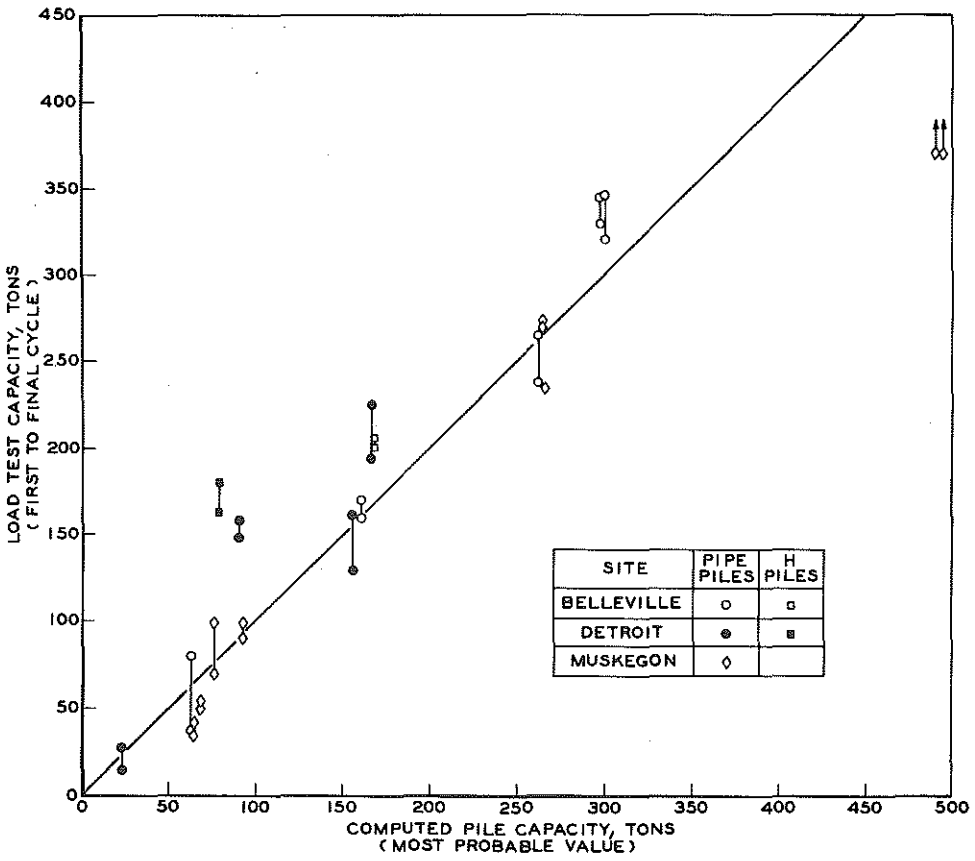

Figure 148. Comparison of computed and measured capacity (yield value or failure load).

The most probable computed capacity represents an assumed combination of resistance factors in the ultimate capacity which appears most representative of pile behavior. With few exceptions, the most probable computed capacity combines cohesive side shear in cohesive soils with minimum frictional side shear in granular materials, and maximum end bearing in the underlying hardpan on rock. In cohesive soils, any additional frictional resistance has been omitted. In friction side shear the coefficient of friction has been taken at unity, subject to later modification in special cases. Frictional side shear under passive lateral

pressure was considered as a possible contribution to ultimate capacity in only one case, an alternate computation of capacity for Belleville LTP 3. For the remaining cases friction is presumed to be a function of active pressure.

First, it is important to note that measured capacity in the final loading cycle for all bearing piles equalled or exceeded predicted capacity, with the exception of Muskegon LTP 9 for which tested capacity was 87 percent of computed capacity based on average end bearing, or 97 percent with minimum end bearing. Second, ultimate capacity of these bearing piles on the first load of the cycle ranged from 82 to 115 percent of computed capacity, except for three piles requiring special consideration. These were Belleville LTP 6 and Detroit LTP's 7 and 8; two were H-piles and the third was a fluted-tapered pile with a relatively small end-bearing area.

Cast-in-place concrete bearing piles driven to refusal in hardpan and stress conditioned under static load, provide an ultimate capacity due to end bearing that exceeds computed capacity by substantial margins. This is shown in Fig. 148 for four pipe piles (Belleville LTP's 4 and 5 and Detroit LTP's 7 and 10). The two other piles with tested capacity substantially above computed capacity in Fig. 148 were the H-piles just mentioned, which developed test loads that could only be accounted for by steel end-bearing approaching the crushing strength of rock at 5,730 to 15,000 psi.

Perhaps one of the outstanding results of the investigation was the conclusive demonstration that bearing piles driven to refusal in highly consolidated and confined granular materials tend to develop end bearing approaching the crushing strength of the granular particles. This confirms previous studies of high-capacity bearing piles in which piles with large bearing areas developed bearing pressures of several hundred tons per square foot, which are eight to ten times the normal bearing values used in past engineering practice.

Several other piles departing somewhat from computed capacities shown in Fig. 148 require only brief comment. Muskegon LTP's 7 and 8 were loaded to the maximum capacity of the testing equipment at 370 tons while the most probable computed capacity exceeded 470 tons. The low-capacity Muskegon friction piles driven in loose sand failed to develop frictional side shear equal to the active lateral pressure, which leads to the conclusion that the coefficient of friction was probably less than the value of one assumed.

CHAPTER TWELVE

DYNAMIC FORMULA STUDY

A principal objective of the hammer performance study was evaluation of the more widely used, representative dynamic pile formulas. It was desired to determine which of these formulas agreed best with actual test capacities, and to indicate any improvements that might be made in the formulas. This study was restricted to include only the project pile driving data and load testing results obtained from the three test sites. For this reason, comparisons and conclusions concerning formulas are at best relative evaluations based on specific hammers, pile types, soil conditions, and similar variables.

Essentially, appropriate pile driving data were applied to the several formulas and estimates of load bearing capacity obtained. These estimates were compared with related pile test loads. The range of indicated safety factors is compared and discussed here.

Initally nine formulas were considered for evaluation, and subsequently two more were included. Although in retrospect, it appears that certain of these formulas essentially duplicate others, the following list of eleven represents the important types in use, or proposed so far, and they are considered here in some detail (abbreviations used in this chapter are given in parenthesis):

1. Engineering News (EN)
2. Hiley
3. Pacific Coast Uniform Building Code (PCUBC)
4. Redtenbacher
5. Eytelwein
6. Navy-McKay
7. Rankine
8. Canadian National Building Code (CNBC)
9. Modified Engineering News (Modified EN)
10. Gates
11. Rabe

Before proceeding with evaluation and comparison of the formulas in terms of conditions at the three sites, a general note of caution must be

stated. It is the consensus of informed engineers that no one dynamic formula, relating dynamic to static resistance, affords a reliable means of estimating the longtime bearing capacity of piles in general. It has been reported that true safety factors may range from less than 1 to 17 when using the Engineering News Formula, and even for the more elaborate formulas of the Hiley type, true safety factors may range by a factor of 5. Thus, unwarranted conclusions should not be drawn concerning the general accuracy or uniformity of results obtained from the several formulas, on the basis of the particular data discussed here.

Presentation and Discussion of Formulas

The following notation is used in the eleven formulas to be discussed:

E_n	Manufacturer's maximum rated energy, ft-lb
S	Set or final average penetration per blow, in.
R_d	Computed design pile load capacity, pounds (derived from dynamic formula)
R_u	Computed ultimate pile load capacity, pounds (derived from dynamic formula)
W_r	Weight of hammer ram, lb
W_p	Weight of pile (including driving appurtenances), lb
L	Total length of pile, ft
C_1	Temporary compression of cap and pile head, in.
$C_2 + C_3$	Temporary compression of pile and ground, in.
e	Coefficient of restitution
A	Net steel cross-sectional area of pile, sq in.
E_L	Modulus of elasticity of steel, 30×10^6 psi
K	Analogous to restitution modulus, e^2

M	Hammer efficiency factor, in. per ft
d	Ratio between developed pile friction at yield point and laboratory-measured unconfined shear strength of soil
B_S	Soil factor (Rabe Formula)
B_L	Pile length factor (Rabe Formula)
B_C	Pile cross-section factor (Rabe Formula)
BPI	Driving resistance, blows per inch of penetration
R_t	Measured (or interpolated) pile yield load, kips (based on static load test)

For brevity, these factors will each be discussed in turn as they first appear in the formulas.

1. Engineering News Formula (Nominal Safety Factor = 6)

$$R_d = \frac{2\ E_n}{S + 0.1} \quad \text{(for single- or double-acting hammers)}$$

The value of energy E_n used in this and succeeding formulas for this study is based on the maximum manufacturer's rating as set forth in the manufacturer's literature. Although these values are often qualified in various ways, only a single maximum value was used for each of the hammers in the comparative analysis. However, rational adjustments of the energy may be desirable in certain practical situations, to compensate for significant variations in steam pressure, length of ram rise, bounce chamber pressure, etc.

The values for set S normally used are the average values obtained during the last 6 in. of driving, or for the actual final inch or less if sudden refusal conditions are encountered.

The basis of the Engineering News Formula is equating the energy available at impact E_n to the energy required to advance the pile through the ground $R_u \times S$, plus energy required to compress the pile, ground, and cap, $R_u \times 0.1$. Given the energy and set, it is then possible to equate for the ultimate capacity R_u, or R_d with designated safety factor.

Although this approach has many theoretical shortcomings, the fact remains that this is the most widely used basis for selecting final blows-per-inch values of light-capacity bearing piles in the United States.

2. Hiley Formula (Nominal Safety Factor = 3)

$$R_d = \frac{4\,E_n}{S + \frac{1}{2}(C_1 + C_2 + C_3)} \times \frac{W_r + e^2\,W_p}{W_r + W_p}$$

The coefficient of restitution e is defined as the ratio of the relative velocity of separation to the relative velocity of approach of the ram and the pile:

$$e = \frac{V'_p - V'_r}{V_r - V_p}$$

A value of $e = 0.45$ was used in the current pile tests for the primary comparisons.

One notes that the expression $\frac{W_r + e^2\,W_p}{W_r + W_p}$ gives a ratio of combined ram-pile kinetic energy before and after impact. This then would define the available energy after impact when multiplied by the initial energy E_n. The factor $1/2\ (C_1 + C_2 + C_3)$ is analogous to the factor 0.1 in the Engineering News Formula. The value of C_1 equals the peak temporary (elastic) compression experienced in the pile head and cap. This was not measured directly in the current study, and consequently test values summarized by Chellis[1] were used. Values of C_1 were set at 0.1 for all hammers in the program, except the McKiernan-Terry DE-30 and DE-40 and the Vulcan No. 1, for which the value was set at 0.15 because of relatively soft cap block material (unconfined wood).

The factor $C_2 + C_3$ was based generally on field measurements, and represents the combined temporary compression of pile and supporting ground. The technique for obtaining this information is indicated in Fig. 149.

An additional computed temporary compression was added for piles having relatively long stub lengths projecting above the measuring point.

---

[1] Chellis, R. D. Pile Foundations. New York: McGraw Hill Book Co., Inc. (1961; 2nd Edition), p. 505 (Table I).

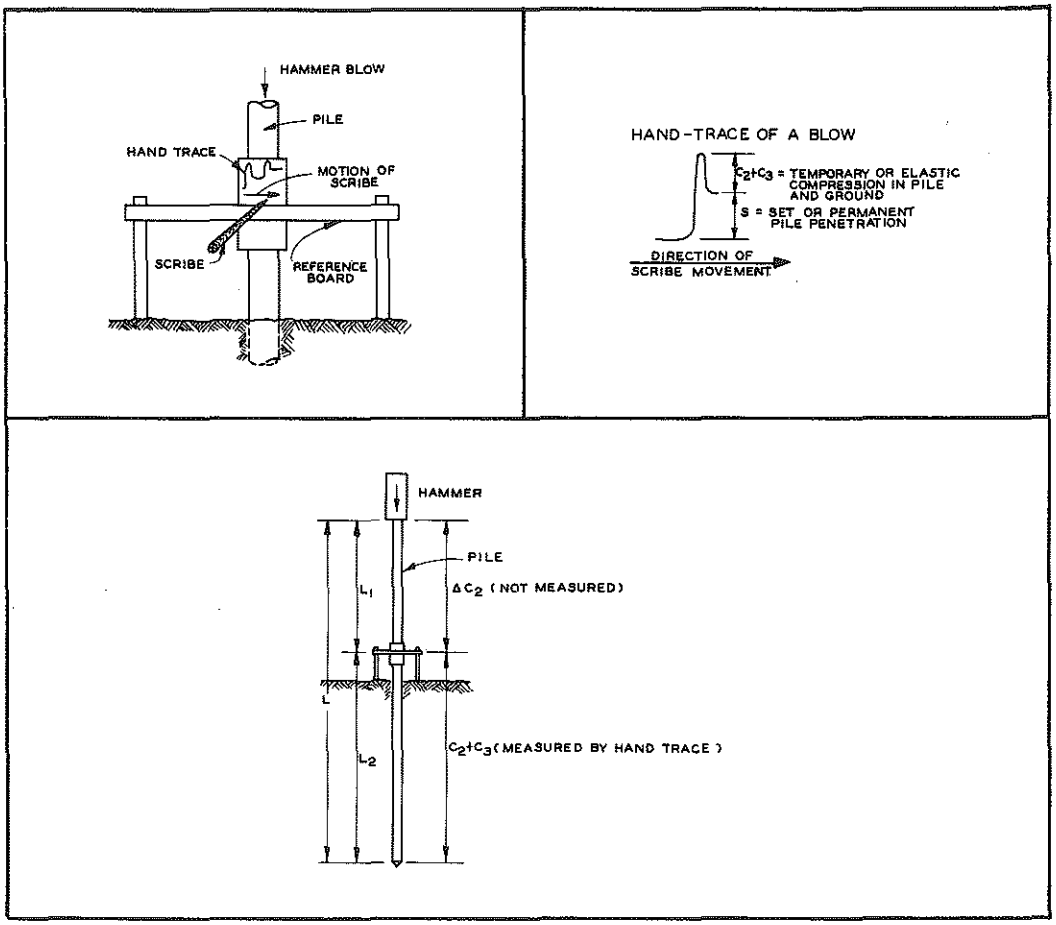

Figure 149. Method of taking manual trace shown schematically (upper left and right), did not include pile length L_1 in the $C_2 + C_3$ portion of the manual trace.

This compression, designated ΔC_2, which is added to C_2 in the Hiley-type formula, is the greater value of those obtained by the following two methods:

Method No. 1. ΔC_2 can be represented by the equation for elastic deformation $\frac{PL_1}{AE_L}$, where L_1 is that portion of the pile above the point where the manually recorded deflection value (hand trace) was taken (Fig. 149). Chellis[2] has computed values of temporary compression C_2 for four different driving conditions (easy, medium, hard, very hard) with values of P/A for steel piles ranging from 7,500 to 30,000 psi.

[2] Ibid, p. 506 (Table II).

At Belleville, driving resistance varied between hard and very hard for reaction piles and for test piles at tip elevation 610. From Chellis,[2] $\underline{P/A}$ = 25,000 psi and $\underline{E_L}$ for steel piles = 30 x 10^6 psi.

$$\Delta C_2 = \frac{PL_1}{AE_L} = \frac{25 \times 10^3}{30 \times 10^6} \times L_1 \text{ (feet)} \times \frac{12 \text{ (inches)}}{1 \text{ (foot)}} = 0.01\ L_1$$

$$\therefore 0.01 \times \text{Stub Length } L_1 \text{ (feet)} = \Delta C_2 \text{ (inches)}$$

At Muskegon, driving resistance varied between easy and medium for piles at tip elevations 530 and 460, respectively. From Chellis,[2] $\underline{P/A}$ = 11,250 psi and $\underline{E_L}$ for steel piles = 30 x 10^6 psi.

$$\Delta C_2 = \frac{PL_1}{AE_L} = \frac{11{,}250}{30 \times 10^6} \times L_1 \text{ (feet)} \times \frac{12 \text{ (inches)}}{1 \text{ (foot)}} = 0.005\ L_1$$

$$\therefore 0.005 \times \text{Stub Length } L_1 \text{ (feet)} = \Delta C_2 \text{ (inches)}$$

Method No. 2. By ratio and proportion a value of $\underline{\Delta C_2}$ (Fig. 149) can be computed as follows:

$$\frac{C_2 \text{ (embedded pile)}}{\Delta C_2 \text{ (pile stub)}} = \frac{L2 \text{ (embedded pile)}}{L_1 \text{ (pile stub)}}$$

$$\Delta C_2 = \frac{C_2\ L_1}{L_2}$$

Chellis[3] has compiled values of temporary compression or quake of the ground $\underline{C_3}$ for the same four driving conditions (easy, medium, hard, and very hard). $\underline{C_3}$ ranges from 0 to 0.10 in. for easy driving, and remains a constant 0.10 in. for all other driving conditions, including those at Belleville and Muskegon:

$$\therefore \Delta C_2 = \left[C_2 + C_3 \text{ (hand trace)} - C_3 \right] \frac{L - L_2}{L_2}$$

$$\Delta C_2 = \left[C_2 + C_3 - 0.10 \right] \frac{L - L_2}{L_2}$$

The Hiley Formula is understood to have acceptance in Great Britain. Its principal advantage is that it allows some flexibility in selecting loss

[3] Ibid, p. 506 (Table III).

factors. Leaving aside the question of precision in the derived capacity value, it does offer an inducement (lower required values for final driving resistance) to the engineer and contractor to use the best in driving practice.

3. Pacific Coast Uniform Building Code Formula (Nominal Safety Factor = 4)

$$R_d = \frac{3\ E_n \times \frac{W_r + K\ W_p}{W_r + W_p}}{S + \frac{48\ R_d\ L}{AE_L}}$$

The factor K is analogous to e^2 in the Hiley Formula, and is specified equal to 0.25 for ordinary practice with steel piles. The temporary compression loss factor $\frac{48\ R_d\ L}{AE_L}$ represents the longitudinal elastic shortening of the pile when subjected to the indicated ultimate driving stress (4 R_d = R_u). Although the cap and supporting soil compressions are not specifically considered, this is compensated for in that pile compression is somewhat overestimated since the peak stress is not likely to be developed over the entire length of the pile in any given instant as is assumed in the formula.

Note that since R_d is a function of R_d, the equation can either be expressed in the quadratic form, or solved by trial and error. The latter method is practical since the final value of R_d computed is not very sensitive to the value of R_d assumed in the factor $\frac{48\ R_d\ L}{AE_L}$.

4. Redtenbacher Formula (Nominal Safety Factor = 3)

$$R_d = \frac{AE_L}{36\ L}\left[-S + \sqrt{S^2 + \left(12\ E_n \times \frac{W_r}{W_r + W_p}\right)\ \frac{2(L)12}{AE_L}}\right]$$

This formula restates the General Pile Energy Formula, or basic equation, for the condition of inelastic impact:

Net work in moving pile = Initial Energy − Energy lost at impact − Energy absorbed in shortening pile elastically

or

$$R_u \times S = 12\ E_n - \frac{12\ E_n\ W_p(1 - e^2)}{W_r + W_p} - \frac{R_u \times R_u L \times 12}{2\ AE_L}$$

Equating for $\underline{e} = 0$ (in elastic impact) for $\underline{R_u}$ involves the solution of the following quadratic equation:

$$R_u^2 \times \frac{12L}{2AE_L} + R_u \times S - 12\ E_n \times \frac{W_r}{W_r + W_p} = 0$$

One may note in this equation that the temporary elastic shortening due to ground quake has not been considered. Also, for the specific conditions of this hammer test program, the assumption of completely inelastic impact is not warranted, based on the apparent response of the more durable cap blocks.

5. Eytelwein Formula (Nominal Safety Factor = 6)

$$R_d = \frac{2\ E_n}{S + 0.1\ \frac{W_p}{W_r}}$$

This formula, although derived from the General Pile Energy Formula, is closely related to the Engineering News Formula, with the impact loss expressed in terms of pile-to-ram weight ratios.

Formula factor $0.1\ \frac{W_p}{W_r}$ does not fully account for energy losses since as pipe wall thickness decreases, impact loss decreases but elastic compression losses increase. The compression losses are not reflected in this formula.

6. Navy-McKay Formula (Nominal Safety Factor = 6)

$$R_d = \frac{2\ E_n}{S\left(1 + 0.3\ \frac{W_p}{W_r}\right)}$$

In this formula, the compression losses are expressed as a function of both set $\underline{S}$ and the ratio $\underline{W_p/W_r}$. This is even less rational than the Eytelwein Formula since it implies that compression losses decrease as set is reduced. Thus, at absolute refusal, $\underline{R_d}$ would approach infinity, which is certainly not a rational solution.

7. Rankine Formula (Nominal Safety Factor = 3)

$$R_d = \frac{2\ AE_L S}{36\ L}\left[\sqrt{1 + \frac{12\ E_n\ (12L)}{S^2\ E_L A}} - 1\right]$$

Referring to the General Pile Energy Formula:

$$S \times R_u = 12\ E_n - 12\ E_n \frac{W_p\ (1 - e^2)}{W_r + W_p} - \frac{R_u}{2} \times \frac{R_u\ L \times 12}{E_L A}$$

when $e = 1$ (perfectly elastic impact) and when the equivalent length for a pure friction pile $= \frac{L}{2}$, then

$$S \times R_u = 12\ E_n - \frac{R_u}{2} \times \frac{R_u\ L \times 12}{2\ E_L A}$$

Expressing this in a quadratic form:

$$\frac{R_u^{\ 2}\ (3L)}{E_L A} + R_u\ S - 12\ E_n = 0$$

The Rankine Formula is thus merely a special case of the General Formula, which includes the Redtenbacher as another limit expression.

8. Canadian National Building Code Formula (Nominal Safety Factor = 3)

$$R_d = \frac{4\ E_n \dfrac{W_r + 0.5\ e^2\ W_p}{W_r + W_p}}{S + \dfrac{3R_d}{2A}\left[\dfrac{12L}{E_L} + 0.0001\right]}$$

This formula has the same general form as the Hiley and PCUBC Formulas with $0.5\ W_p$ taken for effective pile weight under end-bearing conditions and with a small quake and cap compression loss introduced by the factor $0.0001 \times 3\ R_d/2A$. Again, as with the PCUBC formula, either a quadratic or a trial-and-error solution is required, since R_d is a function of R_d.

9. Modified Engineering News Formula (Nominal Safety Factor = 6)

$$R_d = \frac{2\ E_n}{S + 0.1} \times \frac{W_r + e^2\ W_p}{W_r + W_p}$$

This is a variation of the previously discussed Engineering News Formula. For the normal range of e factors and pile-ram weight ratios, it effectively reduces the energy E_n to about 60 percent of the value used in the conventional Engineering News Formula. This formula is currently being used by Michigan State Highway Department, supplanting the formerly specified Engineering News Formula.

10. Gates Formula (Nominal Safety Factor = 3)

$$R_d = 2000 \times \frac{1}{7} \sqrt{E_n} \left[\log \frac{S}{10} \right]$$

or

$$R_d = 2000 \times \frac{1}{7} \sqrt{E_n} \quad \text{ABS} \left[\log \frac{S}{10} \right]$$

This formula[4] is a strictly empirical relationship between hammer energy, final set, and measured design test load, with a safety factor, and is typical of empirical formulas. It is apparent that this relationship does not have rational limits and does not apply to "refusal" conditions when S approaches zero.

11. Rabe Formula (Nominal Safety Factor = 2)

$$R_d = \frac{M \times E_n}{S + C} \times \frac{W_r}{W_r + \frac{W_p}{2}} \times B$$

$$C = \frac{(C_1 + C_2 + C_3)}{2} \quad \text{(by Hiley)}$$

This formula was developed empirically, is more complex than the others, and has been revised periodically. The formula as used in this study is the 1960 version, which at present is the latest. The terms $C_1 + C_2 + C_3$ represent the compression loss in the cap and cushion, in the pile, and in the soil, respectively. The values for these terms are not shown here but are provided in Rabe's published revisions of his formula.[5] Therefore, for convenience in evaluating the Rabe formula, the Rabe value of C has been considered equal to one-half the sum of C's as determined for the Hiley Formula.

In the formula $B = B_S \times B_L \times B_C$, the factor B relates dynamic to static pile bearing capacity. B_S is a soil factor; B_L a length factor, applying to penetration length; and B_C a cross-section factor, applying to average horizontal cross-section of soil displaced by the pile. The values for $B_S \times B_L \times B_C$ are not set forth here but were determined from Rabe's own formula revision.[5] M is a factor incorporating the

---

[4] Gates, M. "Empirical Formula for Predicting Pile Bearing Capacity." Civil Engineering, Vol. 27, No. 3 (March 1957), pp. 183-184.

[5] W. H. Rabe's own imprint (1960) showing revisions of his formula as it had been described in Engineering News-Record, Vol. 60, p. 868 (Dec. 26, 1946).

safety factor 2, the hammer efficiency factor, and a factor of 12 to cause the value of E_n to be expressed in inch-pounds.

INTERPOLATION OF PILE YIELD LOAD VALUES

Comparative data on pile load test capacities are essential in evaluating dynamic formulas. Ideally, this would have involved a complete load test to failure for each of the piles driven, with additional load tests at intermediate depths. However, a total of 88 piles were driven, and costs made proper load testing of such a quantity of piles out of the question.

Actually, load tests were feasible for only about 20 percent of all piles driven. The methods of test and form of load test data were explained and summarized in Chapter 10. The load test data, then, corresponded to only a small fraction of the pile hammer data available, and restricting the formula study to this small body of data would have greatly diminished the value of the analysis. On the other hand, the abundance of detailed information concerning soil conditions and pile driving experience afforded an unusual opportunity for a more extensive formula study.

A general review of the soil boring data indicated relatively uniform stratification and fair agreement in soil test data over each of the sites. It was concluded that under these circumstances it would be possible to obtain static pile load capacity estimates for each pile driven, based on a proper interpolation of the actual load test values. These load capacity estimates would then form a basis for extending the formula analysis to cover a wide range of hammers, pile types, and bearing depths for these different soil conditions. The basis of interpolation differed at each site, reflecting the soil conditions and load test data available.

The procedures for estimating pile bearing capacity to be discussed were designed specifically to obtain interpolated bearing capacities for use in the dynamic formula evaluation. A more general method for determining pile bearing capacity due to side friction in sands and/or clays was discussed in Chapter 11.

Belleville Interpolations

Interpolation of load test values involved the following considerations:

1. Estimates of side shear developed on the piles took into account varying soil strengths and pile pre-excavation depths.

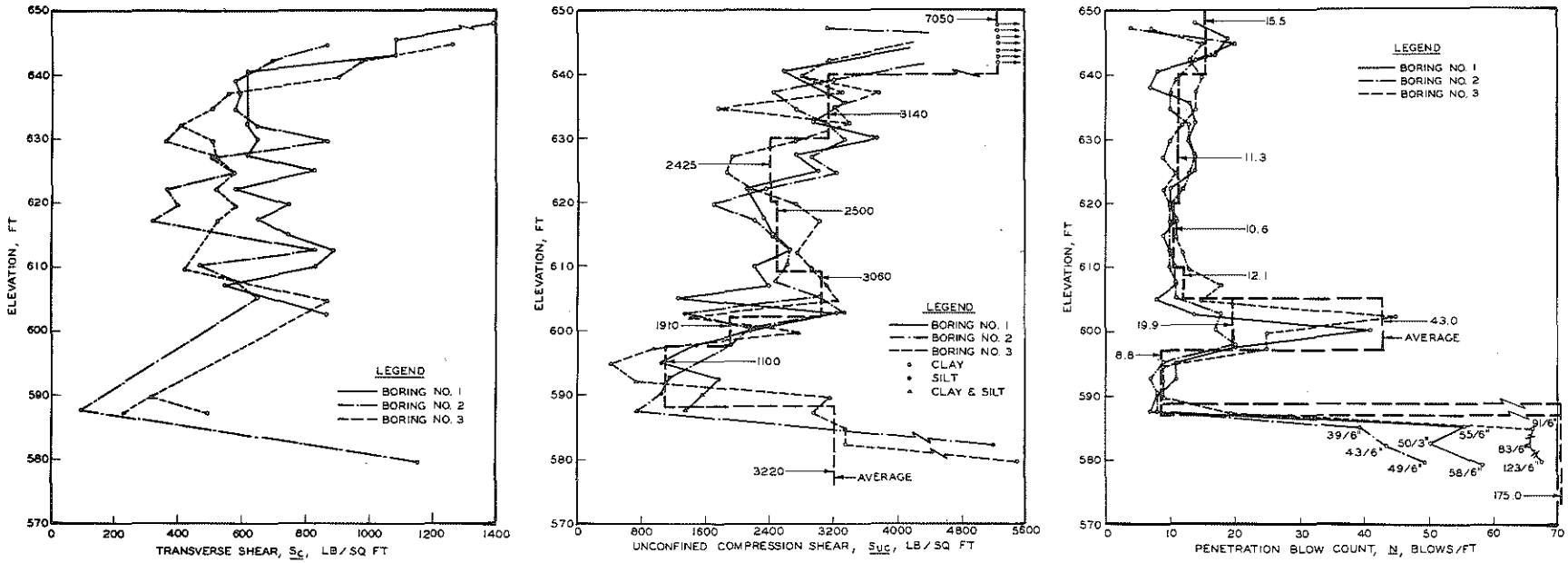

Figure 150. Boring profiles for Belleville shear and penetration resistance.

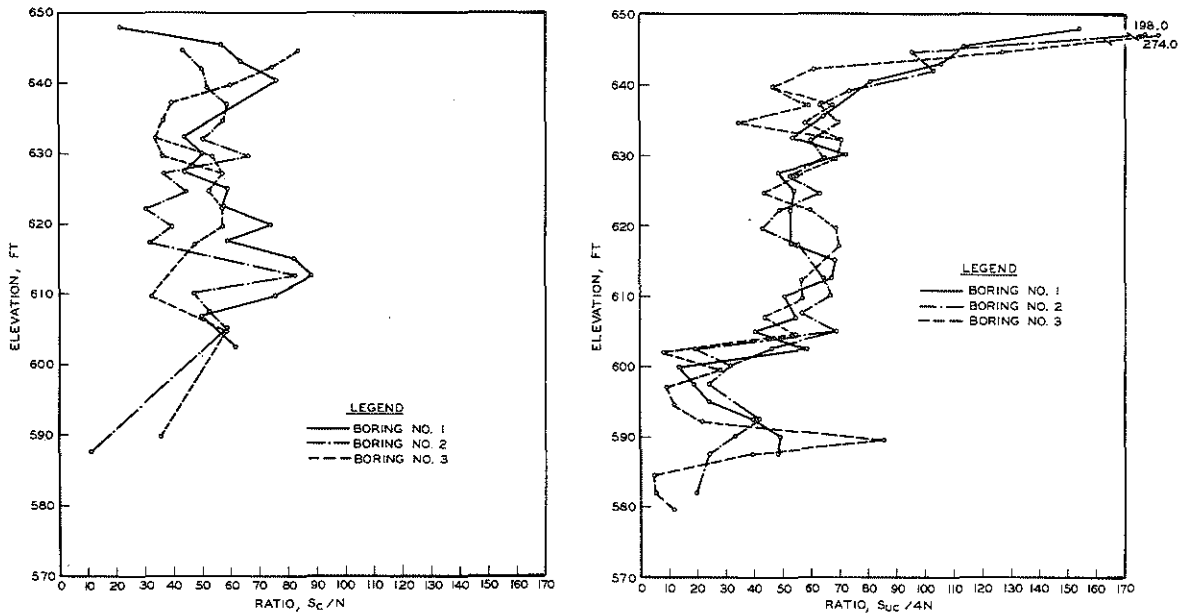

Figure 151. Ratios of transverse shear and one-quarter unconfined compression shear to Belleville boring penetration resistance.

2. The effective failure surface bounding the H-piles was varied depending on soil type and consistency.

3. Estimates of pile end-bearing capacities were based on factors obtained from a previously developed empirical relationship between standard penetration and angle of pressure transmission.

Significant soil strength properties are summarized in Figs. 150 and 151, based on the soils information given in Chapter 1. On the profiles (Fig. 150), transverse and unconfined shear strengths both show considerable variation, normal for these soils; a high-strength crust appears above elevation 640. Ratios of transverse shear strength and unconfined compressive shear strength S_{uc} to boring penetration resistance (Fig. 151) showed a more consistent pattern for the unconfined strength. For this reason, it was concluded that the S_{uc} (unconfined) strength gave a more reliable measure of actual soil resistance in these circumstances and subsequent pile friction estimates were based on average unconfined strength values. Fig. 152 shows the four load test piles in relation to the selected average strength profile.

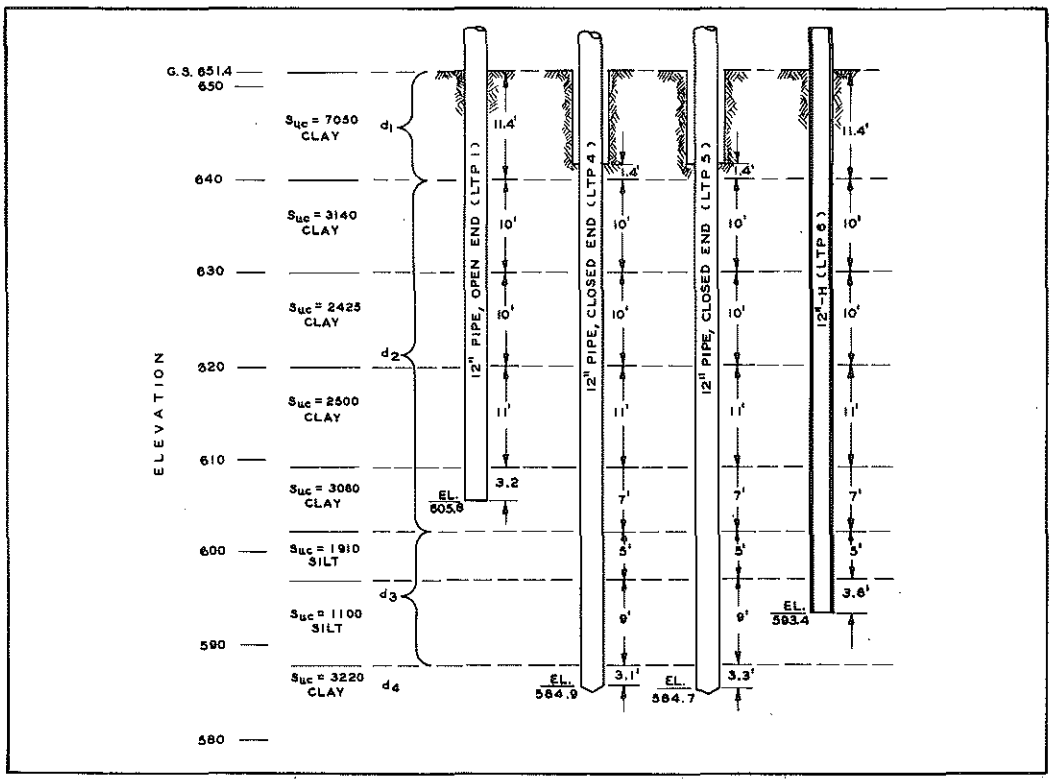

Figure 152. Belleville load test pile profiles.

The soil resistance values Suc in the clay were modified by coefficients d as shown in Fig. 153, based on an empirical relation between unconfined shear strength and mobilized pile side shear at failure. It must be emphasized that these specific d and frictional resistance values are presented only for the purpose of interpolation. However, the relationship presented follows the form of those presented by Peck,[6] Tomlinson,[7] and Woodward, Lundgren, and Boitano,[8] and gives values comparable to theirs. It has been shown that the percent of unconfined shear developed in side shear along the body of a bearing pile at failure varies over a wide range.[6,7,8] Sensitivity of the soil to disturbance, time lapsed between driving and testing, percent of effective pile-soil contact, are all sources of variability in the final value of d.

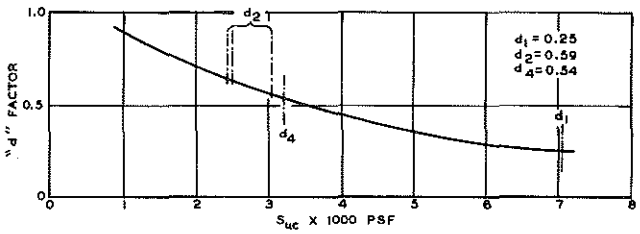

Figure 153. Ratio of developed shear factor "d" and unconfined compressive shearing resistance S_{uc} (Belleville).

Side shear resistance values selected in the silt are shown in the following equations, wherein lateral pressures are set equal to the overburden pressure and the coefficient of friction, steel on silt, is set at 0.33

Elevation 602 to 588

$$S_f = wh\mu = (130 \times 49 + 7 \times 120)\ 0.33 = 2,400 \text{ psf}$$

Elevation 588 to 580

$$S_f' = wh = (130 \times 49 + 18 \times 120)\ 0.33 = 2,830 \text{ psf}$$

The friction values assigned to the silt and clayey silt below elevation 602 are more educated guesses than exact determinations. Equating the overburden weight to the effective horizontal soil stress must not be applied

---

[6] Peck, R. B. "A Study of the Comparative Behavior of Friction Piles." HRB Special Report 36 (1958), p. 33.

[7] Tomlinson, M. J. "The Adhesion of Piles Driven in Clay Soils." Proc., 4th Internat. Conf. Soil Mechanics (London), Vol. 2, pp. 66-71 (1957).

[8] Woodward, R. J., Lundgren, R., and Boitano, J. D. "Pile Loading Tests in Stiff Clays." Proc., 5th Internat. Conf. Soil Mechanics (Paris), Vol. 2, pp. 177-184 (1961).

generally. However, the order of magnitude in assigned friction (2400 to 2830 psf), although quite high, is not unreasonable. The fairly close match between computed and measured pile resistance or capacities lends some support to these specific side shear values, and was the basis for the subsequent interpolations.

Details of capacity computation are as follows:

Computed Load Capacity

LTP 1 (open-end 12-in. diam pipe pile)

$$R_1 = \pi D \left[d_1 \times 7,050 \times 11.4 + d_2 \, (3,140 \times 10 + 2,425 \times 10 + 2,500 \times 11 + 3,060 \times 3.2) \right.$$
$$= 3.14 \times 1 \, (20,100 + 54,900) = 235,100 \text{ lb}$$

LTP 4 (closed-end 12-in. diam pipe pile)

$$R_4 = \pi D \left[d_1 \times 7,050 \times 1.4 + d_2 \, (31,400 + 24,250 + 27,500 + 3,060 \times 7) + S_f \times 14 + (S_f + 3,220 \times d4) \times 3.1 \right] + Q_B$$
$$= 7,750 + 58,200 + 45,000 + 51,100 + 39,800 + 105,800 + 42,200 + Q_B$$

LTP 5 (closed-end 12-in. diam pipe pile)

$$R_5 = R_4 + (S_f + 3,220 \times d_4) \times 0.2 \times 3.14$$
$$= R_4 + 2,700$$

LTP 6 (12-in. H-pile)

Assumed perimeter contact :

Hard clay	El. 651.4 to 640	A = 2 x 1 = 2 sq ft
Plastic clay	El. 640 to 602	A = 4 x 1 = 4 sq ft
Silt	El. 602 to 588	A = 6 x 1 = 6 sq ft

$$R_6 = 2 \times 1 \times 7,050 \times 11.4 \times d_1 + 4 \times 1 \times d_2 \, (31,400 + 24,250 + 27,500 + 21,400) + S_f \times 8.6 \times 6$$
$$= 40,200 + 74,300 + 57,400 + 65,000 + 50,500 + 124,000$$

Bearing Capacity at Various Elevations

El. 609 h = 43 ft

$$Q_B = (8 \, S_{uc}) \, A = 8 \times 3,060 \times 0.785 = \underline{20,000 \text{ lb}}$$

El. 602 $N = 43$ (max), $\cot^5 \theta = 15$, $\cot^4 \theta = 8.6$, $\cot^2 \theta = 2.9$, $K = 9.9$, $h = 50$, $S_{uc} = 1{,}910$ psf, $\sin 2\theta = 0.87$

$$Q_B = \left[\frac{1}{3} \times 9.9 \times 120 \times 0.5 \times 15 + \frac{2 \times 1910}{0.87} (1 + 2.9) + 130 \times 49 (8.6 - 1) \right] A$$

$$= \left[2{,}960 + 18{,}400 + 48{,}400 \right] 0.785 = \underline{53{,}800 \text{ lb}}$$

El. 588 $N = 175$ (avg), $\cot^5 \theta = 60$, $\cot^4 \theta = 26.5$, $\cot^2 \theta = 5.1$, $K = 13.1$, $\sin 2\theta = 0.74$

$$Q_B = \left[\frac{1}{3} \times 13.1 \times 120 \times 0.5 \times 60 + \frac{2 \times 3{,}220}{0.74} (1 + 5.1) + (130 \times 49 + 120 \times 14)(26.5 - 1) \right] A$$

$$= \left[15{,}700 + 53{,}000 + 205{,}000 \right] 0.785 = \underline{215{,}000 \text{ lb}}$$

Evaluation of the H-pile capacity necessitated that the effective contact area be varied with depth and character of the soil. As was noted in Chapter 9, the stiff upper clay trapped between the flanges and adjoining web face of some H-piles was carried down a depth of several feet in some instances, leaving only the two outer faces of the flange in contact with the stiffer upper clay. For this reason, the contact area above elevation 640 was conservatively set as 2 sq ft per lin ft. In the plastic clay, the effective side shear area was set by the minimum bounded perimeter (4 sq ft per lin ft). In the silt, on the other hand, it was considered that failure would involve knifing of the H-section through the granular soil (6 sq ft per lin ft). It may be noted that the end-bearing capacity component for the closed-end pipe piles given above, is based on methods described in the Michigan State Highway Department Field Manual of Soil Engineering, and originally developed by Housel.[9]

Table 31 summarizes load estimates for different depths and pile types. These results are the basis of the interpolated capacity curves for 12-in. pipe piles, both closed-end and open-end, and 12-in. H-section piles shown in Fig. 154. For comparison, the actual load test values are plotted and, with the exception of the deep bearing piles (LTP's 4 and 5), show a good correlation with comparable computed values. Concerning these latter piles, driven under conditions of extremely high standard penetration resistance, it must be recognized that computation of end-bearing values is approximate.

9 Housel, W. S. "Field and Laboratory Correlation of the Bearing Capacity of Hardpan for Design of Deep Foundations." ASTM Proc., Vol. 56 (1956), pp. 1320-1346.

The interpolated values for TP's 7, 10, 11, 14, and 16, at ± 315 tons were based on a preliminary analysis of the LTP 4 and 5 load tests. A subsequent re-interpretation resulted in a somewhat higher assigned yield load (340 to 345 tons) for LTP's 4 and 5. However, this represents only about a 10-percent increase over the previous estimates, and thus the original interpolated values were retained for the formula study. For the shallower depths, where correlations indicate a better agreement, the computed bearing values shown were used in formula comparison.

TABLE 31
COMPUTED BELLEVILLE PILE LOAD CAPACITIES

Pile	Tip Elevation						
	640	630	620	609	602	588	Below 588
LTP-1	31.5 Tons**			117.5 Tons @605.8**			
LTP-4	14 Tons*	43 Tons*	66 Tons*	91 Tons*	111 Tons Above 127 Tons Below	180 Tons Above 260 Tons Below	282 Tons @584.9
LTP-5	14 Tons*	43 Tons*	66 Tons*	92 Tons*	112 Tons Above 128 Tons Below	181 Tons Above 262 Tons Below	283 Tons @584.7
LTP-6	20.1 Tons	57 Tons	86 Tons	118 Tons	144 Tons	205 Tons @593.4	

* Assume average Q_B = 10 Tons
** Open end friction pile.

Detroit Interpolations

When driving bearing piles at Detroit, it was noted that penetration into the bearing strata above bedrock was marked by a sudden and continuing increase in blow count. Consequently, the total depth of penetration into these strata could be estimated on the basis of the pile driving log profile. The relation between actual test load capacity and depth of penetration is shown in Fig. 155 and clearly indicates a good correlation. On this basis, the illustrated interpolated bearing values or "estimated capacities" were obtained. These values in turn were used for the subsequent formula evaluations.

Muskegon Interpolations

The pile load test data given in Chapter 10 indicate that piles bearing at or near elevation 530 (LTP's 2, 3, 4, 5), and those reaching elevation 460 (LTP's 6 and 9), were carried to failure or progressive settlement. LTP's 7 and 8 were extended to the deeper sand hardpan, at elevation 410. It was not possible to reach their load limit with the available reaction system, loads having been carried up to 359 tons without evidence of progressive settlement or failure. Bearing capacity and tip elevation of all the piles carried to failure are shown in Fig. 156.

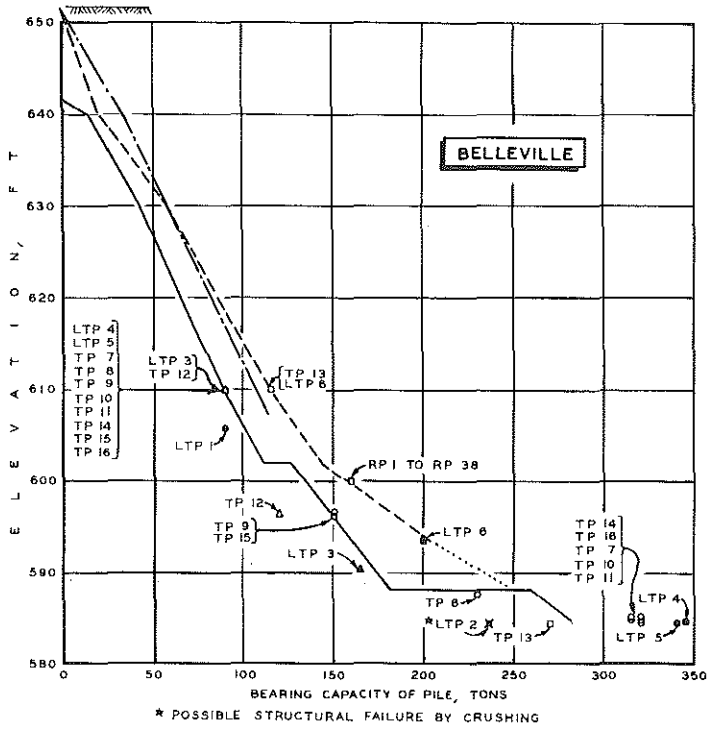

Figure 154. Computed vs. measured pile bearing capacity

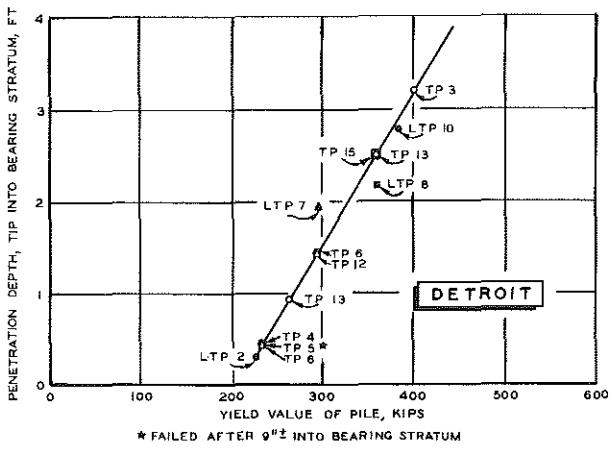

Figure 155. Correlation of pile bearing capacity and penetration into bearing strata.

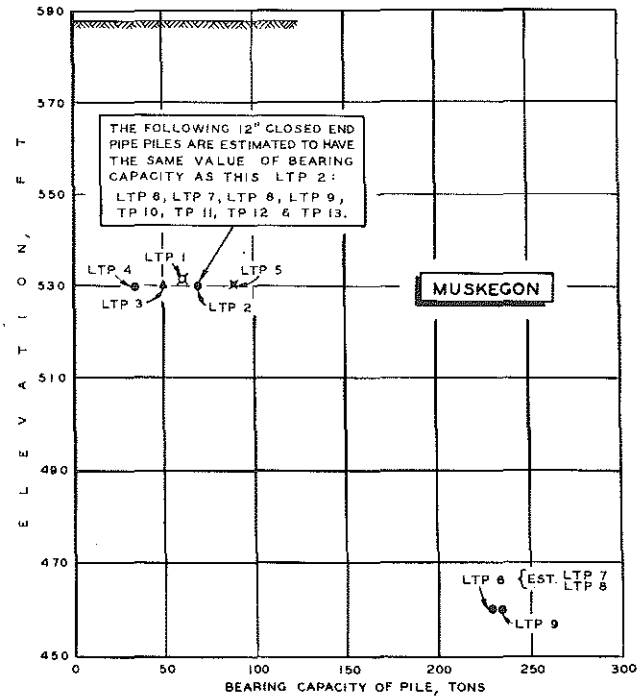

Figure 156 (right). Correlation of measured and estimated pile capacities with depth.

LEGEND (FIGS. 154, 155, 156)

COMPUTED CAPACITY:
- 12" PIPE PILE, CLOSED END
- 12" PIPE PILE, OPEN END
- 12"-53 LB. -H-PILE

MEASURED CAPACITY:
- ● - 12" PIPE PILE, CLOSED END
- ⊖ - 12" PIPE PILE, OPEN END
- ▲ - 12" FLUTED-TAPERED
- ■ - H-PILE
- ✖ - RAYMOND STEP TAPER

ESTIMATED CAPACITY:
- ○ - 12" PIPE PILE, CLOSED END
- ⊖ - 12" PIPE PILE, OPEN END
- △ - 12" FLUTED-TAPERED
- □ - H-PILE

Driving logs of the piles as well as penetration resistance profiles in the Muskegon boring logs show the presence of relatively resistant strata at elevations ± 535 and between elevations 454 and 478. The bearing capacities of LTP's 6 and 9 at elevation 460 shown in Fig. 156 are almost identical (230 tons). Thus, it is reasonable to assign this value as an estimate of bearing capacity of comparable pipe piles when bearing at this depth. As indicated, the 230-ton bearing estimates were assigned to LTP's 7 and 8 for this intermediate elevation.

Determination of a bearing estimate at elevation 530 is complicated by the fact that test pile bearing values range from 35 to 90 tons. However, as noted in Fig. 156, only LTP 2 is actually comparable in all significant respects to the other pipe piles for which a capacity estimate is desired. Its value of 70 tons was assigned to all closed-end pipe piles driven to this elevation, and this load is in line with what might be anticipated when considering all the comparable test loads. For example, the absence of significant end-bearing and probable reduced side friction due to internal jetting during and after driving would account for the low test value of LTP 4 (35 tons). On the other hand, LTP 5 (a corrugated step-tapered pile) had the probable benefit of increasing side shear, reflected in the relatively high load value of 90 tons. LTP 2 and the interpolated pipe piles indicated in Fig. 156 were driven closed-end without jetting, and the 70-ton capacity estimate is intermediate to the extreme values recorded.

ANALYSIS OF DYNAMIC FORMULA CAPACITIES

In the preceding discussion, the 11 formulas chosen for study have been outlined, and the general basis presented for selecting comparative load test values or estimates. Actual results of the formula evaluation are summarized in Tables 32 through 36.

Data are presented in these tables as follows: identifying data (Cols. 1-3), hammer data (Cols. 4-6), pile data (Cols. 7-10), driving data (Cols. 11-13), special Rabe Formula factors (Cols. 14-16), and comparative load test data (Col. 17). The information is grouped so that the primary data, consisting of field driving measurements associated with actual measured pile failure loads, are presented first. Thus, six lines at the top of Table 32, five lines at the top of Table 35, and six lines at the top of Table 36 show the basic data for formula evaluations at Belleville, Detroit, and Muskegon, respectively.

TABLE 32
DYNAMIC PILE DRIVING FORMULA EVALUATION
Belleville Load Test Piles and Test Piles at Refusal

	Pile Number	Hammer Type	Pile Type	Ram Weight, lb	Stroke, ft.	Manufacturer's Rated Energy, ft-lb	Cross-Sectional Pile Area, sq in.	Total Pile Length, ft	Pile Weight, lb Driving Sleeve & Load Cell Wt, lb	Gross Pile Weight, lb	Penetration Resistance/blows/in. at Tip Elevation, ft	C_1, Temporary Compression of Pile Head and Cap, in.	C_2+C_3, Temporary Compression of Pile and Ground, in.	M, Efficiency of Hammer, in./ft (Rabe)	C_4 Factor used in Calculating Compression Loss in Pile (Rabe)	B, Soil Factor (Rabe)	Load Data: R_t, Yield Load Failure, kips	R_a, Computed Ultimate Pile Load Capacity, kips — Ratio: R_a/R_t										R_d, Computed Design Pile Load Capacity, kips										
																		Engineering News	Hiley	Pacific Coast Uniform Building Code	Redtenbacher	Eytelwein	Navy-McKay	Rankine	Canadian National Building Code	Modified Engineering News	Gates	Rabe	Engineering News, SF=6	Hiley, SF=3	Pacific Coast Uniform Building Code, SF=4	Redtenbacher, SF=3	Eytelwein, SF=6	Navy-McKay, SF=6	Rankine, SF=3	Canadian National Building Code, SF=3	Modified Engineering News, SF=3	Gates, SF=3	Rabe, SF = 2
	1	2	3	4	5	6	7	8	9	10	11	12	13	14	15	16	17	18	19	20	21	22	23	24	25	26	27	28	29	30	31	32	33	34	35	36	37	38	39
LOAD TEST CAPACITY	LTP 1 (1)	Vulcan 1	12" Pipe .25" Wall	5000	36.0	15000	9.23	(4) 39.0	1920 2910	4830	11.0 597.0	0.15	0.32	5.00	0.75	0.61	180 (7)	942 5.24	336 1.87	234 1.30	280 1.55	960 5.33	1535 8.53	554 3.08	120 0.66	573 3.19	214 1.19	189 1.05	187	112	58	93	150	256	185	40	96	71	95
	LTP 2	Raymond M15	Raymond Shell	5000	18.0	15000	50.00	64.0	----	10780	36.0 584.3	0.10	0.27	5.25	0.75	0.92	474 (5)	1409 2.97	385 0.81	388 0.82	421 0.89	740 1.56	3935 8.30	1082 2.28	224 0.47	641 1.35	268 0.57	328 0.69	235	128	97	140	123	656	361	75	107	88	164
	LTP 3	McKiernan-Terry DE-30	Fluted taper #7 Gage	2800	96.0	22400 (3)	6.66	81.5	1840 4080	5920	36.0 590.5	0.15	0.80	5.00	0.74	0.88	330	2104 6.37	245 0.74	161 0.49	182 0.55	1124 3.41	5921 17.94	457 1.39	101 0.31	965 2.92	328 0.99	191 0.58	351	82	40	61	187	987	152	34	161	109	95
	LTP 4	Link Belt 312	12" Pipe .25" Wall	3855	30.9	18000 (3)	9.23	81.3	2560 4479	7039	30.0 584.9	0.10	0.80	5.00	0.88	0.92	690	1620 2.35	217 0.31	173 0.25	199 0.29	1000 1.45	4187 6.07	477 0.69	110 0.16	785 1.14	284 0.41	179 0.26	270	72	43	66	167	698	153	37	130	95	90
	LTP 5	Delmag D-12	12" Pipe #7 Gage	2750	98.0	22500 (3)	6.66	80.0	2560 3749	5559	34.0 584.7	0.10	0.65	5.00	0.88	0.92	880	2086 3.07	311 0.46	164 0.24	187 0.27	1166 1.71	5715 8.40	462 0.68	103 0.15	973 1.43	325 0.48	255 0.37	348	104	41	62	194	952	154	34	162	108	127
	LTP 6	Vulcan 1	12 H53	5000	36.0	15000	15.58	72.5	3840 2660	6500	48.0 593.4	0.15	0.40	5.00	0.88	0.78	400	1495 3.74	335 0.84	231 0.58	279 0.70	1197 2.99	6345 15.86	600 1.50	144 0.36	821 2.05	282 0.71	240 0.60	249	112	58	93	199	1058	200	48	137	94	120
INTERPOLATED CAPACITY	TP 7	Vulcan 50C	12" Pipe #7 Gage	5000	15.5	15100	6.66	80.0	1810 2910	4720	40.0 585.1	0.10	0.60	5.25	0.88	0.92	640	1450 2.26	296 0.46	152 0.24	192 0.30	1518 2.37	5648 8.83	378 0.59	100 0.16	888 1.39	274 0.43	254 0.41	242	99	38	64	253	941	126	33	146	91	132
	TP 8	McKiernan-Terry DE-30	12" Pipe #7 Gage	2800	96.0	22400 (3)	6.66	80.0	1810 4080	5890	31.0 587.6	0.15	0.70	5.00	0.88	0.92	460	2032 4.42	270 0.59	163 0.35	183 0.40	1108 2.41	5109 11.11	460 1.00	101 0.22	934 2.03	319 0.69	220 0.48	328	90	40	61	185	851	153	34	156	106	110
	TP 9	Vulcan 1	12" Pipe #7 Gage	5000	36.0	15000	6.66	79.8	1805 2910	4715	55.0 596.5	0.15	0.70	5.00	0.88	0.84	300	1523 5.08	249 0.83	153 0.51	193 0.64	1600 5.33	7717 25.72	380 1.27	100 0.33	934 3.11	287 0.96	193 0.64	254	83	38	64	287	1286	127	33	156	96	97
	TP 10	Delmag D-12	12" Pipe .25" Wall	2750	98.0	22500 (3)	9.23	81.3	2560 3749	6309	75.0 (6) 584.8	0.10	0.65	5.00	0.88	0.92	640	2382 3.72	355 0.55	189 0.30	212 0.33	1112 1.74	11995 18.74	546 0.85	117 0.18	1059 1.65	369 0.58	285 0.45	397	118	47	71	165	1999	182	39	176	123	142
	TP 11	McKiernan-Terry DE-30	12" Pipe .25" Wall	2800	96.0	22400 (3)	9.23	81.3	2560 4080	6640	34.0 584.7	0.15	0.75	5.00	0.88	0.92	640	2077 3.25	246 0.38	186 0.29	205 0.32	1008 1.58	5340 8.34	536 0.84	115 0.18	912 1.42	324 0.51	197 0.31	346	82	46	68	168	890	179	38	152	108	98
	TP 12	Vulcan 1	Fluted taper #7 Gage	5000	36.0	15000	6.66	82.0	1840 2912	4752	40.0 596.3	0.15	0.80	5.00	0.74	0.81	240	1440 6.00	220 0.92	150 0.62	189 0.79	1500 6.25	5603 23.34	372 1.55	99 0.41	880 3.67	273 1.14	165 0.69	240	73	37	63	250	934	124	33	147	91	82
	TP 13 (2)	Delmag D-12	12 H53	2750	98.0	22500 (3)	15.58	80.0	4240 1854	6094	33.0 584.3	0.10	0.62	5.00	0.88	0.85	540	2072 3.84	357 0.66	245 0.45	272 0.50	1072 1.98	5352 9.91	696 1.29	152 0.28	981 1.82	933 1.73	257 0.48	345	119	61	91	179	892	232	51	156	108	133
	TP 14	Vulcan 1	12" Pipe .25" Wall	5000	36.0	15000	9.23	80.8	2540 2912	5452	51.0 585.1	0.15	0.50	5.00	0.88	0.92	630	1505 2.39	305 0.48	174 0.28	216 0.34	1399 2.22	6917 10.98	442 0.70	114 0.18	878 1.40	284 0.45	259 0.41	251	102	44	72	233	1153	147	38	146	95	130
	TP 15	Vulcan 1	12" Pipe .25" Wall	5000	36.0	15000	9.23	80.8	1910 2912	4822	53.0 595.2	0.15	0.50	5.00	0.89	0.84	300	1514 5.05	319 1.06	204 0.68	257 0.86	1561 5.20	7389 24.66	509 1.70	121 0.40	921 3.07	286 0.95	247 0.82	252	106	51	86	260	1233	170	40	154	95	124
	TP 16	Link Belt 312	12" Pipe #7 Gage	3855	30.9	18000 (3)	6.66	80.0	1810 4479	6289	145.0 584.9	0.10	0.35	5.00	0.88	0.92	630	2021 3.21	471 0.75	154 0.25	183 0.29	1270 2.02	21022 33.38	421 0.67	98 0.16	1022 1.62	383 0.56	393 0.62	337	157	39	61	212	3505	140	33	170	121	197

(1) Open-end pile.
(2) Pile driven without load cell assembly.
(3) Manufacturer's maximum hammer rating.
(4) Effective length for friction pile. Total length = 61.1 ft with 3.1 ft earth plug.
(5) Evidence of structural failure due to crushing of concrete.
(6) Estimated
(7) Value at 6th Loading Cycle

TABLE 33
DYNAMIC PILE DRIVING FORMULA EVALUATION
Belleville Load Test Piles and Test Piles at Tip Elevation 610

	Pile and Hammer Data																Load Data	R_u, Computed Ultimate Pile Load Capacity, kips Ratio: R_u/R_t											R_d, Computed Design Pile Load Capacity, kips										
	Pile Number	Hammer Type	Pile Type	Ram Weight, lb	Stroke, in.	Manufacturer's Rated Energy, ft-lb	Cross-Sectional Pile Area, sq in.	Total Pile Length, ft	Pile Weight, lb Driving Head & Load Cell Wt, lb	Gross Pile Weight, lb	Penetration Resistance, blows/in. at Tip Elevation, ft	C_1, Temporary Compression of Pile Head and Cap, in.	$C_2 + C_3$, Temporary Compression of Pile and Ground, in.	M, Efficiency of Hammer, in./ft (Rabe)	C_4, Factor used in Calculating Compression Loss in Pile (Rabe)	E, Soil Factor (Rabe)	R_t, Yield Load Failure, kips	Engineering News	Hiley	Pacific Coast Uniform Building Code	Redtenbacher	Eytelwein	Navy-McKay	Rankine	Canadian National Building Code	Modified Engineering News	Gates	Rabe	Engineering News, SF=6	Hiley, SF=3	Pacific Coast Uniform Building Code, SF=4	Redtenbacher, SF=3	Eytelwein SF=6	Navy-McKay, SF=6	Rankine, SF=3	Canadian National Building Code, SF=3	Modified Engineering News, SF=6	Gates, SF=3	Rabe, SF=2
	1	2	3	4	5	6	7	8	9	10	11	12	13	14	15	16	17	18	19	20	21	22	23	24	25	26	27	28	29	30	31	32	33	34	35	36	37	38	39
INTERPOLATED CAPACITY	LTP 1 (4)	Vulcan 1	12" Pipe .25" Wall	5000	36.0	15000	9.23	(3) 39.0	1920 2910	4830	13.2 610.0	0.15	0.47	5.00	0.75	0.75	150 (6)	1024 6.40	284 1.77	238 1.49	287 1.80	1044 6.53	1842 11.51	569 3.56	121 0.75	623 3.89	222 1.39	197 1.23	171	95	59	96	174	307	190	40	104	74	98
	LTP 2	Raymond M15	Raymond Shell	5000	18.0	15000	50.00	64.0	——	10780	6.0 610.0	0.10	0.45	5.25	0.48	0.61	—— (5)	675 ——	186 ——	282 ——	248 ——	471 ——	656 ——	702 ——	178 ——	307 ——	186 ——	105 ——	113	62	71	83	78	109	234	59	51	62	52
	LTP 3	McKiernan-Terry DE-30	Fluted taper #7 Gage	2800	96.0	22400 (2)	6.66	53.6	1214 4080	5294	4.2 610.0	0.15	0.50	5.00	0.48	0.62	180	795 4.42	210 1.17	173 0.96	178 0.99	629 3.50	720 4.00	449 2.49	98 0.54	380 2.11	208 1.16	116 0.65	133	70	43	59	105	120	150	33	63	69	58
	LTP 4	Link Belt 312	12" Pipe .25" Wall	3855	30.9	18000 (2)	9.23	81.3	2560 4479	7039	6.9 610.0	0.10	0.98	5.00	0.75	0.65	180	882 4.90	217 0.31	173 0.25	199 0.28	1000 1.45	4187 6.07	420 2.33	110 0.16	785 1.14	211 1.17	89 0.50	147	51	40	57	110	180	140	34	71	70	44
	LTP 5	Delmag D-12	12" Pipe #7 Gage	2750	98.0	22500 (2)	6.66	80.0	1810 3749	5559	5.5 610.0	0.10	1.05	5.00	0.75	0.65	180	958 5.32	166 0.92	149 0.83	159 0.88	703 3.91	924 5.14	404 2.25	96 0.53	447 2.48	223 1.24	96 0.53	160	56	37	53	117	154	135	32	74	74	48
	LTP 6	Vulcan 1	12 H53	5000	36.0	15000	15.58	72.5	3840 2660	6500	11.5 610.0	0.15	0.67	5.00	0.75	0.63	230	963 4.19	199 0.86	214 0.93	247 1.07	830 3.61	1489 6.47	535 2.33	136 0.59	529 2.30	216 0.94	115 0.50	160	66	53	82	138	248	178	45	88	72	58
	TP 7	Vulcan 50C	12" Pipe #7 Gage	5000	15.5	15100	6.66	80.0	1810 2910	4720	5.0 610.0	0.10	0.95	5.25	0.75	0.65	180	804 3.36	153 0.85	135 0.75	160 0.89	615 3.42	706 3.92	314 1.74	92 0.51	370 2.06	179 0.99	97 0.54	101	51	33	53	103	118	105	31	62	60	48
	TP 8	McKiernan-Terry DE-30	12" Pipe #7 Gage	2800	96.0	22400 (2)	6.66	80.0	1810 4080	5890	5.2 610.0	0.15	1.05	5.00	0.75	0.65	180	920 5.11	156 0.87	147 0.82	154 0.86	669 3.71	857 4.76	400 2.22	94 0.52	423 2.35	220 1.22	89 0.50	153	52	37	51	111	143	133	31	70	73	46
	TP 9	Vulcan 1	12" Pipe #7 Gage	5000	36.0	15000	6.66	79.8	1725 2910	4635	9.5 610.0	0.15	1.05	5.00	0.75	0.65	180	877 4.87	157 0.87	144 0.80	177 0.98	909 5.05	1338 7.43	346 1.92	96 0.54	540 3.00	207 1.15	94 0.52	146	52	36	59	152	223	115	32	90	89	47
	TP 10	Delmag D-12	12" Pipe .25" Wall	2750	98.0	22500 (2)	9.23	81.3	2560 3749	6309	5.1 610.0	0.10	0.86	5.00	0.75	0.65	180	912 5.07	176 0.99	166 0.92	167 0.93	635 3.53	816 4.53	453 2.52	106 0.59	405 2.25	219 1.22	101 0.56	152	59	41	56	106	136	151	35	68	73	50
	TP 11	McKiernan-Terry DE-30	12" Pipe .25" Wall	2800	96.0	22400 (2)	9.23	81.3	2560 4080	6640	4.2 610.0	0.15	0.90	5.00	0.75	0.65	180	795 4.42	156 0.86	159 0.88	156 0.86	566 3.14	660 3.66	434 2.41	110 0.57	349 1.94	208 1.16	87 0.48	133	52	40	52	94	110	145	34	58	69	44
	TP 12	Vulcan 1	Fluted taper #7 Gage	5000	36.0	15000	6.66	54.4	1214 2912	4126	6.1 610.0	0.15	0.77	5.00	0.48	0.62	180	682 3.79	184 1.02	167 0.93	201 1.11	730 4.06	880 4.89	380 2.11	100 0.55	436 2.42	187 1.04	106 0.59	114	61	42	67	122	147	127	33	73	62	53
	TP 13 (1)	Delmag D-12	12 H53	2750	98.0	22500 (2)	15.58	80.0	4240 1854	6094	4.5 610.0	0.10	0.63	5.00	0.75	0.63	230	838 3.64	207 0.90	204 0.89	198 0.86	608 2.65	790 3.17	540 2.35	132 0.57	377 1.64	212 0.92	115 0.50	140	69	51	66	101	122	180	44	63	71	57
	TP 14	Vulcan 1	12" Pipe .25" Wall	5000	36.0	15000	9.23	61.0	1920 2912	4824	6.8 610.0	0.15	0.84	5.00	0.75	0.65	180	729 4.05	202 1.12	181 1.01	213 1.19	739 4.11	949 5.27	422 2.35	112 0.62	443 2.46	192 1.07	121 0.67	121	67	45	71	123	158	141	37	74	64	61
	TP 15	Vulcan 1	12" Pipe .25" Wall	5000	36.0	15000	9.23	60.8	1910 2912	4822	5.5 610.0	0.15	0.64	5.00	0.75	0.65	180	639 3.55	190 1.06	176 0.98	204 1.13	647 3.59	768 4.27	403 2.24	109 0.61	389 2.16	182 1.01	114 0.63	106	63	44	68	108	128	134	36	65	61	57
	TP 16	Link Belt 312	12" Pipe #7 Gage	3855	30.9	18000 (2)	6.66	80.0	1730 4479	6209	5.5 610.0	0.10	1.25	5.00	0.75	0.65	180	766 4.26	128 0.71	138 0.76	152 0.84	630 3.50	801 4.45	355 1.97	90 0.50	389 2.16	200 1.11	76 0.42	128	43	34	51	105	133	118	30	65	67	38

(1) Pile driven without load cell assembly.
(2) Manufacturer's maximum hammer rating.
(3) Effective length for friction pile. Total length 61.1 ft with 3.1 ft earth plug.
(4) Open-end pile.
(5) No interpolated estimate possible.
(6) Value at 6th Loading Cycle

TABLE 34
DYNAMIC PILE DRIVING FORMULA EVALUATION
Belleville Reaction Piles at Tip Elevation 600

	Pile Number	Hammer Type	Pile Type	Ram Weight, lb	Stroke, in.	Manufacturer's Rated Energy, ft-lb	Cross-Sectional Pile Area, sq in.	Total Pile Length, ft	Pile Weight, lb / Driving Head & Load Cushion Wt, lb	Gross Pile Weight, lb	Penetration Resistance, blows/in at Tip Elevation, ft	C_1, Temporary Compression of Pile Head and Cap, in.	C_2+C_3, Temporary Compression of Pile and Ground, in.	M, Efficiency of Hammer, in./ft (Rabe)	C_t, Factor used in Calculating Compression Loss in Pile (Rabe)	B, Soil Factor (Rabe)	R_t, Yield Load Failure, kips	R_u, Computed Ultimate Pile Load Capacity, kips — Ratio: R_u/R_t										R_d, Computed Design Pile Load Capacity, kips										
																		Engineering News	Hiley	Pacific Coast Uniform Building Code	Redtenbacher	Eytelwein	Navy-McKay	Rankine	Canadian National Building Code	Modified Engineering News	Gates	Rabe	Engineering News, SF=6	Hiley, SF=3	Pacific Coast Uniform Building Code, SF=4	Redtenbacher, SF=3	Eytelwein, SF=6	Navy-McKay, SF=6	Rankine, SF=3	Canadian National Building Code, SF=3	Modified Engineering News, SF=6	Gates, SF=3	Rabe, SF=2
	1	2	3	4	5	6	7	8	9	10	11	12	13	14	15	16	17	18	19	20	21	22	23	24	25	26	27	28	29	30	31	32	33	34	35	36	37	38	39
INTERPOLATED CAPACITY	RP 1	McKiernan-Terry DE-30	12 H53	2800	96.0	22400(1)	15.58	60.0	3180 3834	7014	5.0 600.0	0.15	0.29	5.00	0.88	0.71	320	894 2.79	275 0.86	227 0.71	211 0.66	597 1.86	767 2.40	615 1.92	132 0.41	385 1.20	218 0.68	168 0.53	149	92	57	70	99	128	205	44	64	73	84
	RP 2	Vulcan 50C	12 H53	5000	15.5	15100	15.58	59.0	3120 2660	5780	4.5 600.0	0.10	0.28	5.25	0.88	0.71	320	564 1.76	252 0.79	204 0.64	217 0.68	534 1.67	606 1.89	458 1.43	129 0.40	324 1.01	174 0.54	173 0.54	94	84	51	72	89	101	153	43	54	58	57
	RP 3	Link Belt 312	12 H53	3855	30.9	18000(1)	15.58	60.0	3180 4229	7409	6.0 600.0	0.10	0.56	5.00	0.88	0.71	320	810 2.53	207 0.65	218 0.68	220 0.69	602 1.88	822 2.57	563 1.75	129 0.40	385 1.20	204 0.64	131 0.41	135	69	54	73	100	137	188	43	64	68	66
	RP 4	McKiernan-Terry DE-30	12 H53	2800	96.0	22400(1)	15.58	60.1	3185 3834	7019	8.8 600.0	0.15	0.33	5.00	0.88	0.71	320	1260 3.94	327 1.02	250 0.78	250 0.78	738 2.31	1350 4.22	700 2.19	142 0.44	541 1.69	249 0.78	200 0.62	210	109	62	83	123	225	233	47	90	83	100
	RP 5	Delmag D-12	12 H53	2750	98.0	22500(1)	15.58	60.0	3180 3499	6679	5.2 600.0	0.10	0.35	5.00	0.88	0.71	320	924 2.88	282 0.88	231 0.72	218 0.68	620 1.94	812 2.54	624 1.96	135 0.42	402 1.26	220 0.69	173 0.54	154	94	58	73	103	135	208	45	67	73	86
	RP 6	Vulcan 1	12 H53	5000	36.0	15000	15.58	70.0	3710 2660	6370	7.1 600.0	0.15	0.49	5.00	0.88	0.71	320	750 2.34	216 0.68	205 0.64	229 0.71	672 2.10	924 2.88	495 1.54	132 0.41	414 1.29	194 0.61	141 0.44	125	72	51	76	112	154	165	44	69	65	71
	RP 7	Link Belt 312	12 H53	3855	30.9	18000(1)	15.58	80.0	4240 4229	8469	11.7 600.0	0.10	0.66	5.00	0.88	0.71	320	1164 3.64	210 0.66	206 0.64	216 0.68	708 2.21	1523 4.76	571 1.79	130 0.41	526 1.64	238 0.74	131 0.41	194	70	51	73	116	254	190	43	88	79	55
	RP 8	Delmag D-12	12 H53	2750	98.0	22500(1)	15.58	80.0	4240 3499	7739	6.1 600.0	0.10	0.58	5.00	0.88	0.71	320	1020 3.19	221 0.69	206 0.64	195 0.61	606 1.89	893 2.79	583 1.82	128 0.40	421 1.32	229 0.72	132 0.41	170	74	51	65	101	149	194	43	70	76	66
	RP 9	Vulcan 1	12 H53	5000	36.0	15000	15.58	80.0	4240 2660	6900	10.5 600.0	0.15	0.49	5.00	0.88	0.71	320	924 2.88	233 0.73	200 0.63	229 0.72	774 2.42	1338 4.17	507 1.59	132 0.41	498 1.56	212 0.66	152 0.47	154	76	50	76	129	223	169	44	83	71	76
	RP 10	McKiernan-Terry DE-30	12 H53	2800	96.0	22400(1)	15.58	60.1	3185 3834	7019	6.0 600.0	0.15	0.44	5.00	0.88	0.71	320	1008 3.15	250 0.78	235 0.74	228 0.70	644 2.01	921 2.88	646 2.00	136 0.42	433 1.35	228 0.71	153 0.48	168	83	59	75	107	153	215	45	72	76	76
	RP 11	Vulcan 50C	12 H53	5000	15.5	15100	15.58	61.0	3230 2660	5890	6.0 600.0	0.10	0.39	5.25	0.88	0.71	320	678 2.12	250 0.78	215 0.67	236 0.74	636 1.99	804 2.51	500 1.56	133 0.42	384 1.20	187 0.59	172 0.54	113	83	54	79	106	134	167	44	64	62	86
	RP 12	Delmag D-12	12 H53	2750	98.0	22500(1)	15.58	60.0	3180 3499	6679	8.1 600.0	0.10	0.37	5.00	0.88	0.71	320	1206 3.77	328 1.02	249 0.78	249 0.78	737 2.30	1265 3.95	692 2.18	142 0.44	526 1.64	245 0.77	201 0.63	201	109	62	83	123	211	231	47	88	82	101
	RP 14	Vulcan 50C	12 H53	5000	15.5	15100	15.58	60.0	3180 2660	5840	6.4 600.0	0.10	0.42	5.25	0.88	0.71	320	708 2.22	248 0.78	220 0.69	243 0.76	666 2.08	858 2.68	512 1.61	135 0.42	402 1.25	190 0.59	171 0.53	118	83	55	81	111	143	171	45	67	63	85
	RP 15	Link Belt 312	12 H53	3855	30.9	18000(1)	15.58	60.0	3180 4229	7409	4.9 600.0	0.10	0.38	5.00	0.88	0.71	320	708 2.22	231 0.72	208 0.65	204 0.64	545 1.70	671 2.10	529 1.67	126 0.39	338 1.06	194 0.62	147 0.46	118	77	52	68	91	112	176	42	56	65	73
	RP 16	McKiernan-Terry DE-30	12 H53	2800	96.0	22400(1)	15.58	60.1	3185 3834	7019	6.2 600.0	0.15	0.35	5.00	0.88	0.71	320	1026 3.21	281 0.88	237 0.74	228 0.71	652 2.04	951 2.97	651 2.04	136 0.43	442 1.38	230 0.72	172 0.54	171	94	59	76	109	159	217	45	74	77	86
	RP 17	Vulcan 50C	12 H53	5000	15.5	15100	15.58	60.0	3180 2660	5840	5.3 600.0	0.10	0.34	5.25	0.88	0.71	320	630 1.97	253 0.79	212 0.66	229 0.72	594 1.86	714 2.23	483 1.52	131 0.41	360 1.13	181 0.57	174 0.54	105	84	53	76	99	119	161	44	60	60	87
	RP 18	Link Belt 312	12 H53	3855	30.9	18000(1)	15.58	60.0	3180 4229	7409	6.4 600.0	0.10	0.42	5.00	0.88	0.71	320	840 2.63	247 0.77	221 0.69	225 0.70	620 1.94	877 2.74	573 1.79	131 0.41	401 1.25	207 0.65	157 0.49	140	82	55	75	103	146	191	44	67	69	78
	RP 19	Vulcan 50C	12 H53	5000	15.5	15100	15.58	60.0	3180 2660	5840	7.4 600.0	0.10	0.38	5.25	0.88	0.71	320	768 2.40	275 0.86	224 0.70	253 0.79	720 2.25	990 3.10	533 1.67	137 0.43	438 1.37	197 0.61	189 0.59	128	92	56	84	120	165	178	46	73	66	95
	RP 20	McKiernan-Terry DE-30	12 H53	2800	96.0	22400(1)	15.58	80.0	4240 3834	8074	16.4 600.0	0.15	0.59	5.00	0.88	0.71	320	1668 5.21	254 0.79	226 0.71	232 0.72	769 2.40	236 7.39	667 2.09	138 0.43	681 2.13	284 0.88	151 0.47	278	85	57	77	128	393	222	46	114	95	76

(1) Manufacturer's maximum hammer rating.

TABLE 34 (cont.)
DYNAMIC PILE DRIVING FORMULA EVALUATION
Belleville Reaction Piles at Tip Elevation 600

	Pile Number	Hammer Type	Pile Type	Ram Weight, lb	Stroke, in.	Manufacturer's Rated Energy, ft-lb	Cross-Sectional Pile Area, sq in.	Total Pile Length, ft	Pile Weight, lb / Driving Head & Load Cell Wt, lb	Gross Pile Weight, lb	Penetration Resistance, blows/in. at Tip Elevation, ft	C_1, Temporary Compression of Pile Head and Cap, in.	C_2+C_3, Temporary Compression of Pile and Ground, in.	M, Efficiency of Hammer, in./ft (Rabe)	C_4, Factor used in Calculating Compression Loss in Pile (Rabe)	E, Soil Factor (Rabe)	Load Data: R_y, Yield Load Failure, kips	R_a, Computed Ultimate Pile Load Capacity, kips / Ratio: R_a/R_r										R_d, Computed Design Pile Load Capacity, kips										
																		Engineering News	Hiley	Pacific Coast Uniform Building Code	Redtenbacher	Eytelwein	Navy-McKay	Rankine	Canadian National Building Code	Modified Engineering News	Gates	Rabe	Engineering News, SF=5	Hiley, SF=3	Pacific Coast Uniform Building Code, SF=4	Redtenbacher, SF=3	Eytelwein, SF=6	Navy-McKay, SF=5	Rankine, SF=3	Canadian National Building Code, SF=3	Modified Engineering News, SF=5	Gates, SF=3	Rabe, SF=2
	1	2	3	4	5	6	7	8	9	10	11	12	13	14	15	16	17	18	19	20	21	22	23	24	25	26	27	28	29	30	31	32	33	34	35	36	37	38	39
INTERPOLATED CAPACITY	RP 21	Link Belt 312	12 H53	3855	30.9	18000(1)	15.58	60.0	3180 / 4229	7409	5.2 / 600.0	0.10	0.43	5.00	0.88	0.71	320	738 / 2.31	225 / 0.70	211 / 0.66	209 / 0.65	562 / 1.76	712 / 2.23	540 / 1.69	127 / 0.40	351 / 1.10	197 / 0.62	143 / 0.45	123	75	53	70	94	119	180	42	58	66	71
	RP 22	Vulcan 50C	12 H53	5000	15.5	15100	15.58	80.0	4240 / 2660	6900	7.2 / 600.0	0.10	0.59	5.00	0.88	0.71	320	756 / 2.36	201 / 0.63	192 / 0.60	213 / 0.67	654 / 2.04	924 / 2.89	474 / 1.48	128 / 0.40	408 / 1.27	195 / 0.61	131 / 0.41	126	67	48	71	109	154	158	43	68	65	66
	RP 23	Delmag D-12	12 H53	2750	98.0	22500(1)	15.58	60.1	3185 / 3499	6684	5.3 / 600.0	0.10	0.36	5.00	0.88	0.71	320	936 / 2.93	281 / 0.88	232 / 0.72	220 / 0.69	625 / 1.95	828 / 2.59	627 / 1.96	135 / 0.42	407 / 1.27	221 / 0.69	172 / 0.54	156	94	58	73	104	138	209	45	68	74	86
	RP 24	Link Belt 312	12 H53	3855	30.9	18000(1)	15.58	60.0	3180 / 4229	7409	5.6 / 600.0	0.10	0.43	5.00	0.88	0.71	320	774 / 2.42	232 / 0.72	215 / 0.67	215 / 0.67	583 / 1.82	767 / 2.40	552 / 1.73	128 / 0.40	369 / 1.15	201 / 0.63	147 / 0.46	129	77	54	72	97	128	184	43	61	67	73
	RP 25	Vulcan 50C	12 H53	5000	15.5	15100	15.58	60.0	3180 / 2660	5840	6.2 / 600.0	0.10	0.49	5.25	0.88	0.71	320	696 / 2.18	226 / 0.71	216 / 0.68	241 / 0.75	654 / 2.04	834 / 2.60	508 / 1.59	135 / 0.42	397 / 1.24	189 / 0.59	156 / 0.49	116	75	54	80	109	139	169	45	56	63	78
	RP 26	McKiernan-Terry DE-30	12 H53	2800	96.0	22400(1)	15.58	61.0	3230 / 3834	7064	6.0 / 600.0	0.15	0.38	5.00	0.88	0.71	320	1008 / 3.13	267 / 0.83	234 / 0.73	223 / 0.70	642 / 2.01	918 / 2.87	645 / 2.01	135 / 0.42	432 / 1.35	228 / 0.71	163 / 0.51	168	89	58	74	107	153	214	45	72	76	81
	RP 27	Delmag D-12	12 H53	2750	98.0	22500(1)	15.58	60.1	3185 / 3499	6684	7.2 / 600.0	0.10	0.33	5.00	0.88	0.71	320	1128 / 3.52	332 / 1.04	245 / 0.77	242 / 0.76	707 / 2.21	1124 / 3.51	676 / 2.11	140 / 0.44	492 / 1.54	238 / 0.75	204 / 0.64	188	111	61	81	118	187	228	47	82	79	102
	RP 28	Vulcan 1	12 H53	5000	36.0	15000	15.58	60.0	3180 / 2660	5840	10.2 / 600.0	0.15	0.49	5.00	0.88	0.71	320	908 / 2.83	246 / 0.77	232 / 0.73	270 / 0.84	840 / 2.63	1362 / 4.27	568 / 1.78	141 / 0.44	516 / 1.62	210 / 0.66	161 / 0.50	151	82	58	90	140	227	189	47	86	70	80
	RP 29	Link Belt 312	12 H53	3855	30.9	18000(1)	15.58	60.0	3180 / 4229	7408	6.3 / 600.0	0.10	0.38	5.00	0.88	0.71	320	834 / 2.61	258 / 0.80	220 / 0.69	223 / 0.70	616 / 1.92	862 / 2.70	571 / 1.79	130 / 0.41	397 / 1.24	207 / 0.65	163 / 0.51	139	86	55	74	103	144	190	43	66	69	82
	RP 30	Delmag D-12	12 H53	2750	98.0	22500(1)	15.58	60.0	3190 / 3499	6678	6.4 / 600.0	0.10	0.22	5.00	0.88	0.71	320	1056 / 3.30	371 / 1.16	240 / 0.75	234 / 0.73	676 / 2.11	1000 / 3.12	660 / 2.06	139 / 0.43	458 / 1.43	231 / 0.72	228 / 0.71	176	124	60	78	113	167	220	46	76	77	114
	RP 31	McKiernan-Terry DE-30	12 H53	2800	96.0	22400(1)	15.58	60.0	3180 / 3834	7014	5.8 / 600.0	0.15	0.40	5.00	0.88	0.71	320	1260 / 3.94	297 / 0.93	250 / 0.78	250 / 0.78	738 / 2.31	1351 / 4.22	701 / 2.19	142 / 0.44	541 / 1.69	249 / 0.78	182 / 0.57	210	99	63	83	123	225	234	47	90	83	91
	RP 32	Link Belt 312	12 H53	3855	30.9	18000(1)	15.58	60.0	3180 / 4229	7409	6.1 / 600.0	0.10	0.35	5.00	0.88	0.71	320	816 / 2.55	264 / 0.83	219 / 0.68	221 / 0.69	607 / 1.90	836 / 2.61	566 / 1.77	130 / 0.41	389 / 1.22	205 / 0.64	168 / 0.52	136	88	55	74	101	139	189	43	65	68	84
	RP 33	Vulcan 1	12 H53	5000	36.0	15000	15.58	60.0	4240 / 2660	6900	7.9 / 600.0	0.15	0.68	5.00	0.88	0.71	320	792 / 2.48	178 / 0.56	192 / 0.60	216 / 0.68	678 / 2.12	1008 / 3.13	482 / 1.51	128 / 0.40	426 / 1.33	199 / 0.62	116 / 0.36	132	60	48	72	113	168	161	43	71	66	58
	RP 34	McKiernan-Terry DE-30	12 H53	2800	96.0	22400(1)	15.58	60.0	3180 / 3834	7014	5.0 / 600.0	0.15	0.40	5.00	0.88	0.71	320	894 / 2.78	243 / 0.76	227 / 0.71	211 / 0.66	597 / 1.86	787 / 2.40	615 / 1.93	132 / 0.41	385 / 1.20	218 / 0.68	148 / 0.46	149	81	57	70	98	128	205	44	64	73	74
	RP 35	Delmag D-12	12 H53	2750	98.0	22500(1)	15.58	60.0	3180 / 3499	6679	5.4 / 600.0	0.10	0.38	5.00	0.88	0.71	320	948 / 2.96	276 / 0.86	233 / 0.73	221 / 0.69	631 / 1.97	843 / 2.64	631 / 1.97	135 / 0.42	412 / 1.29	222 / 0.70	170 / 0.53	158	92	58	74	105	141	210	45	69	74	85
	RP 36	Vulcan 1	12 H53	5000	36.0	15000	15.58	60.0	3180 / 2660	5840	7.2 / 600.0	0.15	0.39	5.00	0.88	0.71	320	756 / 2.38	251 / 0.78	224 / 0.70	250 / 0.78	702 / 2.20	960 / 3.00	527 / 1.64	135 / 0.43	432 / 1.35	195 / 0.61	164 / 0.51	126	84	56	83	117	160	176	45	72	65	82
	RP 37	Vulcan 50C	12 H53	5000	15.5	15100	15.58	60.0	3180 / 2660	5840	5.8 / 600.0	0.10	0.38	5.25	0.88	0.71	320	666 / 2.08	251 / 0.78	216 / 0.67	236 / 0.74	624 / 1.95	780 / 2.44	498 / 1.56	132 / 0.41	378 / 1.18	186 / 0.58	172 / 0.54	111	84	54	79	104	130	166	44	63	62	86
	RP 38	Delmag D-12	12 H53	2750	98.0	22500(1)	15.58	60.0	3180 / 3499	6679	6.6 / 600.0	0.10	0.30	5.00	0.88	0.71	320	1074 / 3.36	334 / 1.04	242 / 0.76	236 / 0.74	685 / 2.14	1031 / 3.22	663 / 2.08	139 / 0.43	467 / 1.46	234 / 0.73	205 / 0.64	179	111	60	79	114	172	221	46	78	78	103

(1) Manufacturer's maximum hammer rating.

TABLE 35
DYNAMIC PILE DRIVING FORMULA EVALUATION
Detroit Load Test Piles and Test Piles at Various Elevations

	Pile Number	Hammer Type	Pile Type	Ram Weight, lb	Stroke, in.	Manufacturer's Rated Energy, ft-lb	Cross-Sectional Pile Area, sq in.	Total Pile Length, ft	Pile Weight, lb Driving Head & Load Cell Wt, lb	Gross Pile Weight, lb	Penetration Resistance, blows/in. at Tip Elevation, ft	C_1, Temporary Compression of Pile Head and Cap, in.	C_2 + C_3, Temporary Compression of Pile and Ground, in.	M, Efficiency of Hammer, lb./ft (Rabe)	C, Factor used in Calculating Compression Loss in Pile (Rabe)	B_1, Soil Factor (Rabe)	R_t, Yield Load Failure, kips	R_u, Computed Ultimate Pile Load Capacity, kips — Ratio: R_u/R_t										R_d, Computed Design Pile Load Capacity, kips										
																		Engineering News	Hiley	Pacific Coast Uniform Building Code	Redtenbacher	Eytelwein	Navy-McKay	Rankine	Canadian National Building Code	Modified Engineering News	Gates	Rabe	Engineering News, SF=6	Hiley, SF=3	Pacific Coast Uniform Building Code, SF=4	Redtenbacher, SF=3	Eytelwein, SF=6	Navy-McKay, SF=6	Rankine, SF=3	Canadian National Building Code, SF=3	Modified Engineering News, SF=6	Gates, SF=3	Rabe, SF=3
	1	2	3	4	5	6	7	8	9	10	11	12	13	14	15	16	17	18	19	20	21	22	23	24	25	26	27	28	29	30	31	32	33	34	35	36	37	38	39
LOAD TEST CAPACITY	LTP 1 [4]	Vulcan 1	12" Pipe #7 Gage	5000	36.0	15000	6.66	[3] 55.2	3365 [1] 2934 2910	8309	1.8 519.9	0.15	0.42	5.00	1.00	0.46	60 [5]	275 4.58	108 1.79	106 1.76	95 1.58	249 4.16	216 3.60	239 3.98	67 1.12	138 2.30	132 2.19	45 0.75	46	36	26	32	42	36	30	22	23	44	22
	LTP 2	Vulcan 1	12" Pipe #7 Gage	5000	36.0	15000	6.66	90.0	2940 2910	4950	36.0 510.8	0.15	0.78	5.00	1.00	0.67	226	1409 6.23	220 0.98	142 0.63	178 0.79	1420 6.28	4996 22.11	355 1.57	97 0.43	850 3.76	268 1.19	136 0.60	235	73	35	59	237	833	118	32	142	89	68
	LTP 7	McKiernan-Terry DE-30	Fluted taper #7 Gage	2800	96.0	22400 [2]	6.66	85.3	2384 4080	6464	30.0 508.3	0.15	1.00	5.00	1.00	0.67	295	2016 6.81	196 0.66	154 0.52	172 0.58	1017 3.44	4764 16.10	445 1.50	98 0.33	894 3.02	317 1.07	115 0.39	336	65	38	57	170	794	148	33	149	106	57
	LTP 8	Vulcan 1	12 H53	5000	36.0	15000	15.58	97.0	5150 2660	7810	37.0 508.3	0.15	0.39	5.00	1.00	0.58	360	1417 3.94	311 0.86	193 0.54	227 0.63	982 2.73	4535 12.60	516 1.43	132 0.37	728 2.02	269 0.75	164 0.46	236	104	48	76	164	756	172	44	121	90	82
	LTP 10	Link Belt 312	12" Pipe .23" Wall	3855	30.9	18000 [2]	8.50	90.0	2610 4479	7089	51.0 508.4	0.10	1.02	5.00	1.00	0.68	388	1806 4.65	180 0.46	160 0.41	185 0.48	1061 2.74	7699 18.30	442 1.14	105 0.27	873 2.25	311 0.80	110 0.28	301	65	41	56	210	1262	148	37	156	104	60
INTERPOLATED CAPACITY	TP 3	McKiernan-Terry DE-30	12" Pipe .22" Wall .25" Wall	2800	96.0	22400 [2]	8.50	85.0	2493 4080	6573	30.0 508.7	0.15	1.00	5.00	1.00	0.59	400	2016 5.04	195 0.49	174 0.44	192 0.48	1003 2.51	4732 11.83	502 1.26	110 0.28	889 2.22	317 0.79	100 0.25	336	65	44	64	167	789	167	37	148	106	50
	TP 4	Link Belt 312	12" Pipe #7 Gage	3855	30.9	18000 [2]	6.66	90.0	2040 4479	6519	6.0 510.0	0.10	0.80	5.00	1.00	0.68	235	810 3.45	175 0.74	131 0.56	144 0.61	643 2.74	850 3.66	343 1.46	88 0.38	404 1.72	204 0.87	108 0.46	135	58	33	48	107	143	114	29	67	68	54
	TP 5	Vulcan 50C	12" Pipe #7 Gage	5000	15.5	15100	6.66	84.1	1900 2910	4810	10.2 511.0	0.10	0.72	5.25	1.00	0.67	235	915 3.89	217 0.92	141 0.60	173 0.74	933 3.97	1434 6.10	342 1.45	96 0.41	557 2.37	211 0.90	141 0.60	152	72	35	58	155	239	114	32	93	70	71
	TP 6	Vulcan 1	Fluted taper #7 Gage	5000	36.0	15000	6.66	97.1	2180 2910	5090	7.0 511.0	0.15	0.67	5.00	1.00	0.66	235	741 3.15	195 0.83	127 0.54	152 0.65	736 3.14	965 4.10	306 1.30	91 0.39	443 1.88	193 0.82	119 0.51	124	65	32	51	123	161	102	30	74	64	59
	TP 8	Vulcan 1	Fluted taper #7 Gage	5000	36.0	15000	6.66	97.1	2180 2910	5090	19.0 510.0	0.15	0.67	5.00	1.00	0.66	295	1179 4.00	232 0.79	134 0.45	166 0.56	1164 3.95	2619 8.87	334 1.13	95 0.32	704 2.38	239 0.81	142 0.48	197	77	34	55	194	436	111	32	117	80	71
	TP 12	Delmag D-12	12" Pipe .23" Wall	2750	98.0	22500 [2]	8.11	90.0	2480 3749	6229	6.0 510.0	0.10	1.00	5.00	1.00	0.68	285	1013 3.44	168 0.57	153 0.52	159 0.54	687 2.33	965 3.27	424 1.44	101 0.35	452 1.53	228 0.77	100 0.34	169	56	38	53	114	161	141	34	75	76	50
	TP 13	McKiernan-Terry DE-30	12" Pipe #7 Gage	2800	96.0	22400 [2]	6.66	90.0	2040 4080	6120	8.0 510.0	0.15	1.05	5.00	1.00	0.68	265	1195 4.51	168 0.63	144 0.54	155 0.59	782 2.96	1299 4.89	402 1.52	95 0.36	541 2.04	244 0.92	100 0.38	199	56	36	52	130	216	134	32	90	81	50
	TP 13	McKiernan-Terry DE-30	12" Pipe #7 Gage	2800	96.0	22400 [2]	6.66	90.0	2040 4080	6120	20.0 508.2	0.15	1.05	5.00	1.00	0.68	360	1792 4.98	187 0.52	151 0.42	168 0.47	1001 2.78	3247 9.02	428 1.19	98 0.27	811 2.26	295 0.82	112 0.31	299	62	38	56	167	541	143	33	135	98	56
	TP 15	Delmag D-12	12 H53	2750	98.0	22500 [2]	15.58	96.1	5100 3499	8599	6.0 508.5	0.10	0.50	5.00	1.00	0.58	350	1013 2.89	229 0.65	186 0.53	172 0.49	563 1.61	836 2.39	540 1.54	122 0.35	401 1.14	228 0.65	109 0.31	169	76	47	57	94	139	180	41	67	76	55

(1) Weight of 33.7 ft earth plug.
(2) Manufacturer's maximum hammer rating.
(3) Effective length for friction pile. Total length = 90 ft.
(4) Open-end pile.
(5) Value at 4th Loading Cycle

TABLE 36
DYNAMIC PILE DRIVING FORMULA EVALUATION
Muskegon Load Test Piles and Test Piles at Various Elevations

	Pile Number	Hammer Type	Pile Type	Ram Weight, lb	Stroke, in.	Manufacturer's Rated Energy, ft-lb	Cross-Sectional Pile Area, sq in.	Total Pile Length, ft	Pile Weight, lb Driving Head & Load Cell Wt, lb	Gross Pile Weight, lb	Penetration Resistance, blows/in. at Tip Elevation, ft	C_1, Temporary Compression of Pile Head and Cap, in.	$C_2 + C_3$, Temporary Compression of Pile and Ground, in.	M, Efficiency of Hammer, lb./ft (Hebe)	C, Factor used in Calculating Compression Loss in Pile (Hebe)	E, Soil Factor (Hebe)	R_y, Yield Load Failure, kips	R_u, Computed Ultimate Pile Load Capacity, kips — Ratio: R_u/R_t: Engineering News	Hiley	Pacific Coast Uniform Building Code	Redtenbacher	Eytelwein	Navy–McKay	Rankine	Canadian National Building Code	Modified Engineering News	Gates	Hebe	R_d, Computed Design Pile Load Capacity, kips: Engineering News, SF=6	Hiley, SF=3	Pacific Coast Uniform Building Code, SF=4	Redtenbacher, SF=3	Eytelwein, SF=6	Navy–McKay, SF=6	Rankine, SF=3	Canadian National Building Code, SF=3	Modified Engineering News, SF=6	Gates, SF=3	Hebe, SF=2
	1	2	3	4	5	6	7	8	9	10	11	12	13	14	15	16	17	18	19	20	21	22	23	24	25	26	27	28	29	30	31	32	33	34	35	36	37	38	39
LOAD TEST CAPACITY	LTP 2	Vulcan 1	12" Pipe .23" Wall	5000	36.0	15000	8.50	60.0	1740 2910	4650	8.0 530.0	0.15	0.45	5.00	0.75	0.96	140	800 5.71	261 1.86	181 1.29	217 1.55	826 5.90	1126 8.04	424 3.03	110 0.79	493 3.52	200 1.43	231 1.65	133	87	45	72	138	188	141	37	82	67	116
	LTP 3	Vulcan 1	Fluted taper #7 gage	5000	36.0	15000	6.66	60.5	1380 2910	4270	4.0 530.2	0.15	0.35	5.00	0.52	0.93	100	514 5.14	228 2.28	149 1.49	172 1.72	537 5.37	573 5.73	328 3.28	94 0.94	325 3.25	168 1.68	196 1.96	86	76	37	57	89	96	109	31	54	56	98
	LTP 4	Vulcan 1	12" Pipe .23" Wall	5000	36.0	15000	8.50	60.0	1740 2910	4650	2.0 530.0	0.15	0.45	5.00	0.75	0.75	70	300 4.29	139 1.98	132 1.88	135 1.93	304 4.34	281 4.02	263 3.75	89 1.27	185 2.64	136 1.95	96 1.37	50	46	33	45	51	47	88	30	31	45	48
	LTP 5	Raymond M15	Raymond Shell	5000	18.0	15000	50.00	64.0	10780 ——	10780	6.0 530.0	0.10	0.13	5.25	0.44	0.94	180	675 3.75	291 1.62	282 1.57	248 1.38	471 2.62	636 3.64	702 3.90	178 0.99	307 1.71	186 1.04	253 1.41	113	97	71	83	78	109	234	59	51	62	126
	LTP 6	Delmag D-22	12" Pipe .25" Wall	4850	98.0	39700[1]	9.23	133.5	4190 4505	8695	3.0 460.0	0.10	1.05	5.00	0.80	0.92	460	1099 2.39	255 0.55	188 0.39	192 0.42	929 2.02	929 2.02	470 1.02	137 0.30	537 1.17	252 0.55	212 0.46	183	85	45	64	155	155	157	46	89	84	106
	LTP 9	Vulcan 80C	12" Pipe .25" Wall	8000	16.5	24450	9.23	134.0	4190 4050	8240	5.5 459.8	0.10	0.70	5.25	0.80	0.92	470	1041 2.22	300 0.64	162 0.34	194 0.41	1030 2.19	1233 2.62	391 0.83	128 0.27	620 1.32	233 0.50	268 0.57	174	100	40	65	172	205	130	43	103	78	134
INTERPOLATED CAPACITY	TP 1[4]	Vulcan 1	12" Pipe .23" Wall	5000	36.0	15000	8.50	58.3	2000[3] 1750 2910	6660	5.2 531.6	0.15	0.21	5.00	0.75	0.95	122[2]	616 5.05	263 2.16	162 1.33	177 1.45	553 4.53	669 5.48	391 3.20	97 0.80	335 2.75	180 1.47	230 1.88	103	88	40	59	92	111	130	32	56	60	115
	LTP 6	Delmag D-22	12" Pipe .25" Wall	4850	98.0	39700[1]	9.23	80.0	2520 4505	7025	1.0 530.0	0.10	0.49	5.00	0.75	0.96	140	433 3.09	194 1.39	168 1.20	154 1.10	416 2.97	332 2.37	363 2.59	120 0.86	228 1.63	171 1.22	171 1.22	72	65	42	51	69	55	121	40	38	57	85
	LTP 7	Vulcan 80C	12" Pipe .25" Wall	8000	16.5	24450	9.23	80.0	2520 4050	6570	1.8 530.0	0.10	0.33	5.25	0.75	0.96	140	448 3.20	244 1.74	170 1.21	184 1.32	460 3.29	424 3.03	344 2.46	122 0.87	287 2.05	168 1.20	227 1.62	75	81	42	61	77	71	115	41	48	56	113
	LTP 8	Delmag D-22	12" Pipe .25" Wall	4850	98.0	39700[1]	9.23	80.0	2520 4505	7025	1.0 530.0	0.10	0.55	5.00	0.75	0.96	140	433 3.09	190 1.36	168 1.20	154 1.10	416 2.97	332 2.37	363 2.59	120 0.86	228 1.63	171 1.22	167 1.19	72	63	42	51	69	55	121	40	38	57	83
	LTP 9	Vulcan 80C	12" Pipe .25" Wall	8000	16.5	24450	9.23	80.0	2520 4050	6570	1.7 530.0	0.10	0.41	5.25	0.75	0.96	140	426 3.05	223 1.59	167 1.19	179 1.28	438 3.13	400 2.86	334 2.39	120 0.86	273 1.95	165 1.18	207 1.48	71	74	42	60	73	67	111	40	46	55	104
	TP 10	McKiernan-Terry DE-40	12" Pipe .25" Wall	4000	96.0	32000[1]	9.23	80.0	2520 6160	8680	1.5 530.0	0.15	0.42	5.00	0.75	0.96	140	501 3.58	183 1.31	155 1.11	135 0.96	435 3.10	349 2.49	384 2.74	104 0.75	227 1.62	180 1.29	155 1.11	83	61	39	45	72	58	123	35	38	60	77
	TP 11	McKiernan-Terry DE-40	12" Pipe .25" Wall	4000	96.0	32000[1]	9.23	80.0	2520 6160	8680	1.6 530.0	0.15	0.51	5.00	0.75	0.96	140	530 3.78	183 1.30	159 1.14	140 1.00	456 3.26	372 2.66	398 2.83	107 0.76	241 1.72	164 1.32	154 1.10	88	61	40	47	76	62	132	36	40	61	77
	TP 12	Link Belt 520	12" Pipe .25" Wall	5070	43.2	30000[1]	9.23	80.0	2520 4470	6990	1.5 530.0	0.10	0.51	5.00	0.75	0.96	140	470 3.35	199 1.42	165 1.18	160 1.14	447 3.20	382 2.73	366 2.61	116 0.83	253 1.80	174 1.25	175 1.25	78	66	41	53	75	64	122	39	42	59	88
	TP 13	Link Belt 520	12" Pipe .25" Wall	5070	43.2	30000[1]	9.23	80.0	2520 4470	6990	1.1 530.0	0.10	0.51	5.00	0.75	0.96	140	357 2.55	159 1.14	144 1.03	133 0.95	344 2.46	280 2.00	306 2.19	104 0.74	192 1.37	154 1.10	194 1.00	59	53	36	44	37	47	102	36	32	51	70
	LTP 7	Vulcan 80C	12" Pipe .25" Wall	8000	16.5	24450	9.23	160.0	5040 4050	9090	7.8 460.0	0.10	0.98	5.25	0.80	0.92	460	1286 2.79	253 0.55	151 0.33	181 0.39	1213 2.64	1707 3.71	376 0.82	124 0.27	740 1.61	253 0.55	225 0.49	214	84	38	60	202	284	126	41	123	84	113
	LTP 8	Delmag D-22	12" Pipe .25" Wall	4850	98.0	39700[1]	9.23	160.0	5040 4505	9545	3.2 460.0	0.10	1.28	5.00	0.80	0.92	460	1155 2.51	224 0.49	165 0.36	175 0.38	935 2.03	959 2.08	442 0.96	131 0.28	544 1.18	257 0.56	184 0.40	192	75	41	58	156	160	147	44	91	86	92

(1) Manufacturer's maximum hammer rating.
(2) Based on average test load capacity for LTP 2, 3, 4, and 5.
(3) Weight of 20 ft earth plug.
(4) Open-end pile.

Cols. 18 through 28 show the computed ultimate bearing capacity for the designated formulas (with safety factors excluded), expressed in kips. These values represent theoretical failure load under conditions defined by the first 17 columns. Thus, if a formula is theoretically correct, the computed ultimate bearing capacity listed should agree with the actual or estimated failure loads in Col. 17. To facilitate comparison, the ratio between computed ultimate and measured pile capacity is shown below the computed capacities. Finally, Cols. 29 through 39 show comparable design bearing capacities R_d with appropriate recommended safety factors, ranging from 2 to 6 depending on the formula.

As can be seen, values of the R_u/R_t ratio are only infrequently at or near the theoretical unity figure. For example, ratio values in Col. 18 range from less than 2 to 6 or more for the Engineering News Formula, which means that the computed design bearing value would have a safety factor R_t/R_d of from 3 to less than 1, with respect to actual measured yield or failure load.

Because of the quantity of data (over 1,000 computed bearing values) a further breakdown is desirable. For convenience, the data from Cols. 17 and 29 through 39 in Tables 32 through 36 have been assembled in Figs. 157 through 159 which show the grouping of computed bearing values in terms of actual safety factors expressed as R_t (yield load) divided by R_d (computed design capacity). Because of the great similarity and quantity of H-pile data at Belleville shown in Table 34, these data have been omitted from this comparison.

It will be seen in Figs. 157 to 159 that the ratios of test yield value to computed design capacity (R_t/R_d) are separated by site and formula. The closed symbols refer to actual pile test load yield values and open symbols are based on interpolated yield values. In addition, the design capacities of the test load piles were recomputed based on substituting the average "ENTHRU" values (Chapter 8) for the equivalent factor $E_n \left[\frac{W_r + e^2 W_p}{W_r + W_p}\right]$ in the Hiley, PCUBC, Modified Engineering News, and Rabe Formulas. Connecting lines indicate the trends which accompany such substitutions.

Some of the more pertinent facts shown in Figs. 157 through 159 are the following:

1. Essentially all the computed capacities derived from the Engineering News, Eytelwein, Navy-McKay, and Rankine have true safety factors of less than 2, for piles having R_t values of 200 kips or less.

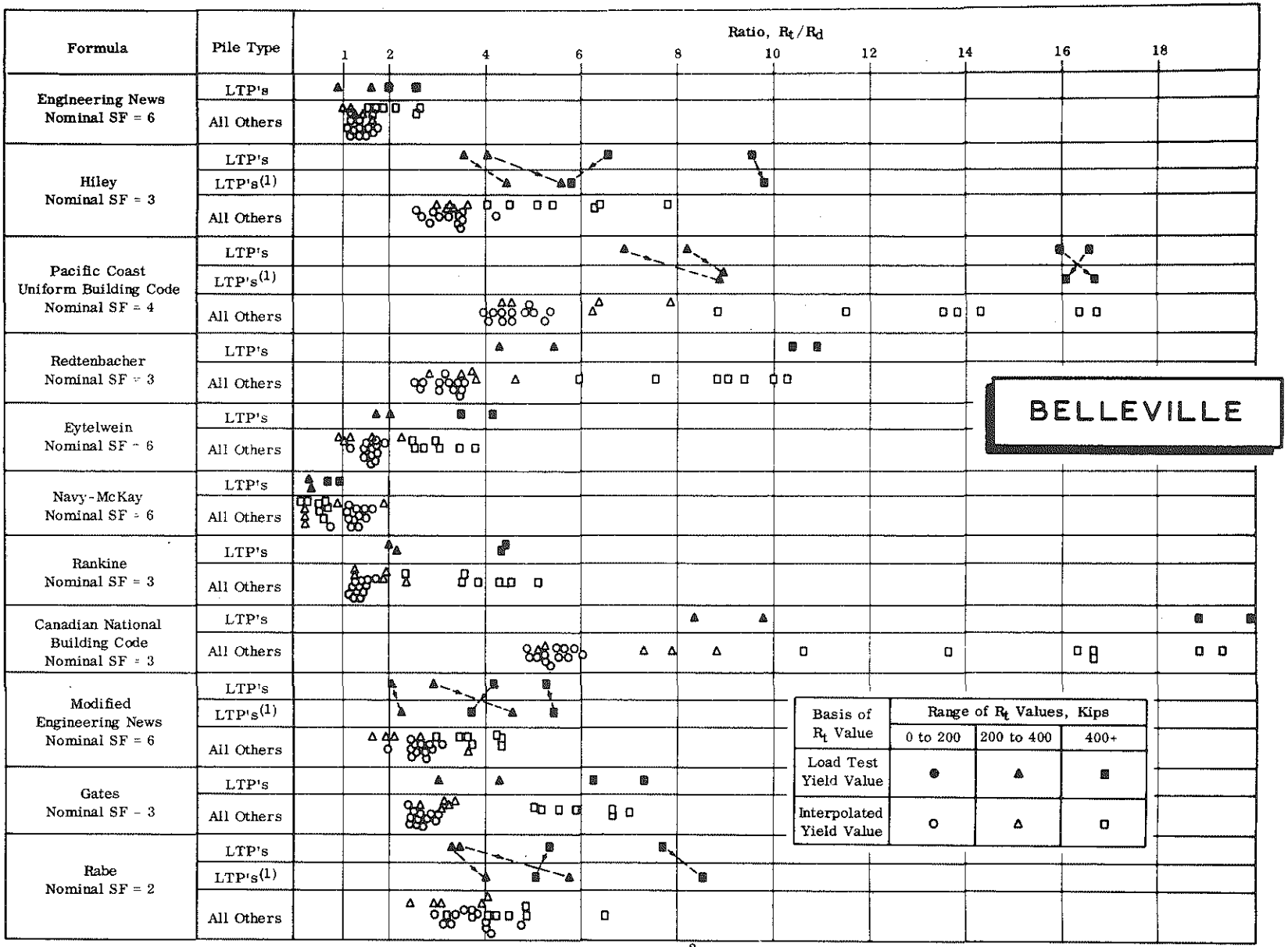

(1) Value obtained when substituting value of "ENTHRU" (Chapter 8) for factor $E_n \frac{W_r + e^2 W_p}{W_r + W_p}$ in appropriate formulas.

Figure 157. Actual safety factors in dynamic formulas (Belleville).

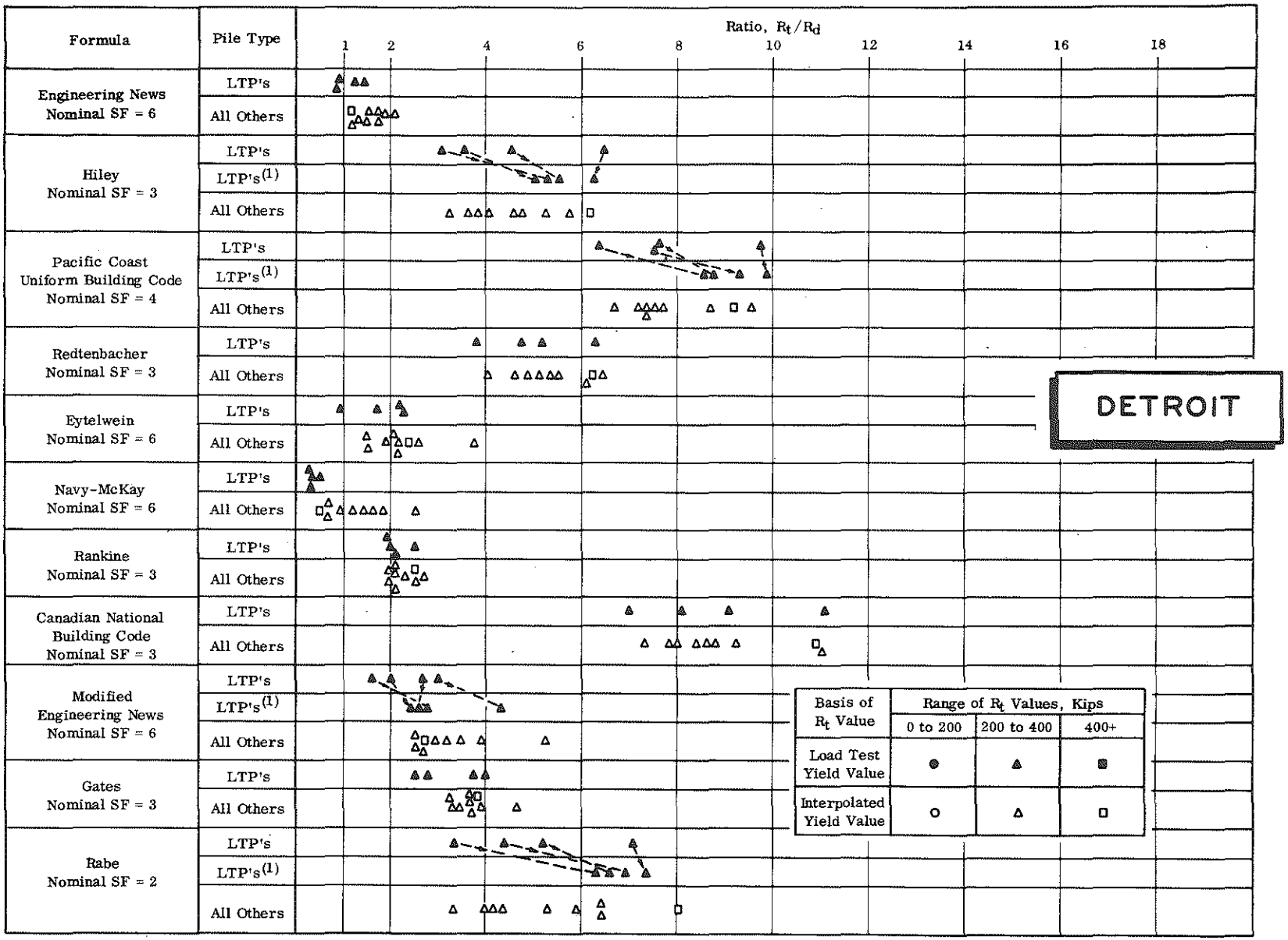

(1) Value obtained when substituting value of "ENTHRU" (Chapter 8) for factor $E_n \frac{W_r + e^2 W_p}{W_r + W_p}$ in appropriate formulas.

Figure 158. Actual safety factors in dynamic formulas (Detroit).

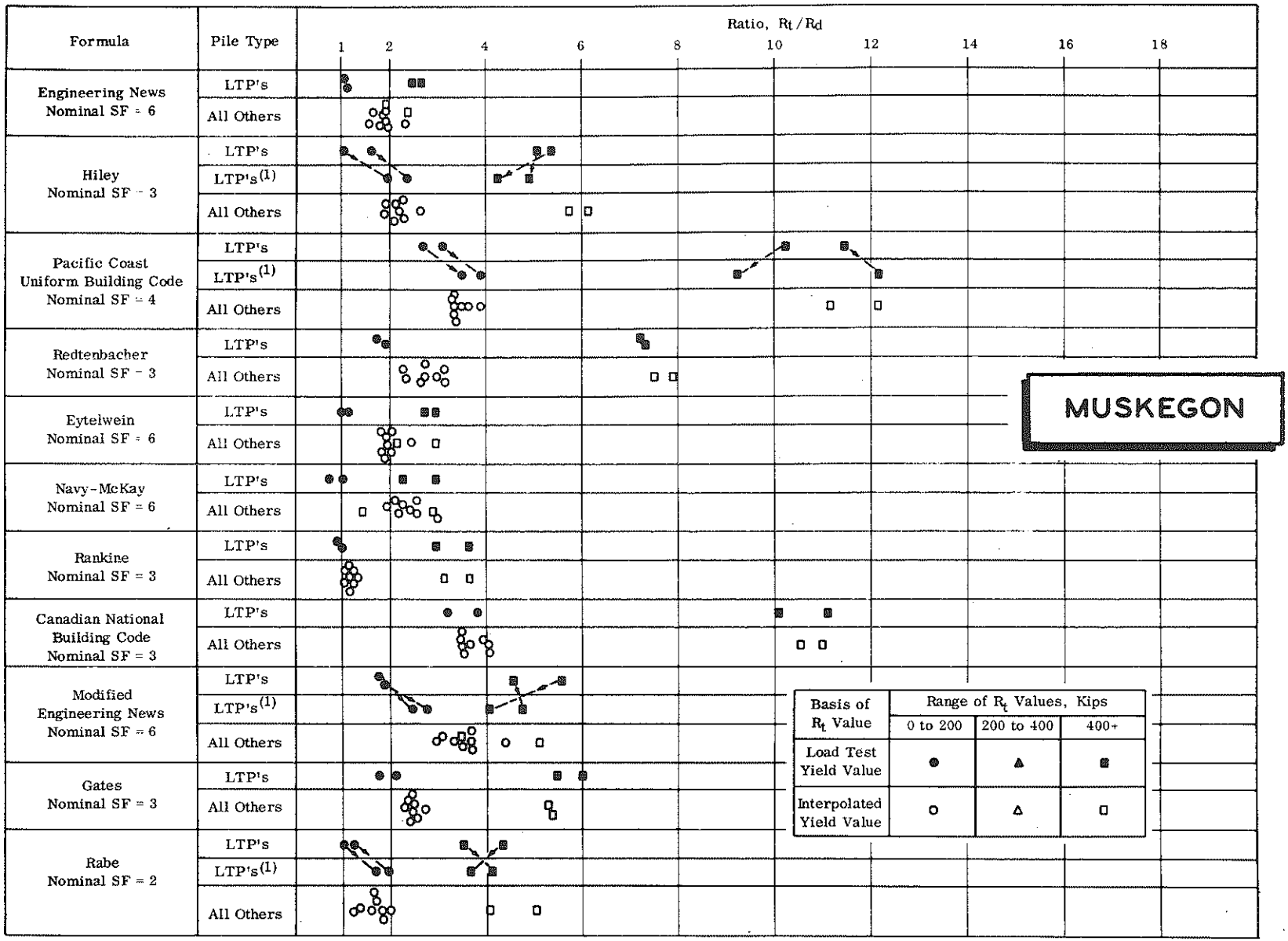

(1) Value obtained when substituting value of "ENTHRU" (Chapter 8) for factor $E_n \frac{W_r + e^2 W_p}{W_r + W_p}$ in appropriate formulas.

Figure 159. Actual safety factors in dynamic formulas (Muskegon).

2. In three out of six instances, the Engineering News Formula gave true safety factors of less than unity with respect to actual measured yield values R_t in the 200- to 400-kip range. Comparable safety factors based on the Modified Engineering News Formula exceed 1.5.

3. The PCUBC and CNBC Formulas show the highest safety factors, generally well in excess of 8 and up to 20 for the Belleville test loads of 400 kips or more.

4. In general, safety factors increase with increasing values of R_t for all the formulas, with a definite grouping of R_t/R_d values associated with differing capacities for the Hiley-type and Gates Formulas at Belleville and particularly at Muskegon.

5. There is a significant reduction in spread of safety factors for the load test piles when using the ENTHRU values in computing capacity at Detroit. Results are inconclusive for Muskegon and Belleville, although there appears to be some evidence that group limits may be narrowed, particularly at Muskegon.

It is also instructive to examine the relation between R_t and R_d (data obtained from Tables 32, 33, 35, and 36, omitting H-piles) for each of the formulas, as shown in Fig. 160. The symbols here identify the points by site and by actual or interpolated load test data. Lines of uniform safety factor are also shown. A general review of the charts suggests that each formula falls into one of the four following categories:

1. The Engineering News, Eytelwein, and Modified Engineering News (Fig. 160), in which points appear fairly evenly distributed within two bounding safety factor limits. Thus, most of the R_t vs. R_d points are distributed between SF = 1 to SF = 3 for the Engineering News, and SF = 1.5 to SF = 6 for the Modified Engineering News Formula. A concentration of lower-valued safety factors may be noted for the lower R_d values; however, the data are not conclusive on this point and may be biased by the large number of interpolated R_t values shown at 140 and 180 kips.

2. The Hiley, Rankine, Gates, Rabe, and especially the Redtenbacher Formulas in which the safety factor increased as the values of R_t and R_d increased. Thus, for the Hiley Formula, piles with values of R_d ranging upward from 50 to 100 kips had true safety factors from about 1.3, whereas for values of R_d from 100 to 150 kips safety factors ranged upward from 3.

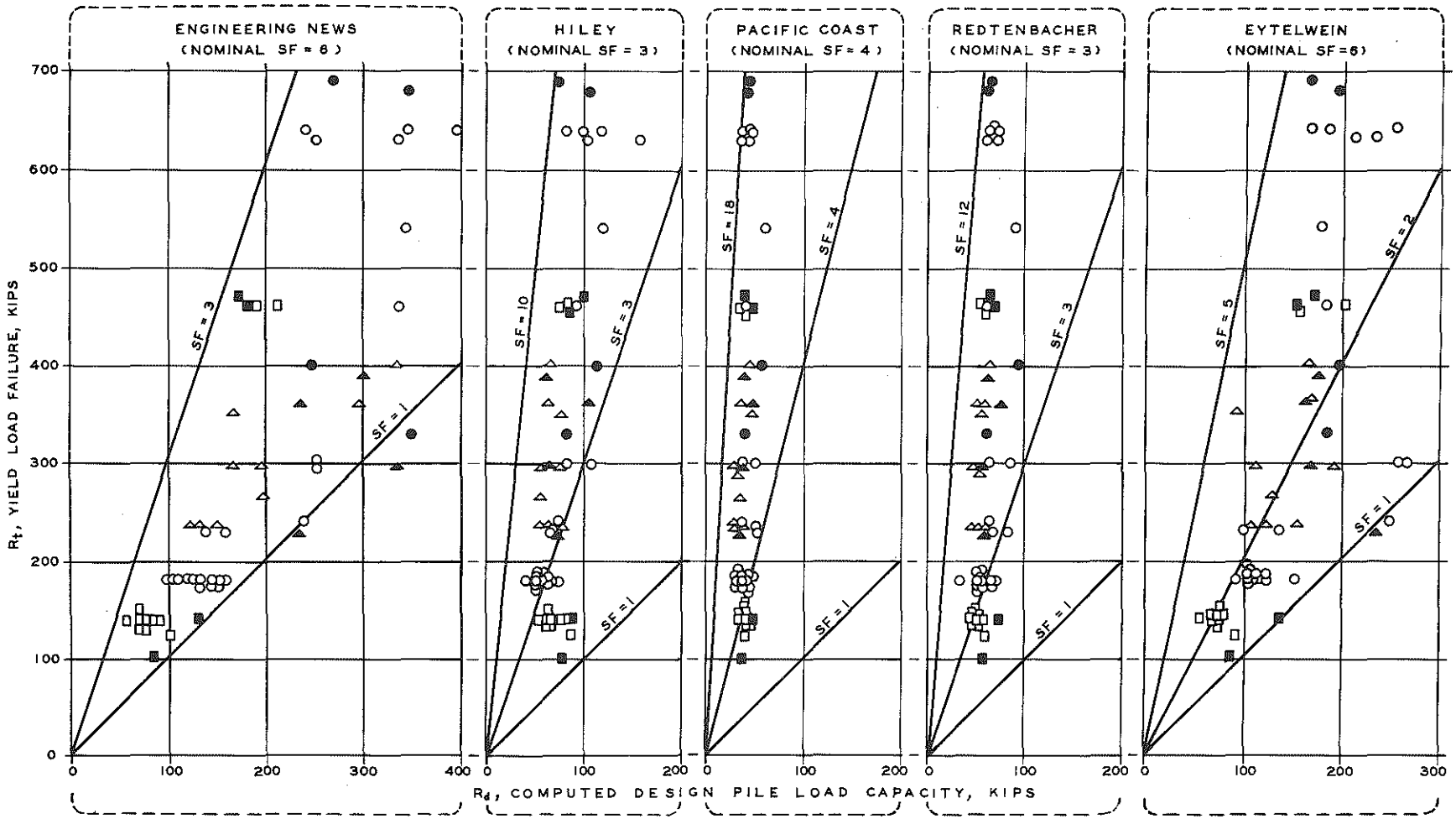

Figure 160. Relation between yield load and formula design capacity.

SITE	ACTUAL YIELD LOAD	INTERPOLATED YIELD LOAD
BELLEVILLE	●	○
DETROIT	▲	△
MUSKEGON	■	□

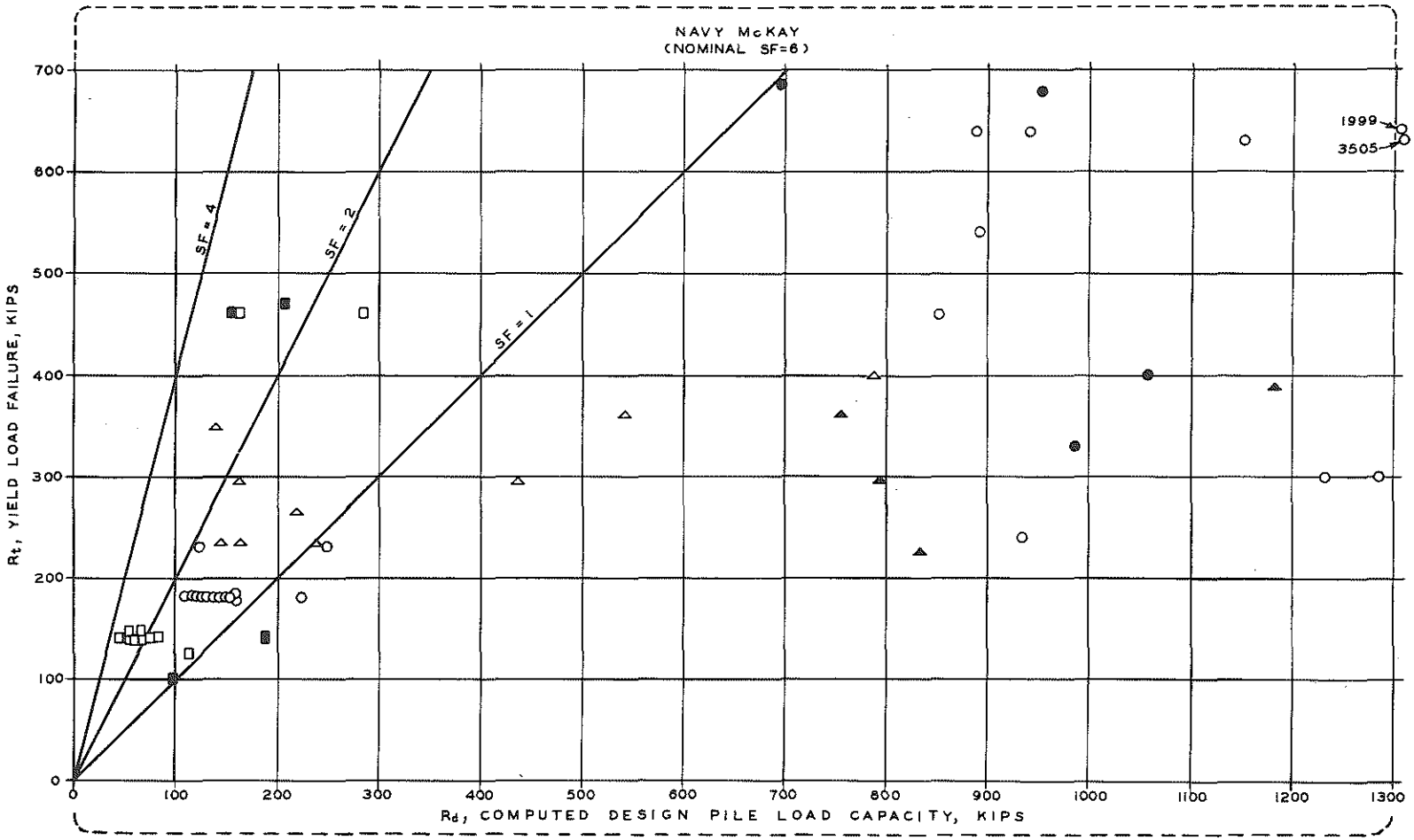

Figure 160 (cont.). Relation between yield load and formula design capacity.

SITE	ACTUAL YIELD LOAD	INTERPOLATED YIELD LOAD
BELLEVILLE	●	○
DETROIT	▲	△
MUSKEGON	■	□

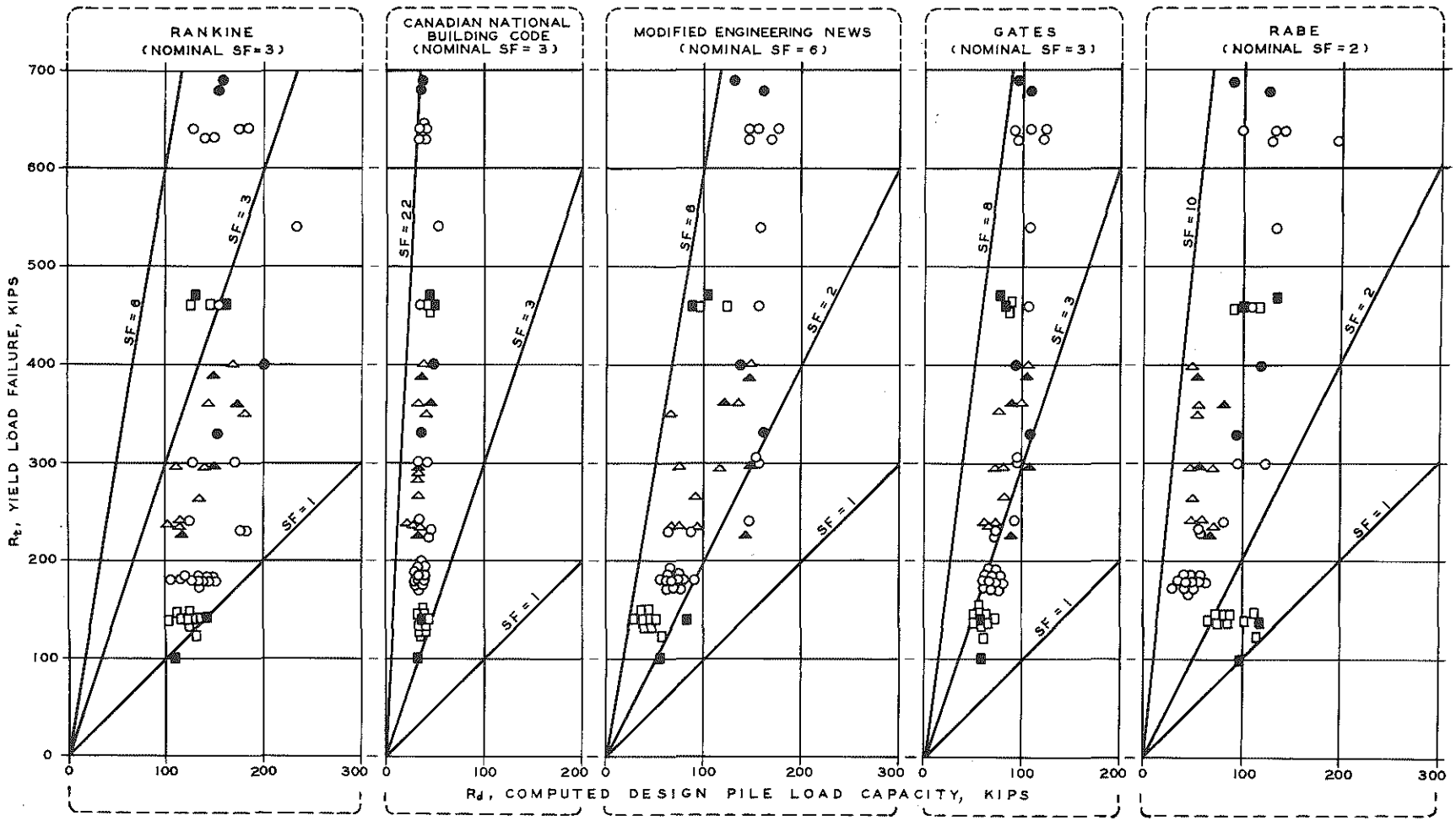

Figure 160 (cont.). Relation between yield load and formula design capacity.

SITE	ACTUAL YIELD LOAD	INTERPOLATED YIELD LOAD
BELLEVILLE	●	○
DETROIT	▲	△
MUSKEGON	■	□

3. The Navy-McKay in which there is general falling off of safety factors for larger values of R_d. This is to be expected since R_d as a limit approaches infinite values as the final set S approaches zero.

4. The PCUBC, CNBC, and possibly the Redtenbacher in which the computed capacity R_d is essentially constant over the range considered, regardless of the associated values of R_t. Thus, for the PCUBC Formula the computed values R_d vary from about 30 to 60 kips whereas R_t is spread from 100 to 700 kips, with no apparent correlation between R_t and R_d in this range.

It is also a characteristic of this fourth category of formulas that each has a fairly definite limit on computed capacity for a given hammer and pile type which is substantially reached under final penetration resistances of 10 or more blows per inch. Thus, it was impossible to achieve a PCUBC design capacity in excess of 35 tons when considering a 12-in. pipe pile or H-pile with a 22,000 ft-lb hammer, even at practical refusal (i.e., 30 blows per in. or more as for TP 13 in Col. 30 to Table 32). Yet, load capacities in excess of 300 tons were measured at Detroit, and design loads of 100 tons by other formulas are not unusual in these circumstances. Conversely, there is no mathematical limit on computed capacity for the third category of formulas, and a majority of the computed design capacities shown in Fig. 160 had true safety factors of less than unity. It must be concluded, therefore, that the third and fourth categories of formulas are of limited usefulness and are not applicable to high-capacity piles driven to high values of final penetration blow count.

There are also upper mathematical limits imposed on R_d values as determined by the first and second categories of formulas. With the exception of the Redtenbacher Formula, these limit loads are in a practical range, generally in excess of 60 tons for a hammer of 15,000 ft-lb or more. The specific limit under any circumstance is a function of length, weight, and compression of pile, soil, etc., particularly for piles of the second formula category, and thus cannot be conveniently indicated here.

With these observations in mind, reference is made to Fig. 161 which shows the range of safety factors falling within successive 200-kip intervals of increasing values of R_t, and represents a compilation of all data in Fig. 160. The upper and lower limits of safety factor are given in each box, and the general magnitude and spread of safety factor limits are also indicated. The open boxes identify formulas and range of yield loads for which safety factors all lie between 1.5 and 6. Note that only

the Modified Engineering News Formula meets this criterion for the entire range of loads and test sites considered. The Gates Formula meets this criterion up to 400 kips, but shows an upper limit of safety factors in excess of 6 in the 400- to 700-kip yield load range. The Redtenbacher Formula also substantially meets the criterion up to 400 kips, but shows safety factors up to 11 for the greater loads.

FORMULA	UPPER & LOWER LIMITS OF TRUE SAFETY FACTOR, R_t/R_d		
	RANGE OF R_t, KIPS		
	0 TO 200	200 TO 400	400 TO 700
ENGINEERING NEWS	1.1 / 2.4	0.9 / 2.1	1.2 / 2.7
HILEY	1.1 / 4.2	3.0 / 6.5	4.0 / 9.8
PACIFIC COAST UNIFORM BUILDING CODE	2.7 / 5.3	4.3 / 9.7	8.8 / 16.5
REDTENBACHER	1.7 / 3.6	2.8 / 6.5	6.0 / 10.9
EYTELWEIN	1.0 / 2.4	1.0 / 3.8	2.2 / 4.1
NAVY-McKAY	0.8 / 3.0	0.2 / 2.5	0.2 / 3.0
RANKINE	0.9 / 1.7	1.3 / 2.7	2.3 / 5.1
CANADIAN NATIONAL BUILDING CODE	3.2 / 6.0	5.1 / 11.1	10.1 / 19.9
MODIFIED ENGINEERING NEWS	1.7 / 4.4	1.8 / 5.2	2.7 / 5.3
GATES	1.8 / 3.0	2.5 / 4.6	3.8 / 7.3
RABE	1.0 / 4.8	2.4 / 7.0	3.2 / 8.0

LEGEND:

= $1.5 < R_t/R_d < 6$

= $1.5 > R_t/R_d < 6$

$\frac{\text{UPPER } R_t/R_d}{\text{LOWER } R_t/R_d} > 4$

= $1.5 < R_t/R_d > 6$

Figure 161. Range of true safety factors, based on Fig. 160).

It is especially noteworthy that the Engineering News Formula showed actual safety factors near or less than unity, and for the current data never exceeded a value of 2.7 for all load ranges. This is in contrast to the nominal safety factor of 6 contained in the formula. Also, the Hiley, Eytelwein, Navy-McKay, Rankine, and Rabe Formulas gave several computed design bearing values with a safety factor less than 1.5 in the 0- to 200-kip range of actual bearing values.

By manipulating the assigned safety factors, all of the formula capacities associated with the diagonally shaded boxes in Fig. 161 could be brought within the criterion range. Only fully shaded box values (notably Navy-McKay) cannot be sufficiently adjusted by a single internal safety factor. Note also that the large range in R_t/R_d ratios for the Hiley and Rabe Formulas preclude bringing all of these capacity values within the 1.5-to-6 safety factor range by a single coefficient, whatever its value. In any event, the arbitrary assignment of safety factors (or in fact any of the formula parameters) is not recommended and is only discussed here to point out inherent limitations to this method of adjusting computed capacities.

Associated with the danger of overestimating safe pile capacities is the problem of underestimating safe bearing values. A formula becomes essentially valueless if it tends to become overly conservative in the range of practical loads. It is apparent from Fig. 161 that the R_t/R_d ratio varies by a factor of 3 or more when considering each of the formulas, applied to all the sites and load ranges. While it is possible to change the average R_t/R_d ratio itself by uniformly adjusting the numerical values of energy, loss factor, etc., or by revising nominal safety factors in the formulas, the percent spread of data would not be significantly reduced by this expedient. This is demonstrated for the case of a typical pipe pile at Belleville, at Detroit, and at Muskegon, in Fig. 162. The ranges of computed capacity are shown when varying the several formula factors over a relatively wide span of values. For example, the upper and lower values of energy for a Link-Belt 312 at Belleville (Fig. 162) which are 18,000 and 13,600 ft-lb, respectivelv, represent the maximum manufacturer's rated and minimum delivered energies (based on indicated chamber pressure recorded at the time of driving, as shown in the pile driving profiles in App. A). Similarly, the range of e factor is shown from perfectly inelastic ($e = 0$) to perfectly elastic ($e = 1$). The range of this factor for the aluminum micarta cap block and steel pile combination is probably not as low as 0.4, and possibly not above 0.8. Thus, the extreme values of associated computed design capacity would be from a 56-kip minimum to a 117-kip maximum. The actual computed value of 78 kips is intermediate, with the 117-kip extreme representing a 50-percent increase over the 78-kip figure. The other curves show similar trends in computed capacities when considering possible variations in the pile compression factor, C_1, e, or E_n. In general, the computed capacities will range by no more than a factor of 1 from the computed value used. That is, by rationally selecting the pile and hammer data in one way or another, a 100-percent difference in computed capacities might be possible, in contrast to a spread of 300 percent or more observed for comparable measured-computed capacity ratios for a given formula.

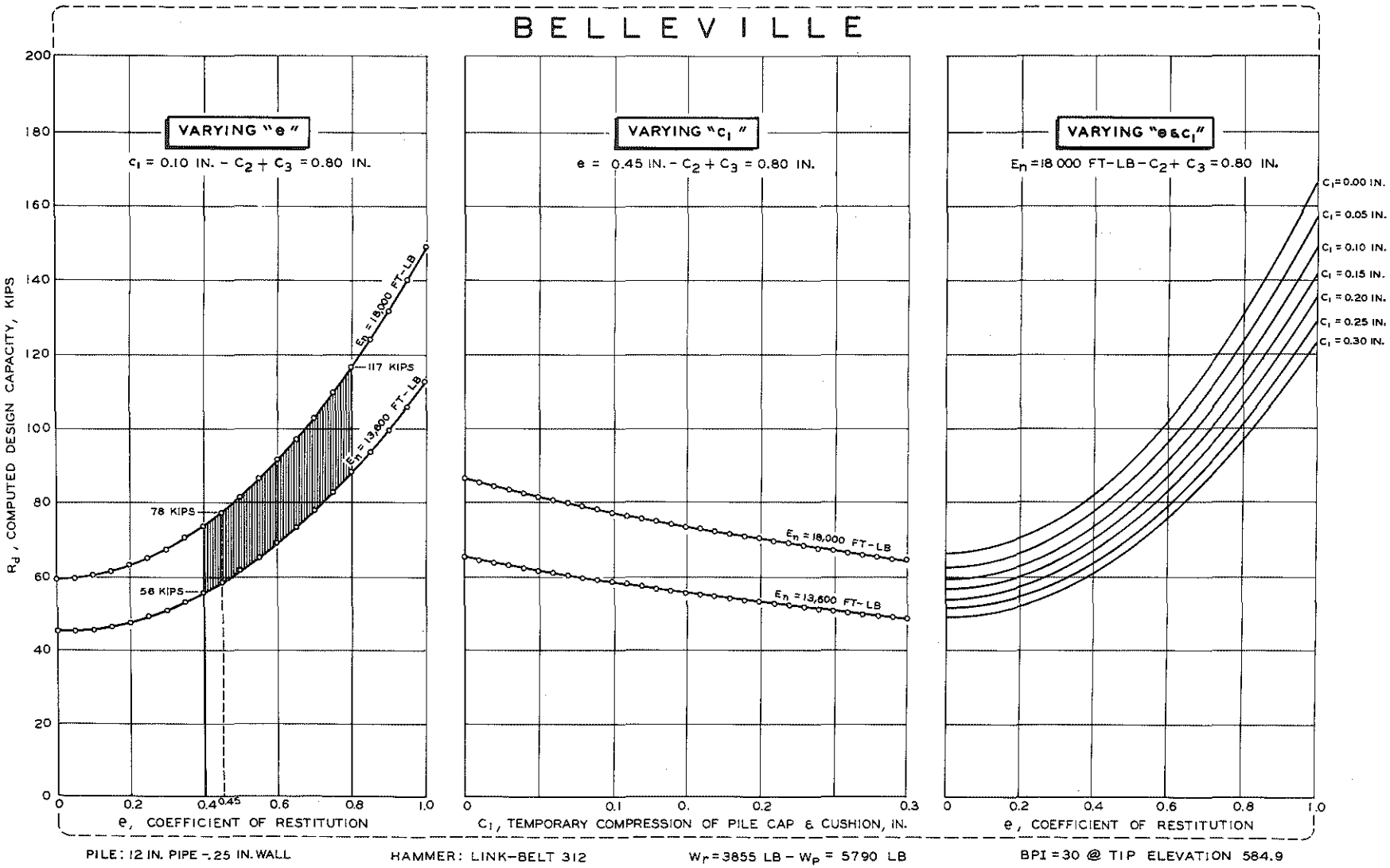

Figure 162. Effect on capacity of varying values in Hiley Formula.

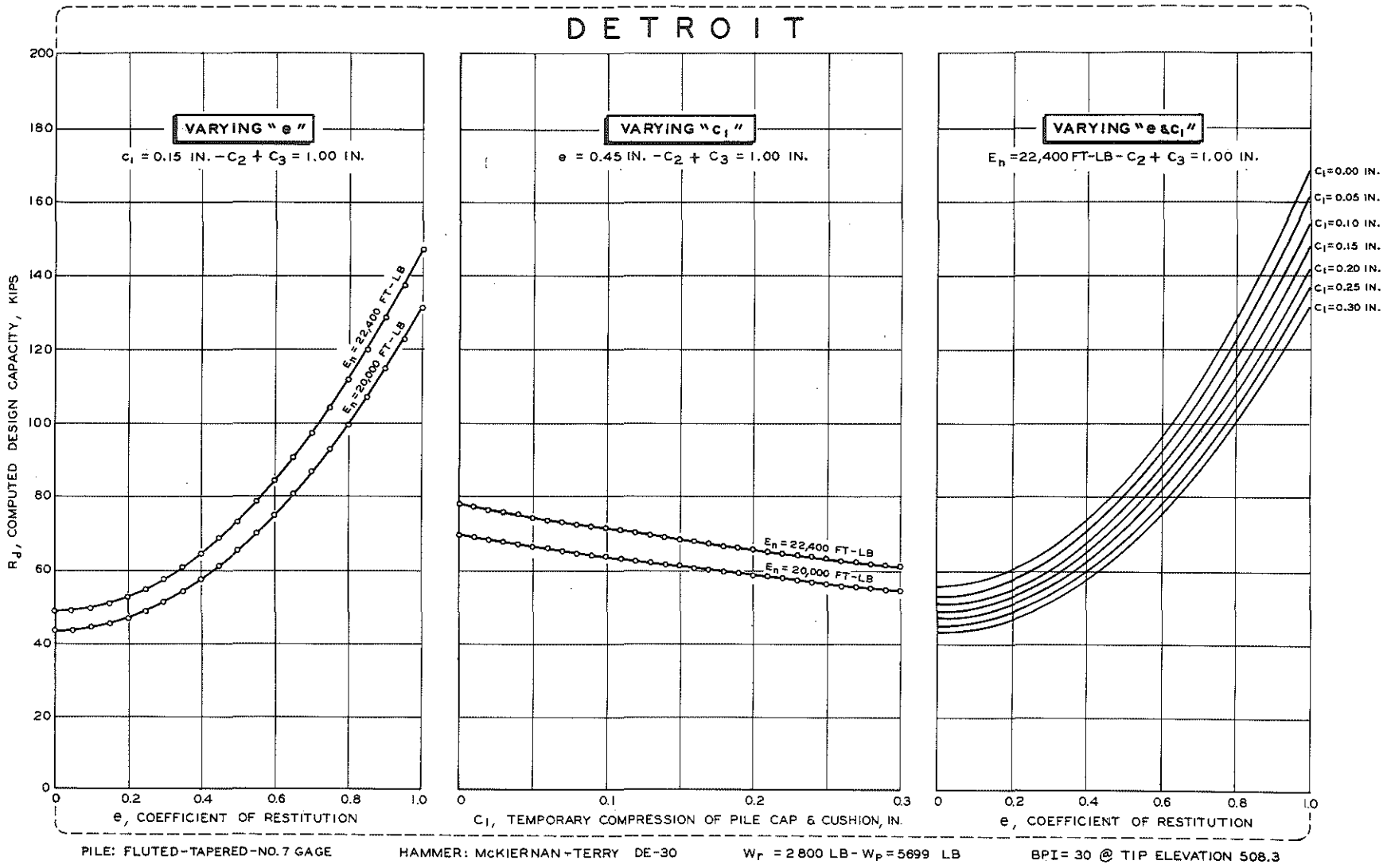

Figure 162 (cont.). Effect on capacity of varying values in Hiley Formula.

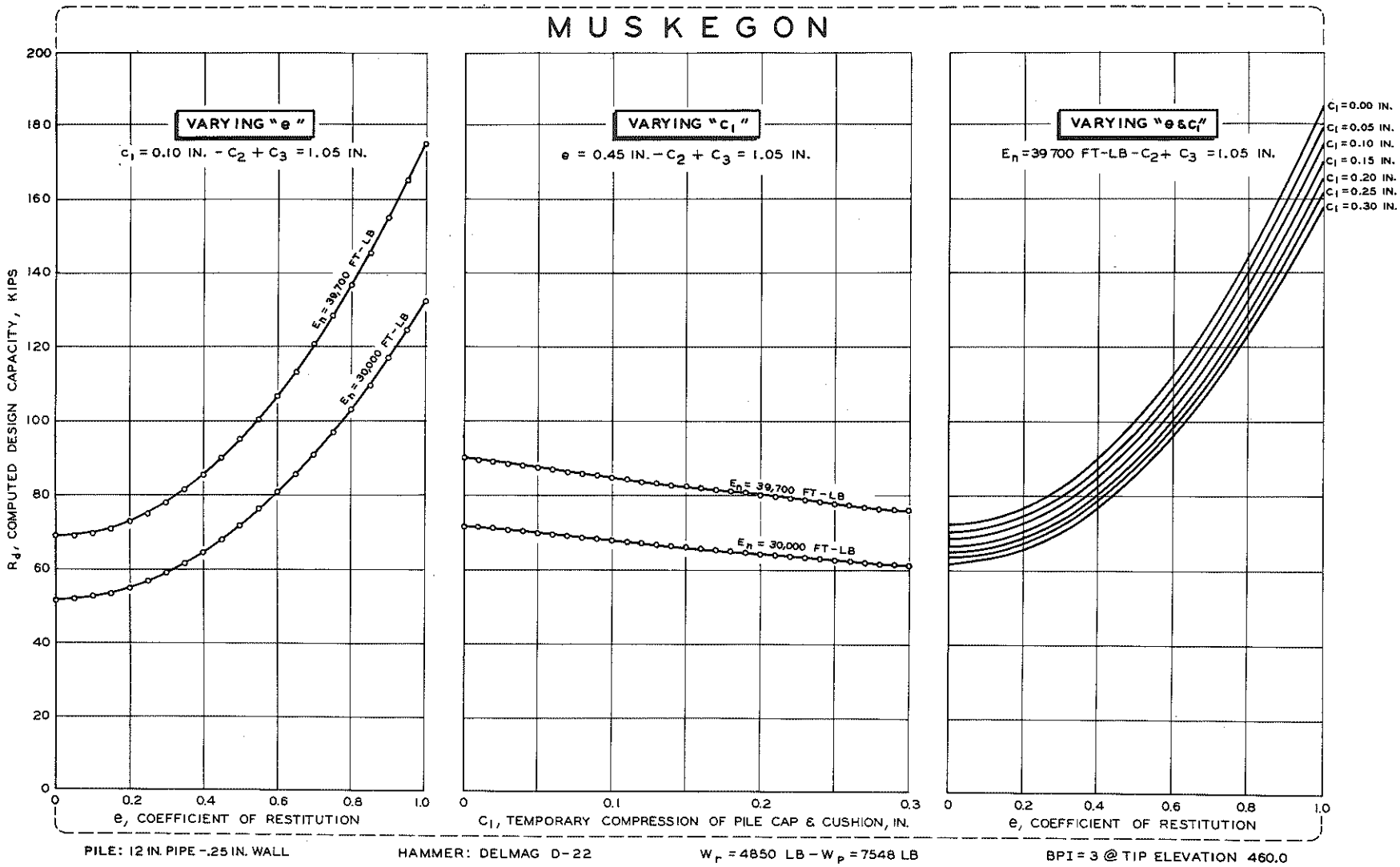

Figure 162 (cont.). Effect on capacity of varying values in Hiley Formula.

Of course, completely arbitrary adjustments in the energy factor, loss factors, etc., could accomplish a perfect match, but such ex post facto management of data is to be avoided. At this point, there seems to be no legitimate simple adjustment to the usual formula factors as presented which would significantly improve the reliability of the formulas for the entire range of test loads involved in this project.

Effect of Hammer Energy Rating on Dynamic Formula Capacities

Although it appears that the spread of safety factors derived from any given formula cannot be reduced significantly by rational selection of energy or loss factors, over the range of conditions of the test program, there is still the question of rating the several hammers on a uniform basis. That is, what should the assigned energy rating be for each hammer, so that the average of each associated computed capacity will be essentially equal for comparable field conditions? This has been attempted by comparing dynamic formula capacities computed by the Modified Engineering News and Gates Formulas for the same site, pile type, and depth of penetration of Figs. 163 and 165, based on Tables 32 through 36.

Each point in Figs. 163 and 165 indicates the computed capacity for a specific pile type at the indicated depth of pile penetration vs. the associated maximum manufacturer's energy rating of the hammer. Large dashed-line symbols show the average computed capacity for each hammer group for H-piles at Belleville, this being the only circumstance where five or more related data were available. The dashed-arrowed lines show the typical relation between changes in assigned energy and computed capacity. Fig. 164 shows the estimated actual safety factor for pipe piles at Detroit, related to maximum hammer energy.

Considering first the H-piles at Belleville (Fig. 163), one notes a 15-kip difference between the extremes of averages of Modified Engineering News formula values (i.e., 64.5 kips for Vulcan 50C and 80 kips for the McKiernan-Terry DE-30). Appropriate plus-and-minus adjustments of about 10 percent or less in rated hammer energies suffice to bring the computed results to a central value of 72 kips. On the other hand, an energy adjustment of 20 percent or more would be required to bring extreme individual results into agreement with the average for the same hammer type.

With the Gates Formula the 18-kip spread between average R_d values (i.e., 62 kips for Vulcan 50C and 80 kips for McKiernan-Terry DE-30) approaches that observed between related data points. As indicated by

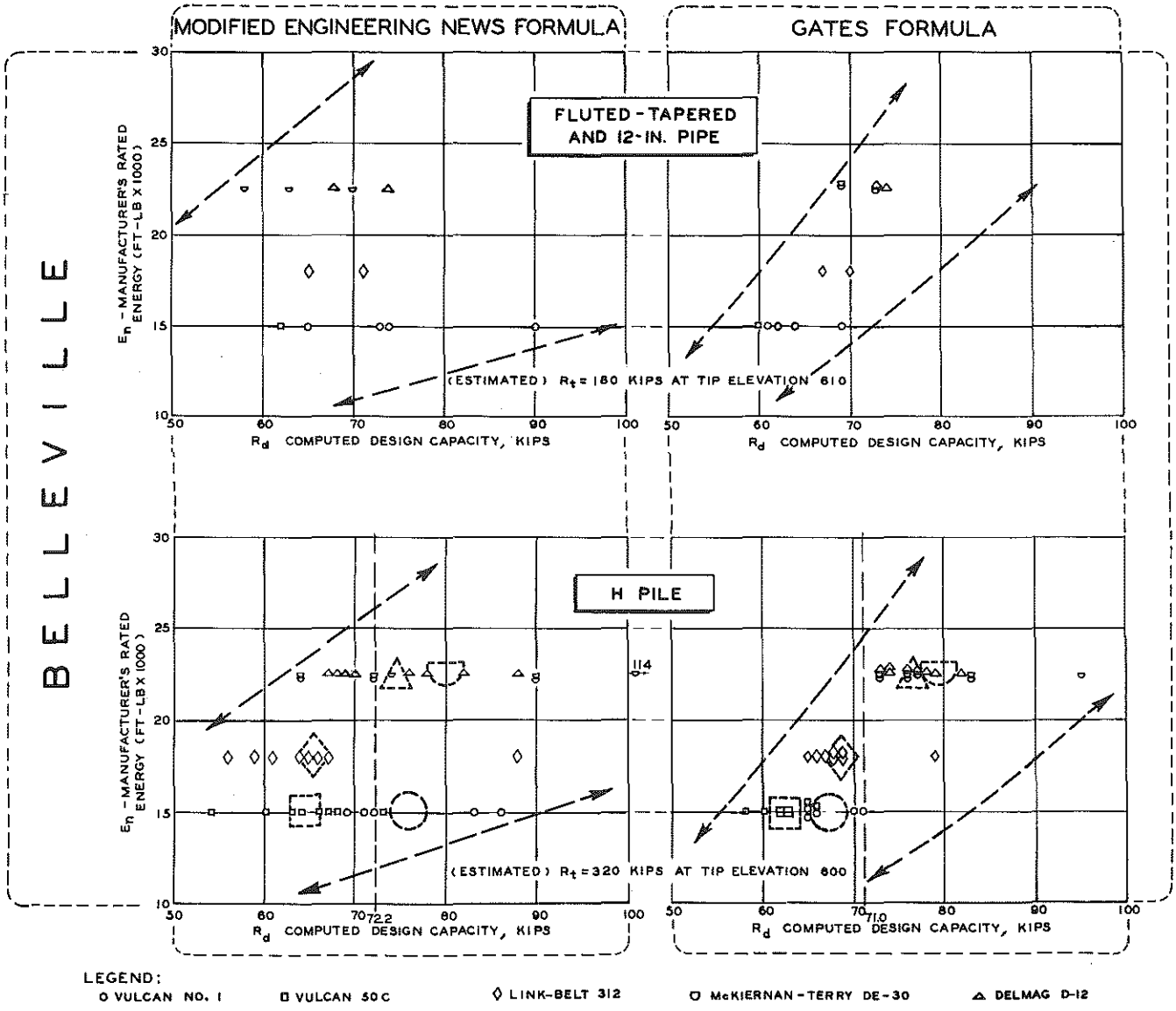

Figure 163. Effect of hammer energy rating on formula design capacities.

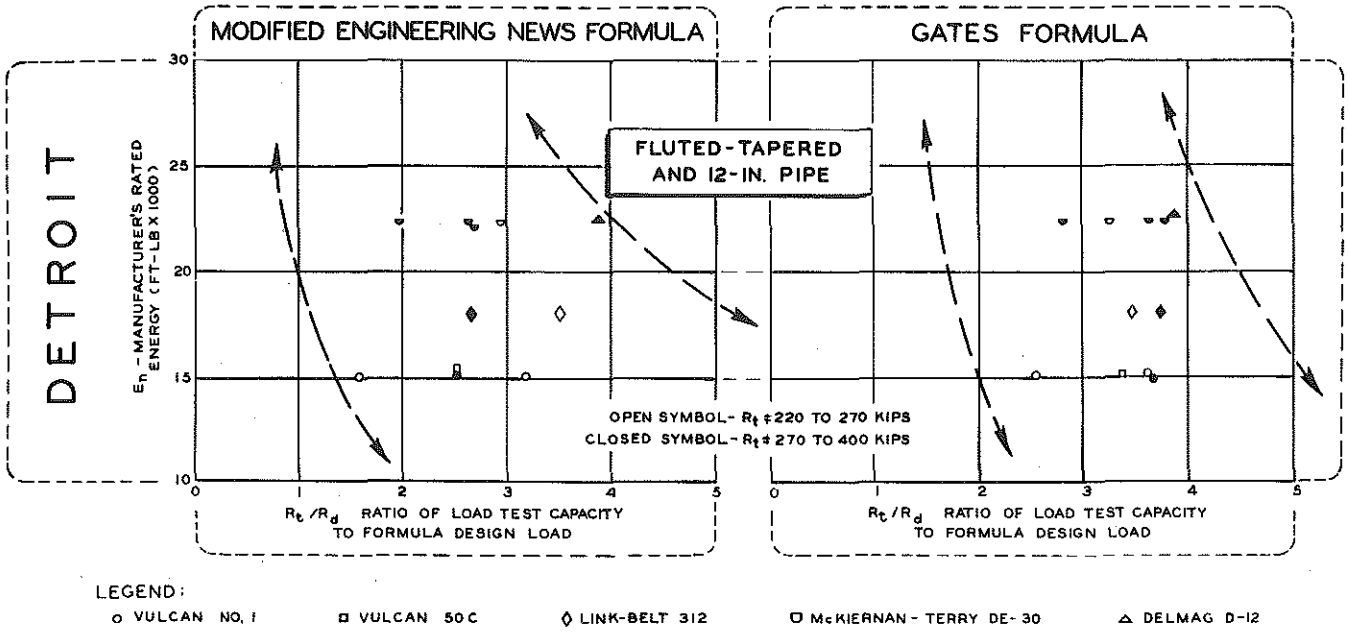

Figure 164. Effect of hammer energy on ratio of load test capacity to formula design load.

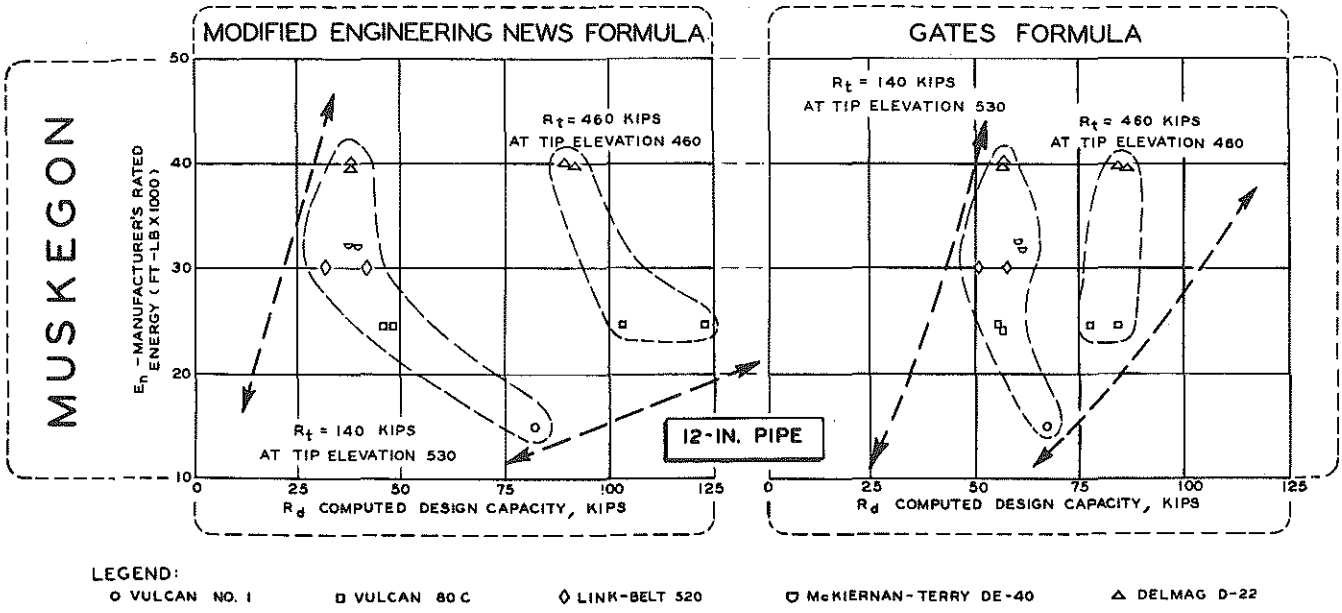

Figure 165. Effect of hammer energy rating on formula design capacities.

the arrowed lines for this formula, the manufacturer's energy rating values must be adjusted by 20 percent or more to bring the extreme average values to a median R_d of 71 kips. That is, the assigned energy for the Vulcan 50C hammer would be increased to about 19,500 ft-lb (i.e., 1.30 x 15,100), and that of the McKiernan-Terry reduced to 18,000 ft-lb (i.e., 0.8 x 22,400) to make the average computed values equal. Lesser energy adjustments would be required for the Vulcan No. 1, Link-Belt 312, and Delmag D-12.

The pipe pile data (Fig. 163) indicate again that the Vulcan No. 1 hammer is perhaps overrated in comparison to the 50C, and it appears that Modified Engineering News design capacities for the three diesel hammers are generally intermediate, with less than a 10-percent adjustment required to equalize all average values of R_d. However, there are insufficient data to make a quantitative comparison with any degree of certainty. Similarly, comparison of the limited number of computed capacities at Muskegon (Fig. 165) shows that adjustments to rated energy values of about 10 percent or less would bring the results in line, with the exception of the single value associated with the Vulcan No. 1 hammer (pile tip at elevation 530).

Because of significant variations in final tip bearing elevations and a consequent wide range in measured and estimated true pile bearing loads R_t at Detroit, computed capacities R_d are compared on the basis of R_t/R_d ratios vs. associated rated energies of hammers (Fig. 164). Limited results suggest that some adjustments in the rated energy are warranted. For example, the McKiernan-Terry DE-30 and Vulcan No. 1 energy ratings would have to be reduced about 10 to 20 percent to bring their average R_t/R_d ratio to a value of 3 in the Engineering News Formula. But data are insufficient to define this adjustment accurately.

It is apparent that differences in computed values arising from possible discrepancies in related energy for various hammers are overshadowed by the range of comparable design values obtained for the same hammers. Even more pronounced is the influence of pile type. Note that although the computed values for the Belleville piles range about a central value of 70 kips, the estimated true yield load is 130 kips for the pipe piles and 320 kips for H-piles. That is, the true safety factor jumps from 2.6 to 4.6 depending on pile type alone, for the Modified Engineering News Formula.

If one substitutes the measured net energy (ENTHRU) delivered into the top of the pile (Table 18) for the factor $E_n \frac{W_r + e^2 W_p}{W_r + W_p}$ in the Modified

Engineering News Formula, somewhat lower average computed values are obtained. This is illustrated in the following table where the R_d values have been shown for Belleville H-piles.

Hammer Type	R_d Average Computed Capacity, kips*	Average $\frac{W_r + e^2 W_p}{W_r + W_p}$	$\frac{\text{ENTHRU}}{E_n}$,	R_d, based on ENTHRU, kips
Vulcan No. 1	76	0.55	0.35	48
Vulcan 50C	64	0.55	----	--
Link-Belt 312	66	0.51	0.43	56
McK-T DE-30	80	0.46	0.26	43
Delmag D-12	75	0.46	0.41	67

* See Fig. 163

It is apparent that the relative scatter in R_d is increased when the average ENTHRU values are introduced. However, this conclusion is counter to the evident reduction in data scatter when ENTHRU values were applied only to load test piles at Detroit (Fig. 158). It is probable, however, that factors other than energy rating dominate final static pile load capacity achieved at Belleville, whereas at Detroit the available energy dictates the depth of pile penetration into hardpan, and consequently the static bearing value achieved. One must conclude that there is no evident advantage in using ENTHRU when computing bearing capacity of Belleville H-piles by the Modified Engineering News Formula.

SUMMARY

Bearing capacities for the several hammers, pile types, and test sites were computed using eleven representative dynamic formulas, and results compared to measured and interpolated pile bearing capacities. For the specific conditions considered, some of the more pertinent findings were as follows:

1. In several instances the Engineering News, Navy-McKay, and Rankine Formula design capacity had a true safety factor of less than unity with respect to test load capacity.

2. In several instances (Hiley, PCUBC, Redtenbacher, CNBC) formula design capacities had a true safety factor of 9 or more with respect to test load capacity.

3. In general, the Modified Engineering News and Gates Formulas gave design capacity values with true safety factors substantially all

falling in the range of 1.5 to 6 with respect to associated test load capacities.

4. Some reduction in scatter of safety factors was observed when appropriate values of ENTHRU were substituted for the factors $E_n \frac{W_r + e^2 W_p}{W_r + W_p}$ in the Hiley, PCUBC, Modified Engineering News, and Rabe Formulas, applied to Detroit load test piles (end-bearing). An improvement is also noted for certain Muskegon data.

CHAPTER THIRTEEN

SUMMARY, SUGGESTIONS FOR FURTHER RESEARCH, AND CONCLUSIONS

Planning of the Michigan Pile Study by various cooperating agencies was initiated in January 1961, and culminated in approval of a project proposal by the Bureau of Public Roads in July 1961. After assignment of personnel to the technical field staff and mobilization of equipment and materials, the field testing program started in October 1961, and continued without interruption through March 1962.

FIELD TESTING PROGRAM

Test Sites

Three test sites were selected, representing a range of soil conditions typical of Michigan pile driving practice. One site involved soft clay overburden (associated with easy driving), characteristic of lake-deposited clays bordering the Great Lakes and connecting channels; another was characteristic of water-worked till clays (associated with moderate-to-heavy driving), also including several sand strata of glacial origin; and a third was of substantially granular character but interbedded with soft, peaty sediments deposited in deep glacial valleys bordering on Lake Michigan and offering a wide range of driving resistance. At all three sites, all piles (except for special shear or friction piles) were driven to practical refusal in the underlying, highly consolidated sand and gravel or hardpan, on which bearing piles or caissons are normally landed in Michigan foundation practice.

Soil Investigation

Routine but comprehensive soil investigations were conducted at each site, consisting of borings with standard field penetration observations and taking of undisturbed samples of cohesive materials for labora-

tory testing. The laboratory tests included two types of shear tests--unconfined compression, widely used in many soil mechanics laboratories, and the "ring shear" test to measure the static yield value, developed at the State Highway Testing Laboratory jointly operated by the Michigan State Highway Department and the University of Michigan. Other conventional tests were also conducted to determine the physical characteristics of representative samples from all test sites. At the respective sites, these tests preceded the pile driving program, and test data were subsequently correlated with pile driving records.

Test Hammers

Pile driving hammers selected for evaluation of performance characteristics included a light and a heavy hammer of each of three makes of diesels (Link-Belt, McKiernan-Terry, and Delmag), and for comparison three Vulcan hammers representative of the air and steam hammers now in common use. In addition, the Raymond internal mandrel hammer was used in driving two special piles.

Test Piles

For the major investigation of pile driving performance, two types of piles were selected--steel pipe and steel H-section. The pipe piles were driven with both open and closed ends. Eighty-eight piles were driven at the three test sites with the ten different makes or models of pile driving hammers. Nearly all the piles were electronically instrumented for dynamic measurement and automatic recording of data during driving. At each site the pile driving schedule and hammer assignments were arranged to provide a dispersed pattern of pile driving so that each hammer would have as closely comparable driving conditions as possible.

Two special but widely used types of piles were also driven to study their driving characteristics and supporting capacity. These were the Union Metal monotube of fluted-tapered section and the Raymond step-taper pile, the latter driven with a Raymond internal mandrel hammer. Neither the Raymond hammer nor these two types of piles were included in the main statistical study of pile hammer characteristics as these special tests did not provide sufficient data for statistical analysis.

Measuring and Recording Procedures

Measuring and recording of data during driving operations involved a number of procedures conventional in pile driving practice, and in ful-

fillment of project objectives also included electronic measurements through the use of transducers (sensing devices converting such physical phenomena as force, acceleration, and deflection into measurable electrical output signals).

A specially designed and calibrated load cell was inserted between the pile driving cap and the top of the pile to measure the force transmitted to the top of the pile. An accelerometer was mounted at the top of the pile in conjunction with the load cell to measure acceleration there during a specific hammer blow. Deflection and penetration of the pile were measured by two methods. Throughout the entire project a manual trace recording assembly was used to obtain a record of deflection and penetration or set for individual hammer blows, at selected intervals for the full pile length. In addition to manual recording, several types of electronically instrumented deflectometers or penetrometers were used experimentally in an attempt to obtain more precise recording of deflection. Only one of these produced reliable results, that being a linear variable differential transformer (LVDT) used at the last test site.

Pile Loading Tests

A supplementary phase of the investigation, equal in practical importance to the study of hammer performance, was the measurement of static supporting capacity of piles at each test site. These tests were to provide the basis for correlating measured supporting capacity with predicted or estimated capacity by two commonly used procedures: first, estimates based on driving resistance translated into load capacity by the conventional dynamic pile formulas; second, estimates based on boring and soil test data gathered from the soil investigation at each site. Nineteen of the 88 piles driven were tested under static load by repetitive loading cycles, for a total of 45 static load tests.

COMPILATION AND ANALYSIS OF DATA

Perhaps the most difficult and time-consuming part of the entire investigation was the almost prohibitive task of compiling and analyzing the tremendous volume of data accumulated in some six months of intensive field operations. After March 1962, following demobilization of field forces and equipment, all available research personnel were assigned to this phase of the study which continued to September 1963, when the first review by all cooperating agencies, including the hammer manufacturers, was scheduled.

This first review led to extensive revisions including the introduction of a second criterion of driving performance, re-analysis of much of the basic data, repetition of computer processing, and rewriting of substantial portions of the first draft of the report. This work continued to May 1964, when a second complete review by all interested parties was arranged. While there was then general agreement on the presentation of the investigation's results, there were still many minor revisions, rechecking of data analysis, and rewriting in completing the report for most effective presentation, a process which continued for several more months.

The conclusions drawn from analysis of the data will be presented in terms of the objectives as outlined in this report's Preface, with emphasis on the three major goals: first, the comparative performance of the pile driving hammers used in this investigation; second, correlation of measured supporting capacity with that computed from driving resistance using various dynamic pile formulas; and third, correlation of static load supporting capacity with estimates based on soil test data.

HAMMER PERFORMANCE

Three main criteria were used in evaluating the comparative performance of the pile driving hammers: first, the number of blows required to drive typical piles a given distance under comparable driving conditions; second, the speed of pile penetration with the various hammers for given piles under comparable conditions; and, third, the effective energy delivered to the top of the pile available for driving the pile.

Blow Count as a Measure of Relative Performance

The first criterion, based on blow count, was embodied in the Blow Count Ratio R, defined as the ratio of the blow count for a specific hammer and specific pile required to drive that pile a given distance divided by the unweighted average blow count of all hammers driving this specific pile type. Blow count data were compiled for 1-ft increments of depth to provide sufficient data in terms of adequately controlled R-values for statistical analysis.

The comparative performance by blow count of the hammers used at each of the three test sites, driving both pipe piles and H-piles, is presented in Fig. 48. Relative performance is shown by relative cumulative

frequency distributions (ogive curves) or graphs, in which R-values less than the par value of 1.0 indicate lower blow count or performance better than average, and R-values greater than 1.0 represent higher blow count or performance poorer than average. These data cannot be adequately summarized in a brief statement; hence, the reader is referred to Fig. 48 and Table 10, where all the data may be studied in concise form.

However, certain comments are necessary as a guide in interpreting blow count ratio data in order to place them in proper perspective. Slower, heavy hammers and lighter, rapid hitting hammers are both shown on the same graph. Obviously, blow count alone is an incomplete measure of relative performance of hammers of widely varying speed, when hammer speed itself is a manufacturer's design objective to increase the rate of penetration.

Penetration Rate as a Measure of Relative Performance

The relative importance of hammer weight and speed led to the introduction of pile penetration rate in feet per minute as a second measure of relative driving performance. Penetration rates were compared by computing a ratio P, defined as the penetration rate for a specific hammer and specific pile for a given distance divided by the unweighted average penetration rate for all hammers driving a specific pile type for the same distance. P-values were again computed for 1-ft increments of depth to provide sufficient data for statistical analysis.

Performance in terms of penetration rate ratios is presented in Fig. 62, and Table 15, to which the reader is referred for comparative study of all hammers used at each of the three sites. Comparative performance in terms of penetration rate is shown by relative cumulative frequency distributions (ogives) in which faster penetration (or performance better-than-average) is represented by P-values greater than the par value of 1.0, and slower penetration (or less-than-average performance) by P-values less than unity.

When judging relative performance by either blow count or penetration rate (as presented in Figs. 48 and 62), it may first be noted that the blow count ratio generally placed higher speed, lighter hammers in a less favorable position than the slower but heavier hammers. This situation was generally reversed, with the lighter, rapid hitting hammers in more favorable position, when penetration rate was used as a measure of hammer performance.

On the other hand, this is not always true and may vary depending on other conditions. For example, under certain soil conditions, where heavy driving resistance is encountered, greater hammer speed may not be as effective as a heavier blow at slower speed. One must conclude then that the selection of one or another of the hammer types under discussion should be determined by the driving conditions under which it is to be operated.

In the second place, the significance of the relative position of ogive curves or the range in R-values for various hammers may be over-emphasized unless it is understood that the spread between hammers may actually represent a relatively small difference in performance. For example, in Fig. 48 for Detroit pipe piles, the spread of the curves represents an average maximum difference of four blows per foot for hammers striking from 50 to 60 blows per minute, or approximately six blows for one hammer striking 50 blows per minute as compared to another hammer striking more than 100 blows per minute. Similar comparisons may be made in the relative performance in terms of penetration rate ratios in Fig. 62 and Table 15.

Relative Performance in Terms of Hammer Energy

Hammer energy actually delivered to the pile, as compared with the manufacturer's rated energy, was the focal point of a major portion of this investigation of pile driving hammers. Even though experimental difficulties were considerable and analytical problems complex, the definite results obtained are believed to be reliable in order of magnitude. A new term, ENTHRU, meaning energy delivered through the load cell to the pile top, was introduced to identify this particular measure of hammer energy and distinguish it from all others.

ENTHRU was measured as the summation of increments of force measured by the load cell multiplied by simultaneous increments of displacement at the pile top during any single hammer blow. This was presumed to be equal to the net energy delivered to the pile. Methods of measurement, experimental difficulties, and techniques by which they were overcome are described in detail in the text and appendices of this report. The results in terms of ENTHRU values are also presented in several different ways, to bring out the relationship of these values to various factors which entered into their determination.

A summary of the ENTHRU measurements for each site-hammer-pile combination is presented in Table 37. The ratio of ENTHRU to the manufacturer's maximum rated energy E_n, has been shown for the

range and average of observed ENTHRU values. Also shown are representative peak values of force and acceleration under a hammer blow, not necessarily in direct quantitative relation to any reported value of ENTHRU, nor are these peaks paired values. More complete presentation of these data is given in tables and figures in the text with accompanying discussion. The reader is urged to consult the text, particularly Pages 130 to 141, to obtain a perspective of the significance and possible limitations of the data developed in this phase of the project.

It should be emphasized that each specific value of ENTHRU is inextricably associated with and affected by the specific conditions under which that determination was made. To draw generalized conclusions regarding hammer performance from the values reported in Table 37 may not only be dangerously misleading, but may result in ignoring some of the most revealing information produced by the investigation on possibilities for improving pile driving practice.

The following factors were found in varying degrees to influence the value of ENTHRU obtained:

1. Available kinetic energy of the hammer at the moment of impact, as controlled by hammer operation.
2. Type of cushion block and its condition (i.e., extent of deterioration).
3. Pile length, rigidity, and mass, as well as mass of the hammer ram.
4. Soil resistance acting on the pile during driving.

Several instances where one or more of these factors apparently had considerable influence on the relative values of ENTHRU obtained have been discussed in Chapter 8 (see particularly Pages 137, 138, and 140), and will not be restated here. Especially worthy of emphasis, however, is the importance of cushion block material in its influence on ENTHRU. For Detroit and Belleville hammers with ordinary oak blocks, average ENTHRU values ranged between 0.26 and 0.39 of the associated maximum manufacturer's rating (Vulcan No. 1 and McKiernan-Terry DE-30). By contrast, the other hammers employing more resistant and durable cushion material (Vulcan 50C, Delmag, and Link-Belt) developed ENTHRU values ranging between 0.41 and 0.65 of the maximum manufacturer's rating.

It seems evident that the relative magnitude of the ENTHRU/E_n ratio between hammers is largely controlled by factors such as the operating condition of the hammer, cushion block material employed, pile types,

and soil conditions under which they were driven. The order of precedence among hammers could well be changed and one might speculate that this order could be completely reversed by selecting other cushion blocks. Certainly some improvement in the proportion of ENTHRU developed could be realized by using a more resistant cushion block, in the case of the Vulcan No. 1 and McKiernan-Terry DE-30.

TABLE 37
HAMMER PERFORMANCE

Site	Hammer	Manufacturer's Maximum Rating E_n, ft-lb	Pile Type	Accepted ENTHRU Determinations	Peak Force, kips	Peak Acceleration, g's	Average ENTHRU, ft-lb	ENTHRU/E_n Ratio		
								Min	Max	Avg
Belleville	Vulcan No. 1	15,000	H-Pile	11	230	90	5,283	0.27	0.45	0.35
			Pipe	5	180	75	5,094	0.26	0.41	0.34
	Link-Belt 312	18,000	H-Pile	27	380	170	7,726	0.28	0.56	0.43
			Pipe	12	440	210	8,226	0.32	0.62	0.46
	McKiernan-Terry DE-30	22,400	H-Pile	22	390	270	5,769	0.19	0.36	0.26
			Pipe	9	490	240	8,682	0.31	0.59	0.39
	Delmag D-12	22,500	H-Pile	30	800[a]	360	9,123	0.19[b]	0.53	0.41
			Pipe	13	690	350	11,870	0.39	0.64	0.53
Detroit	Vulcan No. 1	15,000	H & Pipe	12	200	110	5,339	0.30	0.43	0.36
	Vulcan 50C	15,100	Pipe	3	490	270	9,822	0.55	0.76	0.65
	Link-Belt 312	18,000	H & Pipe	3	200	100	7,554	0.37	0.50	0.42
	McKiernan-Terry DE-30	22,400	H & Pipe	14	370	190	8,417	0.31	0.46	0.38
	Delmag D-12	22,500	H & Pipe	9	600	320	10,033	0.24[c]	0.60	0.45
Muskegon	Vulcan No. 1	15,000	Pipe	10	220	80	6,359	0.32	0.48	0.42
	Vulcan 80C	24,450	Pipe	6	650	310	13,872	0.52	0.64	0.57
	Link-Belt 520	30,000	Pipe	8	560	150	16,637	0.44	0.66	0.55
	McKiernan-Terry DE-40	32,000	Pipe	4	700	310	18,088	0.52	0.65	0.57
	Delmag D-22	39,700	Pipe	9	1,050	470	24,660	0.53	0.78	0.62

[a] Estimated.
[b] Next lowest, 0.32.
[c] Next lowest, 0.35.

The influence of the cushion material can also be gauged by comparing the force traces shown in Fig. 92. At least a five-fold increase in peak driving force is experienced when the oak cushion block is removed from the Vulcan No. 1 hammer. For the McKiernan-Terry DE-40, the peak recorded force increases from 600 to 1,500 kips by omitting the cushion block. In certain cases, it seems probable that a related increase in ENTHRU would occur during the period of time that the peak

force was acting, although the increase may not be computed from these data. Of course, the cushion block also functions to protect the hammer from excess induced stresses, and some kind of buffer will probably always be required to protect both hammer and pile from damage due to impact stresses.

Fig. 76 also indicates that for Belleville soil conditions, hammers with relatively light rams (Delmag and McKiernan-Terry) transfer significantly less energy to heavy H-piles (53 lb per ft) than to comparable lengths of pipe piles (25 to 30 lb per ft). The heavier ram hammers (Vulcan No. 1 and Link-Belt 520) do not show a significant difference in this same regard. These somewhat isolated facts are in line with the theoretical requirements of kinetic energy transfer at impact and tend to support the relationship between the several average values of ENTHRU.

In conclusion, it is believed that the basis developed for evaluating the net energy delivered to the top of a pile during driving (i.e., ENTHRU) is theoretically sound and that the observed values of ENTHRU give an objective and realistic indication of the net energy available for driving a pile under current practice, with the hammers used in this investigation. However, the specific values of ENTHRU determined in the course of driving the project's piles are valid only for the soil-pile-hammer combinations studied, and must be considered tentative until confirmed even for these circumstances. It may also be pointed out that supposedly comparable ENTHRU's varied widely in individual values, indicating uncontrolled factors in either experimental technique or field conditions.

COMPARISON OF MEASURED AND COMPUTED CAPACITY

The second and third major objectives of the investigation involved correlation of supporting capacity under static load a) with estimates of capacity from driving resistance translated into capacity by conventional dynamic pile formulas, and b) with estimates from soil test data. The investigation's results, with reference to these two objectives, will be summarized together to provide a direct comparison between these two basically different methods of predicting capacity and the results of the static load tests.

Pile Load Tests

Field loading tests were conducted on representative piles at all three sites to provide a comprehensive basis for correlating measured and estimated capacity. Static load tests were made using increment loading

with constant time intervals, to permit a yield value determination by extrapolation of rates of settlement following the same control of variables used in laboratory shear tests.

In the case of pile tests, the elastic limit of the pile and soil provides a second basic criterion of ultimate capacity, made available by separating elastic deformation from permanent deformation due to compression of the pile and consolidation of the soil under the pile tip. Settlement of the pile tip was measured by tell-tales resting on the bearing plate at the tip. By means of repetitive loading cycles, the limit of increased bearing developed by stress conditioning can be determined and separated from elastic deformation of the pile and soil.

The two independent measures of the ultimate capacity of the piles under static load--yield value and elastic limit--checked within close limits, confirming similar results in previous investigations. This evidence of the precision and reliability of the criteria derived from load test procedures made it possible to proceed with correlation of measured and computed supporting capacities with greater confidence in the final results.

Correlation with Dynamic Pile Formulas

When the project proposal was formulated early in 1961, eleven typical pile driving formulas were selected for study as representing current practice in estimating supporting capacity from driving resistance. The intent was to include as many of those formulas as possible that had been or were being used in pile driving practice. It was planned to compare estimated capacity from each of these formulas with measured capacity from field loading tests, in order to determine whether the formula provided consistent and reasonably accurate estimates of capacity.

It was recognized that some method of predicting or estimating pile capacity before piles are driven is a practical necessity both for design and for the preparation of construction plans and specifications. A primary objective of the Michigan study then was to determine whether such pile driving formulas were the best available means for such estimates. More specifically, these formulas were to be compared with estimates or predictions based on soil test data from well planned soil investigations.

Chapter 12 of this report is devoted to the dynamic formula study and in it the methods of analysis are described, advantages and disadvantages of each formula are discussed, and comparative results are presented

from several different points of view. The reader may consult the text for those details not covered by this summary.

Figs. 157, 158, and 159 provide the most convenient and comprehensive presentation of comparative results from the formula study for each of the three test sites. These figures show in chart form the ratio of measured capacity from the load tests $\underline{R_t}$, divided by the design capacity $\underline{R_d}$, computed by each of the selected pile driving formulas. Load test values of this ratio are identified to distingush them from interpolated values, which are estimates made by extending the computation from soil test data to all piles driven at each site under comparable driving conditions.

The ratio of R_t/R_d is the horizontal scale and shows the actual safety factors provided by each of the eleven formulas for all piles, including test values and interpolated values. The actual safety factor and the relative position of the plotted values depend directly on the "built-in" safety factor in each formula. For example, in the Engineering News Formula with a safety factor of 6 the actual safety factors range from 1 to 3. This means that the design capacity by the formula is too high and could be dangerous if used in design. This observation is applicable to several of the formulas studied.

On the other hand, for several formulas the actual safety factors are considerably larger than the "built-in" safety factors. This would indicate that those formulas underestimate measured capacity and would be too conservative; as a result of not using enough of the available capacity, they would perhaps be wasteful from the standpoint of cost.

There are two characteristics of the Figs. 157, 158, and 159 charts to which attention is directed. First, if the range of variation or spread in actual safety factors is too great, as is the case in several formulas, the erratic results are evidence that variables which control supporting capacity are not properly related. This would appear to be a weakness in the formulas in interpreting soil conditions or other variable factors of piles or pile driving practices. This sort of discrepancy is presumably theoretical in character and perhaps difficult to correct; at least there are no specific corrective measures to suggest as a result of the current investigation. It may be noted for many of the formulas studied that this dispersion of results occurs in the higher range of test loads (300 to 400 kips and above). Thus, many of the formulas are quite consistent in the low and intermediate ranges of load, but cannot be extended to the high capacity bearing piles.

Second, if the actual safety factors when plotted form a fairly compact group indicating a reasonably consistent evaluation of variable factors in supporting capacity, the position of the group on the horizontal scale is the important consideration. The criterion to be satisfied, for such a compact group of actual safety factors, is that the actual safety factor and the one prescribed by the formula be in agreement. If this were true, the formula would not overestimate or underestimate the true supporting capacity as determined by loading tests. Such discrepancies may be experimental in character and are more readily corrected.

In reviewing the charts under discussion it should be emphasized that actual safety factors of less than 1 are not only in the failure range, but with reference to a high prescribed safety factor indicate a wider range of variation in estimated capacity than is apparent from the arithmetic scale on the chart.

For example, in the Engineering News Formula the computed design capacity tied to a safety factor of 6 is also conditioned by the fact that the manufacturer's maximum rated energy has been used in the formula. In the Michigan Study, ENTHRU, considered as the measure of the net energy available for driving the pile, ranged approximately from 1/3 to 2/3 of the manufacturer's rated energy. If ENTHRU values of this order of magnitude were introduced into the formula, still using a "built-in" safety factor of 6, the true or actual safety factor for the same test loads would be shifted upward. The minimum actual safety factor of 1 would then be changed to range from 1.5 to 3. In other words, the formulas are not necessarily at fault, but the discrepancy rests with the values of energy and perhaps other factors being substituted in the formulas.

With one exception, the other ten formulas under consideration include in their development an impact loss factor of conventional form or other special terms to take the energy losses into consideration. The exception is the Gates Formula, which is an empirical relationship between hammer energy and measured test loads with a specified safety factor.

In charts under discussion there are several of these formulas in which the actual safety factors in the low to intermediate load range are fairly consistent with the prescribed safety factor in the formulas. Except for some scatter in the high capacity range, this is true for the Hiley, Redtenbacher, and Gates Formulas at Belleville and with some qualification at Muskegon where the Rabe Formula may also be included. At Detroit, with the possible exception of the Rankine and Gates Formulas, none of the formulas gave consistent results, possibly because the piles included in that chart are nearly all in the upper range of test loads.

While estimates of pile capacity by the dynamic pile formulas leave much to be desired, there is considerable evidence in their favor, and compelling reasons why they should not be abandoned. It may be true that field loading tests are most reliable to determine supporting capacity, and soil test data most reliable for estimating that capacity, but driving resistance is still the most practical method of estimating capacity and controlling it under job conditions.

Field loading tests are time consuming and expensive and only a limited number can be conducted on any one project. There are many projects for which adequate soil investigations may be impractical for one reason or another. This leaves driving resistance as the most readily available and in many cases the only practical method of job control. Consequently, effort should be continued to improve these formulas in the light of new knowledge and to adapt them to the wide range of field conditions that must be met.

Having come to this conclusion, the Michigan State Highway Department has taken steps to adopt soil test data as the primary basis for design. In addition, a modification of the Engineering News Formula, including a conventional impact loss factor, will be retained for job control and specifications. While the present modification is not entirely satisfactory, the probable revision will provide more accurate appraisal of variable factors controlling energy losses and/or an adjustment in the prescribed safety factor.

Correlation with Soil Test Data

Computations of pile supporting capacity from soil test results are presented in complete detail in Chapter 11, in terms of cohesive side shear, frictional side shear, and point resistance or end bearing. Except for several special control tests, all piles were driven to practical refusal so that point bearing was a major factor in capacity.

Clay soils were treated as purely cohesive in computing cohesive side shear, with the shearing resistance determined by the yield value from laboratory tests of "undisturbed" samples. Frictional side shear was computed for a range of normal pressure from active (or minimum) to passive (or maximum). Computation of these principal pressures was based on the concept of internal stability of granular materials, which defines the relationship between principal pressure or principal stress ratio as a function of mutual support between particles, due to arching action rather than shearing resistance from internal friction.

Quantitatively, internal stability is expressed by the angle of pressure transmission $\underline{\theta}$, and functions of that angle. Curves and tables for translating standard field penetration blow counts into angles of pressure transmission have been developed over a period of years through continued correlation of field and laboratory data. The most recent correlations published in the Michigan State Highway Department's "Field Manual of Soil Engineering" were used in computing pile capacity.

Pile capacities at each site are summarized in the report's tables and graphs, in which the three important factors in total pile capacity--cohesive side shear, frictional side shear, and point resistance or end bearing--are combined. Total computed capacity in tons is given in terms of a minimum and a maximum; the actual capacity is interpolated between these limits. In the graphs, capacities from the load tests are given for the first and final loading cycles, selected from the several test determinations as the most reliable measure of capacity in each case. In general, those selected are the yield values determined by extrapolating the settlement rate. For piles driven to refusal, two values of tip capacity have been computed, based on the range of standard penetration $\underline{N}$ in the hardpan or compact sand. The extent to which tip capacity is mobilized is indicated by comparison with these minimum and maximum values.

It should be emphasized that most of the test piles were primarily bearing piles, intentionally driven to practical refusal (33 blows per inch with a Vulcan No. 1 hammer or equivalent, with $\underline{E_n}$ of 15,000 ft-lb per blow) to develop this potential capacity to the fullest extent possible under field conditions. However, side shear due both to cohesion in the clay and to friction in granular material could not be neglected, since these were substantial factors in total capacity.

Cohesive side shear based on laboratory shear tests has been relatively well established as a basis for computing shear reaction from the field loading tests. In these tests the correlation was considered acceptable but not as close ($\pm$ 10 percent) as expected from previous investigations of purely cohesive clay. Possible reasons for this are discussed in the report text. Special repetitive loading tests were conducted immediately after driving to measure cohesive side shear in the clay. The set-up or recovery from disturbance during driving was some 200 percent in 12 to 13 days. While there was some indication, particularly at Detroit, that some additional strength gain could be expected over a long period of time, it was concluded that a period of two weeks after driving would be a reasonable requirement to permit test piles in these clays to recover from disturbance during driving.

Frictional side shear in granular soils involves evaluation of two unknowns, the normal pressure mobilized on the shear plane and the coefficient of friction. In this investigation it turned out that active lateral pressure and a coefficient of friction of unity gave the best correlation with the load test results. Field conditions generally did not appear to favor developing passive pressure along the sides of the piles, and there was little evidence that such maximum resistance was mobilized. Where granular materials were involved in side shear they were generally not completely consolidated, and with pipe piles and H-piles the volume displacement under static load settlement would be negligible. In only one case (Belleville LTP 3), would the combination of a tapered pile with some volume displacement in a well consolidated sand stratum have produced a reasonable coefficient of friction in combination with passive pressure.

Point resistance or end bearing, computed as tip capacity, is the third and possibly most important factor in total capacity of piles driven to refusal in hardpan. Tip capacity computation follows a procedure formulated over a period of years in development of high-capacity bearing piles in the Detroit metropolitan area. In this procedure, standard penetration has been correlated with internal stability (as previously defined on p. 243) and is applied to both granular materials and granular-cohesive mixtures.

Point resistance or end bearing developed by structurally adequate piles driven to practical refusal equalled or exceeded the computed capacity based on the maximum values of standard penetration recorded in the borings. Test results from this project confirmed previous investigations in that highly consolidated and confined granular or granular-cohesive materials such as the Detroit hardpan developed contact pressures in end bearing which approach the crushing strength of the granular particles or rock. In cast-in-place concrete piles with large end bearing areas, these contact pressures were several hundred tons per square foot, ranging from five to ten times the nominal bearing values for rock widely used in engineering practice.

Representative H-piles tested at each site gave even more striking examples of the potential bearing capacity of highly consolidated and confined granular materials. When the point resistance of these piles is assigned to the actual steel end area, the contact pressures varied from 5,730 to 15,250 psi. Bearing pressures on rock of this magnitude are recognized by AASHO Bridge Specifications, where the maximum design

load for steel piles in point bearing is given as 6,000 psi.[1] This is also confirmed by Chellis who recommends pressures for steel H-piles driven to bearing on rock of 3,000 to 6,000 psi, in relation to the crushing strength of rock ranging from 6,000 to 18,000 psi.

Predictability of Supporting Capacity from Soil Test Data

Direct comparison between measured capacity and that computed from soil test data is given for all load test piles in Tables 25, 27, and 29, and presented graphically in Fig. 148.

First, it is important to note that measured capacity in the final loading cycle for all bearing piles equalled or exceeded the predicted or most probable computed capacity, with the exception of one Muskegon pipe pile not driven to refusal for which the tested capacity was 87 percent of computed capacity based on average end bearing, or 97 percent with minimum end bearing. Second, except for three piles requiring special consideration, ultimate capacity of these bearing piles ranged from 82 to 115 percent of computed capacity in the first loading cycle, and from 87 to 133 percent in the final cycle. Based on the average of all tests on bearing piles, the tested capacity was 99 percent of the computed capacity in the first cycle and 108 percent in the final cycle. Two of the three piles requiring special consideration were H-piles and the third was a fluted-tapered pile with a relatively small end-bearing area, all of which developed exceptionally high bearing pressure at the tip.

SUGGESTIONS FOR FURTHER RESEARCH

Regardless of the contribution that the Michigan Pile Study may make to improvement of pile driving practice, those who worked on the project for several years have often felt that this was only a beginning. There were so many questions yet to be answered, so many ways to extend the scope of the study and improve equipment and experimental technique, that comparisons were constantly being made between what was being done and what might have been done. So, in considering problems faced by the investigation and the difficulties that they presented, the discussion often turned to the many opportunities for improvement in equipment and procedure, and the possibilities offered by approaches to a specific problem other than those used. It is the purpose of this part of

[1] Chellis, Robert D. "Pile Foundations" 2nd Edition. New Yrok: McGraw-Hill (1961), p. 315.

the final chapter to set down for the record some of these points, for the benefit of further research that will doubtless be undertaken by others interested in this field.

Scope and Equipment

In the first place, the investigation covered only three sites which were intended to be representative of considerable areas in Michigan, but nevertheless represented only a small range of the varied soil conditions involved in general pile driving practice. With reference to hammer performance as the major objective of the investigation, it was possible to design the experimental program around only two pile types, which though in wide use by no means cover the field of pile configuration. The number of pile driving hammers used was more adequately representative, particularly with respect to diesels, which were of special interest in the Michigan study. However, with rapid advances being made in pile driving equipment in recent years, a much wider area of interest now requires objective study of a similar nature.

In those areas that represent the general scope of the investigation, it seems obvious that extension of the current study to a much wider range of field conditions is desirable to determine the extent to which the results of this study are generally applicable. In addition, there are several phases of the project where the experience of the research staff has produced specific comments and suggestions.

Measuring and Recording Procedures

The instrumentation conceived, fabricated, and utilized on an experimental basis for this study was reasonably successful in accomplishing the objectives, but left considerable opportunities for improvement that became apparent as the project progressed. Such problems as were encountered may be attributed in part to the absence of previously reported research in the literature, upon which this study's research staff could draw for guide lines, coupled with a lack of provision for a pilot or shakedown study. The following specific recommendations are based on the problems and obstacles encountered, and should be given serious consideration in future projects of this type.

Load Cell. In the opinion of the investigators who designed and used it, the load cell proved entirely satisfactory for the purposes of this study. In order to conduct periodic calibrations, it would be advantageous to have a small load frame, incorporating a hydraulic ram, at the site for check

calibrations of the cell. A capacity of 200,000 to 400,000 lb should prove satisfactory for this purpose. However, some question has been raised by others regarding the behavior of the cell under the dynamic loading involved in pile driving. Those who participated felt that this matter should be clearly resolved by dynamic calibration of the cell under impact conditions simulating pile driving. Development of a pendulum device has been suggested as a possible means of applying a known impact force.

Pile Deflectometer. A transducer of the linear variable differential transformer type (LVDT) as used late in this project gave very satisfactory results and was judged to be an excellent dynamic pile deflectometer. Limitations in the practical, usable linear range (2-in.) of this unit were a handicap, but the units are now available up to and including a 6-ft stroke, However, in any future studies, an attempt should be made to develop a high resolution deflectometer, which will give a continuous pile penetration record and can be affixed without interrupting operations. If a transducer of the LVDT type is used, then an accurate displacement calibrator must be provided for frequent calibration checks during field work.

Accelerometers. Considerable improvements in acceleration measurements are now possible over those made in this study. The acceleration transducers selected should have a range of at least $\pm$ 600 g's, and a minimum natural frequency of 4000 cps; of the units meeting these requirements, the one with the maximum sensitivity and highest resolution should be selected. Consideration should be given to the feasibility of incorporating an accelerometer into the load cell in such a manner and location that it measures accelerations of the pile top, along the cell's vertical axis. In addition to accelerometers located at other points of interest in the pile and hammer system, one unit should definitely be mounted on the pile at the location where deflections are being measured. Provision should be made for an accurate, on-site method of accelerometer calibration. It would be desirable that this by a dynamic calibration rather than static or steady state.

Recording Instrumentation. The oscillographic recording system selected should be of the direct-writing type, capable of a paper speed of at least 80 in. per sec, and incorporating amplifiers and galvanometers whose response is essentially flat to approximately 2000 cps.

An additional and very useful recording system would be an automatic blow-sensing device, to accumulate, display, and record the total and incremented blow count continuously in digital form. Such a device

should discriminate between fully effective blows delivered to the pile, and minor or partially effective blows during warm-up or periods of malfunction.

Other Considerations. Before undertaking a major project, an intensive pilot or shakedown test should be performed using all systems and including pile load tests, as well as reduction and analysis of data obtained. This would facilitate the determination of proper recording procedures and format, most efficient data reduction techniques, correct statistical and other analytical procedures, and sensing and recording instrument accuracies and appropriateness. Also, during this pilot test it would be advisable to perform a study aimed at determining the load cell's effects, if any, on driving characteristics of the hammers studied.

Because of the severe environmental conditions and high accelerations encountered in this type of study, it is mandatory that each item of the transducer system be backed up with a duplicate held in reserve at the site, if costly delays are to be prevented.

In future pile driving studies an attempt should be made to arrive at a system capable of providing a continuous record of simultaneously sensed force, acceleration, and deflection data, along with height of pile hammer ram rise, bounce chamber pressure (where applicable), and the air or steam supply pressure. With the knowledge of the problem parameters obtained from this study it clearly would be a great advantage to select a computer-type instrument that would digitize energy output directly in foot-pounds for each hammer blow. This measurement could be obtained without stopping the hammer, by feeding the load cell and deflectometer and/or accelerometer signals directly to the instrument. The computer would then take simultaneous fraction-second samples of each signal, process them, and integrate the total samples taken so as to give the blow energy in a digitized printout and format. Instrumentation to perform such a function is now commercially available.

Experiment Design

Considering the experience of this study, it is not unreasonable to expect considerable variation of blow count data in any field experiment involving such diverse hammer and pile designs as were included in the present project. No mathematical transformation attempted was successful in relieving the collective effects of unequal, uncontrolled variations among hammers, piles, and penetration depths. If the unequal effects of penetration level on various hammers must be estimated, this

will complicate the problem when hammers of widely varying operating characteristics (such as diesel and steam or air hammers) are to be compared using standard statistical methods. Considering both the degree of performance variability and the different design philosophies from which this variability results, analytical difficulties should be anticipated. If these types are to be compared using standard statistical techniques, then extreme care must be exercised in the field in order that variabilities of hammers involved will be as comparable as possible. It must also be remembered that variability is itself a hammer property of some interest, and even if reduced by controlled experimentation, such control might compromise field performance of the hammer.

Further, it is suggested that the quantity of pile and hammer types compared under the same conditions not be too large, or the magnitude of the test area will introduce undesirable soil variation. To some extent this problem can be alleviated both by maintaining maximum data efficiency through use of equal pile quantities for each comparison, and by "blocking" or grouping the replications (piles of the same type driven with the same hammer). Random location of piles within the blocks minimizes the effects of soil variation (if the data are broken down into depth increments, one cannot, of course, randomize in the same pile locations for successive increments), and makes the experiment more sensitive. Location of the blocks would best be determined by extensive soil borings suggesting regions of similar shear resistance. If several pile types are included, each type would have to appear with each hammer in each block. Thus, it is readily apparent that as the scope of the project is extended, both the test area and the block size also become larger, particularly if pile proximity effects are to be eliminated. However, it should be noted that large block sizes will work against the purpose of blocking itself and be of little additional experimental value.[2]

Measurement of ENTHRU

As was pointed out in Chapter 8, it was not possible from the procedures used on this project definitely to identify all the sources of the wide variation in the ENTHRU or net energy delivered to the pile under apparently similar conditions. Hammer type and operation; soil conditions; pile type, mass, rigidity, and length; and the type and condition of cushion blocks were all factors that affected ENTHRU, but when, how, and how much could not be ascertained with any degree of certainity.

---

[2] For planners of future projects of this type, a useful reference is Owen L. Davies "Design and Analysis of Industrial Experiments." New York: Hafner Publishing Co. (1963: second edition).

The following possibilities are suggested to improve accuracy and reliability in future dynamic measurements:

1. Greater precision in the direct measurement of maximum deflection (limset) at the top of the pile. A properly designed LVDT of greater range, as previously noted, may satisfy this requirement.

2. Assurance that the frequency and magnitude of force and acceleration fluctuations do not exceed response limits of the recording equipment.

3. Provision for securely mounted accelerometers, at both the top and bottom of the load cell.

In addition to improving dynamic measurements, certain modifications in methods of analysis would also be helpful. It is suggested that time ordinates assigned to peak acceleration values be carefully checked against those assigned to peak force. These ordinates should be in close agreement since force and acceleration are, so to speak, mirror images of each other. With improved accuracy in measuring peak acceleration, a small shift in the assigned zero base line should bring the maximum deflection from double integration of the acceleration curve close to the corresponding maximum deflection (limset) measured.

The various problems associated with determination of ENTHRU have perhaps received more attention than any other single phase of the Michigan Study. Reviewers have raised several questions regarding the procedure used in digitizing acceleration data for use in the computer program for double integration of acceleration (Pages 117 through 129).

It was pointed out that the percentage adjustment of acceleration trace ordinates is not equivalent to raising or lowering the zero base line by a constant amount, a method that has been used in problems of this nature in other fields. The procedure used in this project was equivalent to making a positive or negative adjustment in the ordinate of the zero base line, of a magnitude varying as a function of the peak acceleration values in any particular time period. This in effect caused the largest adjustment during the period of maximum acceleration, tapering off toward zero at the end of the impact period. When viewed in terms of the relation between successive ordinates of the acceleration trace, the method of integration may be accurately described as based on determination of the average slope of very small segments (0.0001 sec) of that trace.

It is not the intent in this summary to debate the validity of one or the other of these two methods of adjusting acceleration values, but rather to clarify the distinction between them, and to suggest that this is a vital point in data analysis, deserving further study. However, it may be noted that the method of constant adjustment was the first of several techniques considered, and did not prove satisfactory, resulting in excessive distortions in the terminal portions of the computed deflection. Insofar as the investigators who did this work on the current project are concerned, the selected procedure was recognized as an approximation in order to attain a required result as a project objective. However, they felt that the "trial-and-error" displacement curves and corresponding ENTHRU values in Figs. 67, 68, and 69 were acceptable within practical limits, when the maximum computed deflection is brought into close agreement with the measured value (limset).

Although the limset values from manual trace recordings were subject to possible ground quake effects of the reference beam and uncertainties in the stub length correction, final values were believed to be of the correct order of magnitude. Moreover, these computed values showed good agreement with those measured by the LVDT deflectometer at Muskegon (Fig. 70) and in view of the close match between the ascending portion of the deflection traces, the investigators felt that this confirmation justified their confidence in the general procedure for determining ENTHRU.

Another phase of the energy studies requiring further investigation is the high frequency oscillations in the force and acceleration traces, such as those shown in Fig. 32. The analysis was actually carried through the full range of significant acceleration data, but for several reasons interpretation of the results was somewhat speculative. Partly for this reason and partly because the project had to be completed, this area was omitted in final compilation of data and in the report text. However, certain observations and comments may be presented briefly to cover this omission. First, it may be noted again that the recording oscillograph's chart speed was not great enough for satisfactory resolution of high frequency oscillations. Consequently, the wave forms show up on the trace as closely spaced oscillations that would generally be classified as "hash," except that they do include a number of high peaks that obviously have physical significance. This difficulty with the data suggests higher chart speed in future projects.

The second high peak in many of the force and acceleration traces was the subject of much discussion and speculation as to whether it was a reflected compression wave in the pile, or possibly a tension or rare-

faction wave. Keeping in mind that both force and acceleration were being recorded at the load cell, the consensus was that the second peak was a second impact of the hammer, which in the interval between peaks was not transmitting its peak force. In this connection, it may be noted that the force trace is all on the positive side of the zero base line during this interval; thus, the load cell and hammer were not out of contact with the pile at any time. However, after the first impact the pile may have tended to run away from the hammer, but this generally did not result in separation. At the same time, the hammer, with its residual kinetic energy, caught up with the pile and was again able to transmit very close to the full force of the initial impact.

The subsequent series of oscillations, extending over a longer period of time, were thought to fall into the classification of vibration. Double integration of the acceleration trace gives evidence of compensating displacement, with little if any penetration of the pile. Some force is generally being transmitted to the pile through the load cell, but not enough to drive the pile, so it becomes an ineffective dissipation of energy. This portion of the trace, along with that where the force oscillations are compensating, must also be regarded as dissipation of energy and one of the potential sources of energy loss. It may be speculated that these phenomena may vary considerably with pile type, soil conditions, or other uncontrolled variables, whose analysis would throw further light on the wide variability of ENTHRU values reported in Chapter 8 and summarized in Table 37.

Disturbance by Pile Driving Operations

Two aspects of soil disturbance caused by pile driving operations were investigated as part of the project. These concerned first the temporary loss of shear strength experienced in cohesive soils under the dynamic impact of driving, and second, destruction of side friction resistance in granular materials from jetting.

Shear Strength of Distrubed Clay Soils. It is a matter of common experience that in clay soils classified as cohesive a relatively large loss of shear strength occurs during driving. This is reflected by a reduced value of side shear along the length of the pile, and is a consequence of disturbance caused by the dynamic force of hammer blows. There is no such loss nor in fact any discernible loss, when subjecting the pile to static loads, even after developing large movements (i.e., into progressive displacement). It is characteristic of non-sensitive Detroit and other Great Lakes clays, that they eventually recover nearly their

original shear strength. This recovery or "set-up" was measured by repetitive loading cycles at Belleville and Detroit. It amounted to some 200 percent of the initial pile bearing capacity (4 hr after driving stopped), and was almost complete in approximately two weeks.

Question has arisen whether any attempt was made in the laboratory to correlate this reduction and recovery in cohesive side shear with so-called "remolded" shear strength. No such determinations were made or attempted, as the primary objective of measuring the set-up factor was to determine how long the field loading test should be delayed to ensure development of full pile test load capacity.

There was also a question of whether the degree of remolding and the character of disturbance encountered during actual pile driving are physically related to the usual methods of remolding and compacting clay samples in the laboratory. In a previous investigation, this loss of strength appeared to be more closely related to the shock of the hammer blow than to remolding.[3]

The question of strength fluctuations during and after driving is of considerable practical importance and some thought has been given to determining the relative influence of volume displacement, rapidity and character of hammer blows, and set-up time (for elapsed time periods of a few minutes or more) on developed shear strength. Such a test program would involve driving and periodically load-testing several prototype pile segments of varying diameters, both open and closed end, with supplementary laboratory tests. Ideally, soil conditions should be uniform over the area and to depths involved, and indications are that the Detroit test site essentially meets these requirements.

Pile Jetting. The "controlled jetting" experiment in this project consisted of suspending the jet rod within an open end pipe pile, and reducing the driving resistance by washing out the internal soil plug as it formed during driving. Its purpose was to reduce driving effort by eliminating point resistance, but without disrupting side friction in the uncontrolled manner of conventional side wall jetting. In this way a consistent and possibly predictable amount of side friction may be relied upon when estimating pile bearing capacity.

---

[3] Housel, W. S. Discussion of "Effect of Driving Piles into Soft Clay." ASCE Proc., Vol. 75, No. 10 (December 1949), pp. 1521-1528.

A preliminary trial of the method at Muskegon proved the practicability and effectiveness of this procedure. Fig. 98 gives comparative pile driving resistance profiles, showing a reduction of 50 percent or more in driving resistance while jetting, Fig. 97 shows the equipment used. Some refinement of the volume and velocity of jet flows, and also optimum location of the discharge point, are yet to be determined. However, the equipment cost and operation problems are all within economic limits, and the method should be of great value in reducing the size of hammer and/or required pipe wall thickness when penetrating through or into compact granular strata.

Although the method requires that the pipe to be driven open end during actual jetting, development of final end bearing could be accomplished by removing the jet rod, and driving an internal, closed end sleeve or precast plug by means of a mandrel. Subsequent concreting would effectively combine the resistance afforded by the end bearing sleeve, and the side shear of the pipe pile itself. Further development of this possibility is suggested, where job conditions are appropriate.

CONCLUSIONS

From the background of detailed compilation and discussion of procedures and data in the text and appendices of this report, and the preceding summary, the following conclusions are presented to highlight the more important results of the investigation.

Hammer Performance

Performance of pile driving hammers used in this investigation, both diesel and air or steam powered, was compared by blow count, penetration rate, and net energy delivered to the pile, designated in this investigation as "ENTHRU."

1. Blow Count. The Blow Count Ratio as defined in this report compared the hammers by the number of blows required to drive typical piles a given distance under similar conditions. The differential in relative performance of the hammers by this criterion was not large in terms of the number of blows above or below the average or par value under general driving conditions.

2. Penetration Rate. The Penetration Rate Ratio as defined in this report compared the hammers by the penetration in feet per minute under similar conditions. The differential or spread in relative performance was

also relatively small in terms of feet per minute above or below the average or par value under average driving conditions.

This qualified evaluation of the comparison between hammers by these two criteria of performance is made to place them in their true perspective. There were exceptions to these statements conditioned by such factors as poor hammer operation, which is generally controllable, or by exceptional soil conditions, where selection of a hammer designed for those conditions is important. How significant the differentials in performance are depends upon the conditions under which the hammers are to be used, and there is a sufficiently wide variation in driving conditions to require selectivity in hammer design. Judgment of the significance of the comparison in performance should be made from a careful study of the detailed data and their analysis in the report from the standpoint of selecting hammers designed to meet anticipated variation in driving conditions.

3. Hammer Energy Delivered to the Pile. Hammer energy delivered to the pile, ENTHRU, was the third and most important criterion of driving performance. ENTHRU as measured in this investigation generally varied from about one-third to about two-thirds of the manufacturer's rated energy. The large differential between rated energy and ENTHRU is largely due to energy losses during impact rather than to the mechanical efficiency of the energy-producing mechanism of the hammers. There was little evidence in this investigation upon which to question the manufacturer's rating in this respect. On the other hand, there was much evidence to indicate that the mechanism for transmitting this energy to the pile could be greatly improved.

Analysis of energy data indicated that energy losses were strongly conditioned by numerous variable factors in driving conditions, some of which were uncontrolled and in some cases unidentified by observation techniques used in this investigation. The importance of the energy aspect of pile driving justifies the reader's detailed study of the data and their analysis in the report, and the discussion in the preceding section on suggestions for further research.

Supporting Capacity - Estimates and Test Results

In addition to hammer performance, a second area of interest in the Michigan Pile Study was supporting capacity of piles under static load. This part of the project involved field loading tests and two methods of estimating supporting capacity: a) from driving resistance incorporated

in the conventional dynamic pile formulas; and b) from soil test data from borings and laboratory tests.

1. Field Loading Tests. Field loading tests following the procedures used in this investigation provided an accurate and reliable measure of the supporting capacity of the piles under static load. The basic criteria of ultimate capacity of these piles were the yield value, determined by extrapolation of settlement rates determined by increment loading at constant time intervals, and the elastic limit, determined by precise measurement of the elastic and permanent movement of the pile.

2. Dynamic Pile Formulas. The estimates of supporting capacity by dynamic pile formulas, considering the entire group of eleven formulas, varied through a wide range and could not be used to predict pile capacity with any degree of certainty. The greatest variability occurred in the high capacity range, and except for this deficiency several of the formulas gave fairly consistent results insofar as the range of variation was concerned. However, even with good grouping of points, only a few of the formulas showed reasonably good agreement between the actual safety factor found in the tests and that prescribed in the formulas. Even in these most favorable cases, the predicted capacity could not be compared in accuracy with the more precise estimate obtained from soil test data. The reader should examine the detailed data and discussion in Chapter 12 and in the preceding summary to judge for himself the basis for these general conclusions.

While dynamic pile formulas leave much to be desired as a basis for predicting load capacity, it is strongly recommended that they be retained, as one method of rapid determination of capacity and controlling it under job conditions. Even though field loading tests are much more reliable as a measure of supporting capacity and soil test data much more satisfactory for predicting capacity, dynamic pile formulas will still be needed where load tests and adequate soil investigations are not available. Effort should be directed to improvement of these formulas and selection of those most applicable to field conditions.

3. Soil Test Data. It is concluded that soil test data, consisting of standard penetration measurements taken during sampling and laboratory shear tests with a yield value from ring shear or equivalent yield value from unconfined compression, did provide a reliable and accurate basis of estimating static load capacity in this investigation. This conclusion is supported by a number of other investigations in which similar methods

have been used, and there is much evidence to indicate that this is generally true. The Michigan State Highway Department has already moved in this direction on the basis of results from the current study, by adopting soil test data from well-planned soil investigations for design and adopting a modified Engineering-News Formula for specifications and job control.